ABSTRACT

A mathematical investigation of the simultaneous diffusion of heat and moisture in the non-linear medium of soil is presented. In such a porous medium, the evolution of each diffusing agent is determined both by its own momentary distribution and by the distribution of each associated diffusing agent. Mutual destructive and constructive feedback occurs. Understanding of this complex system assists in the management of soil in adverse conditions. Equally, the governing equations contain features central to the concerns of contemporary mathematics.

The controlling equations are derived from basic physical principles. The resulting simultaneous, non-linear partial differential equations have formed the basis of recent work. Relevant research is reviewed in the areas of laboratory and field experimentation, computer simulation, and analytical and numerical approaches. The equations have been supposed analytically intractable for any generality of coupled flow. On the contrary, simulation indicates that a phenonemon of coupled entrainment occurs in which initial profiles are subsumed into the periodicity of the dominant input variation. The propensity of the system to establish quickly such an asymptotic steady state allows analytical accounts to be formed. Concurrence between simulation, analytical solutions and field observation has been achieved.

Understanding of the general state is acquired through the following intermediate stages. The linear diffusion of a system of n coupled variables under both Dirichlet and Neumann conditions is considered. In the latter case, it is shown that the n variables behave as a composition of n^2 component waves. Periodicity is preserved. For each variable, the amplitude, phase and frequency of each of the n input fluxes is carried into the medium by n wave fronts whose rate of decay and speed of penetration depends solely on the coupling of an individual variable. An alternative derivation of this result using semi-group theory is given. The complementary situation of an individual variable diffusing under non-linear gradients is next addressed. Approximate, but applicable, series solutions may be formed. The non-linearity is accommodated within a stable period by the addition of severely decaying higher harmonics. The heating phase is accelerated whilst the cooling phase is retarded. An increase in the mean oscillation occurs.

Simulation indicates that the full system has an analogous qualitative stability. Input periodicity is retained and no subharmonic, chaotic or catastrophic responses develop. The rigorous analytical establishment of this property is apparently beyond the current state of knowledge of non-linear evolution operators in Banach space. Despite the underlying theoretical uncertainty, series accounts may be formed which concur with both simulation and data from field experiments. A possibility of coupled resonance between the variables is restrained by the exponentially decaying nature of the responses. The agreement between simulation, analysis and field data is illustrated by surface and contour plots of the behaviour for a range of surface conditions and controlling parameters.

COUPLED NON-LINEAR DIFFUSION UNDER PERIODIC BOUNDARY CONDITIONS

Roger Shepherd

A thesis submitted in partial fulfilment of the
requirements of the University of Glamorgan/Prifysgol Morgannwg
for the degree of Doctor of Philosophy

June 1994

CONTENTS

ACKNOWLEDGEMENTS

I should like to thank my supervisors, Dr. R. J. Wiltshire and Professor A. Ryley, for their advice and encouragement during the preparation of this thesis.

The support of a Science and Engineering Council Advanced Studentship Award for the Academic Years 1991-1994 is gratefully acknowledged.

I. ORGANISATION

This opening section sets out the content of the thesis in terms of the material included and the arrangement of that material. The research concerns the simultaneous diffusion of heat and moisture in soil under Dirichlet and Neumann conditions of periodic input at the soil surface. Each of the variables diffuses both under its own gradient and that of its coupled co-variable. Complex patterns of interaction occur and despite intensive investigation by soil physicists during the last forty years, the totality of the behaviour remains only partly understood. A hot and arid thermal and moisture regime produces the most marked cross-coupling effects. The husbandry of soils in these unpropitious conditions would be assisted by further understanding. The practical demand, then, is to find such quantitative accounts as may be feasible.

A separate perspective is gained by considering the set of equations presented by soil physics as an abstract mathematical statement. Indeed, the ubiquitousness of the diffusion process implies that systems of similar form arise in several different contexts. Results in the pure mathematics formulation have bearing on these diverse fields. The equations form a set of coupled, fully non-linear partial differential equations, in which the diffusion coefficients are themselves functions of the dependent variables. The response of the system to periodic input has striking qualitative features; an entrainment effect occurs in which the periodicity of the dominant input variable establishes an identical periodicity at all soil levels and amongst all coupled variables. Transients are quickly collected to this state. It is believed, then, that the true theoretical home for the following enquiries is that of an evolution system in Banach space: to uncover function theoretic constraints for the diffusion coefficients and for the input variation, such that periodicity necessarily occurs. It is believed that any diffusion coefficients smooth in their dependence on the dependent variables will produce this effect. Apart from the formal coherence of such an approach, abstract results are required to provide uniqueness and convergence properties for series solutions. However, such a generally posed system is at present beyond the mathematics of non-linear semi-groups as it is being developed in the United States. Nevertheless, the semi-group approach provides succinct methods of description and solution and is used where appropriate.

From the two preceeding paragraphs, it can be seen that the research lies on the boundary between soil physics and mathematics and responds to two kinds of competing interest. The thesis is generated by an interplay between the two. Taking the word in its dictionary sense as an opinion believed to be true, but which cannot be rigorously established and for which supporting evidence is assembled, the thesis to be presented here may be stated as follows, "that coupled non-linear diffusion in soil, which superficially might be expected to display the profusion of different responses normal in

such non-linear systems: the development of subharmonics, and chaotic or catastrophic behaviour, is, on the contrary, marked by an extreme qualitative stability; a steady state is quickly established which is effectively immune to non-linear disruption." This overview provides the organising theme for the report and the subject matter is selected and arranged around it. Before proceeding to a detailed account of the subject matter, the following observation seems relevant. All soil life is synchronised to circadian rhythms transmitted by diffusion. If these rhythms were grossly corrupted by the transmission mechanism, existing soil life would not be feasible. Diffusion in soil must not merely refrain from producing further harmonic distortion, rather it must regulate the irregularities presented to the soil surface. On teleological Darwinian grounds, then, the periodic stability of coupled diffusion is a reasonable and even unavoidable supposition.

The two aspects of this initial dichotomy between soil physics and mathematics are approached separately. The opening section derives the governing equations from basic physical principles. Although the resulting system is of extreme complexity it is assembled by applying quite elementary physical ideas. A major concern here has been to uncover and make explicit the elaborate chains of interdependency relating the different variables. For any differential equation to have validity, it is evident that a clear causal thread must link dependent to independent variables. In the present organic context, it is easy for a careless treatment to lose this thread amongst the web of inter-relations. Unless all the effects of a variation are collected at each step, the distinction between dependence and independence is lost. The aim is to prevent this kind of inadvertent solecism from entering the basic formulation. Several aspects of the equations have been the subject of controversy. As stated in standard form, the equations tend to underpredict moisture flow. Several enhancement mechanisms have been proposed to counter this discrepancy and are summarised as a rider to the basic derivation.

An alternative formulation is available through the theory of the Thermodynamics of Irreversible Processes. The two lead to essentially the same set of equations and to a certain extent it is immaterial which is used. The thermodynamic approach has, perhaps, greater coherence and economy in its derivation. However, since it results in a phenomenological description, it gives no account of the underlying physical mechanisms present in the transmission process. The former approach, often termed the mechanistic theory, precisely assembles effects from these separate factors to produce an overall formulation. Thus the two are complementary. As outlined above, the essential theme of this thesis is that a certain kind of qualitative behaviour results from coupled diffusion and that quantitative accounts may be formed in consequence; it is desired to assert that this effect is independent not merely of the magnitude of diffusion coefficients, but also, in some sense, independent of their actual functional forms. Since the mechanistic and thermodynamic theories are in qualitative

agreement, from this specialised perspective either may be regarded as redundant. In consequence, the mechanistic theory is adopted throughout.

The two theories were developed in the late 1950's and mid 1960's respectively. Experimental work in the intervening years has attempted to link observation to the theoretical framework. The resulting body of work is far too large to be other than cursorarily surveyed. The initial part of the third section gives an overview of studies in the areas of field and laboratory experiments, computer modelling, and numerical and analytical approaches. Two aspects here seem particularly relevant to the concerns of the thesis and are selected for closer scrutiny. Firstly, the range of mathematical studies addressed to non-linear diffusion is obviously the starting point for the present enquiries and is closely reviewed. Secondly, the series solutions obtained must be validated against field data. Two extended experiments, those by Rose in 1968 and Jackson in 1971, are used for this purpose and are described in detail.

Mathematical enquiries are introduced by considering a system of n coupled variables diffusing down constant gradients under Dirichlet and Neumann boundary conditions. Since general behaviour in the asymptotic state bifurcates from the linear response, close analysis of this case has more relevance than might be supposed for a non-linear system. The Dirichlet situation can be solved by an extension of elementary methods and is carried through for reference purposes and to set out notation. Under Neumann conditions of flux input, the solution initially presents itself as a product of four matrices, with imaginary elements in the second and fourth terms, separated by numerical factors in the first and third. To make physical sense of the expression, it is necessary to show how the imaginary terms will interact; to extract their content from the numerical bracketing. This reconstitution, which effectively seeks to evade the non-commutativity of matrix products, can in fact be achieved be rewriting the product as two higher order matrices, of dimensions n x n^2 and n^2 x n, the first a numerical weighting factor and the second descriptive of n^2 component waves which constitute the behaviour for each variable. This decomposition indicates how input wave characteristics are inherited by each variable in terms of the coupling between them. For physically realistic parameters, two further reductions are possible. The cross-coupling is necessarily weaker than the direct coupling and a sensitivity analysis shows that in the three variable case, four of the waves are numerically negligible. Secondly, for soil in hot and arid conditions, heat predominates and the full complement of nine waves reduces to just three having an observable physical effect. Graphical illustrations of the wave forms and their evolution are given. The matrix manipulations required to produce these results are rather involved and may be carried through far more readily by semi-group theory. In formal terms, the decomposition is a resolution of the identity for a contraction operator in Banach space.

The complementary reduced aspect is then addressed. An individual variable diffusing under a strongly non-linear diffusion coefficient, initially taken as a power of the concentration of the agent and then further generalised, is considered. This form of diffusion occurs in many physical situations, and numerous instances are catalogued. Computer investigations indicate that, without exception, for all initial distributions considered, the behaviour quickly becomes entrained to the input rhythm, representing diurnal fluctuation. "Entrained" is something of a misnomer here, since the system is not forced in the sense of an inhomogeneous equation and is merely responding to a condition on the depth boundary. "Resonance" might be a more accurate descriptive term, but is reserved here for a phenomenon which occurs in the coupled case, when one variable can induce a form of damped resonance in its co-variable. Given the form of the equation, for a variable T, diffusing in time, t, and through depth z, when the diffusion coefficient is the variable raised to a power α:

$$\frac{\partial T}{\partial t} = T^{\alpha}\frac{\partial^2 T}{\partial z^2} + \alpha T^{\alpha-1}\left(\frac{\partial T}{\partial z}\right)^2 \quad ,$$

it is by no means obvious why the equation should have such a propensity to cyclic response; why transient behaviour is indeed so transient. A series solution approach describes the steady state periodicity, but unfortunately excludes transient evolution to that state. It is seen that the non-linearity is accommodated by the addition of severely decaying harmonics, giving an acceleration of the heating phase and a retardation of the cooling phase, within a period which is stabilised, rather than perturbed, by the effects. Transient patterns, necessitating a wide harmonic range, are presumably in some sense captured by the severe convergence of the series. However, it is difficult to express this intuition in formal analytical terms.

Summarising, it is seen that both coupled linear diffusion and individual non-linear diffusion respect input wave characteristics. The first reconciles contradictory fluxes by integrating their forms in a composition of component waves; the second responds to non-linearity by the addition of rapidly decaying harmonics. The essential question to be addressed by research into the full system, then, is whether qualitatively distinct features attach to the behaviour under mutual interaction of these effects. The extreme stability of the system in fact implies that destabilising factors induced by the coupling are restrained to the extent that qualitative uniformity results. This property may be established algebraically, and is, indeed, immediately apparent from the form of the series solutions. Secular terms representing non-linear feedback into the system are present, but are subject to exponential decay. Interaction between the terms increases the order of the exponentials; in consequence, the algebraic mechanisms which normally produce radical bifurcation are too damped to have effect. The system is self-protecting against incursions of non-linear behaviour.

Prior to this investigation it is necessary to assemble the detailed forms of the diffusion coefficients. Surprisingly, nowhere in the literature is this task carried through; separate results distributed amongst the body of research papers are gathered together to be applied in series approximations. Each of the four diffusion coefficients is a function of temperature and moisture content. As these latter vary over possible ranges, each diffusion coefficient can be regarded as mapping out a diffusion co-efficient surface, and equally, the balance between them can be regarded as defining two eigenvalue surfaces. The properties of coupled diffusion then depend on the configuration of these surfaces and, in particular, on their tangent planes at each point associated with a temperature and moisture content coupling. These features are illustrated graphically for the two soils later used for validation against field results. A sensitivity analysis indicates that some aspects of the variation are less decisive than might initially be supposed. These enquiries occupy a separate section.

The series solution for the coupled situation is then derived. It is shown to give good agreement with simulation for physically realistic soils. A possibility of damped resonance between the variables acting in the second harmonic is uncovered by this approach. An interesting feature here is that the resonance is not, as is normally the case, triggered by a constructive interference between the input frequencies, but between the input means. Resonance cannot occur for parameters relevant to soil and is illustrated instead by following system which seemingly is the simplest in which this phenomenon may occur,

$$\frac{\partial}{\partial t}\begin{bmatrix} T \\ \Theta \end{bmatrix} = \frac{\partial}{\partial z}\left\{ \begin{bmatrix} T & 1 \\ 0 & 1 \end{bmatrix} \frac{\partial}{\partial z}\begin{bmatrix} T \\ \Theta \end{bmatrix} \right\} .$$

Other aspects of the wave form evolution: the migration of the mean values, which in the coupled case may either increase, decrease or oscillate; the acceleration of the heating phase and retardation of the cooling phase and the rapid extinction of transients, are illustrated with reference to this case. Analogous effects in soil are of the same order of magnitude as irregularities produced by the non-uniformity of the medium and are not readily observable.

It now remains to show that the theoretical approaches do indeed accurately describe the field observation of soil. Two experiments are chosen for this purpose: the 1968 investigation of Rose in the Australian outback and that of Jackson in 1971 at a site in Arizona. Two initial difficulties must be acknowledged here. Firstly, there is a paucity of data for extended observation of soil. Aligned to this situation, and in all probability in response to it, there is an understandable tendency on the part of researchers to design experiments which monitor soil at dramatic extremes of behaviour. Both Rose and Jackson take soil in an arid, tropical environment, subject the sample to saturation intake of moisture and observe the ensuing development. Their experiments observe not merely infiltration but

inundation and the subsequent re-establishment of long-term normality. They observe natural, but highly exceptional, evolutions. For the present line of approach it would be helpful to have field data not characterised by such extreme discontinuities at the outset.

Secondly, there is a theoretical difficulty in determining appropriate boundary conditions for coupled flow in a semi-desert environment. Heat is evidently transmitted directly into soil with little mediation at the boundary. In contrast, for moisture there is a discontinuity between the dry air at the surface and the residual moisture of the medium. In purely formal terms, under coupled flow both variables are, so to speak, on an equal footing; any solution must contain symmetries consequent on the symmetrical role the variables perform in the equations. Seemingly, then, there is a logical non-sequitur: coupled flow must express symmetry in the medium whilst responding to complete dissymmetry at the boundary. These questions are considered in more detail in section **IX**.3. Evidently, there must exist a boundary layer in which a complex evaporation/distillation budget allows the contradiction to be reconciled. It would be interesting to see if a boundary layer or waiting time solutions may be developed for coupled flow to describe a surface layer in which one variable is continuous whilst its associate is highly discontinuous. This speculation seems the most interesting raised by the present enquiries.

Returning to the reconciliation of theory and experiment, an argument may be advanced that at the surface layer moisture undergoes a phase retardation of $\frac{5\pi}{4}$ in consequence of its negative entrainment to heat flux. As this wave passes through the medium, phase similarity between heat and moisture is re-established. Taking boundary conditions in this form, the series solution may be re-evaluated and can be shown to concur both qualitatively and quantitatively with the separate observations of Rose and Jackson. Wave form evolution, progression and decay can be accurately portrayed, particularly towards the closing period of the experiments when asymptotic periodicity has been attained. Conclusions drawn from the whole body of work and suggestions for potentially productive future lines of enquiry bring the thesis to a conclusion.

II. DERIVATION OF THE COUPLED EQUATIONS

II.1 Introduction.

Classical mathematics, as developed in the seventeenth and eighteenth centuries, was addressed exclusively to the inorganic. Its achievements derive from analysis of behaviour in mechanical terms; an expression of the Enlightenment attitude which saw the universe itself as mechanistic, determined and ordered. In contrast, the most fruitful fields of contemporary mathematics seem applications to biology and environmental systems generally. In moving to an organic substance such as soil, it is apparent that mechanical models are not as immediately applicable. The causal relationships between variables are by no means as clear cut as in traditional areas. What might be termed an ecology of variation is encountered, in which each variable simultaneously affects all the others. Strenuous efforts must be made to ensure that interim equations gather together all side-effects of a variation. The aim, then, is to establish clear causal links between dependent variables of human import, such as moisture and heat content, through interim factors internal to physics such as partial pressures and relative humidities, finally to the space and time co-ordinates of measurement.

Twentieth century soil physics springs from the surprising realisation in early seminal papers (Buckingham **[11]** , Bouyoucos **[8]**) that pressures existing in soil are sufficient to allow moisture to be held and transported in the vapour phase. In referring to coupled flow, the coupling of moisture and heat is in detail a coupling between liquid water, water vapour and heat. The soil matrix forms a three component, two phase system. It will be seen that moisture flow depends on four diffusion coefficients, denoting the response of both liquid and vapour to both moisture and heat gradients, whilst heat flow depends on three diffusion coefficients, describing conduction and the transfer of latent heat by vapour acted on by moisture and heat gradients. This formulation omits numerous additional aspects, such as the transfer of sensible heat, which are quantitatively negligible. In order not to lose sight of the eventual goal among a mass of technicalities, and to establish basic notation, it may be helpful to have a statement of the system to be derived. The remainder of this section will assemble this system from first principles.

$$\frac{\partial \theta_l}{\partial t} = \nabla \cdot ((D_{Tv} + D_{Tl}) \nabla T) + \nabla \cdot ((D_{\theta l} + D_{\theta v}) \nabla \theta_l) + \frac{\partial K}{\partial z} \qquad (2.1)$$

$$C\rho_l \frac{\partial T}{\partial t} = \nabla \cdot ((\lambda + L\rho_l D_{Tv}) \nabla T) + L\rho_l \nabla \cdot (D_{\theta v} \nabla \theta_l) , \qquad (2.2)$$

where the following symbolism is used

θ_l	volumetric liquid content, cm^3/cm^3.
t	time, sec.
$\nabla \cdot$	divergence operator.
D_{Tv}	thermally induced vapour diffusivity, $cm^2/sec/^\circ C$.
D_{Tl}	thermally induced liquid diffusivity, $cm^2/sec/^\circ C$.
∇	gradient operator.
T	temperature, $^\circ C$.
$D_{\theta l}$	isothermal liquid diffusivity, cm^2/sec.
$D_{\theta v}$	isothermal vapour diffusivity, cm^2/sec.
K	hydraulic conductivity, cm/sec.
z	depth (measured downwards), cm.
C	volumetric heat capacity, $cal/cm^3/^\circ C$.
λ	thermal conductivity, $cal/cm/sec/^\circ C$.
L	heat of vaporisation, cal/g.
ρ_l	density of liquid water, g/cm^3.

As stated, this formulation omits diffusion arising from gradients in saline concentration. The inclusion of saline flow is currently the subject of much research activity. Jury, Stolzy and Letey [55] show how the system as a whole may be extended to the three variable case. The methods to be developed below are either addressed to a generally posed system of n variables, or may be extended from two variables to the three at a cost of increased algebraic complexity. Simulation and the validation of results against field data, then, are carried through only for the case of coupled heat and moisture. Equations (2.1) and (2.2), as derived directly from basic physical principles, produce diffusion coefficients which underpredict moisture flow. The various enhancement mechanisms which have been proposed to supplement the basic forms are considered in section II.4.

II.2 Moisture Flow: the Conservation of Mass.

2(i) Introduction.

The section begins by deriving an expression for the flux of soil moisture. Continuity considerations then allow the full differential equation to be formed. The line of argument is as follows: to describe soil water in terms of a potential; to regard flow as seeking to establish equilibrium of that potential; finally to rewrite potential in terms of water content. For the vapour component of moisture flow, an interim expression for vapour pressure is required.

The notion of potential as the fundamental agency of moisture movement is perhaps tautological, since potential itself is defined in terms of various component energies, which are used directly later in the theory. However the development of an argument in such terms is closely analogous to the derivation of other physical theories. The description of potential follows Jury, Letey and Stolzy **[55]**. It should be noted that potential is expressed as energy on a unit weight basis and so has dimensions of length.

2.(ii) Soil Water Potential.

The components contributing to soil water potential are as follows, although, since the report aims to keep the sequence of dependencies clear, it should be remarked that these components are not independent, but will overlap in different contexts. Appropriate combinations are selected for each different use.

Gravitational Potential, z.

This term is the familiar potential energy of elementary kinetics: the energy associated with the water by virtue of its elevation in the soil above some reference level.

Pressure Potential, P

In expending work to overcome pressure differences, water acquires a potential energy. Since the work done in moving a volume of water, V, through a pressure difference, p, is pV, (Edelfson and Anderson **[30]**), when expressed on a unit weight basis, the dimensions are again of length. For water submerged within the water table, the term is positive, denoting work done by hydrostatic pressure. In the context relevant here, of water held within the soil matrix by attractive forces, it is negative, denoting energy expended to attain the current position. This formulation would include work done against differences in atmospheric pressure external to the soil. However, such differences are negligible for soil water movement either with depth or through time, and so pressure potential, for present purposes, reduces to matric potential, that is, the work done by attractive forces in the soil to draw water into the matrix.

Matric Potential ψ.

Matric potential arises from capillary and adsorptive forces within the minute pathways available for water movement within soil. It is perhaps more vividly described as the suction of the soil. The sum $z + \psi$ is the hydraulic head, giving the length of a column of water supported by a soil in tensiometer reading: the historical reason for the use of length as a descriptive unit. It is the large forces which these mechanisms may exert which give soil physics some of its surprising and non-intuitive character.

Osmotic Potential s.

The osmotic potential is the portion of the total potential owing to dissolved solutes in the soil water. The dipole moment of water molecules results in an electrostatic attraction to the solute ions. Thus water is held in a bound state of energy lower than the reference state. Solutes in water affect mainly vapour density and pressure; full consideration of moisture diffusion should ideally take account of their effects. However, the system is considered here solely in terms of the coupling between heat and moisture and detailed results are carried through only for this case.

2.(iii) The Flux of Liquid Movement.

With these definitions of potential, a kinetics of water movement can be formed. The earliest formulation is that of Darcy **[22]**, who found the flux of water percolating through a porous sand bed was directly proportional to the potential head:

$$\frac{q_l}{\rho_l} = -K \nabla \cdot (P + z) , \tag{2.3}$$

where

q_l liquid flux, $g/cm^2/sec.$

K unsaturated hydraulic conductivity, $cm/sec.$

This equation describes saturated flow. For the air/water component mix in unsaturated soils, Buckingham **[11]**, replaced P by the matric potential ψ:

$$\frac{q_l}{\rho_l} = -K(\psi) \nabla \cdot (\psi + z) , \tag{2.4}$$

where K is now a strongly varying function of ψ. This relationship has been exhaustively tested under laboratory conditions (Gardner and Freeman **[35]**, Jackson et al **[47]**, Nielsen et al **[62]**).

The relation (2.4) expresses liquid flux in terms of potential. As outlined initially, the potential is now decomposed in terms of its dependency on moisture content and temperature. Two separate considerations are required. Firstly, the suction that a particular soil has available is a function of its water content. This relation is a fundamental property of the soil, termed its moisture characteristic, and largely determines its everyday horticultural utility. A coarse sandy soil will retain only moderate quantities of moisture and lose that content quickly; its suction characteristic is low for all values of moisture content. The relation can only be determined empirically by experiment. It is perhaps a reflection of the unsatisfactory basis of soil physics that this crucial step linking potential to water content is not amenable to a theoretical analysis. However, Childs and Collis-George **[20]** defined the following diffusivity function via the moisture characteristic curve:

$$D(\theta) = K(\psi)\frac{\partial\psi}{\partial\theta}. \tag{2.5}$$

Secondly, for the range of relatively damp soil in which liquid moves in response to a moisture gradient, suction is due to capillary action, which in turn is proportional to surface tension, (De Vries **[23]**). Hence,

$$\frac{\partial\psi}{\partial T} = \frac{\psi}{\sigma}\frac{d\sigma}{dT}, \tag{2.6}$$

where,

σ surface tension, g/sec^2.

The two equations (2.5) and (2.6) now allow the decomposition of the suction gradient into two component gradients of temperature and moisture content:

$$\frac{q_l}{\rho_l} = -K(\psi)\left\{\frac{\psi}{\sigma}\frac{d\sigma}{dT}\nabla T + \frac{\partial\psi}{\partial\theta_l}\nabla\theta_l + \nabla z\right\}, \tag{2.7}$$

which implicitly defines two of the diffusivities,

$$\frac{q_l}{\rho_l} = -(D_{Tl}\nabla T + D_{\theta l}\nabla\theta_l + \nabla z). \tag{2.8}$$

2.(iv) The Flux of Vapour Movement.

Turning now to moisture contained in the vapour phase, the activating gradient is described by Fick's Law **[32]**,

$$q_v = -D^*\nabla\rho_v, \tag{2.9}$$

where

D^* molecular diffusivity of water vapour in the porous medium, cm^2/sec.

ρ_v density of water vapour, g/cm^2.

Work by Penman **[70]**, Krischner and Rohnalter,**[59]**, Van Bavel, **[87]** and Rollins et al**[80]**, showed that to relate D^* to D_{atm}, the molecular diffusivity in air, requires three phenomenological factors:

α a tortuosity factor, to denote the increased path length, cm/cm.

a the volumetric air content of the porous medium, cm^3/cm^3.

v a mass flow factor, *dimensionless*.

Partington,**[66a]**, showed that for steady diffusion in a closed system,

$$v = \frac{P}{P-p}\,, \tag{2.10}$$

where

p partial pressure of water vapour, $cm.Hg.$

P the actual pressure present, $cm.Hg.$

Note that this use of P differs from its earlier definition as pressure potential. Hence,

$$q_v \;=\; -D_{atm}\alpha \;\; a\,\frac{P}{P-p}\,\nabla\rho_v\,. \tag{2.11}$$

At this stage, vapour flux has been related to a gradient of vapour density. As before, the aim is to decompose this gradient into gradients of temperature and moisture content. Following the early workers cited, a thermodynamic relation (Edelfson and Anderson **[30]**) is introduced,

$$\rho_v \;=\; \rho_o\, h \;=\; \rho_o\, e^{\frac{\psi g}{RT}}, \tag{2.12}$$

where

ρ_o density of saturated water vapour, g/cm^3.

h relative humidity, *dimensionless.*

g acceleration due to gravity, cm/sec^2.

R gas constant of water vapour, $erg/g/^{\circ}C$.

The important paper of Philip and De Vries**[78]**, considered the detailed behaviour of h in two regions, characterised by whether adsorption or capillary action is the dominating force in moisture retention. Using data of Carmen and Raal**[13]**, it was shown that for both regions h is effectively a function of water content alone. By definition, ρ_o depends on temperature alone. Hence the following decomposition is valid, not merely as a formal application of the chain rule, but as an expression of the actual physical realities,

$$\nabla\rho_v \;=\; h\,\frac{d\rho_v}{dT}\,\nabla T \;+\; \rho_o\,\frac{dh}{d\theta_l}\,\nabla\theta_l\,. \tag{2.13}$$

Using (2.12) gives

$$\nabla\rho_v \;=\; h\,\frac{d\rho_o}{dT}\,\nabla T \;+\; \frac{g\rho_v}{RT}\,\frac{\partial\psi}{\partial\theta_l}\,\nabla\theta_l \tag{2.14}$$

and substitution in (2.11) leads finally to

$$q_v \;=\; -D_{atm}\,\alpha a\,\frac{P}{P-p}\left\{\, h\,\frac{d\rho_o}{dT}\,\nabla T \;+\; \frac{g\rho_v}{RT}\,\frac{\partial\psi}{\partial\theta_l}\,\nabla\theta_l \,\right\}, \tag{2.15}$$

or,
$$q_v = - \{ D_{Tv} \nabla T + D_{\theta v} \nabla \theta_l \} . \tag{2.16}$$

Later formulations, e.g. Ghali **[36]**, have included terms for the temperature dependency of h, but are quantitatively negligible. Equations (2.8) and (2.16), then, give the required relation between the two components of moisture flux and the gradients of temperature and moisture content.

2.(iv). The Continuity of Moisture Flux.

Following now De Vries**[23]**, continuity considerations are applied to the two equations for flux, (2.8) and (2.16), to establish the time dependency of moisture variation. Introducing evaporation as the transfer mechanism between the two phases gives

$$\frac{\partial \theta_l}{\partial t} = -\nabla \cdot \left(\frac{q_l}{\rho_l} \right) - E \tag{2.17}$$

$$\frac{\partial \theta_v}{\partial t} = -\nabla \cdot \left(\frac{q_v}{\rho_l} \right) + E \tag{2.18}$$

and adding,

$$\frac{\partial \theta}{\partial t} = -\nabla \cdot \left(\frac{q_m}{\rho_l} \right), \tag{2.19}$$

where

E rate of evaporation, sec^{-1}.

q_m total moisture flux, $g/cm^2/sec.$

θ total volumetric moisture content, cm^3/cm^3.

The assumption that liquid water is in equilibrium with water vapour gives, using (2.12),

$$\theta_v = (s - \theta_l) \frac{\rho_v}{\rho_l} = (s - \theta_l) \frac{\rho_o h}{\rho_l} , \tag{2.20}$$

where s porosity, cm^3/cm^3.

Differentiating (2.20) with respect to time, with the decomposition (2.14) of ρ_v , leads to

$$\frac{\partial \theta_v}{\partial t} = \left\{ \frac{(s-\theta_l)}{\rho_l} \rho_o \frac{gh}{RT} \frac{\partial \psi}{\partial \theta_l} - \frac{\rho_v}{\rho_l} \right\} \frac{\partial \theta_l}{\partial t} + \frac{(s-\theta_l)}{\rho_l} h \frac{d\rho_o}{dT} \frac{\partial T}{\partial t} \tag{2.21}$$

$$= \left\{ \frac{D_{\theta v}}{\alpha v D_{atm}} - \frac{\rho_v}{\rho_l} \right\} \frac{\partial \theta_l}{\partial t} + \frac{(s - \theta_l)}{\rho_l} h \frac{d\rho_v}{dT} \frac{\partial T}{\partial t} , \tag{2.22}$$

where the definition of $D_{\theta v}$ implicit in (2.16) is used. Equation (2.18) now gives an expression for E in terms of the above, and using this value in (2.17) leads finally to

$$\left\{ 1 + \frac{D_{\theta v}}{av D_{atm}} - \frac{\rho_v}{\rho_l} \right\} \frac{\partial \theta_l}{\partial t} + \frac{(s - \theta_l)}{\rho_l} h \frac{d\rho_o}{dT} \frac{\partial T}{\partial t} = -\nabla \cdot \left(\frac{q_m}{\rho_l} \right) = \nabla \cdot \left(\frac{q_v + q_l}{\rho_l} \right)$$

$$= \nabla \cdot \left((D_{\theta l} + D_{\theta v}) \nabla \theta_l \right) + \nabla \cdot \left((D_{Tv} + D_{Tv}) \nabla T \right) + \nabla z , \quad (2.23)$$

where the expressions for flux (2.8) and (2.16) are used. Equation (2.23) represents the full relationship between moisture content and its activating gradients. However Rose, **[81]**, showed that of the four coefficients on the left hand side of (2.23) the second, third and fourth are of the order of magnitude 10^{-3}, 10^{-5} and 10^{-9} of unity respectively. Thus the form quoted initially is reached:

$$\frac{\partial \theta_l}{\partial t} = \nabla \cdot \left((D_{\theta l} + D_{\theta v}) \nabla \theta_l \right) + \nabla \cdot \left((D_{T\theta} + D_{Tv}) \nabla T \right) + \nabla z .$$

II.3 Heat Flow: The Conservation of Energy.

When considering moisture flow, the full derivation was reached in two steps, first by assembling an expression for flux of the two phases and then by applying continuity considerations. Following the De Vries**[23]** formulation for heat flow, which seems to have been universally adopted in later work, the two stages can be coalesced, at perhaps some cost of clarity in depicting the contributory mechanisms. The heat flux can be written directly as

$$q_h = -\lambda \nabla T + L_o q_v + c_p (T - T_o) q_v + c_l (T - T_o) q_l , \quad (2.24)$$

where,

q_h heat flux, $cal/cm^2/sec.$

L_o heat of vaporisation at reference temperature, $cal/g.$

c_p specific heat of water vapour at constant pressure, $cal/g/^oC.$

c_l specific heat of liquid water, $cal/g/^oC.$

T_o reference temperature, ^oC,

and the terms of (2.24) account for respectively: the hypothetical thermal conductivity of the soil in the absence of moisture transport; the transfer of latent heat by vapour; and the transfer of sensible heat by vapour and liquid phases. It is assumed that heat transfer by convection and radiation is negligible, De Vries**[23]**,

The total heat content per unit of volume, then, is given by

$$C_d(T - T_o) + L_o \rho_l \theta_v + c_p \rho_l \theta_v (T - T_o) + c_l \rho_l \theta_l (T - T_o) - \rho_l \int_0^{\theta_l} W . d\theta_l , \quad (2.25)$$

where

C_d thermal capacity of soil in the absence of moisture, $cal/cm^3/^oC.$

W differential heat of wetting, $cal/g.$

and the terms describe: the heat content of the soil matrix in the absence of moisture; the latent heat content in vapour; sensible heat in vapour and liquid phases, and finally the differential heat of wetting. Applying conservation principles, the time differential of (2.25) must equal the spatial differential of (2.24), and so,

$$C_d \frac{\partial T}{\partial t} + L_o \rho_l \frac{\partial \theta_l}{\partial t} + c_p \rho_l (T - T_o) \frac{\partial \theta_v}{\partial t} + c_l \rho_l (T - T_o) \frac{\partial \theta_l}{\partial t} - \rho_l W \frac{\partial \theta_l}{\partial t} =$$

$$\nabla (\lambda \nabla T) - L_o \nabla q_v - c_p q_v \nabla T - c_l q_l \nabla T - c_p (T - T_o) \nabla q_v - c_l (T - T_o) \nabla q_l . \quad (2.26)$$

This somewhat formless expression must now be manipulated to allow the underlying relations between liquid content and temperature and their gradients to become visible. The expressions involving θ_v, W and the flux terms must be recast for their dependence on these factors. Four separate substitutions are necessary, with an expression for E required as an interim step. This last will be derived first.

Reverting to the previous section, the basic continuity equations (2.17) and (2.18) relate the fluxes to the time rate of change they produce. However, this relation involves E, the condensation/evaporation term linking the two phases. Making E the subject of (2.18), and substituting for the time rate of change of vapour content from (2.22), and for q_v from (2.16), it is found that

$$E = \left\{ \frac{D_{\theta v}}{av D_{atm}} - \frac{\rho_v}{\rho_l} \right\} \frac{\partial \theta_l}{\partial t} + \left\{ \frac{s - \theta_l}{\rho_l} h \frac{d \rho_o}{dT} \right\} \frac{\partial T}{\partial t} + \nabla \cdot (- D_{\theta v} \nabla \theta_l - D_{Tv} \nabla T) . \quad (2.27)$$

An expression for the differential heat of wetting (Edelson and Anderson[30]) is

$$W = - \frac{g}{j} \left\{ \psi - T \frac{\partial \psi}{\partial t} \right\}, \quad (2.28)$$

where

j mechanical equivalent of heat, erg/cal.

Further, the latent heats are related by

$$L = L_o - (c_l - c_p) (T - T_o). \quad (2.29)$$

The four substitutions in (2.26) are then successively, for L_o from (2.29), for W from (2.28), and for q_l and q_v from (2.8) and (2.16), using (2.27) to write E explicitly in these last. It is found that

$$\left(C + L (s - \theta_l) h \frac{d\rho_o}{dT} \right) \frac{\partial T}{\partial t} + \left\{ \frac{L\rho_l D_{\theta v}}{\alpha v D_{atm}} - L\rho_v + \rho_l j^{-1} g \left(\psi - T \frac{\partial \psi}{\partial T} \right) \right\} \frac{\partial \theta_l}{\partial t}$$

$$= \nabla \cdot \{ (\lambda + L\rho_l D_{Tv}) \nabla T \} + L\rho_l \nabla \cdot (D_{\theta v} \nabla \theta_l)$$

$$+ \rho_l c_p \{ (D_{\theta v} \nabla \theta_l + D_{Tv} \nabla T) \cdot \nabla T \} + \rho_l c_l \{ (D_{\theta v} \nabla \theta_l + D_{Tl} \nabla T + \boldsymbol{k}) \cdot \nabla T \}, \quad (2.30)$$

where $\boldsymbol{k}$ is the unit downwards vector.

This equation, which is itself a reduction, gives an indication of the complexity of accounting for all mechanisms of heat transfer in soil. A reduction in terms of orders of magnitude is again available (Rose **[81]**), giving the following, where the ignored terms are at least of the order of 10^{-3} of the smallest of those included,

$$C \frac{\partial T}{\partial t} = \nabla \cdot ((\lambda + L\rho_l D_{Tv}) \nabla T) + L\rho_l \nabla \cdot (D_{\theta v} \nabla \theta_l) .$$

Thus the justification of the equations quoted initially is concluded.

II.4 The Enhancement of Water Vapour Diffusion

The theory detailed above was available to soil physicists by the early 1950's. The novelty of the formulation at the time was the unexpectedly prominent role given to vapour transportation. Numerous laboratory investigations were undertaken to test this prediction. (Gurr and others, **[40]**, Taylor and Cavezza, **[84]**, Rollins and others, **[80]**). It was found in all cases by these early experimenters that the theory in fact underpredicted the actual effects of vapour transport. The disparity between theory and observation initiated a major drive in soil physics, which has continued to the present day, to evaluate and understand the exact contribution of the coefficient D_{Tv}, given by equations (2.15-6). In general, experiments have been designed around this goal, with other factors considered in so far they affect vapour movement. Equally, the simple theory described above has been augmented to include additional effects producing vapour transport. These approaches retain the basic formulation in terms of Fick's law modified by pore space geometry. Enhancement of diffusion is shown to occur through effects arising from the simultaneous presence of liquid and vapour phases in the medium.

The 1957 paper of Philip and De Vries **[78]** described two such enhancement mechanisms. Firstly, it was postulated that since the thermal conductivity of water vapour is far lower than either of the conductivities of the liquid or solid phases of the medium, the temperature gradient across a vapour

filled pore cannot be as readily discharged as in the surrounding matrix. The microscopic temperature gradients acting on vapour are thus greater than those recorded macroscopically. Secondly, it was proposed that in a fairly dry medium, transport occurs in a series-parallel fashion across isolated 'islands' of liquid, condensing at the upper meniscus and evaporating at the lower meniscus, in the temperature gradient. The liquid content is then regarded as available for vapour movement in addition to the volumetric air content, increasing the cross section through which flow occurs. In a further elaboration of this theory, Jury and Letey, **[54]**, analysed the heat fluxes present in the successive vapour/liquid/vapour stages of this flow. The lower conductivity of vapour as opposed to liquid results in a further enhancement of the temperature gradient acting on vapour. The remainder of the present section will give the quantitative account of these proposed mechanisms.

The vapour flux density in an air-filled pore is given by the modification of (2.11) to

$$- D_{atm} \frac{P}{P-p} \; h \frac{d\rho_o}{dT} (\nabla T)_a \,, \tag{2.31}$$

where αa is set to one, and $(\nabla T)_a$ denotes the average temperature gradient across all such pores. If now the condensation/re-evaporation mechanism outlined above allows liquid content to transmit vapour, then the total vapour flux density becomes

$$q_v = -(\, a \, + \, \theta_l \,) D_{atm} \frac{P}{P-p} \; h \frac{d\rho_o}{dT} (\nabla T)_a \,. \tag{2.32}$$

An enhancement factor, η, may now be defined by the ratio of the above expression to that given by the simple theory,

$$\eta \;\; = \;\; \frac{a+\theta_l}{\alpha a} \; \frac{(\nabla T)_a}{\nabla T} \,. \tag{2.33}$$

The portion of this term arising from the ratio of temperature gradients is denoted by ζ and may be evaluated by a method of De Vries **[24]** which calculates the thermal conductivity of soil in terms of its constituents. It is found that

$$\zeta = \frac{(\nabla T)_a}{a(\nabla T)_a + \theta_l (\nabla T)_l + (1-a-\theta_l)(\nabla T)_s} \;\; , \tag{2.34}$$

where $(\nabla T)_a$, $(\nabla T)_l$ and $(\nabla T)_s$ are the temperature gradients averaged over the volumes occupied respectively by air, liquid and solid.

The above theory applies to flow when moisture content is too low to allow liquid continuity to exist. Generalising the theory for all values of θ_l , Philip and De Vries argued that as θ_l increases beyond the point of resumption of liquid continuity, denoted by θ_K, then the cross-section available for series-parallel flow would steadily decrease to zero. This property may be denoted by a function $f(a)$, modifying (2.33) to

$$\eta = \frac{a + f(a)\theta_l}{\alpha a} \frac{(\nabla T)_a}{\nabla T} , \tag{2.35}$$

where $f(a) = 1$ for $a \geq a_K$ (a_K denoting the value of a at θ_K) and $f(a)$ -> 0 as a -> 0. A first approximation was proposed as $f(a) = \frac{a}{a_K}$ for $a \leq a_K$.

Validation of the Philip and De Vries model has been an active research area. Jury and Letey **[54]** summarise experiments by Wicks et al **[92]**, Cary and Taylor **[17]**, Hanks et al **[42]** , Cary **[15]**, and Nielsen et al **[62]**, to conclude that an underprediction of up to an order of magnitude between theory and observation is still present. They propose a further enhancement to the temperature gradient acting on vapour flow.

The starting point for this approach is analysis of heat flux within the series-parallel flow. In the vapour region, the heat flux is given by

$$q_h = -\lambda_{as} \left(\frac{dT}{dz}\right)_a + Lq_v , \tag{2.36}$$

where λ_{as} is the thermal conductivity of the saturated air. A thermodynamic analysis derived from Cary **[16]** now indicates that the second term in this expression, for temperatures less than 60^0 centigrade, gives rise to a flow of heat less than that which would occur across liquid water. A corresponding increase of the local temperature gradient across the vapour region occurs. In the Philip and De Vries model, the flow across the liquid island is conceptualised as equivalent to solely vapour transport; in fact, the present more detailed analysis indicates that the liquid acts to shorten the equivalent vapour path. Since,

$$\left(\frac{dT}{dz}\right)_l = \frac{q_h}{\lambda_l} = \frac{\lambda_v}{\lambda_l}\left(\frac{dT}{dz}\right)_v , \tag{2.37}$$

where the subscripts l and v denote gradients and conductivities in the liquid and vapour phases. This modification of path length may now be incorporated into the previous theory.

From the above remarks, the vapour path length for molecules diffusing in a medium where series-parallel flow can occur can be written as

$$l = l_v + \frac{\lambda_v}{\lambda_l} f(a) l_l \,, \tag{2.38}$$

where $f(a)$ is the Philip and De Vries function describing the reduction in liquid available for series-parallel transmission beyond the point of liquid continuity. Equally, the cross-sectional area, A_{vl}, available for vapour transmission by both mechanisms may be written as

$$A_{vl} = A_v + A_l f(a) \,. \tag{2.39}$$

Using, for the moment, only the first of the Philip and De Vries enhancement factors, that derived from the increase in local temperature gradient, the vapour flux is given by

$$q_v \;=\; -D_{atm}\, \alpha a\, \frac{P}{P-p}\; h\, \frac{d\rho_o}{dT}\, \zeta\, \nabla T \,. \tag{2.40}$$

If now the Jury and Letey description of the reduced area and increased path length is incorporated, then this equation becomes

$$q_v \;=\; -D_{atm}\; \frac{P}{P-p}\; h\, \frac{d\rho_o}{dT}\, \left(\frac{A_{vl}}{A}\right)\left(\frac{z}{l}\right) \zeta\, \nabla T \,. \tag{2.41}$$

Since

$$a = \left(\frac{l A_{vl}}{z A}\right), \tag{2.42}$$

defining as a first approximation an augmented version of first Philip and De Vries correction factor by

$$\xi = \left(\frac{a + \theta_l f(a)}{a \;+\; \theta_l \frac{\lambda_v}{\lambda_l} f(a)} \right)^2 , \tag{2.43}$$

by use of (2.42),(and (2.43), it is seen that equation (2.41) becomes

$$q_v \;=\; -D_{atm}\; \frac{P}{P-p}\; h\, \frac{d\rho_o}{dT}\; \xi\, \zeta\, \nabla T \,. \tag{2.44}$$

II.5 Summary.

The section above sets out the standard theory of coupled diffusion in soil. It has been seen that coupled diffusion gives rise to four coefficients, denoting the response of both liquid and vapour to both temperature and moisture concentration gradients. For the purposes of later analysis these coefficients will be termed the primary diffusion coefficients. Four different combinations of the primary coefficients are combined with the conductivity and thermal capacity of soil to produce what may be termed the total diffusion coefficients acting in the equations governing coupled diffusion. It has been seen that the standard formulation tends to underpredict transportation of moisture arising from vapour diffusion; various enhancement mechanisms have been reviewed which have been proposed in the literature to correct the underprediction. In the sequel, the coefficients will be analysed, and their effects calculated, initially in the simple form without enhancement. Simulation and representations of analytically approximated behaviour then show graphically the necessity for enhancement. The additional factors representing increased diffusion may then be introduced progressively into the simulations and analytical descriptions until similarity between prediction and observation is achieved. This method, particularly, has been used in section **VI**. The content of this section may be regarded as theory delivered by soil physics to be subjected to mathematical scrutiny. Techniques to be developed below will produce a quantitative and qualitative description of a periodic steady state to which the transient behaviour of coupled diffusion tends asymptotically.

III. REVIEW OF RELEVANT RESEARCH WORK.

III.1 Field and Laboratory Experiments.

1.(i) Introduction.

The equations derived in the previous section are of extreme complexity. Consequently verifying work undertaken by soil physicists has tended to address reduced aspects of the full generality. Experiments are designed precisely to exclude the complications of the total situation. From the perspective of the present study, which attempts to discover global qualitative properties of behaviour possible to the system, many enquiries are too local, too addressed to specific isolated problems. Thus the task is one of relating various experiments, which touch, or bear upon, analytically derived results, rather than providing direct validation. The partial nature of research in this area of soil physics has been frequently lamented in the literature. Ghali **[36]**, in a recent thesis, in seeking to find data to assess a computer simulation, used the model for various limited sub-sets of controlling conditions, for which there was no shortage of data, but for the full situation of coupled flow, remarked that such data were very rare. A similar, so to speak, piecemeal verification is required for analytical, as for numerical, results.

This reductionist tendency is particularly noticeable in field experiments studying soil in situ. It is an evident platitude to say that all terrestrial life depends ultimately on soil. For countries with poor agrarian resources, such problems as soil erosion and depletion are of crucial importance. It may then seem surprising that research of both abstract significance and material utility has been limited in its scope. The difficulties are two-fold: practical and conceptual. Marshall and Holmes **[64]**, review the various available methods of measurement of soil moisture and conclude that all are either intrusive or destructive. Measurement of attenuation of elementary particles by various forms of emitting probe requires the drilling of separate augur holes for each reading; the soil is sufficiently disturbed to invalidate future data from the immediate vicinity. Equally, the various weighing methods involve destruction of the sample studied. The non-uniformity of soil implies that many duplicated readings must be taken to establish acceptable confidence limits. In sum, then, even such an unambitious goal as to record temperature and moisture content to a modest depth, at moderate sampling intervals of time, over a few diurnal cycles, requires a large area and numerous ancillary staff. Rose**[81-82]**, describes one of the few such studies available.

However, set against more high profile disciplines of physics, such requirements are modest, even trivial. The underlying hindrance to more thorough-going work, as is remarked in many papers

and articles (e.g. Jury, Letey and Stolzy [55], Cary [15], Cass, Campbell and Jones[18]) is the lack of a conceptual frame of reference in which to assess results. Since the governing equations have yielded no generally applicable lines of solution, it is difficult to attach analytical significance to the results produced. A similar tendency may be noted in recent computer modelling of the governing equations. Such work tends to accumulate data in a conceptual void. In the absence of a parallel analytical approach, isolated numerical information does not necessarily cohere into further understanding.

For these various reasons, development of the theory has largely proceeded in the laboratory, where experiments can be designed to truncate the unavoidable complexities of work in the field. For ease of exposition, field and laboratory experiments will be considered together, and since these experiments have led to a further elaboration of the theory given in section two, they will be considered in sequence. The bulk of experiments in soil physics have been primarily addressed to moisture movement, and these will be dealt with first. After this overall summary, two specific experiments, those of Rose [81] and Jackson [52] , will be considered in greater depth, as the most relevant to this thesis. They are used in the sequel to provide numerical field verification of analysis developed.

1.(ii) Moisture Diffusion.

The theory presented above to describe coupled moisture flow was available to soil physicists by the mid-1950's. (Krischner and Rohnalter,[59], van Bavel,[87]). It is generally termed the simple theory. The magnitude of vapour transportation had been previously unexpected. Numerous laboratory experiments (e.g. Gurr et al. [40], Taylor and Cavezza, [84], Rollins et al.,[80]) were undertaken to test this prediction. A typical such early experiment may be briefly described. Taylor and Cavezza subjected columns of soil of various moisture contents to a constant temperature difference in the vertical plane. A dissolved tracer, which could only be carried in the liquid phase, was measured for concentration in the eventual distribution of the liquid, to distinguish the effects of the two phases.

It was found by all experimenters that the theory still underpredicted the actual effects of vapour transport. Many experiments have subsequently been undertaken to evaluate the exact contribution of the coefficient D_{Tv}. In general, experimentation has been organised around this goal, with other factors considered in so far as they affect the observation of vapour movement. The description here will be given in these terms. Various enhancement mechanisms have been proposed to account for the disparity between predicted and observed flow. The important Philip and De Vries [78] paper suggested two such factors, one of which will be described in the context of heat movement, whilst the other proposed that in fairly dry media vapour transport occurs in a across isolated "islands"

of liquid, condensing at the upper meniscus, and evaporating at the lower meniscus, in the temperature gradient. The effective path length is reduced.

This theory has been intensively investigated both in the laboratory (Weeks et al.**[92]**, Hanks, **[42]**, Hadas, **[41]**) and in situ (Rose**[81]**, Cass, Campbell and Taylor, **[19]**). Again typical experiments may be briefly described. Hadas observed soil columns of differing composition and initial water contents under laboratory controlled sinusoidal heat input. Vapour transport was greater than the predicted figure by factors ranging from 0.8 to 8.0. Similarly Rose, in one of the few comprehensive field experiments available, measured soil temperature and moisture content at a site in the Australian outback for a period of six days following inundation. Vapour transport was comparable in magnitude to liquid transport. A series of experiments by Jackson, **[52(b)]**, primarily to discover the processes involved in moisture loss by evaporation, studied the direction of flux movement at varying depth in a desert climate for six weeks after inundation. Complex patterns of movement were found, which could again be accounted for by unexpectedly large vapour movement. A major Russian school, e.g. Abramova**[1]**, following original work by Lebedev, has been directed to the same problem. Russian approaches provide a perspective interesting by their contrast. Thermally induced vapour flow under the permafrost of a Russian winter moves moisture up from warmer and damper soil levels. This may be the main survival mechanism for soil life in such conditions.

The thermodynamic formulation of Cary**[16]**, added further impetus to these studies. As has been outlined above the theory results in a phenomenological description of the diffusion coefficients. An experiment may be regarded as either testing the Philip and De Vries coefficients, or determining the Cary coefficients. Many experiments have been undertaken to this end (Cass, Campbell and Jones **[18]**, Jury and Letey **[54]**, and much work by Cary himself **[15]**). A representative experiment is that of Cary and Taylor **[17]**, in which a steady state temperature difference was induced across horizontal soil samples. The warm and cool side temperatures were provided by water baths contiguous with the sample. The design allowed communication between these two baths, so that the directly induced vapour flux could be measured. Further enhancement mechanisms were proposed through interaction between the two theories by Jury and Letey **[54]**. Finally Ten Berge and Bolt **[85]**, through detailed consideration of the sub-phases present in liquid transport, have questioned the accepted formulation of D_{Tl}.

1.(iii) Heat Diffusion.

Heat movement in coupled diffusion has been less intensively studied than has its counterpart. Immediately obvious reasons may be given for this imbalance. Firstly, most work in soil physics is carried out with agrarian interests either immediately or ultimately in mind. Water

movement is the primary concern. Secondly, as will be seen from the equations (2.1- 2.2) an additional coefficient is present in the former case, which then, theoretically at least, subsumes the latter. Thirdly heat diffusion is dominated by the familiar thermal conductivity term, and so presents fewer novel features. Lastly, it may be said that research has reached a stable consensus view with less controversy attached to the basic formulation.

An early series of papers by De Vries[25], formed a very successful and universally adopted theory by which the thermal conductivity of soil may be calculated as the composition of the individual conductivities of its component materials. The formulation includes the effectively insulating, rather than conducting effects of air in minute capillary pathways. The quantity assembled in this way is termed the hypothetical conductivity, since it supposes conduction in which moisture does not move, a situation unattainable either in the laboratory or under field conditions. This work is summarised in De Vries **[24]**. Measurement of conductivity in early studies thus inadvertently included the latent heat carried by vapour flow, and in practice the two cannot be distinguished. There seem to be no investigations in the literature designed to separate their effects, even though such an experiment would give a conceptually independent, non-standard determination of D_{Tv}.

A further ramification of the De Vries theory leads directly into the central issues of coupled flow. Since the conductivity of the air pathways is much lower than the surrounding matrix, the microscopic temperature gradients cannot be discharged and the consequent vapour flow is increased. This observation provides the first of the series of proposed enhancement mechanisms to account for vapour flow above the simple theory.

Turning now the the research literature it will be seen that most studies belong to the early stages in the development of the theory. Many describe the simple recording of primary data. Belonging to the period before the ideas of Philip and De Vries gained wide dissemination, they lack the theoretical background to have relevance to contemporary work. More recent experiments tend to monitor temperature as a secondary consequence of the primary aim of observing moisture. For the sake of completeness, the following may be briefly touched upon.

The earliest work cited by contemporary accounts is again by Bouyoucos. An early paper **[9]** collects data on soil temperature and speculate on the transport processes involved. It will be seen in the later mathematical sections that the movement of heat into soil in the absence of complicating coupled effects can be readily described by elementary means. In particular, at the soil surface, the input heat follows a diurnal fluctuation superimposed on an annual variation. The subsequent diffusion of this wave can be accounted for by a Fourier analysis. (Carslaw and Jaeger **[14]**, Kirkham and Powers **[57]**). Several long term studies have confirmed this analysis. Fluker **[33]** collected continuous soil

temperatures by thermocouple for a five year period in Texas, and Griffith[39] fitted data to the analysis for an eight year period. Viswandam [89], again in one of the few such studies, viewed coupled flow for its effects on temperature distribution. Thermal diffusivity was found to increase with moisture content, in accordance with the coupled theory. Finally several studies have monitored temperature under a crop cover. Monteith [65], unsurprisingly, found that all variations are damped in these conditions.

1.(iv) Field Verification.

From this necessarily cursory survey, some aspects may be extracted for their relevance to the present analytical approach. Firstly, although the exact numerical determination of the vapour-heat coefficient has been in contention, it has nowhere been suggested that the governing equations do not describe the fundamental agencies by which moisture is moved. The physical circumstances studied have an impressive scope: from frozen Russian steppe to arid Australian outback, water and vapour are carried under gradients of temperature and moisture content. The qualitative nature is unchallenged; only the quantitative detail is in dispute. Useful mathematical work may be undertaken in the absence of consensus. It is possible to frame mathematical studies so that the detailed functional dependence of D_{Tv} on T and θ is left unspecified throughout the body of derivations. Subsequent updating of the theory can then be incorporated at the final stage of analysis. This approach has been used throughout.

Of all the available experiments those of Rose [81] and Jackson [52] are the most relevant to the lines of enquiry followed in the thesis. Both observed soil in an arid desert environment, Rose in the Australian outback and Jackson in Arizona. The papers contain details of the soil characteristics for the two sites, the two differing widely in their properties. Obviously mathematical solutions must be valid under both sets of parameters. The tropical fluctuation in temperature caused extreme gradients approaching $10^{o}\mathrm{K}/cm.$, favouring vapour phase transport against liquid transport. Both experiments monitored moisture profile development subsequent to inundation to saturation levels. Soil at various levels to a depth of 15 $cm.$, in the case of Rose and 30 $cm.$ for Jackson was regularly sampled and plotted against time. The two sets of data are taken as benchmarks against which analytical accounts and computer simulation may be assessed. This verification is carried through in section 8.III.

Mathematical analysis developed in following sections postulates the existence of an asymptotic steady periodic state of diffusion, when transients from an initial profile have decayed, and the medium responds solely to the cyclical input at the surface. In these conditions, quantitative accounts may be formed of such factors as amplitude decay, phase shift, wave form evolution and the upward migration of the means of input variation. Full verification of these results ideally demands a three-fold concurrence between analysis, computer simulation and field data. The scarcity of data for

soil observed in situ in the necessary generality means that field verification is difficult to achieve. The studies of Rose and Jackson, although the most applicable, are in some respects methodologically unsuited to the purpose. Indeed, since they observe evolution subsequent to an initial artificial watering by sprinkler it could be argued that the soil is not monitored in a state which has occurred naturally. Soil in an arid desert climate is subjected to inundation more typical of a tropical maritime regime. However, by taking data from the latter part of each experiment, when it can be assumed that a more standard normality has been resumed, it can be shown that the quantitative descriptions do concur with those observed, in particular with regard to three superimposed effects of the wave evolution of moisture: the movement of a phase retardation of $\frac{5\pi}{4}$ at the surface to a phase shift entrained to that of temperature in the soil depths; the movement of this temperature wave shift by the normal phase lag of diffusion and finally the acceleration of the heating phase and retardation of the cooling phase consequent on the non-linear nature of the diffusion.

III.2 Computer Simulation

The central equations (2.1-2) were derived prior to the widespread availability of computing power. It may be argued that had the theoretical account made its appearance a decade later it would inevitably have been subject to exhaustive testing by computer modelling. The contrary is the case; Jury, Letey and Stolzy[55] remark "only a few simulations have been performed". These simulations tend to be the subject of unpublished Ph.D dissertations at American universities. The present approach provides an account of long-term stable behaviour when transient reaction between an initial profile and surface conditions has been collected to a long-term periodicity. It would be important to determine exactly the manner in which transient evolution is captured by the asymptotic state. In particular, considering all the variety of conditions presented to the soil surface, it is important to determine by what mechanisms the system prevents the occurrence of subharmonic, chaotic or catastrophic responses. A partially developed theoretical reason is suggested in section **X.**, namely that for all parameter values, the system generates a strongly contractive semigroup. However, it would be interesting to see this property illustrated exhaustively by the response of the system to extremes of stimulus. Computer simulation is the ideal medium for such testing, but nowhere in the literature does such a programme seem to have been carried through. For the sake of completeness, the following work should be briefly reviewed.

In common with many other areas of numerical study, the introduction of the Finite Element Method has allowed problems in soil physics with intractable geometries to be studied. Thus, sub-surface sinks and sources, trickle irrigation and lateral inundation have been the subject of recent work. All of these involve various kinds of radial flow which are awkward or impossible to treat

mathematically. Armstrong[3], Baca[4], Ben Asher[7], Sophocleous[83] are examples. A recent and continuing series of papers by Benjamin et. al.[7a] has used the method to study coupled flow under the surface geometry of a ridged soil. Some models have been developed with eventual commercial exploitation as a design goal. It is perhaps surprising, seeing that such models could be programmed with little more than an enhancement of library software, that they tend to address reduced sub-sets of the full situation. Thus the model 'SWATRE', originally engineered by Feddes et al [31], and later modified by Belmans et al [6], is restricted to one-dimensional flow. A useful research project would be to develop software to advise on optimal irrigation scheduling, in terms of rates and periods of application, in arid climates, and which responded to the total complexity of coupled flow. Such software could have commercial viability.

Before leaving the area of computer simulation, one particular study has crucial significance for mathematical ideas to be presented below. Klute and Heerman [58], used the Crank-Nicholson technique to produce a numerical solution for isothermal non-linear moisture diffusion under a periodic boundary condition. Unfortunately, this highly suggestive paper seems to have had no precursors, nor to have elicited any subsequent work. A detailed description and its significance for the present approaches forms the subject matter of section **V**.4. The diffusion coefficient was taken to be strongly concentration dependent, proportional to a high power of moisture content. A hysteresis factor was included. Excluding this last factor, it can be seen that their study addresses numerically exactly the problem for which an analytical line of approach has been found. One is couched in terms of liquid diffusion, the other in terms of heat, but formally the two are identical. Their paper recounts exactly the features which have at least a partial analytical explanation. Within one cycle in their estimation, an initial distribution quickly becomes entrained to the input rhythm, with the non-linearity forming a harmonic distortion within a stable period. The wetting phase is accelerated and drying phase retarded. Thus even under a non-linearity more severe than any considered in the following work, and with hysteresis adding a qualitatively distinct disturbance, the essential features are preserved.

The conclusion of Klute and Heerman is that the highly non-linear form of their observed variation precludes any analytical treatment. It will be argued below that the behaviour of the medium when subjected to a qualitatively similar but quantitatively more temperate regime can indeed be analytically approximated. By design, the Klute and Heerman simulation amounts to destructively testing the system's response. For each quarter of the cycle, the surface is subjected to a constant inundation and then abruptly and effectively discontinuously, for the remainder of the cycle, subjected to levels of drying which would be unlikely to occur in reality. The entire range of the soil characteristic curve is activated within each cycle and the pattern supposed to repeat indefinitely. It will be argued that a similar but more realistic surface variation may be decomposed by the Fourier

Series method, a series solution formed for each of the component sinusoids as the boundary condition for a non-linear diffusion, and the whole recomposed to produce an analytic account. Certainly this approach reveals the qualitative features present in the experimental simulation.

III.3. Numerical and Analytical Approaches.

Crank[21] and Carslaw and Jaegar[14] are frequently cited sources of primary methods of solution of diffusion equations. Since such work is the point of departure for more advanced approaches, a summary of the types of problems for which solutions are possible is of use. Crank considers many forms of diffusion present in different physical contexts, which in turn give rise to different flow geometries and boundary conditions. However, the bulk of the work is addressed to single variable diffusion under a constant coefficient. Solutions are available through constructions involving infinite series of trigonometric, Bessel and Error functions. Such methods can be regarded as a background repertoire of procedures, should any given non-linear diffusion equations be capable of transformation to a more standard form. Two final chapters are devoted firstly to diffusion under a variable coefficient and secondly to coupled flow. In the first, constant boundary conditions only are considered. The second gives some solutions by Henry [44] of a problem occurring in the production of textiles, in which heat and moisture are coupled. The equations have each a form of hydraulic conductivity term involving the first derivative with respect to length. A solution can be found, but only for constant coefficients, and a constant boundary condition. This last removes the dynamic impetus which characterises diffusion in soil.

Carslaw and Jaegar is a similar compendium of solution methods for diffusion equations, with particular reference to soil physics. Again many forms of infinite series are available for particular boundary conditions, and these solutions have been frequently used (e.g.Hadas[41]) in numerical enquiries. It will be seen that section **VI** quotes a standard result from this source as an initial motivating idea. In both these general summaries, it can be seen that the feature of coupled flow to which much of the resulting complexity can be ascribed, that of interacting non-linearity under a fluctuating boundary condition, is nowhere addressed. Either the equations are linearised, or simpler boundary conditions are used. Thus, ironically, solutions are achieved by excluding those aspects which give the behaviour its qualitative character.

A famous series of papers by Philip[72-75], and summarised in [77], gives solutions for steady state behaviour under evaporation. The soil column is then effectively a moisture pump, relaying vapour from the soil depths to the surface layer for evaporation. Solution for several forms of non-linear diffusion coefficients is possible. Again it may be noted that the condition studied is steady state. There would be much interest in trying to determine possible evolutions to that state. Philip [76]

also produced a summary of solutions to the Fokker-Planck equation

$$\frac{\partial \theta}{\partial t} = D\frac{\partial^2 \theta}{\partial z^2} - (A\theta + B)\frac{\partial \theta}{\partial z} \tag{3.1}$$

where D has forms such as

$$D = \frac{a}{(b-\theta)^2} \ , \tag{3.2}$$

describing moisture diffusion with a hydraulic conductivity term. Surprisingly, exact integral solutions are available even to such a generally posed problem, and form a high point of non-linear diffusion enquiries. However, the solutions are for constant moisture concentration infiltration and constant flux moisture infiltration and do not carry over to diffusion marked by response to cyclic boundary conditions.

Finally, it may be convenient to bring together the various techniques by which non-linear equations may be manipulated into more tractable or canonical forms. Methods are summarised in Ames **[2]**, which is a highly impressive synthesis of numerous diverse sources. Ames refers to "the morass of non-linearity", in describing the incoherent assembly of substitutions, decompositions and transformations which are used to find analytical routes into non-linear equations.

Some taxonomy for the different manipulations is possible by considering which aspect of the equation is transformed. Considering first substitutions in the dependent variable, the general category of Kirchoff transformations uses a substitution for the terms in the dependent variable which cause the equation to be non-linear. If such an approach is possible, either an associated linear equation is formed, or a simpler non-linear equation which may admit a series solution, or a solution under restricted conditions. This procedure was used by Gardner**[34]** to produce solutions for steady state flow, and is essentially that of Wiltshire **[94]**. A more general version of the same method is to use an initially unspecified functional transformation for the dependent variable, consider the resulting form, and attempt to solve for the functional transformation to simplify some important aspect of the equation. This method was used to uncover the initial transformation of section **V**.

Similar methods can be applied to the independent variables. The Von Moses **[90]** method introduces new independent variables, related to the originals, but with an additional dependency on some aspect of the equation which will be removed as a consequence of the substitution. Implicit solutions often result from the method, but such solutions may give valuable insight into the behaviour. Strenuous attempts have been made to transform the equations by this method, unfortunately without success.

Finally, one well-known method, that of Boltzman, should be included in any survey. It may be possible to amalgamate the two independent variables into one, so that an ordinary differential

equation results. The method exploits any underlying symmetry in the physical situation addressed, implying that the apparent dependence on two factors is in fact a dependence on one. The method has close connections with Lie Groups, and a general theory can be developed of such similarity transformations, one of the few instances of a unifying theory being available in this field. However, for the method to be at all possible, the symmetry must extend to the boundary and initial conditions, since the two must coalesce under the transformation. Since conditions on the time and depth boundaries here have no functional relation, the method is inapplicable.

In all this area, it can be seen that success requires algebraic insight into the form of the equations, and the aspects of that form which may be exploited to gain solutions. The method might be termed heuristic algorithmic ingenuity, or less pretentiously, proceeding by guesswork in the hope of eventual inspiration. This state of affairs is highly regrettable, but is a side-effect of the novel character of research involving non-linearity. No unifying theory has been produced and enquiries have a tentative or provisional nature.

III.4. Summary.

The present section has reviewed relevant research into coupled diffusion. It has been seen that both field and laboratory experiments have tended to be addressed to the exact role the coefficient D_{Tv} performs in coupled diffusion. Extended field observations have been occasional and this area of soil physics tends to be marked by a shortage of validating data of sufficient generality. In addition, experiments tend to monitor evolution subsequent to a highly discontinuous initial profile, which, from the perhaps narrow perspective of the present study, tends to render the initial periods of these experiments inappropriate to the analytical techniques to be developed. Neverthless, the closing stages of these experiments do allow analysis to be confirmed against observation. Possibly as a consequence of the lack of validating data, there are no published simulations of any generality for coupled diffusion. Recent computer research has tended to use the greater freedom from boundary constraints given by the Finite Element Method and has considered diffusion under unusual flow geometries. Much of this work has been addressed essentially to isothermal diffusion.

The range of techniques by which non-linear differential equations may be approached has been surveyed. It has been seen that no automatic techniques are available and in any particular case only ingenuity can provide methods of solution or approximation. It will be seen in the sequel that the asymptotic stability of the periodic state of coupled diffusion allows the use of extended perturbation techniques to produce approximations to that state to be formed. Further, the stability implies that these approximations are valid for a far wider range of controlling parameters than might initially be supposed for a system exhibiting such extreme non-linearities.

IV. PERIODIC LINEAR DIFFUSION OF COUPLED VARIABLES

IV.1 Introduction.

Mathematical enquiries are now introduced by considering the linear diffusion of coupled variables under periodic boundary conditions. Aspects of behaviour specific to both linear and non-linear diffusion make their appearance in this approach; the analysis is carried through and then attention drawn to the salient features. Both Dirichlet and Neumann conditions are considered. The term Dirichlet is used here since the periodic state defines profiles at each end of the period. Equally, the variables decay to mean values as depth increases. In this way, periodic behaviour implies boundary conditions asserted at all points of the boundary. Since initial profiles are transient, the more formally accurate description of the situation as Cauchy is misleading.

Any of the standard methods of solution of linear partial differential equations may be used. The phasor approach is adopted as perhaps the most direct. The general situation of n coupled variables is addressed. Various extensions, such as considering response to surface input from functions represented by Fourier series, or the decay of initial profiles, which may be expressed by use of Green's functions, are regarded as elementary and are omitted; the main purpose of this initial section is to introduce notation which will be standard throughout.

IV.2 Periodic Behaviour Under Dirichlet Conditions.

The coupled diffusion equations will be written in the form

$$\left.\begin{aligned}
\frac{\partial y_1}{\partial t} &= \kappa_{11}\frac{\partial^2 y_1}{\partial z^2} + \kappa_{12}\frac{\partial^2 y_2}{\partial z^2} + \quad . \; . \; . \quad + \kappa_{1n}\frac{\partial^2 y_n}{\partial z^2} \\
\frac{\partial y_2}{\partial t} &= \kappa_{21}\frac{\partial^2 y_1}{\partial z^2} + \kappa_{22}\frac{\partial^2 y_2}{\partial z^2} + \quad . \; . \; . \quad + \kappa_{2n}\frac{\partial^2 y_n}{\partial z^2} \\
&\quad \ldots\ldots \qquad\qquad \ldots\ldots \qquad\qquad \ldots\ldots \\
\frac{\partial y_n}{\partial t} &= \kappa_{n1}\frac{\partial^2 y_1}{\partial z^2} + \kappa_{n2}\frac{\partial^2 y_2}{\partial z^2} + \quad . \; . \; . \quad + \kappa_{nn}\frac{\partial^2 y_n}{\partial z^2}
\end{aligned}\right\} \qquad (4.1)$$

where each of the diffusion coefficients, κ_{ij}, is constant and $y_i = y_i(z,t)$, with $z = 0$ representing the flat surface and t time. Alternatively,

$$\dot{y}_i = k_{ij} y_j'', \tag{4.2}$$

where a dot represents differentiation with respect to time, a dash with respect to depth, and the tensor summation convention is used. The boundary conditions are then

$$y_i|_{z=0} = y_{iM} + y_{iA}\, cos(\omega t + \beta_i) \tag{4.3}$$

where y_{iM} and y_{iA} are the input mean and amplitude of the surface oscillation of the ith. variable, having phase angle β_i . Input frequency, ω, in the sequel mainly represents daily fluctuation.
The equations may be written in vector form,

$$\dot{\underline{Y}} = \Lambda\, \underline{Y}'', \tag{4.4}$$

where,

$$\Lambda = \begin{bmatrix} \kappa_{11} & \kappa_{12} & \cdots & \cdots & \kappa_{1n} \\ \kappa_{21} & \kappa_{22} & \cdots & \cdots & \kappa_{2n} \\ & \cdots & & \cdots & \\ & \cdots & & \cdots & \\ \kappa_{n1} & \kappa_{n2} & \cdots & \cdots & \kappa_{nn} \end{bmatrix}, \tag{4.5}$$

and

$$\underline{Y} = \begin{bmatrix} y_1 & y_2 & \cdots & \cdots & y_n \end{bmatrix}^T . \tag{4.6}$$

To isolate periodic solutions, $\underline{Y}$ is written in the phasor form

$$\underline{Y} = \Re \left\{ \underline{X}\, e^{i\omega t} \right\} \tag{4.7}$$

where ω is the frequency of the periodic solution, giving

$$i\omega\, \underline{X} = \Lambda\, \underline{X}'' \quad . \tag{4.8}$$

To solve (4.8), standard techniques of eigenvalue decomposition will be used with the aid of the following substitution, where $\boldsymbol{P}$ is the matrix of eigenvectors of Λ,

$$\underline{X} = \boldsymbol{P}\, \underline{U} \tag{4.9}$$

where

$$\underline{U} = \begin{bmatrix} u_1(z), & u_2(z), & \cdots & \cdots & u_n(z) \end{bmatrix}^T . \tag{4.10}$$

Thus (4.8) becomes

$$\boldsymbol{H}\ \underline{\boldsymbol{U}}^{\prime\prime} \;=\; i\,\omega\,\underline{\boldsymbol{U}}\ , \tag{4.11}$$

with

$$\boldsymbol{H} \;=\; \boldsymbol{P}^{-1}\,\boldsymbol{\Lambda}\,\boldsymbol{P} \;=\; \begin{bmatrix} \eta_1 & & & & \\ & \eta_2 & & & \\ & & .. & & \\ & & & .. & \\ & & & & \eta_n \end{bmatrix} \tag{4.12}$$

and η_i are the eigenvalues of $\boldsymbol{\Lambda}$.

It follows, since the widely differing orders of magnitude of the diagonal terms give no repeated eigenvalues, that (4.11) has the form

$$i\,\omega \begin{bmatrix} u_1 \\ u_2 \\ \cdots \\ u_n \end{bmatrix} = \begin{bmatrix} \eta_1 & & & & \\ & \eta_2 & & & \\ & & .. & & \\ & & & .. & \\ & & & & \eta_n \end{bmatrix} \begin{bmatrix} u_1^{\prime\prime} \\ u_2^{\prime\prime} \\ \cdots \\ u_n^{\prime\prime} \end{bmatrix} \tag{4.13}$$

This gives a set of n uncoupled equations for $u_i(z)$ with solutions

$$u_i \;=\; A_i e^{-(1+i)\frac{z}{\Omega_i}}\ , \tag{4.14}$$

where

$$\Omega_i \;=\; \sqrt{\frac{2\eta_i}{\omega}}\ , \tag{4.15}$$

is termed the damping depth and A_i is constant. The negative root of i is taken for decaying waves. Substituting the solution (4.14) into (4.9), and the resulting equation for $\underline{\boldsymbol{X}}$ into (4.7), gives

$$\underline{\boldsymbol{Y}}(z,t) \;=\; \underline{\boldsymbol{Y}}_M \;+\; \Re\left\{ \boldsymbol{P} \begin{bmatrix} A_1 e^{i\omega t-(1+i)\frac{z}{\Omega_1}} \\ \cdots\cdots\cdots \\ A_n e^{i\omega t-(1+i)\frac{z}{\Omega_n}} \end{bmatrix} \right\}, \tag{4.16}$$

where $\underline{\boldsymbol{Y}}_M$ is the vector of means satisfying the null of solution of (4.4).

Asserting now the boundary condition (4.3) in (4.16), it is found that

$$\begin{bmatrix} A_1 \\ A_2 \\ \cdots \\ \\ A_n \end{bmatrix} = P^{-1} \begin{bmatrix} y_{1A}e^{i\beta_1} \\ y_{2A}e^{i\beta_2} \\ \cdots \\ \\ y_{nA}e^{i\beta_n} \end{bmatrix}. \tag{4.17}$$

Taking the real part of (4.16), the solution may thus be written as

$$\underline{Y} = \underline{Y}_M + P \begin{bmatrix} A_1 e^{-\frac{z}{\Omega_1}} cos(\omega t - \frac{z}{\Omega_1} + \beta_1) \\ A_2 e^{-\frac{z}{\Omega_2}} cos(\omega t - \frac{z}{\Omega_2} + \beta_2) \\ \cdots \\ \\ A_n e^{-\frac{z}{\Omega_n}} cos(\omega t - \frac{z}{\Omega_n} + \beta_n) \end{bmatrix} \tag{4.18}$$

where the A_i are defined by equation (4.17).

It is immediately apparent from equation (4.18) that many features of individual linear diffusion carry over into the coupled context. The input sinusoids diffuse into the medium under exponential decay with constant speed of penetration. In the individual case, these properties depend on the magnitude of the diffusion coefficient; here, they are dependent on the coupling between diffusion coefficients. A strong variable, in the sense that its diffusion coefficient is large relative to its associated variables, will give rise to a wave whose decay is slower and whose rate of penetration is greater; it is less impeded by the medium. The input phase shifts do not disturb the periodicity of any individual wave. A sensitivity analysis quantifying these effects will be undertaken in the Neumann case, which in general is more involved and less intuitively apparent. It will be seen in the sequel how these properties are either retained or transformed as more general situations are encountered.

IV.3 Periodic Behaviour Under Neumann Conditions.

Rather more complex behaviour results under the supposition that periodicity is induced by the importation of flux energy, implying a Neumann type of boundary condition. Since only a linear

system is considered, the response is fully available to analysis; in a sense, the behaviour is qualitatively mundane. However, the complexity with which input fluxes are composed within the medium implies that the underlying simplicity would be entirely masked in any physically observable situation. The following approach allows a decomposition which shows these constituent features clearly.

From the analysis, it is seen that the resulting diffusion wave for each of the n variables is a composition of n^2 constituent waves. For a given variable, each of the n input fluxes powers n diffusion waves, each related to the physical characteristics of a single, different variable. A variable responds to the amplitude and phase of each input flux, but its response is mediated by wave forms derived, in terms of rate of decay and speed of penetration, from each separate variable in turn. Thus, the form of equations, setting a mutual dependency between the variables, is mirrored in the form of the solution. For systems with physical relevance, there is likely to be a wide disparity between input fluxes, with one flux dominant and the cross-coupling weaker than the direct coupling. Such indeed is the case for coupled diffusion in soil, other than for a narrow range of values of moisture content; an analysis of the differing magnitudes of the diffusion coefficients will be a subject of section **VI**.2. In this case the solution reduces to a simpler form with interesting properties. Each variable then consists of a main wave, with just two associated subsidiary waves. The main wave, unsurprisingly, is the input flux of the variable carried into the system on a front derived from properties of that variable. The second is the dominant flux wave, and the third a cross-over term with amplitude, frequency and phase determined by the dominant flux, but the wave form itself derived from the considered variable. Since a weaker variable is involved in the first and last of these waves, they will decay more quickly and penetrate more slowly than the second. Thus at a critical depth, the subsidiary wave will become more prominent and the form of the composed wave will be strongly influenced by different wave properties. Graphical illustrations of this kind of behaviour in the three variable case are included. A response of some complexity is thus easily analysed.

The mathematical content is organised in the following way. The general solution reached in the previous section is quoted and the boundary conditions of flux input are incorporated. This solution initially presents itself as a matrix expression of some complexity. In order to uncover the physical significance further manipulation is required. The product of three n x n matrices and a n component vector is rewritten as the product of two higher order matrices. This reconstitution has its own interest in terms of abstract matrix theory and, since the matrix algebra is non-trivial, it is probably best presented as a separate theorem within the body of the derivation. It is then applied to the original expression to produce the analysis of component waves outlined above. A numerical illustration of the matrix recomposition is given as a form of appendix to the present section.

3.(i) Application of the Flux Boundary Conditions.

The preceding section IV.2 has shown that the system given above as (4.4),

$$\dot{\underline{Y}} \;=\; \Lambda\; \underline{Y}'' \,,$$

where Λ is described by (4.5),

$$\Lambda \;=\; \begin{bmatrix} \kappa_{11} & \kappa_{12} & \cdots & \cdots & \kappa_{1n} \\ \kappa_{21} & \kappa_{22} & \cdots & \cdots & \kappa_{2n} \\ & \cdots & & \cdots & \\ & \cdots & & \cdots & \\ \kappa_{n1} & \kappa_{n2} & \cdots & \cdots & \kappa_{nn} \end{bmatrix} ,$$

and $\underline{Y}$ by (4.6), $\qquad \underline{Y} = \begin{bmatrix} y_1 & y_2 & \cdots & \cdots & y_n \end{bmatrix}^T$

has the solution (4.18)

$$\underline{Y}(z,t) \;=\; \underline{Y}_m \;+\; \Re \left\{ P \begin{bmatrix} A_1 e^{i\omega t - (1+i)\frac{z}{\Omega_1}} \\ \cdots\cdots\cdots \\ A_n e^{i\omega t - (1+i)\frac{z}{\Omega_n}} \end{bmatrix} \right\} .$$

Neumann conditions of flux input need now to be applied to this solution.

The flux density $\underline{J}(z,t)$ at any point (z,t) may be defined through the relation

$$\underline{J} \;=\; -\Lambda\; \underline{Y}' \,. \tag{4.19}$$

It will be supposed that the flux density vector is known at $z = 0$, and in particular that

$$\underline{J} \;= \Re \left\{ \begin{bmatrix} J_1 e^{i(\omega t + \beta_1)} \\ \cdots \\ J_n e^{i(\omega t + \beta_n)} \end{bmatrix} \right\} \tag{4.20}$$

allowing for a variety of input flux in terms of phase β_i, amplitude J_i and frequency ω.

Combining equations (4.18), (4.19) and (4.20) with the eigenvector relation $\boldsymbol{\Lambda}\,\boldsymbol{P} = \boldsymbol{P}\,\boldsymbol{H}$ gives

$$\Re\left\{\boldsymbol{\Lambda}\,\boldsymbol{P}\begin{bmatrix}(1+i)\frac{A_1}{\Omega_1}\\ \cdots \\ \cdots \\ (1+i)\frac{A_n}{\Omega_n}\end{bmatrix}e^{i\omega t}\right\} = \Re\left\{\boldsymbol{P}\begin{bmatrix}(1+i)\frac{\eta_1 A_1}{\Omega_1}\\ \cdots \\ \cdots \\ (1+i)\frac{\eta_n A_n}{\Omega_n}\end{bmatrix}e^{i\omega t}\right\} = \Re\left\{\begin{bmatrix}J_1 e^{i(\omega t+\beta_1)}\\ \cdots \\ \cdots \\ J_n e^{i(\omega t+\beta_n)}\end{bmatrix}\right\}. \quad (4.21)$$

The latter pair of identities is a relation through which the arbitrary constants can be evaluated. The following approach allows their values to be substituted directly into the general solution.

Equation (4.18) gives the variation around the mean value, $\underline{\boldsymbol{Y}} - \underline{\boldsymbol{Y}}_m$ as

$$\underline{\boldsymbol{Y}} - \underline{\boldsymbol{Y}}_m = \Re\left\{\boldsymbol{P}\begin{bmatrix}A_1 e^{-(1+i)\frac{z}{\Omega_1}}\\ \cdots \\ A_n e^{-(1+i)\frac{z}{\Omega_n}}\end{bmatrix}e^{i\omega t}\right\}.$$

Rewriting this equation so that the relation of equation (4.21), between arbitrary constants and boundary flux, can be employed gives

$$\underline{\boldsymbol{Y}} - \underline{\boldsymbol{Y}}_m =$$

$$\Re\left\{\boldsymbol{P}\begin{bmatrix}\frac{\Omega_1}{\eta_1(1+i)}e^{-(1+i)\frac{z}{\Omega_1}} & 0 & \cdots & 0\\ \cdots & \frac{\Omega_2}{\eta_2(1+i)}e^{-(1+i)\frac{z}{\Omega_2}} & \cdots & 0\\ \cdots & \cdots & \cdots & \cdots \\ 0 & 0 & \cdots & \frac{\Omega_n}{\eta_n(1+i)}e^{-(1+i)\frac{z}{\Omega_n}}\end{bmatrix}\begin{bmatrix}(1+i)\frac{\eta_1}{\Omega_1}A_1\\ \cdots \\ \cdots \\ (1+i)\frac{\eta_n}{\Omega_n}A_n\end{bmatrix}e^{i\omega t}\right\} \quad (4.22)$$

Incorporating the boundary condition and writing the imaginary denominators in exponential form, gives finally

$$\underline{\boldsymbol{Y}} - \underline{\boldsymbol{Y}}_m = \Re\left\{\,\boldsymbol{P}\,\boldsymbol{A}\,\boldsymbol{P}^{-1}\,\boldsymbol{J}\,\right\}, \quad (4.23)$$

where $\underline{\underline{A}}$ is the diagonal matrix given by

$$\underline{\underline{A}} = \text{diag} \left\{ \frac{\Omega_i}{\sqrt{2\eta_i}} e^{-(1+i)\frac{z}{\Omega_i} - \frac{i\pi}{4}} \right\} \tag{4.24}$$

and $\underline{J}_c$ the vector of input flux in complex form

$$\underline{J} = \left[\begin{array}{ccc} J_1 e^{i(\omega t + \beta_1)} & \cdots & J_n e^{i(\omega t + \beta_n)} \end{array} \right]^T . \tag{4.25}$$

Equation (4.24) gives the general solution (4.18) with incorporated boundary flux conditions. To make physical sense of this equation it is evidently necessary to show how the terms of the imaginary matrix A and the imaginary vector $\underline{J}$ will interact. Naive attempts to write P directly in terms of the eigenvectors of Λ and multiply out lead to expressions of forbidding complexity. Further progress, then, depends on the tractability or otherwise of this matrix expression. The elements of A need to be extracted from the non-commutative bracketing of P and P^{-1} and placed in interaction with the elements of $\underline{J}$. This reconstruction can, in fact, be achieved by rewriting the product PAP^{-1} in terms of higher order matrices. Since this result has its own interest as a property of abstract matrix theory, it may be most appropriate to isolate the theorem as a separate result, before proceeding to clarify equation (4.23) by its application.

3.(ii) A Matrix Decomposition Theorem.

In the context of abstract matrix theory, an expression in the form of equation (4.23) arises in the following way. Consider two vectors $\left[x_1 \ .. \ .. \ x_n \right]^T$ and $\left[X_1 \ .. \ .. \ X_n \right]^T$ and the projection

$$P \begin{bmatrix} x_1 \\ x_2 \\ \cdots \\ x_n \end{bmatrix} = \begin{bmatrix} X_1 \\ X_2 \\ \cdots \\ X_n \end{bmatrix}, \tag{4.26}$$

where P is the matrix of eigenvectors of a matrix Λ. Suppose now that each element of the projected vector undergoes a change of scale, a_i , then it follows that

$$P \begin{bmatrix} a_1 x_1 \\ a_2 x_2 \\ \cdots \\ a_n x_n \end{bmatrix} = P \begin{bmatrix} a_1 & 0 & \cdots & 0 \\ 0 & a_2 & \cdots & 0 \\ & \cdots & \cdots & \\ 0 & 0 & \cdots & a_n \end{bmatrix} P^{-1} \begin{bmatrix} X_1 \\ X_2 \\ \cdots \\ X_n \end{bmatrix} . \tag{4.27}$$

The right hand side of equation (4.27) is evidently the form which occurs in equation (4.23). The aim is to rewrite (4.27) so that the a_i act directly on the X_i. Reforming the matrices in this way, which effectively evades the non-commutativity of matrix products, can only be accomplished through higher order matrices.

Theorem.

If $\boldsymbol{A}$ = diag { a_i } , and $\boldsymbol{P}$ is the matrix of eigenvectors of a matrix $\boldsymbol{\Lambda}$, then $\boldsymbol{P}\,\boldsymbol{A}\,\boldsymbol{P}^{-1}$ may be decomposed in the form

$$\boldsymbol{P}\,\boldsymbol{A}\,\boldsymbol{P}^{-1} = \boldsymbol{L}\,\boldsymbol{F} \tag{4.28}$$

where $\boldsymbol{F}$ is an n^2 x n matrix dependent on the scale factors a_i given by

$$\boldsymbol{F} = \begin{bmatrix} a_1 & \underline{0} & \underline{0} & \cdots & \cdots & \underline{0} \\ \cdots & & & & & \\ a_n & & & & & \\ \underline{0} & a_1 & \underline{0} & \cdots & \cdots & \underline{0} \\ & \cdots & & & & \\ & a_n & & & & \\ & & \cdots & & \cdots & \\ & & \cdots & & \cdots & \\ \underline{0} & \underline{0} & \underline{0} & & \underline{0} & a_1 \\ & & & & & \cdots \\ & & & & & a_n \end{bmatrix} \tag{4.29}$$

where $\underline{0}$ denotes an n-dimensional column null vector, and $\boldsymbol{L}$ is an n x n^2 matrix dependent only on the nature of $\boldsymbol{\Lambda}$. In particular, if $\boldsymbol{L}$ is partitioned into n submatrices each of order n x n, then the sequence of pth. columns in each submatrix is given by the sequence of columns in the n x n matrix given by

$$\frac{\prod_{i=1, i\neq p}^{n} (\boldsymbol{\Lambda} - \eta_i \boldsymbol{I})}{\prod_{i=1, i\neq p}^{n} (\eta_p - \eta_i)} \,. \tag{4.30}$$

Proof

$\boldsymbol{P}$ is composed of the column eigenvectors, denoted by ν_i , of $\boldsymbol{\Lambda}$. If the elements of $\boldsymbol{P}^{-1}$ are denoted by q_{ij} , then direct substitution from the definitions of $\boldsymbol{P}$, $\boldsymbol{A}$, $\boldsymbol{P}^{-1}$, $\boldsymbol{L}$ and $\boldsymbol{F}$ into (4.28), and multiplying

out both sides of the equation, shows that $\boldsymbol{L}$ has the form

$$\boldsymbol{L} = \begin{bmatrix} q_{11}\underline{\nu}_1 & q_{21}\underline{\nu}_2 & \cdots & q_{n1}\underline{\nu}_n & q_{12}\underline{\nu}_1 & q_{22}\underline{\nu}_2 & \cdots & q_{n2}\underline{\nu}_n & \cdots & \cdots & q_{1n}\underline{\nu}_1 & q_{2n}\underline{\nu}_2 & \cdots & q_{nn}\underline{\nu}_n \\ & & & & & & & & & & & & & \\ & & & & & & & & & & & & & \end{bmatrix} \tag{4.31}$$

where $\boldsymbol{L}$ is an n x n^2 matrix.

Note that, if L is partitioned as n submatrices, each of order n x n, the sum of each row is the element of the product $\boldsymbol{P}\ \boldsymbol{P}^{-1}$ for the corresponding row and column. Hence if the a_i' s are equal, $a_i = a$, the $\boldsymbol{LF}$ representation will coalesce into a scalar multiplication by a , as is appropriate.
Since

$$\boldsymbol{\Lambda} = \boldsymbol{P}\ \boldsymbol{H}\ \boldsymbol{P}^{-1} \tag{4.32}$$

it follows that

$$\boldsymbol{\Lambda} = \boldsymbol{L}\ \ \boldsymbol{F}\ |_{a_i = \eta_i} \tag{4.33}$$

and equally, since $\boldsymbol{\Lambda}^m = \boldsymbol{P}\ \boldsymbol{H}^m\ \boldsymbol{P}^{-1}$, where $\boldsymbol{H}^m = \text{diag}\ \{\eta_i{}^m\}$,

$$\boldsymbol{\Lambda}^m = \boldsymbol{L}\ \ \boldsymbol{F}\ |_{a_i = \eta_i{}^m} \ . \tag{4.34}$$

Taking the form of $\boldsymbol{L}$ given by (4.31) and substituting into (4.34), it is seen that each column of $\boldsymbol{\Lambda}^m$ is a linear combination of the $\boldsymbol{\nu}_i$:

$$\boldsymbol{\Lambda}^m = \eta_1{}^m q_{11} \begin{bmatrix} \underline{\nu}_1 & \underline{0} & \cdots & \underline{0} \\ & & & \end{bmatrix} + \eta_2{}^m q_{21} \begin{bmatrix} \underline{\nu}_2 & \underline{0} & \cdots & \underline{0} \\ & & & \end{bmatrix} + \cdots + \eta_n{}^m q_{n1} \begin{bmatrix} \underline{\nu}_n & \underline{0} & \cdots & \underline{0} \\ & & & \end{bmatrix}$$

$$+ \eta_1{}^m q_{12} \begin{bmatrix} \underline{0} & \underline{\nu}_1 & \cdots & \underline{0} \\ & & & \end{bmatrix} + \eta_2{}^m q_{22} \begin{bmatrix} \underline{0} & \underline{\nu}_2 & \cdots & \underline{0} \\ & & & \end{bmatrix} + \cdots + \eta_n{}^m q_{n2} \begin{bmatrix} \underline{0} & \underline{\nu}_n & \cdots & \underline{0} \\ & & & \end{bmatrix}$$

$$+ \cdots$$

$$+ \eta_1{}^m q_{1n} \begin{bmatrix} \underline{0} & \underline{0} & \cdots & \underline{\nu}_1 \\ & & & \end{bmatrix} + \eta_2{}^m q_{2n} \begin{bmatrix} \underline{0} & \underline{0} & \cdots & \underline{\nu}_2 \\ & & & \end{bmatrix} + \cdots + \eta_n{}^m q_{nn} \begin{bmatrix} \underline{0} & \underline{0} & \cdots & \underline{\nu}_n \\ & & & \end{bmatrix}$$

or,

$$\Lambda^m = \sum_{j=1}^{n} \left\{ {\eta_j}^m q_{j1} \begin{bmatrix} \underline{\nu}_j & \underline{0} & \cdots & \underline{0} \end{bmatrix} + {\eta_j}^m q_{j2} \begin{bmatrix} \underline{0} & \underline{\nu}_j & \cdots & \underline{0} \end{bmatrix} + \cdots + {\eta_j}^m q_{jn} \begin{bmatrix} \underline{0} & \underline{0} & \cdots & \underline{\nu}_j \end{bmatrix} \right\}. \quad (4.35)$$

Thus a ring isomorphism is induced between polynomials, $\boldsymbol{p}$, in $\boldsymbol{\Lambda}$ and polynomials in the η_j, given by

$$\boldsymbol{p}(\boldsymbol{\Lambda}) = \sum_{j=1}^{n} \left\{ \boldsymbol{p}(\eta_j) q_{j1} \begin{bmatrix} \underline{\nu}_j & \underline{0} & \cdots & \underline{0} \end{bmatrix} + \boldsymbol{p}(\eta_j) q_{j2} \begin{bmatrix} \underline{0} & \underline{\nu}_j & \cdots & \underline{0} \end{bmatrix} + \cdots + \boldsymbol{p}(\eta_j) q_{jn} \begin{bmatrix} \underline{0} & \underline{0} & \cdots & \underline{\nu}_j \end{bmatrix} \right\}. \quad (4.36)$$

In particular, the polynomial

$$\boldsymbol{p}(\boldsymbol{\Lambda}) = \prod_{i=1, i \neq p}^{n} (\boldsymbol{\Lambda} - \eta_i \boldsymbol{I}) \quad (4.37)$$

induces the polynomials

$$\boldsymbol{p}(\eta_j) = \prod_{i=1, i \neq p}^{n} (\eta_j - \eta_i) \ . \quad (4.38)$$

In the summation through j, each product will contain a zero, other than when $j = p$, and so,

$$\frac{\prod_{i=1, i \neq p}^{n} (\boldsymbol{\Lambda} - \eta_i \boldsymbol{I})}{\prod_{i=1, i \neq p}^{n} (\eta_p - \eta_i)} = \left\{ q_{p1} \begin{bmatrix} \underline{\nu}_p & \underline{0} & \cdots & \underline{0} \end{bmatrix} + q_{p2} \begin{bmatrix} \underline{0} & \underline{\nu}_p & \cdots & \underline{0} \end{bmatrix} + \cdots + q_{pn} \begin{bmatrix} \underline{0} & \underline{0} & \cdots & \underline{\nu}_p \end{bmatrix} \right\} \quad (4.39)$$

Equation (4.39) expresses the columns of $\boldsymbol{L}$ in terms of $\boldsymbol{\Lambda}$ and its eigenvalues. The sequence of pth. columns in each n x n submatrix is given by the sequence of columns of the left hand side of (4.39). This is the form of $\boldsymbol{L}$ necessary to complete the proof. An illustration of the above process for a numerical $\boldsymbol{\Lambda}$ is given as Section **IV.3.**(vii).

□

3.(iii) The Solution Under Flux Input.

Applying the above result to the equation (4.26) gives

$$\underline{Y} - \underline{Y}_m = \Re \{ (L \ F) \ J_c \} = \Re \{ L (F \ J_c) \} \tag{4.40}$$

where the matrix F is given by $$a_i = \frac{\Omega_i}{\eta_i(1+i)} e^{-(1+i)\frac{z}{\Omega_i}} \tag{4.41}$$

and the matrix L is a real matrix defined solely in terms of Λ. The rearrangement of the matrix product in the final term of equation (4.40) gives an n x n^2 matrix L acting on an n^2 x n column vector formed by $F \ J_c$. The behaviour of each variable is thus formed from a composition of n^2 waves, weighted by the elements of L. Taking the real part of the product $F \ J$ leads finally to

$$\underline{Y} - \underline{Y}_m = L \begin{bmatrix} J_1 C_{11}(t,z,\beta_1 - \frac{\pi}{4}) \\ J_1 C_{12}(t,z,\beta_1 - \frac{\pi}{4}) \\ \cdots \\ J_1 C_{1n}(t,z,\beta_1 - \frac{\pi}{4}) \\ J_2 C_{21}(t,z,\beta_2 - \frac{\pi}{4}) \\ J_2 C_{22}(t,z,\beta_2 - \frac{\pi}{4}) \\ \cdots \\ J_2 C_{2n}(t,z,\beta_2 - \frac{\pi}{4}) \\ \cdots \\ \cdots \\ J_n C_{n1}(t,z,\beta_n - \frac{\pi}{4}) \\ J_n C_{n2}(t,z,\beta_n - \frac{\pi}{4}) \\ \\ J_n C_{nn}(t,z,\beta_n - \frac{\pi}{4}) \end{bmatrix} \tag{4.42}$$

where the elements of L are given by equation (4.30) and

$$C_{ij}(t,z,\beta) = \frac{\Omega_j}{\sqrt{2}\eta_j} e^{\frac{-z}{\Omega_j}} \cos\left\{ \omega t - \frac{z}{\Omega_j} + \beta_i \right\} . \tag{4.43}$$

These equations represent the solution of the system (4.4).

3.(iv) Diffusion under a General Lambda Matrix.

It is immediately apparent that the behaviour of each of the n variables is a composition of at most n^2 waves, given by each of the n input fluxes carried into the system by waves reflecting properties of each of the n variables. Examining the form of the $J_i C_{ij}$ terms, it is seen that the influence of the input flux is confined to the amplitude, frequency and phase of the carrying waves, whilst the remaining wave properties relate to the physical characteristics by which the variables are related. The η_i affect the original amplitude, and control the rate of decay and speed of propagation of the waves. In particular, a "weak" variable, in which the coupling coefficient is small, leading to a small associated eigenvalue, will give rise to waves which decay quickly and penetrate slowly.

These n^2 component waves are assigned their relative importance by the elements of the matrix $\boldsymbol{L}$ which, in turn, necessarily, is determined by the form of $\boldsymbol{\Lambda}$. Different kinds of inter-relation between the diffusion coefficients will thus give rise to different characteristic forms for $\boldsymbol{L}$. Each of these could be the subject of rewarding investigation. For present purposes, to illustrate the clarity with which the $\boldsymbol{L}\ \boldsymbol{F}$ reconstitution depicts the behaviour of a complicated system, the most probable form of $\boldsymbol{\Lambda}$, resulting from physically relevant coefficients, will be considered. $\boldsymbol{\Lambda}$ is taken to be strongly diagonally dominant, and in further analysis, a wide divergence in the magnitude of the input fluxes is assumed. As an incidental remark, it is difficult to visualise any possible physical process in which the reverse obtains; in which the secondary side-effects are stronger than the primary effects. Such a system would seem to incorporate a propensity to highly agitated unstable behaviour and, as a mathematical fiction, might be interesting to investigate.

3.(v) Diffusion under a Diagonally Dominant Matrix.

Changing now to notation for the three variable case which motivated the discussion originally, of coupled diffusion in semi desert conditions, where temperature is denoted by T, moisture content by Θ, and salinity content by S, suppose $\boldsymbol{\Lambda}$ is given by

$$\boldsymbol{\Lambda} = \begin{bmatrix} a & \epsilon_{T,\Theta} & \epsilon_{T,S} \\ \epsilon_{\Theta,T} & s & \epsilon_{\theta,s} \\ \epsilon_{S,T} & \epsilon_{S,\Theta} & w \end{bmatrix} \tag{4.44}$$

in which the ϵ terms are small compared to the diagonal terms.

The characteristic equation is then

$$(a-\lambda)(s-\lambda)(w-\lambda) - \epsilon_{s,\Theta}\epsilon_{\Theta,S}(a-\lambda) - \epsilon_{T,\Theta}\epsilon_{\Theta,T}(w-\lambda) - \epsilon_{T,S}\epsilon_{S,T}(s-\lambda)$$

$$+ \epsilon_{T,S}\epsilon_{\theta,T}\epsilon_{S,\theta} + \epsilon_{T,\Theta}\epsilon_{S,T}\epsilon_{\Theta,S} \quad = \quad 0 \quad . \tag{4.45}$$

Neglecting products of ϵ terms gives $\eta_1 = a \qquad \eta_2 = s \qquad \eta_3 = w$. (4.46)

To illustrate the formation of the matrix $\boldsymbol{L}$, the lemma above gives the 3rd., 6th. and 9th. columns of $\boldsymbol{L}$ as the 1st, 2nd and 3rd columns of:

$$\frac{1}{\eta_3{}^2 - \eta_3(\eta_1+\eta_2) + \eta_1\eta_2} \left\{ \; \boldsymbol{\Lambda}^2 - (\eta_1+\eta_2)\,\boldsymbol{\Lambda} + \eta_1\eta_2\,\boldsymbol{I} \; \right\} \tag{4.47}$$

with the remaining columns given by cyclic permutation of the η_k.
Then, to the first order

$$\boldsymbol{\Lambda}^2 \quad = \quad \begin{bmatrix} a^2 & \epsilon_{T,\Theta}(a+s) & \epsilon_{T,S}(a+w) \\ \epsilon_{\Theta,T}(a+s) & s^2 & \epsilon_{\theta,S}(s+w) \\ \epsilon_{S,T}(a+w) & \epsilon_{S,\Theta}(s+w) & w^2 \end{bmatrix} \quad . \tag{4.48}$$

Evaluating $(\eta_1+\eta_2)\boldsymbol{\Lambda}$ and $\eta_1\eta_2\boldsymbol{I}$ and substituting into equation (4.47) gives the 3rd., 6th., and 9th. columns of $\boldsymbol{L}$ as, respectively, the 1st., 2nd. and 3rd. columns of

$$\begin{bmatrix} 0 & 0 & -\frac{\epsilon_{T,S}}{w-a} \\ 0 & 0 & -\frac{\epsilon_{\Theta,S}}{w-s} \\ \frac{\epsilon_{S,T}}{w-a} & \frac{\epsilon_{S,\Theta}}{w-s} & 1 \end{bmatrix} \quad . \tag{4.49}$$

Similarly the full decomposition is

$$\boldsymbol{L} = \begin{bmatrix} 1 & 0 & 0 & \frac{\epsilon_{T,\Theta}}{a-s} & -\frac{\epsilon_{T,\Theta}}{a-s} & 0 & \frac{\epsilon_{T,S}}{a-w} & 0 & -\frac{\epsilon_{T,S}}{a-w} \\ \frac{\epsilon_{\Theta,T}}{a-s} & -\frac{\epsilon_{\Theta,T}}{a-s} & 0 & 0 & 1 & 0 & 0 & \frac{\epsilon_{\Theta,S}}{s-w} & -\frac{\epsilon_{\Theta,S}}{s-w} \\ \frac{\epsilon_{S,T}}{a-w} & 0 & -\frac{\epsilon_{S,T}}{a-w} & 0 & \frac{\epsilon_{\Theta,S}}{s-w} & -\frac{\epsilon_{\Theta,S}}{s-w} & 0 & 0 & 1 \end{bmatrix} \quad (4.50)$$

with

$$\boldsymbol{F}\,\boldsymbol{J} \quad = \quad \begin{bmatrix} \boldsymbol{J}_1 \boldsymbol{C}_{1,2}(t,z,\beta_1 - \frac{\pi}{4}) \\ \boldsymbol{J}_1 \boldsymbol{C}_{1,2}(t,z,\beta_1 - \frac{\pi}{4}) \\ \boldsymbol{J}_1 \boldsymbol{C}_{1,3}(t,z,\beta_1 - \frac{\pi}{4}) \\ \boldsymbol{J}_2 \boldsymbol{C}_{2,1}(t,z,\beta_2 - \frac{\pi}{4}) \\ \boldsymbol{J}_2 \boldsymbol{C}_{2,2}(t,z,\beta_2 - \frac{\pi}{4}) \\ \boldsymbol{J}_2 \boldsymbol{C}_{2,3}(t,z,\beta_2 - \frac{\pi}{4}) \\ \boldsymbol{J}_3 \boldsymbol{C}_{3,1}(t,z,\beta_3 - \frac{\pi}{4}) \\ \boldsymbol{J}_3 \boldsymbol{C}_{3,2}(t,z,\beta_3 - \frac{\pi}{4}) \\ \boldsymbol{J}_3 \boldsymbol{C}_{3,3}(t,z,\beta_3 - \frac{\pi}{4}) \end{bmatrix} \quad (4.51)$$

and $$\boldsymbol{C}_{i,j}(t,z,\beta) \quad = \quad \frac{\Omega_j}{\sqrt{2}\,\eta_j} \; e^{-\frac{z}{\Omega_j}} \; cos \; \left\{ wt - \frac{z}{\Omega_j} + \beta_i \right\} \quad . \quad (4.52)$$

From the form of (4.50) and (4.51), it can be seen that for $\boldsymbol{\Lambda}$ corresponding to likely physical realities the full complement of nine component waves associated with each variable reduces to just five waves having an actual physical effect. The $\boldsymbol{L}$ matrix displays clearly the relative strengths of each of these component waves. The wave related to the uncoupled variable is stressed in the $\boldsymbol{L}$ matrix by a coefficient of one; it is accompanied in its passage through the medium by two pairs of induced waves with equal and opposite $\boldsymbol{L}$ coefficients. In each of these pairs, one wave is the shadow of an

uncoupled variable, whilst its companion wave has mingled characteristics. The amplitude, phase and frequency is derived from input flux; the speed of penetration and rate of decay from the coupling between the variable and the system.

Adhering still to probable physical circumstances, there is likely to be a disparity of orders of magnitude between the strengths of the input fluxes. Self evidently for desert diffusion, the system will be dominated by heat input and analysis reduces to finding the side effects of this single controlling variable. Taking moisture content, which is evidently most important for a practical understanding of desert behaviour, the full complexity collapses to just three relevant waves, those denoted by $\boldsymbol{J}_1\boldsymbol{C}_{11}$, $\boldsymbol{J}_1\boldsymbol{C}_{12}$ and $\boldsymbol{J}_2\boldsymbol{C}_{22}$. The following three graphs illustrate the properties of these waves at different depths as shown by the preceding analysis. The values for the controlling parameters have been taken as follows: a = 7.5, $\epsilon_{T\Theta}$ = 3.7, ϵ_{TS} = 0.01, $\epsilon_{\Theta T}$ = 0.009, s = 0.48, $\epsilon_{\Theta S}$ = 0.01, ϵ_{ST} = 0.01, $\epsilon_{S\Theta}$ = 0.01, w = 0.1, ω = 19.91. (All the preceding with a scale factor of 10^{-8}.) J_1 = 200.0, J_2 = 0.28, J_3 = 0.1.

Fig. **IV**.1 illustrates the theoretical behaviour in the surface layer over a two day cycle. Curve (1) is the resulting moisture content, composed of three waves: curve (2) for the uncoupled value $\boldsymbol{J}_2\boldsymbol{C}_{22}$, with attendant waves (3) $\boldsymbol{J}_1\boldsymbol{C}_{11}$ and (4) $\boldsymbol{J}_1\boldsymbol{C}_{12}$. Input moisture is assumed to fluctuate over an annual cycle, in contrast to the heat input, which is, of course, diurnal. For this short observed period, the uncoupled flux wave (2) is constant relative to variation controlled by $\boldsymbol{J}_1$ input. The overall value for moisture (1) thus treats the uncoupled value as a carrier wave, and fluctuates about its mean value. It is seen that at the surface layer the cross-over wave $\boldsymbol{J}_1\boldsymbol{C}_{12}$ is larger than the dominant flux shadow term $\boldsymbol{J}_1\boldsymbol{C}_{11}$ which, given the negative coefficient in the $\boldsymbol{L}$ matrix, acts to counteract its effects.

At the surface level, the exponential term $e^{-\frac{z}{\Omega_1}}$ controlling rate of decay and the term $-z/\Omega_j$ denoting speed of penetration have, of course, no effect. As is intuitively plausible, the effects of flux are dominant. However, as the waves penetrate the medium, these characteristics, which ultimately depend on the coupling between variables, begin to take effect. This is the situation in Fig **IV**.2, which retains the numbering system of Fig. 1. It can be seen that the $\boldsymbol{J}_1\boldsymbol{C}_{11}$ term has scarcely decayed, whilst at this depth given by $z_1 = \Omega_2\, ln2$, the amplitude of the mixed term $\boldsymbol{J}_1\boldsymbol{C}_{12}$ is reduced to half its original value. Equally the other C_{ij} term for which $j = 2$, giving the uncoupled variable value, has decayed to near zero. The level of moisture thus fluctuates daily around its yearly mean. It is easy to show that at a depth given by

$$z_2 = \frac{\sqrt{2\eta_1\eta_2}}{\omega\,(\sqrt{\eta_1} - \sqrt{\eta_2}\,)}\, ln\sqrt{\frac{\eta_1}{\eta_2}} \tag{4.53}$$

the amplitude of the two induced waves, C_{11} and C_{12} will become equal and opposite. This is the situation in Fig. **IV**.3. However, the differing speeds of penetration of the two waves result in a phase difference of π from their original synchronised behaviour at the surface level. They now act to reinforce each other and the total movement of moisture, at over twice the depth of Fig. **IV**.2., is, in fact, now slightly greater.

3.(vi) Illustration of the *LF* Decomposition for a Product of Real Matrices.

To illustrate the formation of the ***LF*** decomposition in a simple case, consider $\mathbf{\Lambda}$ given by

$$\mathbf{\Lambda} = \begin{bmatrix} 4 & 0 & 1 \\ -2 & 1 & 0 \\ -2 & 0 & 1 \end{bmatrix} . \tag{4.54}$$

The eigenvalues are $\eta_1 = 1$, $\eta_2 = 2$, $\eta_3 = 3$ and $\boldsymbol{P}$, the matrix of eigenvectors, is

$$\boldsymbol{P} = \begin{bmatrix} 0 & -\frac{1}{2} & -1 \\ 1 & 1 & 1 \\ 0 & 1 & 1 \end{bmatrix} . \tag{4.55}$$

Matrix inversion now shows that

$$\boldsymbol{P}^{-1} = \begin{bmatrix} 0 & 1 & -1 \\ 2 & 0 & 2 \\ -2 & 0 & -1 \end{bmatrix} . \tag{4.56}$$

If the scale factors are $a_1 = 2$, $a_2 = 3$ and $a_3 = \frac{1}{2}$, forming the diagonal matrix $\boldsymbol{A}$, then

$$\boldsymbol{P}\,\boldsymbol{A}\,\boldsymbol{P}^{-1} = \begin{bmatrix} -2 & 0 & -\frac{5}{2} \\ 5 & 2 & \frac{7}{2} \\ 5 & 0 & \frac{11}{2} \end{bmatrix} . \tag{4.57}$$

Section **3.**(ii) shows that this matrix can be decomposed as the product of two higher order matrices, $\boldsymbol{L}$ and $\boldsymbol{F}$, with $\boldsymbol{L}$ depending solely on $\mathbf{\Lambda}$, and $\boldsymbol{F}$ solely on $\boldsymbol{A}$. Equation (4.30) gives the 3rd., 6th., and 9th.

columns of $\boldsymbol{L}$ as the columns of

$$\frac{\boldsymbol{\Lambda}^2 - (\eta_1 + \eta_2)\boldsymbol{\Lambda} + \eta_1\eta_2\boldsymbol{I}}{{\eta_3}^2 - \eta_3(\eta_1 + \eta_2) + \eta_1\eta_2} \tag{4.58}$$

with the remaining columns given by cyclic permutation of the η_i.

Evaluating expression (4.58) gives

$$\boldsymbol{\Lambda}^2 = \begin{bmatrix} 14 & 0 & 5 \\ -10 & 1 & -2 \\ -10 & 0 & -1 \end{bmatrix}; \tag{4.59}$$

$$(\eta_1 + \eta_2)\boldsymbol{\Lambda} = \begin{bmatrix} 12 & 0 & 3 \\ -6 & 3 & 0 \\ -6 & 0 & 3 \end{bmatrix}; \quad \eta_1\eta_2\boldsymbol{I} = \begin{bmatrix} 2 & 0 & 0 \\ 0 & 2 & 0 \\ 0 & 0 & 2 \end{bmatrix} \tag{4.60-1}$$

$${\eta_3}^3 - (\eta_1 + \eta_2)\eta_3 + \eta_1\eta_2 = 2 \quad . \tag{4.62}$$

Substitution into (4.58) gives

$$\begin{bmatrix} 2 & 0 & 1 \\ -2 & 0 & -1 \\ -2 & 0 & -1 \end{bmatrix} \tag{4.63}$$

as the 3rd., 6th., and 9th columns of $\boldsymbol{L}$.

Similarly,

$$(\eta_1 + \eta_3)\boldsymbol{\Lambda} = \begin{bmatrix} 16 & 0 & 4 \\ -8 & 4 & 0 \\ -8 & 0 & 4 \end{bmatrix}; \quad \eta_1\eta_3\boldsymbol{I} = \begin{bmatrix} 3 & 0 & 0 \\ 0 & 3 & 0 \\ 0 & 0 & 3 \end{bmatrix} \tag{4.64-65}$$

and

$$\eta_2{}^2 - \eta_2(\eta_1 + \eta_3) + \eta_1\eta_3 \;=\; -1 \tag{4.66}$$

and so

$$\begin{bmatrix} -1 & 0 & -1 \\ 2 & 0 & 2 \\ 2 & 0 & 2 \end{bmatrix} \tag{4.67}$$

are the 2nd., 5th., and 8th. columns of $\boldsymbol{L}$.

Finally,

$$(\eta_2 + \eta_3)\boldsymbol{\Lambda} \;=\; \begin{bmatrix} 20 & 0 & 5 \\ -10 & 5 & 0 \\ -10 & 0 & 5 \end{bmatrix}; \quad \eta_1\eta_3\boldsymbol{I} \;=\; \begin{bmatrix} 6 & 0 & 0 \\ 0 & 6 & 0 \\ 0 & 0 & 6 \end{bmatrix} \tag{4.68-69}$$

and

$$\eta_1{}^2 - \eta_1(\eta_2 + \eta_3) + \eta_2\eta_3 \;=\; 2 \tag{4.70}$$

giving

$$\begin{bmatrix} 0 & 0 & 0 \\ 0 & 1 & -1 \\ 0 & 0 & 0 \end{bmatrix} \tag{4.71}$$

as the 1st., 4th., and 7th. columns of $\boldsymbol{\Lambda}$.

Assembling (4.63), (4.67) and (4.71) gives the decomposition as

$$\boldsymbol{P}\,\boldsymbol{A}\,\boldsymbol{P}^{-1} = \begin{bmatrix} -2 & 0 & -\frac{5}{2} \\ 5 & 2 & \frac{7}{2} \\ 5 & 0 & \frac{11}{2} \end{bmatrix} =$$

$$\begin{bmatrix} 0 & -1 & 2 & 0 & 0 & 0 & 0 & -1 & 1 \\ 0 & 2 & -2 & 1 & 0 & 0 & -1 & 2 & -1 \\ 0 & 2 & -2 & 0 & 0 & 0 & 0 & 2 & -1 \end{bmatrix} \begin{bmatrix} 2 & 0 & 0 \\ 3 & 0 & 0 \\ \frac{1}{2} & 0 & 0 \\ 0 & 2 & 0 \\ 0 & 3 & 0 \\ 0 & \frac{1}{2} & 0 \\ 0 & 0 & 2 \\ 0 & 0 & 3 \\ 0 & 0 & \frac{1}{2} \end{bmatrix} = \boldsymbol{L}\,\boldsymbol{F} \qquad (4.72)$$

IV.4. Summary.

The approaches given above have allowed the periodic state of linear coupled diffusion to be fully described for both Neumann and Dirichlet conditions. The Dirichlet situation for coupled variables leads to an obvious extension of the behaviour for diffusion of an individual variable, in which the eigenvalue associated with each variable now determines the rate of decay and speed of penetration of the variable. The coupling adds no new features to the individual response. Under Neumann conditions, it has been seen that the importation of flux energy leads to more complicated behaviour; conditions on the boundary, in terms of phase angles, amplitudes and periodicity, are retained on transmission in the medium, but only within an involved composition of component waves. It may be said that as more complex forms of coupled diffusion are considered, it is found that input characteristics are respected, but are transmuted into more complex forms. This phenomenon seems generic to coupled diffusion under sinusoidal conditions.

V. PERIODIC NON-LINEAR INDIVIDUAL DIFFUSION

V.1 Introduction.

The previous section has shown how coupled linear diffusion acts as a composition of component waves. An effect, which might be termed a "partition of influence" is observed in which the input fluxes determine the amplitude, phase and period of their associated waves, whilst the rate of decay and speed of penetration is determined by the coupling between variables. The seemingly generic tendency may be noted for diffusion to preserve input sinusoidal characteristics. The phase and frequency of each input flux is inherited by each variable and retained on passage even into the depths of the medium.

The content of this section is summarised by the present writer in **[83(a)]**. The complementary reduced aspect of the full generality is addressed by considering an individual variable diffusing under a non-linear gradient of its concentration. In this situation input wave characteristics are preserved by the addition of severely decaying higher harmonics. It is thus possible to identify two mechanisms, one associated with coupled linear flow, the other with individual non-linear flow, by which the properties of the surface sinusoid are carried into the medium. In particular, neither mechanism disturbs the input period. The response of the full system obviously depends on the reactive properties of the two.

The analysis derives new harmonic series solutions of the heat conduction equation where the thermal diffusivity is assumed to change with temperature. The analysis is carried through with the exact functional dependency initially left unspecified and later specialised to the case of the coefficient varying as a power of temperature. It is believed that this approach gives a compromise between the general and the particular; there is advantage in considering a case where the dependency is sufficiently simple to allow its effects to be readily understood, but sufficiently general to reflect the complexity of transport processes in soil. Work by several soil physicists, summarised in Marshall and Holmes **[64]** and also presented in Ghali **[36]** indicate that taking the coefficient as a power of temperature allows actual behaviour in soil to be adequately modelled. Two points of methodological criticism of the adequacy of this initial model should be made. Firstly, that soil, in addition to its non-linearity is also non-uniform. Any proposed form for the diffusion coefficient will be valid only a severely circumscribed range of values, and so, by implication in a narrow soil layer. Secondly, that in any physically observed diffusion, the variation of the coefficient arising from moisture fluctuation is more significant than that arising from temperature. This inadequacy is remedied in later analysis of coupled flow. For the

present, the following approach should be regarded as essentially qualitative in nature. It establishes that certain characteristics may be regarded as endemic to non-linear individual diffusion. The analysis is carried through and then these features are isolated for review.

The methods of the section provide an analytical comment on the numerical work of Klute and Heerman **[58]** in a Crank-Nicholson simulation on moisture diffusion, where the diffusion coefficient was taken to vary as a high power of moisture concentration. The approach provides a theoretical justification for certain effects noted empirically by Klute and Heerman and thus, in these particular areas, there is concurrence between analysis and observation. However, other conclusions drawn in the paper run counter to the general underlying tenets presented in this thesis, which consequently need to be sustained against the implied contrary view. These questions are considered in the concluding subsection of the chapter.

Finally it should be noted that the generality of the diffusion process implies that equations of similar form arise in the study of several physical problems. Diez, Gratton and Minotti cites **[28]** the following instances of such non-linear diffusion, where the diffusion coefficient depends on a power of the concentration of the diffusing agent, denoted by n:

1) Flow in thin saturated regions in porous media, $n = 1$, (**[79][29][69]**);
2) Percolation of gas through porous media, $n = c_p/c_v \geq 1$, (**[66][37][88]**);
3) Heat conduction by electrons in a plasma, $n = 2.5$, (**[97]**)
4) Viscous gravity currents, $n = 3$, (**[12][46][38]**);
5) Heat conduction by radiation in a multiply ionised gas, $n = 4.5$-5.5, (**[97][71]**)
6) Radiative heat transfer by Marshak waves, $n = 6.5$, (**[62][97][60]**).

The analyses are primarily addressed to specifically non-linear phenomena, such as weak, discontinuous solutions and waiting time behaviour. However none are concerned with transfer in response to a sinusoidal boundary condition, which, as has been remarked, seems to prevent the onset of specifically non-linear phenomena.

V.2. Approximate Solution for Periodic Non-Linear Diffusion

The one dimensional non-linear heat conduction equation will be considered in the standard form,

$$\dot{T} = (\kappa(T)\, T')' , \quad T(0,t) = T_M + T_A cos\omega t \quad , \tag{5.1-2}$$

where $T = T(z,t)$ represents temperature at time t and depth z; κ, the diffusion coefficient, is itself a function of temperature and a dot and dash represent partial differentiation with respect to time and depth respectively. The boundary oscillation has mean T_M and amplitude T_A.

Extensive computer simulation indicates that even under highly non-linear forms of dependence, the non-linearity acts merely to perturb the behaviour around the linear solution. No qualitatively distinct responses emerge and the system seems immune to non-linear disruption. These simulations are implicit in the general modelling of the coupled situation which will be detailed later in section IX. The remarkable qualitative uniformity of response produced by equation (5.1) presents both difficulties and opportunities to analysis. Perturbation treatments are normally valid only for a small range of the controlling parameter. At the extremes of the range different behaviour emerges and the bifurcation is reflected in a failure of convergence of the perturbation series. Here, no such further bifurcation occurs and the perturbation method introduces a constraint inappropriate to the behaviour modelled. However, attempting to establish results for an arbitrary $\kappa(T)$ relation is unlikely to be successful since no existence and uniqueness theorems are available in such a general context. Nevertheless, many different forms have been proposed for the diffusion coefficients present in soil and there is advantage in leaving the functional dependence initially unspecified. The resulting loss of rigour may be justified by the concordance between simulation and analysis for a wide range of functional forms.

Taking the equation (5.1) and writing

$$T(z,t) = T_M + T_V(z,t)\,, \tag{5.3}$$

where $T_V(0,t) \ll T_M$, $\forall t$, then using the truncated form of the Taylor expansion, (5.1) may be rewritten

$$\dot{T_V} = \left((\kappa(T_M) + T_V\kappa'(T_M+\xi))T_V{}'\right)' \tag{5.4}$$

where ξ is, in general, a function of z and t, but satisfies $0 < |\,\xi\,| < |\,T_V\,|$. The method of solution now requires that ξ remain sufficiently small for $\kappa'(T_M)$ to be a good approximation to $\kappa'(T_M+\xi)$ and equally that the system remains qualitatively stable under such a truncation. Obviously for a completely arbitrary κ dependency such an assumption is unsustainable. However simulation indicates that even highly non-linear diffusion does behave in such a way. It will be seen that the assumption produces severely exponentially decaying higher harmonics, and so is internally consistent.

Consider the series $\sum_{i=0}^{\infty} T_i$, where the T_i are defined by

$$\left.\begin{aligned} \dot{T}_0 &= \kappa(T_M){T_0}'' \\ \dot{T}_1 &= \kappa(T_M){T_1}'' + \frac{\kappa'(T_M)}{2}\left({T_0}^2\right)'' \\ \dot{T}_2 &= \kappa(T_M){T_2}'' + \kappa'(T_M)(T_0T_1)'' \\ &\cdots\cdots \\ \dot{T}_i &= \kappa(T_M){T_i}'' + \frac{\kappa'(T_M)}{2}\left(\sum_{r=0}^{i-1} T_r T_{i-1-r}\right)'' \quad (i>0) \end{aligned}\right\} \tag{5.5}$$

under boundary conditions $T_0(0,t) = T_A cos\omega t, \quad T_i(0,t) = 0, i > 0$. On substitution of the function $T_V = \sum T_i$ into (5.4), it can be seen, as follows, that the construction (5.5) exhaustively includes all terms which result from that equation,

$$\sum_{i=0}^{\infty} \dot{T}_i = \kappa(T_M)\sum_{i=0}^{\infty} {T_i}'' + \frac{\kappa'(T_M)}{2}\left\{\left(\sum_{i=0}^{\infty} T_i \sum_{i=0}^{\infty} T_i\right)''\right\} \tag{5.6}$$

$$= \kappa(T_M)\sum_{i=0}^{\infty} {T_i}'' + \frac{\kappa'(T_M)}{2}\left\{\left(\sum_{n=0}^{\infty}\sum_{r=0}^{n} T_r\, T_{n-r}\right)''\right\} \tag{5.7}$$

$$= \kappa(T_M)\sum_{i=0}^{\infty} {T_i}'' + \frac{\kappa'(T_M)}{2}\left\{\left(\sum_{n=1}^{\infty}\sum_{r=0}^{n-1} T_r\, T_{n-1-r}\right)''\right\}. \tag{5.8}$$

Equating, for each i, the term on the L.H.S. of (5.8) to the first term on the R.H.S. and those up to $n = i$ from the second term results in the last equation of (5.5). The purpose of this decomposition is to formalise the notion that the non-linear terms act as feedback into the linear system. It is equivalent to a perturbation analysis without presuppositions for the magnitude of the perturbation.

If, then, the series $T = \sum T_i$ is convergent $\forall\ z, t$, it follows that it converges to an approximate solution to (5.1). The equations (5.5) are soluble by elementary means. The homogeneous part for a T_n gives rise to a term

$$ke^{-\sqrt{n}\alpha z} cos(n\omega t - \sqrt{n}\alpha z) \tag{5.9}$$

where k is to be determined from boundary conditions and α is now a generalised damping depth,

$$\alpha^2 = \frac{\omega}{2\kappa(T_M)}\,. \tag{5.10}$$

The inhomogenous solution arises from compositions of the earlier T_i , and in general contains high order negative exponentials. In addition, the T_i are all zero on the boundary for $i > 0$. These properties induce rapid convergence in the series, and only the first two harmonics have physical impact. The solution, then, is given by

$$\begin{aligned} T_0 = T_M + T_A e^{-\alpha z} cos(\omega t - \alpha z) \\ + \quad \tfrac{1}{2} {T_A}^2 \frac{\kappa'(T_M)}{\kappa(T_M)} \left\{ e^{-\sqrt{2}\alpha z} cos(2\omega t - \sqrt{2}\alpha z) - e^{-2\alpha z} cos(2\omega t - 2\alpha z) \right\} \\ + \quad \tfrac{1}{4} {T_A}^2 \frac{\kappa'(T_M)}{\kappa(T_M)} \left\{ 1 - e^{-2\alpha z} \right\} . \end{aligned} \tag{5.11}$$

When $\kappa(T)$ takes the form

$$\kappa(T) = cT^n \tag{5.12}$$

where c is constant, then the solution (5.11) becomes

$$\begin{aligned} T_0 = T_M + T_A e^{-\alpha z} cos(\omega t - \alpha z) \\ + \quad \tfrac{1}{2} \frac{n\, {T_A}^2}{T_M} \left\{ e^{-\sqrt{2}\alpha z} cos(2\omega t - \sqrt{2}\alpha z) - e^{-2\alpha z} cos(2\omega t - 2\alpha z) \right\} \\ + \quad \tfrac{1}{4} \frac{n\, {T_A}^2}{T_M} \left\{ 1 - e^{-2\alpha z} \right\} . \end{aligned} \tag{5.13}$$

It may appear here that the ${T_A}^2$ term is in some danger of producing failure of convergence in the series. However each subsequent term is multiplied by a factor T_A/T_M, and since $T_A \ll T_M$ in absolute units the convergence is in fact rapid.

V.3. The Properties of the Solution

The behaviour is illustrated by Figs. **V**.1(a-b) and **V**.2(a-b), representing a simulation and the above analytic solution for the equation, when n = 1.5 and 2.0, respectively. In detail, the equation was

$$\frac{\partial T}{\partial t} = \frac{\partial}{\partial z} \left(cT^n \frac{\partial T}{\partial z} \right)$$

$$T(0,t) = T_M + T_A cos\omega t,$$

where T_M= 2.0; T_A= 1.0; $\omega = 2\pi/3600$; $c = 1/36000$. The simulated results were taken from the third cycle with an initial profile constant at T_M. The numerical methods employed throughout will be

described in section **VIII**.3.(i). At five successive levels, namely the surface, 1 cms., 2 cms., and 3 cms. and 4 cms., it can be seen that the wave forms evolve in the way described before reverting to a pure sinusoid. The following features are noticeably present:

(i) Any initial profile, quickly, typically within a a third of a period, becomes entrained to the input surface oscillation and plays no further role in the subsequent development.

(ii) The periodicity of the input sinusoid is strictly preserved on passage through the medium; no subharmonic, catastrophic or chaotic responses emerge.

(iii) There is a retardation of the cooling phase and an acceleration of the heating phase.

(iv) The mean of the variation increases with depth.

This last property has been mentioned by Philip **[77]**, as a consequence of certain, rather different physical considerations which result from an analysis of integral expressions. These characteristics of the behaviour are immediate from (5.13). Evidently the time dependency consists only of multiples of ωt, implying that, in the "steady state" condition, transmission is strictly periodic. All the further terms of the series retain this property and it can be seen how the system dissipates non-linearity and even non-uniformity by the addition of harmonics. The first harmonic recovers the form of the linear solution, except that the damping depth expression is now as given in (5.10). The additional factor of the mean temperature raised to the power alpha is present. A more robust wave is formed as alpha and the mean increase, decaying more slowly and with a greater speed of penetration. Thus soil is more agitated by temperature change in summer, hardly a surprising observation, but one for which linear diffusion, where the wave characteristics are independent of the mean temperature, provides no justification.

These effects are intensified by the action of the second harmonic. The term displaces the stationery values of the first harmonic, accelerating the heating phase and retarding the cooling phase. The following approximate calculation gives a numerical value for this displacement. In both the linear case and the behaviour given by the first harmonic the stationary values are given by

$$\frac{\partial T}{\partial t} \;=\; 0 \;=\; -T_A\,\omega\, e^{-\frac{z}{D}}\, sin\,(\,\omega t \,-\, \tfrac{z}{D}\,)\;. \tag{5.14}$$

where D is the damping depth for the two cases. Obviously, the solutions are given by

$$\omega t \,-\, \tfrac{z}{D} \;=\; n\,\pi \tag{5.15}$$

that is, separated by values of $\frac{\pi}{\omega}$, within the overall translation of the wave at the given depth. Including the second harmonic leads to the equation

$$0 = e^{-\alpha z} sin(\omega t - \alpha z) + \frac{nT_A}{T_M}\left\{e^{-\sqrt{2}\alpha z} sin(2\omega t - \sqrt{2}\alpha z) - e^{2\alpha z} sin(2\omega t - 2\alpha z)\right\} \qquad (5.16)$$

It is easy to see that solutions of (5.14) almost satisfy (5.16), and only the term in $e^{-\sqrt{2}\alpha z}$ prevents their being exact solutions. Since this term is multiplied by a larger negative exponential than the leading term, its contribution will be small. Intuitive reasoning, then, confirms the observation by computer modelling that the displacement of maxima and minima is slight. Taking the sine values as approximated by the first term in their Taylor expansions, valid since the expansion will be close to zero, gives the equivalent of (5.14) as

$$\omega t - \frac{z}{D} = \frac{-\frac{T_A}{T_M}(2-\sqrt{2})\,\alpha z\, e^{(1-\sqrt{2})\alpha z}}{1 - 2n\frac{T_A}{T_M}\left(e^{-\alpha z} - e^{(1-\sqrt{2})\alpha z}\right)} + n\,\pi\ . \qquad (5.17)$$

The displacements are given by the difference between (5.14) and (5.17). The equation refers to the maxima at even n; for the minima, the expansion of the first sine term gives negative values, producing a positive expression in the right hand side of (5.17). Thus the displacement is equal and opposite for maxima and minima. Expression (5.17) obviously has fairly complex behaviour, and as z increases, the negative exponentials in the numerator and denominator become dominant over the linear terms, so that the displacements will themselves increase and then decay. At sufficient depth, a near pure sinusoidal form is re-established. However, in the present context, with physically realistic parameters, these effects are subsumed within the general decay of the wave down to the mean value. The increase in the mean oscillation with depth is described by the final term in (5.13), showing that at sufficient depth an increase occurs given by

$$T_{mean}\big|_{z\to\infty} - T_{mean}\big|_{z=0} = \frac{n\,T_A^{\,2}}{4\,T_M}\,. \qquad (5.18)$$

In summary, then, it may be said that the passage from linearity to non-linearity introduces two new qualitatively distinct features: the migration of the means of variation with depth, and the displacement of maximum and minimum values in time so that the minimum becomes closer to its succeeding maximum. These effects are slight and would in practice be difficult to detect in any physically occurring situation. The non-linearity is accommodated with relatively little disturbance.

V.4. The Klute and Heerman Simulation.

The experiment in the literature which matches most closely the presuppositions of the above analysis is that of Klute and Heerman **[58]**. This paper reports a Crank-Nicolson simulation on Richards' equation

$$\frac{\partial \Theta_l}{\partial t} = \frac{\partial}{\partial z}\left\{ K(\Theta_l)\frac{d\psi}{d\Theta_l}\frac{\partial \Theta_l}{\partial z} \right\} + \frac{dK}{d\Theta_l}\frac{\partial \Theta_l}{\partial z} \tag{5.19}$$

where the hydraulic conductivity, K, is related to volumetric liquid content, Θ_l, by

$$K(\Theta_l) = 740\Theta_l^{6.25} \tag{5.20}$$

and a boundary condition is imposed by a sinusoidal fluctuation in pressure head ψ,

$$\psi(0,t) = 60sin(\tfrac{t}{15}) - 60\ . \tag{5.21}$$

An empirical water content v. pressure head relationship, effectively an inverse hyperbolic tangent, was used with an additional hysteresis factor included.

The four factors catalogued above as typical of non-linear diffusion are all noticeably present in graphical accounts given of the simulation, with the exception that, at the lower soil depths, Klute and Heerman regarded the effects of the initial profile as lingering rather longer than has been found in the present simulations; namely up to three periods in the experimenters' estimation. However, Klute and Heerman's results are frequently regarded as establishing the extreme non-linear character of physically realistic diffusion and, by implication, its mathematical intractability. Since the present approach runs counter to this view, the following points may be usefully made.

The condition (5.21), when interpreted in terms of water content, imposes a wide spectrum of harmonic variation at the boundary. The highly distorted periodic form of the variation visible in the illustrations is not, as it is believed is often supposed, a result of non-linear diffusion; it is not a result of diffusion at all, but is presented to the surface as a consequence of the method of imposition of the boundary condition. It is claimed, then, that the harmonic distortion is a result of sinusoidal fluctuation in pressure expressed, through the moisture characteristic curve in terms of moisture, as a distorted variation at the soil surface. The highly distorted variation within the medium does not result from that same characteristic curve producing extreme non-linear diffusion when acting in the diffusion coefficient. It is present prior to diffusion. It can be seen that the form of the input wave is retained, rather than disturbed, by the non-linearities and is merely modified by the four factors catalogued

above. Even under non-linearities as extreme as those presented by equation (5.19), the further harmonic distortion induced on passage through the medium can only be regarded as slight.

Additionally, it may be noted that the boundary condition (5.21), by design, when acting on the moisture characteristic curve, takes water content from effectively saturation value for a quarter of the cycle through to residual levels for the remainder. The full range of the ψ v. Θ_l variation is activated within each cycle. It seems unlikely that such a regime could occur in reality without depletion of the soil to such an extent that the controlling parameters would become invalid. Diffusion under a more temperate boundary regime can, in fact, be analytically described, certainly to useful orders of approximation, by the method developed above. If the Klute and Heerman situation were adapted to simulation of the following:

$$\frac{\partial \Theta_l}{\partial t} = \frac{\partial}{\partial z}\left\{ K(\Theta_l)\frac{d\psi}{d\Theta}\frac{\partial \Theta_l}{\partial z} \right\} \tag{5.22}$$

$$K(\Theta_l) = 740\Theta_l^{6.25} \tag{5.23}$$

$$\psi(0,t) = 40sin(\tfrac{t}{15}) - 40\ . \tag{5.24}$$

in which the imposed pressure fluctuation does not carry moisture levels to depletion and saturation within each cycle, then it is believed that the above method could account adequately for the behaviour. The computational overhead would be considerable, since approximating the boundary condition would require an extensive Fourier analysis consisting of many terms. However, only one numerically relevant additional harmonic would attach itself to each of the constituent sinusoids on passage through medium, producing little further harmonic distortion.

V.5. Summary.

The above analysis allows non-linear individual diffusion under a sinusoidal boundary condition to be accurately described. It has been seen that the tendency of periodic fluctuation to remain close to the mean of its behaviour allows the non-linearity to be approximated by merely the first term of a Taylor expansion. It will be seen below that even for the extreme non-linearities present in realistic diffusion in soil, which, in the case of some of the diffusion coefficients, lead to gradients in the coefficient of several orders of magnitude, that nevertheless the form of the wave remains close to the mean with a perturbing second harmonic associated with the non-linearity. It is perhaps surprising that complicated functional dependencies in the coefficient are accommodated with so little disruption

to the form arising from the constant case. For the situation of the present chapter, the effects of the considered non-linearity may be summarised as an acceleration of the heating phase, a retardation of the cooling phase, and an increase of the mean. It will be seen that these features are retained, but become more complex, when variables are coupled. In the general case, there will be a migration of the mean which may be either increasing or decreasing, and either advancement or retardation of the maxima and minima. These features, additionally, may vary within one evolution. Nevertheless, it may be noted that more complex factors present in the agencies of diffusion lead to relatively small qualitative implications for the resulting behaviour.

VI. THE DIFFUSION COEFFICIENTS

VI.1 Introduction

Analysis of coupled diffusion in its full generality is now introduced. In the general situation, diffusion is mediated by coefficients which vary with the concentration of the diffusing agents. The nature of this variation is complex in the extreme. It may be verified that each change in T and θ in the standard formulation of the equations induces some forty-five separate changes in the constituent terms of the diffusion expressions. The complexities are such that no useful intuition is possible. If analysis is not to proceed blind, it is important to discern significance amongst the various aspects of the induced variations. The present section, then, develops techniques which amount to a sensitivity analysis by which relative importance of the different agencies may be identified.

It is useful, initially, to distinguish the following forms of dependence on T and θ which occur in the primary diffusion expressions D_{TV}, D_{Tl}, $D_{\theta V}$ and $D_{\theta l}$:

(i) Explicit dependency, in which T or θ are present directly in the functional forms;

(ii) Implicit empirical dependency, referring to factors such as K and ψ, which are in turn functions of the dependent variables, but in which the relation is empirically derived by experiment. No analytical expressions exist for these variables. Derivatives must either be interpolated from data, or from various forms of proposed approximation.

(iii) Implicit theoretical dependency, which category covers terms such as L and ρ_o, which vary with temperature. These quantities have been exhaustively explored in classical physics, and theoretical understanding of their nature is well advanced. However, in the present context, it is often more convenient to use recognised approximations to quantify variation.

(iv) Controversial dependence, by which is meant the enhancement factors for diffusion proposed in the literature. No consensus view concerning these factors has emerged and there seems advantage in carrying through analysis of the diffusion coefficients in a form initially free of the additional uncertainties they represent. The enhancement factors describe postulated microscopic behaviour whose fluctuation in response to external variation is difficult to relate to the macroscopically observable. Since the present approach seeks to assess the change in factors affecting diffusion which, in turn, are brought about by change in the dependent variables, the probable resulting confusion would seem to be non-productive.

The primary diffusion coefficients are combined to produce what may be termed the total diffusion coefficients occurring in the $\mathbf{\Lambda}$ matrix. The resulting expressions are of such forbidding complexity that it is helpful to introduce the following illustrative device, which will be called a "diffusion coefficient surface". As T and θ vary, they induce a sequence of change, initially through the

various forms of dependency catalogued above, relayed through combinations of primary diffusion coefficients, into the total diffusion coefficients forming the $\mathbf{\Lambda}$ matrix. Each of the elements, a, b, r and s of $\mathbf{\Lambda}$ is consequently a function of T and θ. There is, then, a surface associated with each element, as T and θ vary over possible ranges. The removal or inclusion of constituent terms allows their relative importance, which is normally obscured in the algebraic complexities, to be readily assessed. The present section summarises work assessing the coefficients by this technique. As an overall summary of the effects revealed by this line of approach, it may be said that for any individual term variation tends to be brought about either by change in T or by change in θ, with large differences in orders of magnitude existing between the effects of the two variables. For the primary diffusion coefficients, with the exception of D_{TV}, moisture induced variation is more important than temperature induced variation, the effects of which occur mainly in response to category (iii) above, from variation in factors already familiar to classical physics. Indeed, the widely dissimilar results calculated for the proposed enhancement factors may arise from unmonitored local fluctuations of temperature within the sample studied. These various observations are reported in detail in section (**VI**.3). They allow a reduction of the generality given by the basic equations, in which dependencies causing only minor change are suppressed. In consequence analysis of the full situation, which tends to become infeasible owing to the high computational overload involved in accounting for all variation, is facilitated.

It will be seen below that series solution approximations are possible for the asymptotic steady state of coupled diffusion. These solutions, which uncover several qualitative aspects of coupled diffusion and allow description to a degree of approximation which can be verified against physically observed diffusion, involve construction of the partial derivatives with respect to T and θ of the diffusion coefficients. The solutions, in fact, depend on the orientation of the tangent planes to each point of the four diffusion coefficient surfaces. It is, of course, not possible to display such a tangent bundle to a surface graphically. However, the required calculus is carried through in section (**VI**.4). Further, it will be seen that the solution involves in an essential way the eigenvalues and eigenvectors of the $\mathbf{\Lambda}$ matrix, at each point of the variation brought about by change in T and θ. The first of these can be displayed graphically and may be termed an "eigenvalue surface". Underlying algebraic theory to establish that the eigenvalues and eigenvectors have certain properties particular to a coupled diffusion matrix is set out and illustrated by reference to each of the resulting eigenvalue surfaces. It will be seen in the final section of the whole report that these properties provide an indication of how the global qualitative characteristics of non-linear coupled diffusion may be established by semi-group theory.

VI.2 The Primary Diffusion Coefficients

For reference purposes, it may be convenient to bring together the accepted forms of the diffusion coefficients, as presented in Philip and De Vries[78] and de Vries[23]; the opportunity is also taken to set out notation which will be standard throughout. Since the purpose of the present section is to catalogue exhaustively all variation present in coupled diffusion, all underlying dependencies on T and θ will be included explicitly.

Coupled diffusion will be represented in the form

$$\frac{\partial}{\partial t}\begin{bmatrix} T \\ \theta \end{bmatrix} = \frac{\partial}{\partial z}\left\{\begin{bmatrix} a(T,\theta) & b(T,\theta) \\ r(T,\theta) & s(T,\theta) \end{bmatrix}\frac{\partial}{\partial z}\begin{bmatrix} T \\ \theta \end{bmatrix}\right\} \tag{6.1}$$

where the total diffusion coefficients are given by

$$a(T,\theta) = \frac{\lambda(\theta) + L(T)\, D_{TV}(T,\theta)}{C(\theta)} \tag{6.2}$$

$$b(T,\theta) = \frac{L(T)\, D_{\theta V}(T,\theta)}{C(\theta)} \tag{6.3}$$

$$r(T,\theta) = D_{TV}(T,\theta) + D_{Tl}(T,\theta) \tag{6.4}$$

$$s(T,\theta) = D_{\theta V}(T,\theta) + D_{\theta l}(T,\theta) \tag{6.5}$$

and, in turn, the four primary diffusion coefficients are:

$$D_{TV}(T,\theta) = D_{atm}(T)\ \alpha\ (\theta_S - \theta)\ \nu(T,\theta)\ \frac{d\rho_o}{dT}\ e^{\frac{\psi(\theta)g}{RT}} \tag{6.6}$$

$$D_{Tl}(T,\theta) = K(\theta)\ \gamma\ \psi(\theta) \tag{6.7}$$

$$D_{\theta V}(T,\theta) = D_{atm}(T)\ \alpha\ (\theta_S - \theta)\ \nu(T,\theta)\ \frac{g}{RT}\ \rho_o(T)\ e^{\frac{\psi(\theta)g}{RT}}\ \frac{d\psi(\theta)}{d\theta} \tag{6.8}$$

$$D_{\theta l}(T,\theta) = K(\theta)\ \frac{d\psi(\theta)}{d\theta} \tag{6.9}$$

This formulation omits the following features which have been included in some accounts, for example Ghali **[36]**, but which are in practice negligible, representing variation at most of the order 10^{-3} of included terms. The orders of magnitude are given in Rose **[81]**. The following, then, are omitted: conductivity of heat by air and vapour, the differential heat of wetting, conductivity by

liquid, sensible heat present in air and liquid and various mechanical macroscopic phenomena observed in soil, such as the capacity of some soils to swell under infiltration.

The surfaces generated as T and θ vary across possible ranges for the two specimen soils used in field verification, namely the Adelanto loam of the Jackson experiment and the loamy sand of Rose's observations, are given as the following figures. For the soil of the Rose experiment, Figs.**VI**.1-4(a,b) give the primary diffusion coefficients, D_{TV}, $D_{\theta V}$, D_{Tl} and $D_{\theta l}$. The scaling factors are, in sequence, $10^8, 10^5$, 10^8 and 10^5. In order that the liquid diffusivities may be shown in their true relative proportions over a complete range, without resort to logarithmic axes, they are given for θ ranges only to 0.2. Beyond this point, analysis only becomes valid with the inclusion of a hydraulic conductivity term. In each case the surface is given as (a) and the associated contour breakdown as (b). Figs.**VI**.5-8(a,b) duplicate these observations for Adelanto loam. The total diffusion coefficients, a, b, r, s for the Rose soil form Figs.**VI**.9-12(a,b), and those for Adelanto loam are Figs.**VI**.13-16(a,b). Further, the eigenvalue surfaces for each of the two soils are given as, for the Rose soil, Figs.**VI**.17(a,b) and **VI**.18(a,b), and for Adelanto loam as Figs.**VI**.19(a,b)-20(a,b). A property of fundamental importance to coupled diffusion and which will be extensively analysed in Section **VII**.3. here makes its appearance: that over the entire range of possible T, θ variation, the $\mathbf{\Lambda}$ matrix is strongly diagonally dominant, and the two eigenvalues are formed from only minor perturbations of a and s. Visually, little difference is apparent in the surface for η_1 and a, and η_2 and s. Much of the qualitative stability of the system derives from this simple arithmetical observation. These comments will be pursued in section **X**.

As T and θ vary, then, change occurs in the primary and total diffusion coefficients. The following analysis attempts to determine the significant sources of such observed variation. Initial analysis is most conveniently carried out in terms of the categories of dependence mentioned in the introduction.

2.(i) Explicit Functional Dependence.

It can be seen that there are some five explicit appearances of the dependent variables in the functional forms (6.2-5). For the three explicit appearances of T it can be fairly said that they contribute little to the total variation, in comparison both to change induced by moisture content and to change derived from other T dependencies, particularly those of section 2.(iii) below. When T is measured in absolute units, the variation induced even by extreme surface fluctuations present in desert and sub-desert conditions, is slight and will be largely subsumed in the general variation. It is suggested that in many contexts these values can be taken as constant at the mean of the surface conditions. In comparison, the two explicit appearances of θ are responsible for several of the immediately noticeable features of two of the coefficients, $D_{\theta V}, D_{TV}$; in particular, the abrupt decay of the first close to saturation values,

and the near linear decrease of the second for the upper two-thirds of the range. It may be commented that these dependencies, which appear, so to speak, on equal footing in the algebraic statement of the equations, produce widely dissimilar characteristics.

2.(ii) Implicit Empirical Dependence.

This category essentially refers to the occurrence of $\psi(\theta)$, $\frac{d\psi(\theta)}{d\theta}$ and $K(\theta)$ in the equations. These terms are, of course, empirically derived by experiment; there are no theoretical accounts of their nature and in consequence no analytical expressions for the resulting variation. In addition, the terms $\lambda(\theta)$ and $C(\theta)$, which are essentially empirical in nature, although theory has been developed which concurs well with observation, are covered in this sub-section.

$\psi(\theta)$ is present in the exponential expressions for relative humidity and directly in the D_{Tl} expression. The effect of the former is concentrated in the behaviour around residual moisture levels. At this point ψ is increasing rapidly in negative values as moisture level falls. The exponential is evaluated at large negative values, and effectively becomes zero. At levels above this residual amount, the term is dominated by division by R and effectively becomes unity. Thus, the relative humidity term behaves almost as a Heaviside step function. Indeed, there is interest in modelling vapour diffusion by the two controlling functions in its behaviour:

$$\frac{\partial\theta}{\partial t} = \frac{\partial}{\partial z}\left\{\left(\boldsymbol{H}(\theta_R - \theta)\right)(\theta_S - \theta)\,\frac{\partial\theta}{\partial z}\right\} \tag{6.10}$$

where θ_R, θ_S represent residual and saturation values respectively. The series solution to such a representation given in the section above by taking the derivative of the step function as a Dirac δ function, does indeed seem to concur with simulation.

The term $\frac{d\psi}{d\theta}$ occurs in the coefficients $D_{\theta V}$ and$D_{\theta l}$. In the former three significant factors produce the observed functional form. These are the relatively moderate change in suction as moisture increases beyond residual levels, division by the large R term in the denominator and the 'step function' effect of relative humidity. Together they imply that the coefficient $D_{\theta V}$ is significant only for a limited range of θ values. Below this range humidity is effectively zero; above it $\frac{d\psi}{d\theta}$ is not large enough to counter division by R. In some soils, this narrow range amounts almost to a delta function; a pulse of vapour diffusion is triggered at a particular moisture concentration. One of the soils, Pachappa Loam, studied by Jackson in his series of papers, **[48-51]**, noticeably has this quality.

The two remaining coefficients, D_{Tl} and $D_{\theta l}$, which depend on the soil moisture characteristics, can be seen to be formed from an interaction between ψ and K dependencies. K particularly is subject to a variation over many orders of magnitude; obviously hydraulic conductivity is effectively non-existent at residual levels and progresses to the dominant effect as saturation

approaches. ψ equally varies widely, but not over such a pronounced range and with reversed effect, varying from large and negative to small and negative whilst the corresponding change in K is from small and positive to large and positive. The net effect for both coefficients is a monotonic rise from the infinitesimal to the pronounced. Neither of these terms has any T dependency. It may be remarked that there would seem to be some theoretical unreliability in constructing net terms from multiplication of such extreme, and extremely dissimilar, functional forms. In particular, $D_{\theta l}$ is susceptible to the method of calculating an interpolated derivative from data. Alternative methods can give results which vary by as much as an order of magnitude. The nature of these coefficients would seem inheritently too unstable for exact determination.

Theory set out by De Vries originally in **[25]** and summarised in **[24]**, is generally used to determine the two soil thermal property terms, $\lambda(\theta)$ and $C(\theta)$. For the first of these, de Vries gives

$$\lambda(\theta) = \frac{x_w(\theta)\lambda_w + \sum_i k_i x_{s,i}\lambda_i + k_a x_a(\theta)\lambda_a}{x_w(\theta) + \sum_i k_i x_i + k_a x_a(\theta)} \tag{6.11}$$

where,

x	volumetric proportion, *dimensionless.*
λ	thermal conductivity $(cal.cm^{-1}.^oK^{-1}.sec^{-1})$
s, w, a	soil, water, air.
i	soil constituent.
k	shape factor, *dimensionless.*

The k_i are here shape factors dependent on the geometry of a soil grain, generally approximated by an ellipsoid. Unfortunately neither Rose nor Jackson give sufficient detail concerning the constitution of their experimental soils to allow $\lambda(\theta)$ to be calculated directly from (6.11). Instead a standard description of λ variation for soils of the general type occurring in the two experiments has been taken from Marshall and Holmes **[64]**, approximated in each case by two linear interpolations. To summarise the effect of moisture induced variation in λ, it is obvious that, for all ranges, λ is several orders of magnitude larger than its companion coefficient D_{TV} occurring in the term a. Thus the effects of the complex non-linear variation of D_{TV} are, in physically observed diffusion, subsumed within the diffusion induced by λ. In comparison, $\lambda(\theta)$ is more linear in nature, and the moisture dependent change in this term varies over a far smaller range, in practice around a factor of three, between extreme values. These observations, of course, merely confirm in theory the observed nature of heat diffusion in soil as essentially regular, more a linear phenomenon, than moisture diffusion. From a purely mathematical point of view, it may be remarked that if coupled diffusion took place in a

medium with more insulating properties, with λ of the same order of magnitude as the other coefficients, then far more unstable behaviours would be possible in the system. Indeed, the indications given below by which the qualitatively stable nature of coupled diffusion in soil may be established immediately become invalid if λ is diminished by two orders of magnitude.

The theory of volumetric heat capacity and its dependence on moisture content, is again set out definitively in De Vries **[24]**. For $C(\theta)$,

$$C(\theta) = \sum_i x_{s,i} C_i + x_w(\theta) C_w + x_a(\theta) C_a \tag{6.12}$$

where

C volumetric heat capacity $cal/cm^3/^oK$.

Again specimen values have been taken from Marshall and Holmes **[64]**, for the two soils, linearly interpolated. $C(\theta)$ variation increases, again by a factor of around three, between extreme values of the possible ranges. Thus it may be said that $\lambda(\theta)$ and $C(\theta)$ variation largely nullify each other's effects. If a truncated version of the equations is required to lessen the numerical overload, or if reduced interdependencies assist in analytical exploration of the scheme, then these two terms may effectively be taken to be constant, at least in the a coefficient.

2.(iii) Implicit Theoretical Dependency.

These terms occur both in the relations (6.2-5) for the primary diffusion coefficients and in their assembly into the total diffusion coefficients (6.6-9). Since they are all terms familiar in classical physics comment will be restricted to the role their individual variations perform in total variation represented by the diffusion coefficients. References are given for the approximations used in calculation of the coefficient surfaces.

(i) $D_{atm}(T)$ is approximated by the relation (Dorsey **[27]**):

$$D_{atm}(T) = 0.229 \left(\frac{T^oK}{273}\right)^{1.77} \quad cm/sec^2 \tag{6.13}$$

Specimen calculation of values at the limit of ranges which might be encountered even in arid diffusion show that such variation is relatively minor in comparison to other temperature induced factors.

(ii) $\rho_o(T)$ is approximated by the relation given in Kimball et. al. fitted to data in the Smithsonian tables**[56]**,

$$\rho_0(T) = 10^{-6} e^{\left(19.819 - \frac{4975.9}{T^o K}\right)} \quad gm/cm^3 \tag{6.14}$$

It can be seen that taking the range of possible conditions as varying from say 283°K to 333°K, a corresponding change of an order of magnitude occurs. It may be verified that this fluctuation is rather larger than any so far reviewed originating from soil physics proper, and is, in fact, the factor most strongly influencing temperature dependent variation.

(iii) $\nu(T,\theta)$ has been taken to be constant at the value $\nu = 1.023$ by all writers. The following calculation shows that this truncation is indeed valid. ν is given by

$$\nu = \frac{P}{P-p}, \quad dimensionless, \tag{6.15}$$

where P the external pressure is taken as P =1.013 x 10^6 $dynes/cm^2$, and p the partial pressure is given by (Adelson and Edelfson**[30]**)

$$p = RT\rho_o e^{\frac{\psi g}{RT}} \tag{6.16}$$

The partial pressure varies by a factor of less than three for typical ranges, inducing little change in ν. The value $\nu = 1.023$ is taken throughout.

(iv) There is a temperature dependency in the $K(\theta)$ term which has been emphasised by some writers, particularly for thermodynamic purposes, but again for the present mathematical agenda of functional identifying sources of significant variation, $K(T)$ fluctuation again seems negligible, particularly given the orders of magnitude induced by the $K(\theta)$ dependency. An approximation is given by

$$K(T) = K(T_o)\frac{v(T_o)}{v(T)} \tag{6.17}$$

where v expresses the effect of temperature on surface tension. A further approximation (Hardy and Cottingen **[46]**) for v is then

$$log_{10}v = \frac{1301}{998.333 + 8.156(T-20) + 0.0585(T-20)^2} \quad (0 < T < 20^oC) \tag{6.18}$$

$$log_{10}v = \frac{1.3272(T-20) - 0.0101(T-20)^2}{T+105} \quad (20^oC < T) \tag{6.19}$$

It may be verified that over a range of possible values taken as $(280^oK < T < 330^oK)$ these expressions do indeed produce a twofold increase in values for K; however, since K varies typically by a factor of 10^{12} in response to moisture change over possible ranges, the procedure would seem not without a comical aspect. The approximation has not been included in simulation.

(v) An increase in temperature causes a reduction in the latent heat coefficient which may be approximated by

$$L = 597.3 - 0.566(T^oK - 273) \qquad cal/gm \tag{6.20}$$

Values at the limit of temperature ranges may be taken as 591.6 cal/gm and 574.6 cal/gm. In practice, it may be permissible to regard this value as constant as the mean of the range.

VI.3 Reduced Form of the Coupled System.

Taking into account all the differing orders of magnitude of variation present in the system (6.1), as detailed in the above analysis, it is suggested that dependencies on T and θ may be truncated to rather fewer having an observable physical effect. There is, of course, some danger in such a proposed process, since in non-linear work it does not follow that a quantitatively small term does not have qualitatively marked effects. The standard analysis of Duffing's equation for a stiff spring under sinusoidal forcing is the canonical example **[53]**. However, since the complexities of coupled diffusion are so forbidding, there does seem value in carrying out such a reduction. It is suggested, then, that the system (6.1) may be reduced to the following, where the absence of an explicitly noted dependency indicates the variation in the term is not significant:

$$\frac{\partial}{\partial t}\begin{bmatrix} T \\ \theta \end{bmatrix} = \frac{\partial}{\partial z}\left\{ \begin{bmatrix} a(\theta) & b(T,\theta) \\ r(\theta) & s(T,\theta) \end{bmatrix} \frac{\partial}{\partial z}\begin{bmatrix} T \\ \theta \end{bmatrix} \right\} \tag{6.21}$$

where the reduced form of the total diffusion coefficients is given by

$$a(\theta) = \frac{\lambda(\theta) + L(T_M)\, D_{TV}(\theta)}{C(\theta_M)} \tag{6.22}$$

$$b(T,\theta) = \frac{L(T_M)\, D_{\theta V}(T,\theta)}{C(\theta_M)} \tag{6.23}$$

$$r(\theta) = D_{TV}(\theta) + D_{Tl}(\theta) \tag{6.24}$$

$$s(T,\theta) = D_{\theta V}(T,\theta) + D_{\theta l}(\theta) \tag{6.25}$$

and, in turn, the four reduced primary diffusion coefficients are:

$$D_{TV}(\theta) = D_{atm}(T_M)\ \alpha\ (\theta_S - \theta)\ \nu\ \frac{d\rho_o}{dT}\, e^{\frac{\psi(\theta) g}{\overline{RT}_M}} \tag{6.26}$$

For the remaining three coefficients, the appropriate forms are:

$$D_{Tl}(\theta) = K(\theta)\ \gamma\ \psi(\theta) \tag{6.27}$$

$$D_{\theta V}(T,\theta) = D_{atm}(T_M)\ \alpha\ (\theta_S - \theta)\ \nu\ \frac{g}{RT_M}\ \rho_o(T)\ e^{\frac{\psi(\theta)g}{RT_M}}\ \frac{d\psi(\theta)}{d\theta} \tag{6.28}$$

$$D_{\theta l}(\theta) = K(\theta)\ \frac{d\psi(\theta)}{d\theta} \tag{6.29}$$

These reductions allow simplification to be made in later mathematical analysis of coupled diffusion.

VI.4. Derivatives of the Λ Matrix.

Later mathematical approaches require the construction of the two derivatives of the $\mathbf{\Lambda}$ matrix with respect to T and θ. The following notation is introduced,

$$\mathbf{\Lambda}_T = \frac{\partial \mathbf{\Lambda}}{\partial T} = \begin{bmatrix} \dfrac{\partial a(T,\theta)}{\partial T} & \dfrac{\partial b(T,\theta)}{\partial T} \\ \dfrac{\partial r(T,\theta)}{\partial T} & \dfrac{\partial s(T,\theta)}{\partial T} \end{bmatrix}, \tag{6.30}$$

$$\mathbf{\Lambda}_\theta = \frac{\partial \mathbf{\Lambda}}{\partial \theta} = \begin{bmatrix} \dfrac{\partial a(T,\theta)}{\partial \theta} & \dfrac{\partial b(T,\theta)}{\partial \theta} \\ \dfrac{\partial r(T,\theta)}{\partial \theta} & \dfrac{\partial s(T,\theta)}{\partial \theta} \end{bmatrix}. \tag{6.31}$$

These terms are now evaluated.

4.(i) The Primary Diffusion Coefficients.

Taking the four forms for the diffusion coefficients,

$$D_{TV}(T,\theta) = D_{atm}(T)\ \alpha\ (\theta_S - \theta)\ \nu(T,\theta)\ \frac{d\rho_o}{dT}\ e^{\frac{\psi(\theta)g}{RT}} \tag{6.32}$$

$$D_{Tl}(T,\theta) = K(\theta)\ \gamma\ \psi(\theta) \tag{6.33}$$

$$D_{\theta V}(T,\theta) = D_{atm}(T)\ \alpha\ (\theta_S - \theta)\ \nu(T,\theta)\ \frac{g}{RT}\ \rho_o(T)\ e^{\frac{\psi(\theta)g}{RT}}\ \frac{d\psi(\theta)}{d\theta} \tag{6.34}$$

$$D_{\theta l}(T,\theta) = K(\theta)\ \frac{d\psi(\theta)}{d\theta} \tag{6.35}$$

then the derivatives may be evaluated as follows:

(a)

$$\frac{\partial D_{TV}}{\partial T} = \frac{dD_{atm}}{dT}\,\alpha a\nu\frac{d\rho_o}{dT}\,e^{\frac{\psi g}{gT}} + D_{atm}\alpha a\nu\frac{d^2\rho_o}{dT^2}\,e^{\frac{\psi g}{gT}} - D_{atm}\alpha a\nu\frac{d\rho_o}{dT}\,\frac{\psi g}{RT^2}\,e^{\frac{\psi g}{gT}} \tag{6.36}$$

Approximations for the derivatives of D_{atm} and $\frac{d\rho_o}{dT}$ are taken from the expressions (6.13) and (6.14).

(b)

$$\begin{aligned}\frac{\partial D_{\theta V}}{\partial T} = & - D_{atm}\alpha a\nu\frac{\psi g^2}{R^2T^2}\rho_o e^{\frac{\psi g}{gT}}\frac{d\psi}{d\theta} - D_{atm}\alpha a\nu\frac{g\rho_o}{RT^2}\,e^{\frac{\psi g}{gT}}\frac{d\psi}{d\theta} \\ & + D_{atm}\alpha a\nu\frac{g}{RT}\frac{d\rho_o}{dT}\,e^{\frac{\psi g}{gT}}\frac{d\psi}{d\theta} + \frac{dD_{atm}}{dT}\,\alpha a\nu\,\frac{g\rho_o}{RT}\,e^{\frac{\psi g}{gT}}\frac{d\psi}{d\theta}\end{aligned} \tag{6.37}$$

(c)

$$\frac{\partial D_{Tl}}{\partial T} = 0 \tag{6.38}$$

(d)

$$\frac{\partial D_{\theta l}}{\partial T} = 0 \tag{6.39}$$

The derivatives with respect to moisture are:

(a)

$$\frac{\partial D_{TV}}{\partial \theta} = - D_{atm}\alpha\,\nu\,\frac{d\rho_o}{dT}\,e^{\frac{\psi(\theta)g}{RT}} + D_{atm}\alpha\,(\theta_S-\theta)\,\frac{g}{RT}\frac{d\psi}{d\theta}\frac{d\rho_o}{dT}\,e^{\frac{\psi(\theta)g}{RT}} \tag{6.40}$$

(b)

$$\begin{aligned}\frac{\partial D_{\theta V}}{\partial \theta} = & - D_{atm}\alpha\nu\frac{g}{RT}\,\rho_o e^{\frac{\psi(\theta)g}{RT}}\frac{d\psi(\theta)}{d\theta} \\ & + D_{atm}\alpha\,(\theta_S-\theta)\,\nu\,\frac{g^2}{R^2T^2}\,\rho_o e^{\frac{\psi(\theta)g}{RT}}\left(\frac{d\psi(\theta)}{d\theta}\right)^2 \\ & + D_{atm}\alpha\,(\theta_S-\theta)\,\frac{g}{RT}\,\rho_o e^{\frac{\psi(\theta)g}{RT}}\frac{d^2\psi(\theta)}{d\theta^2}\end{aligned} \tag{6.41}$$

(c)

$$\frac{\partial D_{Tl}}{\partial \theta} = K\gamma\,\frac{d\psi}{d\theta} + \frac{dK}{d\theta}\,\gamma\,\psi \tag{6.42}$$

(d)

$$\frac{\partial D_{\theta l}}{\partial \theta} = K\,\frac{d^2\psi}{d\theta^2} + \frac{dK}{d\theta}\,\frac{d\psi}{d\theta} \tag{6.43}$$

The theoretical uncertainty of D_{Tl} and $D_{\theta l}$, which was commented upon in section 2.(ii), is presen even more strongly in these last two derivatives.

4.(iii) The Temperature Derivative.

Given the form of the $\mathbf{\Lambda}$ matrix,

$$\mathbf{\Lambda} = \begin{bmatrix} a(T,\theta) & b(T,\theta) \\ r(T,\theta) & s(T,\theta) \end{bmatrix} \tag{6.44}$$

where the total diffusion coefficients are given by

$$a(T,\theta) = \frac{\lambda(\theta) + L(T)\, D_{TV}(T,\theta)}{C(\theta)} \tag{6.45}$$

$$b(T,\theta) = \frac{L(T)\, D_{\theta V}(T,\theta)}{C(\theta)} \tag{6.46}$$

$$r(T,\theta) = D_{TV}(T,\theta) + D_{Tl}(T,\theta) \tag{6.47}$$

$$s(T,\theta) = D_{\theta V}(T,\theta) + D_{\theta l}(T,\theta) \tag{6.48}$$

it is now possible to determine the form of the derivatives of the $\mathbf{\Lambda}$ matrix.

This derivative is given by

$$\mathbf{\Lambda}_T = \frac{\partial \mathbf{\Lambda}}{\partial T} = \begin{bmatrix} \dfrac{\partial a(T,\theta)}{\partial T} & \dfrac{\partial b(T,\theta)}{\partial T} \\ \dfrac{\partial r(T,\theta)}{\partial T} & \dfrac{\partial s(T,\theta)}{\partial T} \end{bmatrix} \tag{6.49}$$

where the elements are now given by

$$\frac{\partial a}{\partial T} = \frac{L}{C}\frac{\partial D_{TV}}{\partial T} + \frac{dL}{dT}\frac{D_{TV}}{C} \tag{6.50}$$

$$\frac{\partial b}{\partial T} = \frac{dL}{dT}\frac{D_{\theta V}}{C} + \frac{L}{C}\frac{\partial D_{\theta V}}{\partial T} \tag{6.51}$$

$$\frac{\partial r}{\partial T} = \frac{\partial D_{TV}}{\partial T} + \frac{\partial D_{Tl}}{\partial T} = \frac{\partial D_{TV}}{\partial T} \tag{6.52}$$

$$\frac{\partial s}{\partial T} = \frac{\partial D_{\theta V}}{\partial T} + \frac{\partial D_{\theta l}}{\partial T} = \frac{\partial D_{\theta V}}{\partial T} \tag{6.53}$$

and substitution from the equations (6.45-8) gives the full forms.

4.(iv) The Moisture Derivative.

This derivative is given by

$$\mathbf{\Lambda}_\theta = \frac{\partial \mathbf{\Lambda}}{\partial \theta} = \begin{bmatrix} \dfrac{\partial a(T,\theta)}{\partial \theta} & \dfrac{\partial b(T,\theta)}{\partial \theta} \\ \dfrac{\partial r(T,\theta)}{\partial \theta} & \dfrac{\partial s(T,\theta)}{\partial \theta} \end{bmatrix} \tag{6.54}$$

where the elements are

$$\frac{\partial a}{\partial \theta} = \frac{1}{C}\frac{d\lambda}{d\theta} - \frac{dC}{d\theta}\frac{\lambda}{C^2} + \frac{L}{C}\frac{\partial D_{TV}}{\partial \theta} - \frac{L}{C^2}\frac{dC}{D\theta} D_{TV} \tag{6.55}$$

$$\frac{\partial b}{\partial \theta} = \frac{L}{C}\frac{\partial D_{\theta V}}{\partial \theta} - \frac{L}{C^2}\frac{dC}{d\theta} D_{\theta V} \tag{6.56}$$

$$\frac{\partial r}{\partial \theta} = \frac{\partial D_{TV}}{\partial \theta} + \frac{\partial D_{Tl}}{\partial \theta} \tag{6.57}$$

$$\frac{\partial s}{\partial \theta} = \frac{\partial D_{\theta V}}{\partial \theta} + \frac{\partial D_{\theta l}}{\partial \theta} \tag{6.58}$$

and substitution from the equations (6.45-8) gives the full forms.

VI.5. Analysis of Variation in $\mathbf{\Lambda}, \mathbf{\Lambda}_T$ and $\mathbf{\Lambda}_\theta$.

It would be feasible to produce surfaces analogous to those of section (**VI**.2) to display the variation present in $\mathbf{\Lambda}_T$ and $\mathbf{\Lambda}_\theta$. Non-linear diffusion would then be related to the properties of some twelve surfaces. However, such an approach would tend to present far too much information to be readily assimilated. A more accessible approach would seem the tabulation of the results produced by the equations (6.49) and (6.54), as T and θ take on specimen values. $\mathbf{\Lambda}$, $\mathbf{\Lambda}_T$ and $\mathbf{\Lambda}_\theta$ are observed at a representative grid of points in the T,θ plane. For both Adelanto loam and the soil of the Rose experiment, the most complex behaviour is produced within a range of θ values from 0.03 to 0.15; the lines $\theta = 0.03$, 0.07, 0.11, and 0.15 are used. T is taken as varying realistically from 280^oK to 322^oK, again at a division of four steps. The resulting values for the three matrices at the sixteen points are given as Table **VIII**.1. Comment on the values given by this table will be deferred until section **VIII**.2. when algebraic techniques have been developed to discern significance amongst the mass of raw data it presents.

A similar analysis to that of section 4 can obviously be produced for the reduced matrix derived in section 3. Quoting equation (6.20),

$$\frac{\partial}{\partial t}\begin{bmatrix} T \\ \theta \end{bmatrix} = \frac{\partial}{\partial z}\left\{\begin{bmatrix} a(\theta) & b(T,\theta) \\ r(\theta) & s(T,\theta) \end{bmatrix}\frac{\partial}{\partial z}\begin{bmatrix} T \\ \theta \end{bmatrix}\right\}$$

where the reduced form of the total diffusion coefficients is given by

$$\left.\begin{aligned} a(\theta) &= \frac{\lambda(\theta) + L(T_M)\, D_{TV}(\theta)}{C(\theta)} \\ b(T,\theta) &= \frac{L(T_M)\, D_{\theta V}(T,\theta)}{C(\theta)} \\ r(\theta) &= D_{TV}(\theta) + D_{Tl}(\theta) \\ s(T,\theta) &= D_{\theta V}(T,\theta) + D_{\theta l}(\theta) \end{aligned}\right\} \qquad (6.59\text{-}62)$$

and, in turn, the four reduced primary diffusion coefficients are:

$$\left.\begin{aligned} D_{TV}(\theta) &= D_{atm}(T_M)\ \alpha\ (\theta_S - \theta)\ \nu\ \frac{d\rho_o}{dT}\, e^{\frac{\psi(\theta) g}{RT_M}} \\ D_{Tl}(\theta) &= K(\theta)\ \gamma\ \psi(\theta) \\ D_{\theta V}(T,\theta) &= D_{atm}(T_M)\ \alpha\ (\theta_S - \theta)\ \nu\ \frac{g}{RT_M}\ \rho_o(T)\ e^{\frac{\psi(\theta) g}{RT_M}}\ \frac{d\psi(\theta)}{d\theta} \\ D_{\theta l}(T) &= K(\theta)\ \frac{d\psi(\theta)}{d\theta} \end{aligned}\right\} \qquad (6.63\text{-}6)$$

As before, the derivatives may be evaluated for temperature variation:

$$\left.\begin{aligned} \frac{\partial D_{TV}}{\partial T} &= 0 \\ \frac{\partial D_{\theta V}}{\partial T} &= D_{atm}(T_M)\alpha\ (\theta_S - \theta)\ \nu\ \frac{g}{RT_M}\ \frac{d\rho_o}{dT}\, e^{\frac{\psi(\theta) g}{RT_M}}\ \frac{d\psi(\theta)}{d\theta} \\ \frac{\partial D_{Tl}}{\partial T} &= 0 \\ \frac{\partial D_{\theta l}}{\partial T} &= 0 \end{aligned}\right\} \qquad (6.67\text{-}70)$$

and the following forms arise for moisture variation

$$\frac{\partial D_{TV}}{\partial \theta} = -D_{atm}(T_M)\alpha\,\nu\,\frac{d\rho_o}{dT}\,e^{\frac{\psi(\theta)g}{RT_M}} + D_{atm}(T_M)\alpha\,(\theta_S-\theta)\,\frac{g}{RT_M}\,\frac{d\psi}{d\theta}\,\frac{d\rho_o}{dT}\,e^{\frac{\psi(\theta)g}{RT_M}} \tag{6.71}$$

$$\begin{aligned}\frac{\partial D_{\theta V}}{\partial \theta} = & -D_{atm}(T_M)\alpha\nu\frac{g}{RT_M}\,\rho_o e^{\frac{\psi(\theta)g}{RT_M}}\,\frac{d\psi(\theta)}{d\theta} \\ & + D_{atm}(T_M)\alpha\,(\theta_S-\theta)\,\nu\,\frac{g^2}{R^2{T_M}^2}\,\rho_o e^{\frac{\psi(\theta)g}{RT_M}}\left(\frac{d\psi(\theta)}{d\theta}\right)^2 \\ & + D_{atm}(T_M)\alpha\,(\theta_S-\theta)\,\frac{g}{RT_M}\,\rho_o e^{\frac{\psi(\theta)g}{RT_M}}\,\frac{d^2\psi(\theta)}{d\theta^2}\end{aligned} \tag{6.72}$$

$$\frac{\partial D_{Tl}}{\partial \theta} = K\gamma\,\frac{d\psi}{d\theta} + \frac{dK}{d\theta}\,\gamma\,\psi \tag{6.73}$$

$$\frac{\partial D_{\theta l}}{\partial \theta} = K\,\frac{d^2\psi}{d\theta^2} + \frac{dK}{d\theta}\,\frac{d\psi}{d\theta} \tag{6.74}$$

Then the $\mathbf{\Lambda}_T$ is given by

$$\mathbf{\Lambda}_T = \frac{\partial \mathbf{\Lambda}}{\partial T} = \begin{bmatrix} \frac{\partial a(\theta)}{\partial T} & \frac{\partial b(T,\theta)}{\partial T} \\ \frac{\partial r(\theta)}{\partial T} & \frac{\partial s(T,\theta)}{\partial T} \end{bmatrix} = \begin{bmatrix} 0 & \frac{\partial b(T,\theta)}{\partial T} \\ 0 & \frac{\partial s(T,\theta)}{\partial T} \end{bmatrix} \tag{6.75}$$

where,

$$\frac{\partial b}{\partial T} = \frac{L(T_M)}{C(\theta)}\,\frac{\partial D_{\theta V}}{\partial T} \tag{6.76}$$

$$\frac{\partial s}{\partial T} = \frac{\partial D_{\theta V}}{\partial T} \tag{6.77}$$

and $\mathbf{\Lambda}_\theta$ is given by

$$\mathbf{\Lambda}_\theta = \frac{\partial \mathbf{\Lambda}}{\partial \theta} = \begin{bmatrix} \frac{\partial a(T,\theta)}{\partial \theta} & \frac{\partial b(T,\theta)}{\partial \theta} \\ \frac{\partial r(T,\theta)}{\partial \theta} & \frac{\partial s(T,\theta)}{\partial \theta} \end{bmatrix} = \begin{bmatrix} \frac{da(\theta)}{d\theta} & \frac{\partial b(T,\theta)}{\partial \theta} \\ \frac{dr(\theta)}{d\theta} & \frac{\partial s(T,\theta)}{\partial \theta} \end{bmatrix} \tag{6.78}$$

where

$$\frac{\partial a}{\partial \theta} = \frac{1}{C}\frac{d\lambda}{d\theta} - \frac{dC}{d\theta}\frac{\lambda}{C^2} + \frac{L}{C}\frac{\partial D_{TV}}{\partial \theta} - \frac{L}{C^2}\frac{dC}{D\theta}D_{TV} \tag{6.79}$$

$$\frac{\partial b}{\partial \theta} = -\frac{L(T_M)}{C^2(\theta)}\frac{dC(\theta)}{d\theta}D_{\theta V}(T,\theta) + \frac{L(T_M)}{C(\theta)}\frac{\partial D_{\theta V}}{\partial \theta} \tag{6.80}$$

$$\frac{\partial r}{\partial \theta} = \frac{\partial D_{TV}}{\partial \theta} + \frac{\partial D_{Tl}}{\partial \theta} \tag{6.81}$$

$$\frac{\partial s}{\partial \theta} = \frac{\partial D_{\theta V}}{\partial \theta} + \frac{\partial D_{\theta l}}{\partial \theta} \tag{6.82}$$

VI.6. Summary.

The present section has analysed the variation brought to coupled diffusion by the nature of the diffusion coefficients. Four forms of dependency on T and θ have been distinguished. It has been shown that the many sources of theoretical variation present in the coefficients reduce to rather fewer having definite physical effect. In particular, other than for the coefficient $D_{\theta V}$, the effects of temperature are less important than might be supposed. Variation may be easily analysed by coefficient and eigenvalue surfaces. The latter show clearly that for all the possible ranges of T and θ the $\mathbf{\Lambda}$ matrix is diagonally dominant. Later abstract analysis of coupled diffusion will show that this feature is one of the factors inducing the qualitative stability of the system. For analytical approaches the orientation of the tangent planes to each point of the diffusion coefficient surfaces is of importance. The gradient of $\mathbf{\Lambda}$ at each point associated with a (T,θ) pairing may be assessed by the two matrices $\mathbf{\Lambda}_T$ and $\mathbf{\Lambda}_\theta$. Values arising in these matrices have been tabulated and will be analysed when further algebraic techniques have been set out. This line of analysis may be duplicated for reduced matrices which include only numerically important terms.

VII. THE PERIODIC STATE OF COUPLED DIFFUSION

VII.1 Introduction.

The content of this chapter has been summarised for publication and submitted to a relevant journal. Techniques are developed by which the asymptotic stable state of coupled diffusion may be described in both quantitative and qualitative terms. Concordance has been achieved between the analytical solution and behaviour observed in simulation. Each of these aspects is the subject of a sub-section and both are now introduced. For the required three-fold agreement between analysis, simulation and field results, rather different boundary conditions pertain to which both analysis and simulation must be adapted. This area is deferred for separate consideration in section **IX**. It will be seen that analysis uncovers the possibility of a form of induced resonance in the second harmonic occurring between the variables. An interesting and, it is believed unreported, feature here is that resonance is triggered not, as is normally the case, solely by constructive interference between input frequencies, but, in addition, interference between input means. A further aspect of interest is that terms analogous to those occurring in the most familiar instance of resonance, that of harmonic motion forced at its natural period, are here bounded and subject to exponential decay. Hence, even in this extreme instance of potential breakdown of stability, the strongly contractive property of the system ensures that instability is contained. The range of parameter values operable in soil ensure that this phenomenon of coupled resonance cannot, in fact, occur in the medium. However, for pure mathematical interest, examples of simulations for a simple system which displays this feature are included. It will be seen that the onset of resonance causes non-convergence of the numerical scheme.

The theoretical assumptions and limitations of a harmonic series description of coupled diffusion should be stated explicitly. Firstly, such a solution captures only an asymptotic steady state and excludes transient evolution to that state. Equally, the theoretical question of whether any initial profile inevitably follows such an evolution must be regarded as an open question for systems posed in fully non-linear generality. In relation to these observations, it may be said that the phasor method itself, of which the following account is essentially an extension and generalisation, focuses only on harmonic behaviour and gives no information concerning how that state is attained. One parameter group invariance techniques (Ames [2]) may be used to show that certain combinations, limited in number, of boundary and initial conditions each give rise to an associated form of solution; it would be helpful to be able to show that an arbitrary combination of a boundary and initial condition must evolve into one of these available forms. However, in contrast to the theoretical uncertainty, simulation over a range of initial profiles, and with varying functional forms for the diffusion coefficients does progress swiftly to the steady state. The theory of semigroups to be outlined in section **X** indicates that

the system possesses strongly contractive properties. Any functional form imposed at the boundary cannot then give rise to uncontrolled bifurcation; rather its form is preserved and concentrated on passage through the medium, as expressed by its contraction in norm within the Banach space of which it is an element. Thus theoretical indications of the probable uniformity of asymptotic response joined to the actual observation of that response, would seem to establish its existence in practical terms, although such a procedure is evidently not at all rigorous.

The series solutions presume the existence of an asymptotic state and form approximations to it. Even if the above tentative arguments for existence are regarded as sufficiently convincing, it still remains to be seen how adequate are the approximations which result. In fact, the very contractive properties by which existence is indicated equally induce accuracy in the approximation. The solutions depend on approximating each of the diffusion coefficients by its value for the coupled variables at the input mean together with two additional terms representing the orientation of the tangent plane to its associated surface. If the input amplitudes carry the variables sufficiently far from regions where this approximation is valid then inevitably, it would seem, the approximation must fail and may not represent the behaviour even in general qualitative terms. Indeed, for the generality of systems, such an approximation would seem even absurdly inadequate. However, in this context, the strong overall contraction present in the system implies that no permanent bifurcation from mean values may occur. On progression of the input wave through the medium, local tendencies (local here meaning occurring at particular times and soil depths) to depart widely from the mean are constrained to return to it, and thus into regions of values for which the approximation is valid. These intuitive justifications are supported by the close agreement between simulation and analysis.

Assessment of the relevance of the approach to field observation is unfortunately hindered firstly by the scarcity of data of any extended observation of soil carried through in sufficient detail and secondly by the understandable but regrettable fact that experiments have been mainly addressed to evolutions following highly discontinuous and even improbable circumstances at the onset of monitoring. It is hoped that the following comment is not regarded as too casuistical in favour of the present line of argument; but it may be said that if soil were subjected regularly to the kinds of regimes experiments monitor, depletion and erosion would inevitably result. Hence experiments cannot pretend to report naturally occurring behaviour, since the soil characteristic values are not those of a medium in which such evolutions are standard. It may be suggested that if inundation occurred frequently the new soil parameter values for such a depleted medium would imply that periodic regularity would be re-established rather more quickly than the week or so observed in both the experiments of Rose and Jackson.

VII.2 Analytical Description of Coupled Diffusion.

2.(i) Separation into Linear Equations.

Retaining notation as in previous sections, diffusion is considered for the system

$$\dot{Y} = \left(\mathbf{\Lambda}(Y)Y'\right)' \tag{7.1}$$

and boundary conditions are given by

$$Y = Y_M + Y_A \cos\omega t \ , \tag{7.2}$$

where, as before

$$Y = \begin{bmatrix} T \\ \theta \end{bmatrix}, \tag{7.3}$$

and T represents temperature, θ moisture concentration; differentiation with respect to time denoted by a dot and with respect to depth by a dash, and the matrix $\mathbf{\Lambda}$ is now a function of the dependent variables:

$$\mathbf{\Lambda} = \begin{bmatrix} a(T,\theta) & b(T,\theta) \\ r(T,\theta) & s(T,\theta) \end{bmatrix}. \tag{7.4}$$

A series solution for (7.1) may be formed by writing

$$Y(z,t) = Y_M + Y_v(z,t) \ . \tag{7.5}$$

The truncated form of the Taylor expansion in two variables then gives

$$\mathbf{\Lambda}(Y) = \mathbf{\Lambda}(Y_M) + [Y_v \cdot \nabla\mathbf{\Lambda}](Y_M + \Xi). \tag{7.6}$$

In general, Ξ is a vector function of z and t, but satisfies $|\Xi| < |Y_v|$, where $|\cdot|$ is the norm given by the larger absolute value of the vector components. The presupposition of the method is now that the qualitative stability of the system is such that $|\Xi|$ remains sufficiently small under all evolutions for $\mathbf{\Lambda}(Y_M)$ to be a good approximation to $\mathbf{\Lambda}(Y_M + \Xi)$. Differentiation of (7.5), use of (7.6) and substitution into (7.1) leads to

$$\dot{Y}_v = \left(\left(\mathbf{\Lambda}(Y_M) + [Y_v \cdot \nabla\mathbf{\Lambda}](Y_M + \Xi)\right) Y_v'\right)' \ . \tag{7.7}$$

and the assumption of the perturbation represented by Ξ is small gives

$$\dot{Y}_v = \left(\left(\mathbf{\Lambda}(Y_m) + [Y_v \cdot \nabla\mathbf{\Lambda}](Y_m)\right) Y_v'\right)' \ . \tag{7.8}$$

The series decomposition

$$Y_v = \sum_{i=0}^{\infty} Y_i \tag{7.9}$$

on substitution into (7.8) gives

$$\sum_{i=0}^{\infty} \dot{Y}_i = \left(\left\{ \Lambda(Y_m) + \left[\sum_{i=0}^{\infty} Y_i \cdot \nabla \Lambda(Y_m) \right] \right\} \sum_{i=0}^{\infty} Y_i' \right)' \tag{7.10}$$

$$= \Lambda(Y_m) \sum_{i=0}^{\infty} Y_i'' + \sum_{n=0}^{\infty} \sum_{r=0}^{n} \left(\left[Y_r \cdot \nabla \Lambda(Y_m) \right] Y_{n-r}' \right)' \tag{7.11}$$

$$= \Lambda(Y_m) \sum_{i=0}^{\infty} Y_i'' + \sum_{n=1}^{\infty} \sum_{r=0}^{n-1} \left(\left[Y_r \cdot \nabla \Lambda(Y_m) \right] Y_{n-1-r}' \right)' , \tag{7.12}$$

where the Cauchy rearrangement of the product of two infinite series is used in the second equality. Equating for each i the term on the left hand side of (7.12) to the first term on the right hand side and those up to $n = i$ from the second term gives the decomposition:

$$\dot{Y}_i = \Lambda(Y_m) Y_i'' + \sum_{r=0}^{n-1} \left(\left[Y_r \cdot \nabla \Lambda(Y_m) \right] Y_{n-1-r}' \right)' . \tag{7.13}$$

Explicitly, the first three terms are

$$\left.\begin{aligned} \dot{Y}_0 &= \Lambda(Y_m) Y_0'' \\ \dot{Y}_1 &= \Lambda(Y_m) Y_1'' + \left(\left[Y_0 \cdot \nabla \Lambda(Y_m) \right] Y_0' \right)' \\ \dot{Y}_2 &= \Lambda(Y_m) Y_2'' + \left(\left[Y_0 \cdot \nabla \Lambda(Y_m) \right] Y_1' + \left[Y_1 \cdot \nabla \Lambda(Y_m) \right] Y_0' \right)' \end{aligned}\right\} . \tag{7.14}$$

2.(ii) Solution of the Separated Equations.

2.(ii)(a) Solution for the First Harmonic

Considering the first of the equations (7.14), if

$$\dot{Y}_0 = \Lambda(Y_m) Y_0'' , \tag{7.15}$$

then standard methods show the solution is given by

$$Y_0 = \boldsymbol{P}\begin{bmatrix} C_1 u_1 \\ C_2 u_2 \end{bmatrix}, \tag{7.16}$$

where $$u_i = e^{-\alpha_i z}\cos(\omega t - \alpha_i)\,, \qquad \alpha_i{}^2 = \frac{\omega}{2\eta_i} \tag{7.17-8}$$

and

$$\begin{bmatrix} C_1 \\ C_2 \end{bmatrix} = \boldsymbol{P}^{-1}\begin{bmatrix} T_A \\ \Theta_A \end{bmatrix}. \tag{7.19}$$

2.(ii)(b) Solution for the Second Harmonic

Substitution of the solution for Y_0 from (7.16-9) into the second of (7.14)

$$\dot{Y}_1 = \boldsymbol{\Lambda}(Y_m)Y_1{}'' + \Big(\big[Y_0 \cdot \nabla\boldsymbol{\Lambda}(Y_m)\big]\,Y_0{}'\Big)'$$

then gives

$$\begin{bmatrix} \dot{T}_1 \\ \dot{\Theta}_1 \end{bmatrix} = \boldsymbol{\Lambda}(Y_m)\begin{bmatrix} T_1{}'' \\ \Theta_1{}'' \end{bmatrix} + \left(T_0\boldsymbol{\Lambda}_T\begin{bmatrix} T_0{}' \\ \Theta_0{}' \end{bmatrix} + \Theta_0\boldsymbol{\Lambda}_\theta\begin{bmatrix} T_0{}' \\ \Theta_0{}' \end{bmatrix}\right)', \tag{7.20}$$

where $\boldsymbol{\Lambda}_T$ and $\boldsymbol{\Lambda}_\theta$ are the matrices considered in section **VI**.4, defined by

$$\boldsymbol{\Lambda}_T = \frac{\partial}{\partial T}\boldsymbol{\Lambda}\Big|_{Y_m} \quad , \Lambda_\theta = \frac{\partial}{\partial\theta}\boldsymbol{\Lambda}\Big|_{Y_m}. \tag{7.21}$$

Equation (7.20) can be simplified by a second use of eigenvalue decomposition. Substituting

$$\begin{bmatrix} T_1 \\ \Theta_1 \end{bmatrix} = \boldsymbol{P}\begin{bmatrix} v_1 \\ v_2 \end{bmatrix} \tag{7.22}$$

where again $\boldsymbol{P}$ is the eigenvalue matrix of $\boldsymbol{\Lambda}$ evaluated at the input mean, gives

$$\begin{bmatrix} \dot{v}_1 \\ \dot{v}_2 \end{bmatrix} = \begin{bmatrix} \eta_1 v_1{}'' \\ \eta_2 v_2{}'' \end{bmatrix} + \boldsymbol{P}^{-1}\left\{\left((p_{11}C_1u_1 + p_{12}C_2u_2)\boldsymbol{\Lambda}_T\begin{bmatrix} p_{11}C_1u_1{}' + p_{12}C_2u_2{}' \\ p_{21}C_1u_1{}' + p_{22}C_2u_2{}' \end{bmatrix}\right)'\right\}$$

$$+ \boldsymbol{P}^{-1}\left\{\left((p_{21}C_1u_1 + p_{22}C_2u_2)\boldsymbol{\Lambda}_\theta\begin{bmatrix} p_{11}C_1u_1{}' + p_{12}C_2u_2{}' \\ p_{21}C_1u_1{}' + p_{22}C_2u_2{}' \end{bmatrix}\right)'\right\}. \tag{7.23}$$

The p_{ij} here are the elements of $\boldsymbol{P}$. There are, unfortunately, no methods by which this expression can be simplified to a less involved form. The remainder of the present sub-section will be devoted to carrying through the algebra of its solution. Explicitly the equation is

$$\begin{bmatrix} \dot{v}_1 \\ \dot{v}_2 \end{bmatrix} = \begin{bmatrix} \eta_1 v_1'' \\ \eta_2 v_2'' \end{bmatrix} + \begin{bmatrix} A_1 \\ B_1 \end{bmatrix} (u_1 u_1')' + \begin{bmatrix} A_2 \\ B_2 \end{bmatrix} (u_1 u_2')' + \begin{bmatrix} A_3 \\ B_3 \end{bmatrix} (u_2 u_1')' + \begin{bmatrix} A_4 \\ B_4 \end{bmatrix} (u_2 u_2')' \quad (7.24)$$

where the C_i are given by (7.19) and

$$\begin{bmatrix} A_1 \\ B_1 \end{bmatrix} = \boldsymbol{P}^{-1}\boldsymbol{\Lambda}_T \begin{bmatrix} {C_1}^2 {p_{11}}^2 \\ {C_1}^2 p_{11} p_{21} \end{bmatrix} + \boldsymbol{P}^{-1}\boldsymbol{\Lambda}_\theta \begin{bmatrix} {C_1}^2 p_{11} p_{21} \\ {C_1}^2 {p_{21}}^2 \end{bmatrix} \quad (7.25)$$

$$\begin{bmatrix} A_2 \\ B_2 \end{bmatrix} = \boldsymbol{P}^{-1}\boldsymbol{\Lambda}_T \begin{bmatrix} C_1 C_2 p_{11} p_{12} \\ C_1 C_2 p_{11} p_{22} \end{bmatrix} + \boldsymbol{P}^{-1}\boldsymbol{\Lambda}_\theta \begin{bmatrix} C_1 C_2 p_{21} p_{12} \\ C_1 C_2 p_{21} p_{22} \end{bmatrix} \quad (7.26)$$

$$\begin{bmatrix} A_3 \\ B_3 \end{bmatrix} = \boldsymbol{P}^{-1}\boldsymbol{\Lambda}_T \begin{bmatrix} C_1 C_2 p_{12} p_{11} \\ C_1 C_2 p_{12} p_{21} \end{bmatrix} + \boldsymbol{P}^{-1}\boldsymbol{\Lambda}_\theta \begin{bmatrix} C_1 C_2 p_{11} p_{22} \\ C_1 C_2 p_{22} p_{21} \end{bmatrix} \quad (7.27)$$

$$\begin{bmatrix} A_4 \\ B_4 \end{bmatrix} = \boldsymbol{P}^{-1}\boldsymbol{\Lambda}_T \begin{bmatrix} {C_2}^2 {p_{12}}^2 \\ {C_2}^2 p_{12} p_{22} \end{bmatrix} + \boldsymbol{P}^{-1}\boldsymbol{\Lambda}_\theta \begin{bmatrix} {C_2}^2 p_{12} p_{22} \\ {C_2}^2 {p_{22}}^2 \end{bmatrix} \quad (7.28)$$

The equations (7.22-4) will now be solved in terms of the A_i,B_i given by (7.25-8). In practice the highly involved numerical calculations which these solutions demand have been carried through by computer program to produce graphical illustration of the behaviour represented by this analytical solution. These representations will be considered in section **VIII.3**.

2.(ii)(c) Differentiation Formulae.

The manipulations required for solution of (7.22-4) are tedious and rather involved. It is useful to have to hand formulae for the basic differentiations which occur in the solution process. Writing

$$C_{\alpha,n} = e^{-\alpha z} cos(n\omega t - \alpha z) \quad \text{and} \quad S_{\alpha,n} = e^{-\alpha z} sin(n\omega t - \alpha z)\,, \quad (7.29)$$

then it immediately follows that

$$C_{\alpha,n}' = -\alpha(C_{\alpha,n} - S_{\alpha,n})\,; \quad (7.30)$$

$$S_{\alpha,n}' = -\alpha(C_{\alpha,n} + S_{\alpha,n})\,; \quad (7.31)$$

$$C_{\alpha,n}'' = -2\alpha^2 S_{\alpha,n}\,; \quad (7.32)$$

$$S_{\alpha,n}'' = 2\alpha^2 C_{\alpha,n}\,; \quad (7.33)$$

and further,

$$(C_{\alpha,n}C_{\beta,m}{}')' = -\beta(\alpha+\beta)S_{\alpha+\beta,n+m} + \alpha\beta(cos2\beta z C_{\alpha+\beta,n-m} - sin2\beta z S_{\alpha+\beta,n-m}) + \beta^2(cos2\beta z S_{\alpha+\beta,n-m} + sin2\beta z C_{\alpha+\beta,n-m}) . \quad (7.34)$$

In particular, writing $m = n$ in (7.34) gives,

$$(C_{\alpha,n}C_{\beta,n}{}')' = -\beta(\alpha+\beta)S_{\alpha+\beta,2n} + \alpha\beta e^{-(\alpha+\beta)z}cos(\alpha-\beta)z - \beta^2 e^{-(\alpha+\beta)z}sin(\alpha-\beta)z , \quad (7.35)$$

and for $\beta = \alpha$ in (7.34),

$$(C_{\alpha,n}C_{\alpha,m}{}')' = -2\alpha^2 S_{2\alpha,n+m} + \alpha^2\{cos2\alpha z C_{2\alpha,n-m} - sin2\alpha z S_{2\alpha,n-m} + cos2\alpha z S_{2\alpha,n-m} + sin2\alpha z C_{2\alpha,n-m}\} . \quad (7.36)$$

Putting either $\beta = \alpha$ in (7.35), or $m = n$ in (7.36) gives rise to

$$(C_{\alpha,n}C_{\alpha,n}{}')' = -2\alpha^2 S_{2\alpha,2n} + \alpha^2 e^{-2\alpha z} . \quad (7.37)$$

With these various formulae available, if u_i is given by

$$u_i = e^{\alpha_i z}cos(\omega t - \alpha_i z) = C_{\alpha_i,1} \quad (7.38)$$

then the inhomogenous terms occurring in (7.24) may be evaluated as

$$(u_1 u_1{}')' = -2\alpha_1{}^2 e^{-2\alpha_1 z}sin(2\omega t - 2\alpha_1 z) + \alpha_1{}^2 e^{-2\alpha_1 z} ; \quad (7.39)$$

$$(u_1 u_2{}')' = -\alpha_2(\alpha_1+\alpha_2)e^{-(\alpha_1+\alpha_2)z}sin(2\omega t - (\alpha_1+\alpha_2)z) + \alpha_1\alpha_2 e^{-(\alpha_1+\alpha_2)z}cos(\alpha_1-\alpha_2)z - \alpha_2{}^2 e^{-(\alpha_1+\alpha_2)z}sin(\alpha_1-\alpha_2)z ; \quad (7.40)$$

$$(u_2 u_1{}')' = -\alpha_1(\alpha_1+\alpha_2)e^{-(\alpha_1+\alpha_2)z}sin(2\omega t - (\alpha_1+\alpha_2)z) + \alpha_1\alpha_2 e^{-(\alpha_1+\alpha_2)z}cos(\alpha_1-\alpha_2)z + \alpha_1{}^2 e^{-(\alpha_1+\alpha_2)z}sin(\alpha_1-\alpha_2)z ; \quad (7.41)$$

$$(u_2 u_2{}')' = -2\alpha_2{}^2 e^{-2\alpha_2 z}sin(2\omega t - 2\alpha_2 z) + \alpha_2{}^2 e^{-2\alpha_2 z} . \quad (7.42)$$

The following two differentiations are also needed,

$$\left(e^{-(\alpha_1+\alpha_2)z}cos(\alpha_1-\alpha_2)z\right)''$$
$$= 4\alpha_1\alpha_2 e^{-(\alpha_1+\alpha_2)z}cos(\alpha_1-\alpha_2)z + 2({\alpha_1}^2-{\alpha_2}^2)e^{-(\alpha_1+\alpha_2)z}sin(\alpha_1-\alpha_2)z\ ; \quad (7.43)$$

$$\left(e^{-(\alpha_1+\alpha_2)z}sin(\alpha_1-\alpha_2)z\right)''$$
$$= 4\alpha_1\alpha_2 e^{-(\alpha_1+\alpha_2)z}sin(\alpha_1-\alpha_2)z - 2({\alpha_1}^2-{\alpha_2}^2)e^{-(\alpha_1+\alpha_2)z}cos(\alpha_1-\alpha_2)z\ . \quad (7.44)$$

2.(iii) Solution to the Component Equations.

Equation (7.23) may be solved in terms of the following component equations,

$$\dot{w_{11}} = \eta_1 {w_{11}}'' + a(u_1{u_1}')' \quad (7.45)$$
$$\dot{w_{12}} = \eta_1 {w_{12}}'' + b(u_1{u_2}')' \quad (7.46)$$
$$\dot{w_{13}} = \eta_1 {w_{13}}'' + c(u_2{u_1}')' \quad (7.47)$$
$$\dot{w_{14}} = \eta_1 {w_{14}}'' + d(u_2{u_2}')' \quad (7.48)$$

where, for the solution for v_1,

$$a = A_1;\ \ b = A_2;\ \ c = A_3;\ \ d = A_4 \quad (7.49)$$

the A_i being defined by equations (7.25-8). The v_1 required for solution of (7.23) is then given by

$$v_1 = \sum_j w_{1j}\ , \quad (7.50)$$

since it follows that

$$\dot{v}_1 = \sum_j \dot{w}_{1j} = \eta_1 \sum_j {w''}_{1j} + A_1(u_1{u_1}')' + A_2(u_1{u_2}')' + A_3(u_2{u_1}')' + A_4(u_2{u_2}')' \quad (7.51)$$

$$= \eta_1 {v_1}'' + A_1(u_1{u_1}')' + A_2(u_1{u_2}')' + A_3(u_2{u_1}')' + A_4(u_2{u_2}')'\ . \quad (7.52)$$

Thus v_1 satisfies equation(7.24). The solution for v_2 , which is

$$v_2 = \sum_j w_{2j} \quad (7.53)$$

where the w_{2j} are given by

$$\dot{w_{21}} = \eta_2 {w_{21}}'' + a^*(u_1{u_1}')' \quad (7.54)$$
$$\dot{w_{22}} = \eta_2 {w_{22}}'' + b^*(u_1{u_2}')' \quad (7.55)$$
$$\dot{w_{23}} = \eta_2 {w_{23}}'' + c^*(u_2{u_1}')' \quad (7.56)$$
$$\dot{w_{24}} = \eta_2 {w_{24}}'' + d^*(u_2{u_2}')' \quad (7.57)$$

obviously follows from symmetry properties with v_1 by transposing η_1 and η_2 and writing

$$a^* = B_1;\ \ b^* = B_2;\ \ c^* = B_3;\ \ d^* = B_4 \quad (7.58)$$

in the solutions derived, in turn, for w_{21} from that of w_{14}; for w_{22} from w_{13}; for w_{23} from w_{13} and for w_{24} from w_{11}.

The component equations (7.45-8) will now be solved.

2.(iii)(a) Solution to the First Component Equation.

This equation is given by (7.45):

$$\dot{w}_{11} = \eta_1 w_{11}'' + a(u_1 u_1')' \,. \tag{7.45}$$

From (7.39)

$$(u_1 u_1')' = -2\alpha_1^2 e^{-2\alpha_1 z} sin(2\omega t - 2\alpha_1 z) + \alpha_1^2 e^{-2\alpha_1 z} \tag{7.59}$$

For the inhomogeneous equation substitute

$$w_{11} = k_1 e^{-2\alpha_1 z} cos(2\omega t - 2\alpha_1 z) + k_2 e^{-2\alpha_1 z} \tag{7.60}$$

where the k_i are to be determined. Substitution leads to

$$-4\alpha_1^2 \eta_1 k_1 = -8k_1 \eta_1 \alpha_1^2 - 2a\alpha_1^2 \tag{7.61}$$

$$0 = 4\eta_1 \alpha_1^2 k_2 + a\alpha_1^2 \tag{7.62}$$

and so,

$$k_1 = -\frac{a}{2\eta_1} \quad ; \quad k_2 = -\frac{a}{4\eta_1} \,. \tag{7.63-4}$$

Incorporating the homogeneous solution and complying with boundary conditions gives the general solution

$$w_{11} = \frac{a}{2\eta_1}\left\{ e^{-\sqrt{2}\alpha_1 z} cos(2\omega t - \sqrt{2}\alpha_1 z) - e^{-2\alpha_1 z} cos(2\omega t - 2\alpha_1 z) \right\}$$

$$+ \frac{a}{4\eta_1}\left\{ 1 - e^{-2\alpha_1 z} \right\} \tag{7.65}$$

2.(iii)(b) Solution to the Second Component Equation.

The equation is given by (7.46):

$$\dot{w}_{12} = \eta_1 w_{12}'' + b(u_1 u_2')' \,. \tag{7.46}$$

From (7.40)

$$\begin{aligned}(u_1 u_2')' \;&= -\alpha_2(\alpha_1 + \alpha_2) e^{-(\alpha_1 + \alpha_2)z} sin(2\omega t - (\alpha_1 + \alpha_2)z) \\ &+ \alpha_1 \alpha_2 e^{-(\alpha_1 + \alpha_2)z} cos(\alpha_1 - \alpha_2)z \; - \; \alpha_2^2 e^{-(\alpha_1 + \alpha_2)z} sin(\alpha_1 - \alpha_2)z \,. \end{aligned} \tag{7.65}$$

The trial solution for the inhomogeneous part

$$\begin{aligned} w_{12} \;&= \; k_1 e^{-(\alpha_1 + \alpha_2)z} cos(2\omega t - (\alpha_1 + \alpha_2)z) \\ &+ k_2 e^{-(\alpha_1 + \alpha_2)z} sin(\alpha_1 - \alpha_2)z \; + k_3 e^{-(\alpha_1 + \alpha_2)z} cos(\alpha_1 - \alpha_2)z \end{aligned} \tag{7.66}$$

gives, by substitution in (7.46), equating coefficients and using $\omega = 2\eta_1 \alpha_1^2$,

$$\left.\begin{aligned} -4\eta_1{\alpha_1}^2 k_1 &= -2k_1\eta_1(\alpha_1+\alpha_2)^2 - b\alpha_2(\alpha_1+\alpha_2) \\ 0 &= -2k_2\eta_1({\alpha_1}^2-{\alpha_2}^2) + 4k_3\eta_1\alpha_1\alpha_2 + b\alpha_1\alpha_2 \\ 0 &= 4k_2\eta_1\alpha_1\alpha_2 + 2k_3\eta_1({\alpha_1}^2-{\alpha_2}^2) - b{\alpha_2}^2 \end{aligned}\right\} \tag{7.67}$$

(7.67(a)) implies

$$k_1 = \frac{\frac{b}{\eta_1}\alpha_2(\alpha_1+\alpha_2)}{4{\alpha_1}^2 - 2(\alpha_1+\alpha_2)^2}\,. \tag{7.68}$$

For k_2 and k_3 , equations (7.67(b)) and (7.67(c)) can be written

$$\begin{bmatrix} 2({\alpha_1}^2-{\alpha_2}^2) & -4\alpha_1\alpha_2 \\ -4\alpha_1\alpha_2 & -2({\alpha_1}^2-{\alpha_2}^2) \end{bmatrix} \begin{bmatrix} k_2 \\ k_3 \end{bmatrix} = \begin{bmatrix} \frac{b}{\eta_1}\alpha_1\alpha_2 \\ -\frac{b}{\eta_1}{\alpha_2}^2 \end{bmatrix} \tag{7.69}$$

and so,

$$\begin{bmatrix} k_2 \\ k_3 \end{bmatrix} = \frac{-1}{4({\alpha_1}^2+{\alpha_2}^2)^2} \begin{bmatrix} -2({\alpha_1}^2-{\alpha_2}^2) & 4\alpha_1\alpha_2 \\ 4\alpha_1\alpha_2 & 2({\alpha_1}^2-{\alpha_2}^2) \end{bmatrix} \begin{bmatrix} \frac{b}{\eta_1}\alpha_1\alpha_2 \\ -\frac{b}{\eta_1}{\alpha_2}^2 \end{bmatrix} \tag{7.70}$$

$$= \frac{1}{2({\alpha_1}^2+{\alpha_2}^2)} \begin{bmatrix} \frac{b}{\eta_1}\alpha_1\alpha_2 \\ -\frac{b}{\eta_1}{\alpha_2}^2 \end{bmatrix}. \tag{7.71}$$

Incorporating the homogeneous solution, and meeting the boundary condition gives as general solution

$$w_{12} = \frac{\frac{b}{\eta_1}\alpha_2(\alpha_1+\alpha_2)}{2(\alpha_1+\alpha_2)^2 - 4{\alpha_1}^2} \left\{ e^{-\sqrt{2}\alpha_1 z}\cos(2\omega t - \sqrt{2}\alpha_1 z) \quad - e^{-(\alpha_1+\alpha_2)z}\cos(2\omega t - (\alpha_1+\alpha_2)z) \right\}$$

$$+ \frac{\frac{b}{\eta_1}\alpha_1\alpha_2}{2({\alpha_1}^2+{\alpha_2}^2)} \left\{ e^{-(\alpha_1+\alpha_2)z}\sin(\alpha_1-\alpha_2 z \right\} + \frac{\frac{b}{\eta_1}{\alpha_2}^2}{2({\alpha_1}^2+{\alpha_2}^2)} \left\{ 1 - e^{-(\alpha_1+\alpha_2)z}\cos(\alpha_1-\alpha_2)z \right\}. \tag{7.72}$$

2.(iii)(c) Solution to the Third Component Equation

Equation (7.46) may obviously be solved directly by exploiting its symmetry properties with (7.45). However, carrying through the manipulation in detail provides a useful check for internal consistency. The equation to be solved is

$$\dot{w}_{13} = \eta_1 w_{13}'' + c(u_2 u_1')' \,, \tag{7.47}$$

and from equation (7.41)

$$\begin{aligned}(u_2u_1')' = & -\alpha_1(\alpha_1+\alpha_2)e^{-(\alpha_1+\alpha_2)z}sin\big(2\omega t-(\alpha_1+\alpha_2)z\big) \\ & + \alpha_1\alpha_2 e^{-(\alpha_1+\alpha_2)z}cos(\alpha_1-\alpha_2)z \;+\; {\alpha_1}^2 e^{-(\alpha_1+\alpha_2)z}sin(\alpha_1-\alpha_2)z \,. \end{aligned} \tag{7.73}$$

The trial solution

$$\begin{aligned} w_1 \;=\; & k_1 e^{-(\alpha_1+\alpha_2)z}cos\big(2\omega t-(\alpha_1+\alpha_2)z\big) \\ & + k_2 e^{-(\alpha_1+\alpha_2)z}sin(\alpha_1-\alpha_2)z \;\; + k_3 e^{-(\alpha_1+\alpha_2)z}cos(\alpha_1-\alpha_2)z \end{aligned} \tag{7.74}$$

gives, by substitution in (7.47), equating coefficients and using $\omega = 2\eta_1{\alpha_1}^2$,

$$\left.\begin{aligned} -4\eta_1{\alpha_1}^2 k_1 &= -2k_1\eta_1(\alpha_1+\alpha_2)^2 - c\alpha_1(\alpha_1+\alpha_2) \\ 0 &= -2k_2\eta_1({\alpha_1}^2-{\alpha_2}^2) + 4k_3\eta_1\alpha_1\alpha_2 + c\alpha_1\alpha_2 \\ 0 &= 4k_2\eta_1\alpha_1\alpha_2 \;+\; 2k_3\eta_1({\alpha_1}^2-{\alpha_2}^2) \;+\; c{\alpha_1}^2 \end{aligned}\right\} \tag{7.75}$$

(7.75(a)) implies

$$k_1 = \frac{\frac{c}{\eta_1}\alpha_1(\alpha_1+\alpha_2)}{4{\alpha_1}^2 - 2(\alpha_1+\alpha_2)^2} \,. \tag{7.76}$$

For k_2 and k_3 , equations (7.75(b)) and (7.75(c)) can be written

$$\begin{bmatrix} 2({\alpha_1}^2-{\alpha_2}^2) & -4\alpha_1\alpha_2 \\ -4\alpha_1\alpha_2 & -2({\alpha_1}^2-{\alpha_2}^2) \end{bmatrix} \begin{bmatrix} k_2 \\ k_3 \end{bmatrix} \;=\; \begin{bmatrix} \frac{c}{\eta_1}\alpha_1\alpha_2 \\ \frac{c}{\eta_1}{\alpha_1}^2 \end{bmatrix} \tag{7.77}$$

and so,

$$\begin{bmatrix} k_2 \\ k_3 \end{bmatrix} = \frac{-1}{4({\alpha_1}^2+{\alpha_2}^2)^2} \begin{bmatrix} -2({\alpha_1}^2-{\alpha_2}^2) & 4\alpha_1\alpha_2 \\ 4\alpha_1\alpha_2 & 2({\alpha_1}^2-{\alpha_2}^2) \end{bmatrix} \begin{bmatrix} \frac{c}{\eta_1}\alpha_1\alpha_2 \\ \frac{c}{\eta_1}{\alpha_1}^2 \end{bmatrix} \tag{7.78}$$

$$= \frac{-1}{2(\alpha_1{}^2+\alpha_2{}^2)} \begin{bmatrix} \frac{c}{\eta_1}\alpha_1\alpha_2 \\ \\ \frac{c}{\eta_1}\alpha_1{}^2 \end{bmatrix}. \tag{7.79}$$

Incorporating the homogeneous solution, and meeting the boundary condition gives as general solution

$$w_{13} = \frac{\frac{c}{\eta_1}\alpha_1(\alpha_1+\alpha_2)}{2(\alpha_1+\alpha_2)^2-4\alpha_1{}^2}\left\{ e^{-\sqrt{2}\alpha_1 z}cos(2\omega t-\sqrt{2}\alpha_1 z) \quad -e^{-(\alpha_1+\alpha_2)z}cos(2\omega t-(\alpha_1+\alpha_2)z)\right\}$$

$$-\frac{\frac{c}{\eta_1}\alpha_1\alpha_2}{2(\alpha_1{}^2+\alpha_2{}^2)}\left\{e^{-(\alpha_1+\alpha_2)z}sin(\alpha_1-\alpha_2)z\right\}+\frac{\frac{c}{\eta_1}\alpha_1{}^2}{2(\alpha_1{}^2+\alpha_2{}^2)}\left\{1-e^{-(\alpha_1+\alpha_2)z}cos(\alpha_1-\alpha_2)z\right\} \tag{7.80}$$

2.(iii)(d) Solution to the Fourth Component Equation.

The equation to be solved is

$$\dot{w}_{14} = \eta_1 w_{14}'' + d(u_2u_2')' \,. \tag{7.48}$$

From (7.42)

$$(u_2u_2')' = -2\alpha_2{}^2e^{-2\alpha_2 z}sin(2\omega t-2\alpha_2 z)+\alpha_2{}^2e^{-2\alpha_2 z} \,. \tag{7.81}$$

For the inhomogeneous equation substitute

$$w_{14} = k_1e^{-2\alpha_2 z}cos(2\omega t-2\alpha_2 z)+k_2e^{-2\alpha_2 z} \,, \tag{7.82}$$

where the k_i are to be determined. Using now $\omega = 2\eta_2\alpha_2{}^2$, substitution leads to

$$-4\alpha_2{}^2\eta_2 k_1 = -8k_1\eta_1\alpha_2{}^2-2d\alpha_2{}^2 \tag{7.83}$$

$$0 = 4\eta_1\alpha_2{}^2k_2+d\alpha_2{}^2 \tag{7.84}$$

and so,

$$k_1 = -\frac{d}{4\eta_1-2\eta_2} \quad ; \quad k_2 = -\frac{d}{4\eta_1} \,. \tag{7.85-6}$$

Incorporating the homogeneous solution and complying with boundary conditions gives the general solution

$$w_{14} = \frac{d}{4\eta_1-2\eta_2}\left\{e^{-\sqrt{2}\alpha_1 z}cos(2\omega t-\sqrt{2}\alpha_1 z)-e^{-2\alpha_2 z}cos(2\omega t-2\alpha_2 z)\right\}$$

$$+\frac{d}{4\eta_1}\left\{1-e^{-2\alpha_2 z}\right\} \tag{7.87}$$

Exploiting the property mentioned after equation (7.57) the functions w_{2i} may now be given as

$$w_{21} = \frac{a^*}{4\eta_2 - 2\eta_1}\left\{e^{-\sqrt{2}\alpha_2 z}cos(2\omega t - \sqrt{2}\alpha_2 z) - e^{-2\alpha_1 z}cos(2\omega t - 2\alpha_1 z)\right\}$$

$$+\frac{a^*}{4\eta_2}\left\{1 - e^{-2\alpha_1 z}\right\} \; ; \tag{7.88}$$

$$w_{22} = \frac{\frac{b^*}{\eta_2}\alpha_2(\alpha_1+\alpha_2)}{2(\alpha_1+\alpha_2)^2 - 4{\alpha_2}^2}\left\{ e^{-\sqrt{2}\alpha_2 z}cos(2\omega t - \sqrt{2}\alpha_2 z) \;\; - e^{-(\alpha_1+\alpha_2)z}cos\big(2\omega t - (\alpha_1+\alpha_2)z\big)\right\}$$

$$-\frac{\frac{b^*}{\eta_2}\alpha_1\alpha_2}{2({\alpha_1}^2+{\alpha_2}^2)}\left\{ - e^{-(\alpha_1+\alpha_2)z}sin(\alpha_1-\alpha_2)z\right\} + \frac{\frac{b^*}{\eta_2}{\alpha_2}^2}{2({\alpha_1}^2+{\alpha_2}^2)}\left\{1 - e^{-(\alpha_1+\alpha_2)z}cos(\alpha_1-\alpha_2)z\right\} ; \tag{7.89}$$

$$w_{23} = \frac{\frac{c^*}{\eta_2}\alpha_1(\alpha_1+\alpha_2)}{2(\alpha_1+\alpha_2)^2 - 4{\alpha_2}^2}\left\{ e^{-\sqrt{2}\alpha_2 z}cos(2\omega t - \sqrt{2}\alpha_2 z) \;\; - e^{-(\alpha_1+\alpha_2)z}cos\big(2\omega t - (\alpha_1+\alpha_2)z\big)\right\}$$

$$+\frac{\frac{c^*}{\eta_2}\alpha_1\alpha_2}{2({\alpha_1}^2+{\alpha_2}^2)}\left\{ - e^{-(\alpha_1+\alpha_2)z}sin(\alpha_1-\alpha_2)z\right\} + \frac{\frac{c^*}{\eta_2}{\alpha_1}^2}{2({\alpha_1}^2+{\alpha_2}^2)}\left\{1 - e^{-(\alpha_1+\alpha_2)z}cos(\alpha_1-\alpha_2)z\right\} ; \tag{7.90}$$

$$w_{24} = \frac{d^*}{2\eta_2}\left\{e^{-\sqrt{2}\alpha_2 z}cos(2\omega t - \sqrt{2}\alpha_2 z) - e^{-2\alpha_2 z}cos(2\omega t - 2\alpha_2 z)\right\}$$

$$+\frac{d^*}{4\eta_2}\left\{1 - e^{-2\alpha_2 z}\right\} \; . \tag{7.91}$$

The starred constants are here given by (7.58) and (7.25-8). The various constituent terms derived above may now be assembled to produce the full solution for the second harmonic. Note that under the notation used in this approach, the first harmonic is given by T_o and θ_o and so forth. The second harmonic, is, then

$$\begin{bmatrix} T_1 \\ \Theta_1 \end{bmatrix} = \boldsymbol{P}\begin{bmatrix} v_1 \\ v_2 \end{bmatrix} \tag{7.92}$$

where $\boldsymbol{P}$ is matrix of eigenvectors calculated at the input means, and v_1 is given by

$$v_1 = \sum_j w_{1j} \; . \tag{7.93}$$

where the w_{1j} are described by equations (7.65), (7.72), (7.80) and (7.87); the constants a, b, c, d are

equal respectively to the A_1, A_2, A_3, A_4 of equations (7.25-8). Equally,

$$v_2 = \sum_j w_{2j} \tag{7.94}$$

where the w_{2j} are described by equations (7.88-91), and the constants a^*, b^*, c^*, d^* are equal respectively to the B_1, B_2, B_3, B_4 of equations (7.25-8).

VII.3 Properties of Eigenvalue Decomposition Occurring in Coupled Diffusion

Before proceeding to an analysis of the second harmonic present in coupled diffusion, as shown by the solution (7.92-4), when illustrated by values occurring in the $\mathbf{\Lambda_T}$ and $\mathbf{\Lambda_\theta}$ matrices, certain properties of the eigenvalue decomposition are required. Although these observations are entirely elementary, they are, in fact, fundamental to the nature of coupled diffusion in soil, and will be used below, in section **X**, to determine the semigroup representation of the possible behaviours.

3.(i) Eigenvalue and Eigenvector Properties.

Considering the matrix $\mathbf{\Lambda}$, given by

$$\mathbf{\Lambda} = \begin{bmatrix} a & b \\ r & s \end{bmatrix} \tag{7.95}$$

then the eigenvalues associated with $\mathbf{\Lambda}$ are given by

$$\eta_i = \frac{(a+s) \pm \sqrt{(a+s)^2 - 4(as - br)}}{2} \tag{7.96a}$$

$$= \frac{(a+s) \pm \sqrt{(a-s)^2 + 4br}}{2} \tag{7.96b}$$

Since the entries in a diffusion matrix are necessarily positive it is immediate from the form (7.96b) that the eigenvalues occurring in coupled diffusion are real; secondly, since for all T, θ values $as \gg br$, it is evident from (7.96a) that the eigenvalues will be close to a and s respectively, and both will be positive. It will be seen below that these simple properties truncate drastically the possible qualitative evolutions of the system. Further, as may be verified from the table **VIII**.1., all T, θ variation retains the property that $a \gg s$ and $a - s \gg br$. Using the binomial expansion, it is seen that in coupled diffusion the eigenvalues are perturbed from a and s by

$$\eta_1 = a + \frac{br}{a-s} \tag{7.97}$$

$$\eta_2 = s - \frac{br}{a-s} \tag{7.98}$$

It then follows that the eigenvector matrices may be approximated as

$$\boldsymbol{P} = \begin{bmatrix} 1 & -\frac{b}{a-s} \\ \frac{r}{a-s} & 1 \end{bmatrix} \tag{7.99}$$

and

$$\boldsymbol{P^{-1}} = \begin{bmatrix} 1 & \frac{b}{a-s} \\ -\frac{r}{a-s} & 1 \end{bmatrix} \tag{7.100}$$

For regions of T, θ variation outside the sudden increase of $D_{\theta V}$ values around what may be called the impulsive behaviour of the coefficient at residual levels, it is permissible to regard the off diagonal terms in both these matrices as small; however, such a property cannot be asserted globally for all T, θ. In fact, the property that $a - s < b$ demarcates a region in which greater qualitative variety is possible to the system.

3.(ii) Implications for the Second Harmonic.

The properties of the eigenvectors allow an analysis in terms of orders of magnitude of the complicated component expressions of the second harmonic. It seems most useful to carry through such an analysis for values of the coefficients in which development of a subharmonic might be most likely to occur, that is, around the rapidly changing values for the coefficient $D_{\theta V}$. The term $\frac{b}{a-s}$ will then be large and changing rapidly. Such an analysis probes the nature of the stability of the system of coupled diffusion and its harmonic series representation. Specimen values for a hot, arid regime are taken from Adelanto loam at a temperature mean of $308°K$ and a moisture value of 0.03. The three $\boldsymbol{\Lambda}$ matrices, taking values from Table **VIII**.1. are then:

$$\boldsymbol{\Lambda} = \begin{bmatrix} 1.6\text{E}-3 & 7.6\text{E}-2 \\ 1.8\text{E}-8 & 4.2\text{E}-5 \end{bmatrix} \; ; \; \boldsymbol{\Lambda}_T = \begin{bmatrix} 3.09\text{E}-7 & 1.1\text{E}-1 \\ 1.9\text{E}-10 & 3.2\text{E}-6 \end{bmatrix} \; ; \; \boldsymbol{\Lambda}_\theta = \begin{bmatrix} 1.3\text{E}-2 & -3.5\text{E}+1 \\ 1.1\text{E}-7 & -1.9\text{E}-2 \end{bmatrix}$$

In particular, it would be helpful to determine whether the relatively large terms in the $\boldsymbol{\Lambda}_\theta$, which are, of course, consequent on the rapid increase of $D_{\theta V}$, are large enough to disturb the system when evaluated in all the many permutations of different expressions present in equations (7.92-4). Writing

$$\epsilon_T = \frac{b}{a-s}; \quad \epsilon_\theta = \frac{r}{a-s} \; ,$$

where, in the particular behaviour studied, this notation carries no implication for the magnitude of these terms, although in general behaviour they will be small, then, writing all terms in orders of magnitude, $\epsilon_T = 10^{-5}, \epsilon_\theta = 10^2$, and following the general line of the solution for the second harmonic gives

$$\begin{bmatrix} C_1 \\ C_2 \end{bmatrix} = \boldsymbol{P}^{-1}\begin{bmatrix} T_A \\ \Theta_A \end{bmatrix} = \begin{bmatrix} 1 & \epsilon_T \\ -\epsilon_\theta & 1 \end{bmatrix}\begin{bmatrix} T_A \\ \Theta_A \end{bmatrix} = \begin{bmatrix} T_A + \epsilon_T \theta_A \\ \Theta_A \end{bmatrix}, \qquad (7.101)$$

where, as in all the current section, calculations are truncated in terms of orders of magnitude. For the equations (7.25-8), namely,

$$\begin{bmatrix} A_1 \\ B_1 \end{bmatrix} = \boldsymbol{P}^{-1}\boldsymbol{\Lambda}_T \begin{bmatrix} C_1^2 p_{11}^2 \\ C_1^2 p_{11} p_{21} \end{bmatrix} + \boldsymbol{P}^{-1}\boldsymbol{\Lambda}_\theta \begin{bmatrix} C_1^2 p_{11} p_{21} \\ C_1^2 p_{21}^2 \end{bmatrix}$$

$$\begin{bmatrix} A_2 \\ B_2 \end{bmatrix} = \boldsymbol{P}^{-1}\boldsymbol{\Lambda}_T \begin{bmatrix} C_1 C_2 p_{11} p_{12} \\ C_1 C_2 p_{11} p_{22} \end{bmatrix} + \boldsymbol{P}^{-1}\boldsymbol{\Lambda}_\theta \begin{bmatrix} C_1 C_2 p_{21} p_{12} \\ C_1 C_2 p_{21} p_{22} \end{bmatrix}$$

$$\begin{bmatrix} A_3 \\ B_3 \end{bmatrix} = \boldsymbol{P}^{-1}\boldsymbol{\Lambda}_T \begin{bmatrix} C_1 C_2 p_{12} p_{11} \\ C_1 C_2 p_{12} p_{21} \end{bmatrix} + \boldsymbol{P}^{-1}\boldsymbol{\Lambda}_\theta \begin{bmatrix} C_1 C_2 p_{11} p_{22} \\ C_1 C_2 p_{22} p_{21} \end{bmatrix}$$

$$\begin{bmatrix} A_4 \\ B_4 \end{bmatrix} = \boldsymbol{P}^{-1}\boldsymbol{\Lambda}_T \begin{bmatrix} C_2^2 p_{12}^2 \\ C_2^2 p_{12} p_{22} \end{bmatrix} + \boldsymbol{P}^{-1}\boldsymbol{\Lambda}_\theta \begin{bmatrix} C_2^2 p_{12} p_{22} \\ C_2^2 p_{22}^2 \end{bmatrix}$$

it may be verified, by tedious substitution, that all terms involving $p_{12} = \epsilon_T$ become negligible. Substituting further $p_{11} = p_{22} = 1$, $p_{12} = \epsilon_\theta$, and the expressions for the C_i from (7.101), gives

$$\begin{bmatrix} A_1 \\ B_1 \end{bmatrix} = \boldsymbol{P}^{-1}\boldsymbol{\Lambda}_T \begin{bmatrix} (T_A + \epsilon_\theta \theta_A)^2 \\ 0 \end{bmatrix} + \boldsymbol{P}^{-1}\boldsymbol{\Lambda}_\Theta \begin{bmatrix} 0 \\ 0 \end{bmatrix} \qquad (7.101)$$

$$\begin{bmatrix} A_2 \\ B_2 \end{bmatrix} = \boldsymbol{P}^{-1}\boldsymbol{\Lambda}_T \begin{bmatrix} e_\theta T_A \theta_A + e_\theta^2 \theta_A^2 \\ T_A \theta_A + e_\theta \theta_A^2 \end{bmatrix} + \boldsymbol{P}^{-1}\boldsymbol{\Lambda}_\Theta \begin{bmatrix} 0 \\ 0 \end{bmatrix} \qquad (7.102)$$

$$\begin{bmatrix} A_3 \\ B_3 \end{bmatrix} = \boldsymbol{P}^{-1}\boldsymbol{\Lambda}_T \begin{bmatrix} e_\theta T_A \theta_A + e_\theta {}^2 \theta_A {}^2 \\ 0 \end{bmatrix} + P^{-1}\boldsymbol{\Lambda}_\Theta \begin{bmatrix} T_A \theta_A + e_\theta \theta_A {}^2 \\ 0 \end{bmatrix} \quad (7.103)$$

$$\begin{bmatrix} A_4 \\ B_4 \end{bmatrix} = \boldsymbol{P}^{-1}\boldsymbol{\Lambda}_T \begin{bmatrix} \epsilon_\theta {}^2 \theta_A {}^2 \\ \epsilon_\theta \theta_A {}^2 \end{bmatrix} + \boldsymbol{P}^{-1}\boldsymbol{\Lambda}_\Theta \begin{bmatrix} \epsilon_\theta \theta_A {}^2 \\ \theta_A {}^2 \end{bmatrix} \quad (7.104)$$

This reduction allows the coefficients A_i, B_i to be evaluated in terms of orders of magnitude. Taking the values for the Λ matrices given above, it is found that

$$\boldsymbol{P}^{-1}\boldsymbol{\Lambda}_T = \begin{bmatrix} 1 & 10^2 \\ 10^{-5} & 1 \end{bmatrix} \begin{bmatrix} 10^{-7} & 10^{-1} \\ 10^{-10} & 10^{-5} \end{bmatrix} = \begin{bmatrix} 10^{-7} & 10^{-1} \\ 10^{-10} & 10^{-5} \end{bmatrix} \quad (7.105)$$

$$\boldsymbol{P}^{-1}\boldsymbol{\Lambda}_\theta = \begin{bmatrix} 1 & 10^2 \\ 10^{-5} & 1 \end{bmatrix} \begin{bmatrix} 10^{-2} & 10^{+1} \\ 10^{-6} & 10^{-2} \end{bmatrix} = \begin{bmatrix} 10^{-2} & 10^{+1} \\ 10^{-6} & 10^{-2} \end{bmatrix} \quad (7.106)$$

Taking now values for T_A and θ_A again in very broad dimensional terms, with T_A as 10^1 and θ_A as 10^{-2} (considering the low presupposed mean value), it is seen that the equations (7.101-4) become:

$$\begin{bmatrix} A_1 \\ B_1 \end{bmatrix} = \boldsymbol{P}^{-1}\boldsymbol{\Lambda}_T \begin{bmatrix} 10^2 \\ 0 \end{bmatrix} + \boldsymbol{P}^{-1}\boldsymbol{\Lambda}_\Theta \begin{bmatrix} 0 \\ 0 \end{bmatrix} \quad (7.107)$$

$$\begin{bmatrix} A_2 \\ B_2 \end{bmatrix} = \boldsymbol{P}^{-1}\boldsymbol{\Lambda}_T \begin{bmatrix} 10 \\ 10^{-1} \end{bmatrix} + \boldsymbol{P}^{-1}\boldsymbol{\Lambda}_\Theta \begin{bmatrix} 0 \\ 0 \end{bmatrix} \quad (7.108)$$

$$\begin{bmatrix} A_3 \\ B_3 \end{bmatrix} = \boldsymbol{P}^{-1}\boldsymbol{\Lambda}_T \begin{bmatrix} 10 \\ 0 \end{bmatrix} + \boldsymbol{P}^{-1}\boldsymbol{\Lambda}_\Theta \begin{bmatrix} 10^{-1} \\ 0 \end{bmatrix} \quad (7.109)$$

$$\begin{bmatrix} A_4 \\ B_4 \end{bmatrix} = \boldsymbol{P}^{-1}\boldsymbol{\Lambda}_T \begin{bmatrix} 10 \\ 10^{-2} \end{bmatrix} + \boldsymbol{P}^{-1}\boldsymbol{\Lambda}_\Theta \begin{bmatrix} 10^{-2} \\ 10^{-4} \end{bmatrix} \quad (7.110)$$

giving, finally,

$$\begin{bmatrix} A_1 \\ B_1 \end{bmatrix} = \begin{bmatrix} 10^{-5} \\ 10^{-8} \end{bmatrix} + \begin{bmatrix} 0 \\ 0 \end{bmatrix} \tag{7.111}$$

$$\begin{bmatrix} A_2 \\ B_2 \end{bmatrix} = \begin{bmatrix} 10^{-2} \\ 10^{-6} \end{bmatrix} + \begin{bmatrix} 0 \\ 0 \end{bmatrix} \tag{7.112}$$

$$\begin{bmatrix} A_3 \\ B_3 \end{bmatrix} = \begin{bmatrix} 10^{-6} \\ 10^{-9} \end{bmatrix} + \begin{bmatrix} 10^{-3} \\ 10^{-7} \end{bmatrix} \tag{7.113}$$

$$\begin{bmatrix} A_4 \\ B_4 \end{bmatrix} = \begin{bmatrix} 10^{-3} \\ 10^{-7} \end{bmatrix} + \begin{bmatrix} 10^{-3} \\ 10^{-6} \end{bmatrix} \tag{7.114}$$

The A_i and B_i values, when substituted into the solutions (7.93) are subject to multiplication by the difference between two rapidly decaying exponential functions which, by design, is zero at the boundary. The maximum value for this difference is of the order of 10^{-2}. It may seem, then, that the second harmonic is negligible. However, these terms are also subject to division by various combinations of eigenvalues and damping depths. For a narrow soil layer, close to the surface, when the exponential terms give a maximum value, the resulting terms are, in fact, of significance. Under these very limited conditions, it is seen that the development of subharmonic behaviour is indeed possible. These comments will be resumed below and illustrated for simulated behaviour. It may be quickly verified that outside the peak values conveyed to $\mathbf{\Lambda}_T$ and $\mathbf{\Lambda}_\theta$ by the behaviour of $D_{\theta V}$ around residual levels of moisture, the second harmonic represents only a small perturbation from the first harmonic. The decomposition in terms of orders of magnitude allows an easy identification of factors which may be expected to lead to a second harmonic influence on behaviour. For both heat and moisture, it is required, as a prerequisite, that b should be of comparable magnitude to a. If this condition is not present then obviously neither of the matrices $\boldsymbol{P}$ or $\boldsymbol{P}^{-1}$ will contain terms large enough to produce significant values. If the condition is met, it is seen that the largest terms in the expressions (7.111-4) arise from, for moisture, $\frac{\partial s}{\partial T}$ and $\frac{\partial s}{\partial \theta}$. In turn, the large values in the derivative of this coefficient arise from $\frac{\partial D_{\theta V}}{\partial T}$ and $\frac{\partial D_{\theta V}}{\partial \theta}$. In a sense, analysis merely confirms the obvious. For temperature, $\frac{\partial b}{\partial T}$ has the greatest significance, resulting from the large values of $\frac{\partial D_{\theta V}}{\partial T}$. It is interesting to observe that there is some inherent incompatibility in these two conditions, since, assuming behaviour occurs for moisture values larger than the rapid decay of $D_{\theta V}$, the derivatives in the second condition will be large and negative. The first condition will quickly become inapplicable. The normally harmonic progression can only be disturbed within narrow parameter limits.

VII.4. Summary.

The methods given above allow the periodic state of coupled diffusion to be described. It has been seen that, despite the quantiative complexity of the terms which result from this analysis, in qualitative terms the behaviour is relatively simple: a first harmonic is perturbed from sinusoidal behaviour by a second harmonic which under general conditions adds a slight disturbance to it. Under some conditions and for some soils, particularly those with large impulsive $D_{\theta V}$ values occurring at high moisture concentration values, the second harmonic can become large enough to influence the behaviour significantly. It will be seen below that Adelanto loam, the soil used by Jackson for many field investigations, comes into this category. In addition, it should be said that for exceptionally low moisture values, those occuring below peak values of $D_{\theta V}$, analysis, confirmed by simulation, indicates that the second harmonic may dominate the response. However, such residual moisture values, when effectively moisture content is entirely vapour, may be beyond the limits of validity of the theory. For moisture concentration values above this peak, behaviour is controlled by the balance between the two harmonics. In these circumstances, there is migration of the means and of the maxima and minima of the variations. Depending on complicated relationships between the various constants which occur in section **VII**.2., these migrations, for the means, may be either an increase or a decrease, and for the stationary values, accelerations or retardations. These comments will be followed through in the next section, when the analysis of the present section is illustrated by values occuring in the Λ matrices for two specific soils.

VIII. QUANTITATIVE DESCRIPTION OF COUPLED DIFFUSION.

VIII.1 Introduction.

Analytical lines of approach to the problem of coupled diffusion have been set out above. However, the resulting analytical approximations are highly complex, both as algebraic expressions and as a consequence of the variation of parameter values substituted from the $\mathbf{\Lambda}$ matrices. The purpose of the present section is to discern salient aspects of the behaviour initially concealed within these complexities. The variation in $\mathbf{\Lambda}$, $\mathbf{\Lambda}_T$ and $\mathbf{\Lambda}_\theta$ matrices for the two studied soils is reviewed. Representative values leading to features which typify the general behaviour are studied in greater depth. These features are then illustrated by graphical depictions of both simulated behaviour and the behaviour given by the solutions. There is good agreement between simulation and analysis.

VIII.2 Variation in the $\mathbf{\Lambda}$, $\mathbf{\Lambda}_T$ and $\mathbf{\Lambda}_\theta$ Matrices.

It may be said of the general application of the computer to mathematical problems that there is a certain danger that the resulting profusion of data tends to obscure, rather than clarify, the underlying features. The present comments attempt to reduce the mass of information concerning the three $\mathbf{\Lambda}$ matrices, given as Table **VIII**.1, to those aspects which have physical effect. Variation is considered for soils under a hot, arid regime. Moisture concentration values are taken from 0.03 to 0.15, with extension in some instances to 0.2. For completeness, the review includes features which are obvious from consideration of the diffusion coefficient surfaces given as Figs. **VI**.1-20.

The tables for the two soils give a cross-section for four different temperatures as moisture levels increase. It is immediately apparent that the effect of increasing temperature is merely to intensify qualitative features which are already present in each sequence of increasing moisture values. As a simplifying overstatement, it is generally true that any balance between parameter values for a given temperature will be present for all temperatures, under a slightly perturbed moisture value: no new features emerge as temperature increases. As an illustration of this comment, the point at which the coefficient b becomes of equal magnitude to the coefficient a, for the soil of Rose, at the coolest temperature of the range, occurs slightly above 0.03; at the hottest temperature it occurs at about 0.04. The increase in temperature merely shifts this significant point slightly. It should be noted equally that there is no temperature induced behaviour specific to a given soil; the significant variations occur through standard physical parameters common to all soils. Thus, to assist in management of the detail of Table **VIII**.1., effectively only moisture variation need be considered.

If, then, both tables are considered at the specimen temperature value of 294°K the most immediately obvious feature is that variation in range occurs in response to the coefficients $D_{\theta V}$ and D_{TV}, and what have been termed their 'impulsive' and 'Heaviside function' behaviours respectively. The rapid increase and decrease of $D_{\theta V}$ occurs at very residual moisture values for the Rose soil, and the table covers its behaviour from below its maximum to values for which it no longer has effect. This decrease is, of course, reflected in the large negative $\frac{\partial b}{\partial \theta}$ values. In contrast, the peak for Adelanto loam occurs rather later, and has a wider spread of moisture concentrations. The table values cover its behaviour from just below the peak to regions when it is still of significance. Since, as was shown above, the development of any subharmonic influence on behaviour requires, simultaneously, a b value comparable to that of a, and large values for either of $\frac{\partial D_{\theta V}}{\partial \theta}$ or $\frac{\partial D_{\theta V}}{\partial T}$, it might be expected that Adelanto loam is a particularly suitable medium for its occurrence. There is evidence to this effect in a study by Jackson**[52(b)]** in which a third harmonic in transient redistribution behaviour is discernable. The features of the $D_{\theta V}$ variation obviously equally have an effect on the coefficient r, except that here the influence of $D_{\theta l}$ gradually becomes felt as $D_{\theta V}$ decreases. The minimum value for b occurs around 0.08 for the Rose soil and around 0.13 in the Adelanto loam case.

The coefficient a has perhaps the simplest behaviour and shows a gradual increase in the whole moisture range. Its derivative with respect to temperature is obviously negligible and the above analysis of section **VII**.3. would seem to indicate that its derivative with respect to moisture equally does not enter into the determining mechanisms. In the tabulated values, D_{TV} for the Rose soil is observed at larger moisture values than its sudden increase in the 'Heaviside effect', giving a gradual decline; in the Adelanto case the step occurs at around 0.04. Theoretically, there should be a tendency to subharmonic behaviour around these specific values. However, the rise occurs at such a specific moisture value when the content is very low that its effects would be difficult to observe physically. The choice of the grid of representative points for both soils here misses the extreme behaviour of D_{TV}. As indicated by the low derivative values, the consequent behaviour for a and r does not have qualitatively marked features.

Turning now from from the derivative properties of the diffusion coefficients to the properties of their values, two simultaneous changes in their relative balances are discernible as moisture levels increase. As the peak of $D_{\theta V}$ values is traversed, s initially diminishes in relation to a, and then, as the coefficient $D_{\theta l}$ begins to have effect, begins to increase in respect to it. This movement continues beyond the values which the tables catalogue up till the point when, to model the situation accurately, a hydraulic conductivity term would be required. For the initial part of this movement, when s is decreasing with respect to a, the movement of b obviously parallels that of s. There is a movement from b initially being larger than a to its gradually becoming infinitesimal in comparison.

The coefficient r shows only a slight decrease over the range and so is not a determining factor in the general behaviour.

VIII.3. Comparison of Analytical and Simulated Behaviour of Coupled Diffusion

The previous section gave some observations concerning the variation in the balance between different elements of the $\mathbf{\Lambda}$ matrices as T and θ traverse possible ranges. Using the analytical approximation of section **VII**, it possible to see how these variations affect observed coupled diffusion. Simulated evolutions are given for specimen values of T and θ means imposed at the boundary which illustrate how the interaction between $\mathbf{\Lambda}$, $\mathbf{\Lambda}_T$ and $\mathbf{\Lambda}_\theta$ affects the resulting behaviour. These simulations are compared with graphical plots of the solutions from section **VII**. It is shown that for all evolutions other than those very limited ranges when the second harmonic can become dominant, there is good agreement between analysis and simulation. The section opens with some comments on the numerical method employed for simulation.

3.(i) Numerical Methods of Simulation.

Finite difference methods have been employed throughout in simulation. Justification for this choice is now given. A highly non-linear system, such as that representing coupled diffusion, gives particular difficulties to numerical simulation. Ideally, a method is required with good convergence properties, freedom from instability, ease of programming and which makes as minimal demand as possible on C.P.U. time. For a fully non-linear system, these requirements are evidently incompatible. Methods with good convergence properties, such as the Crank-Nicholson method, various forms of predictor-corrector and the Runge-Kutta methods give either interim transcendental equations for the node points, requiring further numerical methods for their solution at each node point as the grid is traversed, or else lead to such programming complexities that the method becomes unwieldy. All recent simulations on the equations ([4][3][31]) have used the finite element method; however, these simulations were addressed to non-Cartesian flow geometries, such as trickle irrigation. For the essentially rectilinear Cartesian situation of the present enquiries, the finite element method introduces inappropriate geometrical complexities. Despite evident drawbacks the finite difference method, then, has seemed the most suitable. Further, the enquiry of this thesis has been regarded as essentially mathematical in character, with simulation providing secondary support for the analytical approximations uncovered. Throughout, other than for the narrow band when rapidly changing coefficient values render the methods only partly applicable, good agreement has been achieved between simulation and analysis. The necessity for more elaborate numerical methods has not, therefore, arisen. The main liability of finite difference methods is that the poor convergence properties require a fine mesh size, leading inevitably to slow running times, and, potentially, to the build up of rounding

errors. The concordance between analysis and simulation indicates that rounding error build-up has not in fact occurred. In general, it can be said that the contractive properties of the evolutions, which will be detailed in section **X**, allow confidence to placed in the finite difference method when applied in this context. Its convergence properties arise naturally as a consequence of approximation to the exponential representation of its infinitesimal generator **[68]**. When that generator is contractive, convergence becomes more severe. These comments will be resumed in section **X**.

Details of the parameters used in simulation are now given. Simulation was carried through in the units given in the derivation of section **II**. The largest of the diffusion coefficients, a, is then of the order of 10^{-3}. Simulation to a depth of $50cms$, at which level the daily temperature wave has decayed, if carried out at the relatively coarse mesh size of $0.5cms$ for depth, then requires a subdivision, to simulate a two day period, of this period by 10,000. Simulation to a depth of $20cms$, with a mesh of $0.1cms$ for depth, requires some 100,000 steps. The terminal running time in this second case is then some 76 hours, which is a reflection of the involved nature of the calculations for each diffusion coefficient at each point of the grid. In practice, the following sets of simulations have been carried through by simulation to a depth of $25cms$, with a mesh of 0.3, requiring 30,000 steps. Specimen values, particularly those in which subharmonic developments are evidently more possible, have been simulated with the finer mesh of 0.1 and 100,000 time divisions steps. No difference was discernible for the two different mesh sizes. In addition, numerous simulations have been carried out to survey the entire range of evolutions possible to the system, under varying boundary inputs and initial profiles. The simulations included here have been abstracted from this mass of data to illustrate significicant features.

In detail, the simulation used can be represented by, in the notation of previous sections,

$$\begin{aligned} \boldsymbol{Y}_{r+1,s} &= \boldsymbol{Y}_{r,s} + \frac{h}{k^2}\left\{\boldsymbol{\Lambda}(\boldsymbol{Y}_{r,s})\left(\boldsymbol{Y}_{r,s+1} - 2\boldsymbol{Y}_{r,s} + \boldsymbol{Y}_{r,s-1}\right)\right\} \\ &\quad + \frac{h}{k^2}\left\{\left(\boldsymbol{\Lambda}(\boldsymbol{Y}_{r,s+1}) - \boldsymbol{\Lambda}(\boldsymbol{Y}_{r,s})\right)\left(\boldsymbol{Y}_{r,s+1} - \boldsymbol{Y}_{r,s}\right)\right\} \end{aligned} \tag{8.1}$$

where r and s are grid points in the time and depth directions respectively, and h and k are the time- and depth steps. All the functional dependencies catalogued in section **VI**.2. were used to evaluate the $\boldsymbol{\Lambda}(\boldsymbol{Y})$ variation at each step. The surface boundary conditions was asserted at the $s = 0$ value for traversal of the grid. At the lower depth boundary, there is perhaps some uncertainty over the appropriate boundary condition to enforce: it is necessary for simulation to detect the increase in mean value predicted by the abstract theory, although in many evolutions this increase will be small. For simulation purposes, to provide confirmation of the analytical approach and so necessarily independent

of it, there is, of course, no ab initio expectation of the actual value of this increase. A form of Neumann condition was asserted, in which each successive time traversal was forced, at the lower boundary, to be equal to the previous traversal. This condition ensures the behaviour converges to a constant value whilst making no presupposition about that value. It will be seen that this condition displays the development of the non-linear effects detailed above: the increase in mean values and the acceleration of wetting and retardation of drying cycles. For further confirmation a second method was employed in which simulation was carried through, at a necessarily coarser mesh size, to a depth twice that of the previous method. At this depth decay to the mean was enforced. When behaviour at the original maximum depth was then observed, an increase in mean equal both to the analytical prediction and to that found under the above "Neumann" conditions was found. These features are illustrated graphically in the following figures.

3.(ii) Specimen Analytical and Simulated Results.

Coupled diffusion is illustrated first by behaviour which might be termed 'regular', in which there is no assumed moisture fluctuation at the boundary. All the terms which potentially induce subharmonic behaviour for moisture in equations (7.25-8) then become zero. Graphical depictions for both temperature and moisture as both surface and contour plots are given in the following figures. A commentary on the features uncovered by analysis and illustrated by simulation is appended to each group. Details of the controlling parameters for each figure are summarised, and for convenience the details of the $\mathbf{\Lambda}$ matrices are included. The notation is used: T_M, T_A, temperature mean and amplitude respectively of the input surface variation; θ_M, θ_A, moisture mean and amplitude of the input surface vacation. The component plots for each considered evolution follow the same sequence, which is given explicitly only in the first case.

Figure **VIII.**1(a-h)

The soil of Rose; $T_M = 300$; $\theta_M = 0.2$; $T_A = 20$; $\theta_A = 0.0$

a) Simulated Temperature surface plot; b) Simulated Temperature contour plot;
c) Analytical Temperature surface plot; d) Analytical Temperature contour plot;
e) Simulated Moisture surface plot; f) Simulated Moisture contour plot;
g) Analytical Moisture surface plot; h) Analytical Moisture contour plot;

$\mathbf{\Lambda}$		$\mathbf{\Lambda}_T$		$\mathbf{\Lambda}_\theta$	
2.84E-3	2.76E-7	2.24E-7	1.18E-8	4.21E-3	-2.09E-5
8.76E-8	2.59E-4	2.25E-10	1.01E-11	2.09E-6	2.76E-3

Figure **VIII.2**(a-h)

The soil of Rose; $T_M = 300$; $\theta_M = 0.15$; $T_A = 20$; $\theta_A = 0.0$

Λ		Λ_T		Λ_θ	
2.60E-3	1.80E-6	3.12E-7	7.76E-8	5.23E-3	-5.75E-5
5.67E-8	8.41E-5	2.82E-10	5.97E-11	8.70E-7	1.00E-2

Figure **VIII.3**(a-h)

The soil of Rose; $T_M = 300$; $\theta_M = 0.1$; $T_A = 20$; $\theta_A = 0.0$

Λ		Λ_T		Λ_θ	
2.30E-3	2.68E-5	4.23E-7	1.16E-6	6.68E-3	-1.99E-3
5.86E-8	1.06E-5	3.38E-10	7.90E-10	-1.34E-7	8.24E-4

These figures show purely temperature induced variation in moisture since no fluctuation in moisture at the surface is assumed. Obviously such a static surface moisture distribution would be unlikely to occur in practice, and this case is included for its illustrative value in this limiting case. As moisture values fall from 0.2 to 0.1, the a and s coefficients of Λ become more unequal, and s is eventually dominated by a; at 0.1, the diffusion of moisture by the isothermal agencies, s, is too weak to have effect, and movement is solely induced by temperature. The decay of the temperature wave then automatically implies the decay of the moisture wave and so maximum moisture movement occurs immediately below the surface. As the soil becomes damper, s values increase, resulting in a more even balance between thermal and isothermal diffusion. Maximum movement occurs then at a deeper soil level. This change is obviously expressed mathematically by the more equal eigenvalues acting in the damping depth expressions allowing diffusion resulting from η_2 to have effect. No non-linear effects are observable in these evolutions.

Subsequent figures will show only moisture variation since in all cases the temperature variation is effectively a simple decaying sinusoid. The component figures are now:

a) Simulated Moisture surface plot; b) Simulated Moisture contour plot;

c) Analytical Moisture surface plot; d) Analytical Moisture contour plot;

Figure **VIII.4**(a-d)

The soil of Rose; $T_M = 300$; $\theta_M = 0.2$; $T_A = 5$; $\theta_A = 0.01$

Λ		Λ_T		Λ_θ	
2.84E-3	2.76E-7	2.24E-7	1.18E-8	4.21E-3	-2.09E-5
8.76E-8	2.59E-4	2.25E-10	1.01E-11	2.09E-6	2.76E-3

Figure **VIII**.5(a-d)

The soil of Rose; $T_M = 300$; $\theta_M = 0.15$; $T_A = 5$; $\theta_A = 0.01$

Λ		Λ_T		Λ_θ	
2.60E-3	1.80E-6	3.12E-7	7.76E-8	5.23E-3	-5.75E-5
5.67E-8	8.41E-5	2.82E-10	5.97E-11	8.70E-7	1.00E-2

Figure **VIII**.6(a-d)

The soil of Rose; $T_M = 300$; $\theta_M = 0.1$; $T_A = 5$; $\theta_A = 0.01$

Λ		Λ_T		Λ_θ	
2.30E-3	2.68E-5	4.23E-7	1.16E-6	6.68E-3	-1.99E-3
5.86E-8	1.06E-5	3.38E-10	7.90E-10	-1.34E-7	8.24E-4

These figures, in which a moisture fluctuation is now assumed at the boundary under a minimal temperature variation, are intended to be taken in conjunction both with the preceding and with the following set, which give evolutions for identical parameters for the Adelanto soil. In comparison with the former set, diffusion is now almost entirely an isothermal process. The more temperate boundary conditions, combined with the absence of any enhancement factors in the thermally induced coefficients give a simple decay of the imposed moisture wave. The increase of s with the moisture mean implies that at higher moisture values the wave penetrates further into the soil. At low values, the wave is rapidly extinguished, showing graphically the requirement of coupled agencies to explain movement of moisture at lower depths. As enhancement factors increase movement will penetrate further into the soil, but will tend to be synchronised with the temperature wave, rather than $\frac{5\pi}{4}$ out of phase with it. An illustration of this kind of behaviour will be given in the next section. When the figures are compared with those following for Adelanto loam they may be taken to demonstrate the very precise conditions needed for the onset of non-linear behaviour. Indeed, out of the six cases in only one, the variation for $\theta_M = 0.15$ for Adelanto loam, can the second harmonic be said to be relevant. For the Rose group, although the values in the $\mathbf{\Lambda}$ derivative matrices are large enough to produce non-linearity, the relatively small values of b in comparison to a, leading to a small $\frac{b}{a-s}$ term in the $\boldsymbol{P}$ and $\boldsymbol{P}^{-1}$ matrices which occur in the construction of the second harmonics, removes these terms from physical impact.

Figure **VIII**.7(a-d)

Adelanto Loam; $T_M = 300$; $\theta_M = 0.2$; $T_A = 5$; $\theta_A = 0.01$

Λ		Λ_T		Λ_θ	
2.64E-3	3.78E-5	2.24E-7	1.68E-6	4.21E-3	-4.79E-3
4.80E-8	1.06E-4	2.25E-10	1.44E-9	5.62E-7	1.56E-3

Figure **VIII**.8(a-d)

Adelanto Loam; $T_M = 300$; $\theta_M = 0.15$; $T_A = 5$; $\theta_A = 0.01$

Λ		Λ_T		Λ_θ	
2.60E-3	9.98E-4	3.11E-7	5.58E-5	5.28E-3	3.78E-2
4.95E-8	4.07E-5	2.80E-10	4.27E-8	-3.51E-8	6.54E-3

Figure **VIII**.10(a-d)

Adelanto Loam; $T_M = 300$; $\theta_M = 0.1$; $T_A = 20$; $\theta_A = 0.01$

Λ		Λ_T		Λ_θ	
2.30E-3	3.16E-3	4.16E-7	3.17E-4	6.84E-3	-2.71E-1
5.51E-8	5.21E-6	3.30E-10	2.13E-7	-7.87E-8	-1.22E-4

In the above it should be noted that the apparently anomalous values for $\frac{\partial s}{\partial \theta}$ and $\frac{\partial s}{\partial T}$ when $\theta_M = 0.1$, which are negative when s itself is apparently increasing, are caused by the fact that at this point s is traversing the ambiguous contours, shown in Fig.**VI**.12.(b), when $D_{\theta l}$ and $D_{\theta V}$ are of equal positive and negative magnitude. The three component figures illustrate the precise conditions needed for the incursion of non-linear effects, which are plainly visible in Fig.**VIII**.8.(a-d). At $\theta_M = 0.2$, the b value has decayed sufficiently for the large $\frac{\partial s}{\partial \theta}$ to have no effect. The evolution at this value is effectively linear. To illustrate this part point further, it may be noted that for all the Rose values, the differentials with respect to moisture are at least an order of magnitude larger than those in the Adelanto set; however, the earlier decay of $D_{\theta V}$ leading to smaller b values in the former case again prevents subharmonic onset. At $\theta_M = 0.1$, although s is now of comparable magnitude to a, the balance between the two isothermal coefficients implies that the gradients are again small and diffusion is again linear. The two outer evolutions, included here to illustrate the conditions needed to trigger subharmonics, are, in fact, highly atypical for this soil, which is prone to non-linear perturbation throughout its range. The upper instance of linearity, at $\theta_M = 0.2$, is caused by the fact that this value lies at the slackening off of increase in $D_{\theta l}$ at medium moisture values which some soils show. However, midway between these two values, at $\theta_M = 0.15$, the required parameter balance is struck and the incursion of a second harmonic is noticeable in both simulation and the analytical approximation. Cross sections of the surface for both analysis and simulation are given as Fig **VIII**.9. An evolution for $\theta_M = 0.18$ is given later as Fig.**IX**.13. and an even more pronounced subharmonic is observed. As a further illustration, a plot is given, at an increased scale as Fig.**VIII**.11.(a-b), for the following data:

Adelanto loam, $T_M = 300$; $\theta_M = 0.08$; $T_A = 20$; $\theta_A = 0.02$.

Λ		Λ_T		Λ_θ	
2.93E-3	8.71E-2	4.56E-6	1.49E-2	6.56E-3	-6.19E0
5.45E-7	5.64E-5	3.41E-9	9.46E-9	5.85E-7	-3.60E-3

VIII.4. Coupled Second Harmonic Resonance.

In the solutions to the constituent equations given in section **VII**.2.(iii), it may be noted that two expressions occur in the denominators which give rise to a coupled resonance effect in the second harmonic. That is, from equations (7.80) and (7.87), if either

$$4{\alpha_1}^2 - 2(\alpha_1 + \alpha_2)^2 = 0 \tag{8.2}$$

or

$$4\eta_1 - 2\eta_2 = 0 \tag{8.3}$$

then the solutions apparently become infinite. Using

$${\alpha_i}^2 = \frac{\omega}{2\eta_i}$$

in (8.2) it is found that the two expressions give rise to ratios between eigenvalues

$$\frac{\eta_1}{\eta_2} = (3 - 2\sqrt{2}) \quad ; \quad \frac{\eta_1}{\eta_2} = (3 + 2\sqrt{2}) \quad ; \quad \frac{\eta_1}{\eta_2} = \frac{1}{2} \tag{8.4-6}$$

at which resonance occurs in the first variable. Since the η_i perform symmetrical roles in the equations these relations may be reversed to find conditions for resonance in the second variable. An unusual feature here is that since the η_i are controlled by the input means, resonance is not triggered solely by interference between boundary amplitudes, as obviously is normally the case, but requires, in addition, interference between boundary means.

In saying that the solutions apparently become infinite, the construction here is analogous to the equation

$$\frac{d^2u}{dt^2} + \omega^2 u = cos\omega_1 t \tag{8.7}$$

which gives rise to an apparently infinite expression if $\omega_1 = \omega$ is substituted in the inhomogenous term in the general solution

$$u = Acos\omega t + Bsin\omega t + \frac{1}{\omega^2 - {\omega_1}^2} cos\omega_1 t \ . \tag{8.8}$$

The true expression for resonance is, of course,

$$u = A cos\omega t + B sin\omega t + \frac{t}{2\omega} sin\omega t \ . \tag{8.9}$$

In the case of coupled diffusion, at resonant values given by equations (8.2) and (8.3), the solution then consists of complicated expressions of the form $ze^{-\alpha_i z} sin(\omega t - \alpha_i z)$. Since it is obvious from equations (8.4-6) that coupled resonance is not possible when the eigenvalues differ by an order of magnitude the phenomenon cannot occur in soil and so the line of enquiry has not been pursued in depth. However, it is interesting to note that the damping given by the negative exponential ensures that even if resonance could occur in soil the behaviour would nevertheless be bounded and stable.

An illustration of resonance is now given for the following system, which seemingly is the simplest in which it may occur:

$$\begin{bmatrix} T \\ \theta \end{bmatrix} = \frac{\partial}{\partial z} \left\{ \begin{bmatrix} T & 1 \\ 0 & 1 \end{bmatrix} \frac{\partial}{\partial z} \begin{bmatrix} T \\ \theta \end{bmatrix} \right\} \tag{8.10}$$

$$T(0,t) = T_M + T_A cos\omega t \quad ; \quad \theta(0,t) = \theta_M + \theta_A cos\omega t \ . \tag{8.11-12}$$

Following the analytical methods of section **VII**.2, the system (8.10) gives rise to the matrices, which are now exact rather than approximations

$$\boldsymbol{P} = \begin{bmatrix} 1 & \frac{-1}{T_M - 1} \\ 0 & 1 \end{bmatrix} ; \qquad \boldsymbol{P}^{-1} = \begin{bmatrix} 1 & \frac{1}{T_M - 1} \\ 0 & 1 \end{bmatrix} ; \tag{8.13-14}$$

$$\boldsymbol{\Lambda}_T = \begin{bmatrix} 1 & 0 \\ 0 & 0 \end{bmatrix} ; \qquad \boldsymbol{\Lambda}_\theta = \begin{bmatrix} 0 & 0 \\ 0 & 0 \end{bmatrix} . \tag{8.15-16}$$

The constants C_i derived from the boundary amplitudes are then given by equation (7.19)

$$\begin{bmatrix} C_1 \\ C_2 \end{bmatrix} = \begin{bmatrix} 1 & \frac{1}{T_M - 1} \\ 0 & 1 \end{bmatrix} \begin{bmatrix} T_A \\ \theta_A \end{bmatrix}$$

and the constants appearing in the separated equations given by (7.25-8) are

$$\begin{bmatrix} A_1 \\ B_1 \end{bmatrix} = \boldsymbol{P}^{-1} \boldsymbol{\Lambda}_T \begin{bmatrix} {C_1}^2 {p_{11}}^2 \\ {C_1}^2 p_{11} p_{21} \end{bmatrix} + \boldsymbol{P}^{-1} \boldsymbol{\Lambda}_\Theta \begin{bmatrix} {C_1}^2 p_{11} p_{21} \\ {C_1}^2 {p_{21}}^2 \end{bmatrix} = \begin{bmatrix} {C_1}^2 \\ 0 \end{bmatrix} \tag{8.17}$$

$$\begin{bmatrix} A_2 \\ B_2 \end{bmatrix} = \boldsymbol{P}^{-1}\boldsymbol{\Lambda}_T \begin{bmatrix} C_1C_2p_{11}p_{12} \\ C_1C_2p_{11}p_{22} \end{bmatrix} + \boldsymbol{P}^{-1}\boldsymbol{\Lambda}_\Theta \begin{bmatrix} C_1C_2p_{21}p_{12} \\ C_1C_2p_{21}p_{22} \end{bmatrix} = \begin{bmatrix} -\frac{C_1C_2}{T_M - 1} \\ 0 \end{bmatrix} \qquad (8.18)$$

$$\begin{bmatrix} A_3 \\ B_3 \end{bmatrix} = \boldsymbol{P}^{-1}\boldsymbol{\Lambda}_T \begin{bmatrix} C_1C_2p_{12}p_{11} \\ C_1C_2p_{12}p_{21} \end{bmatrix} + \boldsymbol{P}^{-1}\boldsymbol{\Lambda}_\Theta \begin{bmatrix} C_1C_2p_{11}p_{22} \\ C_1C_2p_{22}p_{21} \end{bmatrix} = \begin{bmatrix} -\frac{C_1C_2}{T_M - 1} \\ 0 \end{bmatrix} \qquad (8.19)$$

$$\begin{bmatrix} A_4 \\ B_4 \end{bmatrix} = \boldsymbol{P}^{-1}\boldsymbol{\Lambda}_T \begin{bmatrix} {C_2}^2{p_{12}}^2 \\ {C_2}^2p_{12}p_{22} \end{bmatrix} + \boldsymbol{P}^{-1}\boldsymbol{\Lambda}_\Theta \begin{bmatrix} {C_2}^2p_{12}p_{22} \\ {C_2}^2{p_{22}}^2 \end{bmatrix} = \begin{bmatrix} {C_2}^2\left(\frac{-1}{T_M - 1}\right)^2 \\ 0 \end{bmatrix} \qquad (8.20)$$

From these equations, it is apparent that resonance is a genuine coupled phenomenon, and attaches to the non-linear effects set out in section **IV.**, for individual non-linear diffusion, only when an additional coupled variable is present. If $C_2 = 0$, representing the behaviour when second variable is constant, then all the terms in equations (8.17-20) become zero, other than the first for A_1, for which the denominator derived in section **VII.**2.(iii).(a) is positive definite. The three conditions for resonance of equations (8.4-6) are all nullified by A_2, A_3 and A_4 becoming zero. Further, it may be noted that resonance is not dependent on the coupled variable being non-linear.

The phenomenon of coupled resonance has proved difficult to observe since its onset tends to disturb the approximating numerical scheme. Taking input parameters for the system (8.10) as: $T_A = 0.05$; $\theta_A = 0.01$; $\theta_M = 0.2$, then since $\eta_1 = T_M$ and $\eta_2 = 1$, equation (8.4) indicates that one case of resonance occurs if the input mean for T is given by

$$T_M = \eta_1 = \eta_2(3 - 2\sqrt{2}) = 0.1715$$

Fig.**VIII.**12(a-b) illustrates the behaviour at $T_M = 0.19$; already some resonance seems to be developing around the second harmonic just below the surface slightly beyond $t = \pi$. At $T_M = 0.18$, the numerical scheme is sufficiently disturbed to cause floating overflow in the computer program. There would be interest in exploring this phenomena by a more stable scheme than the finite difference method. In order to illustrate the onset, values produced by the scheme have been artificially limited to produce a maximum absolute value of 0.3. Obviously the maximum values produced should be of the order of $T_M + T_A + \theta_A = 0.25$. It is seen from Fig.**VIII.**13(a-b) that convergence is disturbed by large negative values on the second harmonic. Finally, Fig.**VIII.**14(a-b) shows the evolution when $\theta_A = 0$, indicating that linearity is resumed when disturbing input from the second variable is not present.

VIII.5. Summary.

The analytical lines of solution given in section **VII.** have been illustrated for the range of values occuring in the coefficient matrix and its derivatives. It has been seen that this approach allows the main features of coupled diffusion to be described. As the balance between the terms a and s changes, so equally does the relative balance beween thermally induced and isothermal diffusion. The balance between a, b and the derivatives of s controls the onset of subharmonic incursion. It has been seen that only if particular conditions hold between these parameters will the second harmonic become large enough to have significance. These features have been illustated by simulation and graphical depictions of the analytically predicted behaviour for a range of boundary conditions chosen to typify the essential features. The possibility of a form of resonance induced between the variables in the second harmonic has been explored. The dominance of temperature diffusion over moisture diffusion in soil ensures this phenonemon cannot occur in the medium. However, for generally posed diffusion, if the two main diffusing mechanism are of equal efficiency in transportation, then coupled resonance will occur extensively for, in all, six different ratios between these coefficients. Despite resonance, the response nevertheless remains bounded by the presence of decaying exponential terms. It is suggested that the transient evolution of such systems may show very complex patterns, as different forms of resonance are evoked by the varying means on redistribution.

TABLE VIII.1. The Λ, Λ_T and Λ_θ Matrices at Specimen (T, θ) Values.

A) The Soil of the Rose (1968) Experiment.

Λ		Λ_T		Λ_θ	
TM = 2.80E+02	MM = 3.00E-02				
1.71794E-03	2.89608E-03	6.15779E-07	5.76901E-04	1.04863E-02	-3.82123E-01
5.96709E-08	1.63079E-06	3.86141E-10	3.09914E-07	4.96969E-08	-1.72017E-04
TM = 2.80000E+02	MM = 7.00000E-02				
2.08174E-03	8.62104E-05	4.97462E-07	1.20158E-05	7.93140E-03	-1.14794E-02
5.66059E-08	2.97113E-06	3.53557E-10	7.28766E-09	-1.20452E-07	9.69291E-04
TM = 2.80000E+02	MM = 1.10000E-01				
2.36666E-03	4.49378E-06	3.93230E-07	6.17348E-07	6.39927E-03	-3.26400E-04
5.05553E-08	1.56630E-05	3.10968E-10	4.16570E-10	-8.71229E-08	1.22379E-03
TM = 2.80000E+02	MM = 1.50000E-01				
2.59912E-03	5.34337E-07	3.07885E-07	7.33306E-08	5.27777E-03	-1.70473E-05
5.14063E-08	8.41324E-05	2.68092E-10	5.44837E-11	8.92261E-07	1.00962E-02
TM = 2.94000E+02	MM = 3.00000E-02				
1.72662E-03	6.92890E-03	6.23838E-07	8.22925E-04	1.04457E-02	-9.15392E-01
6.51815E-08	3.83706E-06	4.01063E-10	4.49558E-07	4.32635E-08	-4.56763E-04
TM = 2.94000E+02	MM = 7.00000E-02				
2.08875E-03	2.05672E-04	5.03248E-07	1.27091E-05	7.89074E-03	-2.73877E-02
6.16483E-08	3.04477E-06	3.66751E-10	7.88078E-09	-1.35469E-07	9.59692E-04
TM = 2.94000E+02	MM = 1.10000E-01				
2.37220E-03	1.07198E-05	3.97786E-07	6.41994E-07	6.36619E-03	-7.78624E-04
5.49901E-08	1.56673E-05	3.22559E-10	4.43076E-10	-1.02400E-07	1.22349E-03

TM = 2.94000E+02 MM = 1.50000E-01

2.60345E-03 1.27464E-06 3.11451E-07 7.61644E-08 5.25047E-03 -4.06656E-05

5.52297E-08 8.41330E-05 2.78085E-10 5.78808E-11 8.76970E-07 1.00962E-02

TM = 3.08000E+02 MM = 3.00000E-02

1.73540E-03 1.53169E-02 6.30448E-07 1.29835E-03 1.04040E-02 -2.02588E+00

7.08998E-08 8.49625E-06 4.15802E-10 7.21453E-07 3.61632E-08 -1.05882E-03

TM = 3.08000E+02 MM = 7.00000E-02

2.09583E-03 4.53480E-04 5.07906E-07 1.37775E-05 7.84965E-03 -6.03887E-02

6.68742E-08 3.19986E-06 3.79788E-10 8.80215E-09 -1.51045E-07 9.39474E-04

TM = 3.08000E+02 MM = 1.10000E-01

2.37779E-03 2.36337E-05 4.01451E-07 6.75067E-07 6.33276E-03 -1.71662E-03

5.95863E-08 1.56763E-05 3.34013E-10 4.80739E-10 -1.18234E-07 1.22286E-03

TM = 3.08000E+02 MM = 1.50000E-01

2.60783E-03 2.81015E-06 3.14320E-07 7.99066E-08 5.22290E-03 -8.96541E-05

5.91921E-08 8.41341E-05 2.87959E-10 6.26657E-11 8.61122E-07 1.00961E-02

TM = 3.22000E+02 MM = 3.00000E-02

1.74426E-03 3.16060E-02 6.35646E-07 2.16842E-03 1.03611E-02 -4.18473E+00

7.68232E-08 1.76856E-05 4.30368E-10 1.22522E-06 2.84090E-08 -2.24759E-03

TM = 3.22000E+02 MM = 7.00000E-02

2.10297E-03 9.33532E-04 5.11464E-07 1.54857E-05 7.80820E-03 -1.24321E-01

7.22816E-08 3.50501E-06 3.92678E-10 1.02998E-08 -1.67174E-07 8.99693E-04

TM = 3.22000E+02 MM = 1.10000E-01

2.38343E-03 4.86483E-05 4.04246E-07 7.22403E-07 6.29907E-03 -3.53357E-03

6.43419E-08 1.56940E-05 3.45338E-10 5.38050E-10 -1.34618E-07 1.22162E-03

TM = 3.22000E+02 MM = 1.50000E-01

2.61225E-03 5.78447E-06 3.16508E-07 8.51839E-08 5.19509E-03 -1.84546E-04

6.32920E-08 8.41365E-05 2.97721E-10 6.98953E-11 8.44724E-07 1.00961E-02

B) Adelanto Loam

Λ Λ_T Λ_θ

TM = 2.80000E+02 MM = 3.00000E-02

1.63157E-03 1.25881E-02 2.73232E-07 2.12221E-02 1.23061E-02 -5.70130E+00

1.34978E-08 6.84855E-06 1.58953E-10 1.13527E-05 8.76590E-07 -3.05252E-03

TM = 2.80000E+02 MM = 7.00000E-02

2.06389E-03 4.25623E-03 4.60041E-07 1.49182E-03 8.60051E-03 -1.75569E-01

4.58036E-08 3.56388E-06 3.20758E-10 9.01093E-07 2.14910E-07 4.48141E-07

TM = 2.80000E+02 MM = 1.10000E-01

2.36344E-03 6.44818E-04 3.87418E-07 1.17189E-04 6.50525E-03 -2.77382E-02

4.79315E-08 4.93570E-06 3.05015E-10 7.89429E-08 -8.11276E-08 2.57264E-04

TM = 2.80000E+02 MM = 1.50000E-01

2.59828E-03 2.92241E-04 3.06426E-07 4.43262E-05 5.32253E-03 1.12080E-02

4.40348E-08 4.02556E-05 2.66429E-10 3.29121E-08 -1.48129E-08 6.52807E-03

TM = 2.94000E+02 MM = 3.00000E-02

1.63553E-03 3.23266E-02 2.92006E-07 4.96103E-02 1.24564E-02 -1.47451E+01

1.58251E-08 1.76356E-05 1.73528E-10 2.68998E-05 9.76648E-07 -7.96027E-03

TM = 2.94000E+02 MM = 7.00000E-02

2.07039E-03 1.02567E-02 4.67964E-07 2.69612E-03 8.58208E-03 -4.26795E-01

5.03898E-08 7.26208E-06 3.34371E-10 1.65214E-06 2.17634E-07 -1.43970E-04

TM = 2.94000E+02 MM = 1.10000E-01

2.36890E-03 1.54145E-03 3.92320E-07 1.57440E-04 6.47486E-03 -6.63989E-02

5.22836E-08 5.55054E-06 3.16680E-10 1.07944E-07 -9.38243E-08 2.32308E-04

TM = 2.94000E+02 MM = 1.50000E-01

2.60260E-03 6.97609E-04 3.10079E-07 5.12784E-05 5.29631E-03 2.67316E-02

4.78350E-08 4.05617E-05 2.76442E-10 3.88527E-08 -2.89043E-08 6.54049E-03

TM = 3.08000E+02 MM = 3.00000E-02

1.63974E-03 7.62111E-02 3.09782E-07 1.09462E-01 1.26051E-02 -3.49849E+01

1.83569E-08 4.19824E-05 1.88154E-10 6.01702E-05 1.07904E-06 -1.91109E-02

TM = 3.08000E+02 MM = 7.00000E-02

2.07699E-03 2.28223E-02 4.74691E-07 5.07371E-03 8.56198E-03 -9.57167E-01

5.51652E-08 1.51250E-05 3.47803E-10 3.15403E-06 2.19580E-07 -4.53694E-04

TM = 3.08000E+02 MM = 1.10000E-01

2.37442E-03 3.40493E-03 3.96319E-07 2.34573E-04 6.44397E-03 -1.46851E-01

5.67979E-08 6.84793E-06 3.28203E-10 1.63804E-07 -1.07109E-07 1.79576E-04

TM = 3.08000E+02 MM = 1.50000E-01

2.60696E-03 1.53895E-03 3.13032E-07 6.39623E-05 5.26974E-03 5.89250E-02

5.17746E-08 4.12067E-05 2.86335E-10 4.96337E-08 -4.35664E-08 6.56665E-03

TM = 3.22000E+02 MM = 3.00000E-02

1.64420E-03 1.66777E-01 3.26502E-07 2.27046E-01 1.27515E-02 -7.70049E+01

2.10936E-08 9.30063E-05 2.02804E-10 1.26548E-04 1.18343E-06 -4.26200E-02

TM = 3.22000E+02 MM = 7.00000E-02

2.08368E-03 4.73756E-02 4.80257E-07 9.48342E-03 8.54035E-03 -2.00115E+00

6.01274E-08 3.07293E-05 3.61065E-10 5.98062E-06 2.20766E-07 -1.07319E-03

TM = 3.22000E+02 MM = 1.10000E-01

2.37999E-03 7.02112E-03 3.99440E-07 3.75100E-04 6.41265E-03 -3.03154E-01

6.14726E-08 9.40496E-06 3.39594E-10 2.66724E-07 -1.20974E-07 7.55175E-05

TM = 3.22000E+02 MM = 1.50000E-01

2.61136E-03 3.16962E-03 3.15303E-07 8.64760E-05 5.24289E-03 1.21275E-01

5.58519E-08 4.24763E-05 2.96115E-10 6.88912E-08 -5.87920E-08 6.61811E-03

IX. VALIDATION OF ANALYSIS AGAINST FIELD DATA

IX.1. Introduction.

The analytical method presented in the previous section is now considered for the insight it may yield into the observed phenomena of coupled diffusion in soil. Two experiments are used for this purpose: the 1968 observations of Rose [81-82] and those of Jackson in 1973 [52]. These experiments yare described. The immediate application of the approximate solution of section **VII.** is prevented by two factors present in physical diffusion which the analytical model does not accommodate. Firstly, as has been remarked above, all reported observation of soil is subsequent to highly discontinuous initial conditions. The initial phase monitors transient redistribution prior to the resumption of steady conditions. The early stages of the Jackson experiment, in particular, show a transfer from high moisture concentrations at the surface and dryer below to the reverse, which, of course, normally obtains. This redistribution, in which hydraulic conductivity rather than diffusion is the controlling agency, required a week. Day 9 has thus been selected from the observations for comparison with the analytical approach. The soil in the Rose experiment, it has been suggested, is more "regular" than that of Jackson, in the sense that the values in its associated $\mathbf{\Lambda}_T$ and $\mathbf{\Lambda}_\theta$ matrices are small in comparison to the $\mathbf{\Lambda}$ matrix. It might be expected that this soil will show less complex qualitative phenomena in diffusion. Such is the case, and the observed evolution in the Rose experiment is effectively damped, decaying sinusoids. Day 4 from these observations has been selected for comment.

The second failing of the analytical approximation lies in the inappropriate boundary conditions which it assumes. Physically observed diffusion responds to boundary conditions which are difficult to assimilate within analytical models. Indeed, there are no mathematical approaches whatsoever in the literature in which boundary conditions are realistically asserted. A sub-section is devoted to adapting the solutions originally obtained to these considerations. As depth increases, soil becomes damper as the water table is approached. The water table is imposed upon the system by the surrounding physical configuration and is extraneous to the processes modelled. The increase in mean moisture concentration was studied in early approaches by Gardiner [34] and by Philip [72-75] for isothermal conditions. These methods may be adapted to the coupled case by assuming, as is the case, that temperature evolution is little affected by the coupling from moisture. The resulting expressions for mean moisture concentration in terms of depth require numerical integration, and have been carried through by computer to yield an accurate description of the increasing profile of the means for both experiments. However, the increase in mean invalidates the assumptions of the analytical method, that expansion of the non-linear $\mathbf{\Lambda}$ matrix about a constant mean is valid. Strictly speaking, then, the analytical approximations are accurate only when the evolutions are suspended sufficiently far above

the water table for there to be no increase in mean consequent on approach to it. Such cannot be said to be the case in the present context. However, by taking the values of the mean as depth increases from the extended Gardner method, and using the mean associated with the mid-point of the depth studied to compute the matrices which occur in the analytical method, $\mathbf{\Lambda}, \boldsymbol{P}$, $\boldsymbol{P}^{-1}$, $\mathbf{\Lambda}_T$ and $\mathbf{\Lambda}_\theta$, it is found that there is close agreement between analysis, simulation, and observation. It should be remarked that the analytical method enforces agreement at the surface and when variation has decayed, and so the mean of the concentrations at the mean depth is the most critical in determining behaviour.

The boundary condition at the surface is consequent on the complicated evaporation-distillation balance which must hold in the upper region of the soil. Although theory has been developed to describe this equilibrium, it again adds factors extraneous to the agencies modelled in coupled diffusion and is difficult to assimilate analytically. Arguments will be developed to indicate that a phase shift of $\frac{5\pi}{4}$ in moisture variation against temperature variation might be expected. The abrupt increase in moisture concentration at the surface at around 3 p.m., and the abrupt decrease at around 3 a.m., is perhaps the most immediately noticeable feature of both Rose's and Jackson's studies. It is suggested that this shift is consequent on the continuity of temperature between the desert air and the soil in comparison to the discontinuity of moisture between the two media. The phase shift can be understood and quantified but without an extended examination of conditions around the soil surface it is not possible the estimate the resulting amplitude in moisture. Such an examination seems rather removed from the essential purposes of this thesis and neither of the studies carry sufficient data for it be feasible. It therefore seems permissible, for both simulation and analysis, to take the observed amplitude as an imposed boundary condition for which the resulting evolutions can be studied. This is the approach which has been used.

The various points mentioned above, together with the effects revealed by the analytical solution allow a general description of moisture diffusion in the coupled case. In all some eight qualitative factors may be catalogued which can be expected to occur as a moisture wave progresses through soil in the steady state. The analytical approaches allow these factors to be quantified. A subsection is devoted to these comments, which can be regarded as a summary of the understanding reached by the present enquiry. Some of the effects would be expected to be immediately discernible in any profile evolution and may be regarded as the salient features; others may be expected to be small and will be masked by stochastic effects brought about the non-uniformity of the medium and experimental error. The remainder of the section then shows how all the salient features are present in the observations of Rose and those of Jackson. In particular, the absence of any subharmonic development in the Rose case, and its occurrence in the Jackson experiment when moisture mean

values around 0.15 are attained is very noticeable. Graphical illustrations of the simulation of these two experiments and the analytical approximation are given and a three way validation between simulation, analysis and observation forms the subject of the closing sub-section. It is shown that to concur with observed data, both experiments require the addition of enhancement factors. If the theory is left in the simple state prior to the additional enhancement factors suggested by Philip and de Vries, then that theory seriously underpredicts moisture movement in both experiments. Rose used his data to deduce values for the enhancement factors at various soil levels. In general it was found that enhancement of at least one order of magnitude was required. The Jackson experiment included no analysis of the data in those terms, but it seems that a similar order of enhancement is equally required in this case. The material from this chapter has been summarised and submitted for publication to a relevant journal.

IX.2. Description of the Two Validating Experiments

Jackson's paper **[52]** describes two experiments; the second and more extended, which took place in March 1971, has been used for validation purposes. The site was the U.S. Water Conservation Laboratory at Phoenix, Arizona. The water characteristic and hydraulic conductivity of the soil, Adelanto loam were quoted by Jackson from field data by Brust, Van Bavel and Stirk **[10]**. The diffusion coefficients calculated from these values have, of course, been extensively analysed in section VI.2. Maximum and minimum air temperatures ranged from 17^o to 24^oC and -2^o to 5^oC, respectively. The average of the these values has been taken for simulation and analysis. The site was inundated with approximately 10 *cms.* of water prior to monitoring. Samples were taken at 0.5 hr. intervals for three separate periods representing 2-17 days, 22-24 days and 36-38 days after initial watering, for the 0 to 0.5 *cm.* layer, and in 1 *cm.* increments to $5cms.$, and in $2cm.$ increments to 9 *cms.* The measurement was performed gravimentrically. Temperature variation was recorded by thermocouple at 7 depths in the $0 - 10cm$ layer and at four further depths down to 128 *cms.* In addition, meteorological data including solar and net radiation, wind speed, air temperature and vapour pressure, was recorded. Data concerning the physical composition of the soil does not seem to have been included in the paper, and specimen values for the thermal characteristics of a loam soil have been taken from Marshall and Holmes **[64]**.

The Rose experiment took place at the CSIRO plant introduction nursery at Alice Springs in the Northern Territory, Australia. The soil was a loamy sand with percentages of sand, silt and clay of 73.5, 15.0 and 11.5 respectively. These values have been used to calculate the thermal characteristics of the soil. Water content was measured gravimentrically in 0.5 inch depths to 2 inches, and in 1 inch intervals to 6 inches. Rose used a theoretical relationship to describe the relation between hydraulic

conductivity and water content, shown to give good agreement with experimental values taken from the site. Soil temperature profiles were taken with a duplicated array of seven thermistors, fixed at the soil surface and at depths of 0.4, 1, 2, 4, 7 and 13 inches below the surface. On day 4, which will be used subsequently for analysis, temperature at the surface varied between 10^o and 50^oC. These values have been taken for the temperature mean and amplitude. The site was thoroughly watered prior to observation, and readings for temperature and moisture content continued for six days.

IX.3. Adaption of Boundary Conditions.

3.(i) The Lower Boundary Condition.

The adaption of the analytical solution to a situation in which an increase in moisture mean is imposed by the presence of a water table, or, in general, by factors present in the physical configuration in which diffusion occurs and so not assimilated in the processes modelled, will now be carried through. The method is essentially that of Gardner **[34]** for isothermal diffusion except that the analysis of orders of magnitude occurring in the diffusion coefficients given in section **VI**.2. allow the conclusion that this process is valid even in coupled diffusion. Assuming that fluctuation is approximately sinusoidal at all soil levels allows this variation to be simply described by a mean term with an additional amplitude term. However, the mean term is now assumed to vary with depth. Writing the means as $T^*(z), \theta^*(z)$, then as these means do not vary with time, they will approximately satisfy the equation

$$\begin{bmatrix} 0 \\ 0 \end{bmatrix} = \frac{d}{dz}\left\{ \begin{bmatrix} a(T^*,\theta^*) & b(T^*,\theta^*) \\ r(T^*,\theta^*) & s(T^*,\theta^*) \end{bmatrix} \frac{d}{dz} \begin{bmatrix} T^* \\ \theta^* \end{bmatrix} \right\} \tag{9.1}$$

where the boundary conditions are now

$$T^*(0) = T_S, \quad T^*(w) = T_W, \tag{9.2-3}$$

$$\theta^*(0) = \theta_S, \quad \theta^*(w) = \theta_W. \tag{9.4-5}$$

If the assumption is made that the increase in T^* is small, then the T dependencies in a and s may be approximated by constant values. The coefficient r will be too small to have effect, if the variation in T^* is also small. The only term in which such an approximation is not valid is b. However, since the temperature dependency originates mainly in the increase of ρ_o with temperature, the system may be decoupled as

$$\begin{bmatrix} 0 \\ 0 \end{bmatrix} = \frac{d}{dz}\left\{ \begin{bmatrix} a(T_S,\theta^*) & \rho_o(T^*)b_\theta(\theta^*) \\ 0 & s(T_S,\theta^*) \end{bmatrix} \frac{d}{dz} \begin{bmatrix} T^* \\ \theta^* \end{bmatrix} \right\}, \tag{9.6}$$

where $b_\theta(\theta)$ represents the remaining terms in b. The solution to the second of these equations is

$$z\,(\theta^*) \quad = \quad w \left\{ \frac{\int_{\theta_S}^{\theta^*} s(T_s, \theta')d\theta'}{\int_{\theta_S}^{\theta_W} s(T_s, \theta')d\theta'} \right\} \tag{9.7}$$

giving the depth at which a given moisture mean between θ_S and θ_W will occur. Since the upper equation is now expressible only in terms of T and z it could, theoretically, be solved by the integrating factor method. However, all studies indicate that no observable increase in T occurs and so this approach will not be pursued. Numerical integrations for equation (9.7) have been carried out for the two relevant days: day seven of the Jackson experiment and day four of the Rose experiment. The resulting profiles are given as Figs.**IX**.1-2, where depth in *cms.* is given as the x coordinate, and mean moisture concentration as the y coordinate. These predicted levels match observation closely.

3.(ii) The Upper Boundary Condition.

The following observations allow a phase retardation for moisture in relation to temperature to be ascribed to surface boundary conditions. Equally, they show that an evolution in that phase retardation must occur as the moisture wave penetrates the medium and sufficient depth is reached. For ease of exposition, this secondary effect will be considered first. It is then shown how these two additional factors may be incorporated in the analytical solution so that their implications may be quantified. The persistence of the temperature wave to a far greater depth than the moisture wave induced by isothermal moisture diffusion, as represented by the differing magnitudes of a and s, implies that at a sufficient depth moisture fluctuation will be synchronised to temperature fluctuation. In order to gain insight into the interaction of heat and moisture at the soil surface, it is instructive to consider their coupling at a depth when isothermal diffusion is assumed to be no longer present. The significance of this approach for surface conditions will become apparent as the argument proceeds. Heat flow, obviously, occurs from high heat concentration to low heat concentration, with the maximum flux occurring for the greatest temperature gradient. By the standard argument, for sinusoidal waves, the downward movement of heat occurs at a $\frac{\pi}{4}$ phase retardation with respect to temperature. Since moisture and heat are synchronised, the downward movement of moisture flux occurs in phase with heat flux: heat carries moisture with it, if no isothermal phenomenon is present. However, this downward movement of flux does not imply that the concentrations decrease. Within the translation of the wave as whole as it progresses into the medium, downward flux for heat and so for moisture occurs between the equivalent of 3.00 a.m. and 3.00 pm. For most of this period the soil is heating and so equally moisture levels are increasing. Obviously each of heat and moisture flux is constantly replenished from the levels above as it migrates downwards, leading to an increase in concentration.

If this situation is now contrasted with that obtaining at the surface, it is seen that concentration/flux relationship for heat is unaffected: downward movement of heat flux occurs between 3.00 and 15.00 hours, whilst temperature increases from 0.00 to 12.00 hours: the increasing warmth activates the downward flux. However, for moisture, in a dry desert environment, little replenishment is possible from the air above, whilst its downward migration is still enforced by the movement of heat flux. Presumably advection will be slight in these circumstances. If no source of moisture is present at the surface, so that diffusion is isothermal, the above argument leads to the conclusion that moisture concentration will be negatively synchronised to heat flux, that is $\frac{5\pi}{4}$ in retardation with respect to temperature. Minimum moisture levels would be expected to occur at 3.00 p.m., and maximum at 3.00 a.m. In studying both the Rose and Jackson data, abrupt minima and maxima do, in fact, occur at these times.

From these comments, an additional factor would be expected to be present in moisture wave form evolutions as the soil is penetrated. The moisture wave will originate $\frac{5\pi}{4}$ in retardation to temperature and evolve until it is eventually in synchronisation with it. Since isothermal diffusion has usually entirely decayed by a depth at which the phase lag for temperature evolution is not noticeable, the implication is that the maxima and minima of moisture traverse a nine hour phase lag within the medium, typically by a depth of $20cms$. From this depth onwards moisture and temperature are in phase. This evolution occurs independently of, and is superimposed on, the evolutions resulting from the balance between a and s values commented on in section **VIII**.3.(ii), and any attendant non-linear subharmonics. The analytical solution may be easily adapted to accommodate this additional factor, which reduces to adding an a phase lag term of $\frac{5\pi}{4}$ in the solution u_2 of the first harmonic.

IX.4. Qualitative Description of Moisture Wave Evolution

Bringing together the understanding gained by the analytical solution of section **VII**. as it responds to coefficients representing the variation in diffusion coefficients described in section **VI**.4., the following phenomena should be present, whether observable or not, in the evolution of a moisture wave through soil.

1. The wave should originate $\frac{5\pi}{4}$ in retardation with respect to the imposed temperature variation at the surface.

2. At a sufficient depth, when isothermal diffusion has ceased, moisture will be in phase with temperature.

3. The evolution between these two states will be controlled by the relative balance of the coefficients a and s; for large s with respect to a, the $\frac{5\pi}{4}$ retardation will persist further into the medium.

4. The effects will be subject to the normal phase lag of diffusion; a small s, implying a slow rate of penetration, will bring about a marked "cornering" phenomena in the lines of maxima or minima of moisture values as they change over from their initial slow penetration to synchronisation with the rapid penetration of temperature.

5. Superimposed upon these effects they may be non-linear perturbation by a second harmonic. The development of subharmonics is dependent on their being, simultaneously, large values of b in relation to those of a, together with large values of $\frac{\partial r}{\partial \theta}$, $\frac{\partial s}{\partial \theta}$ or $\frac{\partial s}{\partial T}$. If this is the case, assuming that the region of abrupt decay in $D_{\theta V}$ occurs at residual moisture values, so that non-linear behaviour results from the later increase of s or b as $D_{\theta l}$ takes effect, then additional phenomena will be observed. The qualitative nature of these responses are controlled by the exact balance between the a^*,b^*,c^* and d^* of section **VII**.2.(iii), and may, theoretically, be determined by close inspection of the constituent equations. Under the generality of all possible behaviours of the system, wetting and drying phases may be either retarded or accelerated, means may either increase or decrease, and these effects may all be present at different depths for the same evolution. However, considering the most relevant kinds of evolution, those in which impulsive $D_{\theta V}$ behaviour has already subsided, the second harmonic will have the following consequences:

6. There will be an acceleration of the wetting phase and retardation of the drying phase.

7. The mean of the variation will increase.

8. For some particular values, these non-linear effects may be large enough to disturb the basic sinusoidal pattern to the extent that two minima and two maxima in each cycle are observed.

IX.5. Validation of Simulation and Analysis by Field Data.

5.(i) The 1968 Experiment of Rose.

Data in the Rose paper gives the history of water content for day 4 of the experiment in three plots, namely for the layers 0-1.27$cms.$, 2.54-3.81$cms.$ and 12.7-15.2$cms.$ For each of these three depths the profile is one of a sinusoidal fluctuation superimposed upon a slow decay in mean value with time. Unfortunately, the Rose experiment did not monitor the evolution for a sufficient period for the mean at each level to stabilise and so some transient redistribution persists. Nevertheless it will be seen that the theory developed provides a good explanation of the resulting behaviour. Assuming that the amplitudes, and the mean at the mid-point of a cycle, are at least similar to those which would occur in the steady state, the three levels may be represented as: Level1: mean 0.05, amplitude 0.02; Level 2: mean 0.09, amplitude 0.01; Level 3: mean 0.14, amplitude 0.005. Further, the phase lags at the three levels, taking noon as a reference point, are: Level 1: +3 hrs; Level 2: +3.5hrs., Level 3: +5hrs. Given

the first of these levels as approximating to surface conditions, the further two should be recoverable from analysis.

Rose calculated values for $D_{\theta l}$ directly in situ and compared the values with those obtained theoretically from the ψ-θ and K-θ curves. The comparison is given as a figure in the paper. The values obtained theoretically by the present writer are rather smaller than those of Rose; however, $D_{\theta l}$ is obviously extremely sensitive to any error in reading or interpolating values from graphs. Both of the figures in the paper giving the ψ and K values are very small and calculations stemming from them cannot be regarded as reliable. For this reason, the $D_{\theta l}$ values have been taken directly from the paper rather than calculated independently.

Fig.**IX**.6(a-b) gives a surface plot and contour breakdown for the analytical prediction of evolution down to the 3 *cm.* level. For this set of plots simulation agreed closely with analysis and so only one specimen set of simulation results, for the second level, has been given. Using the principle outlined in section **IX**.3(i), the input mean was taken from Fig **IX**.1. at 1.5 *cms.* The $\mathbf{\Lambda}$ matrices were:

$\mathbf{\Lambda}$		$\mathbf{\Lambda}_T$		$\mathbf{\Lambda}_\theta$	
2.16E-3	8.56E-5	4.76E-7	3.75E-6	7.43E-3	-1.94E-2
6.21E-8	5.11E-5	3.61E-10	2.42E-9	-1.63E-7	-4.00E-4

The result obviously gives a good approximation to observed behaviour, although amplitudes are perhaps slightly underpredicted and the phase lag overpredicted. The discrepencies are probably within experimental and theoretical error, but for this level of the soil, where the means are increasing rapidly, a more probable cause is the underestimation of $D_{\theta l}$ inherent in the theoretical approach. The phenomena are confined to the first harmonic and almost entirely isothermal. For none of the Rose approximations does b reach a sufficient value to cause harmonics, even though the differential $\frac{\partial s}{\partial \theta}$ would otherwise be large enough to do so. Equally, Rose found that the calculations for ζ and ξ, the two enhancement factors detailed in the paper, resulted in unity for this layer. Simulation and analysis indicates that no enhancement is required to reproduce observation for this layer.

In contrast, superficial examination of the history for the lower layer immediately indicates that thermal agencies now have effect. A decay in amplitude from 0.15 to 0.01 in 3 *cms.* would obviously result in extinction of the behaviour at a depth of 15*cms.*, were the same agency only available for transport. Equally, Rose's calculations show that at several of the intervening layers, which were monitored but not presented graphically, enhancement greater than an order of magnitude was required. For one layer a value in excess of a hundred was required. The three sets of plots, Figs. **IX**.7(a-b), **IX**.8(a-d) and **IX**.9(a-b), give evolutions down to 15 *cms* with enhancement factors of 1, 10 and 50 respectively. In the second of these plots (c) and (d) give the simulations. It should be remarked that contouring packages can be somewhat arbitrary in the placing of contours, particularly when

ambiguous terrain with low gradients is surveyed, and the difference in contour distribution between (b), for analysis, and (d) for simulation in Fig.**IX**.8., tends to over-emphasise differences between the two. Visually, the two surfaces are effectively identical; an impression confirmed by examination of the numerical results. Only differences of the order of 0.005 are present between simulation and analysis. In addition, of course, the simulation will include some redistribution in consequence of the constant initial profile, whose transients have not entirely decayed within the first cycle.

Input means are taken at the 7.5 *cm.* level. The three matrices were:

(i) No Enhancement

Λ		Λ_T		Λ_θ	
2.55E-3	2.41E-6	3.32E-7	1.03E-7	5.48E-3	-6.64E-5
5.47E-8	4.38E-4	2.93E-10	7.80E-11	3.41E-7	5.24E-3

(ii) Enhancement = 10.0

Λ		Λ_T		Λ_θ	
3.16E-3	2.41E-5	3.32E-6	1.04E-6	1.66E-3	-6.64E-4
5.07E-7	4.38E-4	2.93E-9	7.80E-10	-1.40E-6	5.24E-3

(iii) Enhancement = 50.0

Λ		Λ_T		Λ_θ	
5.90E-3	1.20E-4	1.66E-5	5.19E-6	-1.53E-2	-3.23E-3
2.52E-6	4.38E-4	1.46E-8	3.90E-9	-9.14E-6	5.24E-3

It should be noted that in these figures, enhancement has no effect on the s coefficient, nor its moisture derivative, since $D_{\theta l}$ is the determining agency for these moisture levels. The temperature derivative, is, of course, entirely controlled by vapour diffusion. Equally, enhancement does not increase the b coefficient to a point where subharmonic behaviour is evoked. In the first of these plots it is apparent that the unenhanced thermal vapour contribution is not sufficient to produce fluctuation down to the required level. The simple theory would lead to no discernible movement below 9 *cms.* As enhancement increases, more moisture movement is induced, and amplitudes are predicted exactly with enhancement slightly larger than 10. Further increase in enhancement, as was remarked above, to a point where in the soil depths this agency becomes dominant, causes variation to be synchronised to temperature. Fig.**IX**.9(b). shows clearly the movement from the negative synchronisation with heat flux at the surface, to the positive synchronisation with temperature as diffusion proceeds. However, this

movement then causes the phase lag to be overestimated in comparison with observation. Again, the probable underestimation of $D_{\theta l}$, combined with a rather lower value for enhancement would produce exact duplication of both amplitudes and phase-lag.

5.(ii) The 1971 Experiment of Jackson.

For behaviour as complex as that of day 9 of the Jackson experiment in which there may well be stochastic elements derived from the non-uniformity of the medium, it is probably a mistaken and even a ludicrous endeavour to attempt to match analytically derived results too closely. The following comments should then be regarded as essentially qualitative in nature, in which main features of the evolutions are recovered by analysis. Simulation and analysis reproduce the basic qualitative forms observed in the Jackson data, and several factors are reproduced with quantitative accuracy. The experiment produced data for some 8 levels, although the forms of the wave for the lower four may be regarded as identical. The results may be summarised as follows: (i) level one, the surface: mean 0.06; amplitude 0.02, phase shift with respect to noon 2 *hrs.*; (ii) level 2, 1 *cm.*, mean 0.1, amplitude, 0.02, phase shift + 4 *hrs.*; (ii) level three, 3 *cms.*, mean 0.21, amplitude, 0.005, phase shift -2 *hrs.*; (iv) level 4, 7 *cms.*, mean 0.23, amplitude 0.002, no phase shift since the maxima occurred at noon. This final pattern persisted to the limit of the depth measured. However, the behaviour at all levels other than the surface was disturbed by the influence of non-sinusoidal patterns: in particular both maxima and minima show a tendency to have associated subsidiary peaks and troughs. The behaviour cannot be regarded as at all regular.

Two analytically derived figures, both with the input moisture mean taken from Fig.**IX**.2. at 3.0*cms.*, showing evolution down to 6.0*cms.* are given, the first with no enhancement factor, and the second with an enhancement factor of 10, as Figs.**IX**.11(a,b)-12(a,b). Enhancement is required to produce variation down to 6 *cms.* The following features of this plot, which accord with those of the Jackson data, can be noted. Firstly, the entrainment of the thermally induced moisture variation at the lower level is now in phase with temperature. In so far as variation in Jackson's data can be discerned at the lowest levels it is unquestionably in phase with temperature, and peaks slightly after noon. This phenomena is equally noticeable in the analytically derived results. Secondly, the decay in amplitude is predicted closely. A cross-section of the surface in Fig.**IX**.12. at five levels: the surface, 0.5, 1.0, 3.0 and 6.0 *cms.*, is given as Fig.**IX**.14(a-b). The amplitudes have decayed to 0.005 *cm.* at the 6 *cms* level; decay at the intervening levels is accurately portrayed. Thirdly, and perhaps most importantly, taken in conjunction with the Rose figures, the Adelanto loam displays a far greater prevalence to non-linear forms of response. The tendency of maxima, in particular, throughout the Jackson data, to bifurcate into double peaks is very noticeable in the field data, and occurs in analysis. A overall comparison

between simulation and analysis down to 15 *cms.* is given as Fig. **IX.** 13.(a-d). The simulations tended not to show the full detail of subharmonic development, which is often only of the order of 0.005 *cms.* and is thus difficult to detect within, typically, less then ten depth-steps. Amplitude decay, phase shift, and the transition to synchronisation with temperature at the lower depths however are accurately portrayed. It therefore seems permissible to assert that the kind of analytical model developed in section **VII.**, if incorporated with a stochastic element to recognise the non-uniformity of the medium would lead to all the features of the behaviour being reproduced in analysis.

IX.6. Summary.

The content of this section provides a demonstration of the agreement between simulation, analysis and observed behaviour of coupled diffusion in the field. The lower boundary condition has been adapted to accommodate the varying mean as depth increases, whilst the adaption of the upper condition has been shown to bring about a movement from negative synchronisation with heat flux at the surface to positive synchronisation with heat concentration in the soil depths. The former considerations allow the increasing means to be numerically evaluated; these evaluations have been shown to concur with observed moisture levels. Two validating experiments, those of Rose in 1968 and Jackson in 1971 have been described. The soil of the Rose experiment might be expected to produce relatively simple evolutions whilst that of Jackson would be more prone to subharmonic developments. Within reasonable bounds for experimental error and stochastic effects, the analytical approach developed in previous sections is shown to account for both qualitative and quantitatives feature of the behaviour.

X. THE SEMIGROUP APPROACH TO COUPLED DIFFUSION

X.1 Introduction

An underlying theme of this thesis has been the assertion that coupled diffusion in soil is remarkable for the qualitative stability it displays. Despite the involved, non-linear functional dependencies present in the diffusion coefficients, the resulting behaviour is no more complex than a perturbed exponentially decaying sinusoid; it seems that all initial profiles are drawn into this kind of evolution, and even, further, that the property is not dependent on the detailed forms of the diffusion coefficients. The present section attempts to establish this property rigorously by the use of semigroup methods. It will be seen that the techniques required lie on the boundary of this developing theory and it has not been possible to prove the opening assertion so that absolute confidence may be placed upon it. It is believed that this failure is not a consequence of weaknesses in the theory, nor in its application to the particular problem, rather that it reflects the actual nature of coupled diffusion: that there is the slight possibility, and the possibility is very slight, that under some evolutions the stability is not certain. Since the theory concerns global qualitative properties it gives no local information to locate how these putative unstable evolutions may occur. It must be said that none has been identified. However, the abstract approach implies that coupled diffusion retains an intruiging theoretical uncertainty.

Despite this failing, semigroup theory does yield much valuable information concerning coupled diffusion and allows the development of intuitive insight into its nature. Many of the properties attendant on the relative balance between the a, b, r and s coefficients of the $\mathbf{\Lambda}$ matrix are immediately obvious under this approach. It is assumed that the reader may have no detailed familiarity with the method. The required theory, which amounts to no more than application of three standard theorems, is quoted and illustrated. The initial case of constant diffusion coefficients is considered and gives an interesting application of the basic theory. This particular example does not seem to have figured anywhere in the literature; it gives valuable insight into the method, since the central theorem does not seem immediately applicable; in seeking to find the additional conditions required for application, it is found that they are precisely those needed to ensure the global stability of the system. By the use of an additional theorem, it can be shown that a property possessed by a varying quasi-linear operator at all points of its available range is transferred to all evolutions within that range. The constant properties then apply to the varying case. It is found that although the behaviour is bounded for all evolutions, the required property of contraction can only be shown for 'most' evolutions. The system fails a sufficient test for contraction under some conditions. There is no available necessary test and so the question remains open. Equally this colloquial use of the word

'most' to assert that contraction occurs for most evolutions, cannot be extended to the technical condition of 'almost all' evolutions, since if expansive, but bounded, evolutions occur, they will occur for more than a nowhere dense set of initial and boundary conditions.

X.2 Basic Semigroup Theory.

Elementary semigroup theory is set out in **[96]** and **[95]**; more advanced, in which semi-, quasi- and fully non-linear operators are considered, in **[67]** and **[61]**. The relevant theory of contractive semigroups, with occasional references to bounded semigroups, may be summarised as follows. A contractive semigroup describes properties analogous to exponential decay in a more general context. The context is a Banach space X, a normed vector space complete under its specified norm: all Cauchy convergent sequences converge to a member of the space. The semigroup, in this context the solution to a partial differential equation, under boundary and initial conditions, is normally unobtainable explicitly. It is a one parameter family of operators, $T(t)$, carrying an initial state in X through its evolution in X. The semigroup properties are then

$$\left.\begin{aligned} T(0) &= I \\ T(t_2)T(t_1) &= T(t_2+t_1) \end{aligned}\right\} \qquad (10.1)$$

I is here the identity operator. The second property is an algebraic statement of the principle of scientific determinism: that an initial state, evolved through a time t_1, then regarded as an initial state for a further evolution through a time t_2 determines the same state as a continuous evolution through time $t_1 + t_2$.

The theory concerns the relations between $T(t)$ and its generating operator A, effectively the operator in the right hand side of an evolution equation:

$$\frac{d}{dt}x(t) = Ax(t) \qquad (10.2)$$

$$x(0) = x_0 \qquad x_0 \in X \ ; \ A: X \to X. \qquad (10.3)$$

Here, $x(t)$ is the Banach space valued function of t, to which the initial state x_o is conveyed by the operators $T(t)$, the semigroup generated by A. A third operator occurs in the theory, $R(\lambda, A)$, the resolvent of A, giving the solution for x_1 in terms of x_2 , for those λ for which the solution of the following equation is uniquely defined

$$(\lambda I - A)x_1 = x_2 \ , \qquad x_1, x_2 \in X \ . \qquad (10.4)$$

The power of the method lies in the fact that the spectral properties of A induce qualitative properties in $T(t)$, which are then known to be valid even if $T(t)$ cannot be derived analytically. The result which initiated the whole theory is the Hille-Yosida theorem **[45]**:

Theorem (Hille-Yosida)

If X is a Banach space and A an operator with range and domain in X, then A is the generator of a contractive semigroup $\| T(t) \| < 1$, $\forall\ t$, if and only if,

H-Y (i) A is closed, with domain dense in X;

H-Y (ii) The resolvent set, $\rho(A)$, of A includes $\Re^+$;

H-Y(iii) $\forall \lambda \in \Re^+,\ \| R(\lambda, A) \| < \frac{1}{\lambda}$.

If the third condition is replaced by

H-Y(iv) $\forall \lambda \in \Re^+,\ \| R(\lambda, A) \| < \frac{M}{\lambda},\ M > 1 \in \Re^+,$

then the semigroup is not contractive, but bounded.

The following example, adapted from Hille[45] by specifically identifying the required topological properties, provides a clarifying instance of these ideas.

Example 1

Consider the Banach space of real numbers, under the norm of absolute value, and the operator $A = a \in \Re$ of simple multiplication. The real numbers are a valid, if degenerate, Banach space since they form a one dimensional vector space and all convergent sequences, by the defining property of real numbers, converge to a real number. Multiplication carries $\Re$ into $\Re$, is defined on the whole of X, not merely a dense subset, and is a closed operation since the multiple of a limit of a sequence is equal to the limit of the multiples of the sequence. Condition H-Y (i) applies.

The equation

$$\frac{dx}{dt} = ax, \qquad x(0) = x_0 \tag{10.5}$$

has the solution

$$x = e^{at} x_o \tag{10.6}$$

and the operator defined by

$$[T(t)]x_o = e^{at} x_o \tag{10.7}$$

evidently satisfies the semigroup properties. For H(ii) to hold

$$(\lambda - a)x_1 = x_2 \tag{10.8}$$

must have a solution for all $\lambda > 0$, which forces a to be negative. For such an a and for positive λ,

$$\| R(\lambda, A) \| = |\frac{1}{\lambda - a}| < \frac{1}{\lambda} \tag{10.9}$$

Thus all three conditions for contraction are met for a negative a, and in this instance the theorem provides actual exponential decay in T. Further, the beautiful relationship, which holds between semigroups and their resolvents,

$$R(\lambda, A) = \int_0^\infty e^{-\lambda \xi} T(\xi).d\xi \tag{10.10}$$

that the resolvent is the Laplace transform of the semigroup, is seen to be true.

Example 2

The second example is included for illustrative purposes, and to introduce an analysis required in considering coupled diffusion. If X is now a two dimensional vector space of real numbers, and $A = \Lambda$ is the operator of matrix multiplication, then analysis of the equation

$$\frac{d}{dt}\begin{bmatrix} x_1 \\ x_2 \end{bmatrix} = \Lambda \begin{bmatrix} x_1 \\ x_2 \end{bmatrix} \quad , \quad \boldsymbol{x} = \boldsymbol{x}_0 \in X \tag{10.11}$$

gives a semigroup depiction of the kind of system normally analysed by phase plane methods. It might be expected that a contractive semigroup will here correspond to a stable node or spiral. Such is the case, except that the stringent condition for a contractive semigroup demands that the property holds globally rather than locally around the node or centre. The topological requirements are again satisfied vacuously. A vector norm is provided by $\| \boldsymbol{x} \| = \sqrt{x_1^2 + x_2^2}$. A matrix norm is given by

$$\| A \| = \max_i \sum_j | a_{ij} | \ , \tag{10.12}$$

where the a_{ij} are the elements of A.

For the algebraic requirements of Hille-Yosida, if

$$(\lambda \boldsymbol{I} - \Lambda)\, \boldsymbol{x} = \widetilde{\boldsymbol{x}} \ , \qquad \boldsymbol{x}, \widetilde{\boldsymbol{x}} \in X \tag{10.13}$$

is to have a solution for all λ, $Re(\lambda) > 0$, then the real parts of both eigenvalues must be negative. If $\Lambda = \boldsymbol{P} \boldsymbol{H} \boldsymbol{P}^{-1}$, where the the standard notation is used, equation (10.11) has the solution

$$\begin{bmatrix} x_1 \\ x_2 \end{bmatrix} = \boldsymbol{P} \begin{bmatrix} C_1 e^{\eta_1 t} \\ C_2 e^{\eta_2 t} \end{bmatrix} \quad ; \quad \begin{bmatrix} C_1 \\ C_2 \end{bmatrix} = \boldsymbol{P}^{-1} \boldsymbol{x}_0 \tag{10.14}$$

and it may be verified that the semigroup defined by

$$[T(t)]\, \boldsymbol{x}_o = \boldsymbol{P} \boldsymbol{C}^T \cdot \begin{bmatrix} e^{\eta_1 t} \\ e^{\eta_2 t} \end{bmatrix} \quad ; \quad \boldsymbol{C} = \boldsymbol{P}^{-1} \boldsymbol{x}_o \tag{10.15-6}$$

satisfies the semigroup properties.

If the real parts of the η_i are negative then either a stable node or spiral is formed. However, in seeking to establish condition H-Y(iii), it is found, considering only real negative eigenvalues,

$$\begin{aligned} \| R(\lambda, \Lambda) \| &= \| (\lambda \boldsymbol{I} - \Lambda)^{-1} \| \qquad (10.17) \\ &= \| \left(\boldsymbol{P} (\lambda \boldsymbol{I} - \boldsymbol{H}) \boldsymbol{P}^{-1} \right)^{-1} \| \\ &= \| \boldsymbol{P} (\lambda \boldsymbol{I} - \boldsymbol{H})^{-1} \boldsymbol{P}^{-1} \| \\ &\leq \| \boldsymbol{P} \| \, \left| \left(\frac{1}{\lambda - \eta^*} \right) \right| \, \| \boldsymbol{P}^{-1} \| \qquad (\eta^* = max(\eta_i),\ \eta_i < 0) \\ &\leq \| \boldsymbol{P} \| \, \| \boldsymbol{P}^{-1} \| \left(\frac{1}{\lambda} \right) \qquad (10.18) \end{aligned}$$

Thus, in the general case, only H-Y(iv) applies, leading to boundedness rather than contraction since $\| \boldsymbol{P} \| \, \| \boldsymbol{P}^{-1} \| < 1$ is not true in general, e.g. $\boldsymbol{P} = \boldsymbol{I}$. For coupled diffusion it will be seen that an extra term occurs in the equivalent of (10.18) making the condition easier to resolve in favour of contraction. However, pursuing the ordinary differential equation case, in seeking to find why trajectories which evidently have a form of exponential decay do not necessarily lead to a contractive semigroup, it is instructive to consider a matrix whose phase plane is at the furthest remove from those occurring in coupled diffusion. If in equation (10.11) $\boldsymbol{\Lambda}$ is given by

$$\boldsymbol{\Lambda} = \frac{1}{3}\begin{bmatrix} -7 & 2 \\ -2 & -2 \end{bmatrix} \quad \text{then} \quad \boldsymbol{P} = \begin{bmatrix} 1 & 2 \\ 2 & 1 \end{bmatrix} \quad \text{and} \quad \boldsymbol{P}^{-1} = \frac{1}{3}\begin{bmatrix} -1 & 2 \\ 2 & -1 \end{bmatrix} \tag{10.19-21}$$

The solution is given by

$$\begin{bmatrix} x_1 \\ x_2 \end{bmatrix} = \begin{bmatrix} \frac{1}{3}(-a+2b) \\ \frac{2}{3}(-a+2b) \end{bmatrix} e^{-t} + \begin{bmatrix} \frac{2}{3}(2a-b) \\ \frac{1}{3}(2a-b) \end{bmatrix} e^{-2t} \tag{10.22}$$

where a and b are the initial values of x_1 and x_2. Thus solutions emerge from parallel to $x_2 = 2x_1$ and become asymptotic to $x_2 = \frac{x_1}{2}$. It is immediately apparent that evolutions beginning with small positive x_2 are initially expansive as part of an eventual contractive movement. Indeed for $x_2 = 0$, the solutions locally have the property, from equation (10.19) for $\boldsymbol{\Lambda}$ substituted into equation (10.11), that since $\frac{dx_2}{dx_1} = \frac{2}{7}$ the solutions are obviously increasing.

If the case is considered for which $\| \boldsymbol{P} \| \, \| \boldsymbol{P}^{-1} \| = 1$, by taking both $\boldsymbol{P}$ and $\boldsymbol{P}^{-1}$ to be identity matrices, then obviously the system uncouples and the resulting node is a star, in which, for negative eigenvalues, all trajectories are obviously stable. This degenerate case gives two independent contractive semigroups. A slight perturbation to

$$\boldsymbol{P} = \begin{bmatrix} 1 & \epsilon_1 \\ 0 & 1 \end{bmatrix} \tag{10.23}$$

leads to

$$\boldsymbol{P}^{-1} = \begin{bmatrix} 1 & -\epsilon_1 \\ 0 & 1 \end{bmatrix} \quad ; \tag{10.24}$$

and

$$\boldsymbol{\Lambda} = \begin{bmatrix} -\omega_1{}^2 & \epsilon_1(\omega_1{}^2 - \omega_2{}^2) \\ 0 & -\omega_2{}^2 \end{bmatrix} \tag{10.25}$$

where the eigenvalues are now written as $-\omega_1{}^2, -\omega_2{}^2$ to emphasise the contractive property. The stability of this system may be decided by the use of a Lyapunov function. Taking

$$V = x_1{}^2 + x_2{}^2 \tag{10.26}$$

then

$$\dot{V} = 2x_1\dot{x_1} + 2x_2\dot{x_2} \tag{10.27}$$

$$= -2\left(\omega_1{}^2x_1{}^2 - \epsilon_1(\omega_1{}^2 - \omega_2{}^2)x_1x_2 + \omega_2x_2{}^2\right) \tag{10.28}$$

which may be written as

$$\dot{V} = 2\omega_1{}^2x_2{}^2\left\{ - \left(\frac{x_1}{x_2} - \frac{\epsilon_1}{2}\left(1 - \frac{\omega_2{}^2}{\omega_1{}^2}\right)\right)^2 - \frac{\omega_2{}^2}{\omega_1{}^2} + \frac{\epsilon_1{}^2}{4}\left(1 - \frac{\omega_2{}^2}{\omega_1{}^2}\right)^2\right\} \tag{10.29}$$

It is now apparent that no matter how small the value of ϵ_1, x_i and ω_i pairings may be found such that $\dot{V}$ is not negative definite. If $\omega_2{}^2$ is taken sufficiently small in relation to $\omega_1{}^2$, the final two terms will together be positive; an initial value sufficiently close to the line

$$x_2 = \frac{2x_1}{\epsilon_1}\frac{\omega_1{}^2}{\omega_1{}^2 - \omega_2{}^2} \tag{10.30}$$

will then give a positive $\dot{V}$, and $\boldsymbol{x}$ will move initially outwards from the point and thus increase initially in the Euclidean norm. However, if the ω_i are specified, then only for an ϵ_1 satisfying

$$\epsilon_1{}^2 > \frac{4\,\omega_1{}^2\omega_2{}^2}{\left(\omega_1{}^2 - \omega_2{}^2\right)^2} \tag{10.31}$$

will the system necessarily produce a departure from globally contractive behaviour. $\| \boldsymbol{P} \| \, \| \boldsymbol{P}^{-1} \|$ is, of course, greater than unity for the system (10.25) and so the procedure of finding a bound for the norm of $\| (\lambda \boldsymbol{I} - \boldsymbol{\Lambda})^{-1} \|$ in terms of the norm of $\boldsymbol{P}$ and its inverse only provides a sufficient test for contraction. The bulk of evolutions in coupled diffusion pass this sufficient test; but the above analysis indicates that failure is not decisive.

X.3. Semigroup Derivation under Neumann Conditions.

Before proceeding to a semigroup analysis of coupled diffusion for both the linear and non-linear cases, it is helpful to see how the theory may be used to simplify the derivation of an earlier result. Section **IV**.3. gave a description of coupled flow for n variables diffusing under constant coefficients for conditions of Neumann input. It was seen that each variable behaved as a composition of n^2 component waves, whose relative weighting was described by an n x n^2 matrix. A involved piece

of matrix manipulation was required to establish this result. The notation of semigroup theory may be used to give a more economical derivation. In strict terms, the derivation does not use semigroup theory proper, merely its notation, since the solution is not constructed for an arbitary initial state, but for the particular initial state associated with periodic behaviour.

It was shown in section IV.3. that the n x n matrix, now denoted by χ_p, formed from the sequence of pth. columns of the matrix $\boldsymbol{L}$, defined as above, is given by equation (4.50)

$$\chi_p = \frac{\prod_{j \neq p} (\Lambda - \eta_j \boldsymbol{I})}{\prod_{j \neq p} (\eta_p - \eta_j)} \quad .$$

An important idea in the theory of Banach algebras is that of the "resolution of the identity". For the algebra of n x n matrices, this notion becomes the spectral decomposition of the matrix, carried through as follows. Associate with an n x n matrix, n matrices Λ_i defined by

$$\Lambda_i = \boldsymbol{P}\, \boldsymbol{H}_i\, \boldsymbol{P}^{-1} \,, \tag{10.32}$$

where $\boldsymbol{H}_i$ is a null matrix other than for ith. eigenvalue in the (i,i)th. position. The Λ_i then generate a commutative ring with identity under the composition properties,

$$\left.\begin{aligned} &\text{(i)} \quad \Lambda_i \Lambda_j = \delta_{ij} \eta_i \Lambda_i \\ &\text{(ii)} \quad \sum_i \Lambda_i = \Lambda \\ &\text{(iii)} \quad \sum_i \frac{\Lambda_i}{\eta_i} = \boldsymbol{I} \end{aligned}\right\} \tag{10.33-35}$$

and by iteration of (i),

$$\text{(iv)} \quad \Lambda_i^{\,n} = \eta_i^{\,n-1} \Lambda_i \,. \tag{10.36}$$

The expression (4.50) may now be recast in terms of the matrices Λ_i . Taking

$$\chi_p = \frac{\prod_{j \neq p} (\Lambda - \eta_j \boldsymbol{I})}{\prod_{j \neq p} (\eta_p - \eta_j)}$$

and substituting in the numerator for Λ by (ii), and for $\boldsymbol{I}$ by (iii) gives

$$\chi_p \;=\; \frac{\displaystyle\prod_{j\neq p}\left\{\sum_{i=1}^{n}\left(1-\frac{\eta_j}{\eta_i}\right)\Lambda_i\right\}}{\displaystyle\prod_{j\neq p}(\eta_p-\eta_j)} \;. \tag{10.37}$$

Since the Λ_i are orthogonal, interchanging the product and summation in the numerator results in

$$\chi_p \;=\; \frac{\displaystyle\sum_{i=1}^{n}\left\{\prod_{j\neq p}\left(1-\frac{\eta_j}{\eta_i}\right)\Lambda_i\right\}}{\displaystyle\prod_{j\neq p}(\eta_p-\eta_j)} \;. \tag{10.38}$$

For each value of i, the product term in the numerator includes a zero, other than when $i = p$, and so

$$\chi_p = \frac{\displaystyle\prod_{j\neq p}\left(1-\frac{\eta_j}{\eta_p}\right)\Lambda_p}{\displaystyle\prod_{j\neq p}(\eta_p-\eta_j)} \;=\; \frac{\displaystyle\prod_{j\neq p}(\eta_p-\eta_j)\,\frac{\Lambda_p}{\eta_p}}{\displaystyle\prod_{j\neq p}(\eta_p-\eta_j)} \;=\; \frac{{\Lambda_p}^{n-1}}{{\eta_p}^{n-1}} \;. \tag{10.39}$$

It then follows that

$$\chi_p \;=\; \frac{\Lambda_p}{\eta_p} \;. \tag{10.40}$$

The last identity is a consequence of property (iv) above. An illustration of the formation of the $\boldsymbol{L}$ matrix using this representation is given at the close of the current sub-section. It is now shown that expressions of the form (10.40) arise naturally in the solution of evolution equations under Neumann conditions.

It is required to solve the equation

$$\dot{y} = \Lambda\, y'' \tag{10.41}$$

under the boundary condition

$$\Lambda y'\big|_{z=0} \;=\; \Re\left\{\boldsymbol{J}e^{i\omega t}\right\}, \tag{10.42}$$

where y is a vector of functions, each individually $R^2 \rightarrow R$, and $\boldsymbol{J}$ is the flux density vector of section IV.3. The appropriate general solution to (10.41) is

$$y \;=\; \Re\left\{\left(e^{\sqrt{i\omega}\;z\Lambda^{-\frac{1}{2}}}y_0\right)e^{i\omega t}\right\}. \tag{10.43}$$

where y_0 is a constant vector. Although the expression (10.43) bears obvious affinities with semigroup

representations, it cannot strictly be regarded as a semigroup for y in terms of t, since the initial state is not arbitrary if (10.42) is to be simultaneously satisfied, which leads, as will be shown, to a predetermination of y_0. Differentiating (10.42) gives

$$y'|_{z=0} = \Re\left\{ \left(\sqrt{i\omega}\boldsymbol{\Lambda}^{-\frac{1}{2}}\right) y_0\, e^{i\omega t} \right\} \tag{10.44}$$

and asserting the boundary condition, it follows that

$$y_0 = (i\omega)^{-\frac{1}{2}}\ \boldsymbol{\Lambda}^{-\frac{1}{2}}\ \boldsymbol{J}\ . \tag{10.45}$$

The solution is then

$$y = \Re\left\{ e^{\sqrt{i\omega}z\boldsymbol{\Lambda}^{-\frac{1}{2}}} (i\omega)^{-\frac{1}{2}}\boldsymbol{\Lambda}^{-\frac{1}{2}}\boldsymbol{J}\ e^{i\omega t} \right\}\ . \tag{10.46}$$

This solution may now be manipulated to show its identity with that derived in section **IV**.3. (Equation 4.23). Since

$$\boldsymbol{\Lambda}^{-\frac{n}{2}} = \boldsymbol{P}^{-1}\boldsymbol{H}^{-\frac{n}{2}}\boldsymbol{P}\ , \tag{10.47}$$

expanding the exponential term in (10.46) and substituting for $\boldsymbol{\Lambda}^{-\frac{n}{2}}$ from (10.47) gives

$$y = \Re\left\{ (i\omega)^{-\frac{1}{2}} \left(\sum_{n=0}^{\infty} \frac{(i\omega)^{\frac{n}{2}} z^n}{n!}\, \boldsymbol{P}^{-1}\boldsymbol{H}^{-\frac{n}{2}}\boldsymbol{P} \right) \boldsymbol{P}^{-1}\boldsymbol{H}^{-\frac{1}{2}}\ \boldsymbol{P}\ \boldsymbol{J} \right\} \tag{10.48}$$

$$= \Re\left\{ \boldsymbol{P}^{-1} \left((i\omega)^{-\frac{1}{2}} \left\{ \sum_{n=0}^{\infty} \frac{(i\omega)^{\frac{n}{2}} z^n}{n!}\, \boldsymbol{H}^{-\frac{n}{2}} \right\} \boldsymbol{H}^{-\frac{1}{2}} \right) \boldsymbol{P}\ \boldsymbol{J} \right\}\ . \tag{10.49}$$

The round bracket is now seen to be the matrix $\boldsymbol{A}$ given by

$$\boldsymbol{A} = diag\left(\frac{1}{\sqrt{\eta_i \omega}}\, e^{\sqrt{\frac{i\omega}{\eta_i}}z - \frac{i\pi}{4}} \right), \tag{10.50}$$

which occurred when the solution was given in the form $\boldsymbol{P}^{-1}\ \boldsymbol{A}\ \boldsymbol{P}\ \boldsymbol{J}$. Reconstituting this expression in the form $\boldsymbol{LF}$, where $\boldsymbol{L}$ is formed from the set of matrices $\boldsymbol{\chi}_p$, namely the sequence of columns

$$\{p\ ,\ p+n\ ,\ p+2n\ ,\ \ .\ .\ .\ \ ,p+n^2-n\}$$

of $\boldsymbol{L}$ being the columns of $\boldsymbol{\chi}_p$, and if $\boldsymbol{F}$ is as defined above as equation (4.29), composed of the

elements $\{a_n\}$ of $\boldsymbol{A}$, then

$$\boldsymbol{LF} = \sum_{p=1}^{n} a_p \boldsymbol{\chi}_p \quad , \tag{10.51}$$

and since,

$$\boldsymbol{P}^{-1}\boldsymbol{A}\boldsymbol{P} = \boldsymbol{LF} \tag{10.52}$$

it follows that, since $\boldsymbol{A}$ is diagonal,

$$\boldsymbol{I} = \boldsymbol{P}\Big(\sum_{p} \boldsymbol{\chi}_p\Big)\boldsymbol{P}^{-1} \tag{10.53}$$

giving finally

$$\boldsymbol{\chi}_p = \frac{\boldsymbol{\Lambda}_p}{\eta_p} \tag{10.54}$$

by the property ((10.35 (iii)) above.

X.4. Alternative Derivation of the *LF* Matrices Using Spectral Decomposition.

In the approach of the previous section to the formation of the $\boldsymbol{LF}$ matrices it was shown that the matrices $\boldsymbol{\chi}_i$ may be written as

$$\boldsymbol{\chi}_i = \frac{\boldsymbol{\Lambda}_i}{\eta_i} = \frac{1}{\eta_i}\left(\boldsymbol{P}\boldsymbol{H}_i\boldsymbol{P}^{-1}\right). \tag{10.55}$$

This method will now be illustrated for the same numerical $\boldsymbol{\Lambda}$ as that of section **IV**.3.

For $\boldsymbol{\Lambda}$ given by

$$\boldsymbol{\Lambda} = \begin{bmatrix} 4 & 0 & 1 \\ -2 & 1 & 0 \\ -2 & 0 & 1 \end{bmatrix}, \tag{10.56}$$

the eigenvalues are $\eta_1 = 1$, $\eta_2 = 2$ and $\eta_3 = 3$, whilst

$$\boldsymbol{P} = \begin{bmatrix} 0 & -\frac{1}{2} & -1 \\ 1 & 1 & 1 \\ 0 & 1 & 1 \end{bmatrix} \tag{10.57}$$

and

$$\boldsymbol{P}^{-1} = \begin{bmatrix} 0 & 1 & -1 \\ 2 & 0 & 2 \\ -2 & 0 & -1 \end{bmatrix}. \tag{10.58}$$

The expressions for the χ_i are then

$$\chi_1 = \begin{bmatrix} 0 & -\frac{1}{2} & -1 \\ 1 & 1 & 1 \\ 0 & 1 & 1 \end{bmatrix} \begin{bmatrix} 1 & 0 & 0 \\ 0 & 0 & 0 \\ 0 & 0 & 0 \end{bmatrix} \begin{bmatrix} 0 & 1 & -1 \\ 2 & 0 & 2 \\ -2 & 0 & -1 \end{bmatrix}$$

$$= \begin{bmatrix} 0 & 0 & 0 \\ 0 & 1 & -1 \\ 0 & 0 & 0 \end{bmatrix} \tag{10.59}$$

$$\chi_2 = \frac{1}{2}\left\{ \begin{bmatrix} 0 & -\frac{1}{2} & -1 \\ 1 & 1 & 1 \\ 0 & 1 & 1 \end{bmatrix} \begin{bmatrix} 0 & 0 & 0 \\ 0 & 2 & 0 \\ 0 & 0 & 0 \end{bmatrix} \begin{bmatrix} 0 & 1 & -1 \\ 2 & 0 & 2 \\ -2 & 0 & -1 \end{bmatrix} \right\}$$

$$= \begin{bmatrix} -1 & 0 & -1 \\ 2 & 0 & 2 \\ -2 & 0 & 2 \end{bmatrix} \tag{10.60}$$

$$\chi_3 = \frac{1}{3}\left\{ \begin{bmatrix} 0 & -\frac{1}{2} & -1 \\ 1 & 1 & 1 \\ 0 & 1 & 1 \end{bmatrix} \begin{bmatrix} 0 & 0 & 0 \\ 0 & 0 & 0 \\ 0 & 0 & 3 \end{bmatrix} \begin{bmatrix} 0 & 1 & -1 \\ 2 & 0 & 2 \\ -2 & 0 & -1 \end{bmatrix} \right\}$$

$$= \begin{bmatrix} 2 & 0 & 1 \\ -2 & 0 & -1 \\ -2 & 0 & -1 \end{bmatrix} \tag{10.61}$$

These matrices are seen to agree with those derived previously.

X.5. Semigroup Properties of Linear Coupled Diffusion.

5.(i) Contractive Properties.

Turning now to the use of semigroup theory proper, considering initially coupled diffusion under constant coefficients, the system may be described as

$$\left.\begin{aligned} \frac{\partial}{\partial t}\boldsymbol{u} &= \frac{\partial^2}{\partial z^2}\,\boldsymbol{\Lambda}\,\boldsymbol{u} \\ \boldsymbol{u}(0,z), \boldsymbol{u}(t,0) &\in X \end{aligned}\right\} \tag{10.62}$$

where $\boldsymbol{\Lambda}$ is a matrix of positive elements, normed as before, and X is the Banach space of vectors of bounded, twice differentiable functions, each $R^2 \rightarrow R$, normed in any suitable fashion, say the supremum of the individual components, over z and t. This norm only recognises as convergent those sequences which are uniformly convergent, implying that such sequences converge to a continuous function and the space is complete.

Defining $\boldsymbol{v} = \boldsymbol{P}^{-1}\boldsymbol{u}$, where $\boldsymbol{P}$ is the matrix of eigenvectors of $\boldsymbol{\Lambda}$, then the eigenvalue properties of $\boldsymbol{\Lambda}$ imply that $\boldsymbol{v} \in X$. Define further operators $\mathfrak{H} = \frac{\partial^2}{\partial z^2}\boldsymbol{H}$, and $\mathfrak{H}_n = \frac{\partial^2}{\partial z^2}\boldsymbol{H}_n$, where $\boldsymbol{H}$ is the eigenvalue matrix of $\boldsymbol{\Lambda}$, and $\boldsymbol{H}_n$ is a null matrix other than the $nth.$ eigenvalue in the $(n,n)th.$ place. The system can then be written in uncoupled form as

$$\left.\begin{aligned} \frac{d}{dt}v_n &= \mathfrak{H}_n v_n \\ \boldsymbol{v}(0,z) = \boldsymbol{P}^{-1}\boldsymbol{u}(0,z), \boldsymbol{v}(t,0) &= \boldsymbol{P}^{-1}\boldsymbol{u}(t,0) \in X \end{aligned}\right\} \tag{10.63}$$

Differential operators are unbounded but closed, and since the differentiable Weierstrass approximation polynomials are dense in X, condition H-Y (i) is met. For the spectral properties of the operators $\mathfrak{H}_n$, consider the equations

$$\left.\begin{aligned} (\lambda - \mathfrak{H}_n)v_n &= g_n \\ \boldsymbol{g}(z) = \boldsymbol{P}^{-1}\boldsymbol{u}(t,0) &\in X \end{aligned}\right\} \tag{10.64}$$

For $\lambda > 0$, writing $\lambda = \omega^2$, the theory of Green's functions gives the solution to (10.64) as

$$v_n = \int_0^\infty \frac{1}{2\omega}\left\{ e^{-\frac{\omega}{\sqrt{\eta_n}}|\,z-z'\,|} - e^{-\frac{\omega}{\sqrt{\eta_n}}(z+z')} \right\} g_n(z').dz' \tag{10.65}$$

Since ω may be taken real and positive and $\sqrt{\eta_n}$ is real by the properties of $\boldsymbol{\Lambda}$ discussed in section VII.3. and may be taken positive for decaying waves, $v_n \in X$, and so $\lambda > 0$ lies in the resolvent set of

each $\mathfrak{H}_n$. Condition H-Y (ii) is met.

Further,

$$\| \boldsymbol{u} \| \leq \| \boldsymbol{P} \| \, \| \boldsymbol{v} \|$$

$$\leq \| \boldsymbol{P} \| \left| \frac{1}{2\omega} \left\{ \int_0^z e^{-\frac{\omega}{\sqrt{\eta_n}}(z-z')} .dz' + \int_z^\infty e^{-\frac{\omega}{\sqrt{\eta_n}}(z'-z)} .dz' + \int_0^\infty e^{-\frac{\omega}{\sqrt{\eta_n}}(z+z')} .dz' \right\} \right| \| \boldsymbol{P}^{-1} \| \, \| \boldsymbol{g} \|$$

$$= \| \boldsymbol{P} \| \left| \frac{\sqrt{\eta_n}}{2\omega^2} \left\{ 1 - e^{-\frac{\omega}{\sqrt{\eta_n}}z} + 1 + e^{-\frac{\omega}{\sqrt{\eta_n}}z} \right\} \right| \| \boldsymbol{P}^{-1} \| \, \| \boldsymbol{g} \|$$

$$= \| \boldsymbol{P} \| \, \| \boldsymbol{P}^{-1} \| \left| \frac{\sqrt{\eta_n}}{\lambda} \right| \| \boldsymbol{g} \| \qquad (10.66)$$

where the maxima are taken over the η_n in the last three expressions. The above argument is adapted to one-dimensional coupled diffusion from Pazy **[68]**, where it is applied to the wave equation in one variable for n dimensional waves. Thus,

$$\| R(\lambda, \mathfrak{H}) \| \leq \max_n \left\{ \| \boldsymbol{P} \| \, \| \boldsymbol{P}^{-1} \| \, | \sqrt{\eta_n} | \right\} \frac{1}{\lambda} \qquad (10.67)$$

given the expressions for $\boldsymbol{P}$ and $\boldsymbol{P}^{-1}$ in **VII**.3.(i) and the eigenvalues which occur for the $\boldsymbol{\Lambda}$ matrix, it is immediately apparent, by the Hille-Yosida theorem, that for "most" evolutions in the constant case, the resulting semigroup will be contractive. The condition that

$$\| \boldsymbol{P} \| \, \| \boldsymbol{P}^{-1} \| \, | \sqrt{\eta_n} | < 1 \qquad (10.68)$$

will be examined further below. However, the present argument may be continued to show that the semigroup is in fact analytic.

5.(ii) Analytic Properties.

Again the underlying argument is from Pazy **[68]**. A theorem of Hille**[45]** may be quoted as follows.

Theorem (Hille)

$T(t)$ can be extended to an analytical semigroup in a sector $\Delta_\delta = \{z: \, | \, arg z \, | \, < \delta\}$ if and only if $\exists \, \delta, 0 < \delta < \frac{\pi}{2}, M > 0$, such that

H(i) $\rho(\boldsymbol{A}) \in \Sigma = \{\lambda: \, | \, arg \lambda \, | \, < \frac{\pi}{2} + \delta\} \cup 0$

H(ii) $\| R(\lambda, \boldsymbol{A}) \| < \frac{M}{| \lambda |}, \lambda \in \Sigma, \lambda \neq 0$

For the analytic properties, if λ is now considered as complex, then the above argument to equation (10.66) may be retained, with the absolute value bars now representing moduli. Writing

$$\omega = |\omega|(cos\theta + isin\theta) \tag{10.69}$$

where θ is the argument of ω, equation (10.66) may be adapted to read

$$\| \boldsymbol{u} \| \leq \| \boldsymbol{P} \| \left\{ \frac{1}{2|\omega|}(I_1 + I_2 + I_3) \right\} \| \boldsymbol{P}^{-1} \| \, \| \boldsymbol{g} \| \tag{10.70}$$

where the I_i are the integrals

$$I_1 = \int_0^z e^{-\frac{|\omega| cos\theta}{|\sqrt{\eta_n}|}(z - z')} .dz' \tag{10.71}$$

$$I_2 = \int_z^\infty e^{-\frac{|\omega| cos\theta}{|\sqrt{\eta_n}|}(z' - z)} .dz' \tag{10.72}$$

$$I_3 = \int_0^\infty e^{-\frac{|\omega| cos\theta}{|\sqrt{\eta_n}|}(z + z')} .dz' \tag{10.73}$$

Evaluating these integrals it is found, again taking the maximum of the η_n, that

$$\| \boldsymbol{u} \| \leq \| \boldsymbol{P} \| \frac{\sqrt{|\eta_n|}}{|\omega|^2 cos\theta} \| \boldsymbol{P}^{-1} \| \, \| \boldsymbol{g} \| = \| \boldsymbol{P} \| \frac{\sqrt{|\eta_n|}}{|\lambda| cos(arg\frac{\lambda}{2})} \| \boldsymbol{P}^{-1} \| \, \| \boldsymbol{g} \| \tag{10.74}$$

and so,

$$\| R(\lambda, \mathfrak{H}) \| \leq \left\{ \| \boldsymbol{P} \| \frac{\sqrt{|\eta_n|}}{cos(arg\frac{\lambda}{2})} \| \boldsymbol{P}^{-1} \| \right\} \frac{1}{|\lambda|} \tag{10.75}$$

Thus for $0 < |arg\lambda| < \pi$, the above inequality supplies a positive M defined by

$$M = \frac{\sqrt{|\eta_n|}}{cos(arg\frac{\lambda}{2})} \| \boldsymbol{P} \| \, \| \boldsymbol{P}^{-1} \| < \infty , \tag{10.76}$$

establishing that the semigroup is analytic by the Hille criteria.

X.6. Extension to the Quasi-Linear Case.

X.6.(i). Introduction.

The relatively simple context discussed above, for $\boldsymbol{A}$ constant, is now extended to the system

$$\left.\begin{aligned} &\frac{du(t)}{dt} + \boldsymbol{A}(t,u)u = 0 \\ &u(0) = u_0 \quad u, u_0 \in \boldsymbol{X}, \end{aligned}\right\} \tag{10.77}$$

in which $\boldsymbol{A}$ is a varying operator function both of time and the dependent variable, u. The approach follows work essentially by Kato **[55(a)]**. It will be seen that a far more elaborate technical framework is required to convey the properties of such a generally posed system. Much of the resulting theory is concerned with establishing preliminary conditions required for the existence and uniqueness of solutions. In contrast, the present enquiry seeks qualitative information about the solutions, in particular their properties of boundedness and contraction. The applicable content needs to be extracted from the pure mathematical character of the relevant proofs. By choosing a sufficiently specialised Banach space, namely assuming that all functions are infinitely differentiable, it is possible to ensure that preliminary conditions are satisfied automatically. Since the proofs are constructive, their qualitative content remains valid. There seems value in retaining initially the full generality of the pure mathematical results, even if the subsequent choice of the Banach space renders much of its complexity redundant. The following terminology is required for the statement of proofs.

Mild Solutions.

In the initial survey of semigroup theory presented above it was stated that a semigroup $\boldsymbol{T}(t)$, generated by an infinitesimal generator $\boldsymbol{A}$, applied to u_0, provides the solution to the differential equation

$$\frac{du}{dt} = \boldsymbol{A}u, \qquad u(0) = u_0. \tag{10.78}$$

However, if u_0 does not belong to the domain of $\boldsymbol{A}$, then the right hand side of the equation has no meaning at the initial condition. Nevertheless, $\boldsymbol{T}(t)u_0$ may itself be defined, (in fact, the abstract theory guarantees it is defined) and can be regarded as a solution, termed the mild solution. As an illustration, consider the semigroup,

$$[\boldsymbol{T}(t)]u(\xi) = u(t+\xi)\ . \tag{10.79}$$

If u is infinitely differentiable, then the infinitesimal generator is the differentiation operator, since then

$$[e^{t\boldsymbol{A}}]u(\xi) = \left[\sum_{n=0}^{\infty} \frac{t^n \boldsymbol{A}^n}{n!}\right] u(\xi) = \sum_{n=0}^{\infty} \frac{t^n}{n!} \frac{d^n u(\xi)}{d\xi^n} \;=\; u(\xi + t) \tag{10.80}$$

by the Taylor expansion. However, if u is merely say continuous, then the differential equation

$$\frac{\partial x}{\partial t} = \frac{\partial x}{\partial \xi}\,, \quad x(0,\xi) = u(\xi) \tag{10.81}$$

has no meaning at the initial condition. However, the function $x = u(\xi + t)$ is defined and can be taken to be a mild solution. Mild solutions may be regarded as the "natural" form of generalised solution provided by semigroup theory. They provide an interim position between classical, i.e. sufficiently differentiable solutions, and weak, or distributional solutions. Standard theory (Pazy[67]) shows that all mild solutions are weak solutions, and mild solutions given by analytical or differentiable semigroups are classical solutions. Much of contemporary theory is concerned with establishing additional conditions required for a mild solution in fact to be a classical solution.

Evolution Systems

Kato's results concerning the system (10.77) assume a time dependency in the operator in addition to that given by its dependence on u. Obviously, for coupled diffusion in soil, other than a situation such as, say, a soil in the process of erosion, the time dependency of the diffusive mechanisms is totally accounted for by variation in the dependent variables. Thus Kato's results provide a greater generality than is required in the present context. The theoretical framework, when specialised by the removal of time dependence, becomes more tractible. However, for statement of the general results, the following terminology is required.

An evolution system $\boldsymbol{U}(t,s)$ is a two parameter family of bounded linear operators provided the following three conditions are met

$$\left.\begin{array}{rl} \text{(i)} & \boldsymbol{U}(s,s) = \boldsymbol{I}; \\ \text{(ii)} & \boldsymbol{U}(t,r)\boldsymbol{U}(r,s) = \boldsymbol{U}(t,s); \\ \text{(iii)} & (t,s) \to \boldsymbol{U}(t,s) \text{ is strongly continuous.} \end{array}\right\} \tag{10.82}$$

Evolution systems provide the setting for study of the equation

$$\left.\begin{array}{c} \dfrac{du(t)}{dt} = \boldsymbol{A}(t)u(t) \\ u(s) = x \end{array}\right\}. \tag{10.83}$$

In general no simple conditions can be stated to guarantee the existence of a solution to (10.82), whether mild or classical. However, if a solution exists, then it is given by

$$u(t) = \boldsymbol{U}(t,s)x \tag{10.84}$$

where $\boldsymbol{U}$ is the evolution system generated by (10.83). However, any evolution system can be reduced to a semigroup $\boldsymbol{T}(t)$ by means of

$$\boldsymbol{T}(t-s) = \boldsymbol{U}(t,\mathrm{s})\,. \tag{10.85}$$

It is immediate that any U satisfying (10.82, i-iii) will give rise to a T satisfying the semigroup properties (10.1). Such a $T(t-s)$ will only provide solutions to (10.83) if the time dependency of $\boldsymbol{A}$ is

constant: equation (10.85) expresses the idea that the evolution system then only depends on the elapsed time since the initial condition. The reduction (10.85) will allow complicated results from the theory of equation (10.83) to be simplified.

The following three definitions, of stability, invariant subspaces and admissible subspaces are required in the theory to be developed.

Stability

A family $\{\boldsymbol{A}(t)\}$ of infinitesimal generators is called stable if there are constants $M \geq 1$, and ω, termed stability constants, such that

(i) $\rho(\boldsymbol{A}(t)) \supset (\omega, \infty]$

(ii) $\left\| \prod_{j=1}^{k} R(\lambda: \boldsymbol{A}(t_j)) \right\| \leq M(\lambda - \omega)^{-k}$ for every finite sequence $0 \leq t_1 \leq t_2 \ldots \leq t_k$.

It is immediate, (Pazy[67]), by the Hille-Yosida theorem, that a family of infinitesimal generators of contractive semigroups satisfies (i) and (ii) with stability constants $M = 1, \omega = 0$.

Invariant Subspaces.

If X is a Banach space, Y a subspace of X, and $\boldsymbol{S}: D(\boldsymbol{S}) \subset X \to X$, is a linear operator in X, then the subspace Y is an invariant subspace if $\boldsymbol{S}: D(\boldsymbol{S}) \cap Y \to Y$.

In the sequel it will be seen that it is possible, if X is taken to be functions infinitely differentiable, to choose $Y = X$, ensuring that the whole space is invariant.

Admissible Subspaces

If $\boldsymbol{T}(t)$ is a semigroup on X, with $\boldsymbol{A}$ its infinitesimal generator, a subspace Y of X is termed $\boldsymbol{A}$-admissible if it is an invariant subspace of $\boldsymbol{T}(t)$ and the restriction of $\boldsymbol{T}(t)$ to Y is a semigroup in Y.

Again, if Y may be identified with X, then Y is automatically $\boldsymbol{A}$-admissible.

X. 6. (ii). The Abstract Results.

Kato provides conditions that the system given above as (10.77)

$$\left.\begin{aligned} &\frac{du(t)}{dt} + \boldsymbol{A}(t,u)u = 0 \\ &u(0) = u_0 \quad u_0 \in \boldsymbol{X}, \end{aligned}\right\},$$

should have a mild solution. The present section will set out these conditions, and extract from the three theorems by which the result is established qualitative information concerning the solution which results as a side-effect of the constructive nature of the proofs. The following section will show that the

conditions of the theorem are met by coupled diffusion, and that if differentiability conditions are assumed the mild solution is, in fact, a classical solution.

The manner of Kato's proof is as follows. It is shown that under the conditions given below as K(i)-(iii) the system

$$\left.\begin{aligned} \frac{du(t)}{dt} + \boldsymbol{A}(t,u)v = 0 \\ v(0) = u_0 \quad v,\ u,\ u_0 \in \boldsymbol{X}, \end{aligned}\right\}, \tag{10.82}$$

has a mild solution. If such is the case it defines a mapping

$$v \rightarrow u = F(u) \tag{10.83}$$

of the space of continuous X-valued functions into itself. If then a further condition, given as K(iv) below, is satisfied, the mapping acts as a Banach contraction, whose fixed point provides a solution to the original system (10.77).

The framework for the required conditions is as follows: X and Y are Banach spaces such that: Y is densely and continuously embedded in X, and $B \subset X$ is a subset of X such that for some T, and $t \leq T$, every $(t,b) \in [0,T]$ x B implies $A(t,b)$ is the infinitesimal generator of a semigroup $S_{t,b}(s)$ on X. The conditions are:

K(i) The family $\{\boldsymbol{A}(t,b)\}$, $(t,b) \in [0,T]$ x B is stable;

K(ii) Y is $\boldsymbol{A}(t,b)$-admissible for $(t,b) \in [0,T]$ x B;

K(iii) For $(t,b) \in [0,T]$ x B, $D(A(t,b)) \supset Y$, $\boldsymbol{A}(t,b)$ is a bounded linear operator from Y to X, and $t \rightarrow \boldsymbol{A}(t,b)$ is continuous in the $B(Y,X)$ norm, $\| \ \|_{Y \rightarrow X}$, for every $b \in B$;

K(iv) There is a constant L such that $\left\| \boldsymbol{A}(t,b_1) - \boldsymbol{A}(t,b_2) \right\|_{Y \rightarrow X} \leq L \left\| b_1 - b_2 \right\|$.

The three theorems by which the properties of (10.77) are established are now quoted. Comment on their reduction for application to coupled diffusion, under the three additional properties that the diffusion operators are time-independent; that the semi-group families occurring in the proofs are all contractive; and that the underlying Banach space will be assumed to have sufficient differentiability properties will be deferred until the following sub-section. The first theorem assures the existence of an evolution system for (10.82).

Theorem A (Kato)

Let $B \subset X$ and let $\{\boldsymbol{A}(t,b)\}, (t,b) \in [0,T]$ x B be a family of operators satisfying the conditions K1-3. If $u \in C([0,T]: X)$ has values in B then there is a unique evolution system $U_u(t,s)$ in X satisfying

$$\text{(i)} \qquad \left\| \boldsymbol{U}_u(t,s) \right\| \leq M e^{\omega(t-s)}; \tag{10.84}$$

(ii) $$\frac{\partial^+}{\partial t}\boldsymbol{U}_u(t,s)w\Big|_{t=s} = \boldsymbol{A}(s,u(s))w \quad \text{for } w \in Y; \tag{10.85}$$

(iii) $$\frac{\partial}{\partial s}\boldsymbol{U}_u(t,s)w = -\boldsymbol{U}_u(t,s)\boldsymbol{A}(s,u(s))w \quad \text{for } w \in Y. \tag{10.86}$$

□

The second theorem establishes the contractive nature of the mapping (10.83):

Theorem B (Kato)

Let $B \subset X$ and let $\{\boldsymbol{A}(t,b)\}$, $(t,b) \in [0,T]$ x B, satisfy K(iv). There is a constant C_1 such that for every $u, v \in C([0,T]: X)$ with values in B and every $w \in Y$ we have

$$\left\| \boldsymbol{U}_u(t,s)w - \boldsymbol{U}_v(t,s)\, w \right\| \;\leq\; C_1 \,\|\, w \,\|_Y \int_s^t \left\| u(\tau) - v(\tau) \right\| d\tau \tag{10.87}$$

□

The final, summarising, result is then:

Theorem C (Kato)

Let $u_0 \in Y$ and let $B = \{x: \| x - u_0 \| \leq r \;,\; r > 0\}$. If $\{\boldsymbol{A}(t,b)\}, (t,b) \in [0,T]$ x B satisfy K(i)-(iv), then the initial value problem

$$\left.\begin{aligned} \frac{du(t)}{dt} + \boldsymbol{A}(t,u)u = 0 \\ u(0) = u_0 \end{aligned}\right\}, \tag{10.88}$$

has a unique mild solution $u \in C([0,T]: X)$ with $u(t) \in B$. □

X.6.(iii). Application to Coupled Diffusion.

The underlying purpose of the above series of theorems is to find minimal differentiability conditions on the boundary such that solutions should still exist. For the present purpose, much of the subtlety of such an approach is not relevant: for applications it is permissible to frame the study so that existence is assured, and collect the qualitative content from theorems **XI.**4.(A-C). The Banach space X will be chosen to be a vector of functions, x_1, x_2, each $R \to R$, bounded and infinitely differentiable. It is desired to show that the full generality of coupled diffusion acts as a contraction on this space. The conditions K(i-iv) and the three theorems are now considered in this setting; it will be seen that the result follows almost immediately: inevitably so, given the strong assumptions.

The system to be considered is, then,

$$\left.\begin{aligned} \frac{du}{dt} + \boldsymbol{A}(u)u = 0 \\ u(0) = u_0 \quad ,\; u_0 \in X \end{aligned}\right\}, \tag{10.89}$$

where $X = BC^{\infty}[0,\infty)$ x $BC^{\infty}[0,\infty)$. In this context, the criteria to be met in K(i-iv) may be treated as follows:

Stability.

The extensive analysis of section **VI** showed that as T and θ vary over possible ranges, the matrix $\mathbf{\Lambda}$ remains diagonally dominant; combined with the results of ***X***.2., it follows that "almost all" values for u substituted into (10.89) produce contraction, and thus the family of infinitesimal generators in (10.89) is stable, with stability constants $M = 1$; $\omega = 0$. The term "almost all" is used here since section ***X***.3.(i) indicated that there remains some doubt over the contractive properties for some isolated ranges of values. It has not proved possible to remove this uncertainty in the present approach.

Invariance and Admissibility.

Kato's theorems are framed in terms of a subspace Y and a subset B of X: this to allow for the possibility that the operator $\boldsymbol{A}(t,u)$ may not be defined over the whole of the underlying Banach space. However, with the maximum differentiability conditions assumed at the outset in the present approach, it is possible to identify both Y and B with X. Y is then invariant and $\boldsymbol{A}$-admissible.

The Conditions K(i-iv)

Turning now to the conditions K(i-iv), it is seen that K(i) and K(ii) are satisfied immediately; for K(iii), which comprises in fact two conditions, boundedness is assured by the differentiability of the underlying space, whilst the continuous dependence on t is satisfied vacuously since $\boldsymbol{A}$ is constant in its t dependency. The Lipschitz condition K(iv) follows again from differentiability of elements of X.

For the three theorems of Kato, in this context, the lack of time dependency reduces Theorem A to the existence of a family of semigroups. Using (10.85),

$$\boldsymbol{T}_u(t-s) = \boldsymbol{U}_u(t,s) \ ,$$

when t is substituted for the elapsed time, $t-s$, conclusion (i) of the theorem is

$$\left\| \boldsymbol{T}_u(t) \right\| < 1; \qquad \forall u \in X \tag{10.90}$$

indicating that the family is contractive. Further, the mild solution to (10.82),

$$v = \boldsymbol{T}_u(t)u_0$$

either by the fact that u_0 necessarily belongs to the domain of $\boldsymbol{A}$, or by the analyticity of $\boldsymbol{T}_u$ established in **XI**.5.(ii), is in fact a classical solution. The Banach contraction result of Theorem B now becomes:

$$\left\| \boldsymbol{T}_u(t)w - \boldsymbol{T}_v(t)w \right\| \ \leq \ C_1 \left\| w \right\|_X \int_s^t \left\| u(\tau) - v(\tau) \right\| d\tau \tag{10.91}$$

providing, by Theorem C, a fixed point which is a classical solution to the original system (10.77). This solution is constructed by a doubly contractive process and thus provides a contraction on u_0.

X.7. Summary.

The analysis of previous sections, supported by computer simulation, indicates that relatively little qualitative variety occurs to the responses of coupled diffusion as controlling parameters vary. The present section attempts to establish this property in rigorous terms by the use of semigroup theory; in particular, by showing that all possible evolutions are contractive, that is, exponential decay occurs in the norm of all evolutions, implying, in turn, that subharmonic or chaotic developments are necessarily limited in their effects. Semigroup theory has been briefly reviewed. The simplest case of a contractive semigroup has been given for illustrative purposes. A method of analysing the norm of resolvents of coupled equations has been derived; by considering the case of linear coupled ordinary differential equations, it is shown that this method only provides a sufficient test for contraction. The equivalent analysis for coupled diffusion shows that contraction occurs for most parameter values; however, there remains a possibility that for some evolutions, particularly those for which moisture levels are around the peak in $D_{\theta V}$, expansion is possible to the system. However, if enhancement factors, well within the order of magnitude of those proposed in the literature, supplement diffusion then contraction is assured. Enhancement factors may therefore have a decisive significance for the qualitative properties of coupled diffusion in addition to the quantitative effects which are normally regarded as a rationale for their existence. Further theorems are given by which it is indicated how these properties for constant diffusion coefficients may be extended to the quasi-linear case in which the diffusive mechanisms are functions of the dependent variables.

XI. GENERAL SUMMARY.

The foregoing thesis has addressed mathematical questions raised by the coupled flow of moisture and heat in soil. The fundamental equation governing moisture distribution was derived through modified versions of Darcy's and Fick's Laws for liquid and vapour flows respectively, conservation principles then being applied to deduce time variation. De Vries' approach through the local heat balance in soil was used to derive the equation for heat diffusion. Various proposed enhancement factors to account for the underprediction of vapour flow by the simple theory were discussed. This exposition of the underlying physical theory formed the subject matter of section **II**. Relevant research was summarised in the following section, covering the areas of field and laboratory experiments, computer simulation and numerical and analytical approaches. It was seen that the abstract account given by physical theory, which should, theoretically, govern all possible behaviours of the system, had not been related, in any general or global sense, either to observed data or to computer simulation. The present work has attempted, where feasible, to form such relations.

Understanding was attained through the following intermediate stages. Section **IV** considered the periodic coupled variation of variables responding to linear coefficients. Standard techniques of eigenvalue decomposition in the context of the phasor method were used to obtain an analytical solution for this behaviour. Under Dirichlet conditions the solution was obtained straightforwardly. For Neumann conditions, a form of matrix reconstitution was required. It was seen that periodicity was preserved, with complicated inheritance by each variable, determined by its diffusive properties relative to the co-variables, of input amplitudes and phase angles. The following section considered non-linear diffusion for an individual variable. Here periodicity was again retained, in this case by the addition of severely exponentially decaying higher harmonics. The thesis may be summarised by saying that no additional phenomena accrete to the behaviour of coupled non-linear diffusion by the interaction of these effects.

Further consideration of the equations requires detailed analysis of the functional forms of the diffusion coefficients present in coupled variation. Primary and total diffusion coefficients were distinguished. It was suggested that their nature could most readily be understood by the graphical device of a diffusion coefficient surface, displaying the variation related to a T-θ plane. Such surfaces were given for the two soils to be studied subsequently. The features of the functional dependencies which control the most salient aspects of the variation were set out. Each of the coefficients may thus be reduced to a form in which only essential dependencies are retained.

Section **VII.** then turned to consideration of the full coupled situation. Simulation indicates that, despite the severe non-linearities present in the coefficients, the resulting behaviours only represent slight perturbations of the linearised system around the solutions for such systems, as considered in section **IV.** The perturbation is formed from coupled higher harmonics, severely decaying with depth, analogous to those of section **V.** A straightforward uncoupling of the system into component equations for each of the higher harmonics may then be formed. The detailed algebra was carried through, and uncovered the possibility of coupled resonance in the second harmonic. The magnitude of the parameters required implies that the phenomenon cannot occur in soil, but remains a theoretical possibility in more insulating mediums.

The following two sections compared the analytical approximation formed by truncating the series at the second term with observed behaviour, initially in comparison with computer simulation. The susceptibility or otherwise of the system to incursion by second harmonics may be readily gauged by comparison of the orders of magnitude of the elements of three matrices. These effects were illustrated for a range of boundary conditions and controlling parameters. For validation against field data, two experiments, those of Rose in 1968 and the Jackson paper of 1973 were used. The former of these shows a remarkable resistance to the incursion of non-linear effects; this property may be detected by the analysis developed. The Jackson observations, in comparison, show greater qualitative variety, although still essentially formed around simple decaying sinusoids. The propensity of this soil not to respond with such regular behaviour, whether caused by non-linearity or non-uniformity of the medium, may again be detected analytically. Illustrations of these properties were again given.

The non-linearity of the basic system would lead to the a priori assumption that diverse qualitative behaviours should be observed in its evolutions. Simulation indicates that such is not the case; if the assumption is made that all evolutions are perturbed from the linearised solutions, then quantitative accounts may be readily formed of that perturbation. However, this approach rests on the assumption, and provides no justification, internal to the analysis, that no greater variety is possible. Semigroup methods, particularly those associated with contractive semigroups, were used in section **X** to attempt to provide such a justification. Basic theory was reviewed and two illustrations given. The second of these showed that a test for contraction was only a sufficient test: it was possible for a system to fail this sufficient test and yet, nevertheless, only give rise to contractive evolutions. The enquiry of section **VI** concerning the orders of magnitude present in the coefficient matrix showed that, other than for a small range, all evolutions would pass the sufficiency test, giving a good indication that coupled diffusion is inherently restrained from wildly unstable behaviour. However, the assertion cannot be made for all evolutions, indicating that the system retains some features not uncovered and accounted

for by the foregoing analysis.

The present enquiry indicates several general areas and various specific topics which might be productive for further study. There are obvious extensions and generalisations of the mathematical methods given above. It is easily seen that more general surface conditions, such that they may be represented by a Fourier series, can be accommodated within the techniques set out. Each component term would then diffuse as if it were sinusoidal input acting in isolation; the resulting diffusion would then be a superposition of the resulting waves. For non-linear individual diffusion, each component sinusoid would acquire companion higher harmonics, exponentially decaying. The Klute and Heerman [58] experiment, in particular, may well be describable analytically by such means. A complementary analogous extension would be to consider arbitrary initial profiles by the method of Green's functions. It would be useful to show that an initial distribution survives in its effects only for a limited period of time. However, the most generally posed situation, of an arbitrary initial profile, under arbitrary surface conditions, even arbitrary periodic conditions, for non-linear diffusion would seem an analytical impossibility. The semigroup approach indicates that there may be possible interactions in this generality unlike any of those encountered in the present work. Enquiries to locate these possible evolutions would seem a productive, if speculative, area.

Much present research activity is directed towards coupled diffusion in which various dissolved solutes also diffuse. Since the present approaches are carried through, at least initially, for n variables, or else could be adapted to such a context at the cost of increased algebra, it is likely that much of present work is of direct relevance to this situation. Further, it seems that the qualitative properties of the resulting extended diffusion matrix, in terms of diagonal dominance, may still hold, and thus the qualitative nature of the diffusion should be retained. Since dissolved solutes include the nutritional requirements of plant life, it seems that the earlier teleological arguments may be applied in this context also: that no wildly disturbed evolutions are feasible since soil life would be adversely affected.

The phenomenon of coupled second harmonic resonance described in section **VIII**, although of no relevance to the behaviour of soil, seems to have interest from a pure mathematical standpoint. In particular, the role of means in triggering its occurrence, to the best of the writer's knowledge, seems not to have been remarked upon in any studies of partial differential equations. In an evolution in which transient redistribution of means occurs, corresponding, say, to a low mean assumed at the depth boundary, under sinusoidal input with a larger mean at the surface, it would seem that local "hot spots" (in literal terms, if the diffusing variable were visualised as heat) should occur as the evolution passes through the triggering mean values. The complexity of the resulting behaviour should be worthy of further study, and seems, in fact, to be the most interesting raised by the present enquiry.

REFERENCES

1. **Abramova, J.**, Movement of Water Vapour in Soil, Soviet Soil Sci. 1963, pp. 952-963. (1963).

2. **Ames, P.**, Non-Linear Partial Differential Equations in Engineering, Academic Press, New York. (1965).

3. **Armstrong, T.E.**, A Computer Model for Moisture Distribution in Stratified Soils under a Trickle Source, Trans. ASAE, pp 1704. (1983).

4. **Baca**, Finite Element Models for Simultaneous Heat and Moisture Transfer, Seminaires sur L'Irrigation Localise, Italy, p 57. (1978).

5. **Bell, E. C.**, Men of Mathematics, Penguin. (1953).

6. **Belmans, C. et al.**, Simulation Model of Water Balance of a Cropped Soil, J. Hydrol. Vol 63, pp271. (1983).

7. **Ben Asher**, Radiation and Energy Balance of Sprinkler and Trickle Irrigated Fields. Assom. J. Vol 70(4), pp368. (1978).

7a. **Benjamin, J.G., et. al.,** Coupled Water and Heat Transport in Ridged Soils, Soil Sci. Am J., **54**,963-968, (1990).

8. **Bouyoucos, G. J.**, The Effect of Soil Temperature on the Movement of Water Vapour. J. Agr.Res. Vol.5. (1915).

9. **Bouyoucos, G. J.**, Soil Temperature, Michigan Agr. College Expt. Sta. Tech. Bull., 17. (1918).

10. **Brust K. J., Van Bavel C. H. M., and Stirk G. B.,** Hydraulic Properties of a Clay Loam Soil, Soil Sci. Amer.Proc. **32.** 322-326. (1968).

11. **Buckingham**, Studies in the Movement of Soil Moisture. U.S. Dept. Agr. Bur. Soils. Bull. 38. (1915).

12. **Buckmaster J.**, Viscous Sheets Advancing over Dry Beds. J. Fluid Mech. **81**. 735-756 (1977).

13. **Carmen,P.C.& Raal**, F.A.,Physical Adsorption of Gases in Porous Solids,1. Proc.Roy.Soc.Lond. 209A. (1951).

14. **Carslaw, H.S. & Jaeger, J.C.**, Conduction of Heat in Solids. Clarendon Press, Oxford. (1959).

15. **Cary, J.W.**, Soil Moisture Transport Due to Thermal Gradients. Proc. Soil Soc. Amer. 30. (1966).

16. **Cary, J. W.**, Onsager's Relation and the Non-isothermal Diffusion of Water Vapour. J. Phys. Chem. 67, 126-9. (1963).

17. **Cary, J.W. & Taylor, S.A.**, The Interactions of the Simultaneous Diffusion of Heat and Water Vapour. (1962).

18. **Cass, Campbell & Jones.**, Enhancement of Thermal Water Vapour Diffusion in Soil, Soil Sci. Soc. Am. J. **48**. 25-32. (1984).

20. **Childs & Collis-George**, The permeability of Porous Materials. Proc. Roy. Soc. Lond. 201, 392-405. (1950).

21. **Crank, J.**, Mathematics of Diffusion. Oxford University Press. (1956).

22. **Darcy, M.**, Les Fontaines Publiques de la ville de Dijon. Belmont, Paris. (1834).

23. **De Vries, D.A.**, Simultaneous Transfer of Heat and Moisture in Porous Media. Amer. Geophys.Union. Vol 32(5) pp.909.(1959).

24. **De Vries, D.A.**, Thermal Properties of Soils, in Physics of Plant Environment, W.R. Van Wyle, North-Holland, Amsterdam. (1963).

25. **De Vries**, Het Warmtegelerdings Vermogen van Grond. Landsbouwhogeschool, Wageningen 52, pp73. (1952).

26. **De Vries**, Transfer Processes in the Plant Environment in 'Heat and Mass Transfer in the Biosphere', Ed. De Vries & Afgan, John Wiley and Sons, (1975).

27. **Dorsey, N. E.**, Properties of Ordinary Water Substance, Reinhold Publ. Corp. (1940).

28. **Diez J.A., Gratton J., and Minotti F.**, Self-Similar Solutions of the Second Kind of Nonlinear Diffusion-Type Equations, Quart. Appl. Maths. **50**. 401-414 (1992).

29. **Eagleson P.S.**, Dynamic Hydrology. McGraw-Hill. New York. (1970).

30. **Edlefsen,W.E. & Anderson, B.C.**, The Thermodynamics of Soil Moisture, Hilgardia, Vol 15(2), (1943).

31. **Feddes J., et. al.**, Simulation of Field Water Flux and Crop Yield. Centre of Agricultural Publishing and Documentation. Wageningen, The Netherlands. (1978).

32. **Fick, A.**, Uber Diffusion. Annalen Der Physik. (Leipzig) Vol. 170. pp. 39. (1855).

33. **Fluker, K.**, Soil Temperatures, Soil Sci. Soc. Am. Proc. 21, 400-420. (1953).

34. **Gardner, W.R.**, Some Steady State Solutions of the Unsaturated Moisture Flow Equation. Soil Sci., 85, 228-232. (1958).

35. **Gardner, W.R. & Fireman, M.**, Laboratory Studies of Evaporation. Soil. Sci. 85, 244-9. (1958).

36. **Ghali,S.G.**, Mathematical Modelling of Moisture Dynamics., Ph.D.Thesis.Southampton Univ., (1986).

37. **Gilding B.H. and Peletier L.A.**, On a Class of Similarity Solutions of the Porous Media Equation. J. Math. Anal. Appl. **55**. 351-364. (1976).

38. **Gratton J. and Minotti F.**, Self-Similar Viscour Gravity Currents: Phase Plane Formalism. J.Fluid Mech. **210**. 155-182 (1990).

39. **Griffith.** Analysis of Soil Temperature Variation, Soil Sci. Soc. Am. Proc., 32, 54-67. (1953).

40. **Gurr, C.G., et al.**, Movement of Water in Soil due to a Temperature Gradient. Soil Sci. 74, 335-345. (1952).

41. **Hadas, A.**, Simultaneous Flow of Water and Heat. Soil Sci. Soc. Am. Proc. 32, 297-301. (1953).

42. **Hanks et al.**, Evaporation of Water from Soils. Soil Sci. Soc. Am. Proc. 31, 593-598. (1952).

43. **Hayashi**, Non-Linear Oscillations in Physical Systems. Mc.Graw-Hill, New York. (1964).

44. **Henry, D.S.H.**, Proc. Roy. Soc. Lond. 171A 215. (1939).

45. **Hille E. and Phillips R.S.**, Functional Analysis and Semigroups, Amer. Math. Soc. Colloq. **31**., Providence, RHode Island. (1957).

46. **Huppert H.E.**, The Propagation of Two-Dimensional Viscous Gravity Currents over a Rigid Horizontal Surface. J. Fluid Mech. **210**. 43-58. (1982).

47. **Jackson, R.D., et al.**, On Diffusion Laws Applied to Porous Materials. USDA-ARS Bull. (1963).

48. **Jackson, R.D.,** Water Vapor Movement in Relatively Dry Soil,Soil Sci.Soc.Am.Proc.28,172-176. (1964).

49. **Jackson, R.D.** Water Vapor Movement in Relatively Dry Soil,Soil Sci.Soc.Am.Proc.28,464-466. (1964).

50. **Jackson, R.D.,** Water Vapor Movement in Relatively Dry Soil,Soil Sci.Soc.Am.Proc.28,467-470. (1964).

51. **Jackson, R.D.,** Water Vapor Movement in Relatively Dry Soil,Soil Sci.Soc.Am.Proc.29,144-148. (1964).

52. **Jackson, R.D.,** Diurnal Changes in Soil Water Content During Drying, in Field Soil Water Regime, Spec. Publ. No.5. Soil Sci. Soc. Am., Madison, Wisconsin. (1973).

52b. **Jackson, R. D.,** Diurnal Soil Water Time- Depth Flux Patterns. Soil Sci. Soc. Am. Proc. 37, 505-509. (1973).

53. **Jordan & Smith,** Non-Linear Ordinary Differential Equations. Clarendon Press, Oxford. (1987).

54. **Jury & Letey,** Water Vapor Movement in Soil: Reconciliation of Theory and Experiment, Soil Sci. Soc. Amer. Proc. 43, 823-827. (1979).

55. **Jury, W.A., Letey, J. & Stolzy, L.H.,** Flow of Water and Energy Under Desert Conditions, in Water in Desert Ecosystems. Ed. Thames & Evans, Dowden, Hutchinson, & Ross, Inc. (1981).

55(a). **Kato, T.,** Quasi-linear Equations of Evolution, Lecture Notes in Mathematics, Springer-Verlag, (1975), 25-70.

56. **Kimball, B.A. et. al.,** Seasonal Effects on Soil Drying After Irrigation, Proc. of Arizona Section, AWRA, Hydrol. Section, Vol. 1. (1971).

57. **Kirkham and Powers,** Advanced Soil Physics. Wiley Interscience, New York. (1972).

58. **Klute & Heerman,** Soil Water Profile Development Under a Periodic Boundary Condition. Soil Sci., Vol. 117, No. 5. (1973).

59. **Krischer, O. & Rohnalter, H.,** Warmleitung und Dampf Diffusion im Feuchten Gutern, Verein. Deut. Ing. Forschungs. Left. 402, (1940).

60. **Larsen E. W. and Pomraning G. C.,** Asymptotic Analysis of Nonlinear Marshak Wave. SIAM J. Appl. Math. **39.** 201-212. (1980).

61. **Martin, R.H.,** Nonlinear Operators and Differential Equations in Banach Space., John Wiley and Sons, New York, (1976).

62. **Neilsen, D.R., et al.,** Experimental Consideration of Diffusion Analysis in Unsaturated Flow Problems. Soil. Sci. Am. Proc. 39, 37-43. (1975).

63. **Marshak R. E.,** Effect of Radiation on Shock Wave Behaviour. Phys. Fluids **1**. 24-29. (1958).

64. **Marshall and Holmes,** Soil Physics, Cambridge University Press, (1988).

65. **Monteith,** The Heat Balance of Soils Beneath Crops. Unesco Ariel Zones, Res. (1960).

66. **Muskat M.,** The Flow of Homogeneous Fluids through Porous Media. McGraw-Hill, New York. (1937).

66a. **Partington, J. R.,** Advanced Treatise on Physical Chemistry, Longmans, Green & Co., London, pp., 943, (1949).

67. **Pazy A.,** Semigroups of Linear Operators and Applications to Partial Differential Equations. Springer Verlag, New York (1983).

68. **Pazy, A.,** A Class of Semi-Linear Equations of Evolution, Israel J. Math. **20.** (1975).

69. **Peletier L.A.,** Applications of Non-Linear Analysis in the Physical Sciences, Chap. 2: The Porous Media Equation. Pitman Adv. Publ. Progr., Boston. (1981).

70. **Penman, H.L. & Schofield, R.R.,** Gas and Vapour Movement in Soil. J. Agr. Sci. 30, 437-462. (1940).

71. **Pert G. J.,** A class of Similar Solutions of the Nonlinear Diffusion Equation. J. Phys. A. **10**. 583-593. (1977).

72. **Philip, J. R.,** The Theory of Infiltration, 1. Soil Sci, 83, 345-357. (1957).

73. **Philip, J. R.,** The Theory of Infiltration, 2. Soil Sci, 83, 435-448. (1957).

74. **Philip, J. R.,** The Theory of Infiltration, 3. Soil Sci, 84, 251-264. (1957).

75. **Philip, J. R.,** The Theory of Infiltration, 4. Soil Sci, 84, 421-438. (1957).

76. **Philip, J.R.,** Recent Progress in the Solution of Non-Linear Diffusion Equations, Soil Sci. V.117, No.5. (1974).

77. **Philip, J.R.,** An Integral Relation and its Physical Consequences, Aust. J. Phys., **26**, 513-519, (1973).

78. **Philip, J.R. & De Vries, D.A.,** Moisture Movement in Porous Materials Under a Temperature Gradient. Trans. Am. Geophys. Un 38, 222-32. (1958).

79. **Polubarinova-Kochina P.Y.,** Theory of Ground Water Movement. Princeton Univ. Press. Princeton, N.Y., (1962).

80. **Rollins et. al.,** Movement of Soil Moisture under a Thermal Gradient. Highway Res. Board Proc. 33. (1934).

81. **Rose, C.W.,** Water Transport in Soil with a Daily Temperature Wave, 1. Aust. J. Soil Res., 6, 31-44. (1968).

82. **Rose, C.W.,** Water Transport in Soil with a Daily Temperature Wave, 2. Aust. J. Soil Res., 6, 44-55. (1968).

83. **Sophocleous,** Analysis of Heat and Moisture Flow in Unsaturated/Saturated Media, Nat. Res. Res. Vol 15, p. 1195. (1979).

83(a). **Shepherd, R., & Wiltshire, R. J.,** A Periodic Solution to a Non-Linear Diffusion Equation, Transport in Porous Media (to appear), (1994).

84. **Taylor, S.A. & Cavezza, L.,** The Movement of Soil Moisture in Response to Temperature Gradients, Soil Sci. Soc. Amer. Proc., 18 351-358 (1954).

85. **Ten Berge & Bolt.** Transport in Porous Media, 3, 35-49, (1988).

86. **Thomson.,J. M.T.,** An Introduction to Non-Linear Dynamics, Appl. Math. Modelling, 8,157-167 (1984).

87. **Van Bavel, C.H.M.,** Gaseous Diffusion and Porosity in Porous Media. Soil Sci. 73, 91-104, (1952).

88. **Vasquez J.L.,** Free Boundary Problems: Theory and Application, Vol 1, Pitman Adv. Publ. Progr., Boston (1983).

89. **Viswandam,** The Thermal Diffusivity of Soil at Tropical Stations in the Southern Hemisphere, Pure and Applied Geophys. 101, 247-260. (1953).

90. **Von Moses,** Bermerkungen zur Hydrodynamik, 2, Math. Mech., 7, 425. (1943).

91. **Weast R.D., Melvin A.J., and Beyer W.M.,** CRC Handbook of Chemistry and Physics, CRC Press, Inc., Florida. (1983).

92. **Weeks et. al.**, Water and Salt Transport in Soil Resulting from Thermal Gradients. Soil Sci. Soc. Amer. Proc. 30 428-33. (1980).

93. **Wierenga, P.J.**, Soil Temperature Profiles during Infiltration and Redistribution of Cool and Warm Irrigation Water, Wat. Res. Res., Vol 6(1), pp. 230. (1970).

94. **Wiltshire., R. J.,** Earth Surface Processes and Landforms, 8, 547-555 (1983).

95. **Yosida, K.,** Functional Analysis, Springer Verlag, New York. (1980).

96. **Zaidman S. D.,** Abstract Differential Equations, Pitman Research Notes in Math. **36**. (1976).

97. **Zel'dovich Ya.B. and Raizer Yu.P.**, Physics of Shock Waves and High Temperature Hydrodynamics Phenomena. Academic Press. New York. (1966).

APPENDIX: ILLUSTRATIVE FIGURES

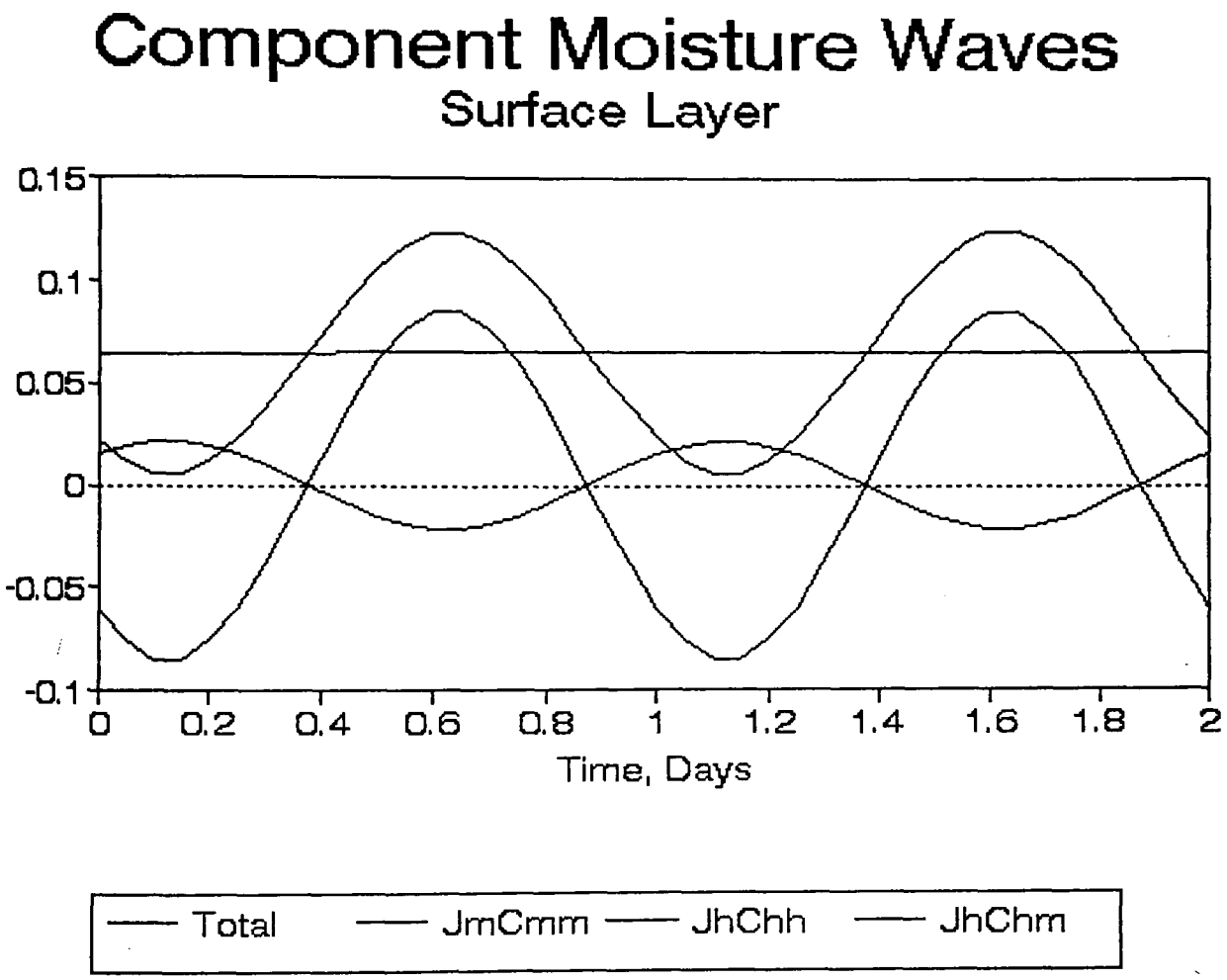

Fig. IV.1. Coupled Linear Diffusion under Flux Input; Surface Layer.
Time, Days v. Moisture Content, Dimensionless.
J_iC_{ik} as text, *p.* 50.

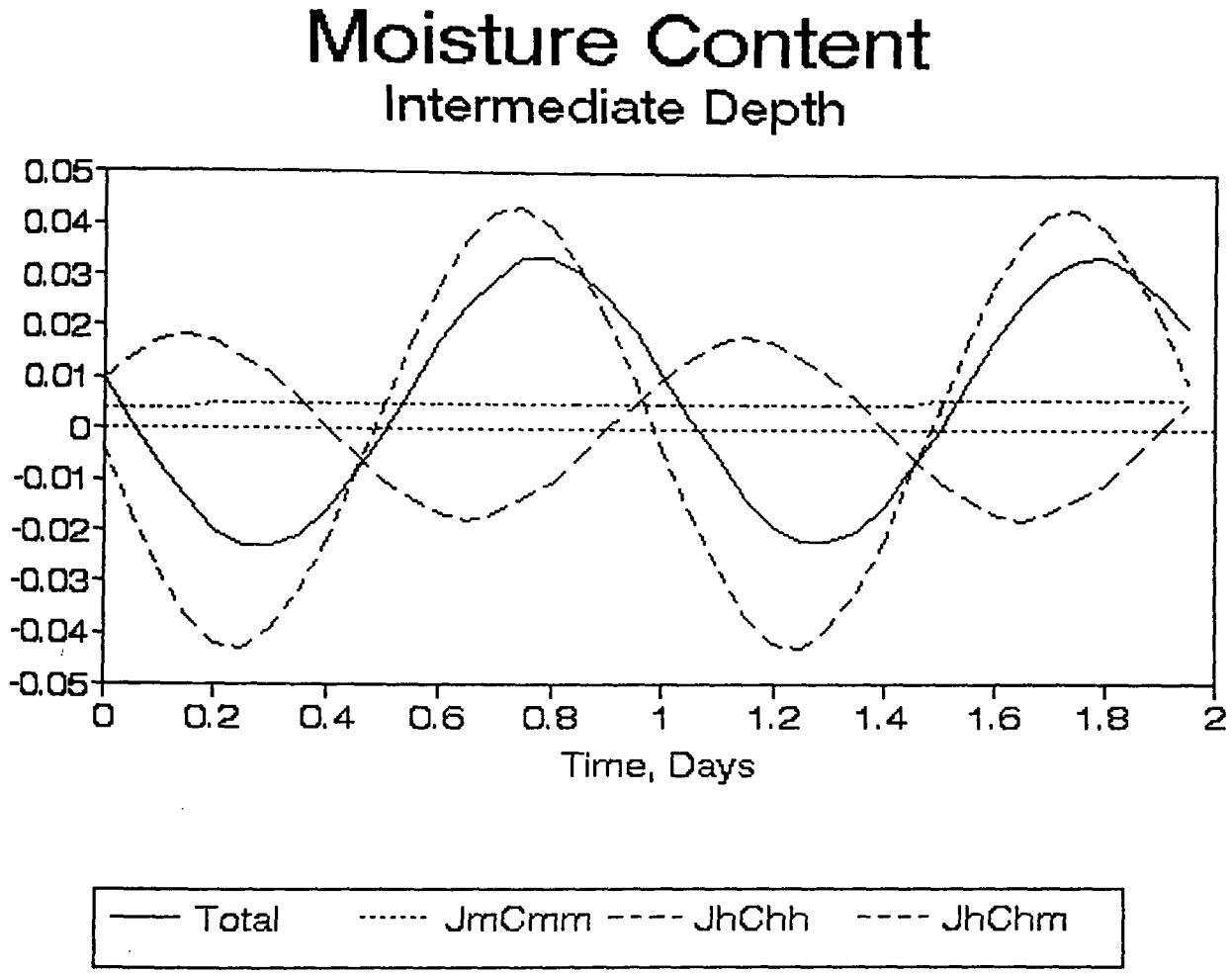

Fig. IV.2. Coupled Linear Diffusion under Flux Input; Intermediate Layer.
Time, Days v. Moisture Content, Dimensionless.
$J_i C_{ik}$ as text, *p.* 50.

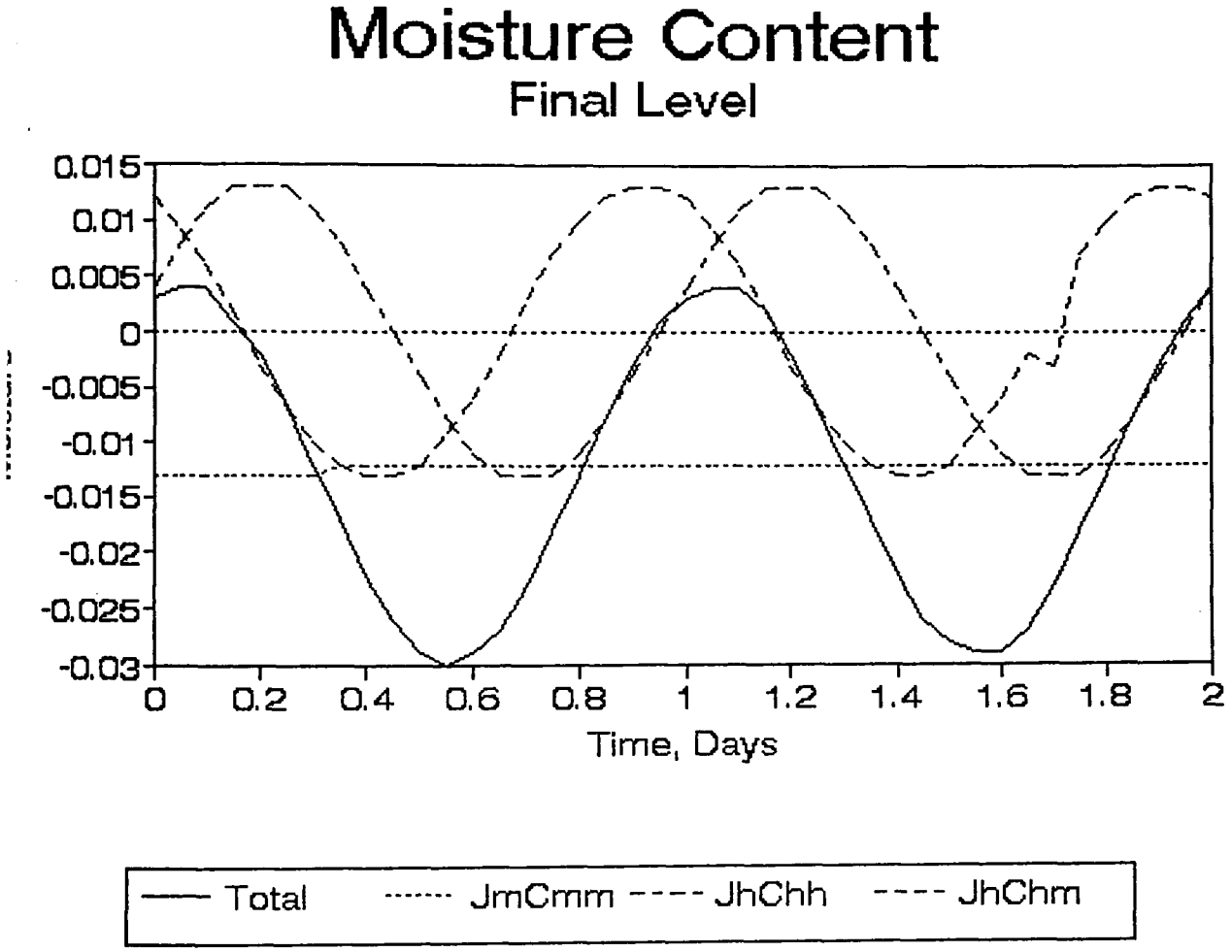

Fig. IV.3. Coupled Linear Diffusion under Flux Input; Final Layer.
Time, Days v. Moisture Content, Dimensionless.
J_iC_{ik} as text, *p.* 50.

YYYY

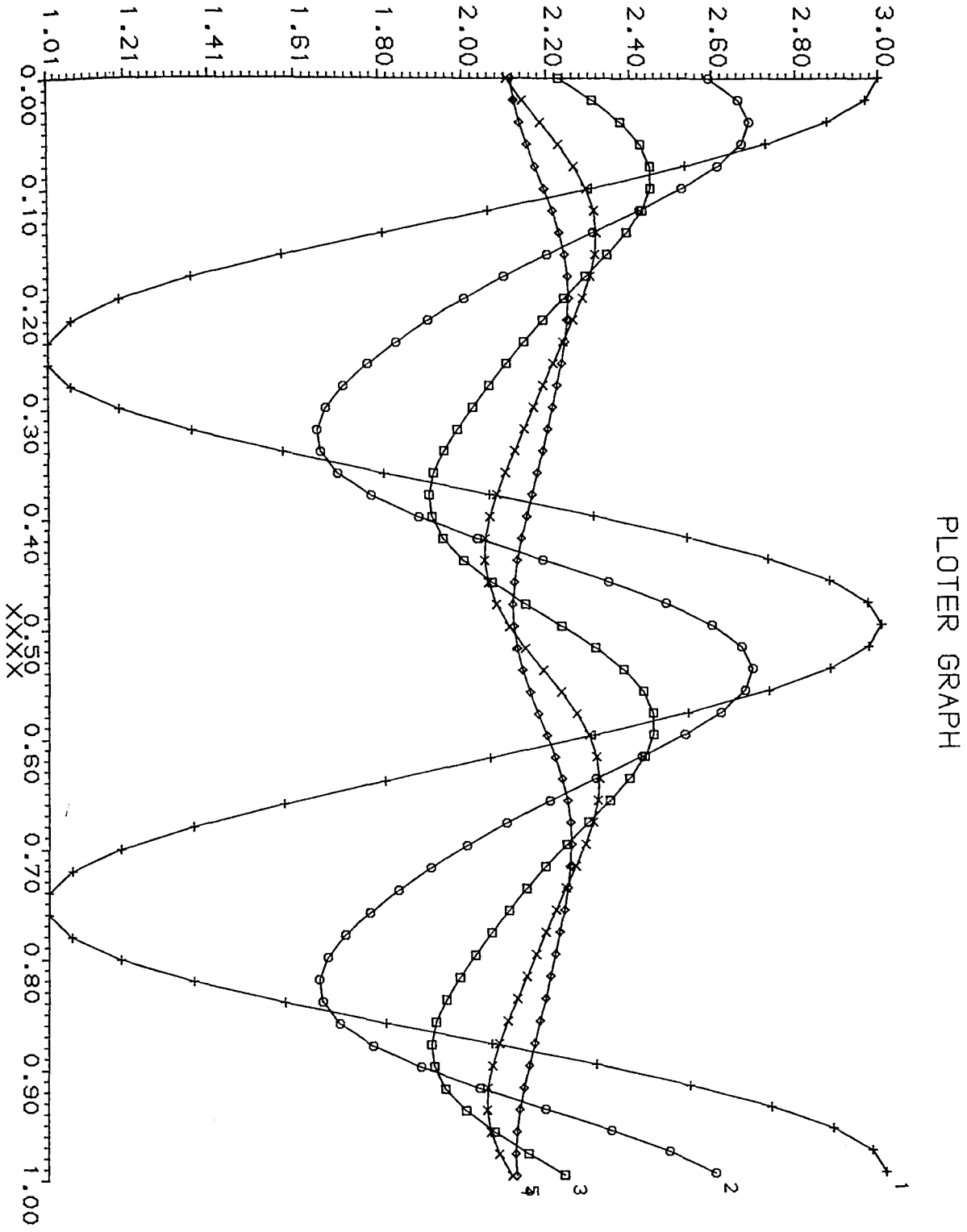

Fig. V.1.(a). Analytical Solution for Individual Non-Linear Diffusion. ($\alpha = 1.5$).
Time, 2 Cycles, against the dependent variable, dimensionless.
Surface Layer, depth = 1, 2, 3 & 4, dimensionless.

YYYY

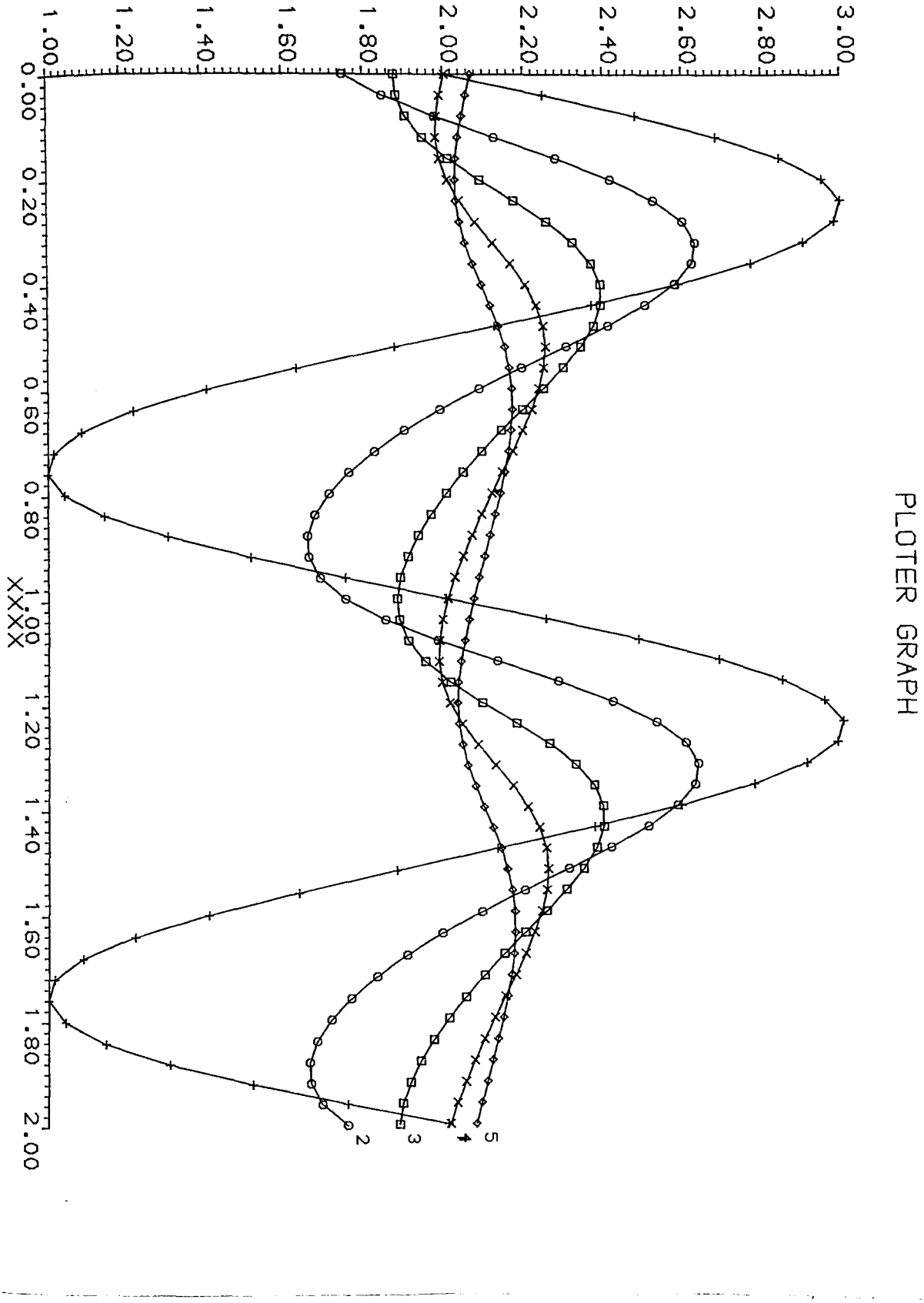

Fig. **V**.1.(b). Simulation for Individual Non-Linear Diffusion. ($\alpha = 1.5$).
Time, 2 Cycles, against the dependent variable, dimensionless.
Surface Layer, depth = 1, 2, 3 & 4, dimensionless.

YYYY

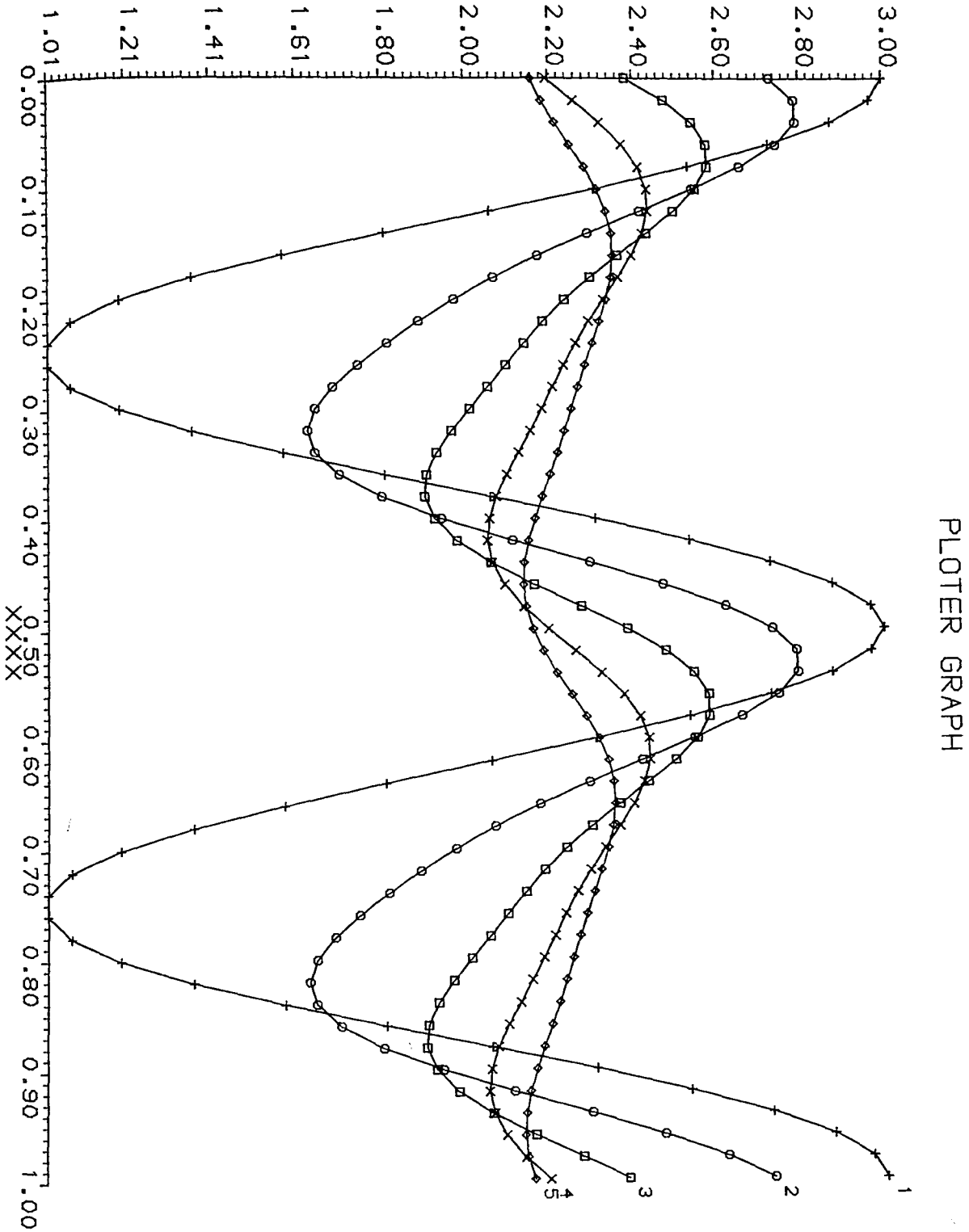

Fig. V.2.(a). Analytical Solution for Individual Non-Linear Diffusion. ($\alpha = 2.0$). Time, 2 Cycles, against the dependent variable, dimensionless. Surface Layer, depth = 1, 2, 3 & 4, dimensionless.

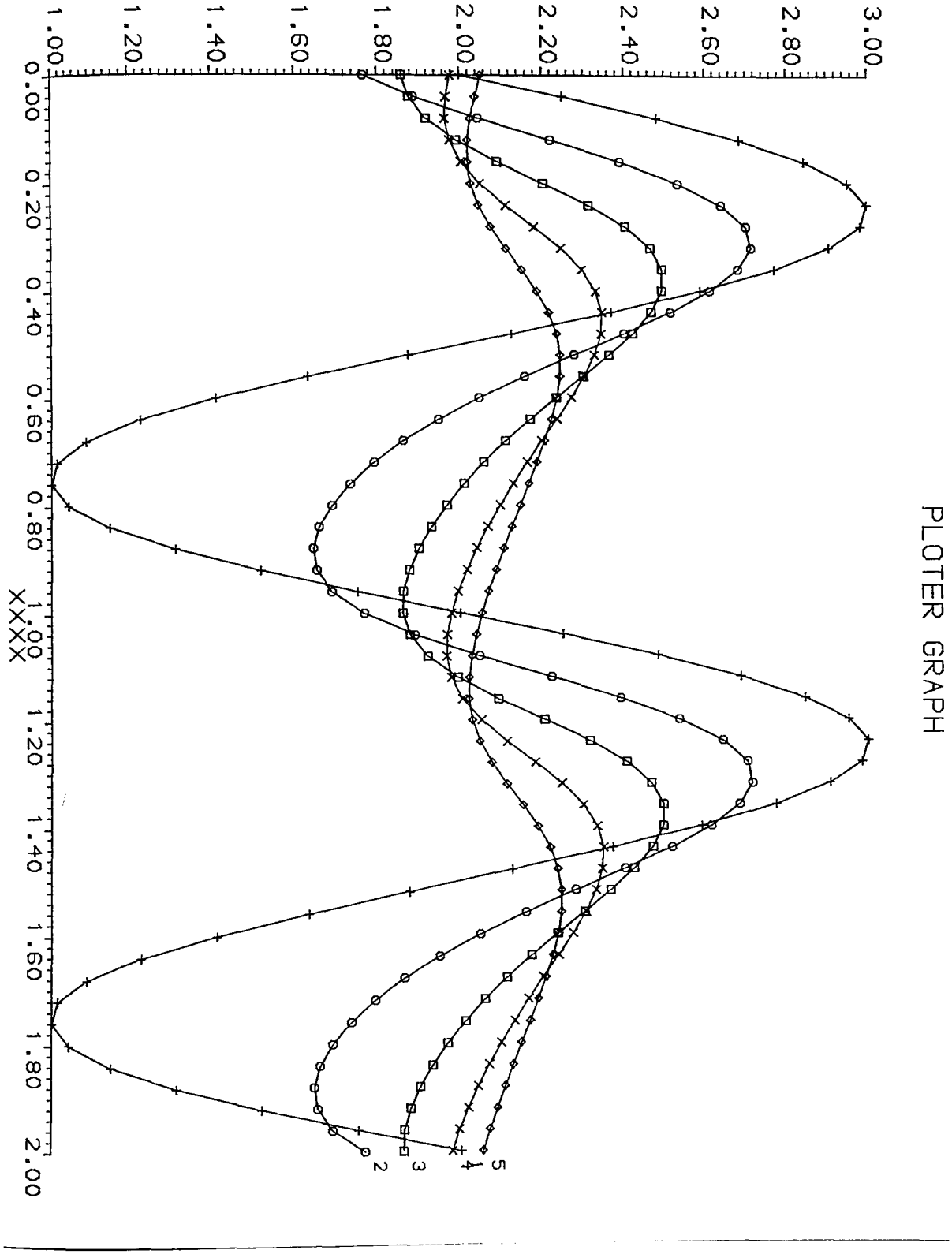

Fig. V.2.(b). Simulation for Individual Non-Linear Diffusion. ($\alpha = 2.0$).
Time, 2 Cycles, against the dependent variable, dimensionless.
Surface Layer, depth = 1, 2, 3 & 4, dimensionless.

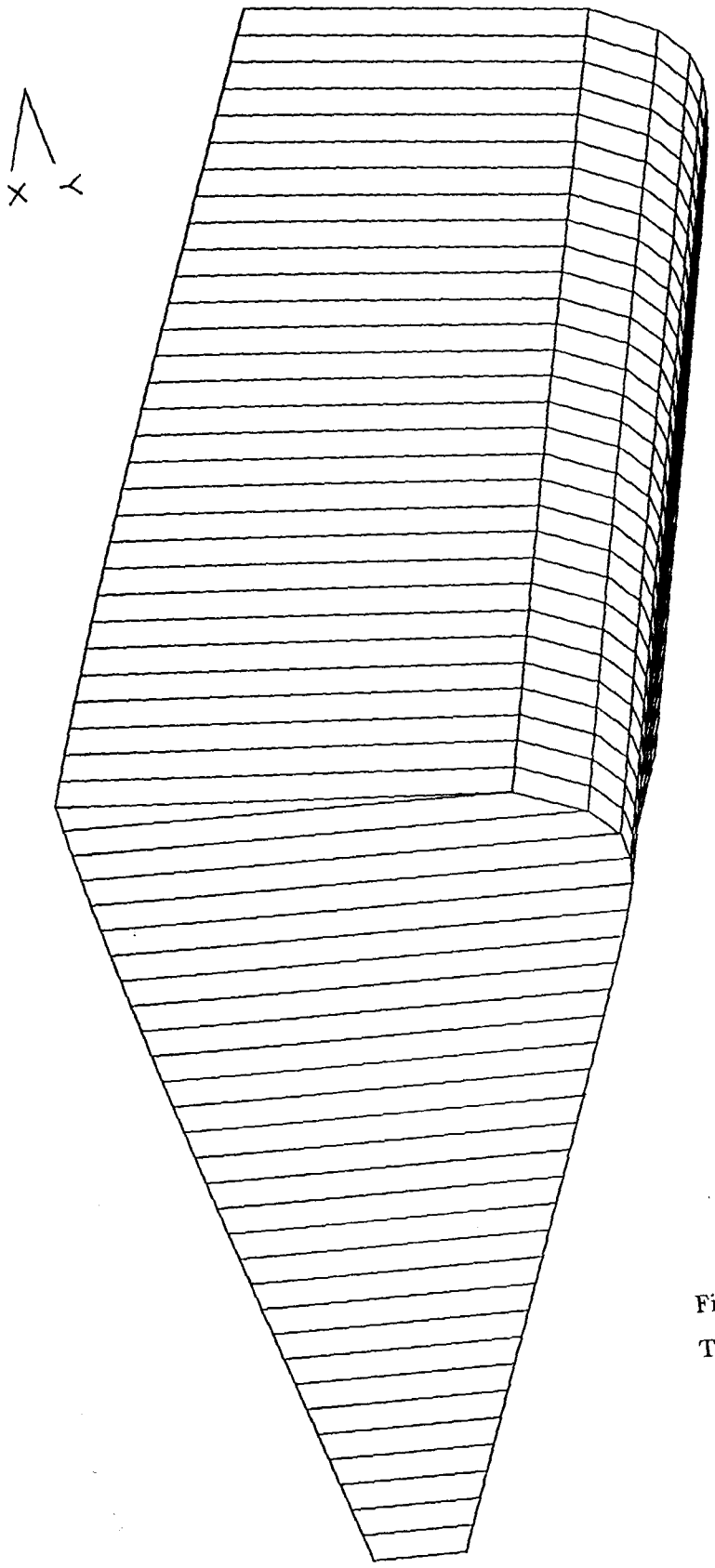

Fig. VI.1.(a) Primary Diffusion Coefficients The Rose Soil. D_{TV}x10^8 Surface Plot.

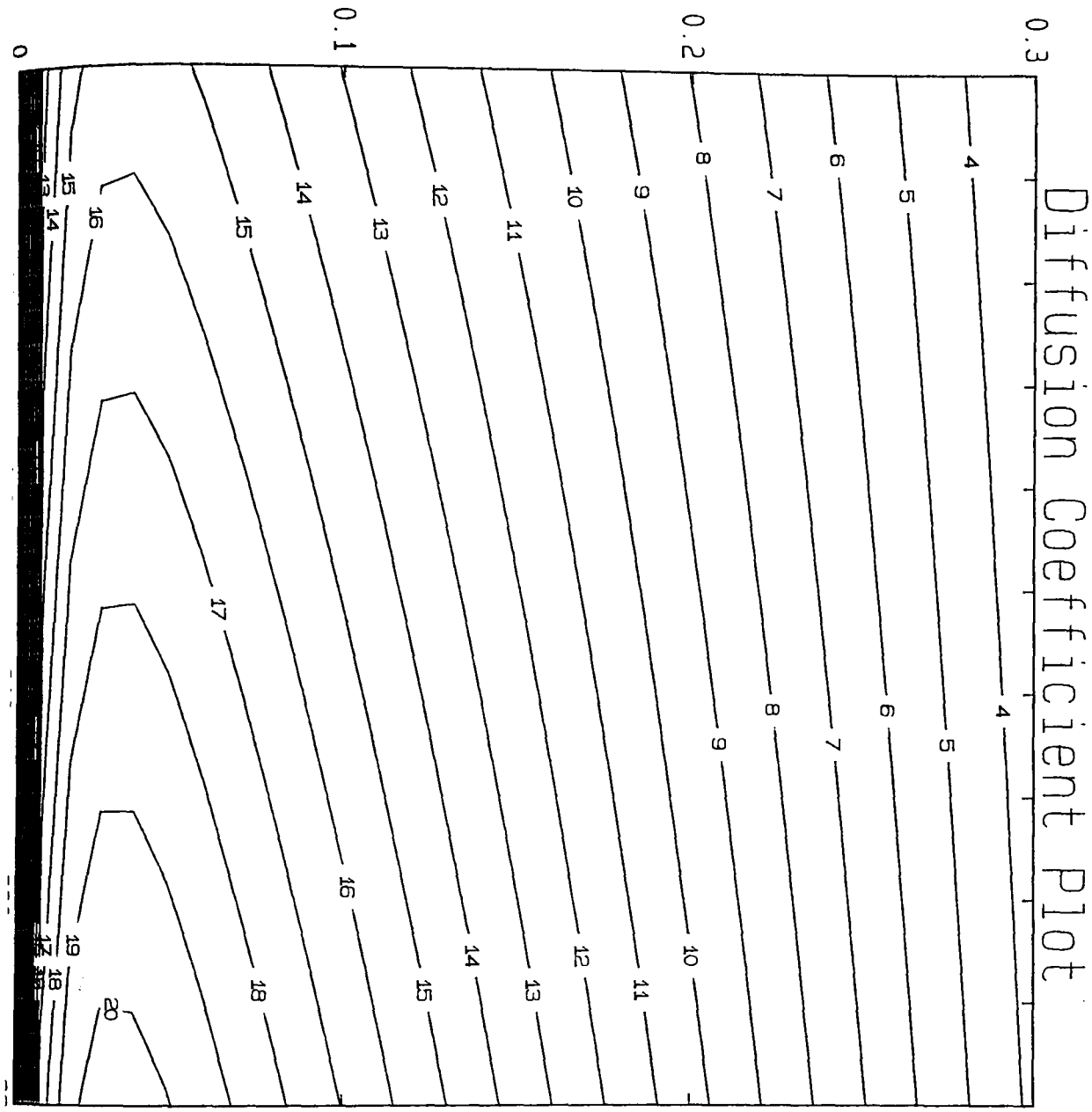

CONTOUR KEY	
1	0.1670
2	0.5011
3	0.8351
4	1.1692
5	1.5033
6	1.8373
7	2.1714
8	2.5054
9	2.8395
10	3.1736
11	3.5076
12	3.8417
13	4.1757
14	4.5098
15	4.8438
16	5.1779
17	5.5120
18	5.8460
19	6.1801
20	6.5141

Fig. VI.1.(b) Primary Diffusion Coefficients for the Rose Soil. Contour Plot. Temperature, ^{o}K, v. Moisture Content, Dimensionless, v. D_{TV} $cm^2/sec/^{O}K$ x 10^8 .

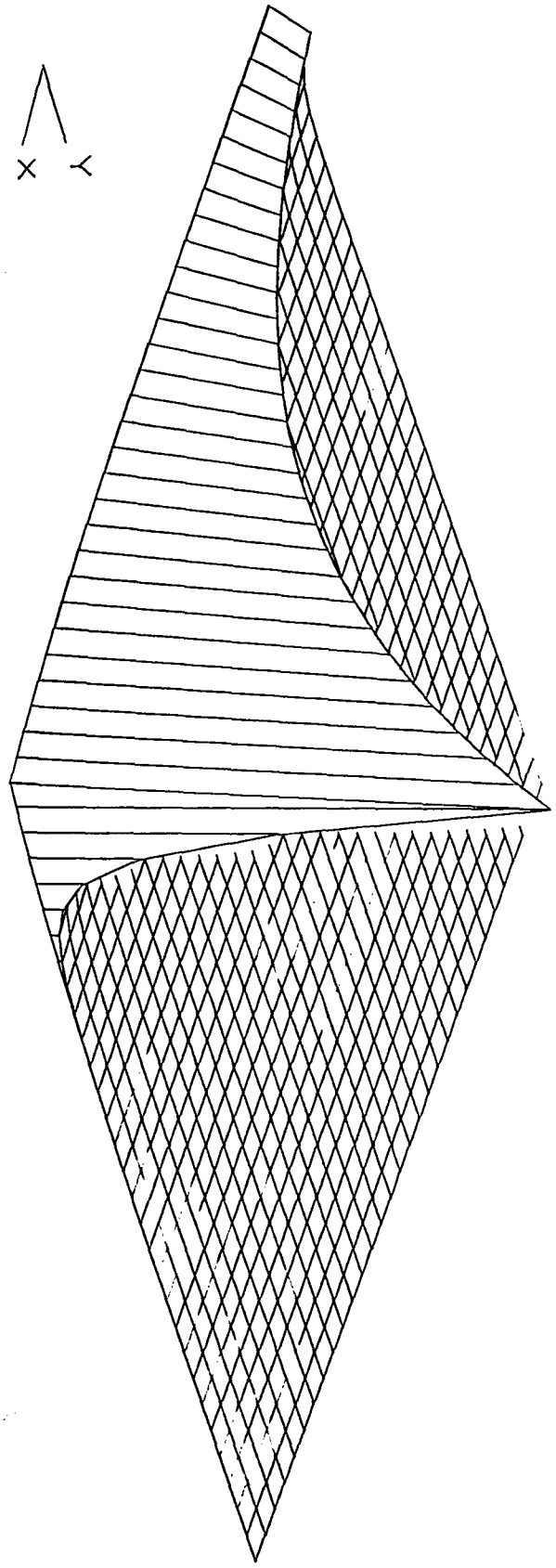

Fig. **VI**.2.(a) Primary Diffusion Coefficients. The Rose Soil. $D_{\theta V}$x10^5 Surface Plot.

CONTOUR KEY	
1	1.7920
2	5.3759
3	8.9599
4	12.5438
5	16.1278
6	19.7118
7	23.2957
8	26.8797
9	30.4636
10	34.0476
11	37.6315
12	41.2155
13	44.7994
14	48.3834
15	51.9674
16	55.5513
17	59.1353
18	62.7192
19	66.3032
20	69.8871

Fig. VI.2.(b) Primary Diffusion Coefficients for the Rose Soil. Contour Plot. Temperature, ^{o}K, v. Moisture Content, Dimensionless, v. $D_{\theta v}\ cm^2/sec/^{O}K$ x 10^5 .

Fig. VI.3.(a) Primary Diffusion Coefficients.
The Rose Soil. D_{Tl}x10^8 Surface Plot.

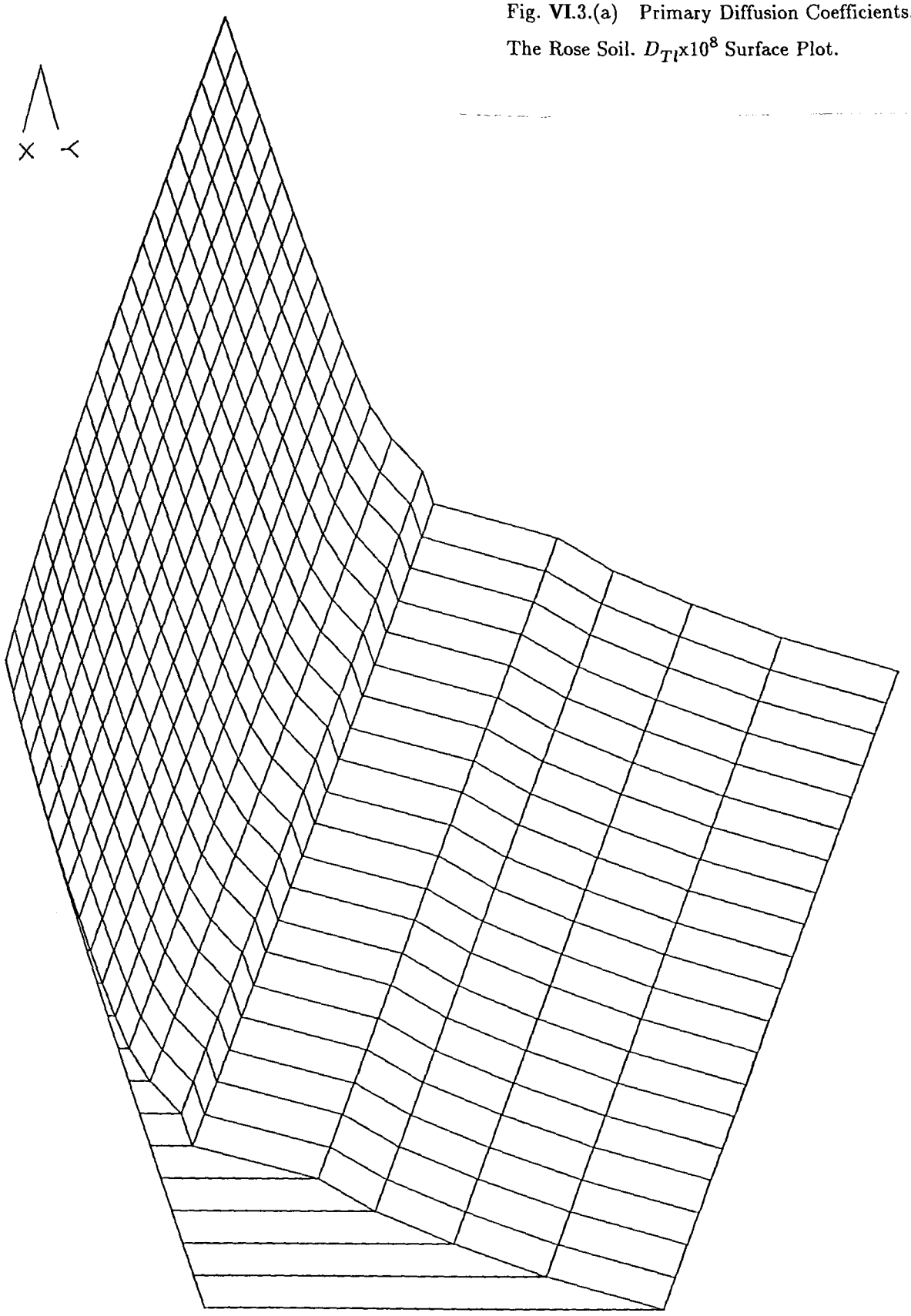

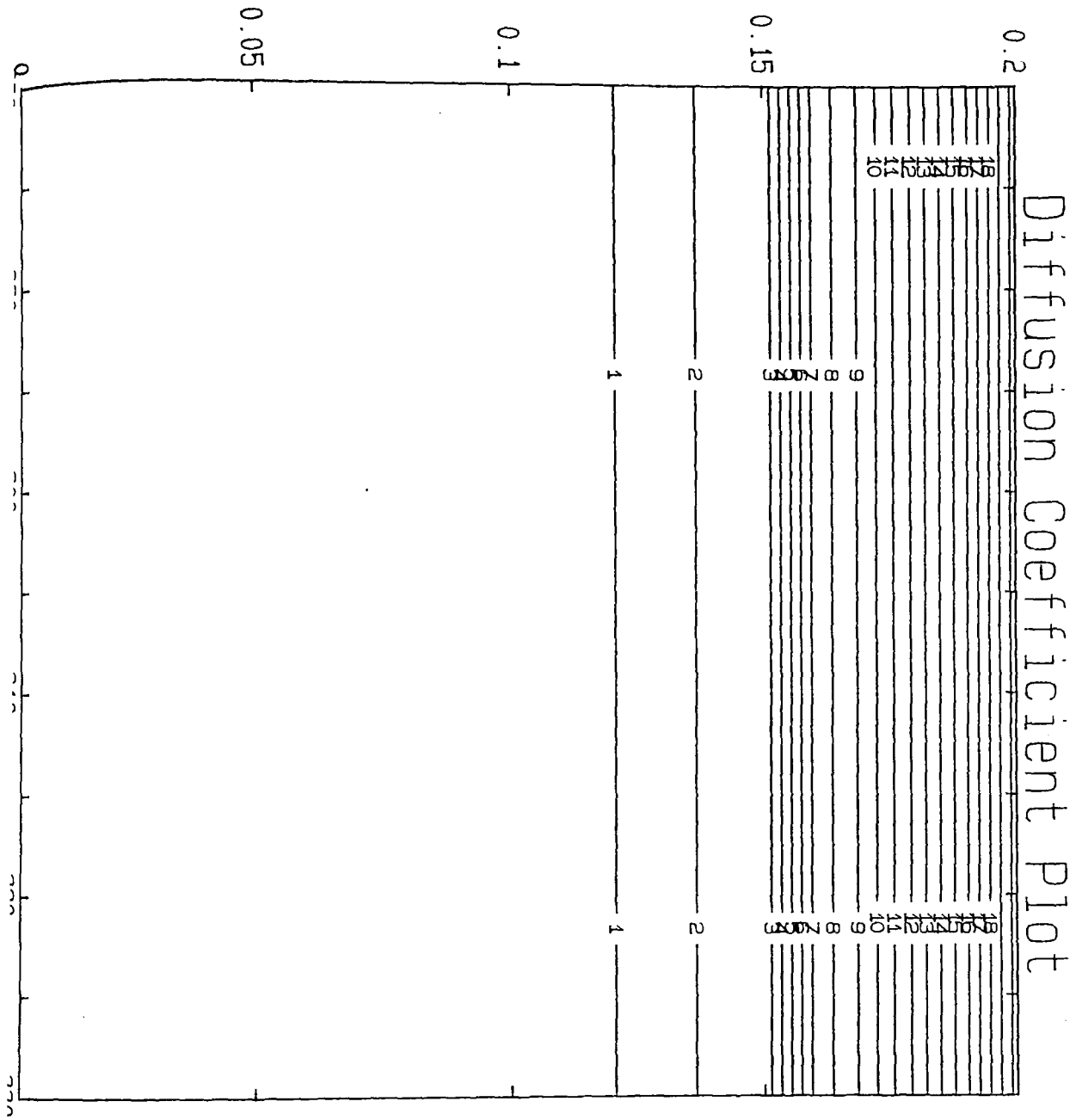

CONTOUR KEY	
1	0.1223
2	0.3670
3	0.6117
4	0.8564
5	1.1011
6	1.3458
7	1.5905
8	1.8352
9	2.0799
10	2.3246
11	2.5693
12	2.8140
13	3.0587
14	3.3034
15	3.5480
16	3.7927
17	4.0374
18	4.2821
19	4.5268
20	4.7715

Fig. VI.3.(b) Primary Diffusion Coefficients for the Rose Soil. ContourPlot. Temperature, ^{o}K, v. Moisture Content, Dimensionless, v. $D_{Tl}\ cm^2/sec/^{O}K$ x 10^8 .

Fig. VI.4.(a) Primary Diffusion Coefficients.
The Rose Soil. $D_{\theta l}$x10^5 Surface Plot.

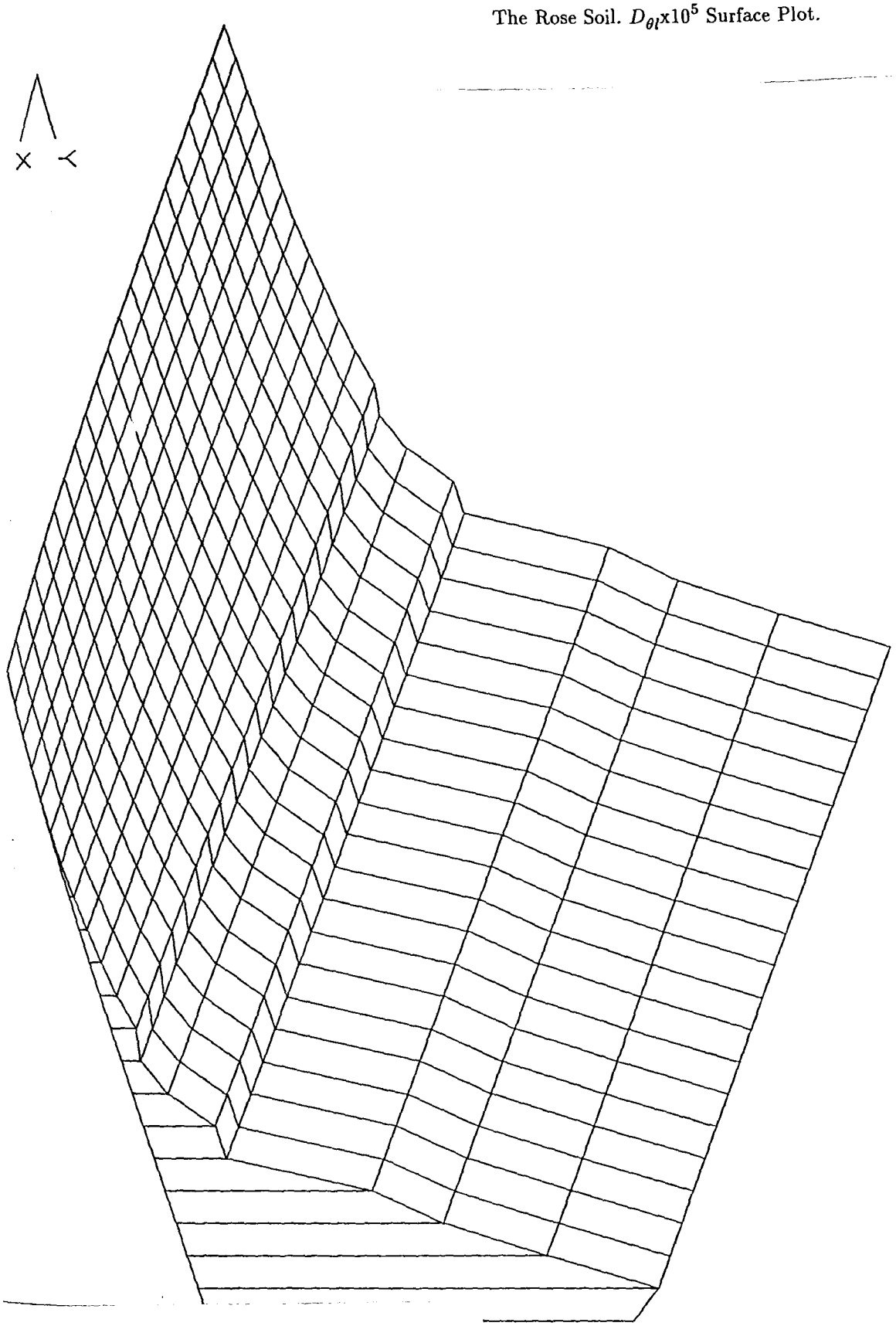

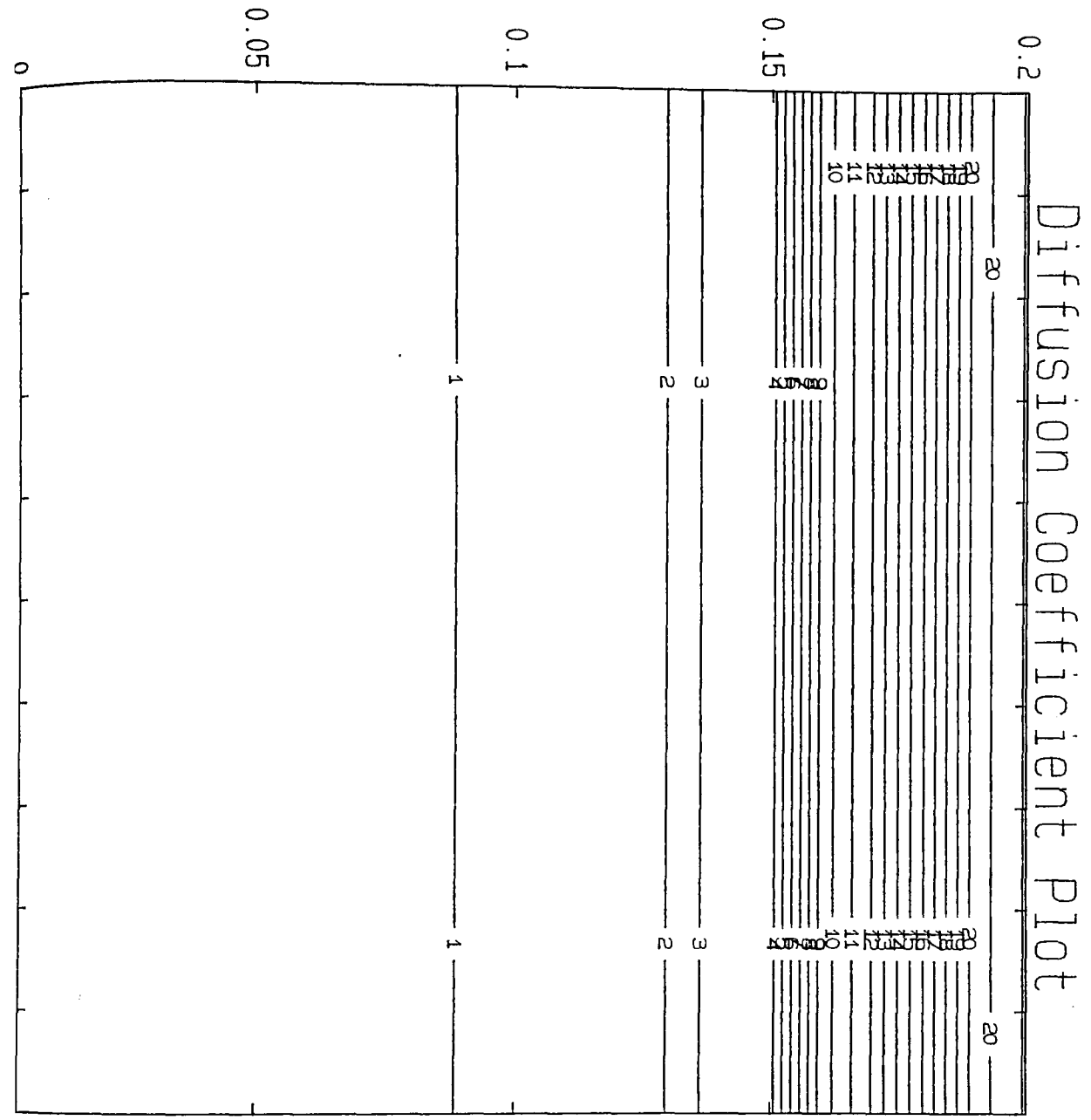

CONTOUR KEY	
1	0.0705
2	0.2115
3	0.3525
4	0.4935
5	0.6345
6	0.7756
7	0.9166
8	1.0576
9	1.1986
10	1.3396
11	1.4806
12	1.6216
13	1.7626
14	1.9036
15	2.0446
16	2.1857
17	2.3267
18	2.4677
19	2.6087
20	2.7497

Fig. VI.4.(b) Primary Diffusion Coefficients for the Rose Soil. Contour Plot. Temperature, ^oK, v. Moisture Content, Dimensionless, v. $D_{\theta l}$ cm^2/sec x10^5 Contour Plot.

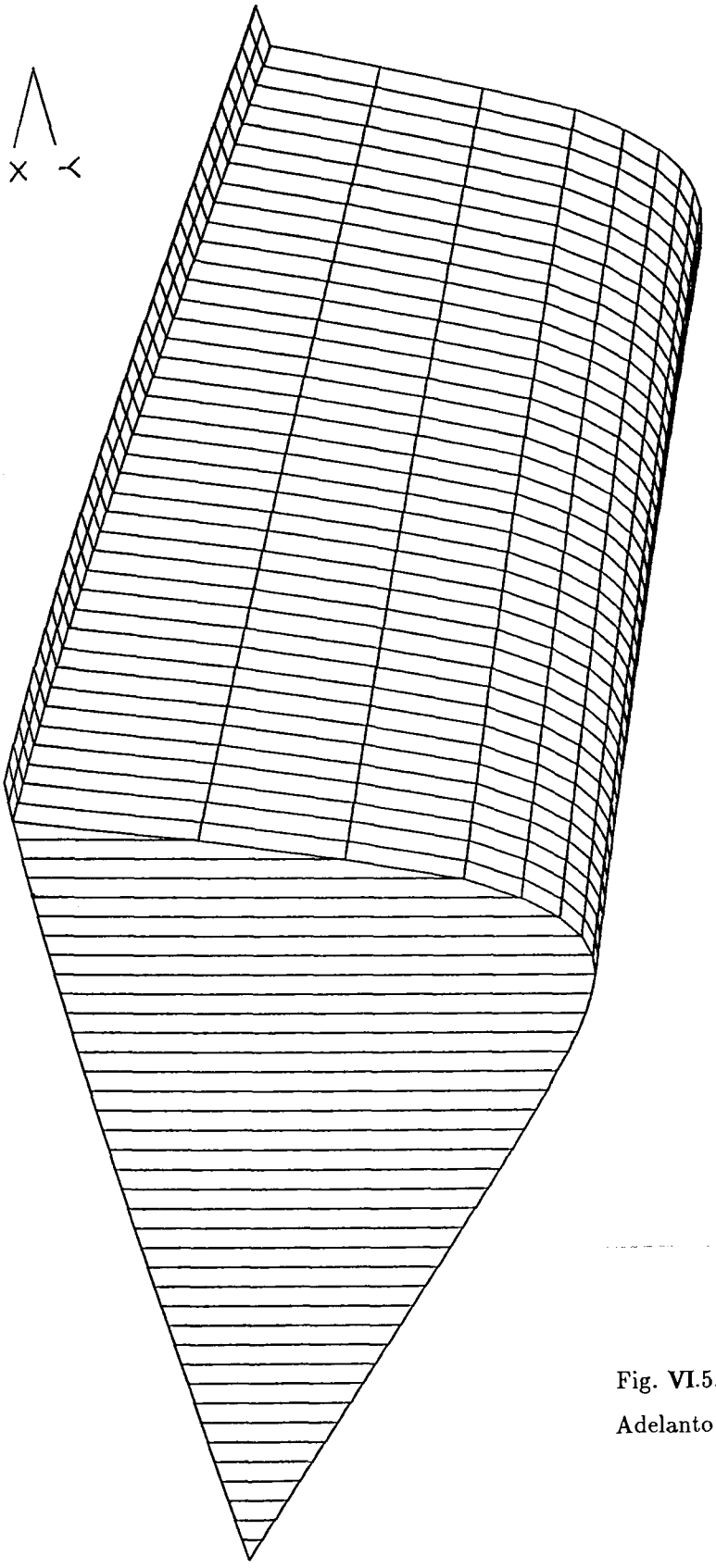

Fig. VI.5.(a) Primary Diffusion Coefficients. Adelanto Loam. D_{TV}x10^8 Surface Plot.

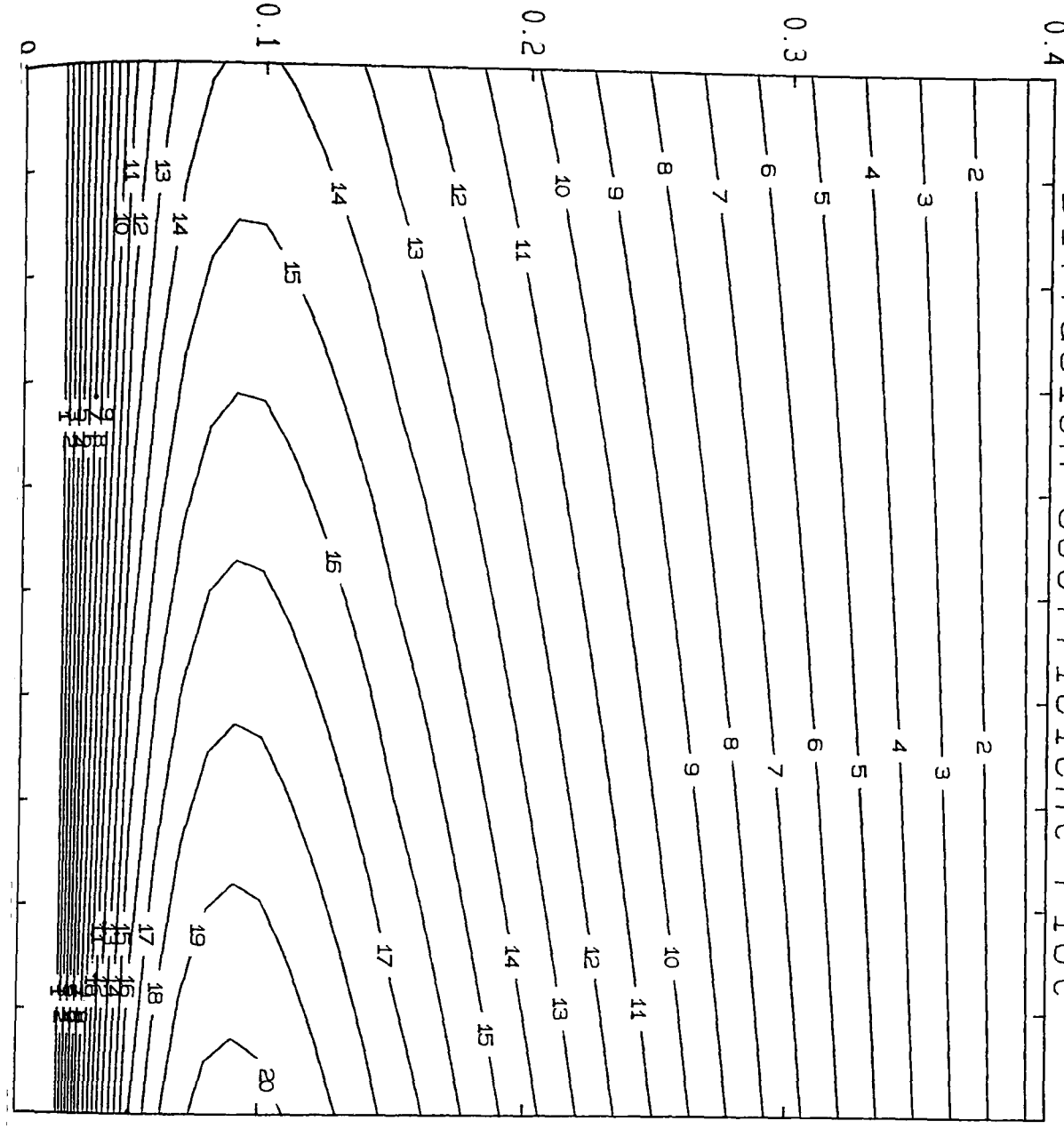

CONTOUR KEY	
1	0.1721
2	0.5162
3	0.8604
4	1.2045
5	1.5487
6	1.8928
7	2.2370
8	2.5811
9	2.9252
10	3.2694
11	3.6135
12	3.9577
13	4.3018
14	4.6460
15	4.9901
16	5.3343
17	5.6784
18	6.0226
19	6.3667
20	6.7109

Fig. VI.5.(b) Primary Diffusion Coefficients Adelanto Loam. Contour Plot.
Temperature, ^oK, v. Moisture Content, Dimensionless, v.
D_{TV} $cm^2/sec/^oK$ x 10^8 .

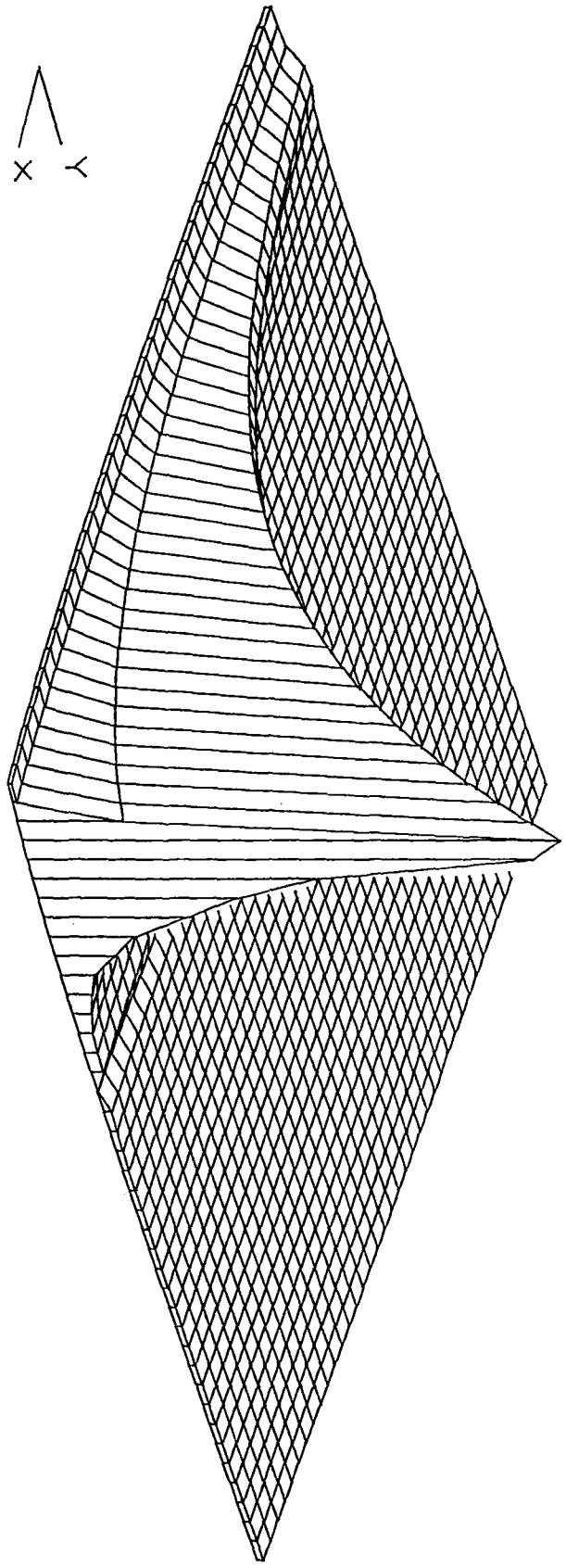

Fig. VI.6.(a) Primary Diffusion Coefficients. Adelanto Loam. $D_{\theta V}$x10^5 Surface Plot.

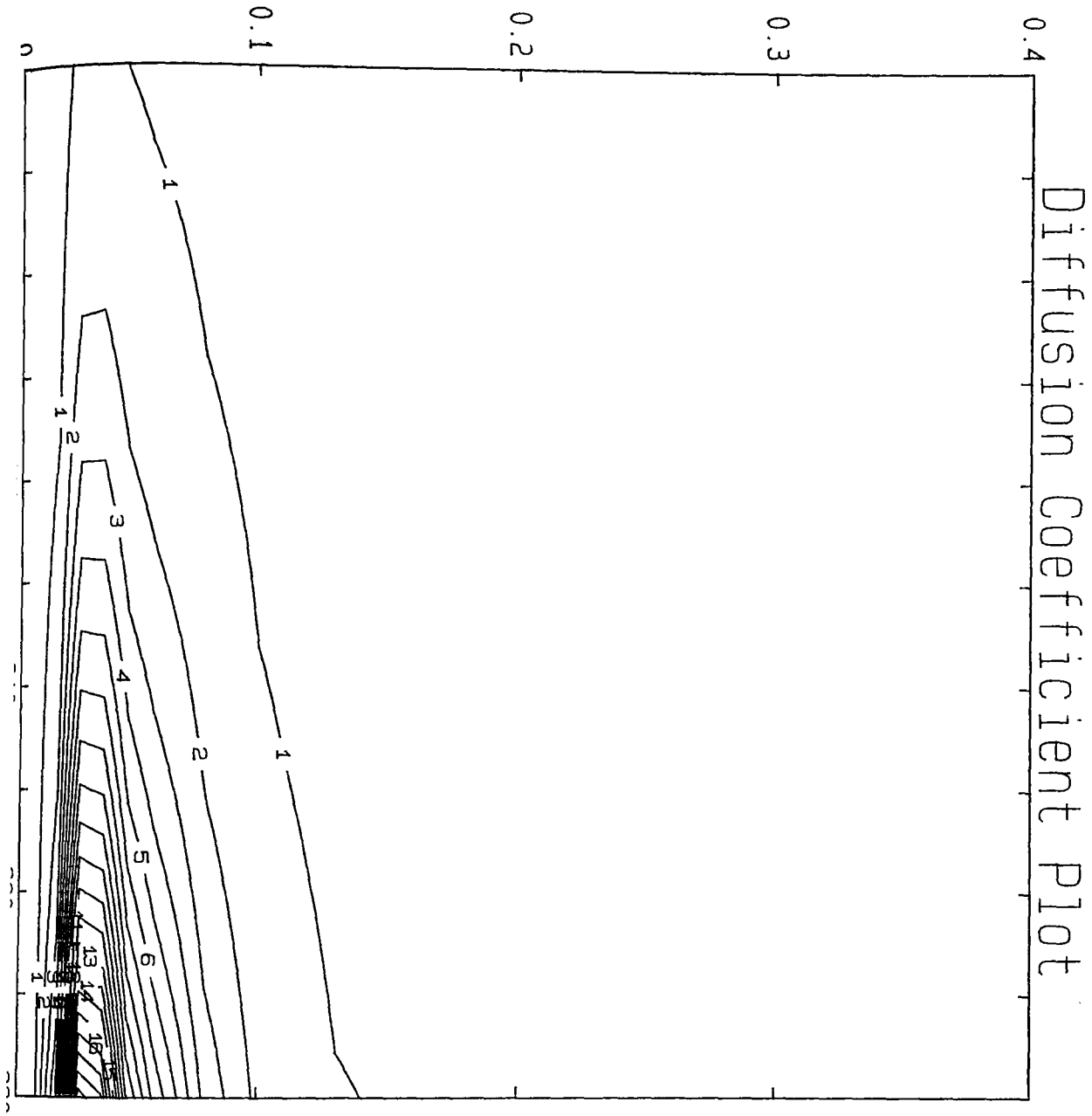

CONTOUR KEY	
1	6.1808
2	27.8117
3	49.4425
4	71.0734
5	92.7043
6	114.3352
7	135.9661
8	157.5970
9	179.2279
10	200.8587
11	222.4896
12	244.1205
13	265.7514
14	287.3823
15	309.0132
16	330.6441
17	352.2749
18	373.9058
19	395.5367
20	417.1676

Fig. VI.6.(b) Primary Diffusion Coefficients for Adelanto Loam. Contour Plot. Temperature, ^{o}K, v. Moisture Content, Dimensionless, v. $D_{\theta V}$ cm^2/sec x 10^5 .

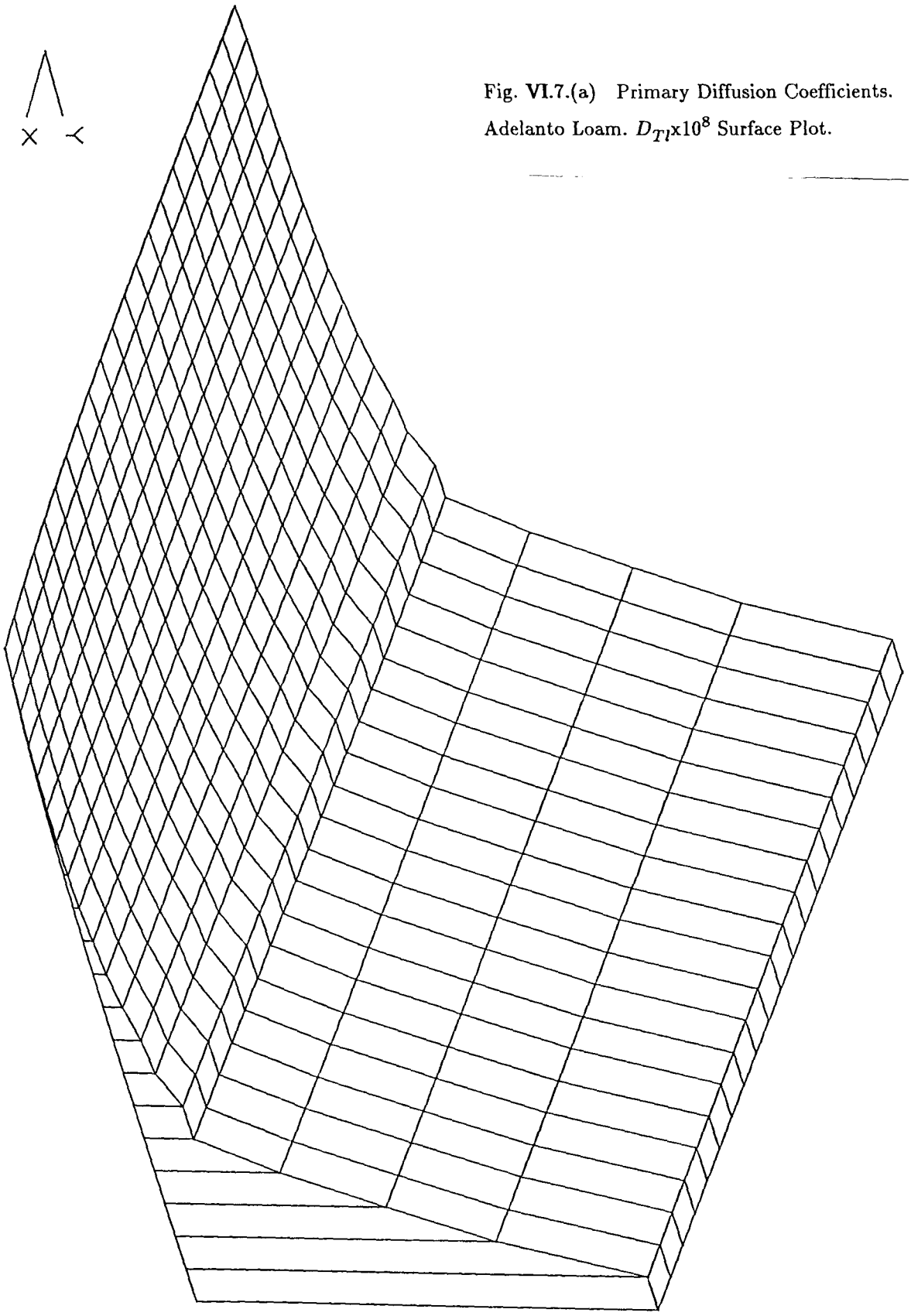

Fig. VI.7.(a) Primary Diffusion Coefficients.
Adelanto Loam. D_{Tl}x10^8 Surface Plot.

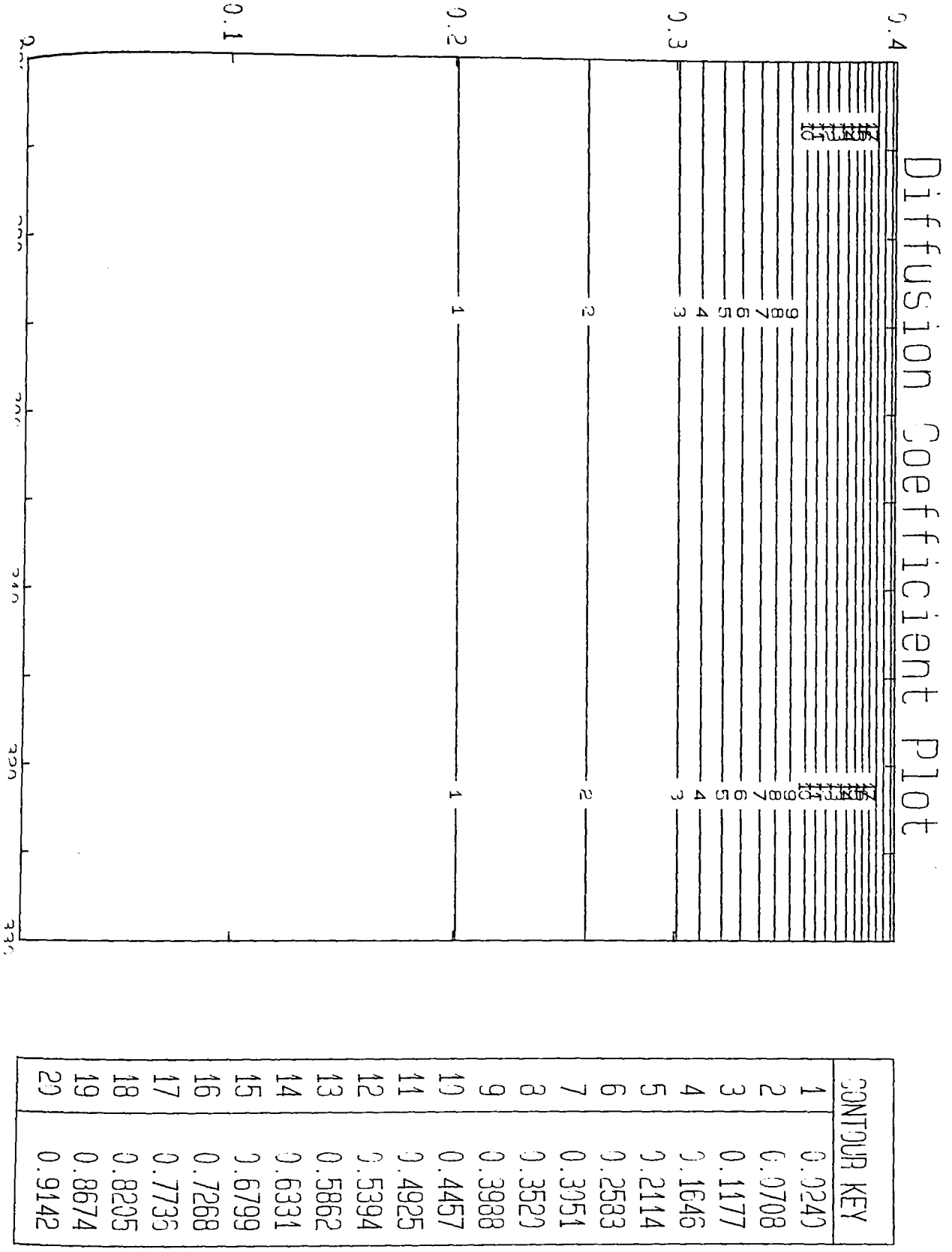

CONTOUR KEY	
1	0.0240
2	0.0708
3	0.1177
4	0.1646
5	0.2114
6	0.2583
7	0.3051
8	0.3520
9	0.3988
10	0.4457
11	0.4925
12	0.5394
13	0.5862
14	0.6331
15	0.6799
16	0.7268
17	0.7736
18	0.8205
19	0.8674
20	0.9142

Fig. VI.7.(b) Primary Diffusion Coefficients for Adelanto Loam. Contour Plot. Temperature, ^{o}K, v. Moisture Content, Dimensionless, v. $D_{Tl}\ cm^2/sec$ x 10^8 .

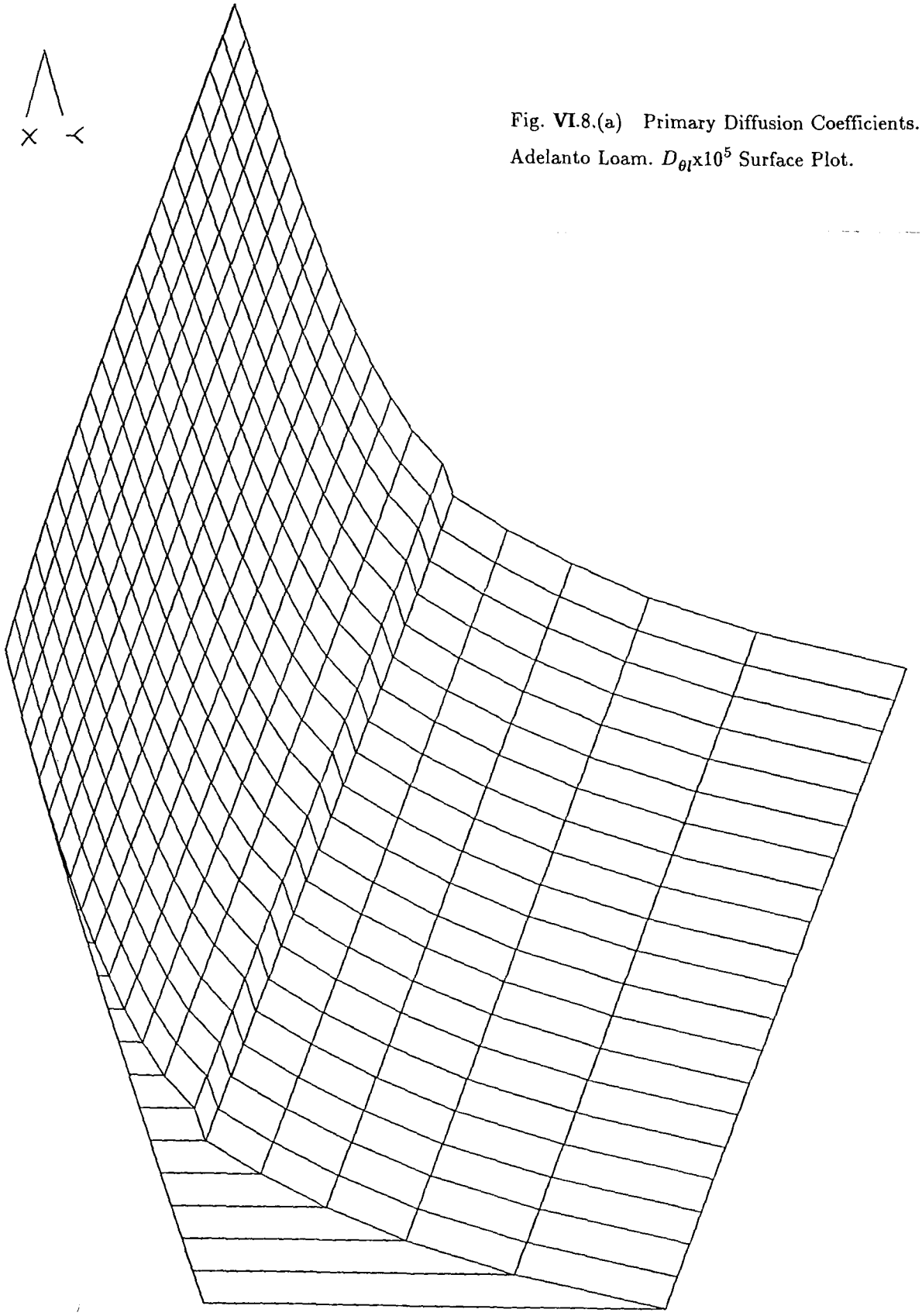

Fig. VI.8.(a) Primary Diffusion Coefficients. Adelanto Loam. $D_{\theta l}$x10^5 Surface Plot.

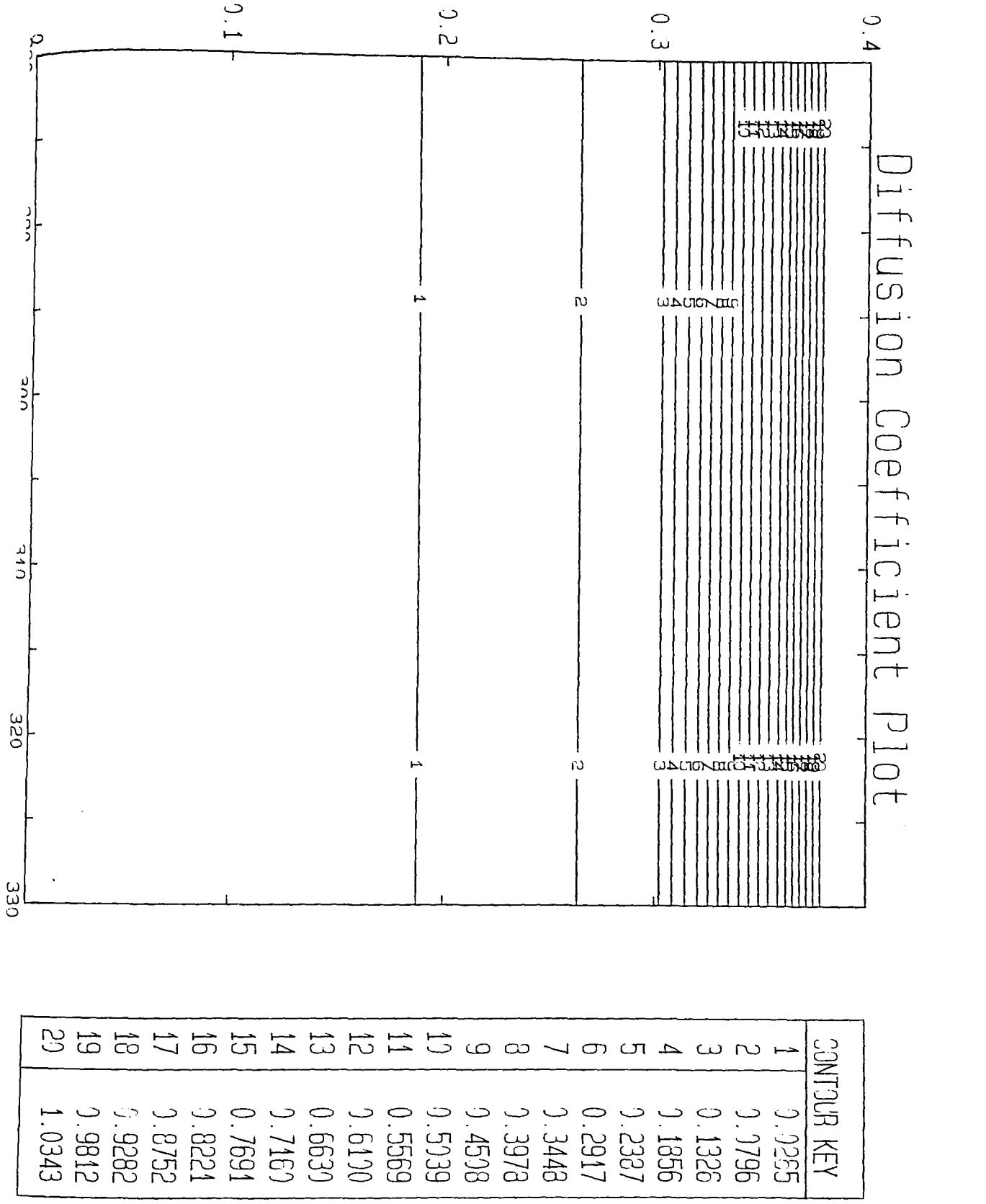

Fig. VI.8.(b) Primary Diffusion Coefficients for Adelanto Loam. Contour Plot. Temperature, ^{o}K, v. Moisture Content, Dimensionless, v. $D_{Tl}\ cm^2/sec/^{o}K$ x 10^5 .

Fig. VI.9.(a) Total Diffusion Coefficients.
The Rose Soil. a x10^3 Surface Plot.

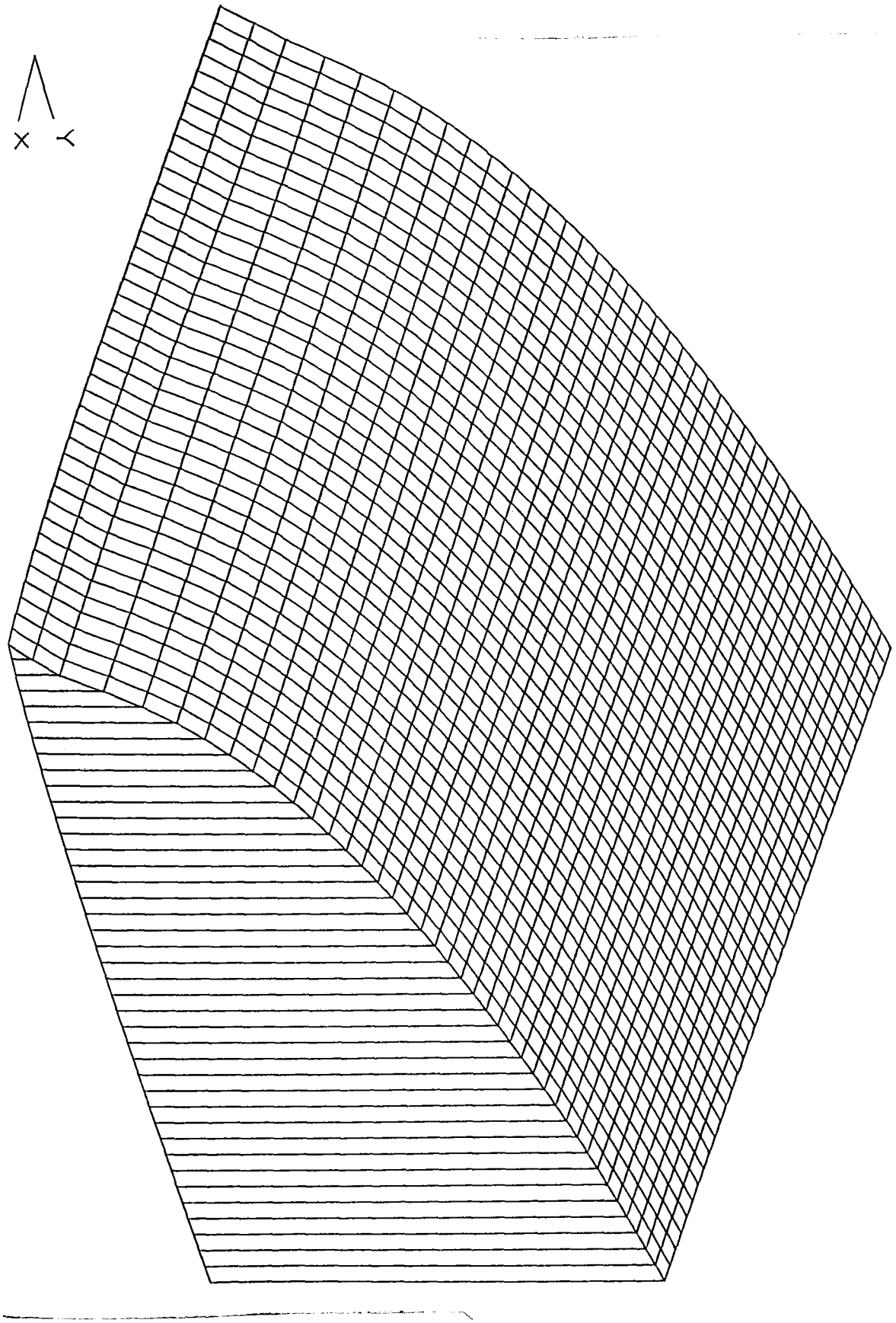

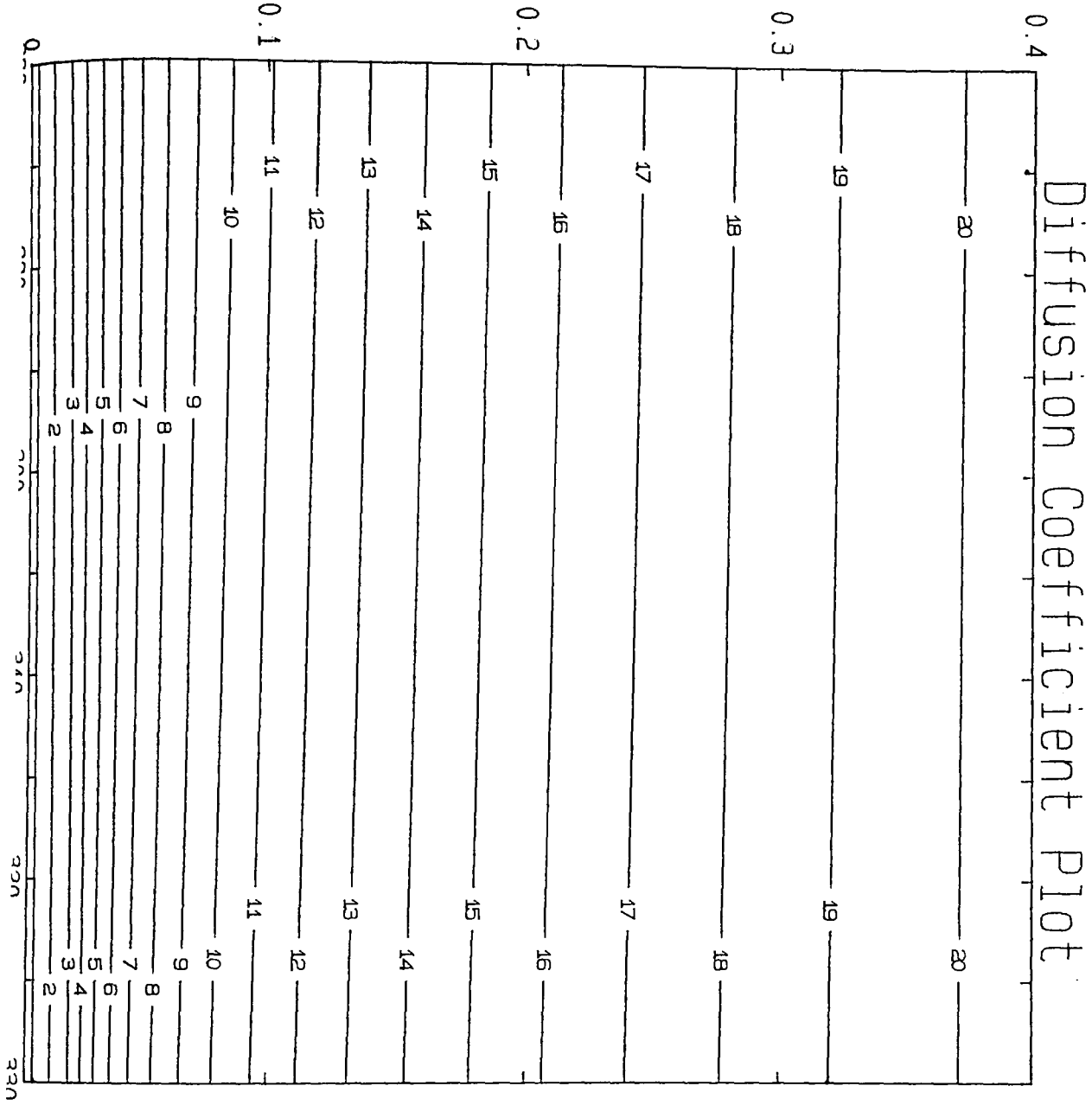

CONTOUR KEY	
1	275.8009
2	281.9487
3	288.0965
4	294.2443
5	300.3921
6	306.5399
7	312.6877
8	318.8355
9	324.9833
10	331.1311
11	337.2789
12	343.4267
13	349.5745
14	355.7223
15	361.8701
16	368.0179
17	374.1657
18	380.3135
19	386.4613
20	392.6091

Fig. VI.9.(b) Total Diffusion Coefficients for the Rose Soil.Contour Plot.
Temperature, ^oK, v. Moisture Content, Dimensionless, v.
a $cal/cm/sec/^oK$ x 10^3

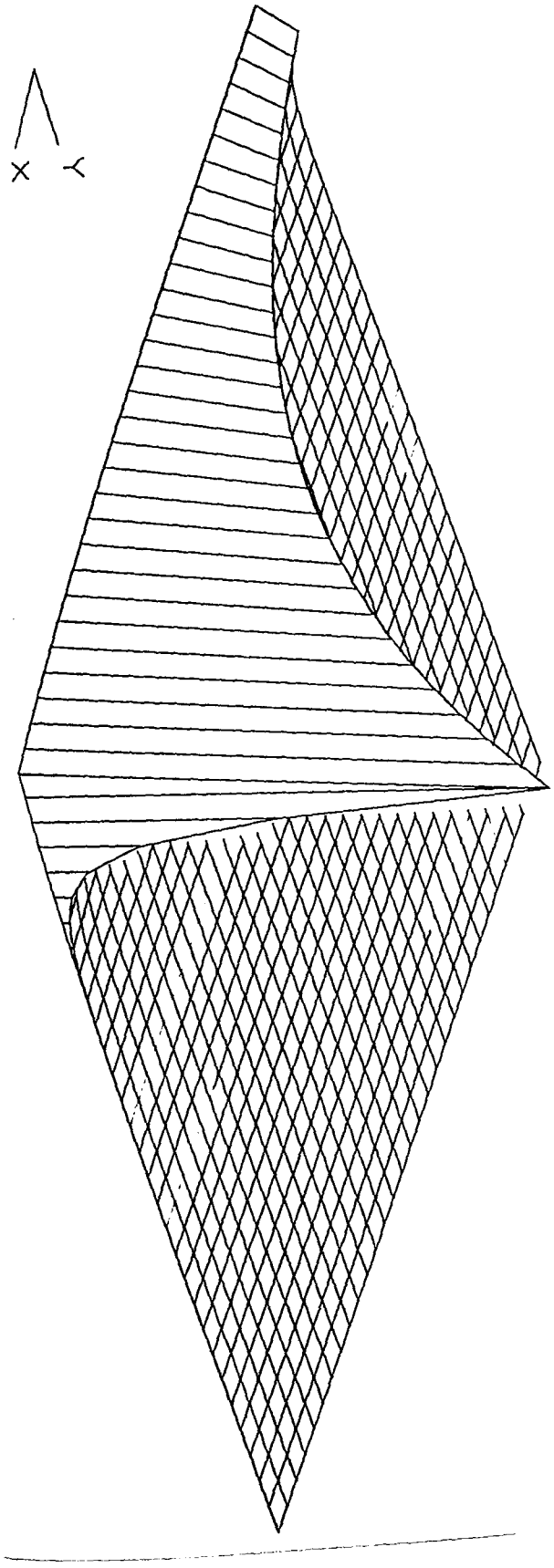

Fig. **VI**.10.(a) Total Diffusion Coefficients.
The Rose Soil. b x10^5 Surface Plot.

CONTOUR KEY	
1	3.7321
2	11.1964
3	18.6606
4	26.1249
5	33.5891
6	41.0534
7	48.5176
8	55.9819
9	63.4461
10	70.9104
11	78.3746
12	85.8389
13	93.3031
14	100.7674
15	108.2316
16	115.6959
17	123.1601
18	130.6244
19	138.0886
20	145.5529

Fig. VI.10.(b) Total Diffusion Coefficients for the Rose Soil.Contour Plot.
Temperature, ^{o}K, v. Moisture Content, Dimensionless, v.
b $cal/cm/sec$ x 10^{5}

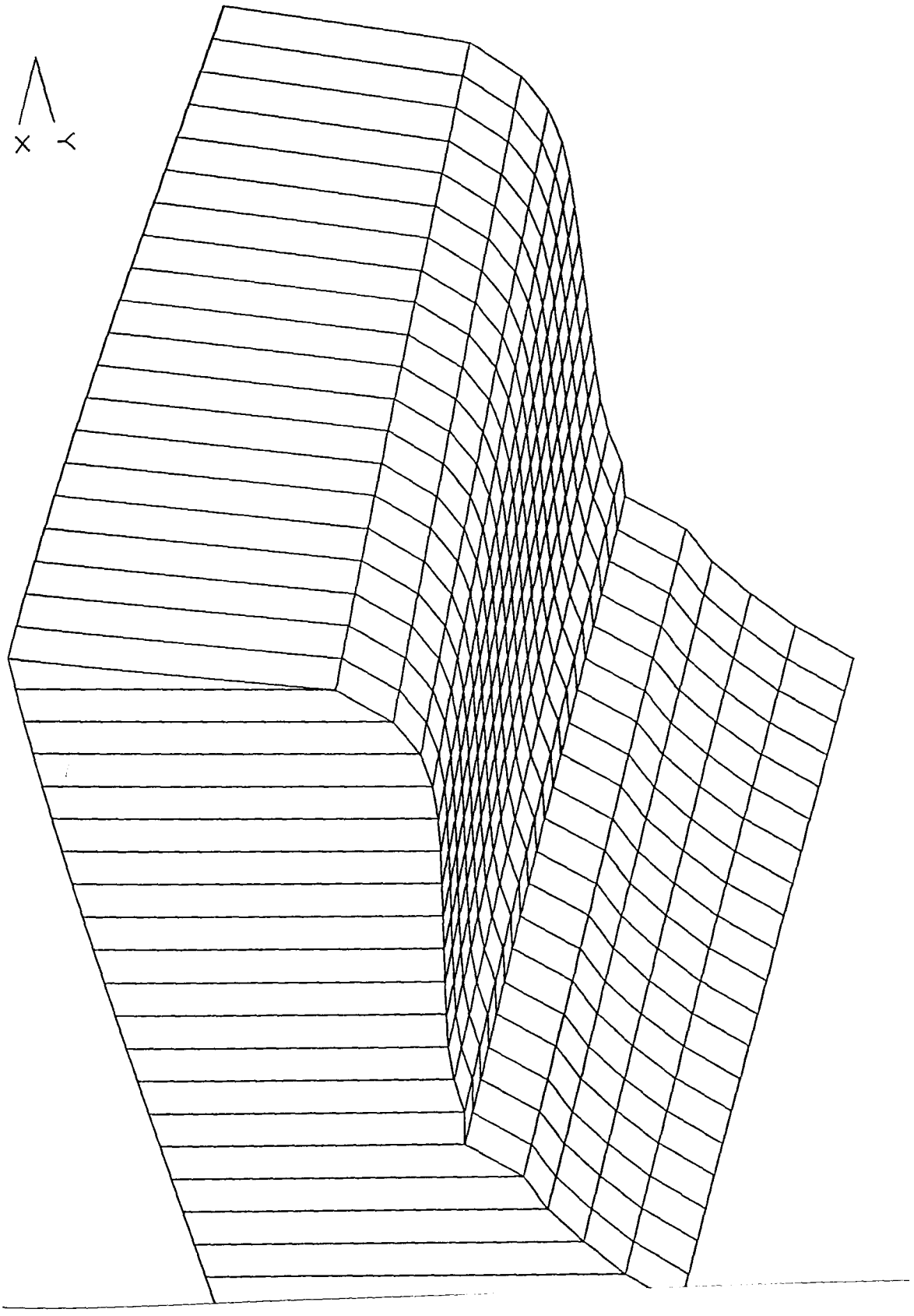

Fig. VI.11.(a) Total Diffusion Coefficients.
The Rose Soil. r x10^8 Surface Plot.

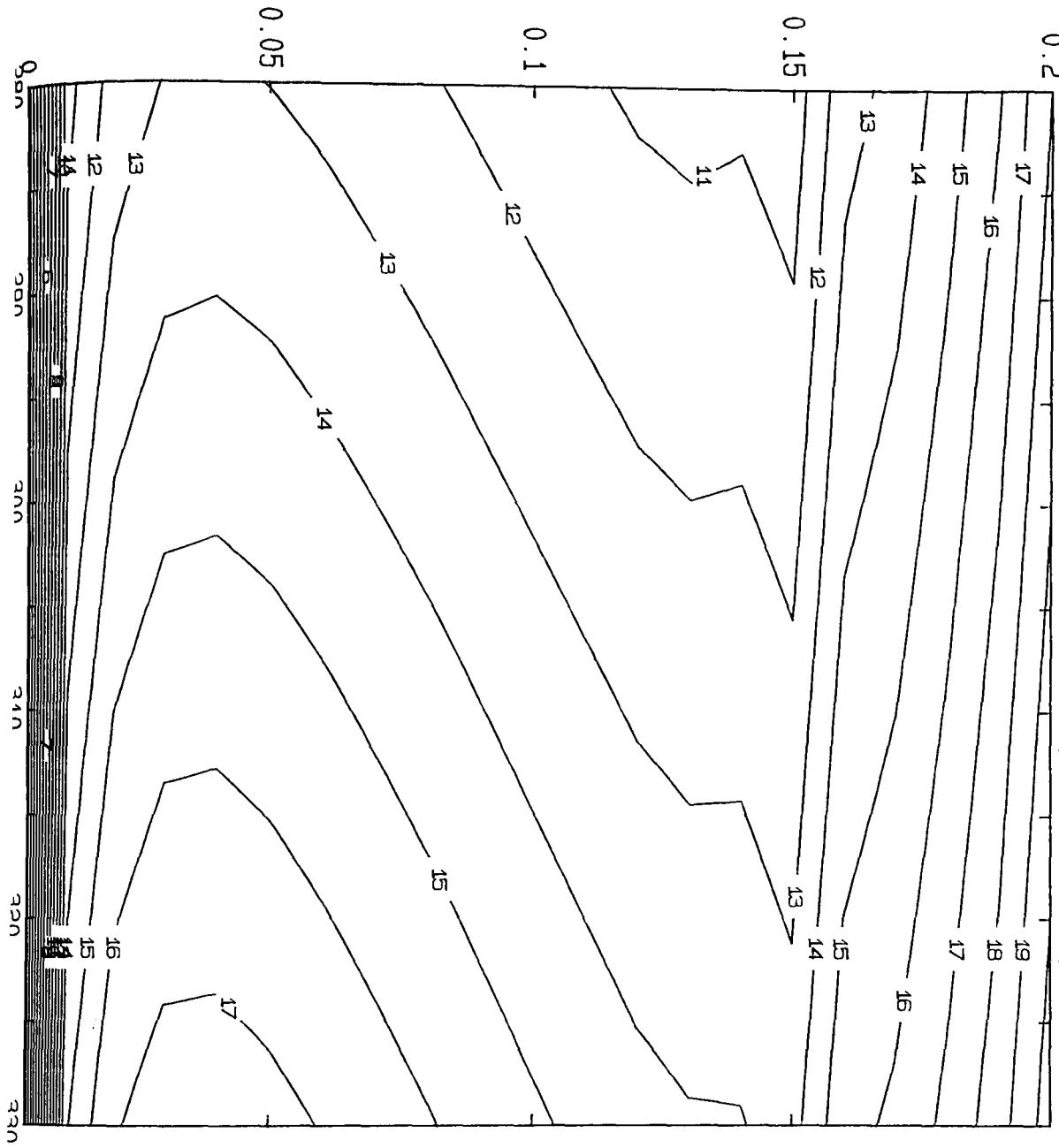

CONTOUR KEY	
1	0.2379
2	0.7138
3	1.1897
4	1.6655
5	2.1414
6	2.6172
7	3.0931
8	3.5690
9	4.0448
10	4.5207
11	4.9966
12	5.4724
13	5.9483
14	6.4242
15	6.9000
16	7.3759
17	7.8517
18	8.3276
19	8.8035
20	9.2793

Fig. **VI**.11.(b) Total Diffusion Coefficients for the Rose Soil. Contour Plot. Temperature, ^{o}K, v. Moisture Content, Dimensionless, v. $r\ cal/cm/sec/^{o}K$ x 10^{8}

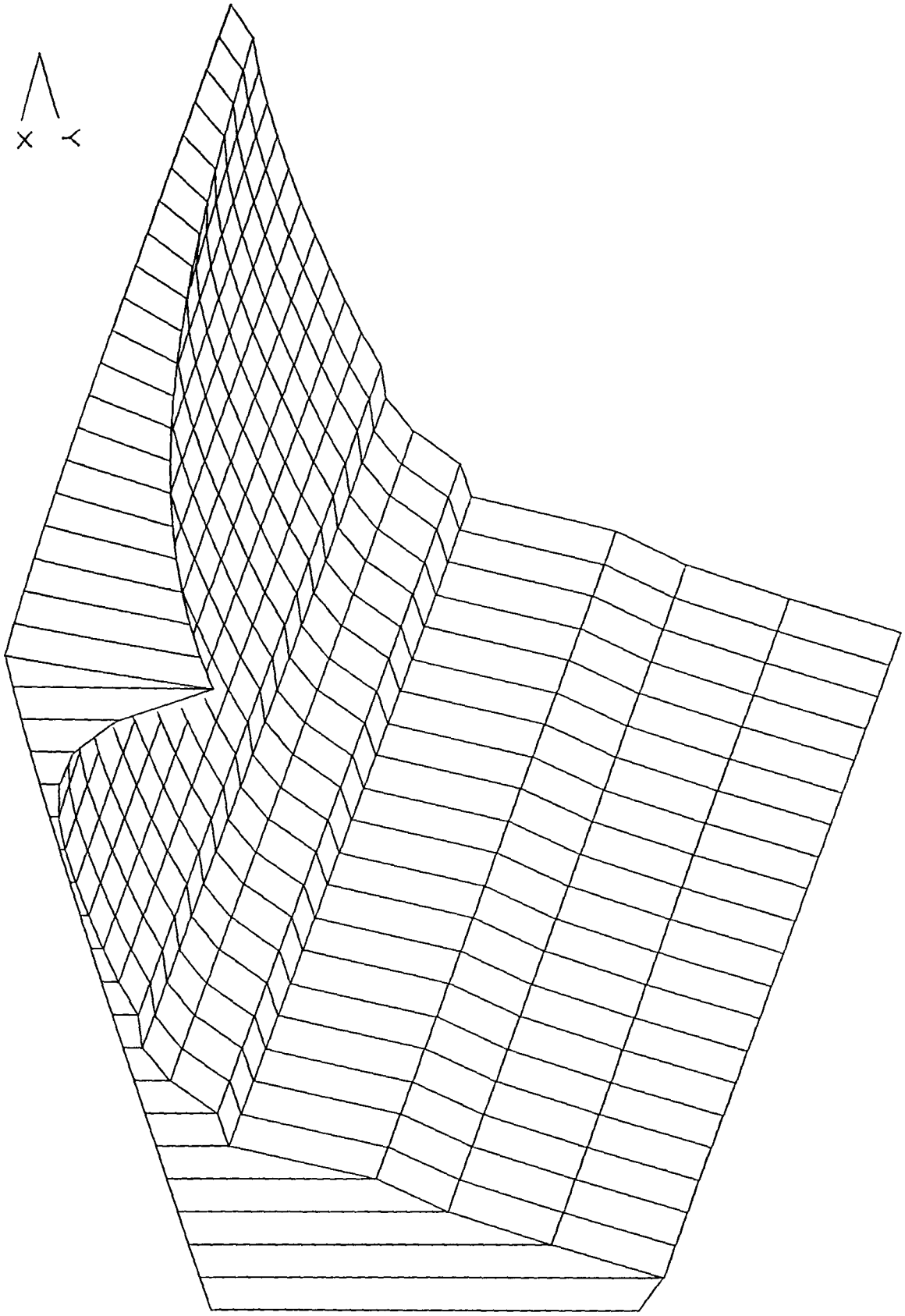

Fig. VI.12.(a) Total Diffusion Coefficients.
The Rose Soil. s x10^5 Surface Plot.

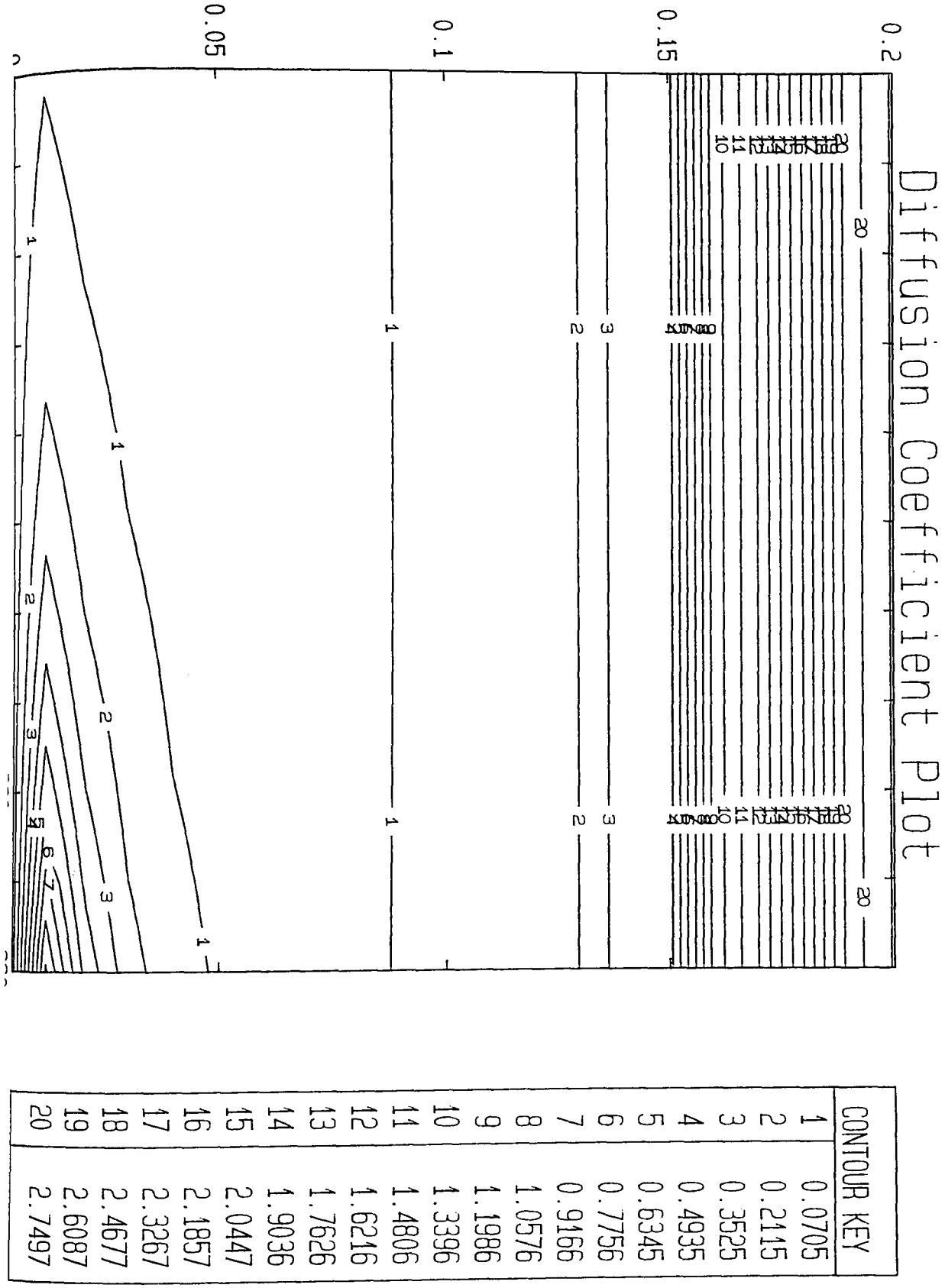

CONTOUR KEY	
1	0.0705
2	0.2115
3	0.3525
4	0.4935
5	0.6345
6	0.7756
7	0.9166
8	1.0576
9	1.1986
10	1.3396
11	1.4806
12	1.6216
13	1.7626
14	1.9036
15	2.0447
16	2.1857
17	2.3267
18	2.4677
19	2.6087
20	2.7497

Fig. VI.12.(b) Total Diffusion Coefficients for the Rose Soil. Contour Plot. Temperature, ^{o}K, v. Moisture Content, Dimensionless, v. s $cal/cm/sec$ x 10^{5}

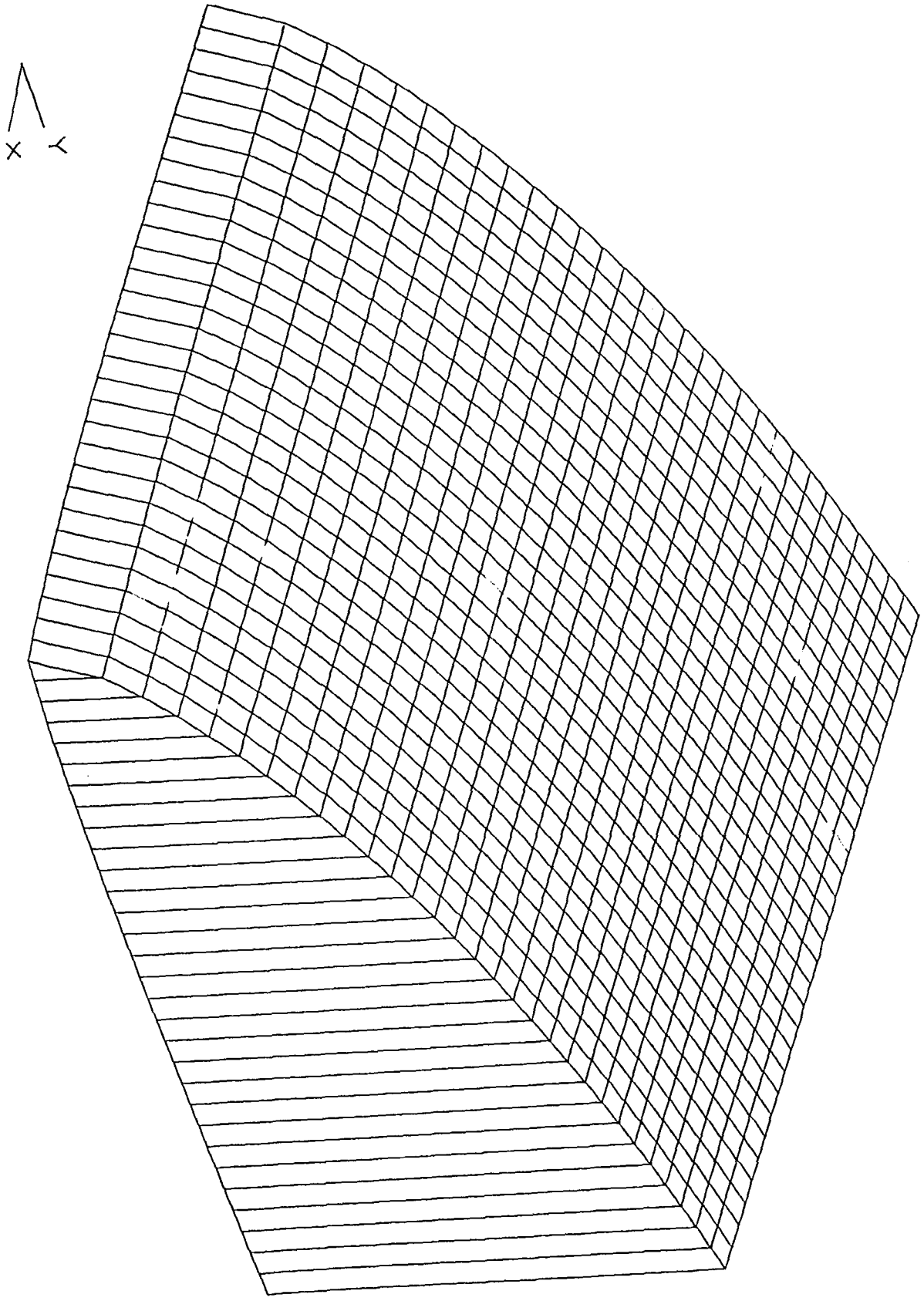

Fig. VI.13.(a) Total Diffusion Coefficients. Adelanto Loam. a x10^3 Surface Plot.

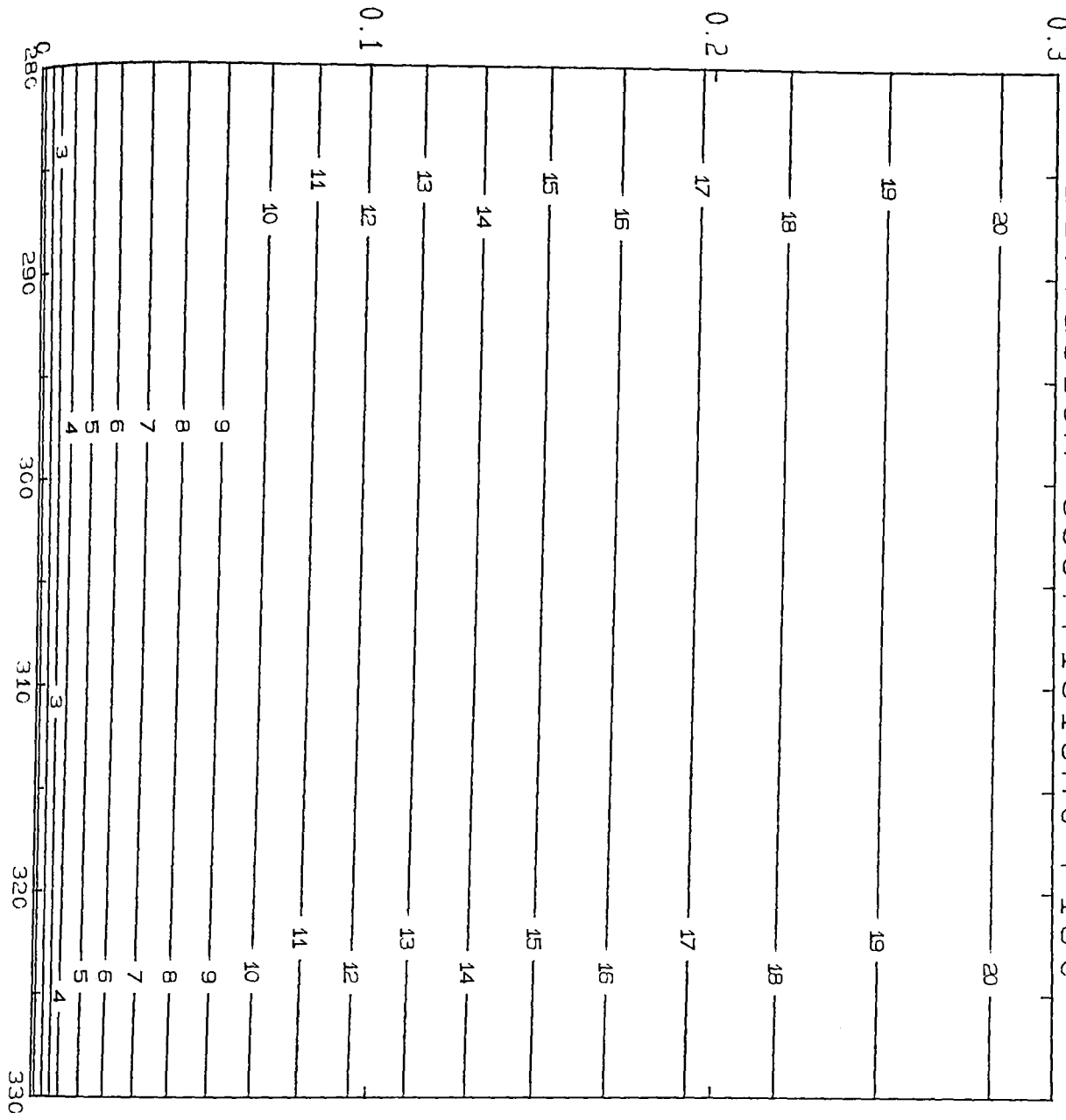

CONTOUR KEY	
1	2.7547
2	2.8096
3	2.8644
4	2.9193
5	2.9742
6	3.0291
7	3.0839
8	3.1388
9	3.1937
10	3.2485
11	3.3034
12	3.3583
13	3.4131
14	3.4680
15	3.5229
16	3.5777
17	3.6326
18	3.6875
19	3.7424
20	3.7972

Fig. VI.13.(b) Total Diffusion Coefficients for Adelanto Loam. Contour Plot. Temperature, ^oK, v. Moisture Content, Dimensionless, v. $a\ cal/cm/sec/^oK \times 10^{3}$

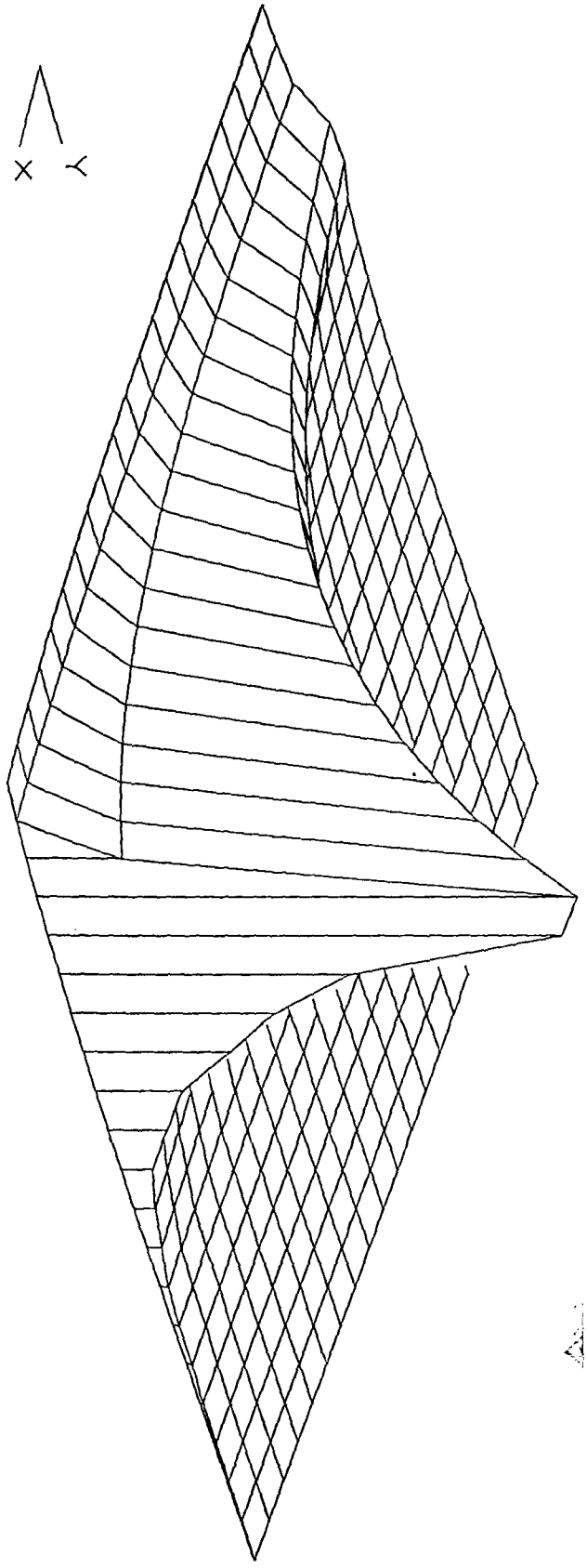

Fig. VI.14.(a) Total Diffusion Coefficients. Adelanto Loam. b x10^5 Surface Plot.

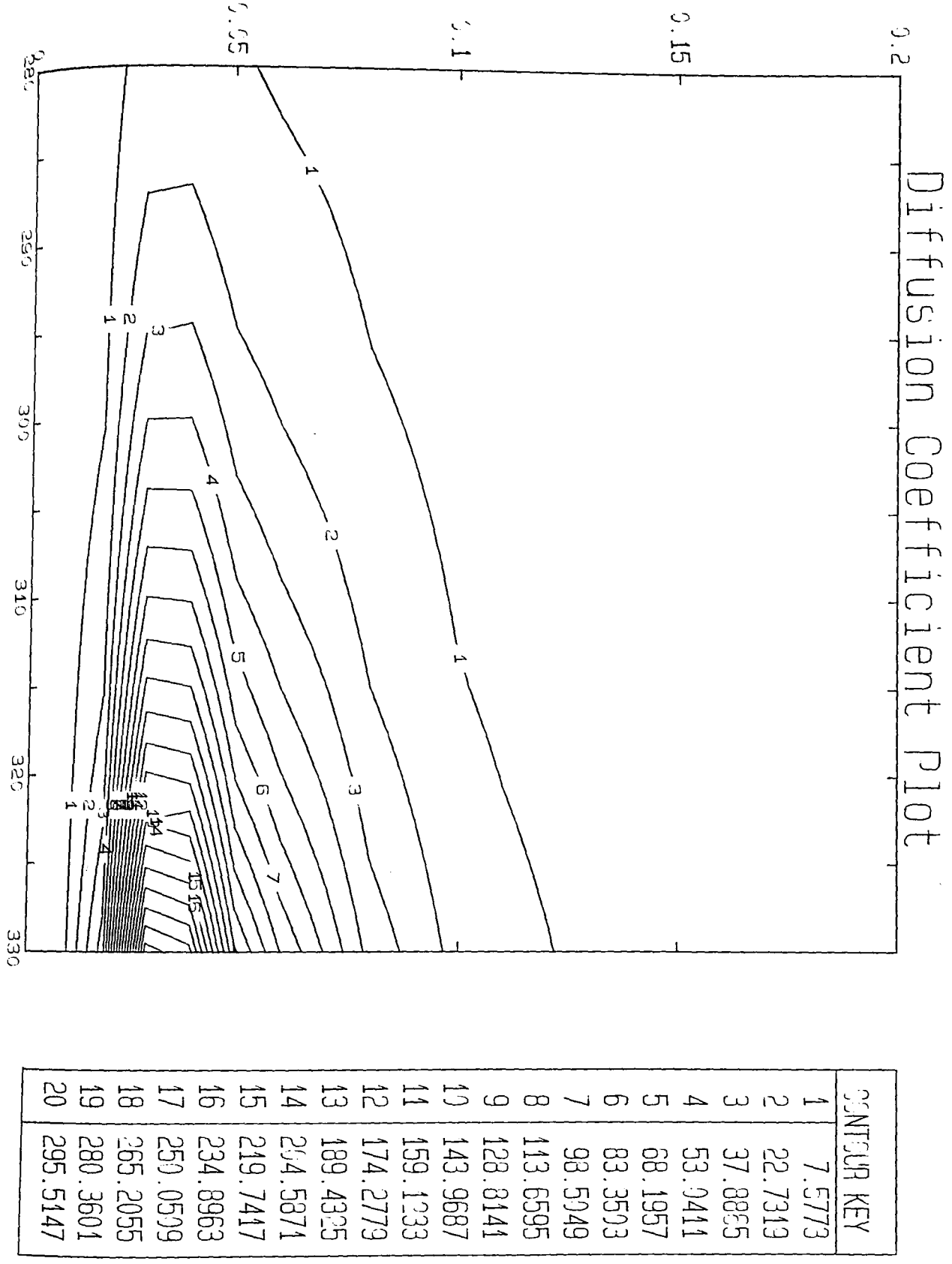

CONTOUR KEY	
1	7.5773
2	22.7319
3	37.8865
4	53.0411
5	68.1957
6	83.3503
7	98.5049
8	113.6595
9	128.8141
10	143.9687
11	159.1233
12	174.2779
13	189.4325
14	204.5871
15	219.7417
16	234.8963
17	250.0509
18	265.2055
19	280.3601
20	295.5147

Fig. VI.14.(b) Total Diffusion Coefficients for Adelanto Loam. Contour Plot.
Temperature, ^{o}K, v. Moisture Content, Dimensionless, v.
b $cal/cm/sec$ x 10^{5}

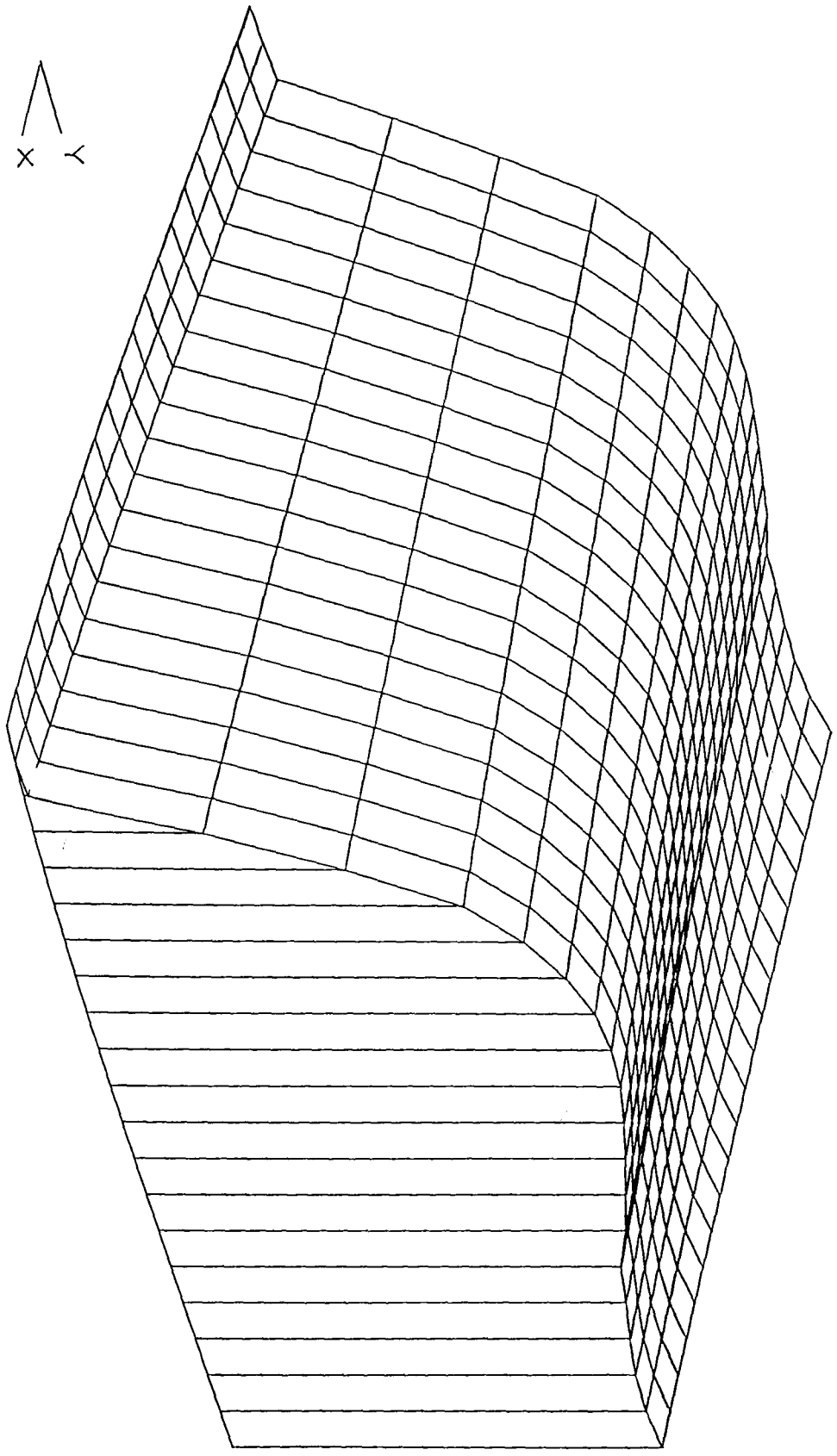

Fig. VI.15.(a) Total Diffusion Coefficients.
Adelanto Loam. r x10^8 Surface Plot.

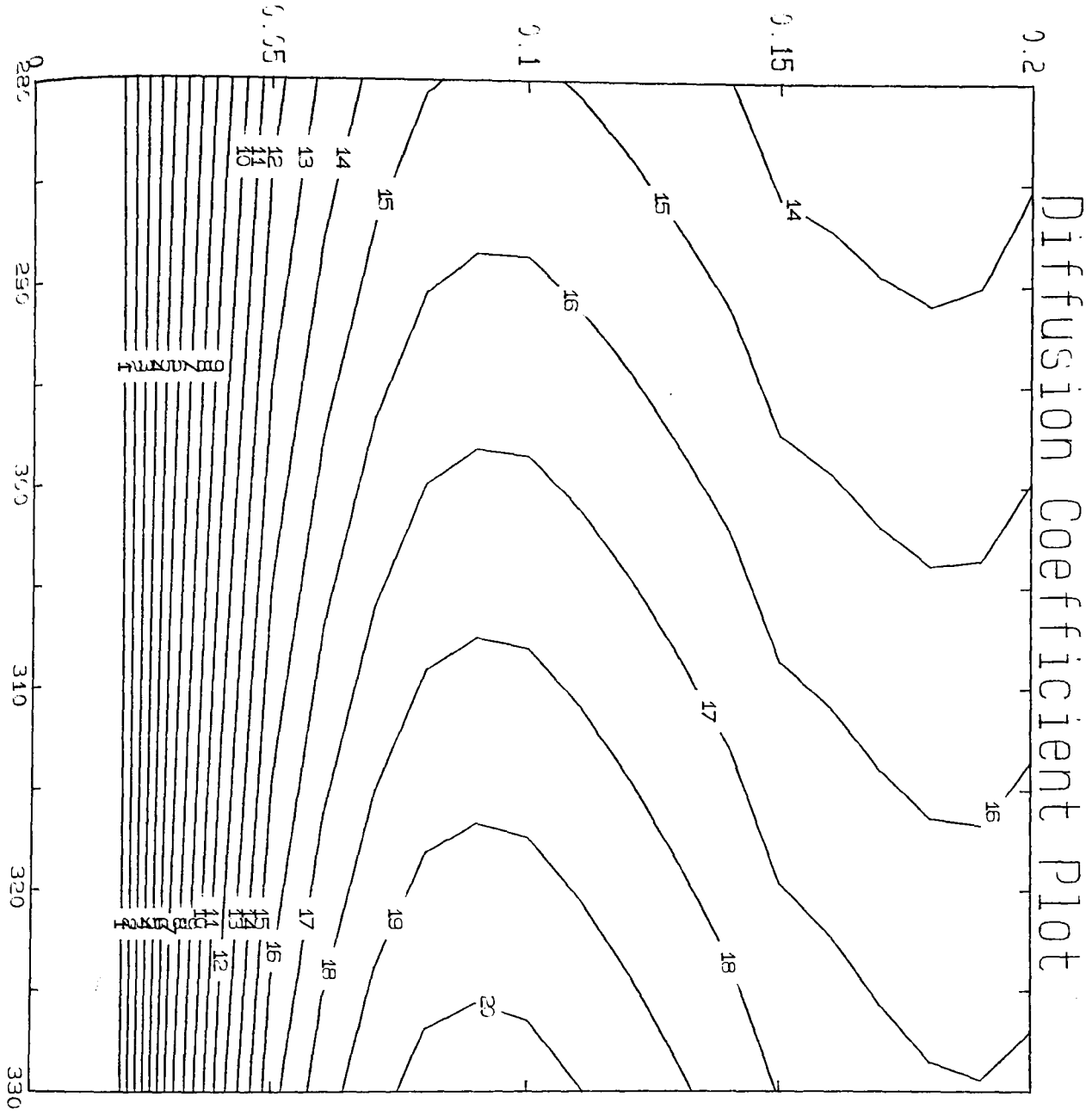

CONTOUR KEY	
1	0.1666
2	0.4987
3	0.8309
4	1.1630
5	1.4951
6	1.8272
7	2.1593
8	2.4914
9	2.8235
10	3.1556
11	3.4877
12	3.8198
13	4.1519
14	4.4840
15	4.8161
16	5.1482
17	5.4804
18	5.8125
19	6.1446
20	6.4767

Fig. VI.15.(b) Total Diffusion Coefficients, Adelanto Loam. Contour Plot. Temperature, ^oK, v. Moisture Content, Dimensionless, v. $r\ cal/cm/sec/^oK$ x 10^{8}

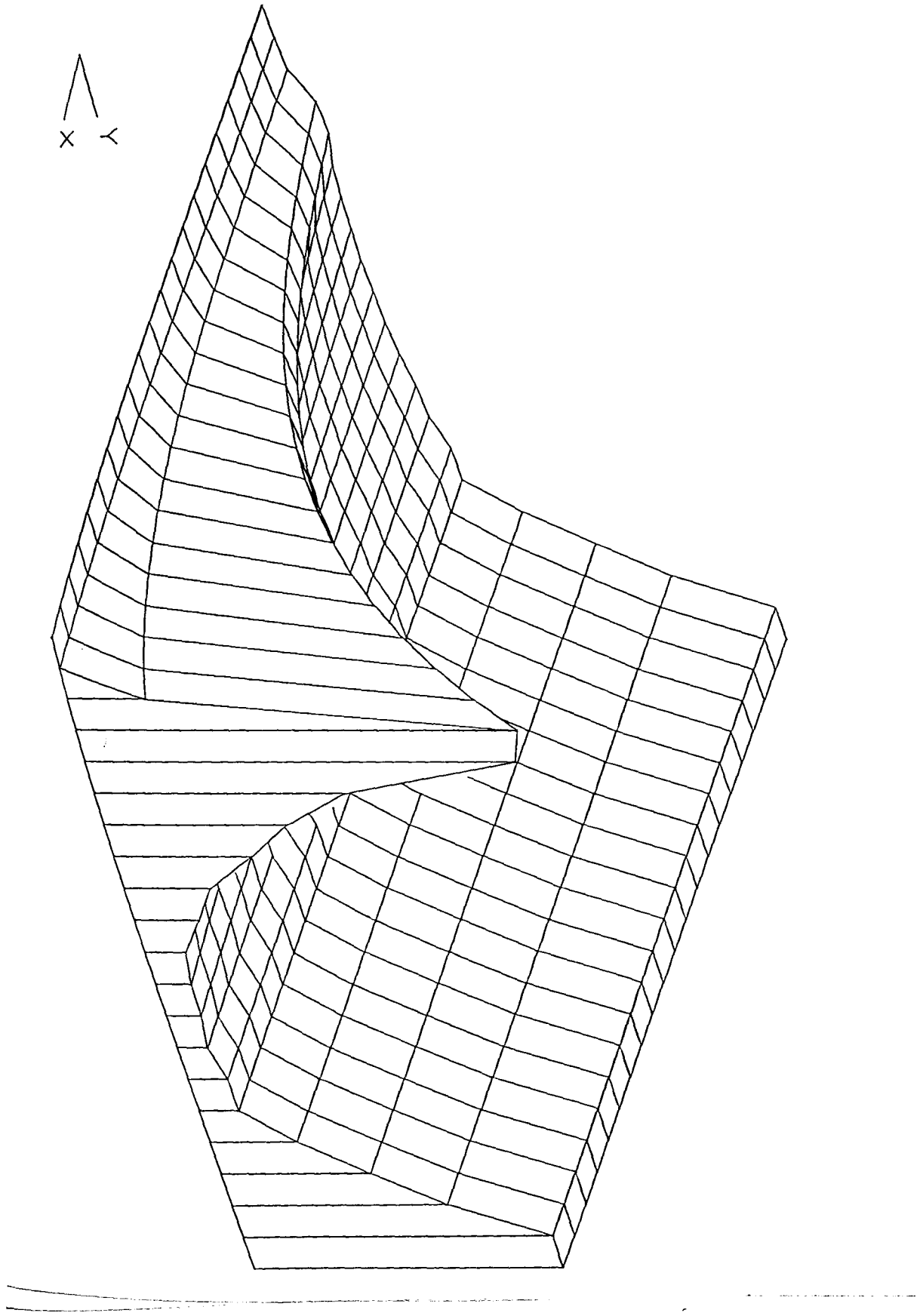

Fig. VI.16.(a) Total Diffusion Coefficients.
Adelanto Loam. s x10^5 Surface Plot.

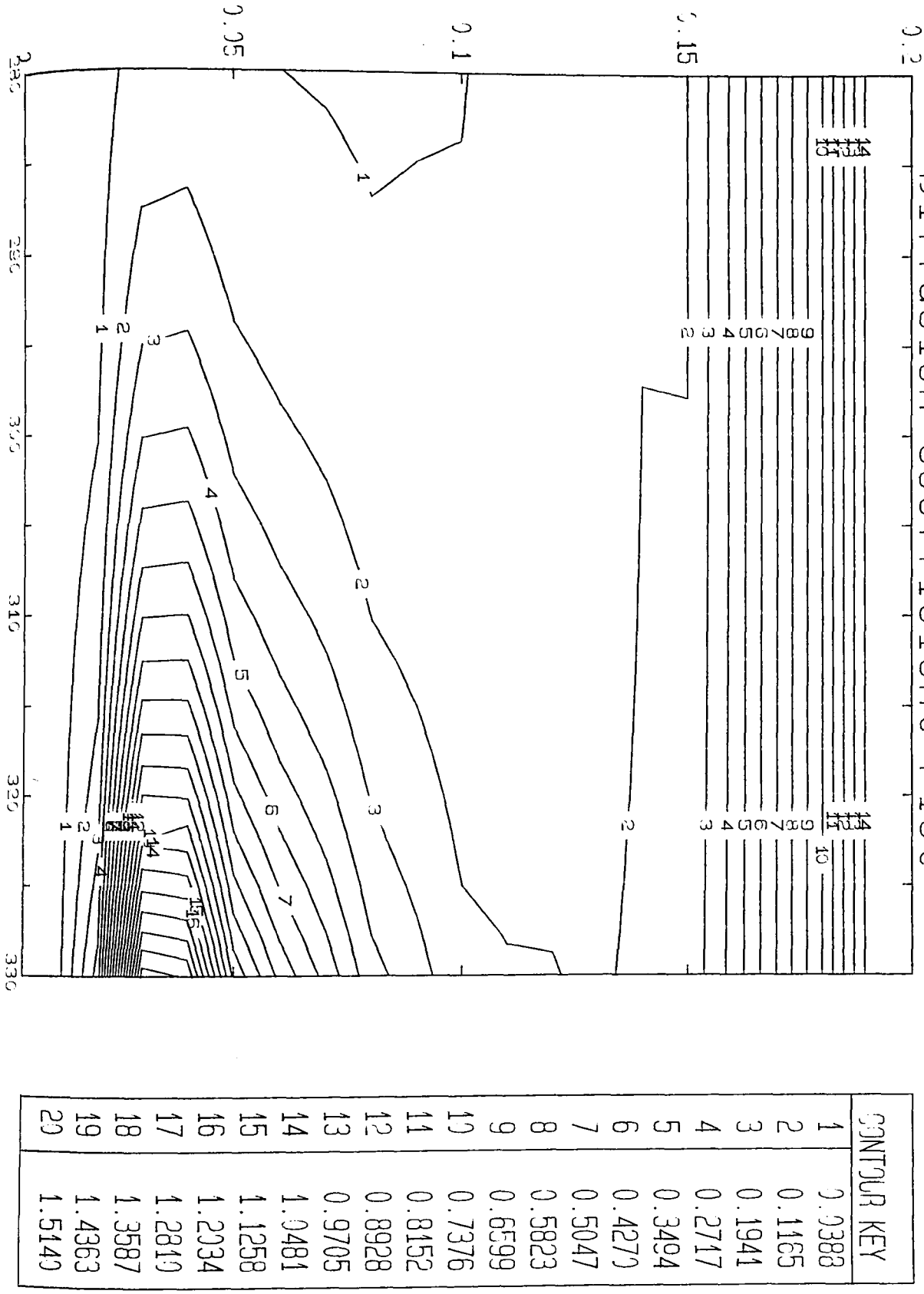

CONTOUR KEY	
1	0.0388
2	0.1165
3	0.1941
4	0.2717
5	0.3494
6	0.4270
7	0.5047
8	0.5823
9	0.6599
10	0.7376
11	0.8152
12	0.8928
13	0.9705
14	1.0481
15	1.1258
16	1.2034
17	1.2810
18	1.3587
19	1.4363
20	1.5140

Fig. VI.16.(b) Total Diffusion Coefficients, Adelanto Loam. Contour Plot.
Temperature, ^{o}K, v. Moisture Content, Dimensionless, $\dot{v}$.
s $cal/cm/sec$ x 10^{5}

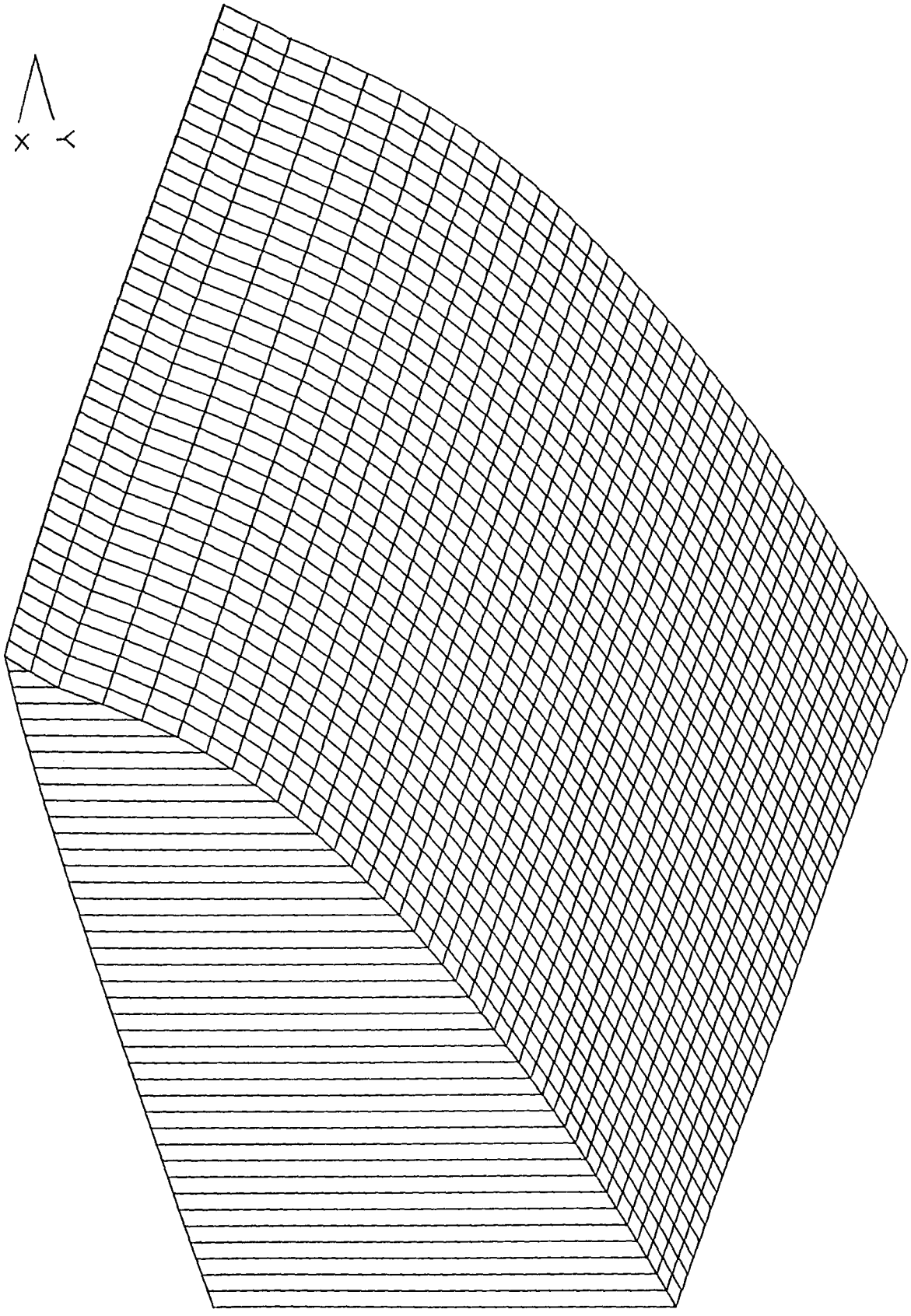

Fig. VI. 17(a) Eigenvalue Surfaces.
The Rose Soil, η_1 x 10^3, Surface Plot.

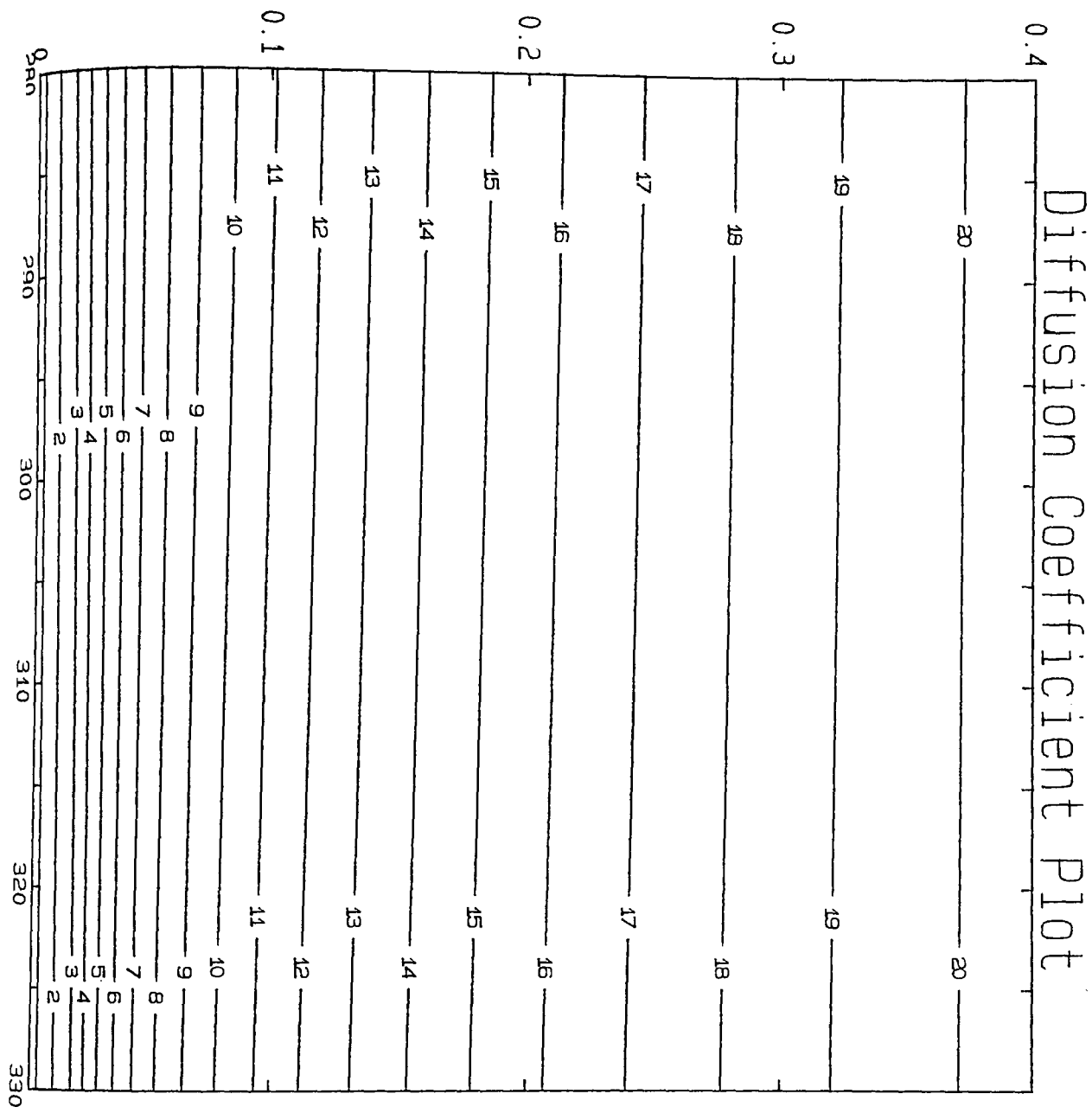

CONTOUR KEY	
1	2.7580
2	2.8195
3	2.8810
4	2.9424
5	3.0039
6	3.0654
7	3.1269
8	3.1884
9	3.2498
10	3.3113
11	3.3728
12	3.4343
13	3.4957
14	3.5572
15	3.6187
16	3.6802
17	3.7417
18	3.8031
19	3.8646
20	3.9261

Fig. VI. 17(b) Eigenvalue Surfaces for the Rose Soil, Contour Plot.
Temperature, ^{o}K, v. Moisture Content, Dimensionless, v.
η_1 *dimensionless* x 10^{3}.

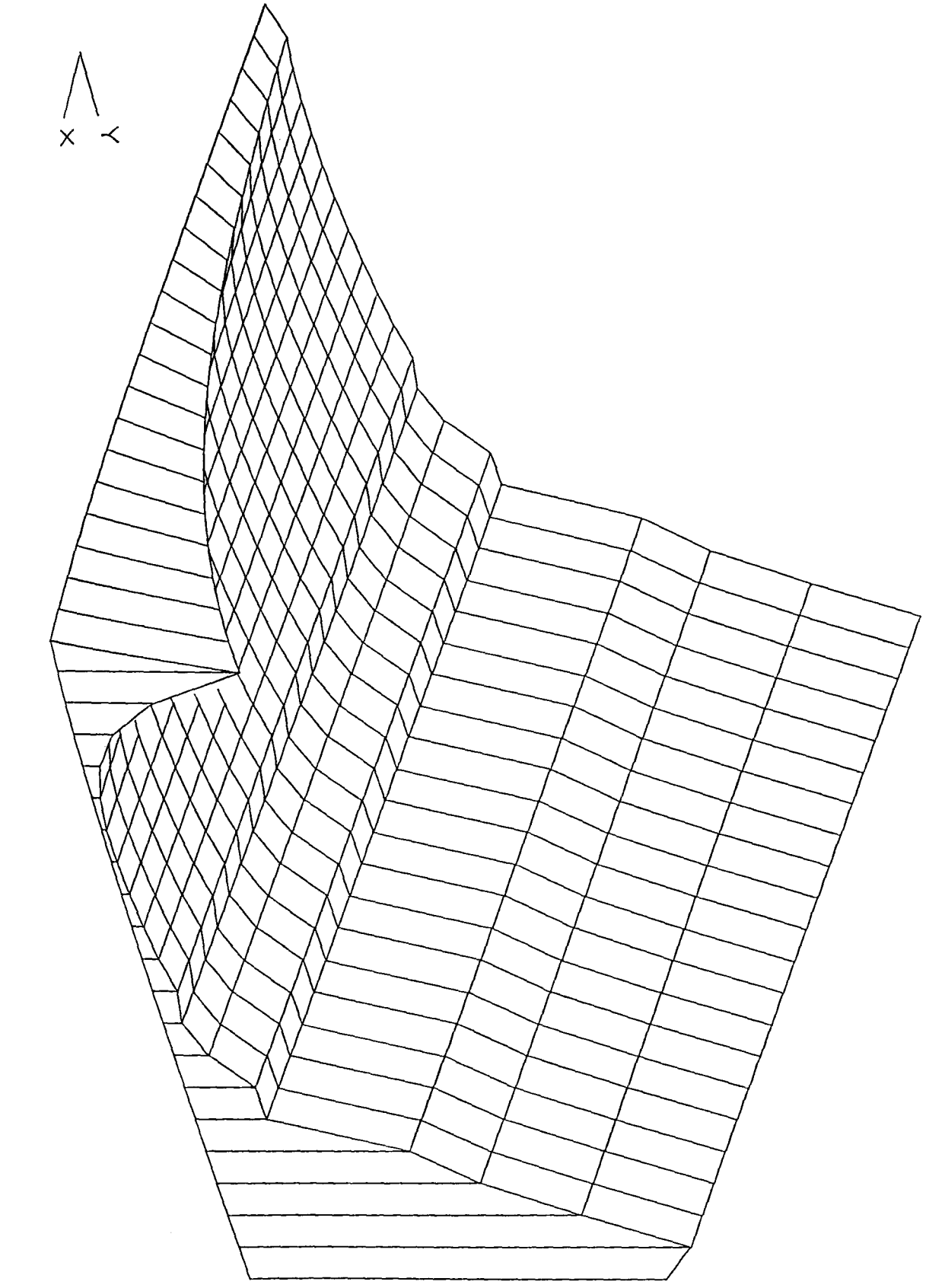

Fig. **VI.** 18(a) Eigenvalue Surfaces.
The Rose Soil, η_2 x 10^5, Surface Plot.

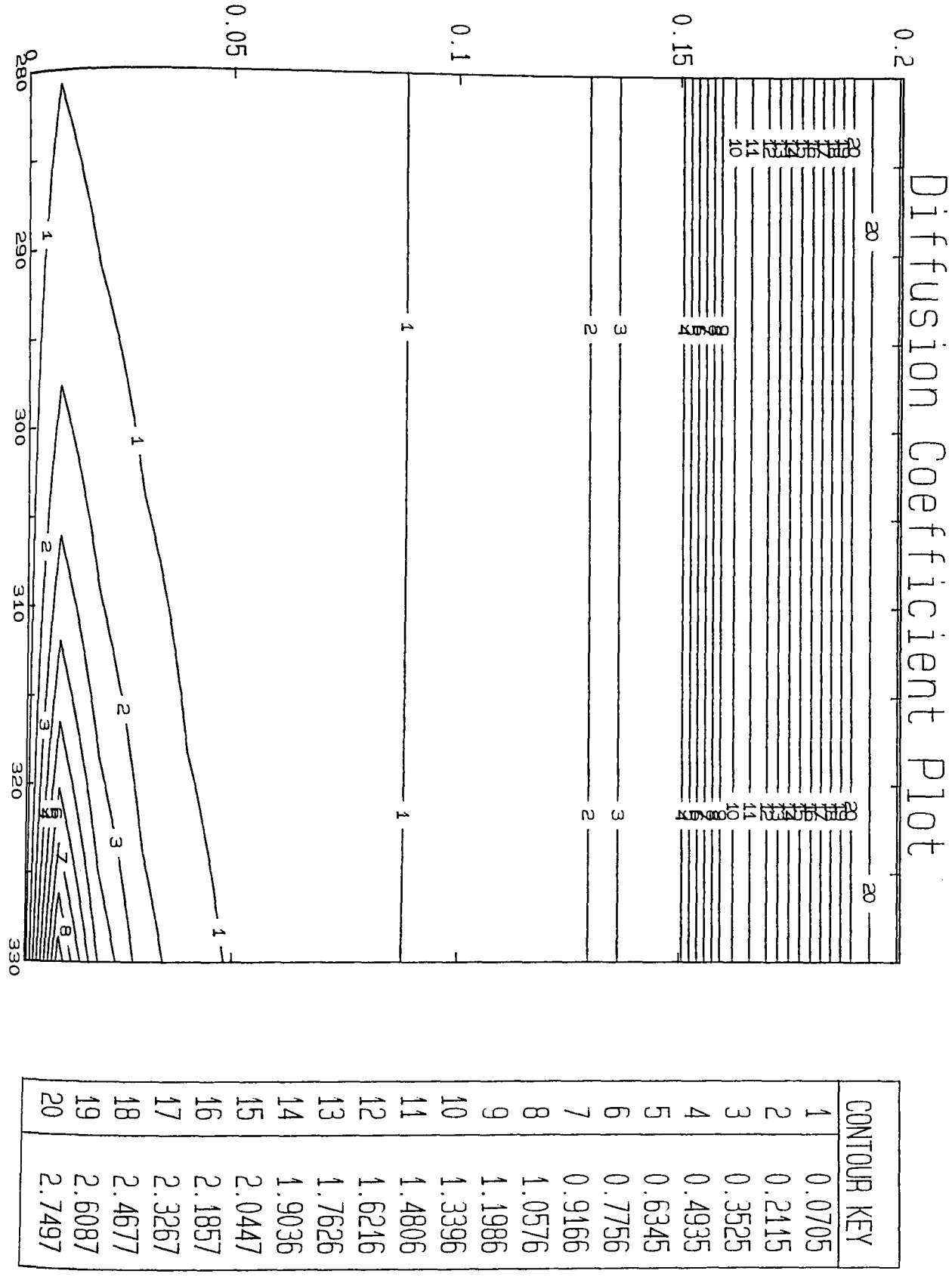

CONTOUR KEY	
1	0.0705
2	0.2115
3	0.3525
4	0.4935
5	0.6345
6	0.7756
7	0.9166
8	1.0576
9	1.1986
10	1.3396
11	1.4806
12	1.6216
13	1.7626
14	1.9036
15	2.0447
16	2.1857
17	2.3267
18	2.4677
19	2.6087
20	2.7497

Fig. **VI.** 18(b) Eigenvalue Surfaces for the Rose Soil, Contour Plot. Temperature, ^{o}K, v. Moisture Content, Dimensionless, v. η_2 *dimensionless* x 10^{5}.

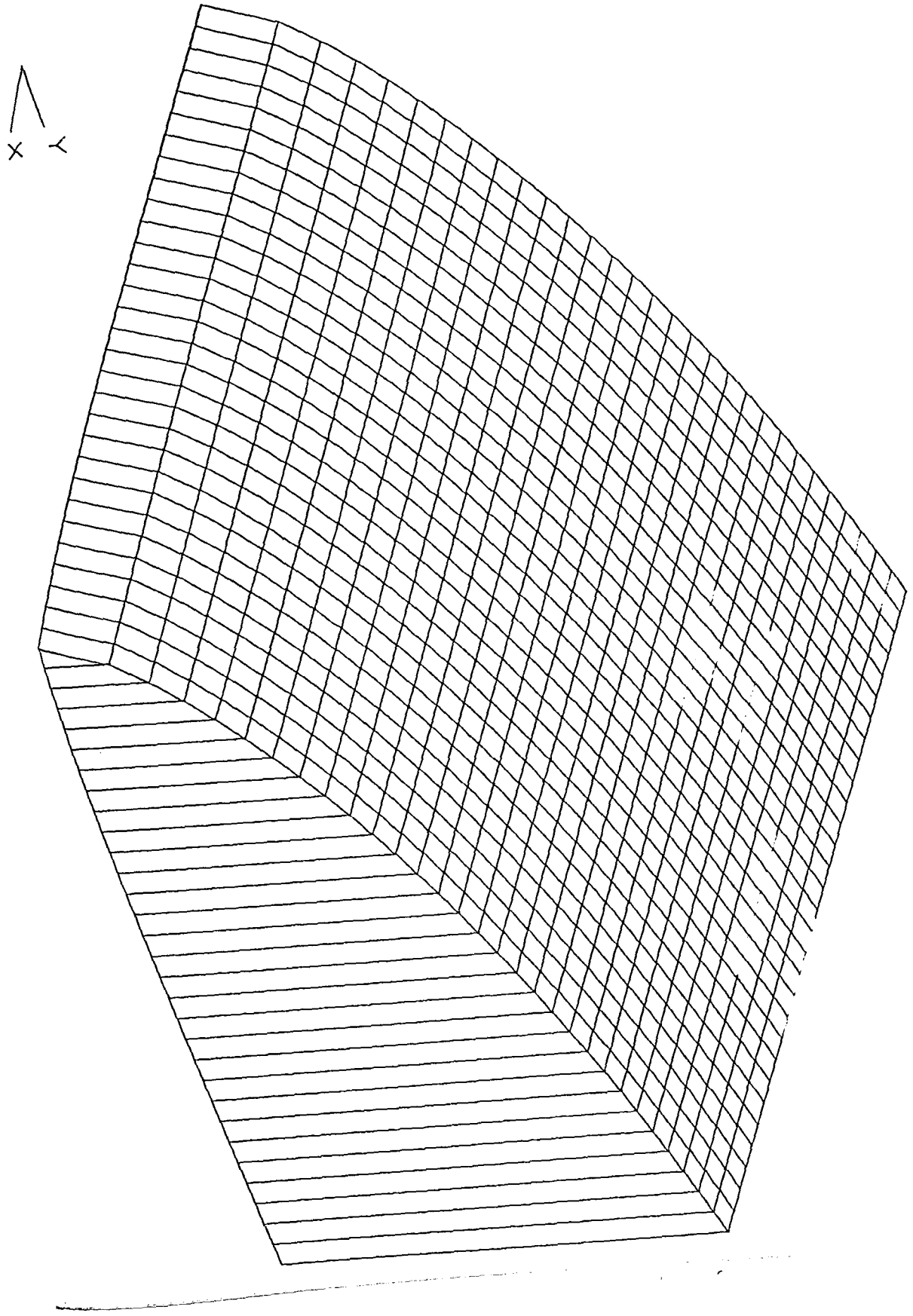

Fig. VI. 19(a) Eigenvalue Surfaces.
Adelanto Loam, η_1 x 10^3, Surface Plot.

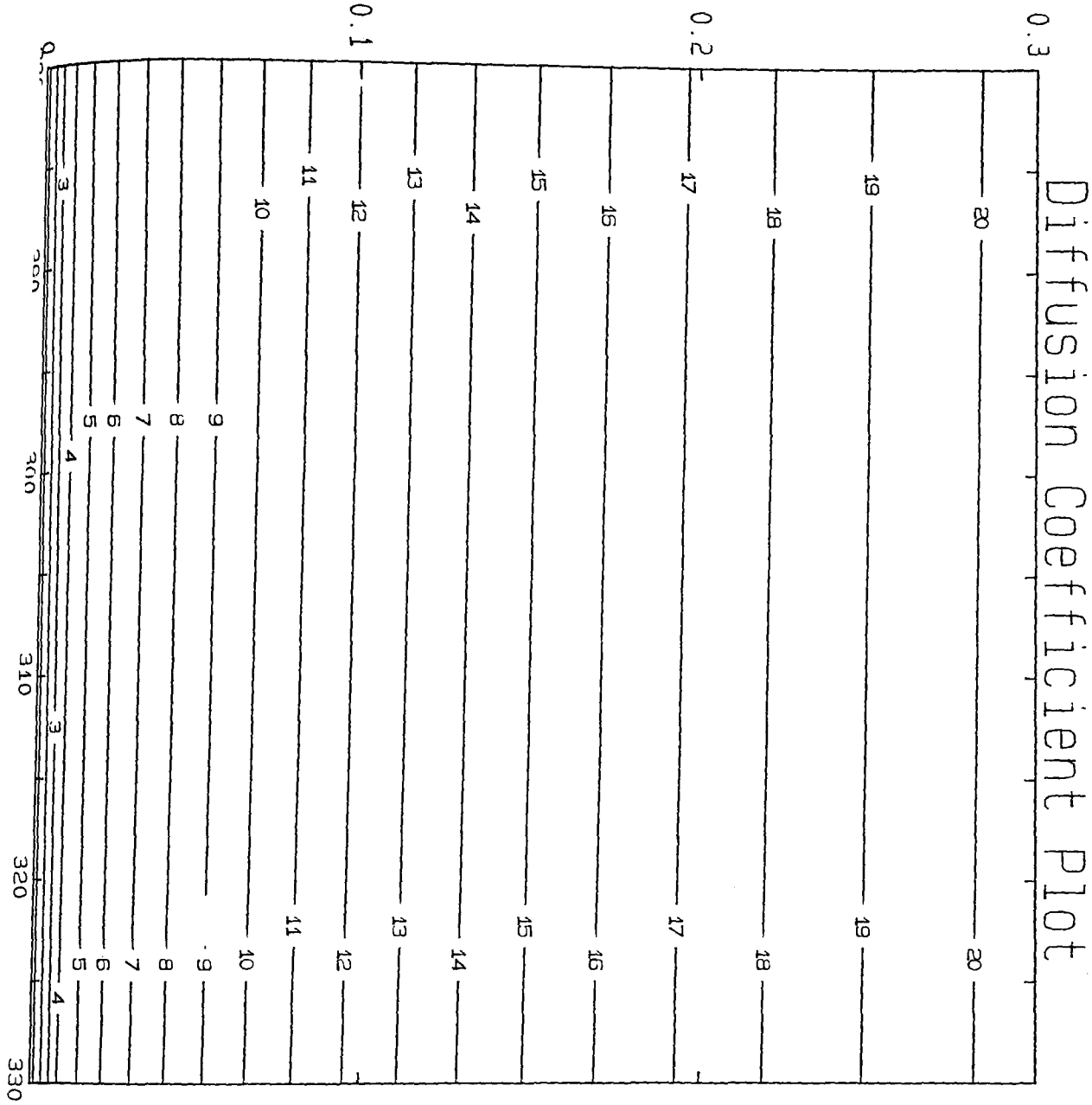

CONTOUR KEY	
1	2.7547
2	2.8096
3	2.8644
4	2.9193
5	2.9742
6	3.0291
7	3.0839
8	3.1388
9	3.1937
10	3.2485
11	3.3034
12	3.3583
13	3.4131
14	3.4680
15	3.5229
16	3.5777
17	3.6326
18	3.6875
19	3.7424
20	3.7972

Fig. VI. 19(b) Eigenvalue Surfaces for Adelanto Loam, Contour Plot.
Temperature, ^{o}K, v. Moisture Content, Dimensionless, v.
η_1 *dimensionless* x 10^{3}.

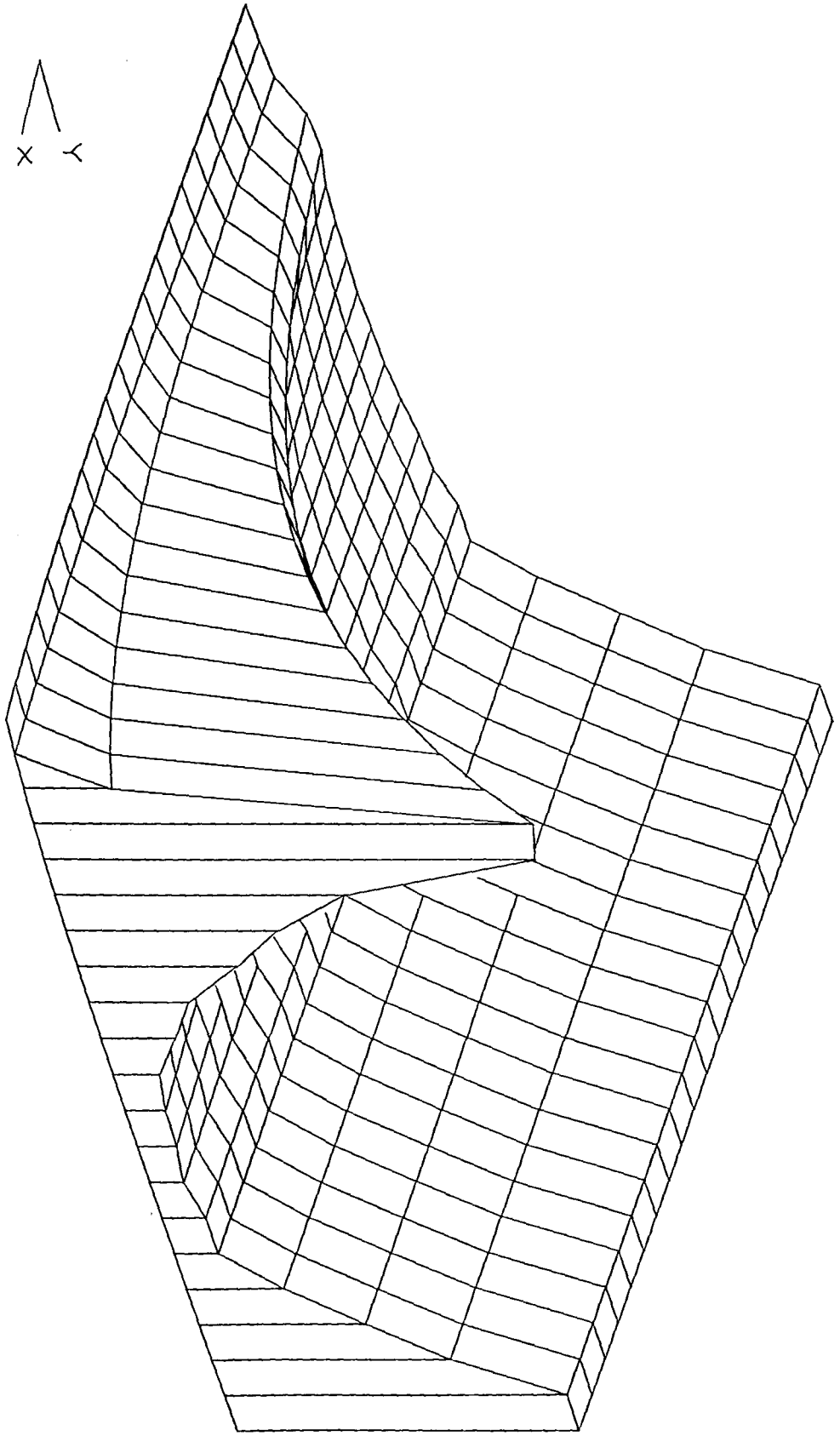

Fig. VI. 20(a) Eigenvalue Surfaces.
Adelanto Loam, η_2 x 10^5, Surface Plot.

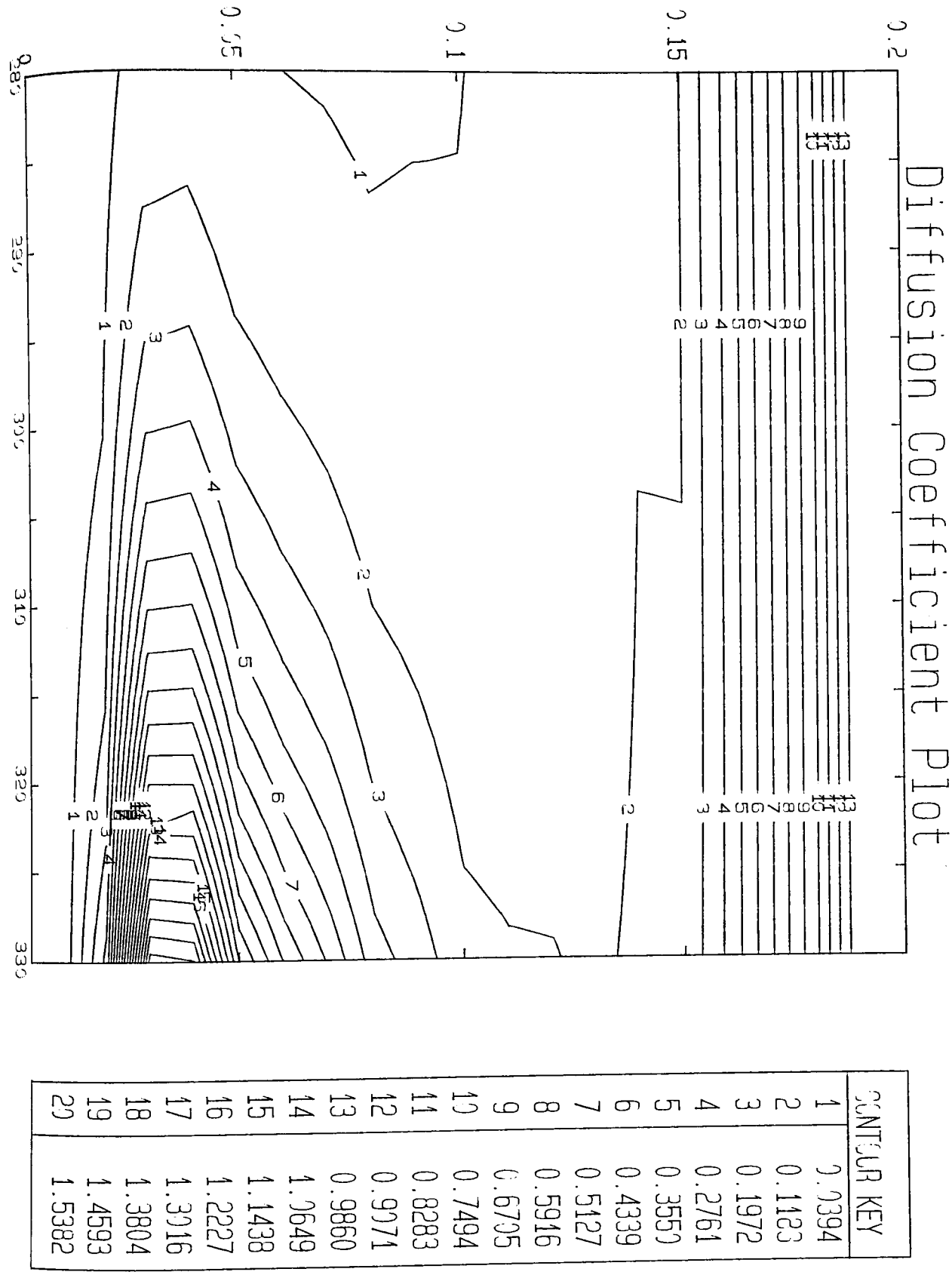

CONTOUR KEY	
1	0.0394
2	0.1123
3	0.1972
4	0.2761
5	0.3550
6	0.4339
7	0.5127
8	0.5916
9	0.6705
10	0.7494
11	0.8283
12	0.9071
13	0.9860
14	1.0649
15	1.1438
16	1.2227
17	1.3016
18	1.3804
19	1.4593
20	1.5382

Fig. VI. 20(b) Eigenvalue Surfaces for Adelanto Loam, Contour Plot. Temperature, ^{o}K, v. Moisture Content, Dimensionless, v. η_2 *dimensionless* x 10^{5}.

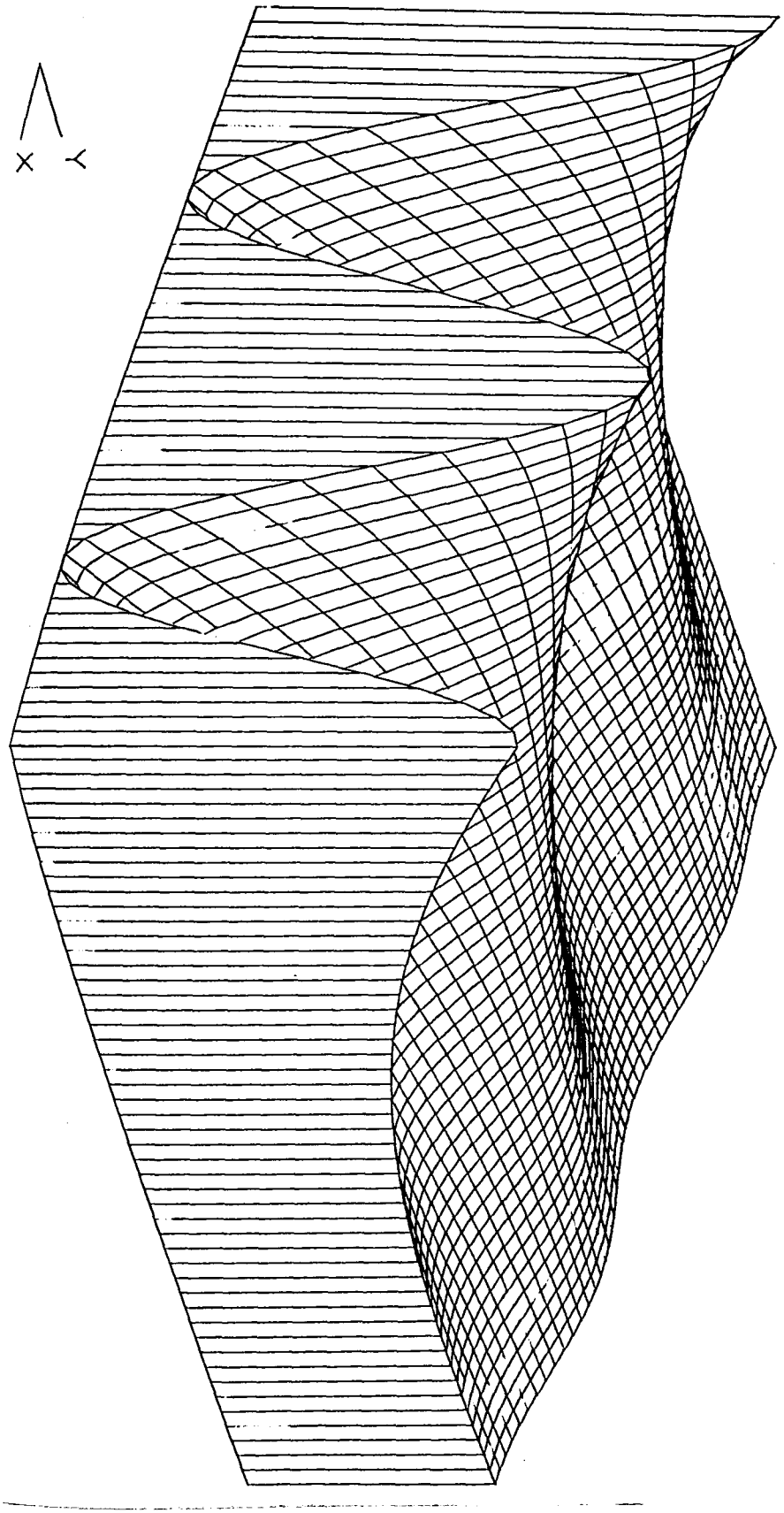

Fig. VIII.1.(a). Simulation. Temperature.

The Rose Soil,

$T_M = 300$; $T_A = 20$; $\theta_M = 0.2$; $\theta_A = 0.0$.

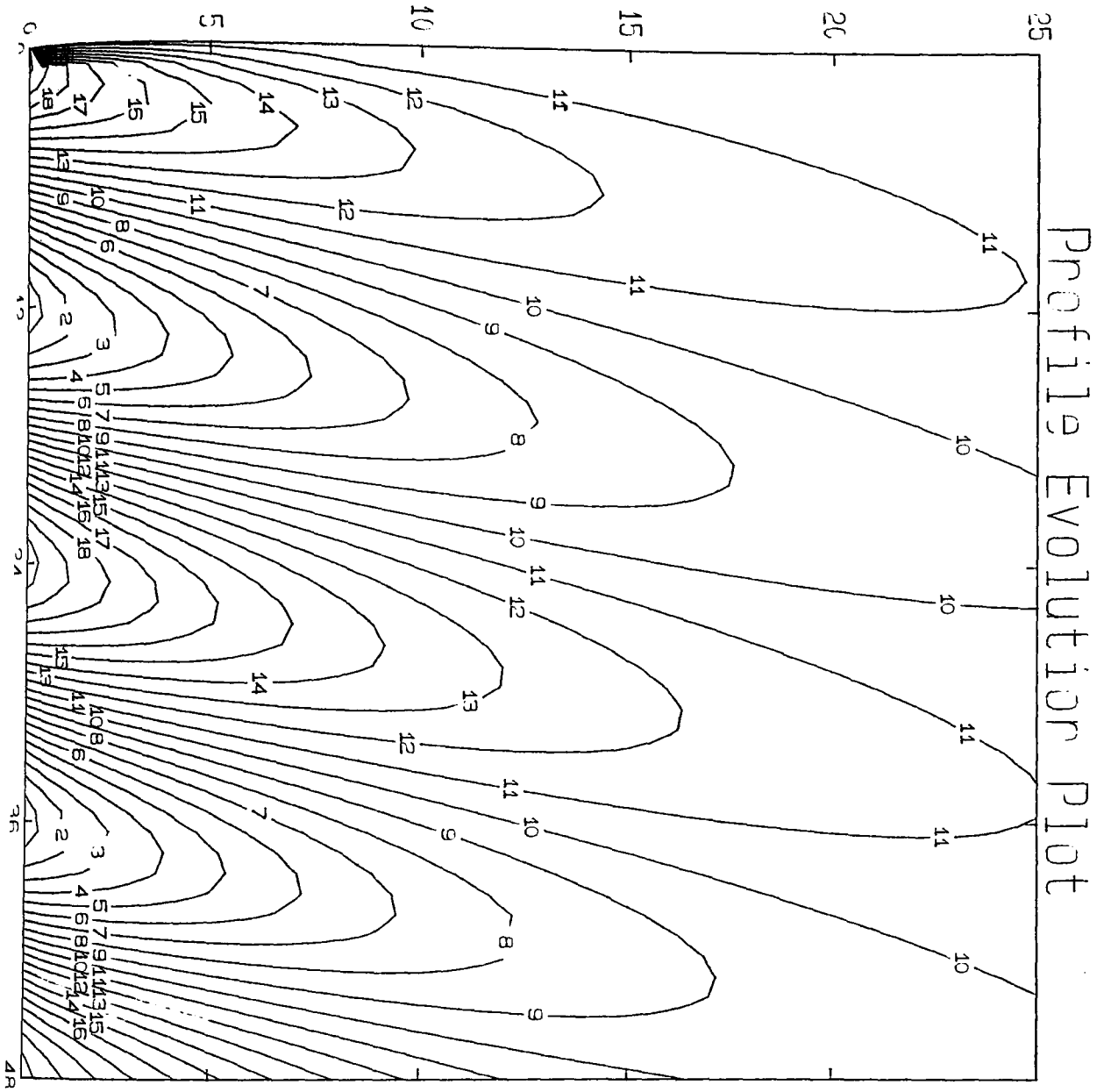

CONTOUR KEY	
1	281.1541
2	283.1462
3	285.1383
4	287.1304
5	289.1224
6	291.1145
7	293.1066
8	295.0988
9	297.0909
10	299.0830
11	301.0751
12	303.0672
13	305.0592
14	307.0514
15	309.0435
16	311.0356
17	313.0277
18	315.0198
19	317.0119
20	319.0039

Fig. VIII.1.(b). Simulation. Temperature. The Rose Soil,
Time, *hrs.* v. Depth, *cms.* v. Temperature, ^oK.
$T_M = 300$; $T_A = 20$; $\theta_M = 0.2$; $\theta_A = 0.0$.

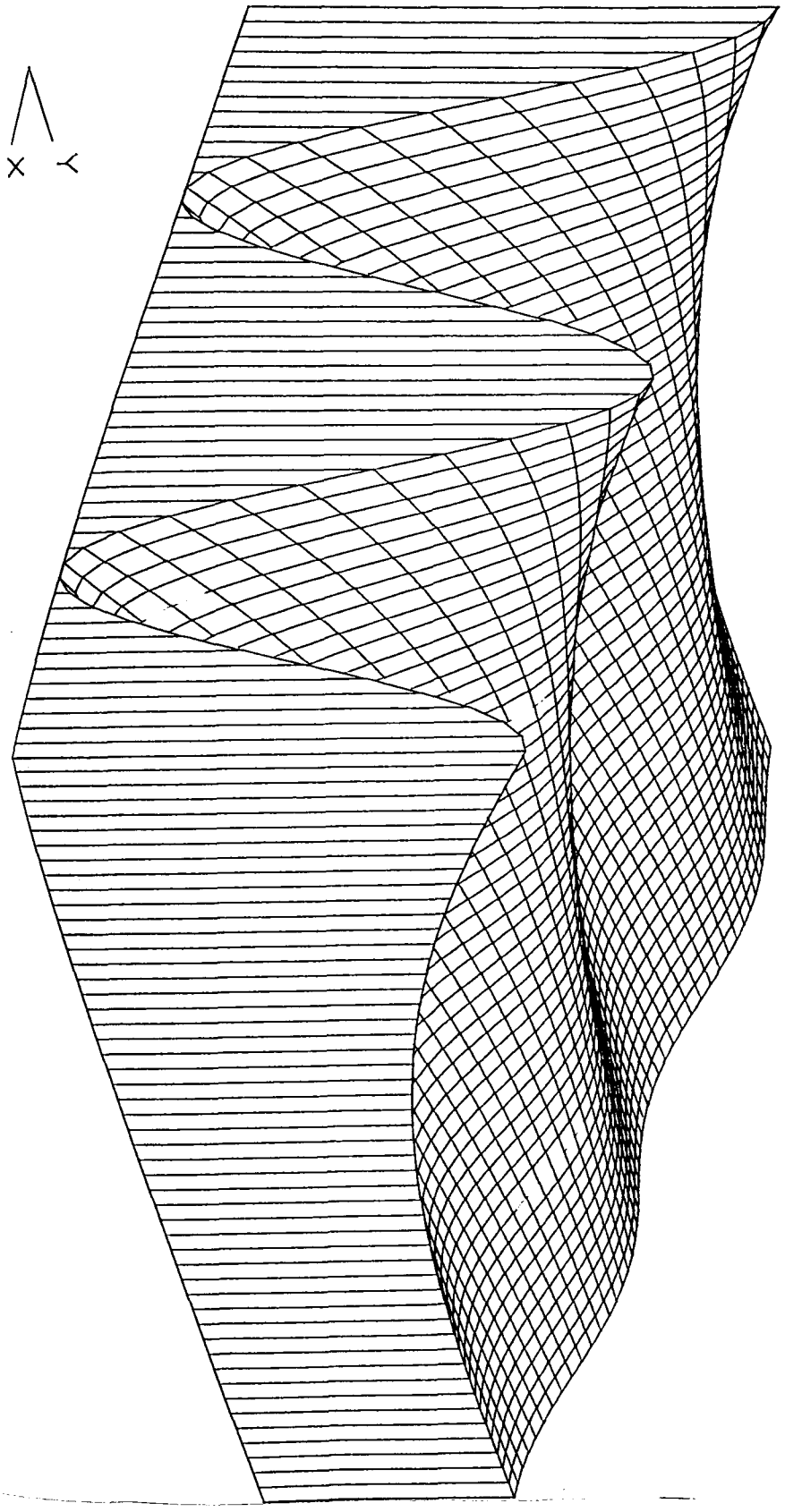

Fig. VIII.1.(c). Analysis. Temperature.

The Rose Soil,

$T_M = 300$; $T_A = 20$; $\theta_M = 0.2$; $\theta_A = 0.0$.

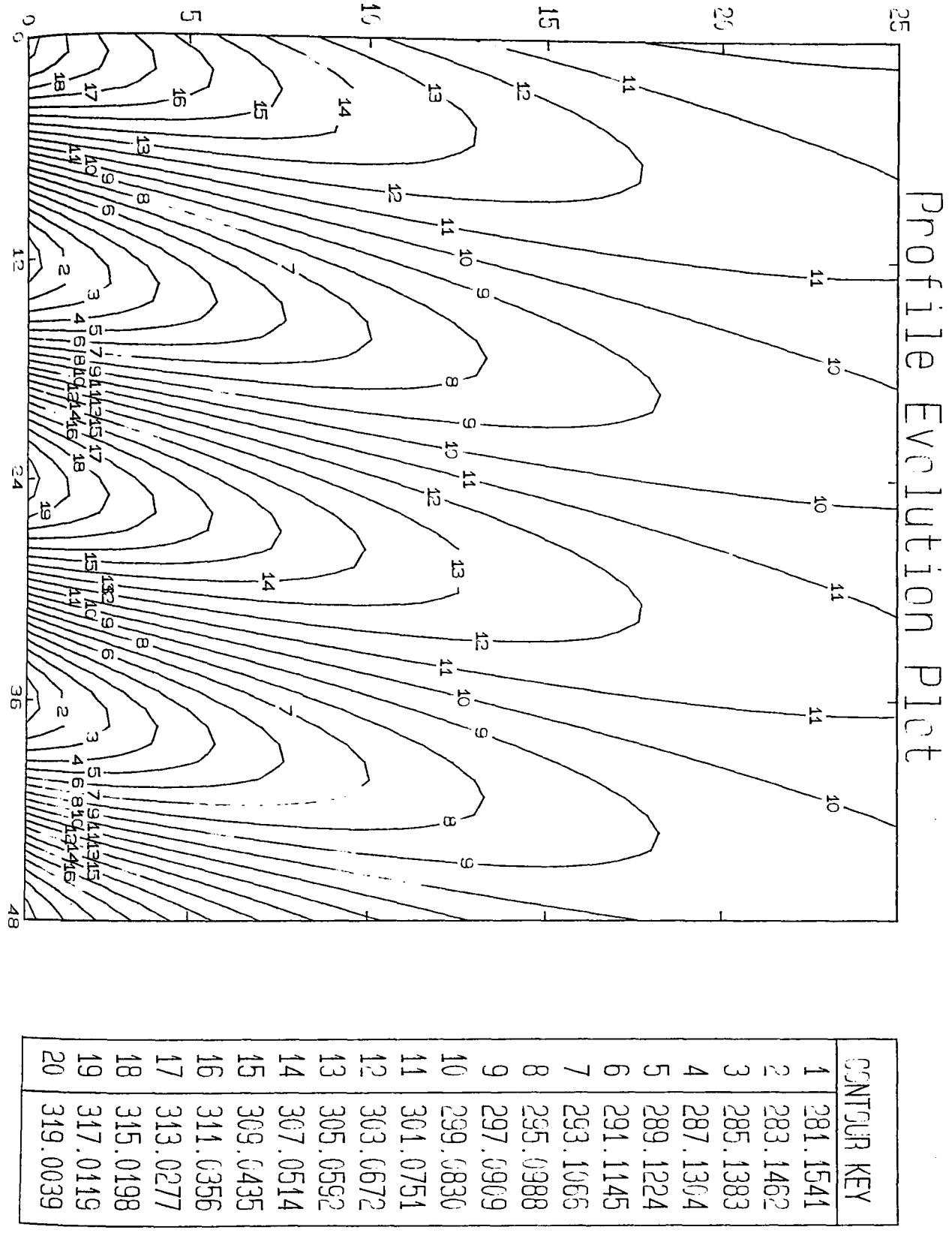

CONTOUR KEY	
1	281.1541
2	283.1462
3	285.1383
4	287.1304
5	289.1224
6	291.1145
7	293.1066
8	295.0988
9	297.0909
10	299.0830
11	301.0751
12	303.0672
13	305.0592
14	307.0514
15	309.0435
16	311.0356
17	313.0277
18	315.0198
19	317.0119
20	319.0039

Fig. VIII.1.(d). Analysis. Temperature. The Rose Soil,
Time, *hrs.* v. Depth, *cms.* v. Temperature, ^oK.
$T_M = 300$; $T_A = 20$; $\theta_M = 0.2$; $\theta_A = 0.0$.

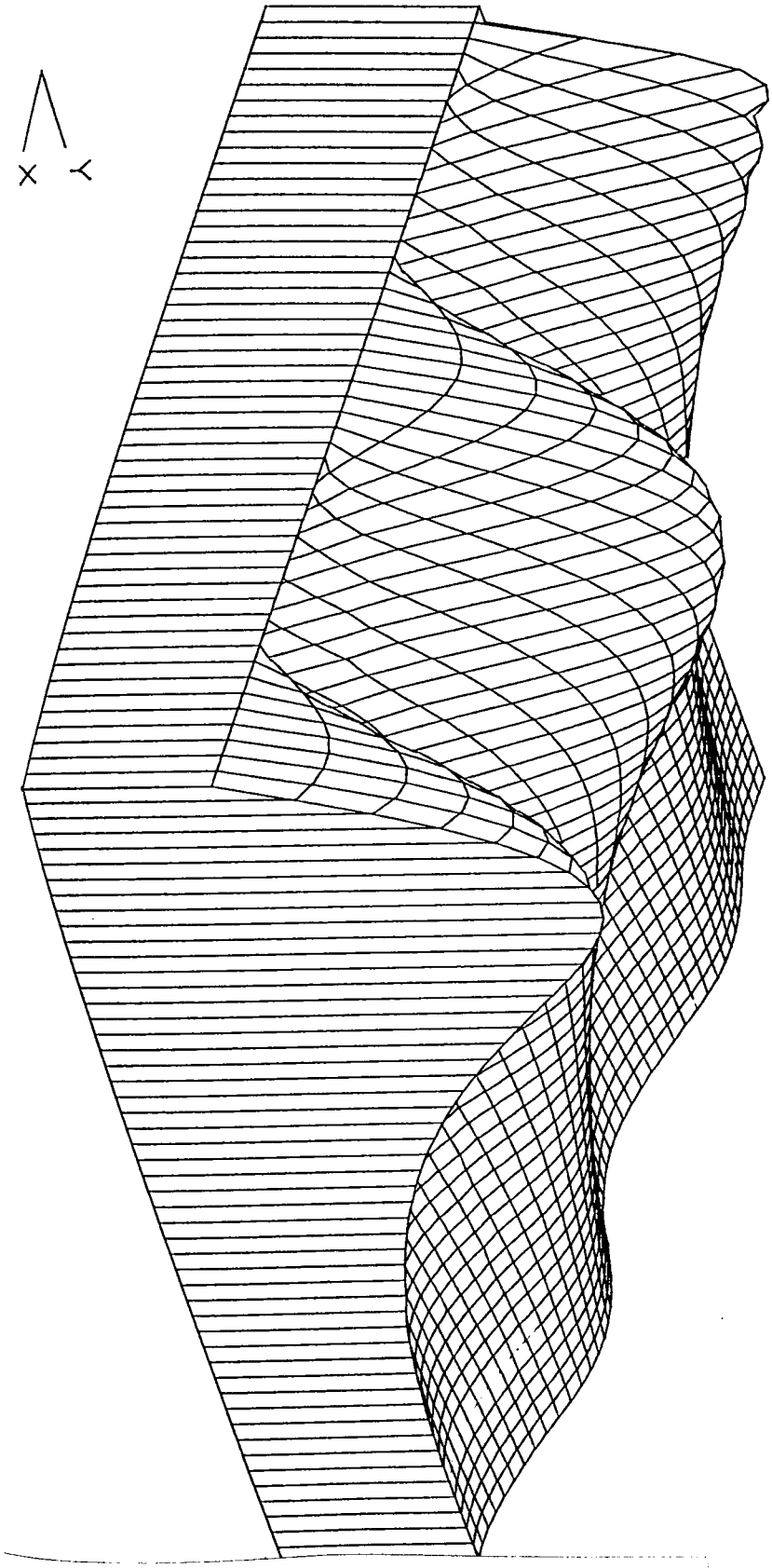

Fig. VIII.1.(e). Simulation. Moisture.

The Rose Soil,

$T_M = 300$; $T_A = 20$; $\theta_M = 0.2$; $\theta_A = 0.0$.

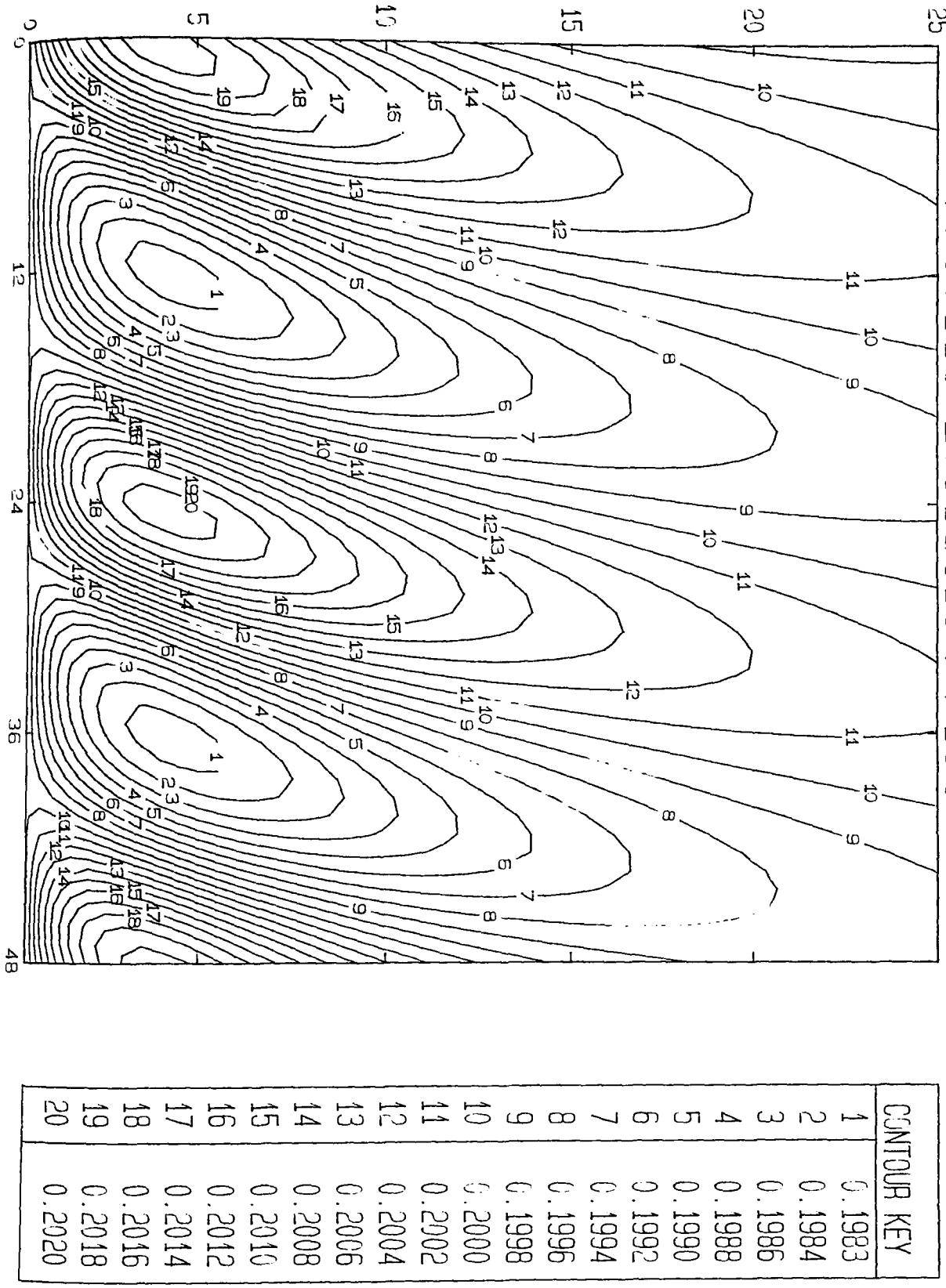

CONTOUR KEY	
1	0.1983
2	0.1984
3	0.1986
4	0.1988
5	0.1990
6	0.1992
7	0.1994
8	0.1996
9	0.1998
10	0.2000
11	0.2002
12	0.2004
13	0.2006
14	0.2008
15	0.2010
16	0.2012
17	0.2014
18	0.2016
19	0.2018
20	0.2020

Fig. **VIII**.1.(f). Simulation. Moisture. The Rose Soil,
Time, *hrs.* v. Depth, *cms.* v. Moisture, *dimensionless.*
$T_M = 300$; $T_A = 20$; $\theta_M = 0.2$; $\theta_A = 0.0$.

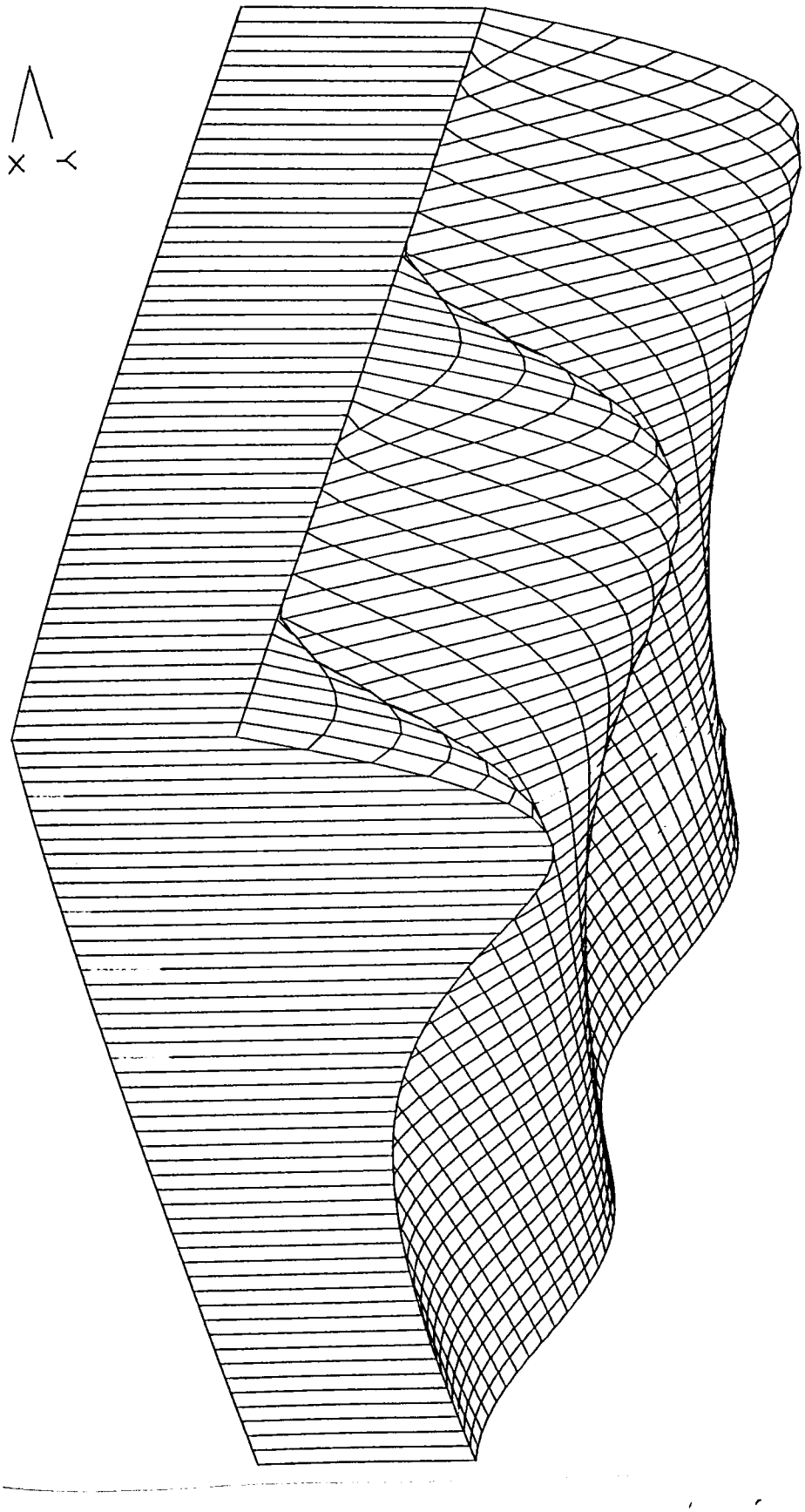

Fig. VIII.1.(g). Analysis. Moisture.

The Rose Soil,

$T_M = 300$; $T_A = 20$; $\theta_M = 0.2$; $\theta_A = 0.0$.

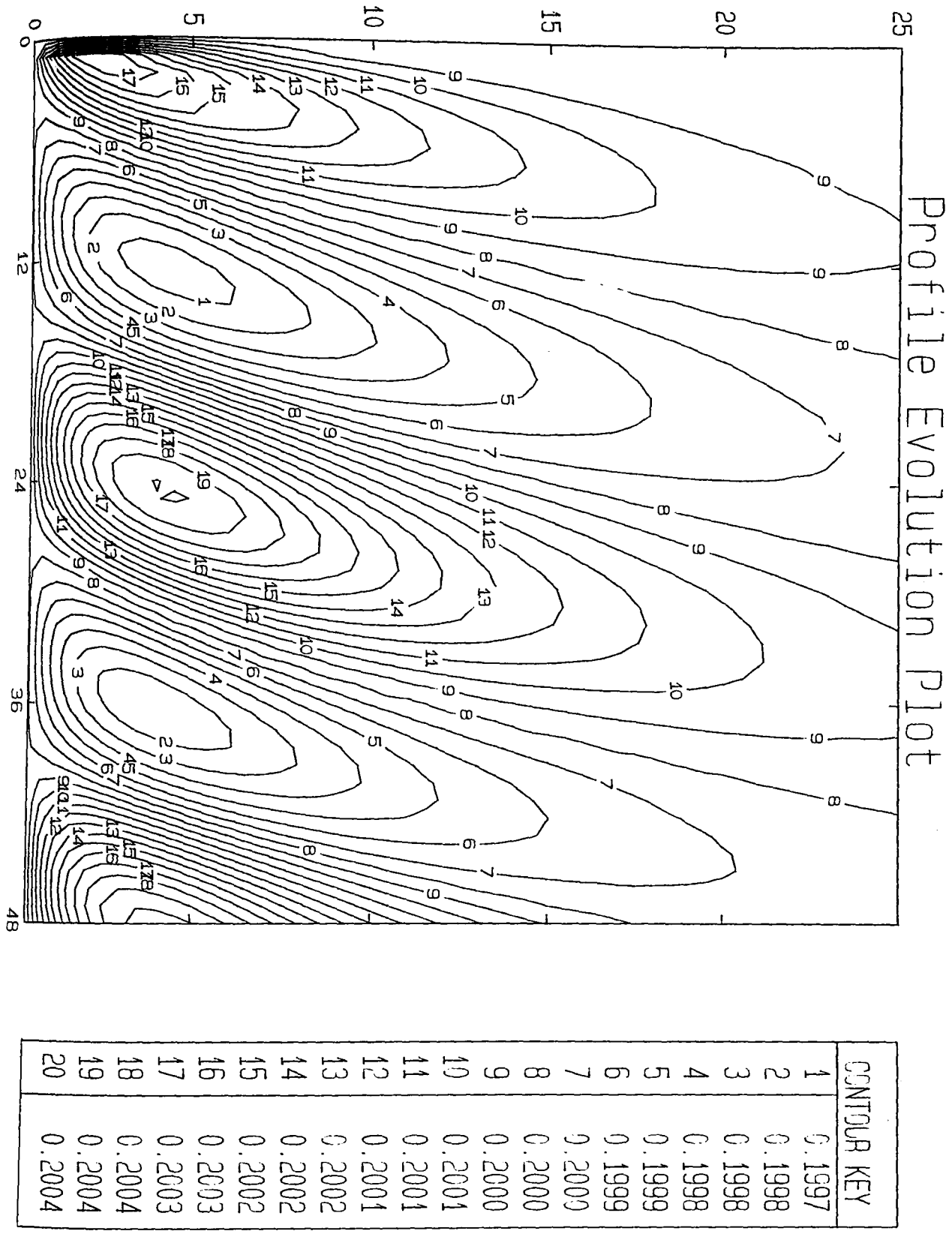

CONTOUR KEY	
1	0.1997
2	0.1998
3	0.1998
4	0.1998
5	0.1999
6	0.1999
7	0.2000
8	0.2000
9	0.2000
10	0.2001
11	0.2001
12	0.2001
13	0.2002
14	0.2002
15	0.2002
16	0.2003
17	0.2003
18	0.2004
19	0.2004
20	0.2004

Fig. VIII.1.(h). Analysis. Moisture. The Rose Soil,
Time, *hrs.* v. Depth, *cms.* v. Moisture, *dimensionless.*
$T_M = 300$; $T_A = 20$; $\theta_M = 0.2$; $\theta_A = 0.0$

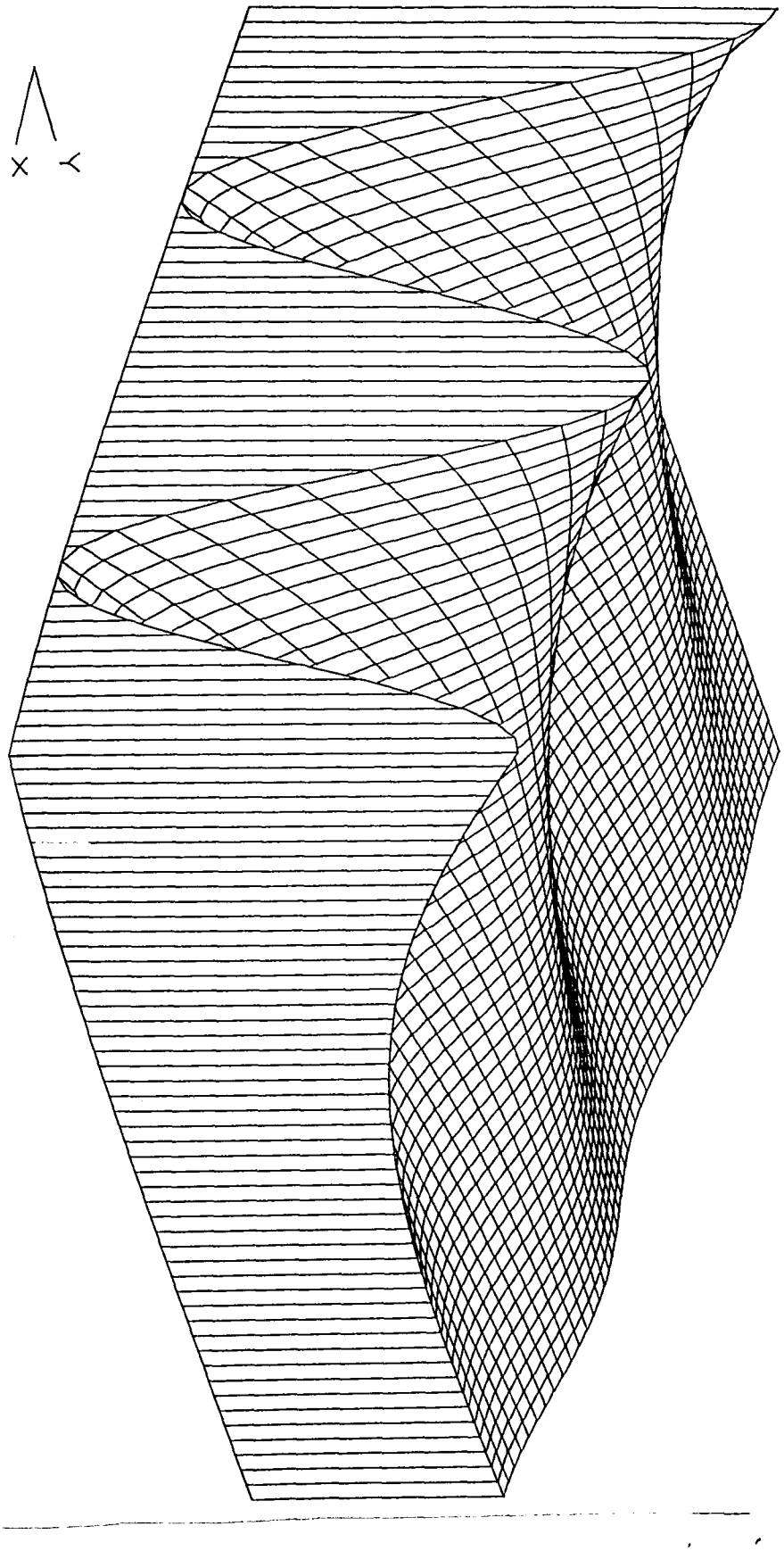

Fig. VIII.2.(a). Simulation. Temperature.

The Rose Soil,

$T_M = 300$; $T_A = 20$; $\theta_M = 0.15$; $\theta_A = 0.0$.

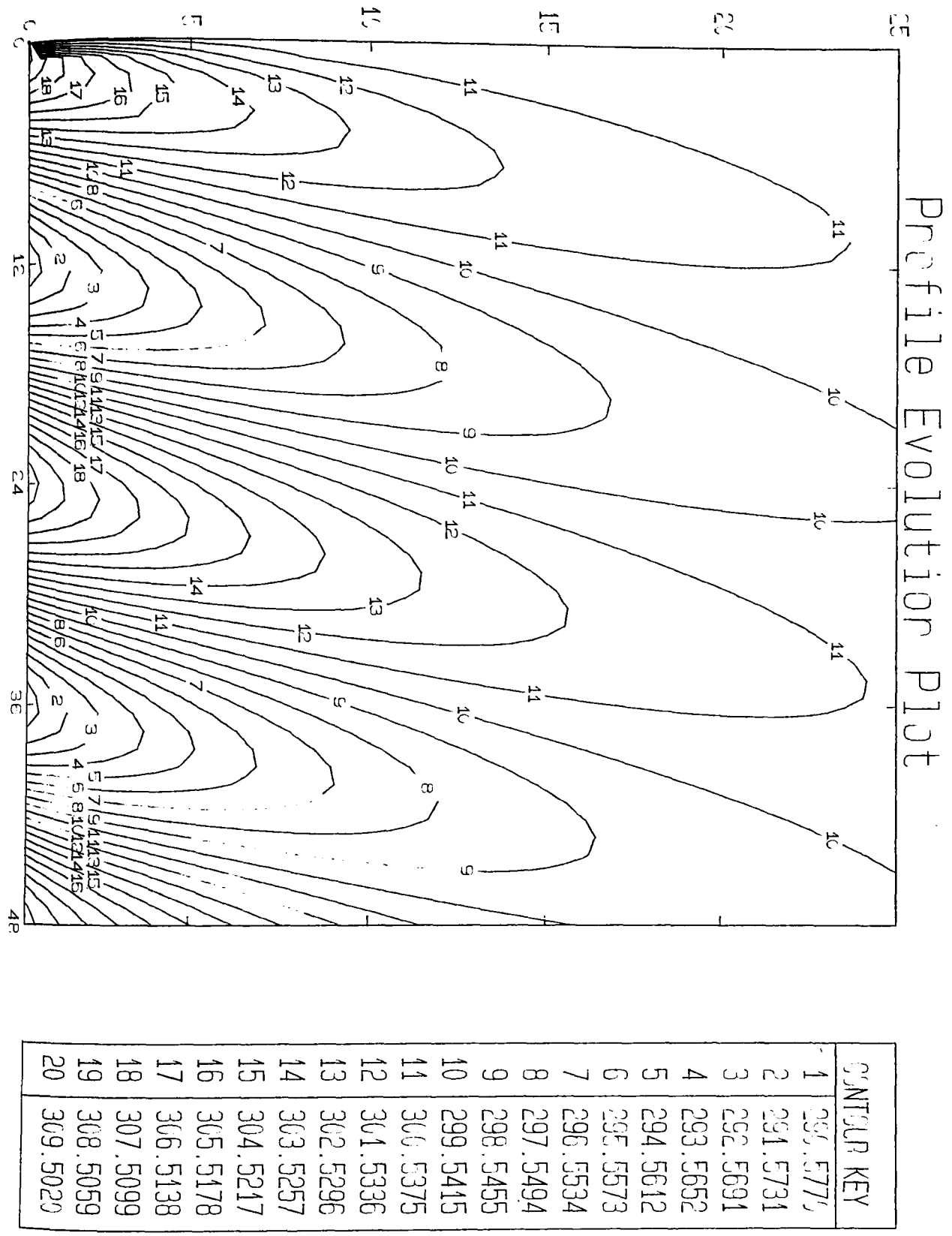

Fig. **VIII**.2.(b). Simulation. Temperature. The Rose Soil, Time, *hrs*. v. Depth, *cms*. v. Temperature, ^oK.
$T_M = 300$; $T_A = 20$; $\theta_M = 0.15$; $\theta_A = 0.0$.

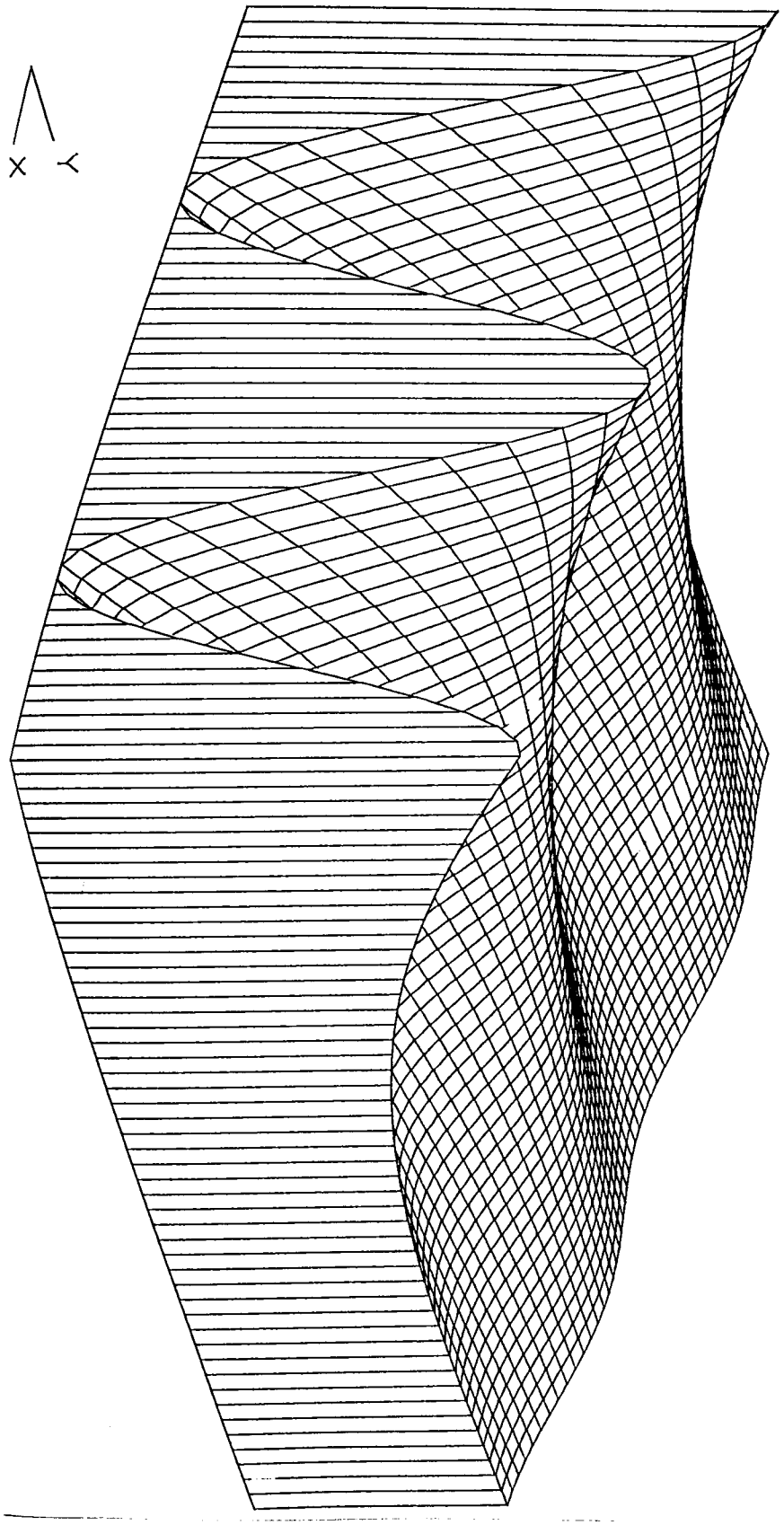

Fig. VIII.2.(c). Analysis. Temperature.

The Rose Soil,

$T_M = 300$; $T_A = 20$; $\theta_M = 0.15$; $\theta_A = 0.0$.

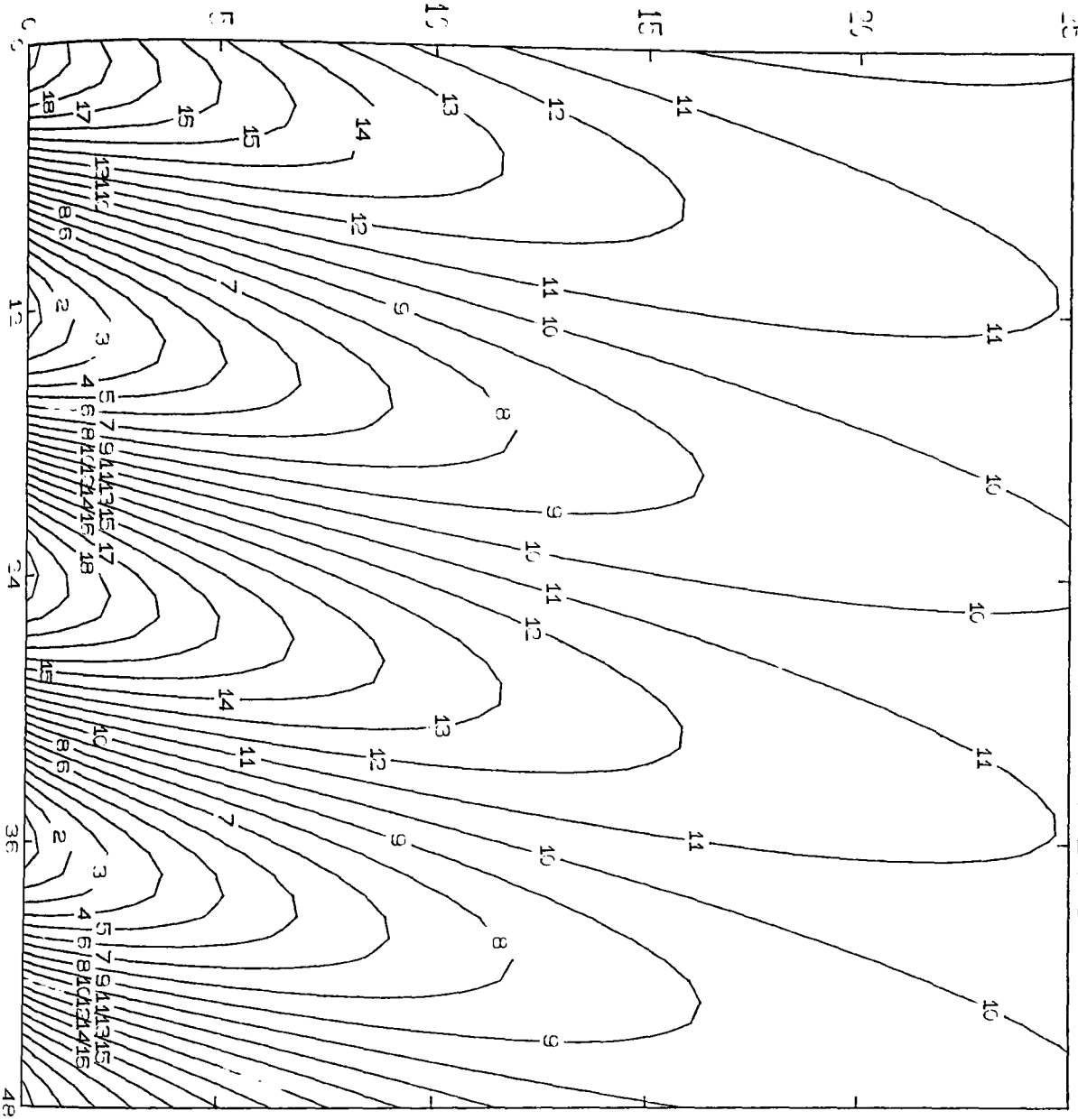

CONTOUR KEY	
1	281.1541
2	283.1462
3	285.1383
4	287.1304
5	289.1224
6	291.1145
7	293.1066
8	295.0988
9	297.0909
10	299.0830
11	301.0751
12	303.0672
13	305.0592
14	307.0514
15	309.0435
16	311.0356
17	313.0277
18	315.0198
19	317.0119
20	319.0039

Fig. VIII.2.(d). Analysis. Temperature. The Rose Soil,
Time, *hrs.* v. Depth, *cms.* v. Temperature, ^oK.
$T_M = 300$; $T_A = 20$; $\theta_M = 0.15$; $\theta_A = 0.0$.

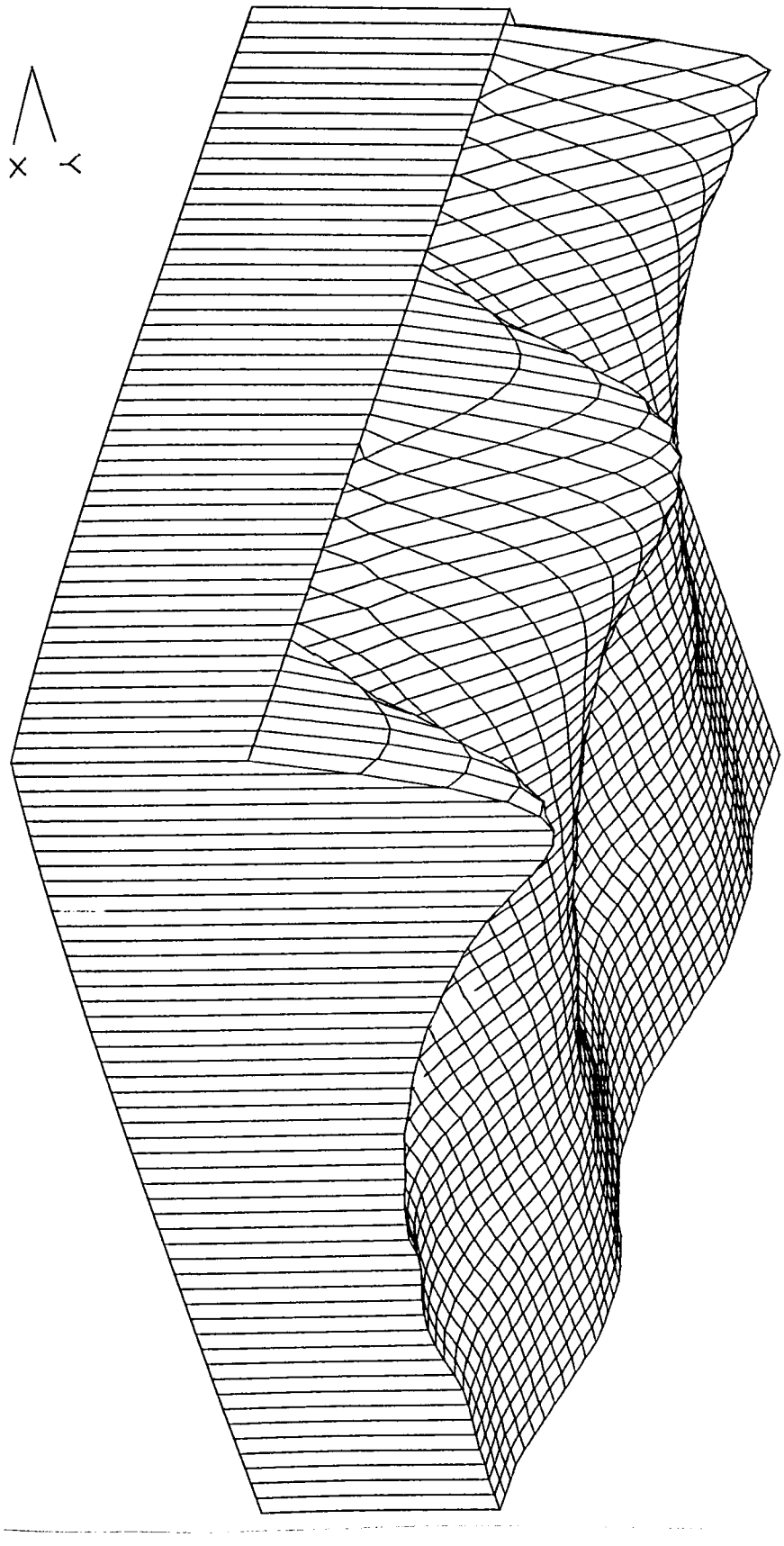

Fig. VIII.2.(e). Simulation. Moisture.

The Rose Soil,

$T_M = 300$; $T_A = 20$; $\theta_M = 0.15$; $\theta_A = 0.0$.

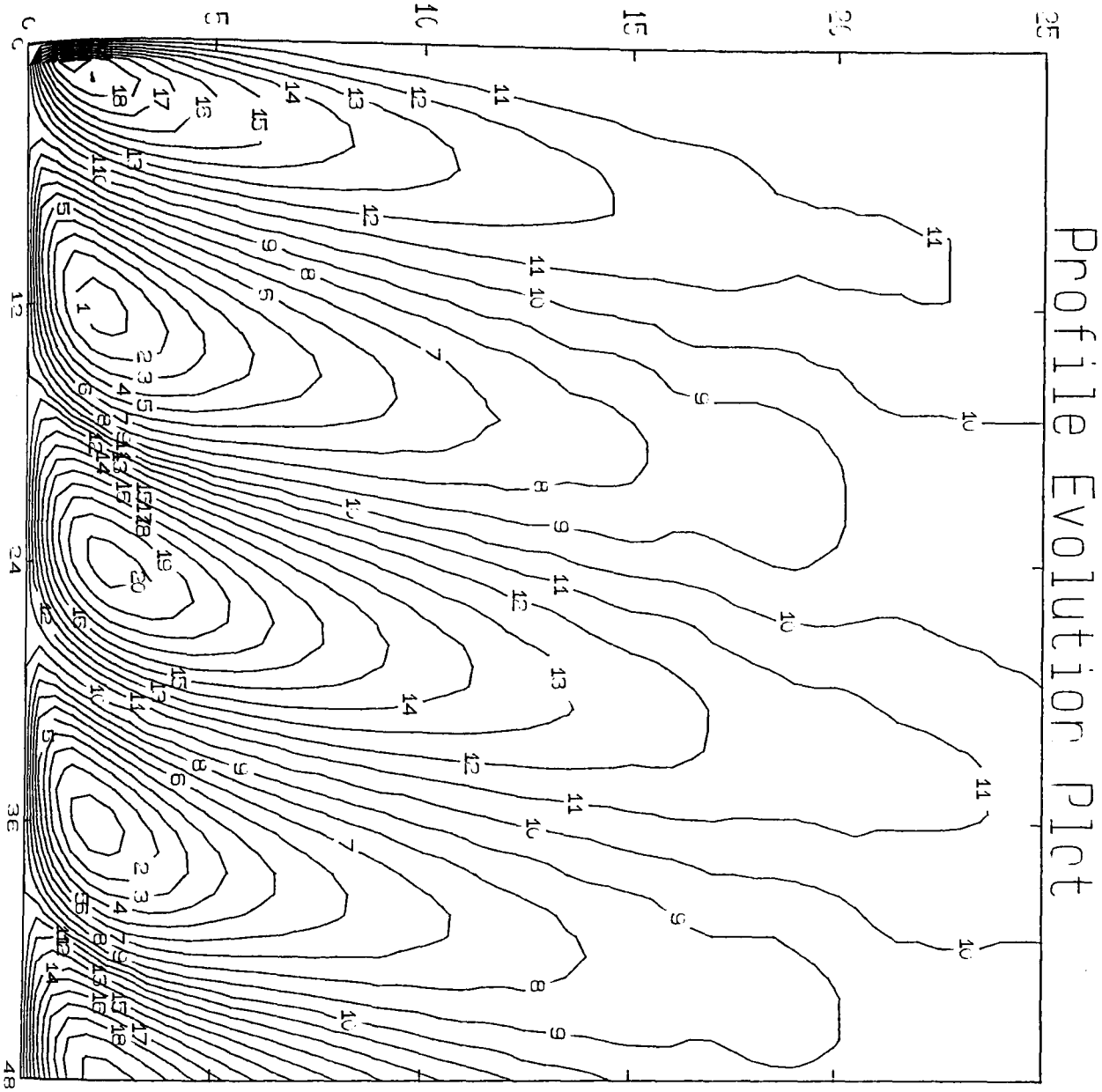

CONTOUR KEY
1 0.1499
2 0.1499
3 0.1499
4 0.1499
5 0.1499
6 0.1499
7 0.1499
8 0.1500
9 0.1500
10 0.1500
11 0.1500
12 0.1500
13 0.1500
14 0.1501
15 0.1501
16 0.1501
17 0.1501
18 0.1501
19 0.1501
20 0.1502

Fig. **VIII.2.**(f). Simulation. Moisture. The Rose Soil,
Time, *hrs.* v. Depth, *cms.* v. Moisture, *dimensionless.*
$T_M = 300$; $T_A = 20$; $\theta_M = 0.15$; $\theta_A = 0.0$.

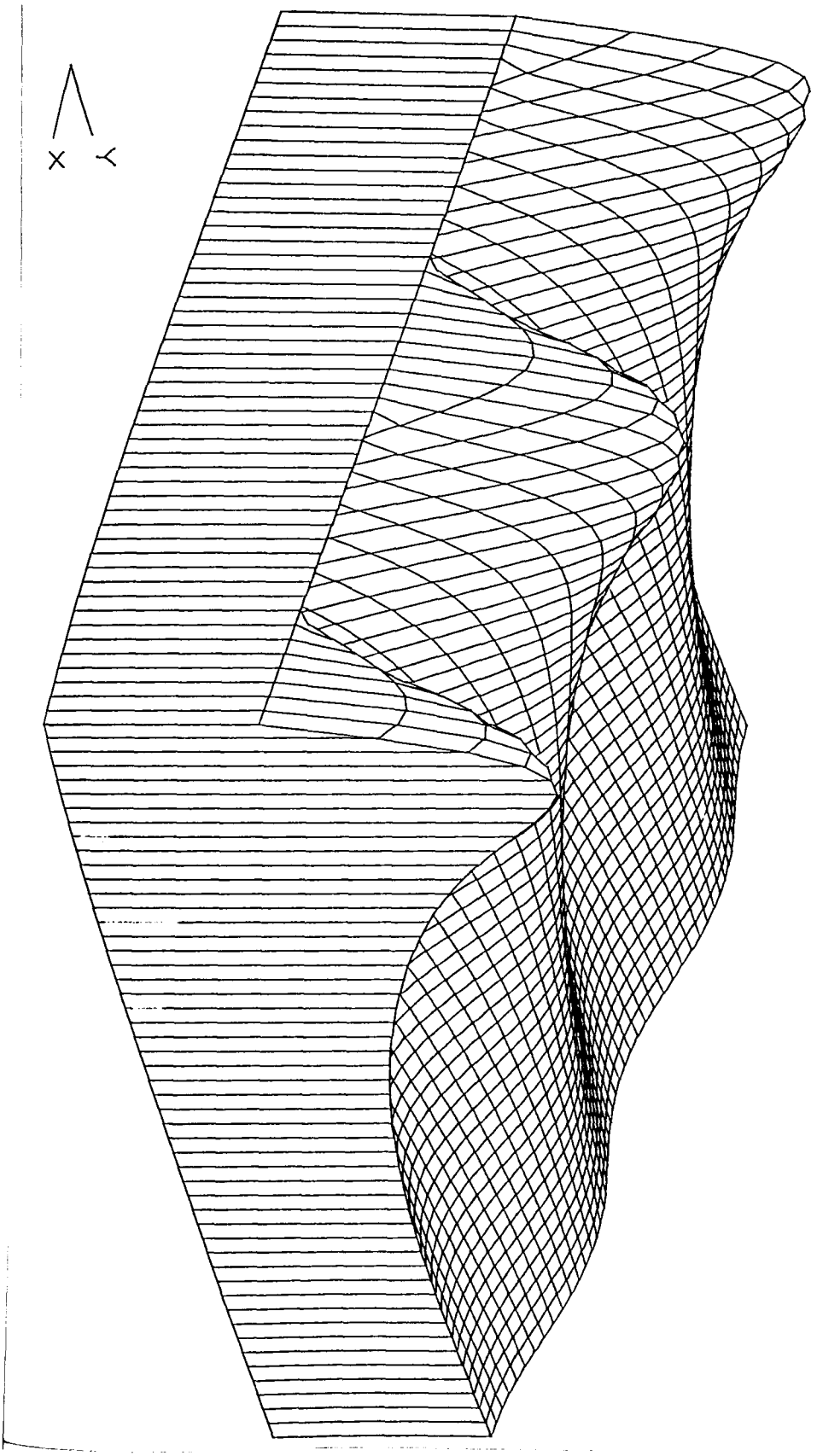

Fig. VIII.2.(g). Analysis. Moisture.

The Rose Soil,

$T_M = 300$; $T_A = 20$; $\theta_M = 0.15$; $\theta_A = 0.0$.

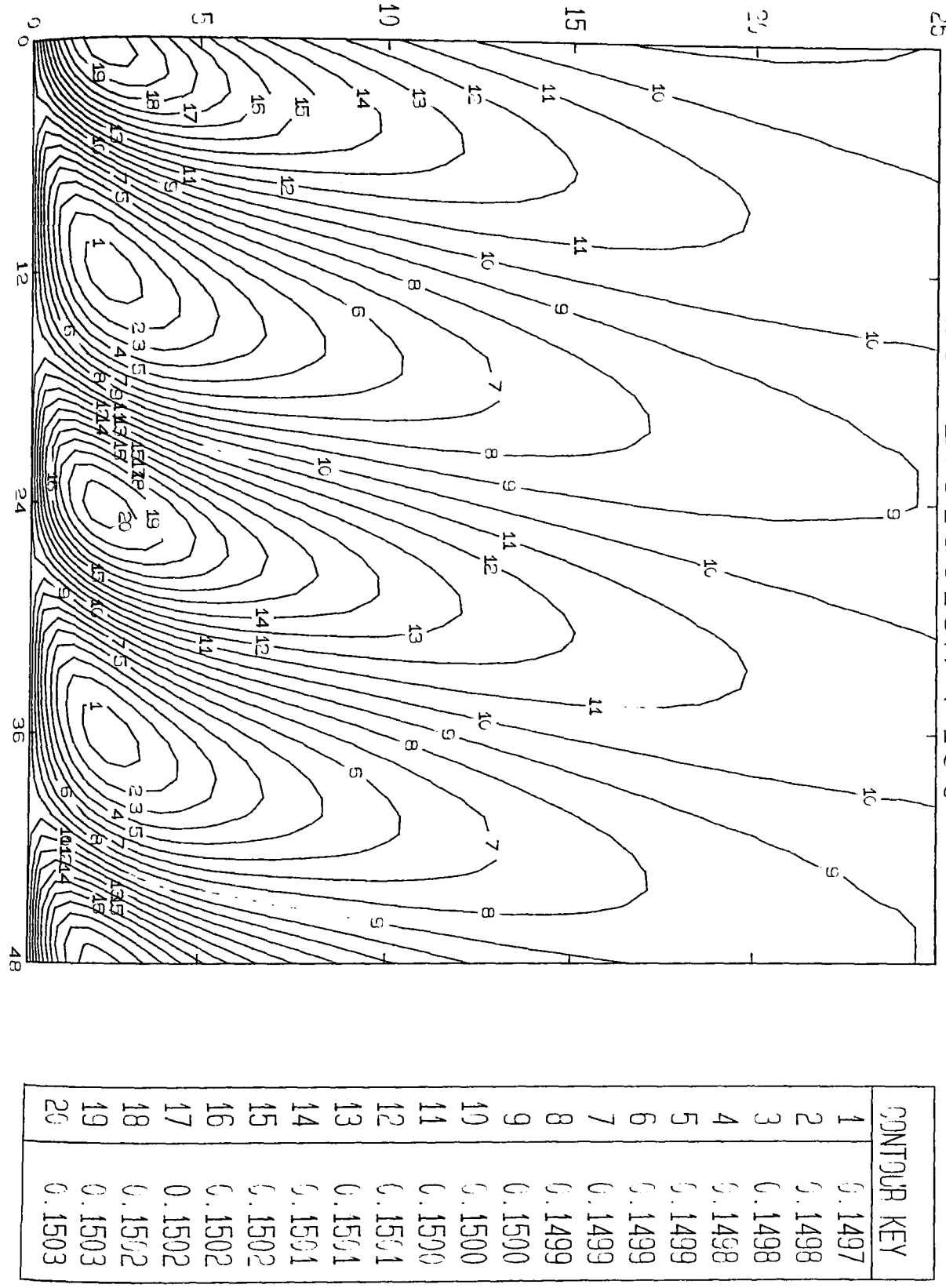

CONTOUR KEY	
1	0.1497
2	0.1498
3	0.1498
4	0.1498
5	0.1499
6	0.1499
7	0.1499
8	0.1499
9	0.1500
10	0.1500
11	0.1500
12	0.1501
13	0.1501
14	0.1501
15	0.1502
16	0.1502
17	0.1502
18	0.1502
19	0.1503
20	0.1503

Fig. **VIII**.2.(h). Analysis. Moisture. The Rose Soil,
Time, *hrs.* v. Depth, *cms.* v. Moisture, *dimensionless.*
$T_M = 300$; $T_A = 20$; $\theta_M = 0.15$; $\theta_A = 0.0$

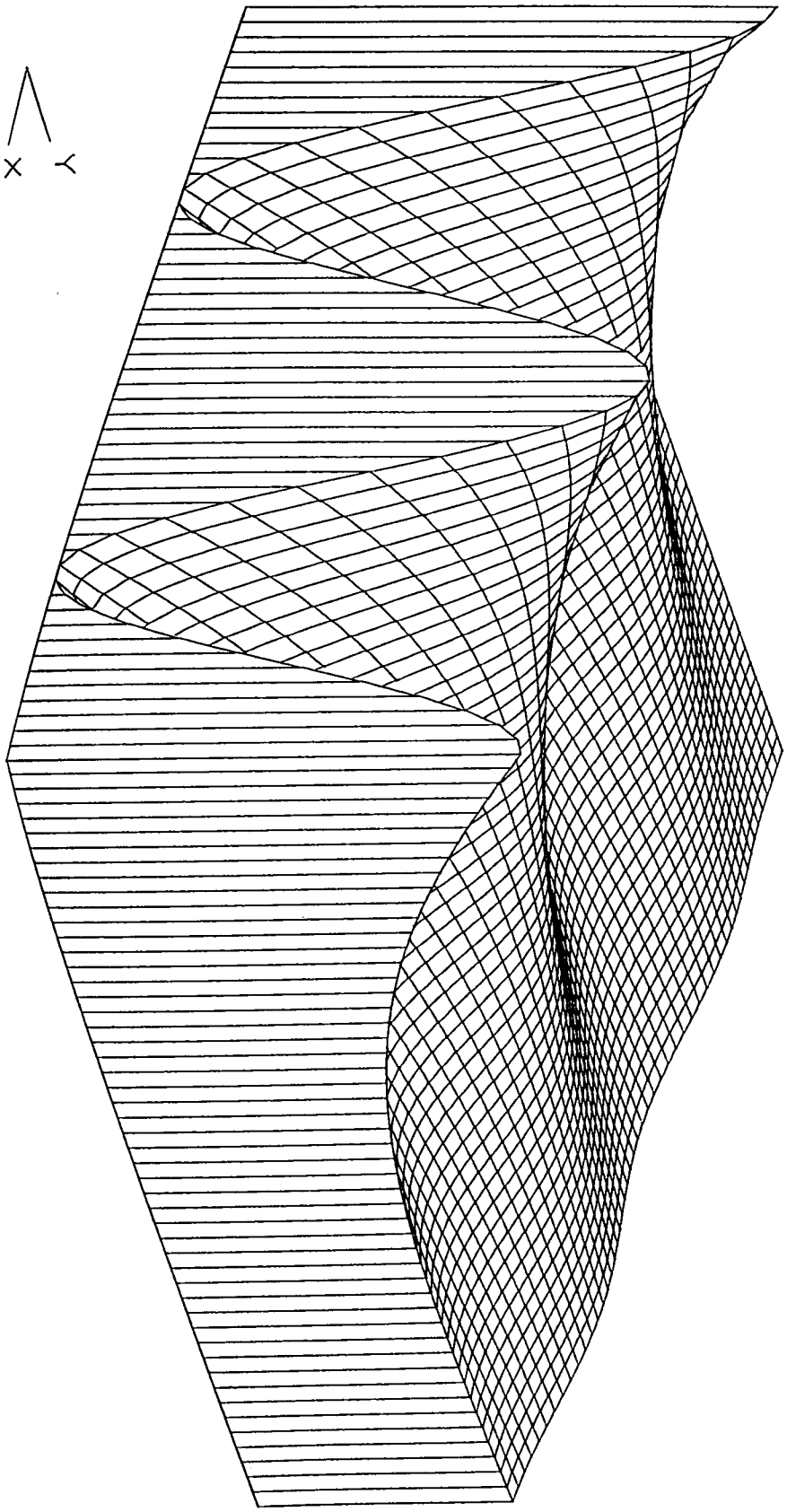

Fig. VIII.3.(a). Simulation. Temperature.

The Rose Soil,

$T_M = 300$; $T_A = 20$; $\theta_M = 0.1$; $\theta_A = 0.0$.

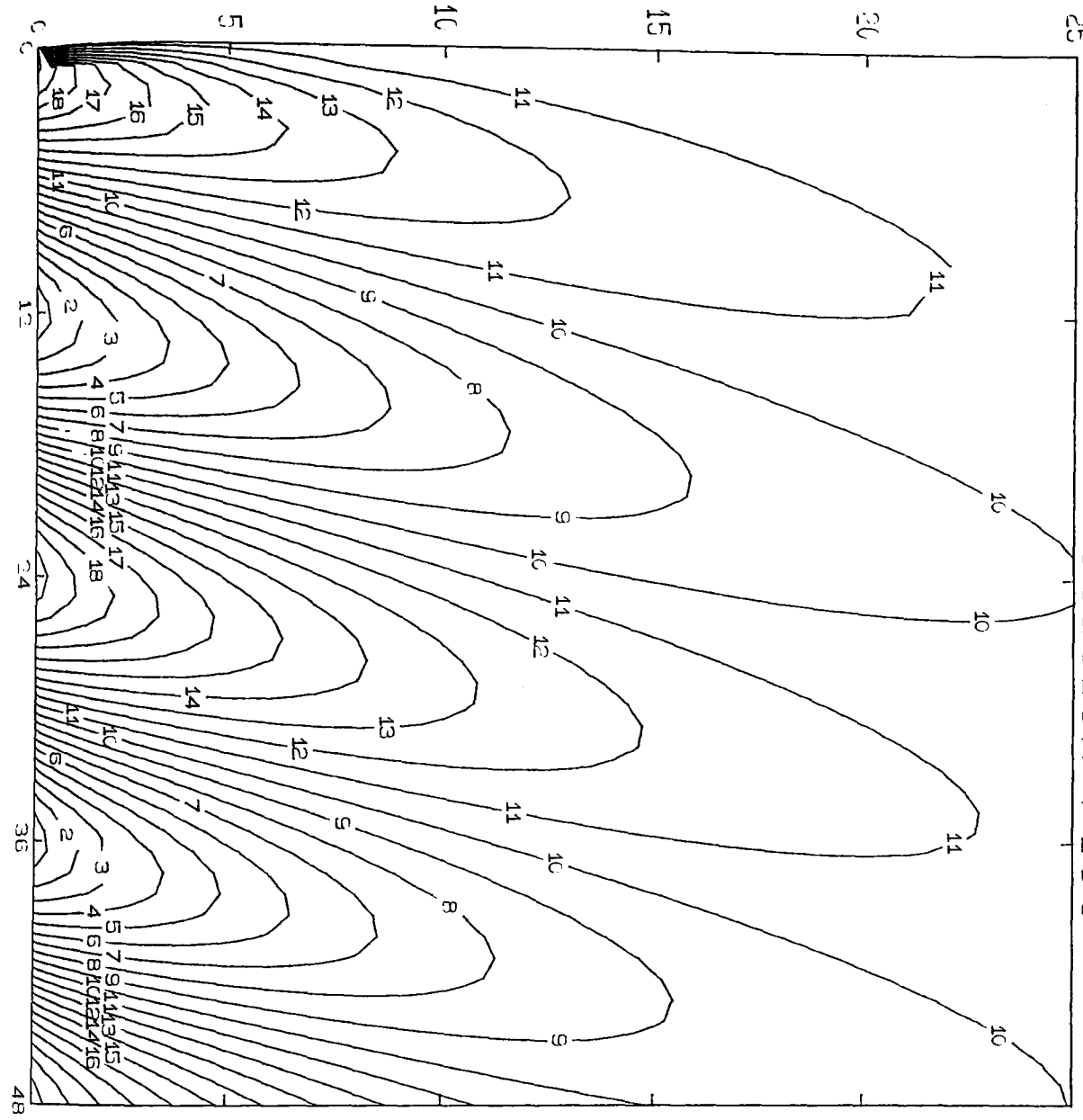

CONTOUR KEY	
1	290.5770
2	291.5731
3	292.5691
4	293.5652
5	294.5612
6	295.5573
7	296.5534
8	297.5494
9	298.5455
10	299.5415
11	300.5375
12	301.5336
13	302.5296
14	303.5257
15	304.5217
16	305.5178
17	306.5138
18	307.5099
19	308.5059
20	309.5020

Fig. VIII.3.(b). Simulation. Temperature. The Rose Soil,
Time, *hrs.* v. Depth, *cms.* v. Temperature, ^oK.
$T_M = 300$; $T_A = 20$; $\theta_M = 0.1$; $\theta_A = 0.0$.

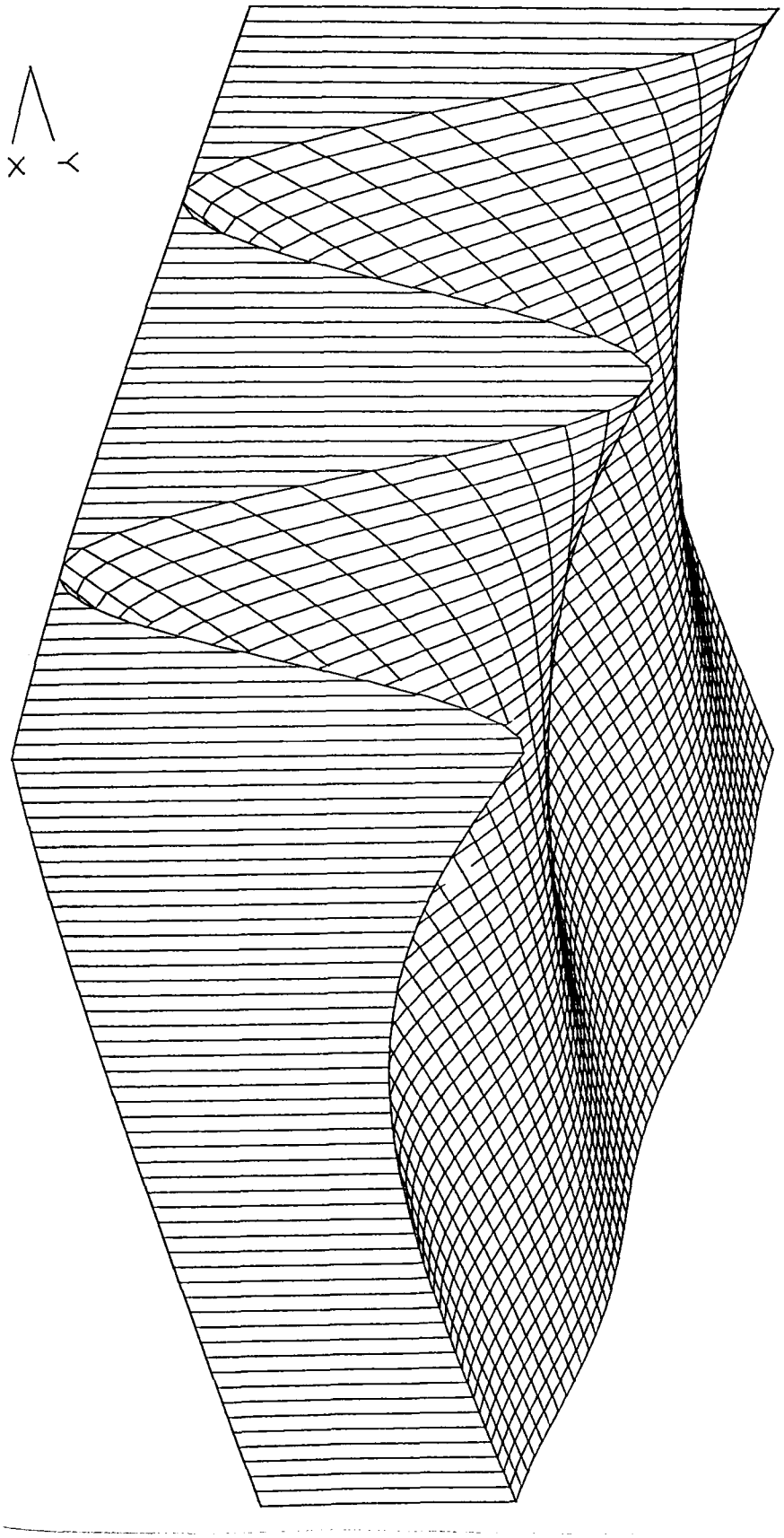

Fig. VIII.3.(c). Analysis. Temperature.

The Rose Soil,

$T_M = 300$; $T_A = 20$; $\theta_M = 0.1$; $\theta_A = 0.0$.

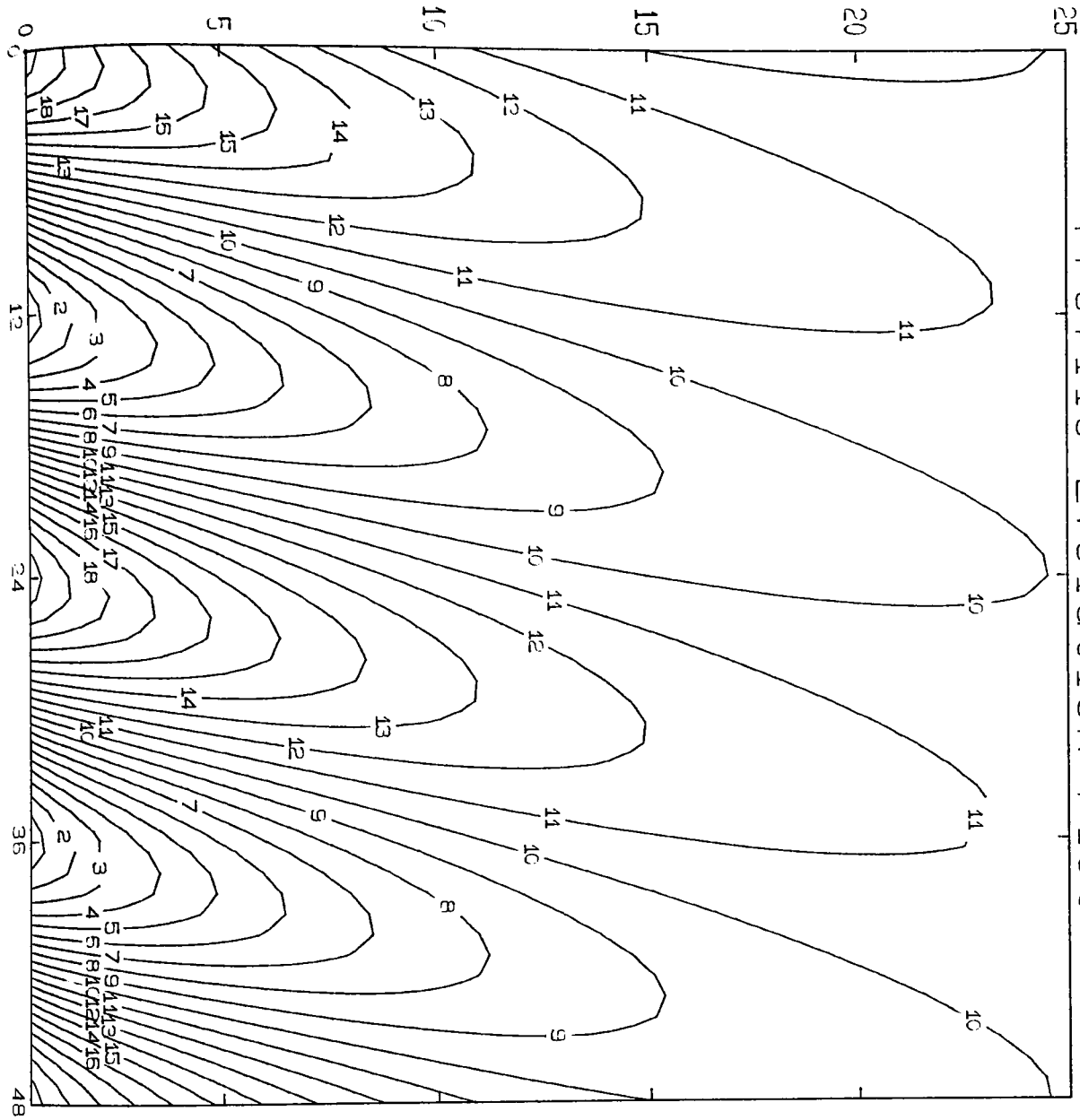

CONTOUR KEY	
1	281.1541
2	283.1462
3	285.1383
4	287.1304
5	289.1224
6	291.1145
7	293.1066
8	295.0988
9	297.0909
10	299.0830
11	301.0751
12	303.0672
13	305.0592
14	307.0514
15	309.0435
16	311.0356
17	313.0277
18	315.0198
19	317.0119
20	319.0039

Fig. VIII.3.(d). Analysis. Temperature. The Rose Soil,

Time, *hrs.* v. Depth, *cms.* v. Temperature, ^oK.

$T_M = 300$; $T_A = 20$; $\theta_M = 0.1$; $\theta_A = 0.0$.

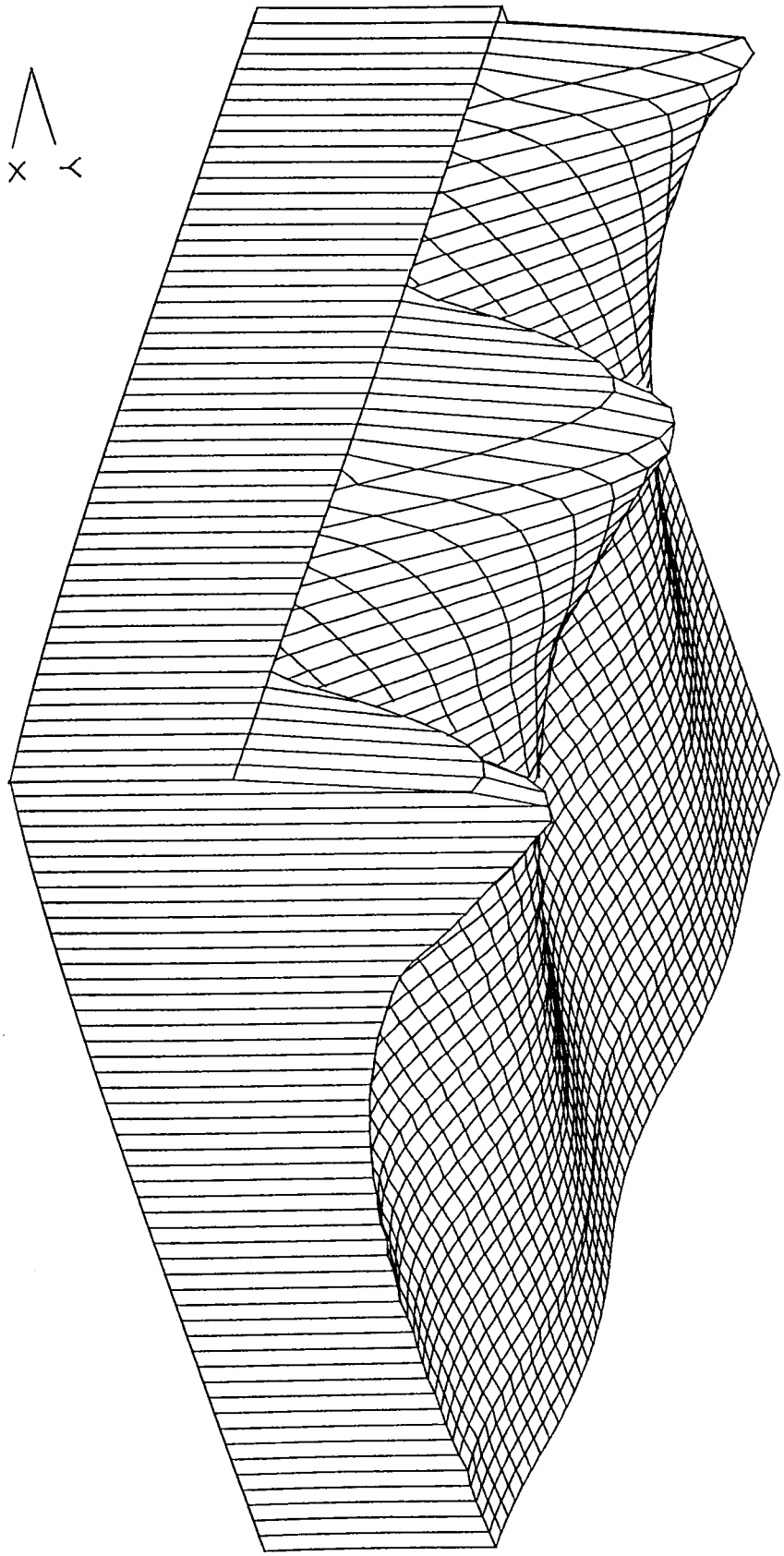

Fig. **VIII**.3.(e). Simulation. Moisture.

The Rose Soil,

$T_M = 300$; $T_A = 20$; $\theta_M = 0.1$; $\theta_A = 0.0$.

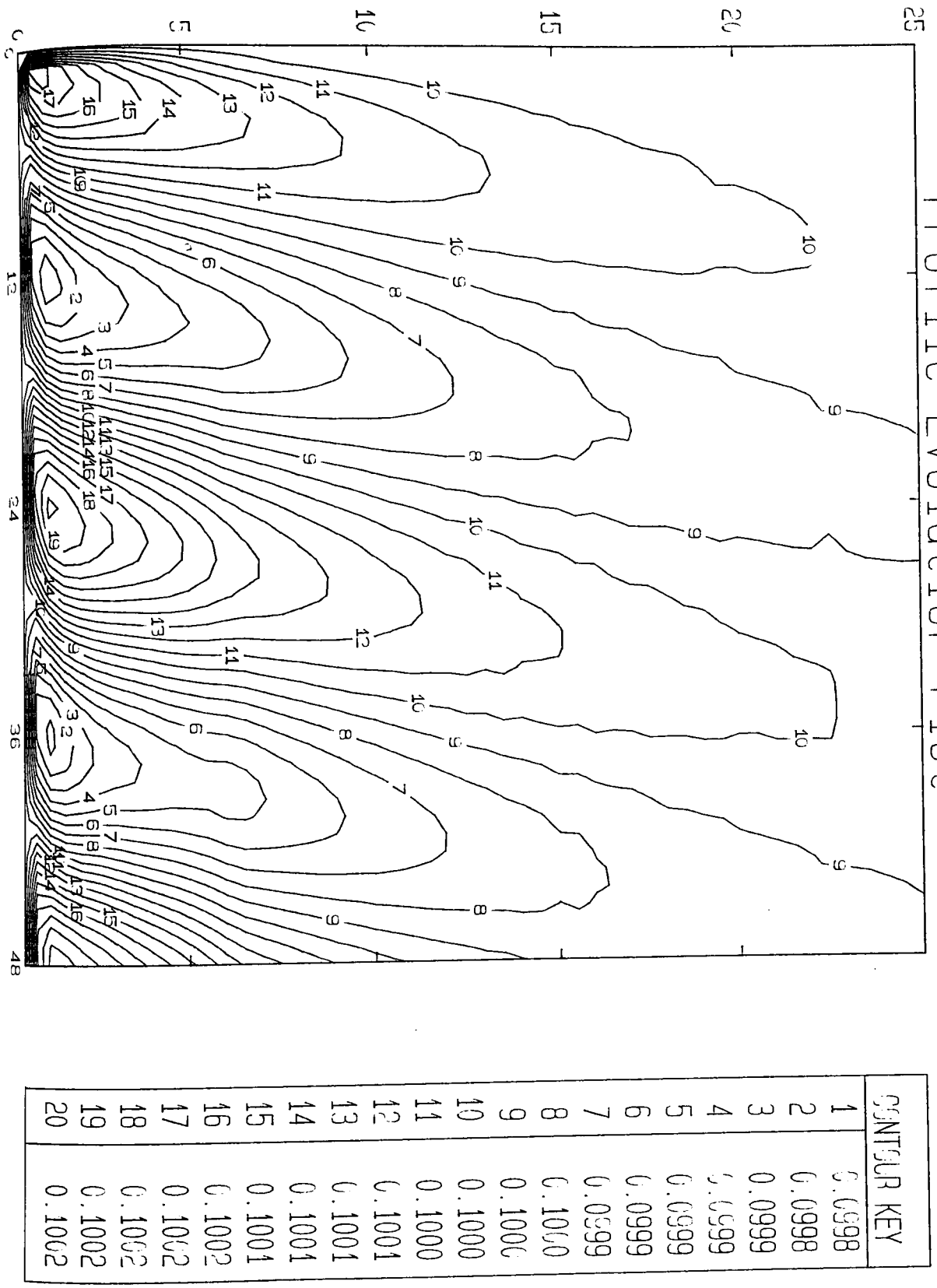

Fig. VIII.3.(f). Simulation. Moisture. The Rose Soil, Time, *hrs.* v. Depth, *cms.* v. Moisture, *dimensionless.* $T_M = 300$; $T_A = 20$; $\theta_M = 0.1$; $\theta_A = 0.0$.

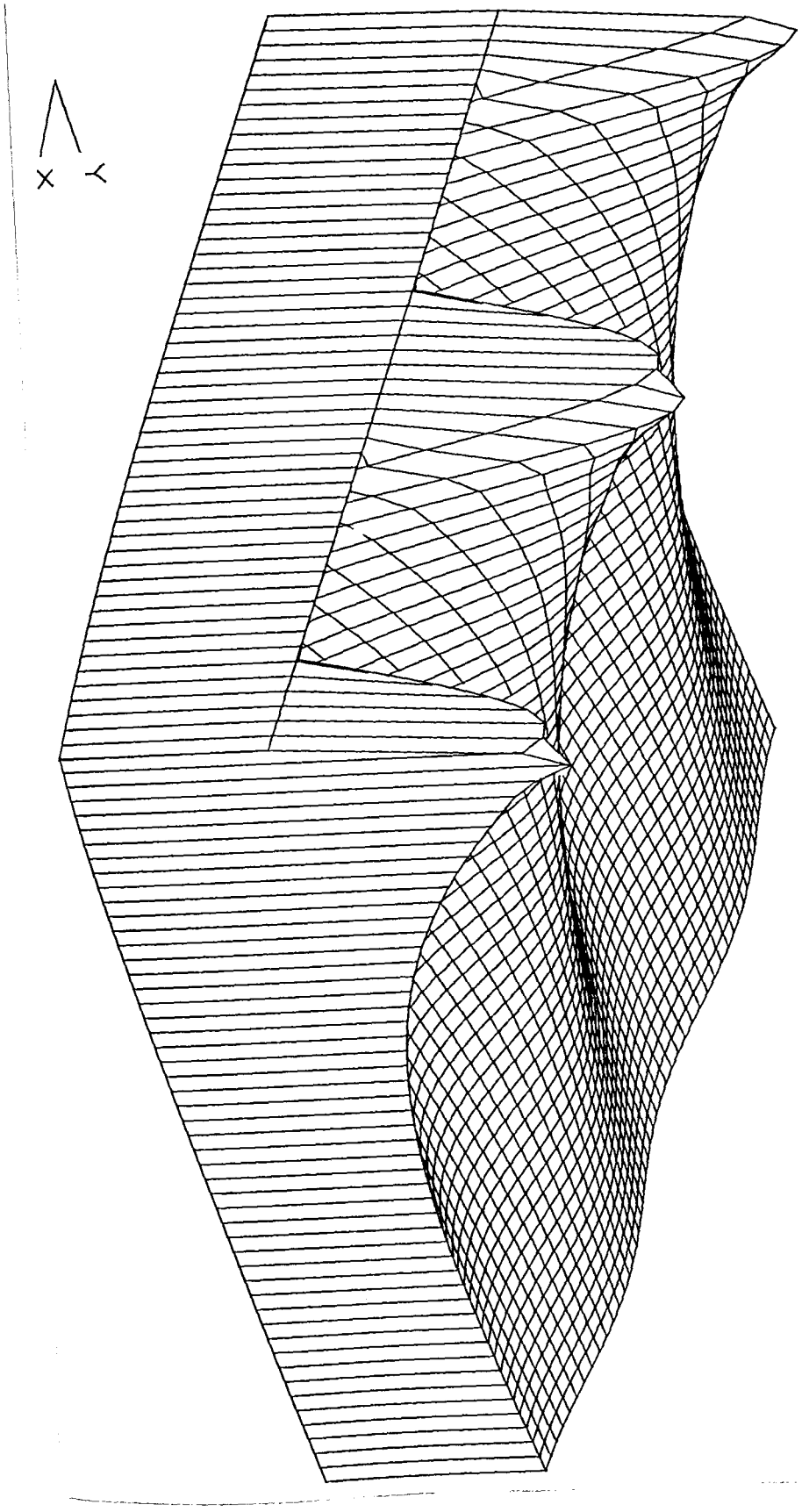

Fig. VIII.3.(g). Analysis. Moisture.

The Rose Soil,

$T_M = 300$; $T_A = 20$; $\theta_M = 0.1$; $\theta_A = 0.0$.

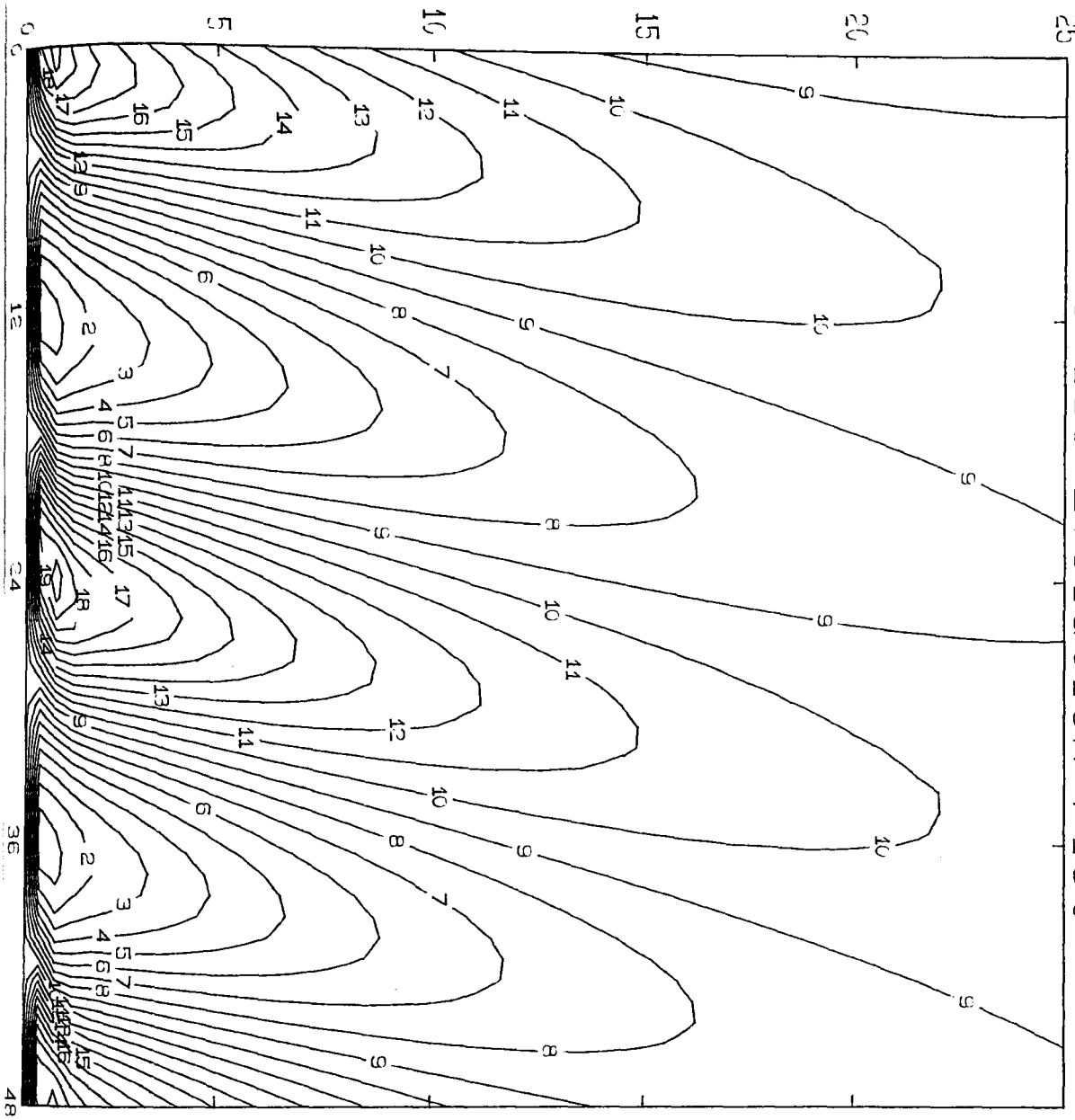

CONTOUR KEY
1 0.0996
2 0.0997
3 0.0997
4 0.0998
5 0.0998
6 0.0998
7 0.0999
8 0.0999
9 0.1000
10 0.1000
11 0.1001
12 0.1001
13 0.1002
14 0.1002
15 0.1003
16 0.1003
17 0.1003
18 0.1004
19 0.1004
20 0.1005

Fig. VIII.3.(h). Analysis. Moisture. The Rose Soil,
Time, *hrs.* v. Depth, *cms.* v. Moisture, *dimensionless.*
$T_M = 300$; $T_A = 20$; $\theta_M = 0.1$; $\theta_A = 0.0$

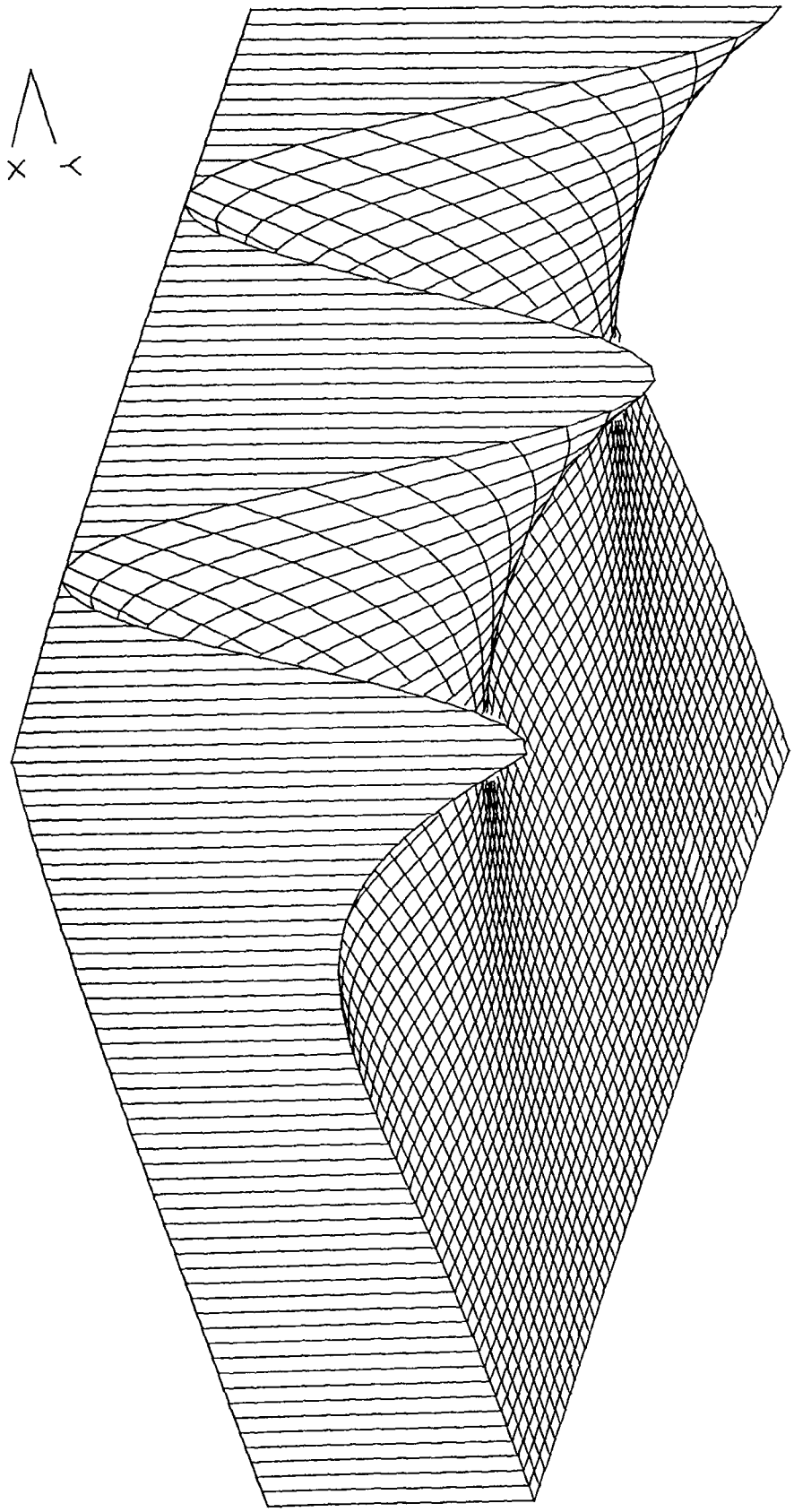

Fig. VIII.4.(a). Simulation. Moisture.

The Rose Soil,

$T_M = 300$; $T_A = 5$; $\theta_M = 0.2$; $\theta_A = 0.01$.

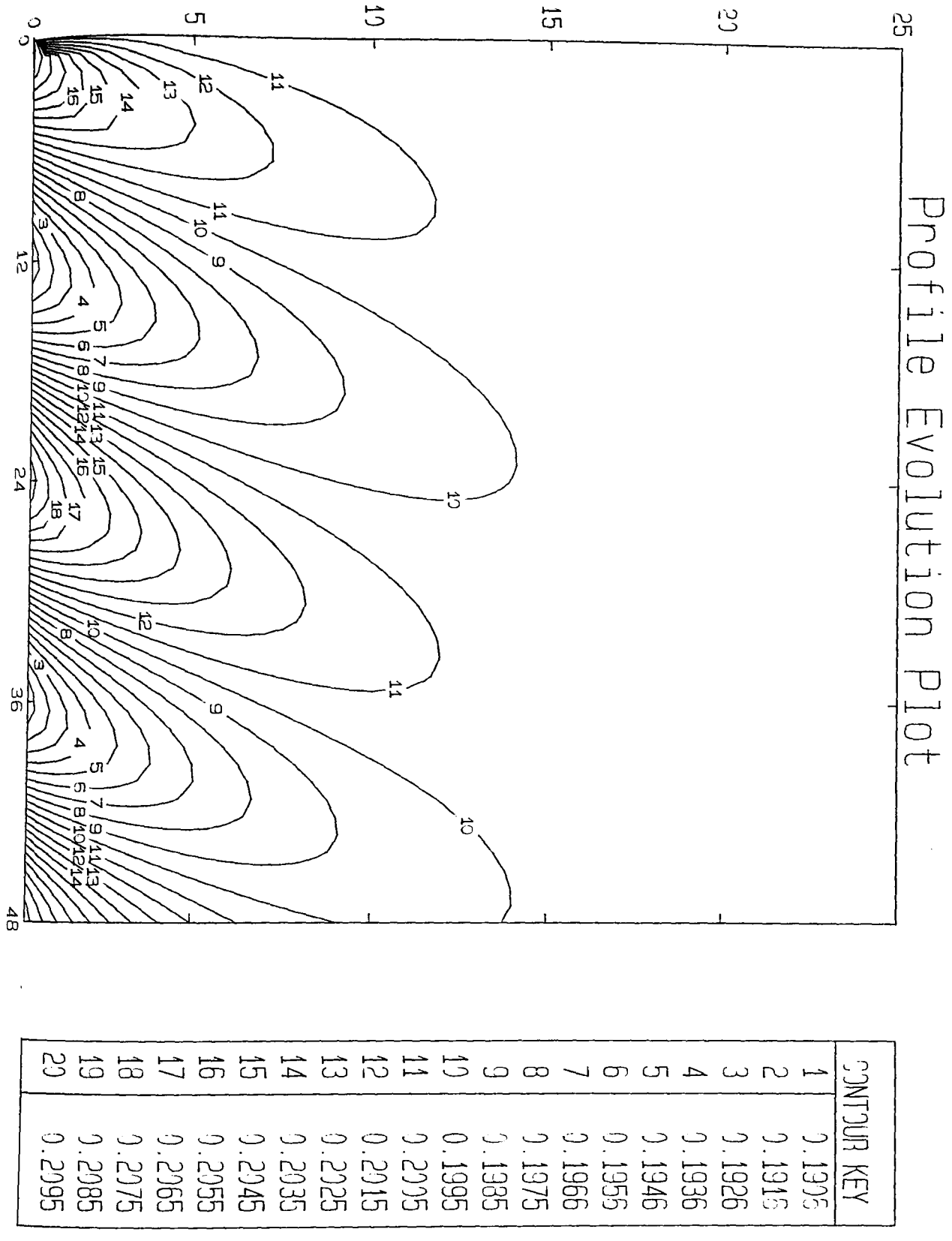

CONTOUR KEY
1 0.1905
2 0.1915
3 0.1926
4 0.1936
5 0.1946
6 0.1956
7 0.1966
8 0.1975
9 0.1985
10 0.1995
11 0.2005
12 0.2015
13 0.2025
14 0.2035
15 0.2045
16 0.2055
17 0.2065
18 0.2075
19 0.2085
20 0.2095

Fig. VIII.4.(b). Simulation. Moisture. The Rose Soil,
Time, *hrs.* v. Depth, *cms.* v. Moisture, *dimensionless.*
$T_M = 300$; $T_A = 20$; $\theta_M = 0.2$; $\theta_A = 0.01$.

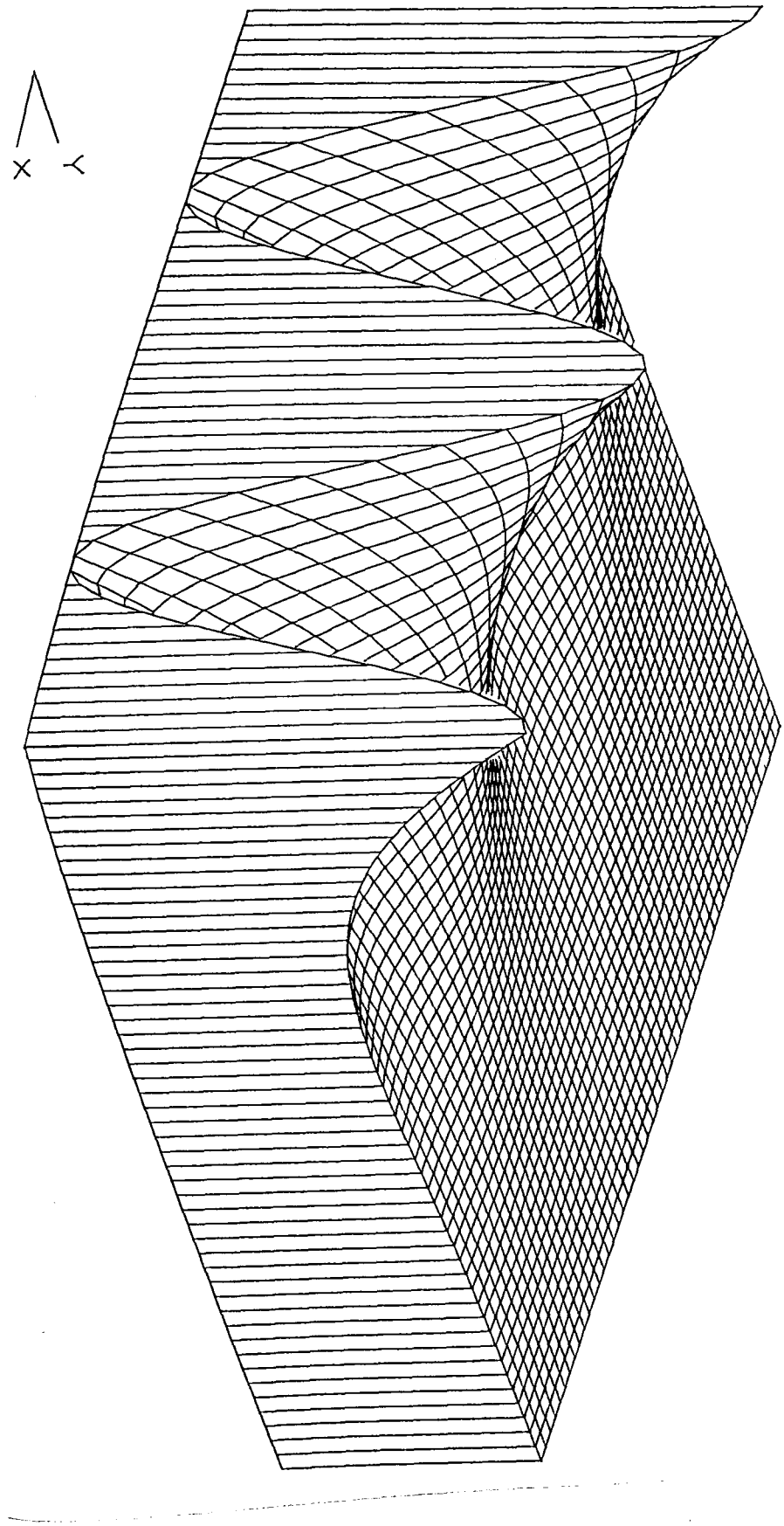

Fig. VIII.4.(c). Analysis. Moisture.

The Rose Soil,

$T_M = 300$; $T_A = 5$; $\theta_M = 0.2$; $\theta_A = 0.01$.

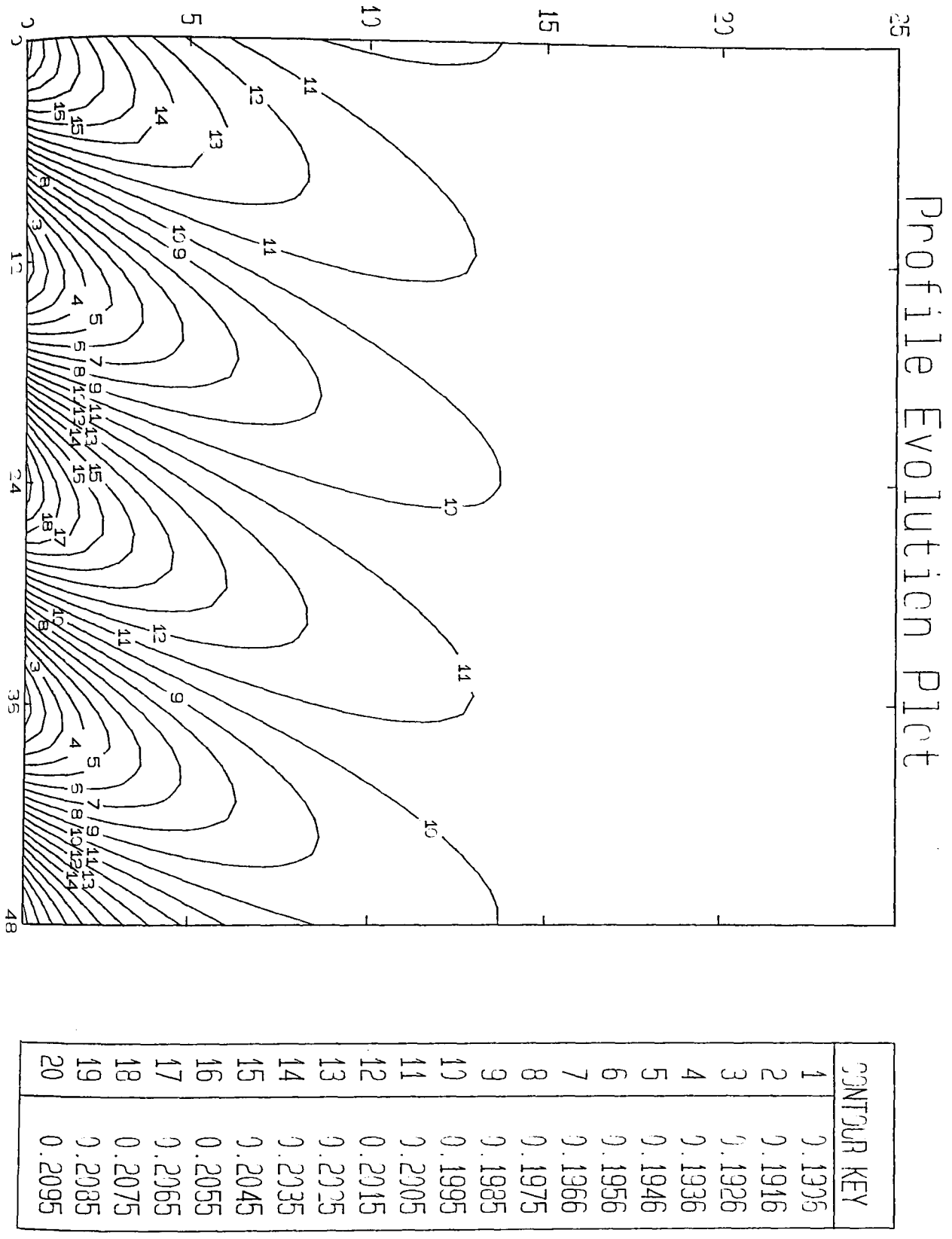

Fig. VIII.4.(d). Analysis. Moisture. The Rose Soil,
Time, *hrs.* v. Depth, *cms.* v. Moisture, *dimensionless.*
$T_M = 300$; $T_A = 20$; $\theta_M = 0.2$; $\theta_A = 0.01$.

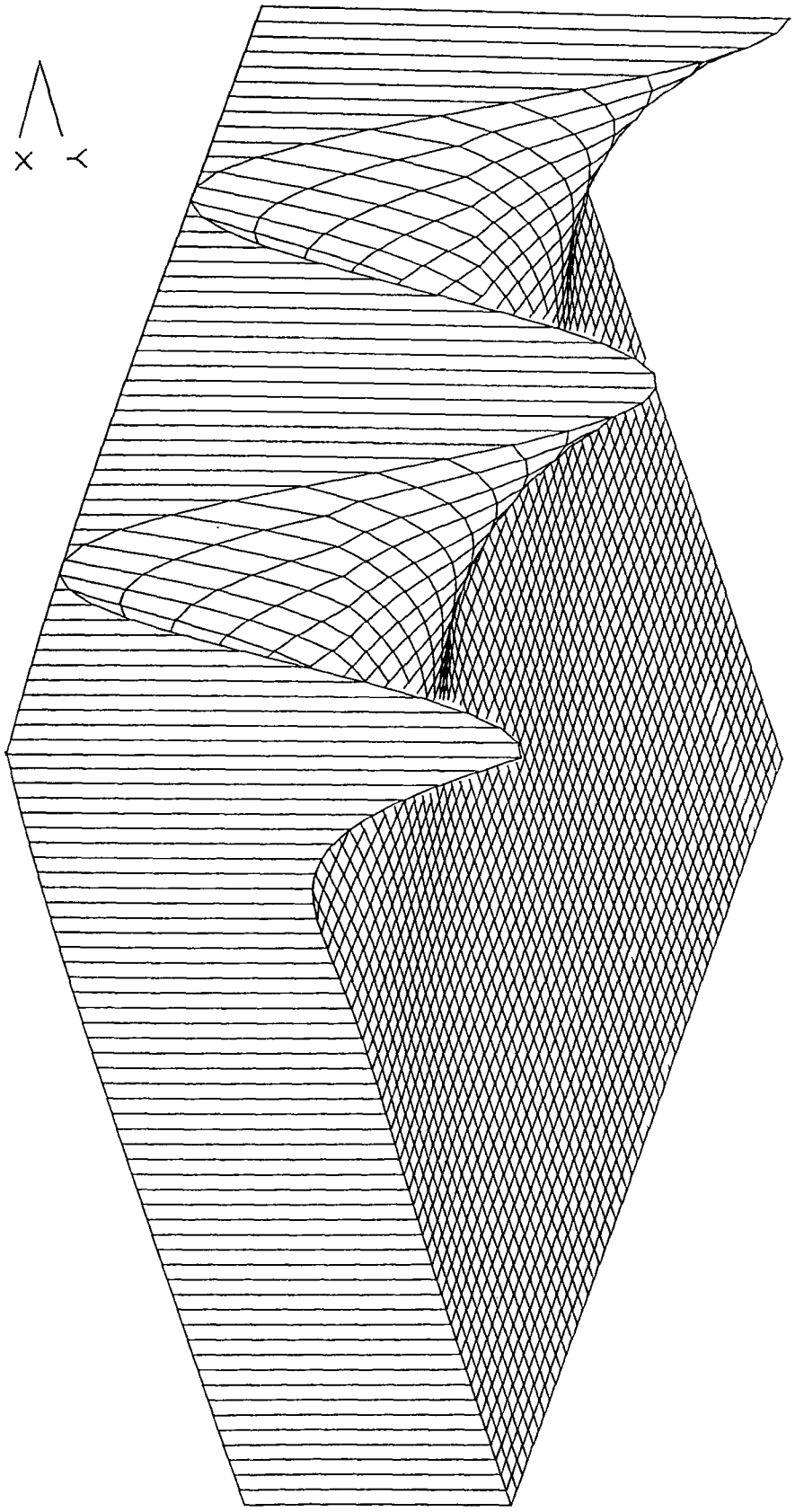

Fig. VIII.5.(a). Simulation. Moisture.

The Rose Soil,

$T_M = 300$; $T_A = 5$; $\theta_M = 0.15$; $\theta_A = 0.01$.

CONTOUR KEY
1 0.1406
2 0.1416
3 0.1426
4 0.1436
5 0.1446
6 0.1456
7 0.1466
8 0.1475
9 0.1485
10 0.1495
11 0.1505
12 0.1515
13 0.1525
14 0.1535
15 0.1545
16 0.1555
17 0.1565
18 0.1575
19 0.1585
20 0.1595

Fig. VIII.5.(b). Simulation. Moisture. The Rose Soil, Time, *hrs.* v. Depth, *cms.* v. Moisture, *dimensionless.* $T_M = 300$; $T_A = 20$; $\theta_M = 0.15$; $\theta_A = 0.01$.

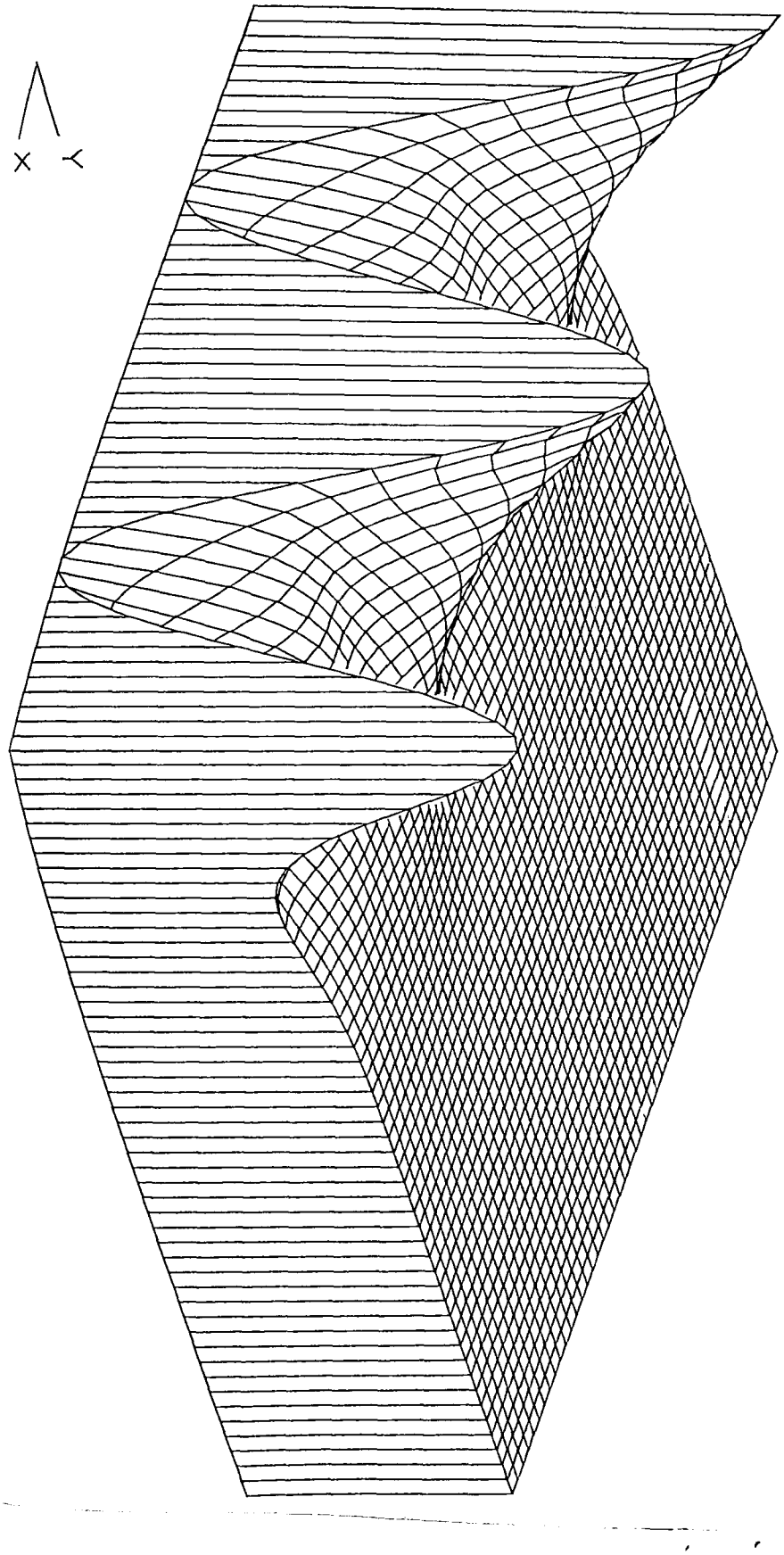

Fig. VIII.5.(c). Analysis. Moisture.

The Rose Soil,

$T_M = 300$; $T_A = 5$; $\theta_M = 0.15$; $\theta_A = 0.01$.

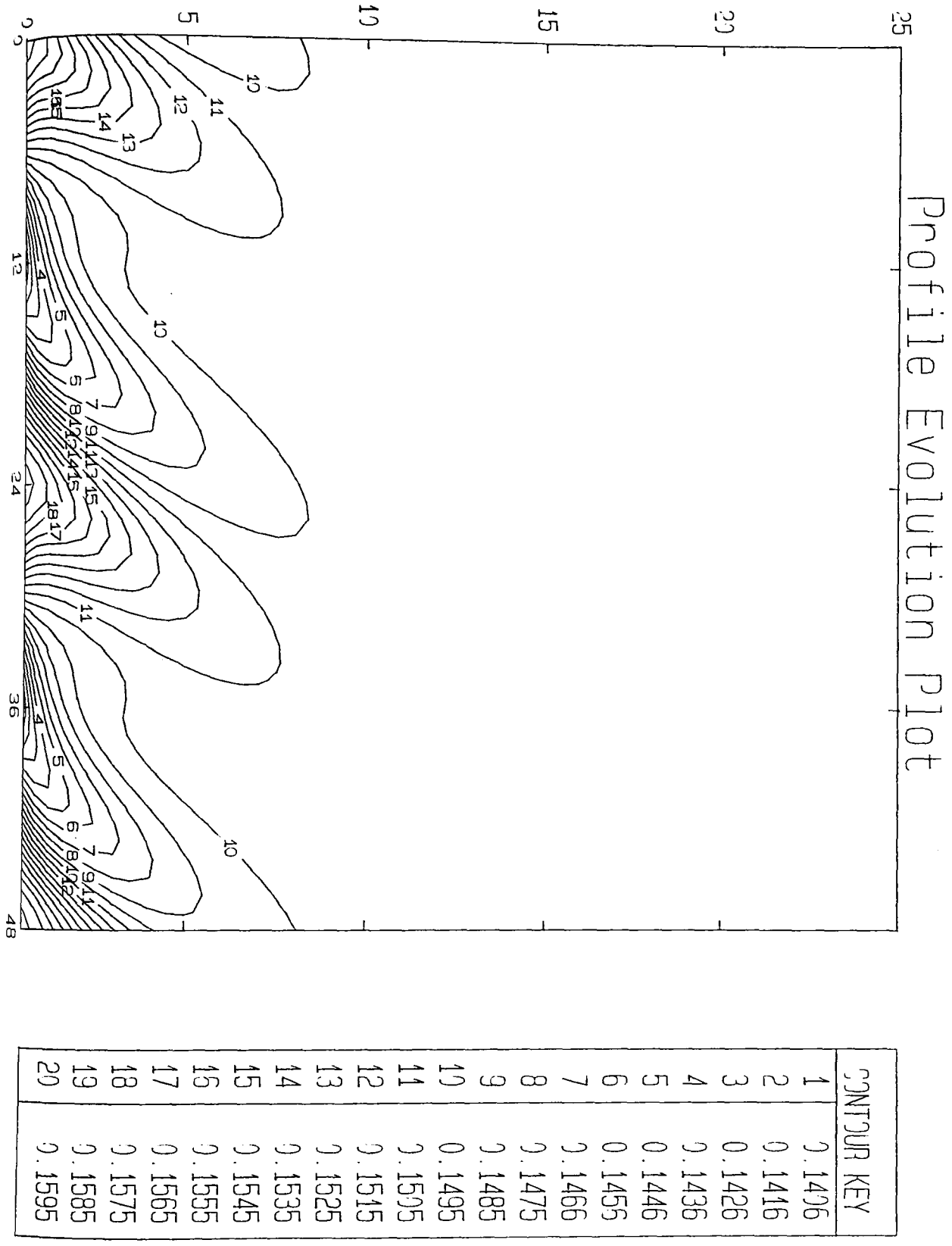

CONTOUR KEY	
1	0.1406
2	0.1416
3	0.1426
4	0.1436
5	0.1446
6	0.1456
7	0.1466
8	0.1475
9	0.1485
10	0.1495
11	0.1505
12	0.1515
13	0.1525
14	0.1535
15	0.1545
16	0.1555
17	0.1565
18	0.1575
19	0.1585
20	0.1595

Fig. VIII.5.(d). Analysis. Moisture. The Rose Soil,
Time, *hrs.* v. Depth, *cms.* v. Moisture, *dimensionless.*
$T_M = 300$; $T_A = 20$; $\theta_M = 0.15$; $\theta_A = 0.01$.

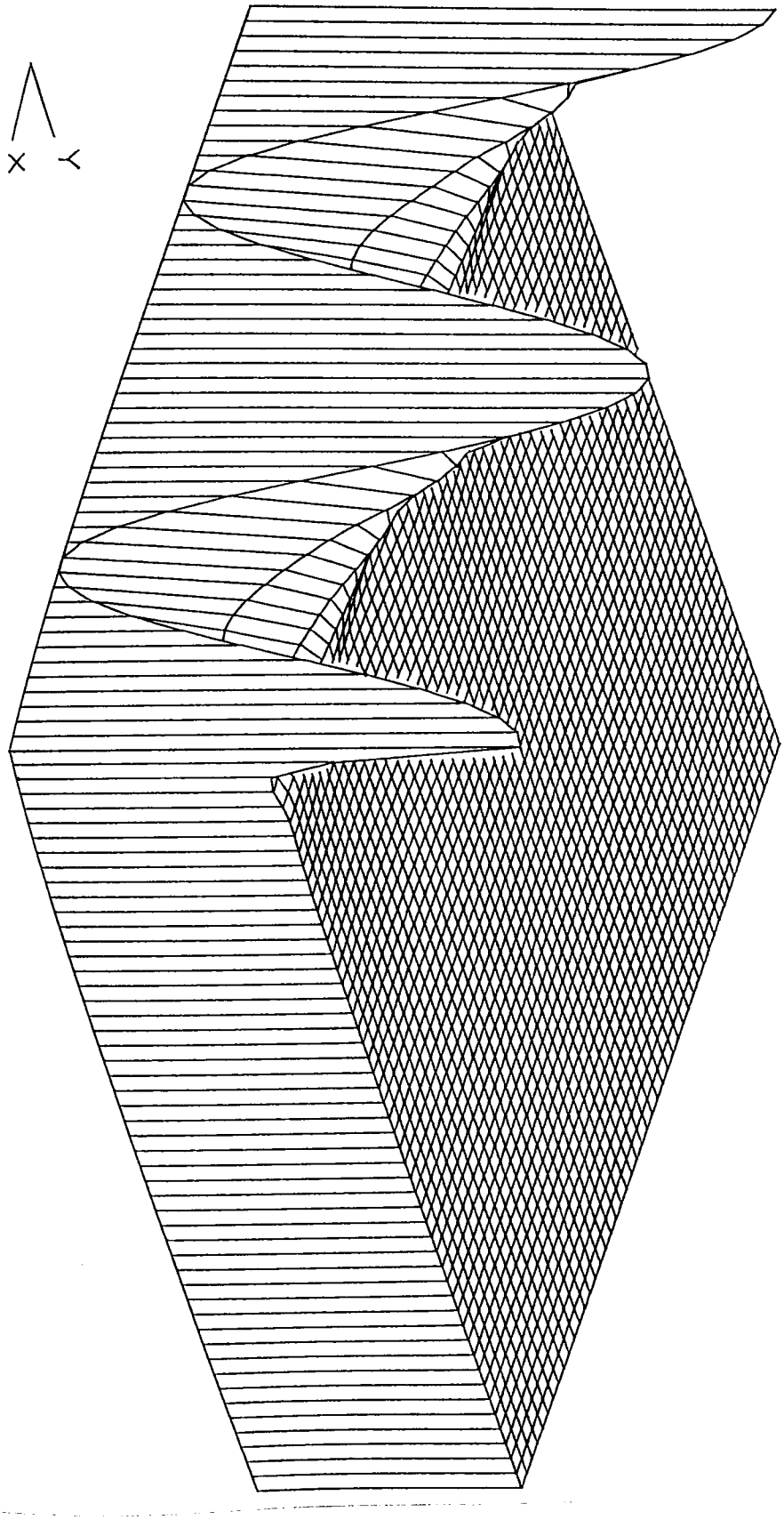

Fig. **VIII**.6.(a). Simulation. Moisture.

The Rose Soil,

$T_M = 300$; $T_A = 5$; $\theta_M = 0.1$; $\theta_A = 0.01$.

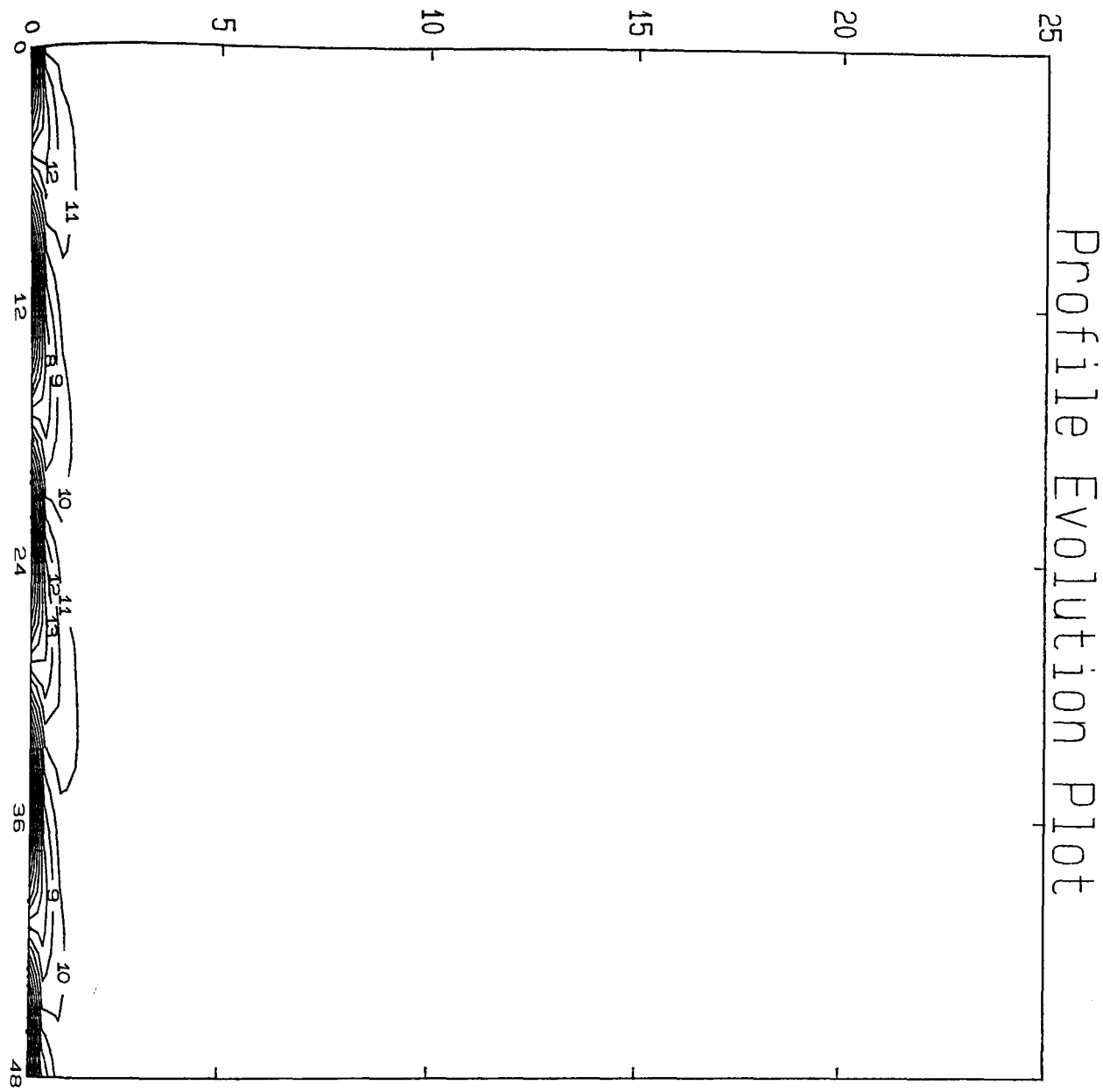

CONTOUR KEY	
1	0.0906
2	0.0916
3	0.0926
4	0.0936
5	0.0946
6	0.0956
7	0.0966
8	0.0975
9	0.0985
10	0.0995
11	0.1005
12	0.1015
13	0.1025
14	0.1035
15	0.1045
16	0.1055
17	0.1065
18	0.1075
19	0.1085
20	0.1095

Fig. **VIII**.6.(b). Simulation. Moisture. The Rose Soil, Time, *hrs.* v. Depth, *cms.* v. Moisture, *dimensionless.* $T_M = 300$; $T_A = 20$; $\theta_M = 0.1$; $\theta_A = 0.01$.

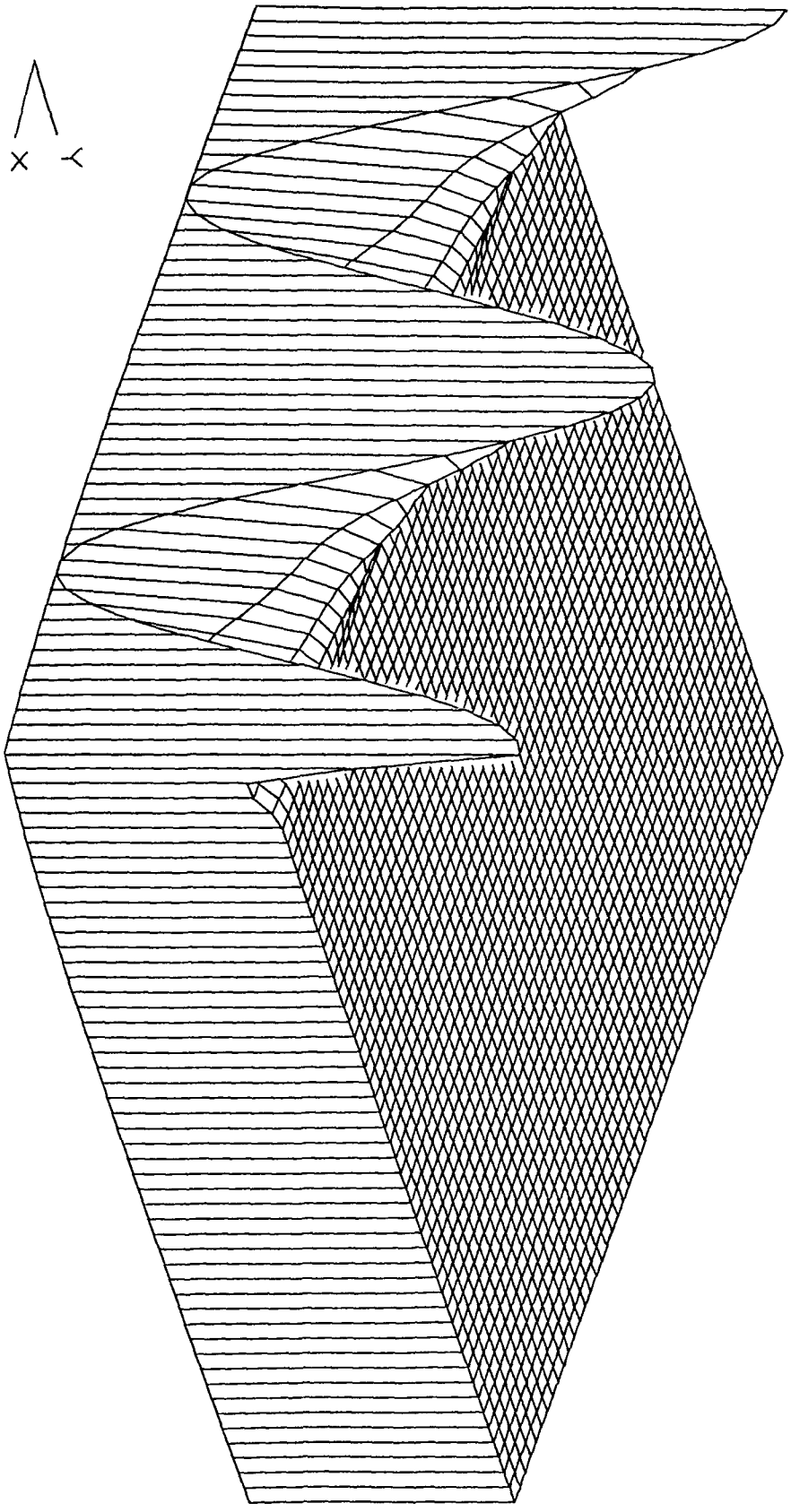

Fig. VIII.6.(c). Analysis. Moisture.

The Rose Soil,

$T_M = 300$; $T_A = 20$; $\theta_M = 0.1$; $\theta_A = 0.01$.

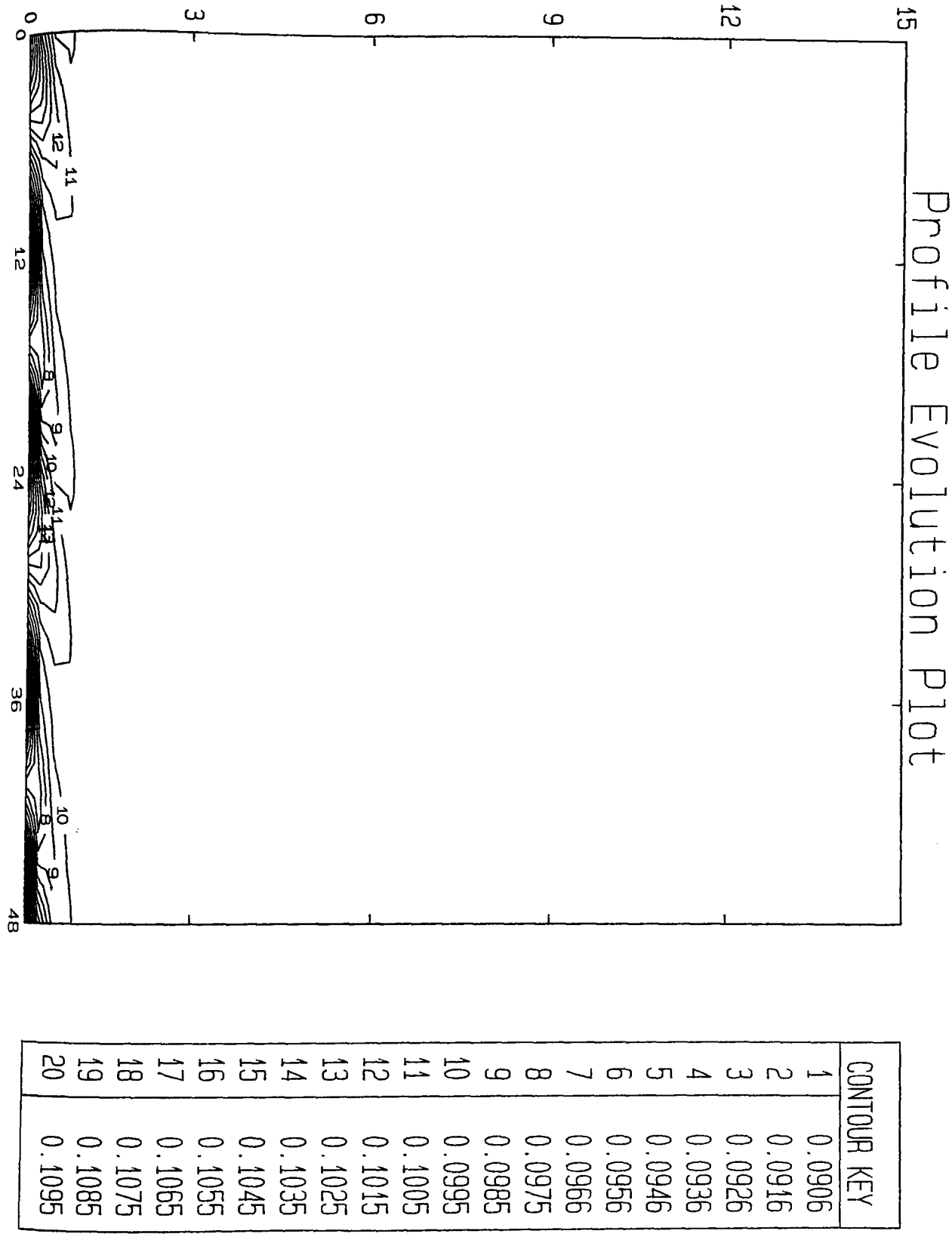

CONTOUR KEY	
1	0.0906
2	0.0916
3	0.0926
4	0.0936
5	0.0946
6	0.0956
7	0.0966
8	0.0975
9	0.0985
10	0.0995
11	0.1005
12	0.1015
13	0.1025
14	0.1035
15	0.1045
16	0.1055
17	0.1065
18	0.1075
19	0.1085
20	0.1095

Fig. **VIII**.6.(d). Analysis. Moisture. The Rose Soil,
Time, *hrs.* v. Depth, *cms.* v. Moisture, *dimensionless.*
$T_M = 300$; $T_A = 20$; $\theta_M = 0.1$; $\theta_A = 0.01$.

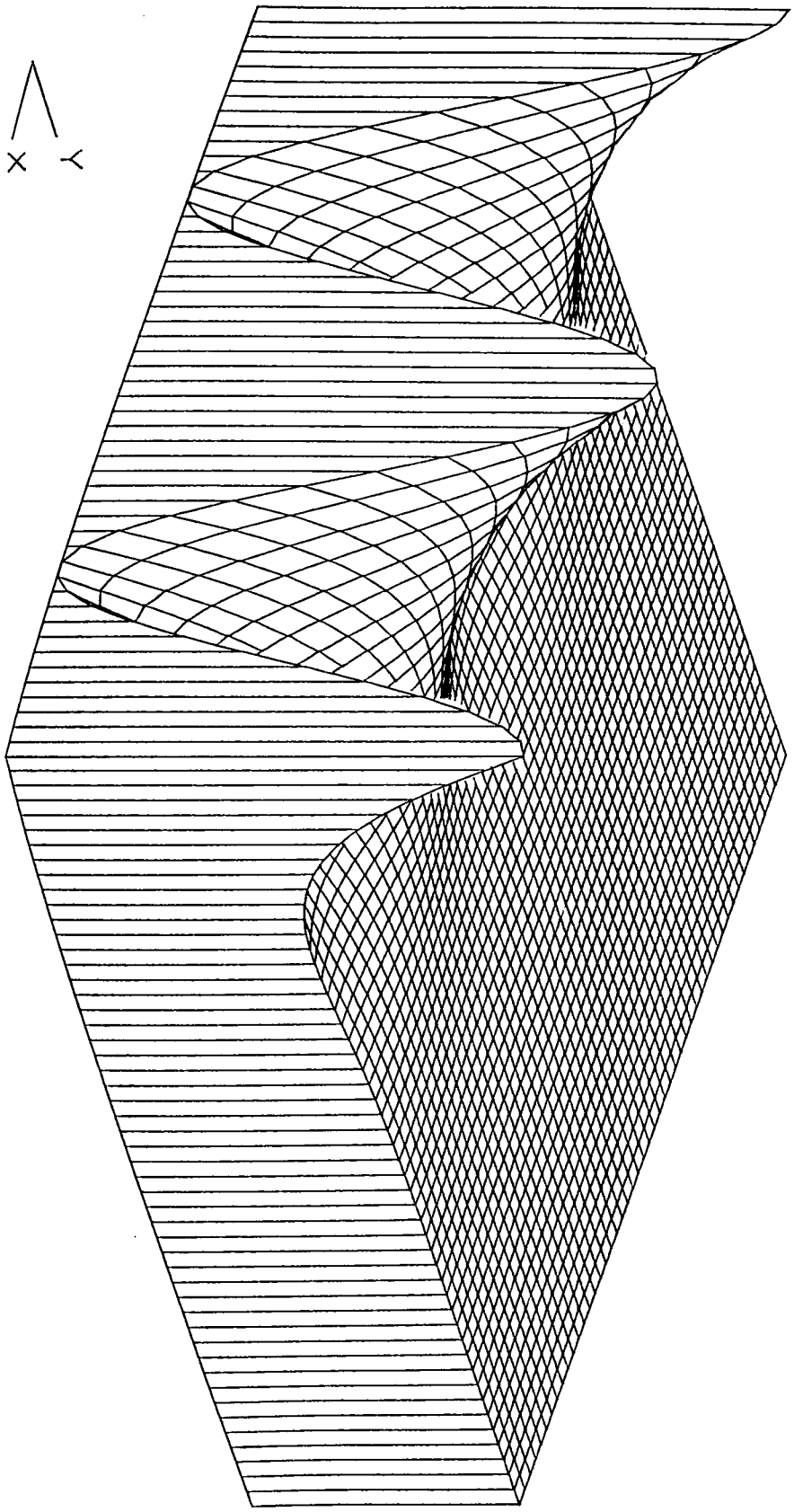

Fig. VIII.7.(a). Simulation. Moisture.

Adelanto Loam,

$T_M = 300$; $T_A = 5$; $\theta_M = 0.2$; $\theta_A = 0.01$.

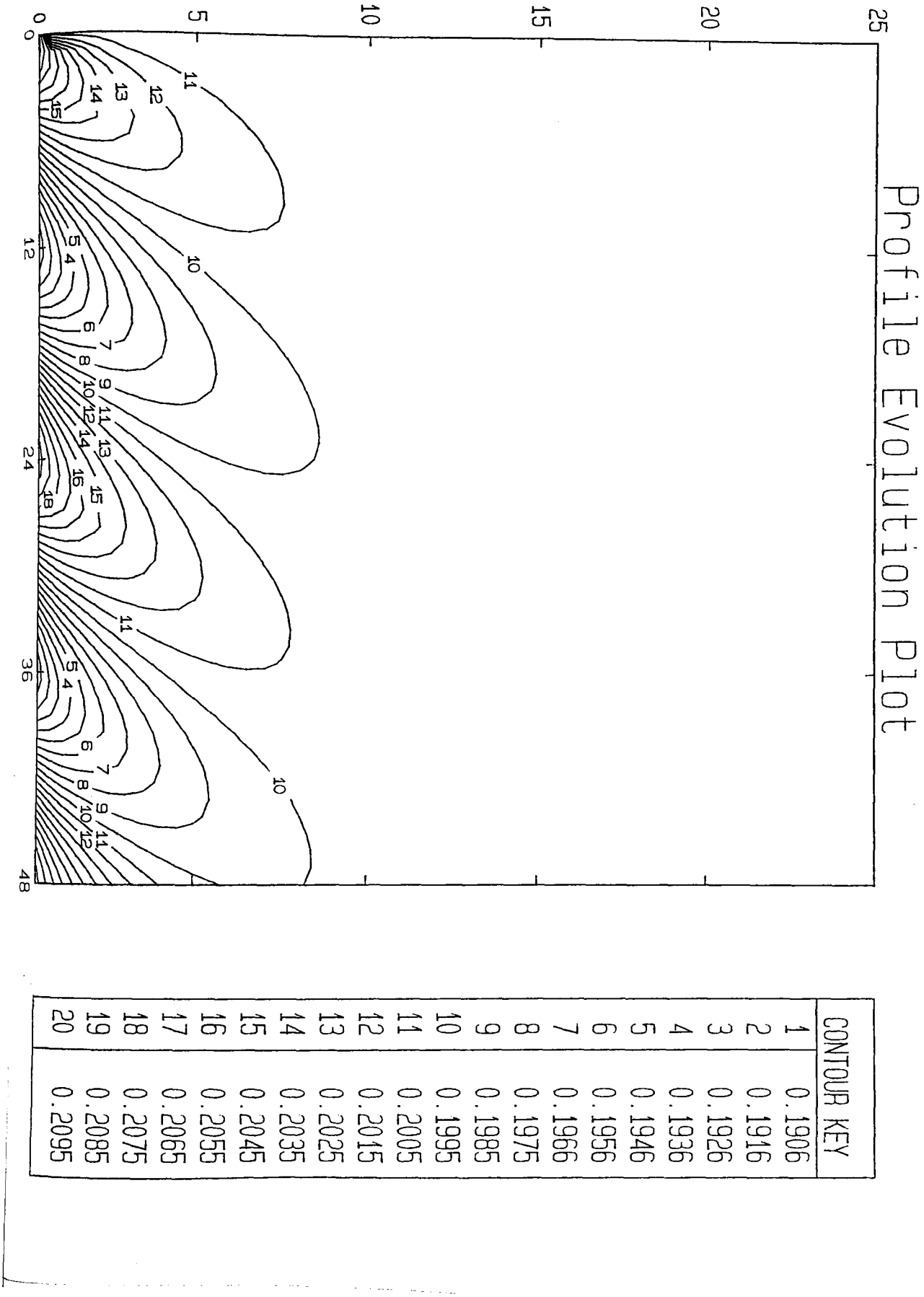

Fig. VIII.7.(b). Simulation. Moisture. Adelanto Loam, Time, *hrs.* v. Depth, *cms.* v. Moisture, *dimensionless.* $T_M = 300$; $T_A = 20$; $\theta_M = 0.2$; $\theta_A = 0.01$.

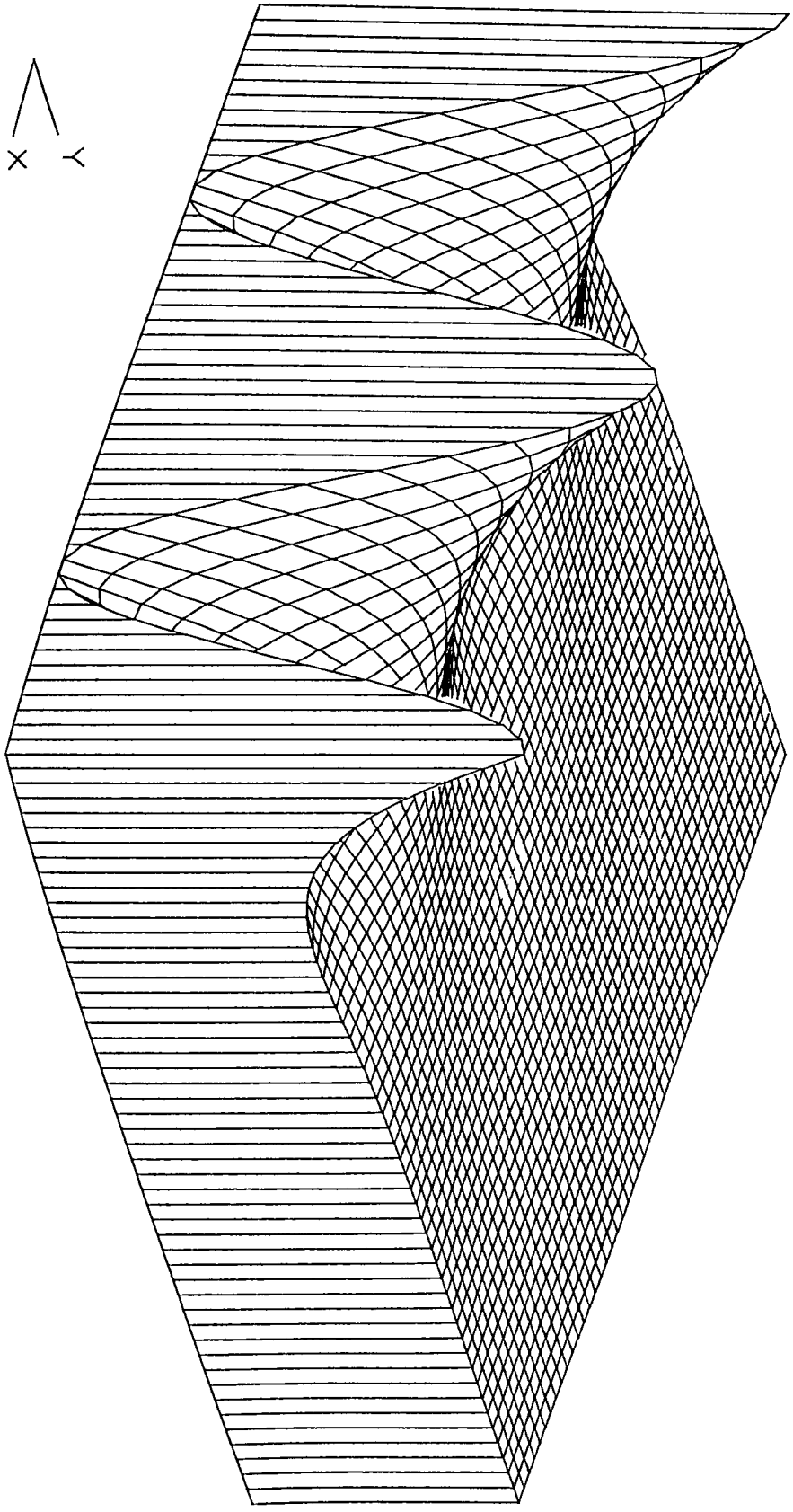

Fig. VIII.7.(c). Analysis. Moisture.

Adelanto Loam,

$T_M = 300$; $T_A = 5$; $\theta_M = 0.2$; $\theta_A = 0.01$.

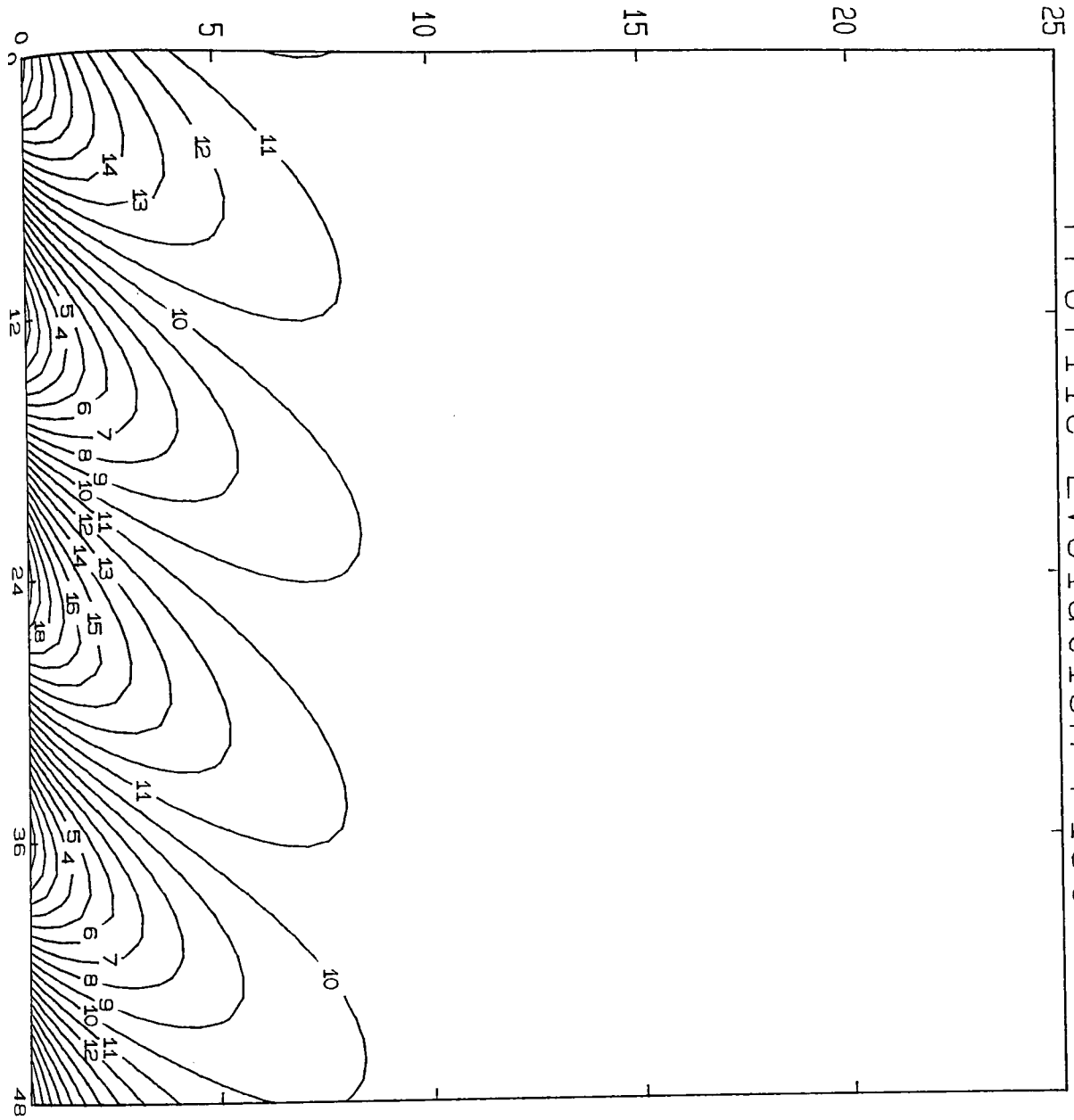

CONTOUR KEY	
1	0.1906
2	0.1916
3	0.1926
4	0.1936
5	0.1946
6	0.1956
7	0.1966
8	0.1975
9	0.1985
10	0.1995
11	0.2005
12	0.2015
13	0.2025
14	0.2035
15	0.2045
16	0.2055
17	0.2065
18	0.2075
19	0.2085
20	0.2095

Fig. VIII.7.(d). Analysis. Moisture. Adelanto Loam,
Time, *hrs.* v. Depth, *cms.* v. Moisture, *dimensionless.*
$T_M = 300$; $T_A = 20$; $\theta_M = 0.2$; $\theta_A = 0.01$.

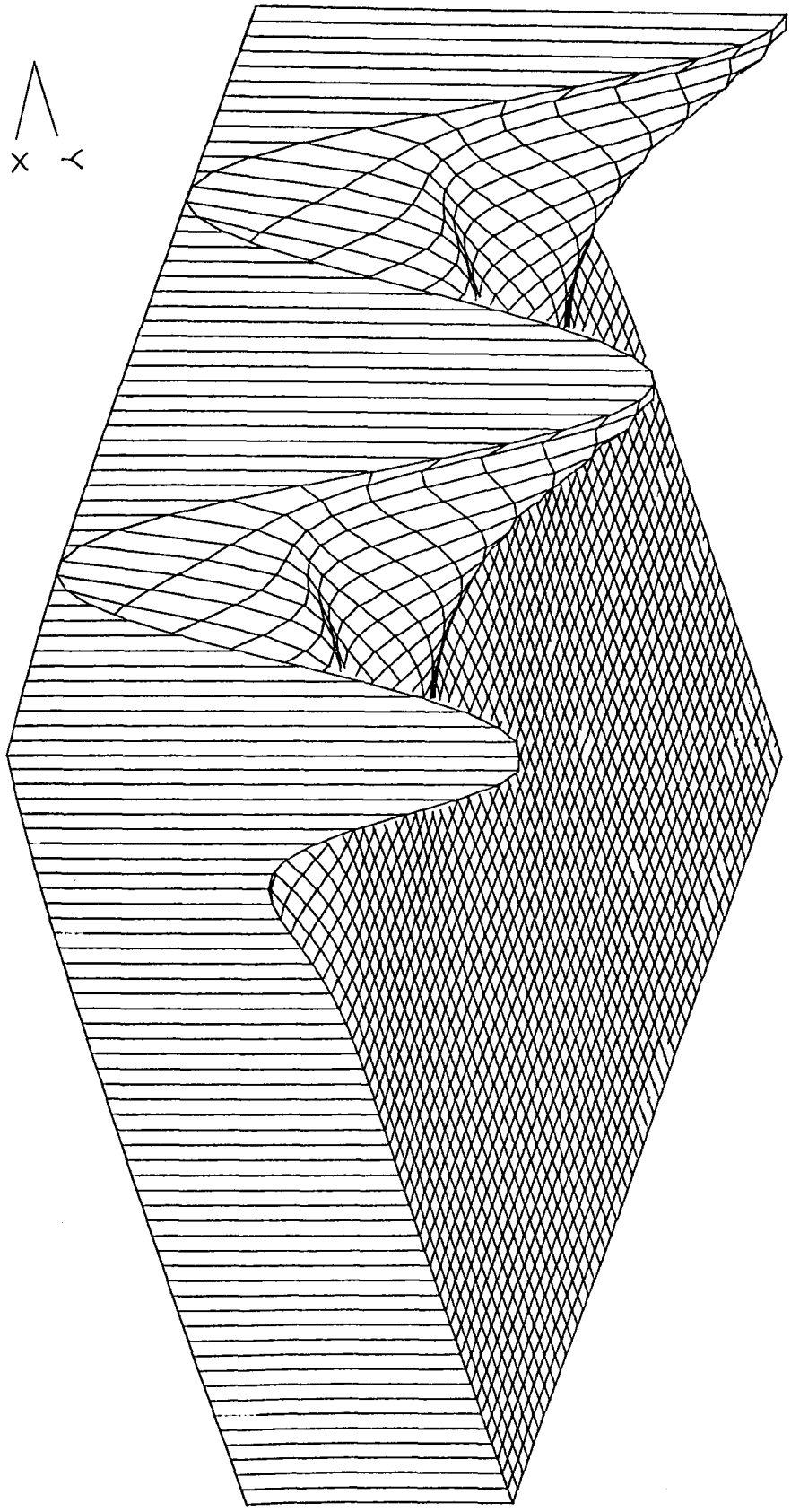

Fig. VIII.8.(a). Simulation. Moisture.

Adelanto Loam,

$T_M = 300$; $T_A = 5$; $\theta_M = 0.15$; $\theta_A = 0.01$.

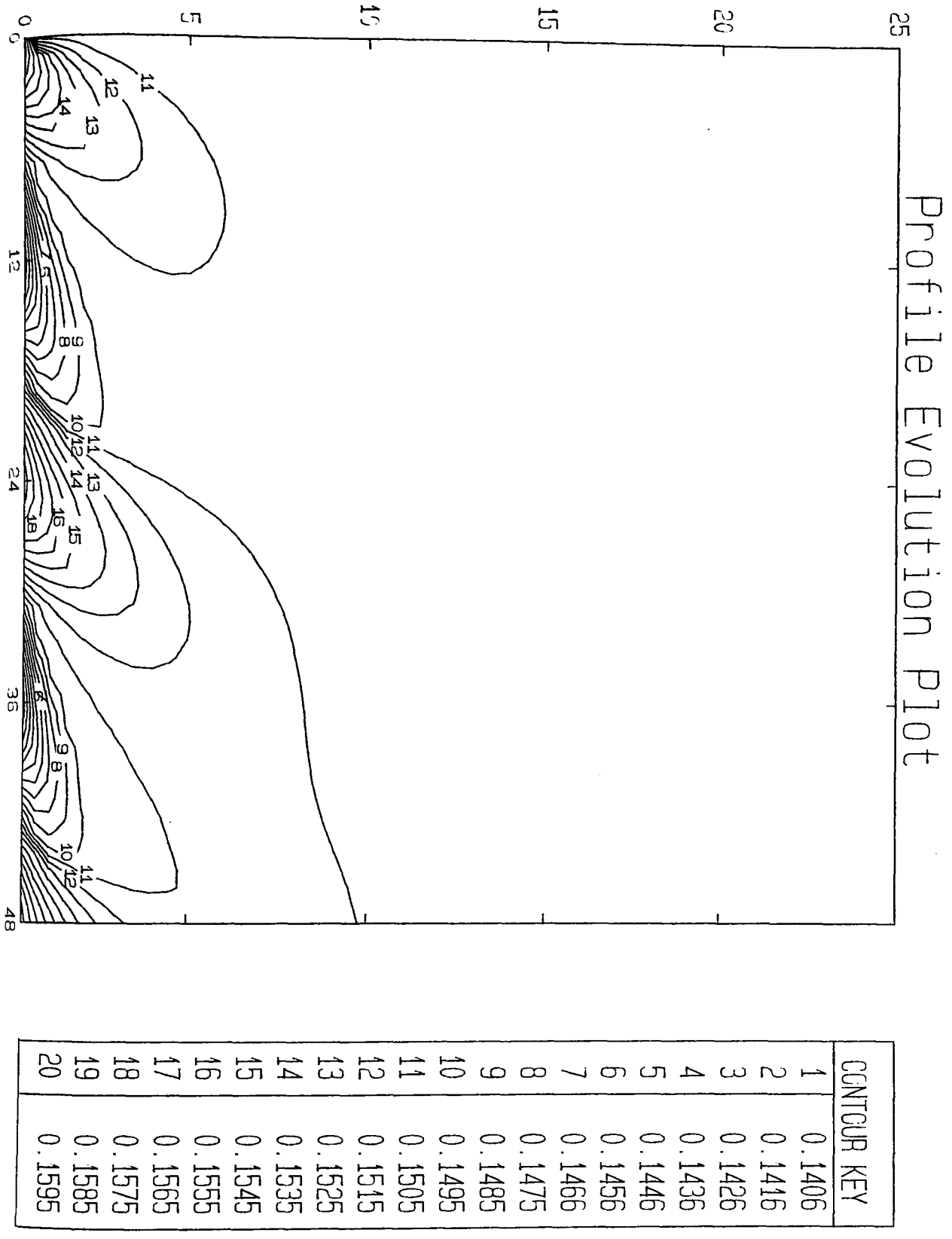

CONTOUR KEY	
1	0.1406
2	0.1416
3	0.1426
4	0.1436
5	0.1446
6	0.1456
7	0.1466
8	0.1475
9	0.1485
10	0.1495
11	0.1505
12	0.1515
13	0.1525
14	0.1535
15	0.1545
16	0.1555
17	0.1565
18	0.1575
19	0.1585
20	0.1595

Fig. **VIII**.8.(b). Simulation. Moisture. Adelanto Loam, Time, *hrs.* v. Depth, *cms.* v. Moisture, *dimensionless.* $T_M = 300$; $T_A = 20$; $\theta_M = 0.15$; $\theta_A = 0.01$.

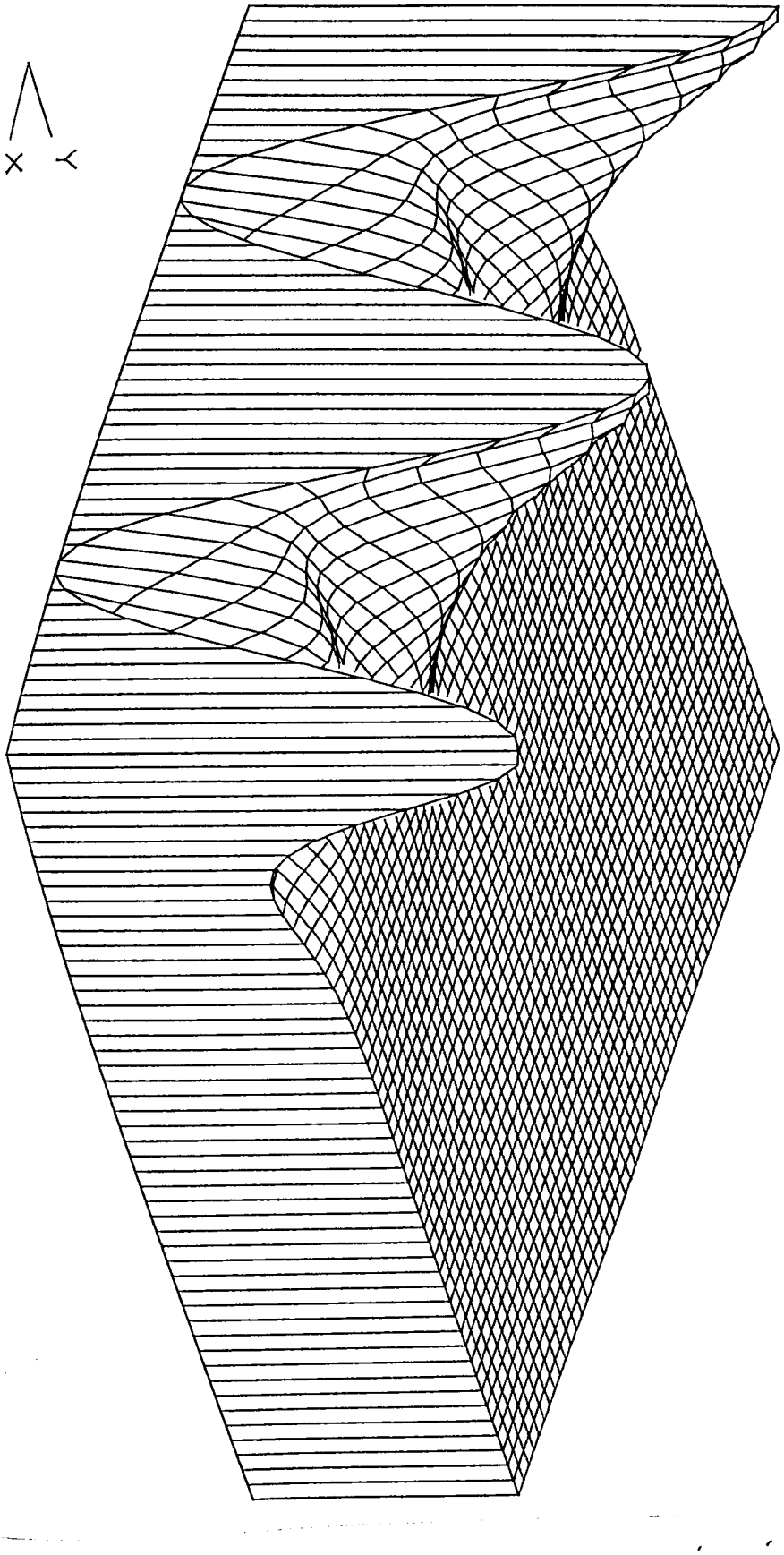

Fig. VIII.8.(c). Analysis. Moisture.

Adelanto Loam,

$T_M = 300$; $T_A = 5$; $\theta_M = 0.15$; $\theta_A = 0.01$.

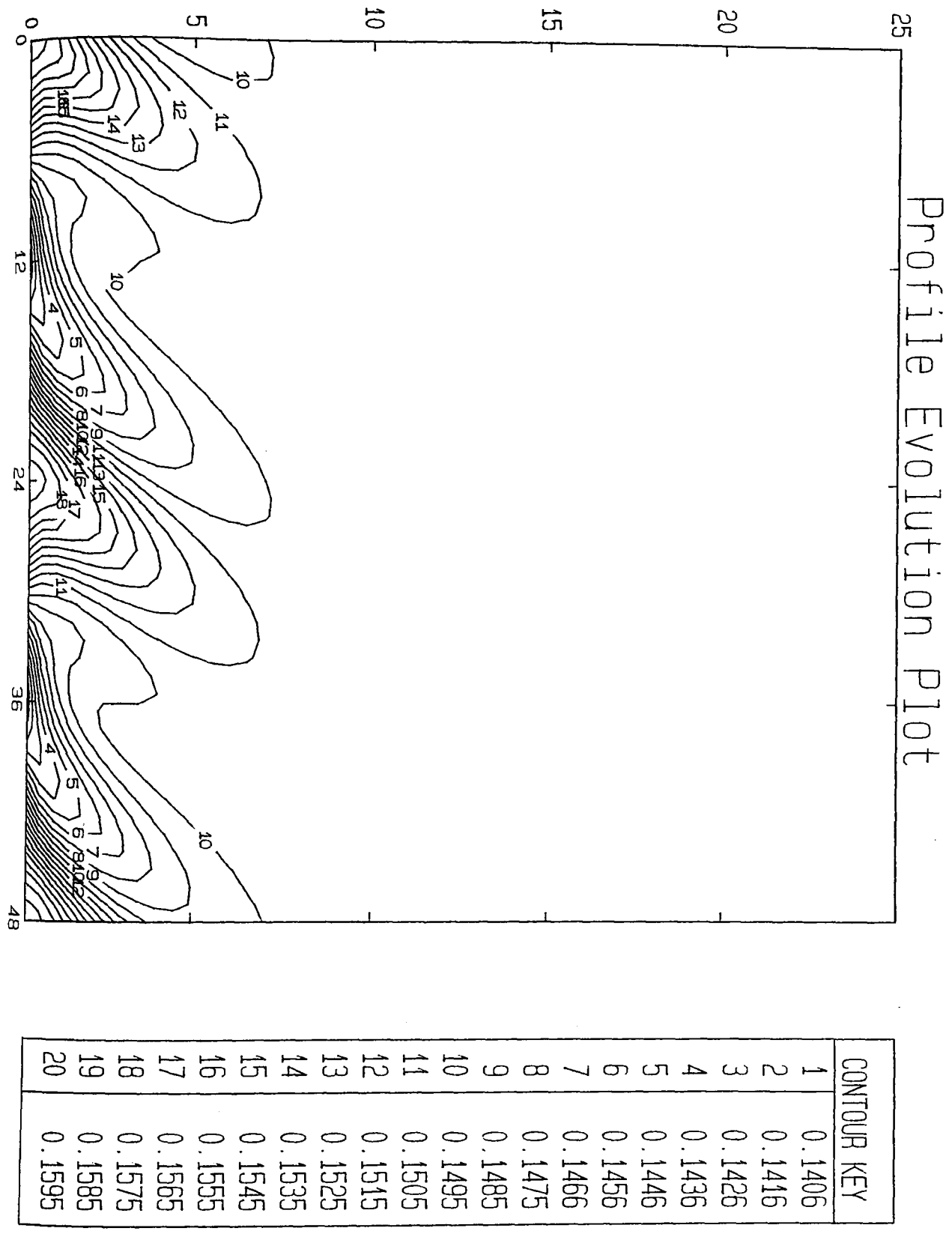

CONTOUR KEY
1 0.1406
2 0.1416
3 0.1426
4 0.1436
5 0.1446
6 0.1456
7 0.1466
8 0.1475
9 0.1485
10 0.1495
11 0.1505
12 0.1515
13 0.1525
14 0.1535
15 0.1545
16 0.1555
17 0.1565
18 0.1575
19 0.1585
20 0.1595

Fig. VIII.8.(d). Analysis. Moisture. Adelanto Loam,
Time, *hrs.* v. Depth, *cms.* v. Moisture, *dimensionless.*
$T_M = 300$; $T_A = 20$; $\theta_M = 0.15$; $\theta_A = 0.01$.

YYYY

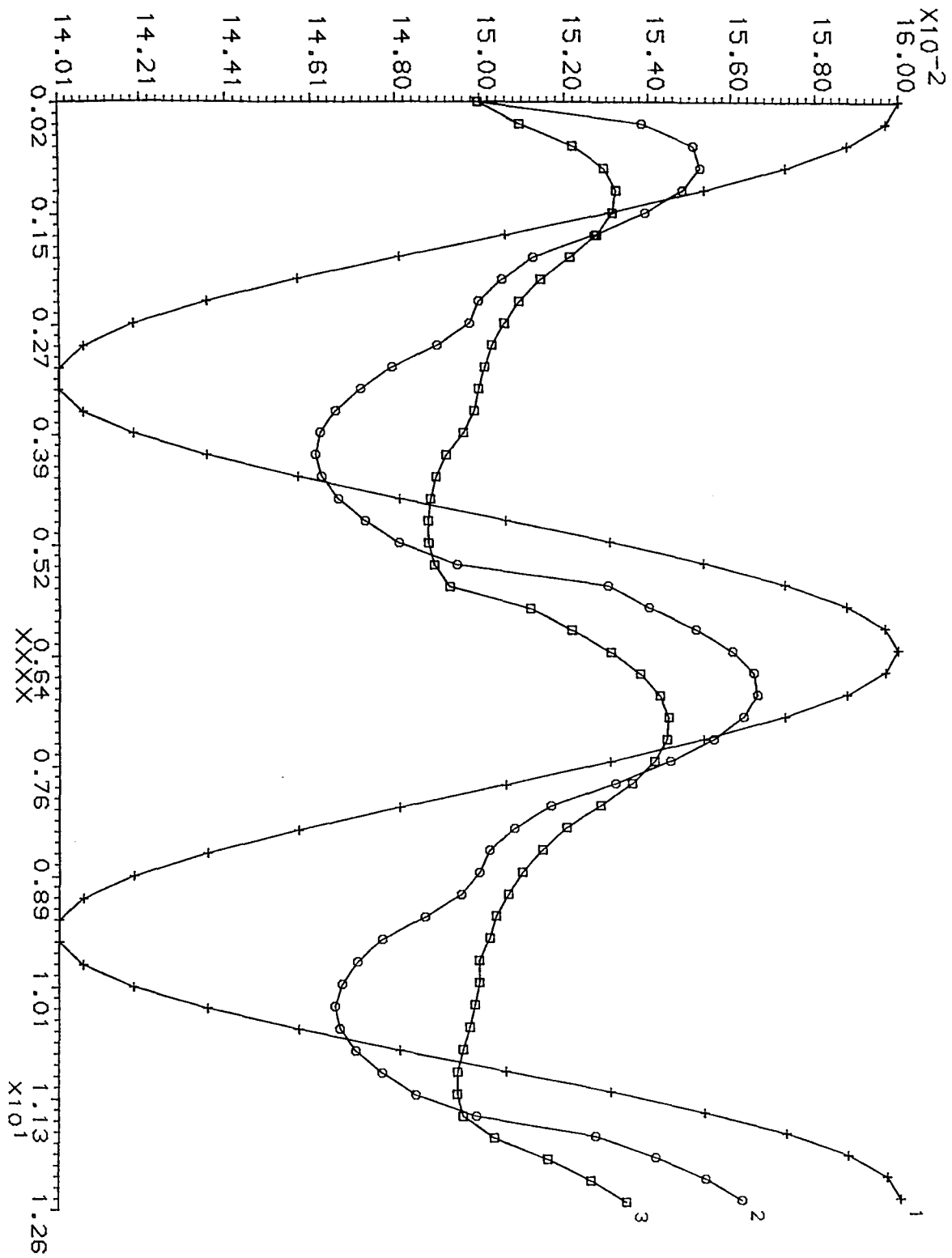

Fig. VIII.9.(a) Cross Sections of the Simulated Behaviour of Fig. VIII.8.(a)
Time, 2 Cycles (4π) v. Moisture, *dimensionless*.
Surface, 3 *cms.*, and 5 *cms.*

YYYY

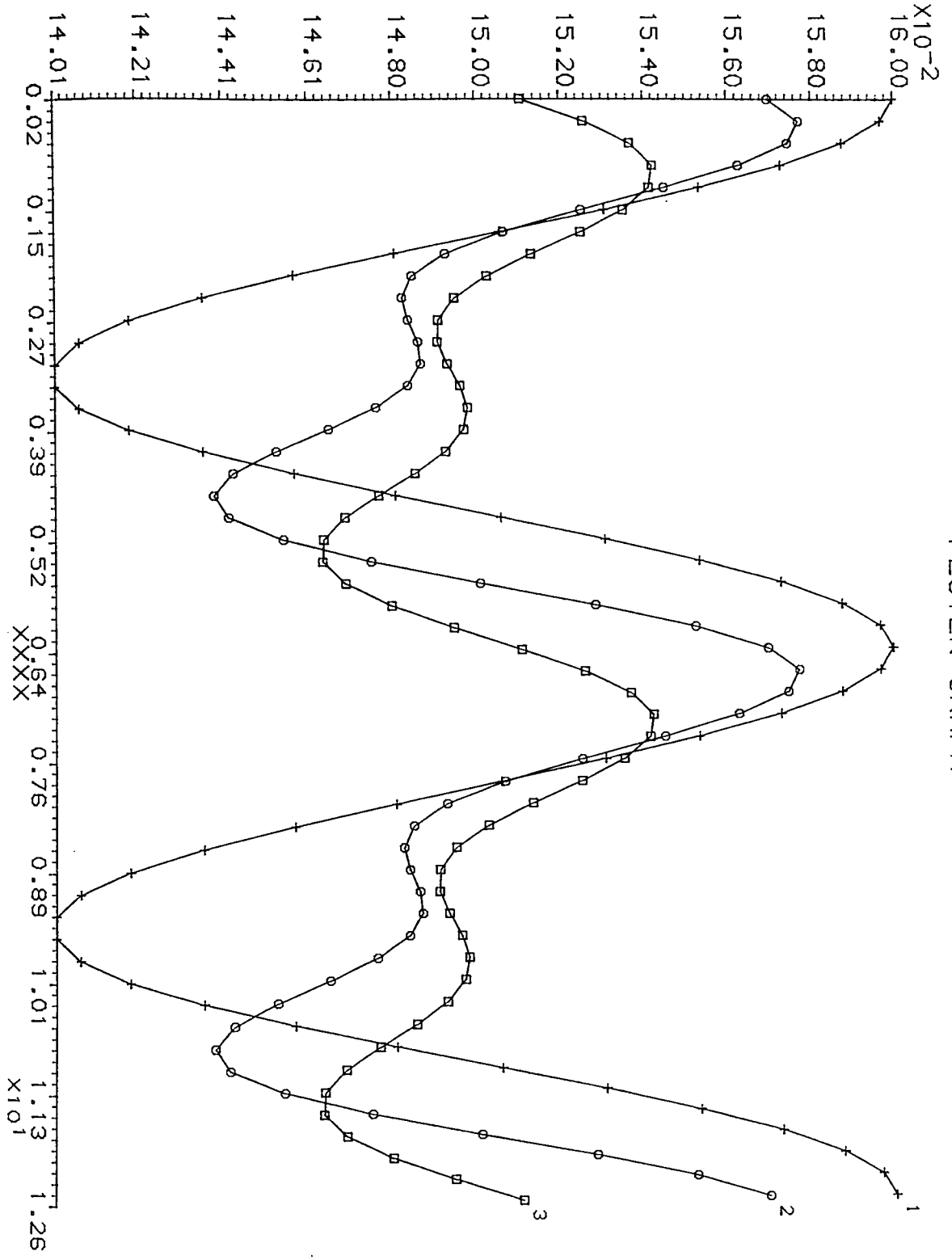

Fig. VIII.9.(b) Cross Sections of the Analytical Behaviour of Fig. VIII.8.(c)
Time, 2 Cycles (4π) v. Moisture, *dimensionless*.
Surface, 3 *cms*., and 5 *cms*.

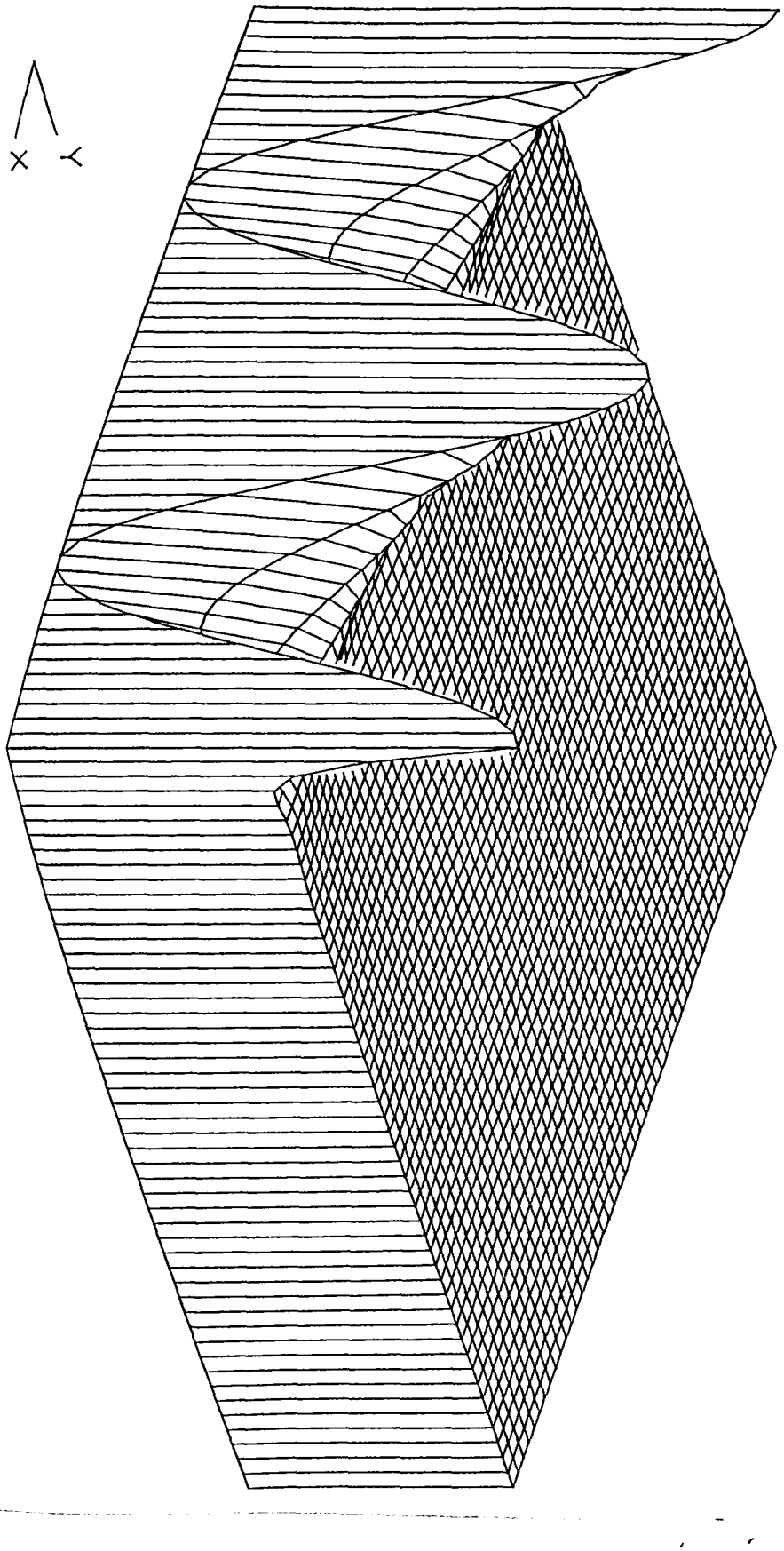

Fig. VIII.10.(a). Simulation. Moisture.

Adelanto Loam,

$T_M = 300$; $T_A = 5$; $\theta_M = 0.1$; $\theta_A = 0.01$.

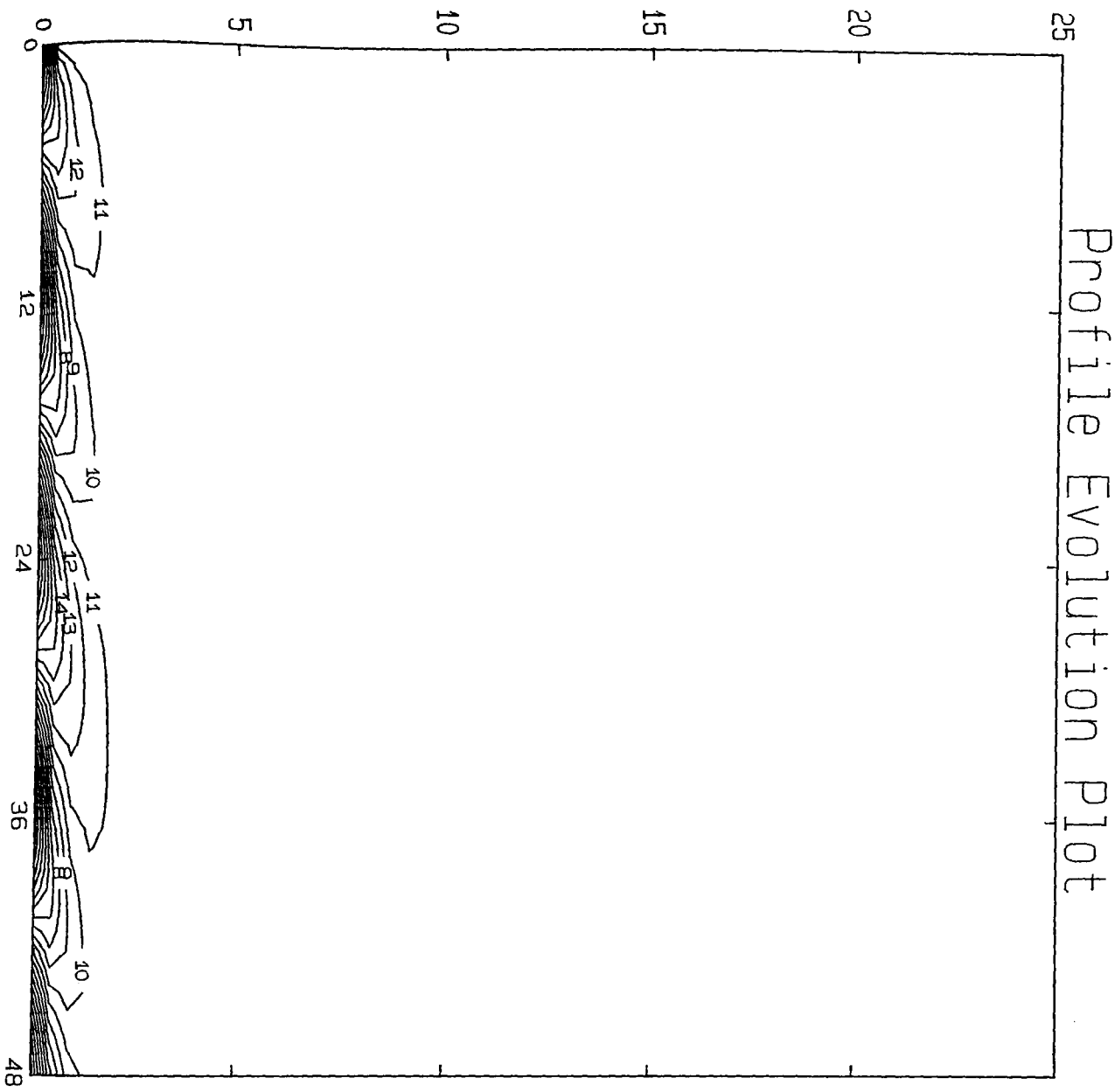

CONTOUR KEY	
1	0.0906
2	0.0916
3	0.0926
4	0.0936
5	0.0946
6	0.0956
7	0.0966
8	0.0975
9	0.0985
10	0.0995
11	0.1005
12	0.1015
13	0.1025
14	0.1035
15	0.1045
16	0.1055
17	0.1065
18	0.1075
19	0.1085
20	0.1095

Fig. VIII.10.(b). Simulation. Moisture. Adelanto Loam, Time, *hrs.* v. Depth, *cms.* v. Moisture, *dimensionless.* $T_M = 300$; $T_A = 20$; $\theta_M = 0.1$; $\theta_A = 0.01$.

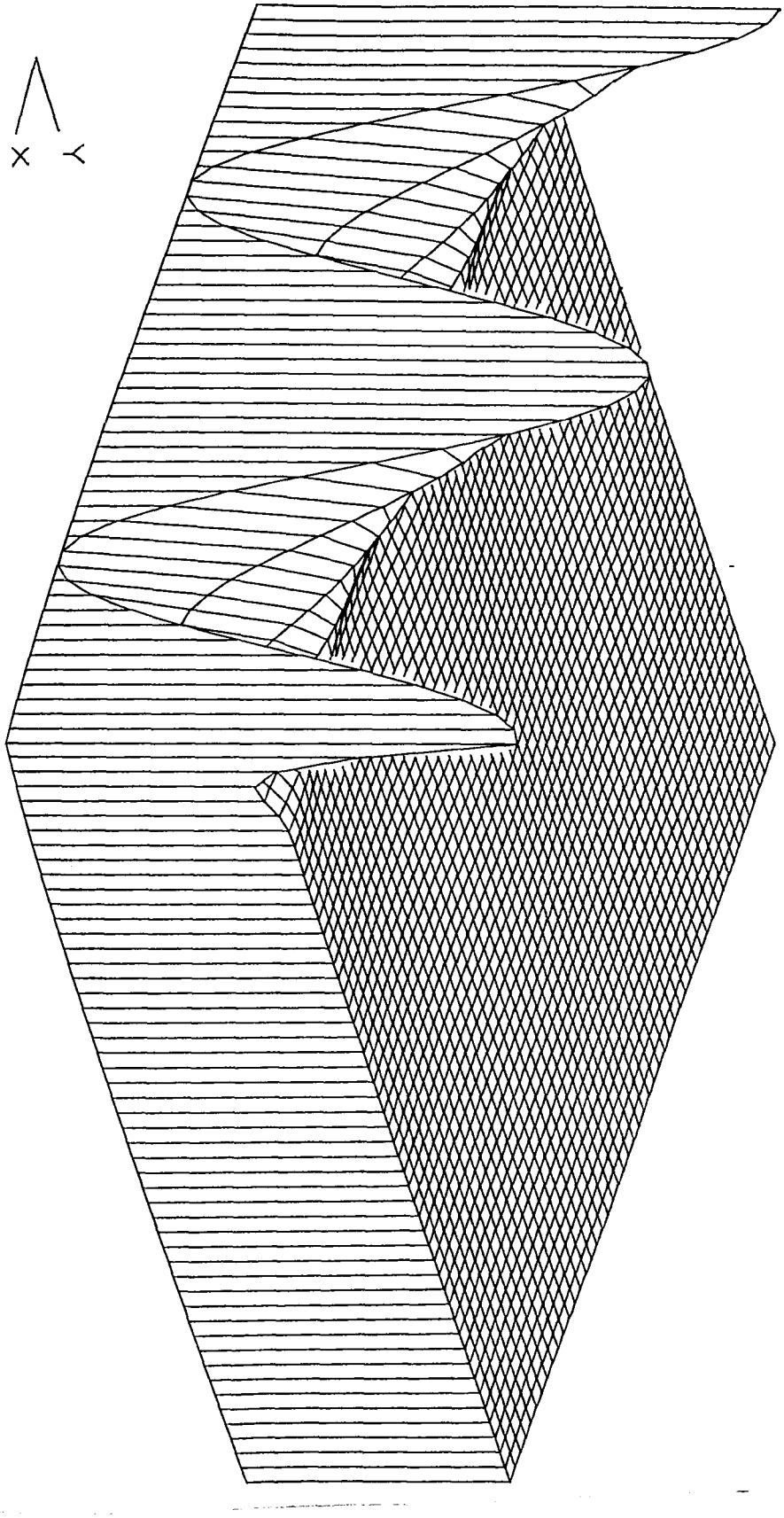

Fig. VIII.10.(c). Analysis. Moisture.

Adelanto Loam,

$T_M = 300$; $T_A = 5$; $\theta_M = 0.1$; $\theta_A = 0.01$.

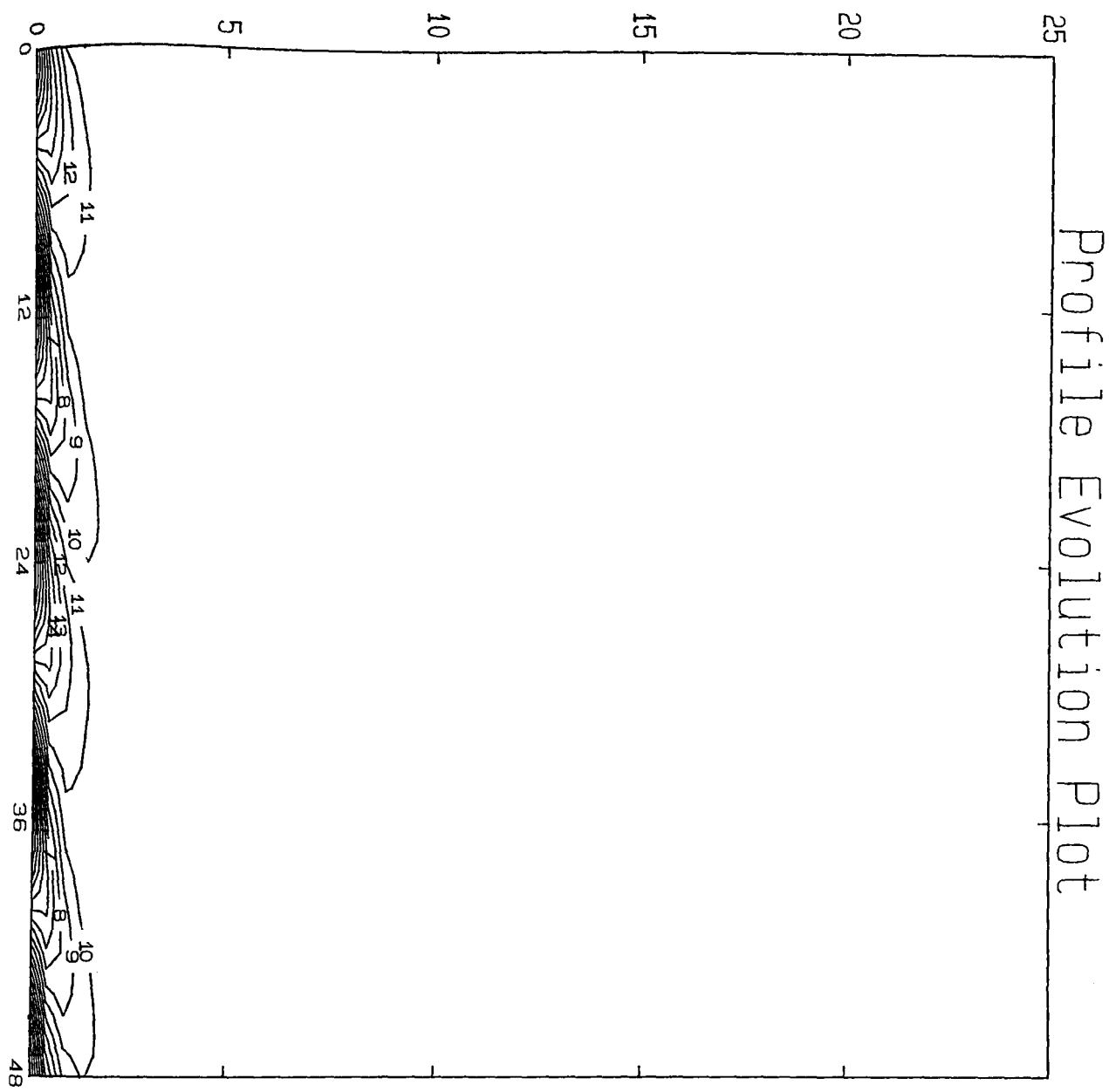

CONTOUR KEY	
1	0.0906
2	0.0916
3	0.0926
4	0.0936
5	0.0946
6	0.0956
7	0.0966
8	0.0975
9	0.0985
10	0.0995
11	0.1005
12	0.1015
13	0.1025
14	0.1035
15	0.1045
16	0.1055
17	0.1065
18	0.1075
19	0.1085
20	0.1095

Fig. VIII.10.(d). Analysis. Moisture. Adelanto Loam, Time, *hrs.* v. Depth, *cms.* v. Moisture, *dimensionless.* $T_M = 300$; $T_A = 20$; $\theta_M = 0.1$; $\theta_A = 0.01$.

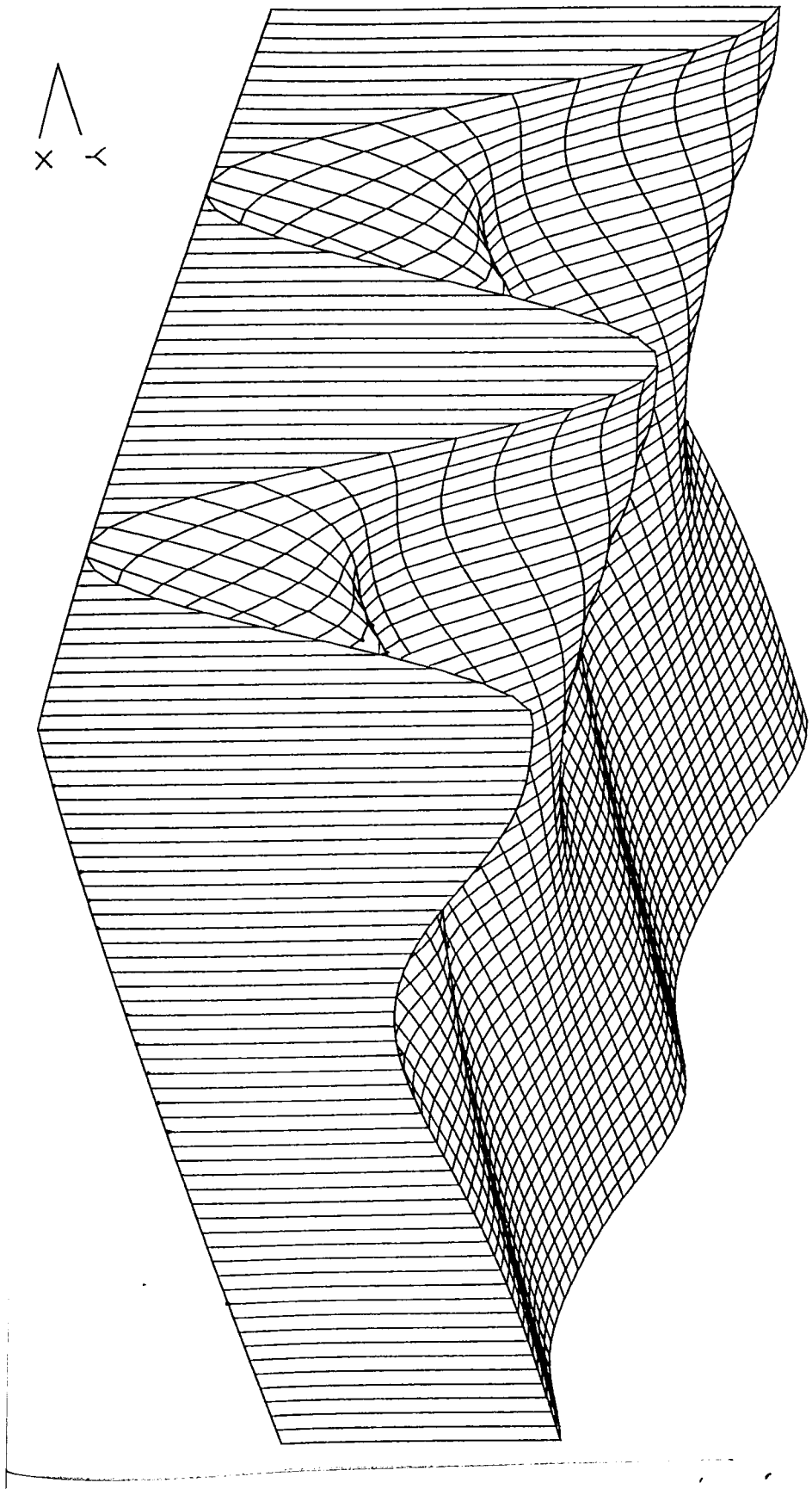

Fig. VIII.11.(a). Analysis. Moisture.

Adelanto Loam,

$T_M = 300$; $T_A = 5$; $\theta_M = 0.08$; $\theta_A = 0.01$.

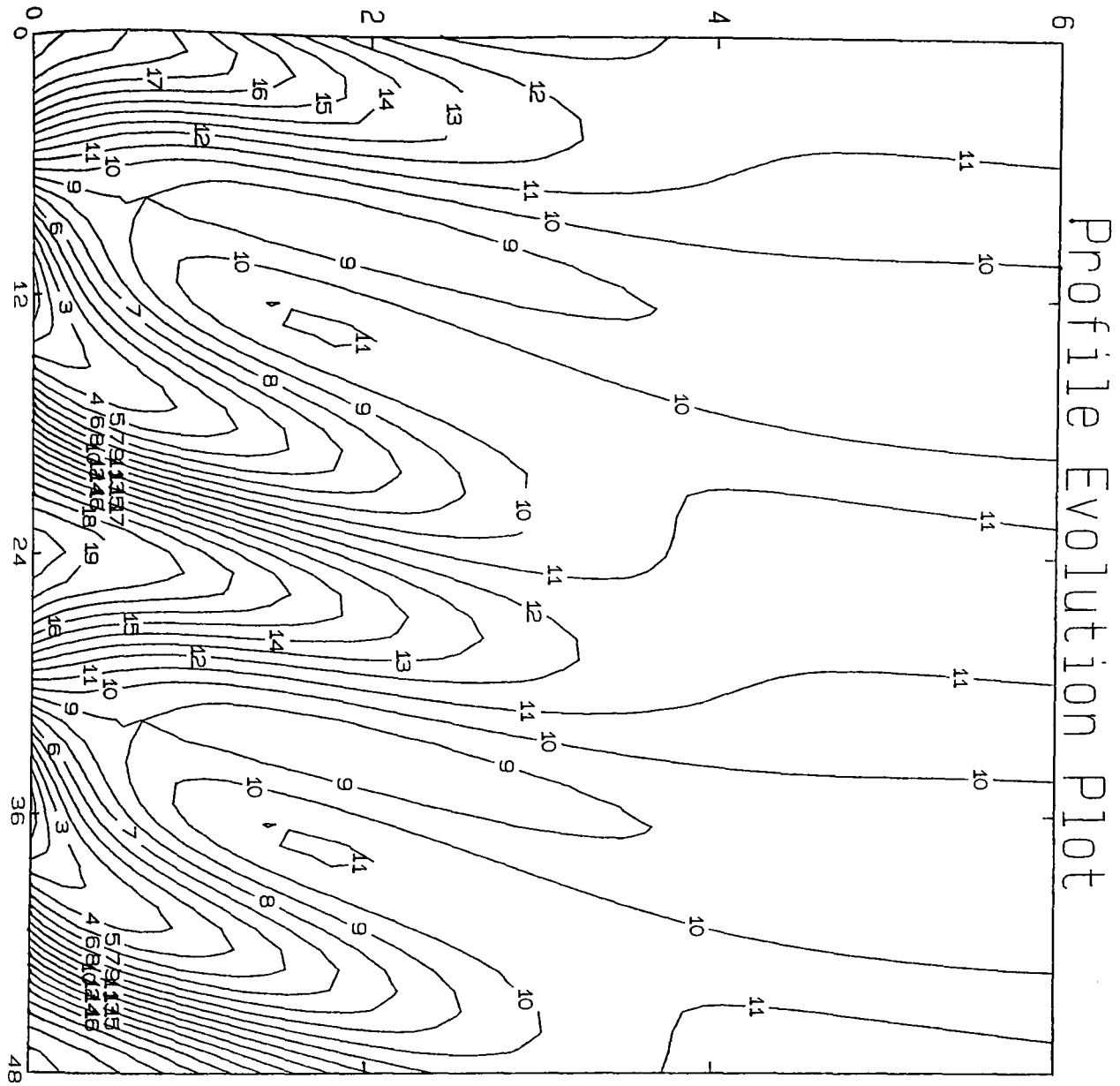

CONTOUR KEY	
1	0.0612
2	0.0631
3	0.0651
4	0.0671
5	0.0691
6	0.0711
7	0.0731
8	0.0751
9	0.0771
10	0.0791
11	0.0811
12	0.0831
13	0.0851
14	0.0871
15	0.0890
16	0.0910
17	0.0930
18	0.0950
19	0.0970
20	0.0990

Fig. VIII.11.(b). Analysis. Moisture. Adelanto Loam,
Time, *hrs.* v. Depth, *cms.* v. Moisture, *dimensionless.*
$T_M = 300$; $T_A = 20$; $\theta_M = 0.08$; $\theta_A = 0.02$.

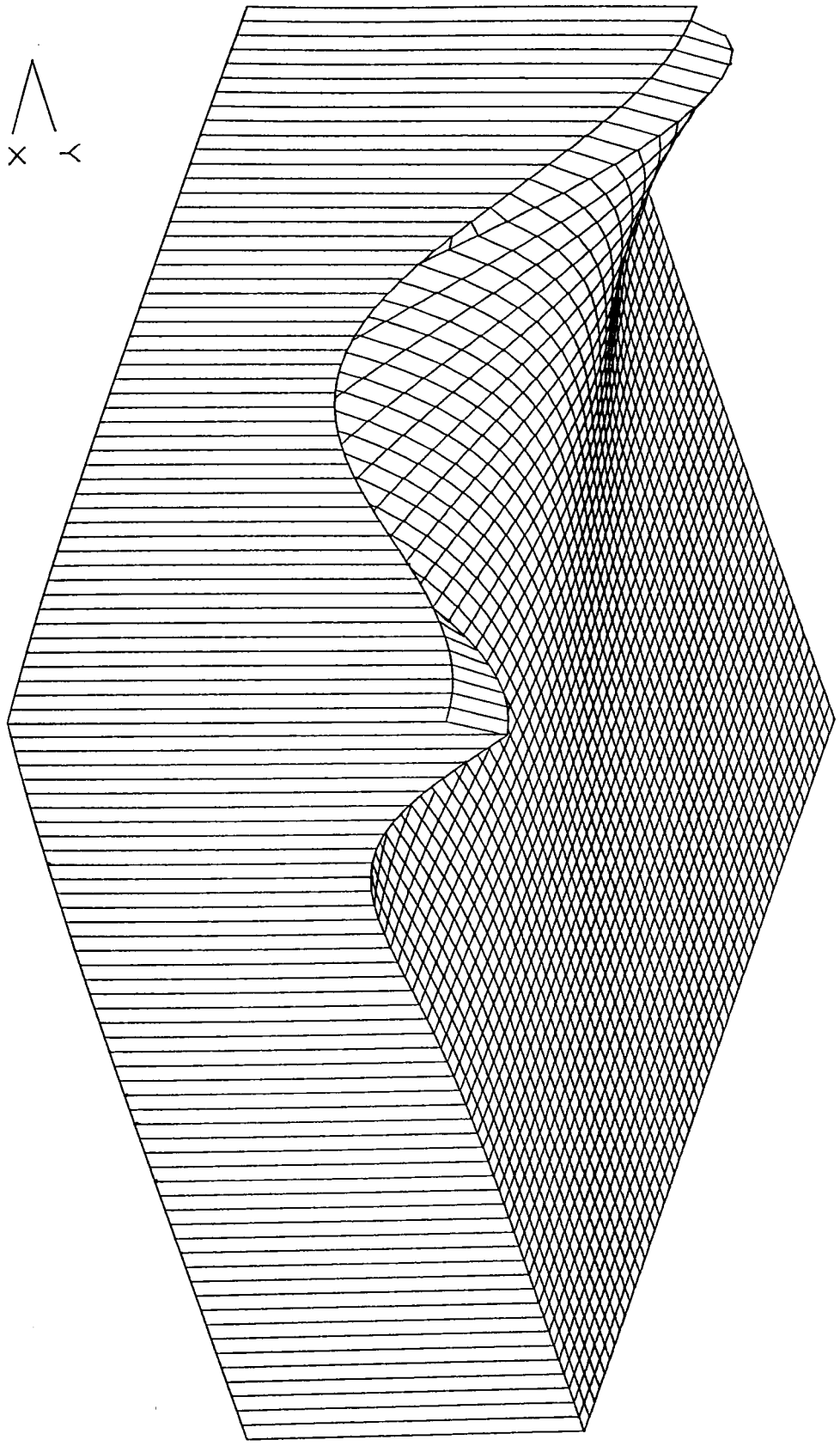

Fig. **VIII**.12.(a). 2nd. Harmonic Resonance,
$T_M = 0.19$; $T_A = 0.05$; $\theta_M = 0.2$; $\theta_A = 0.01$.

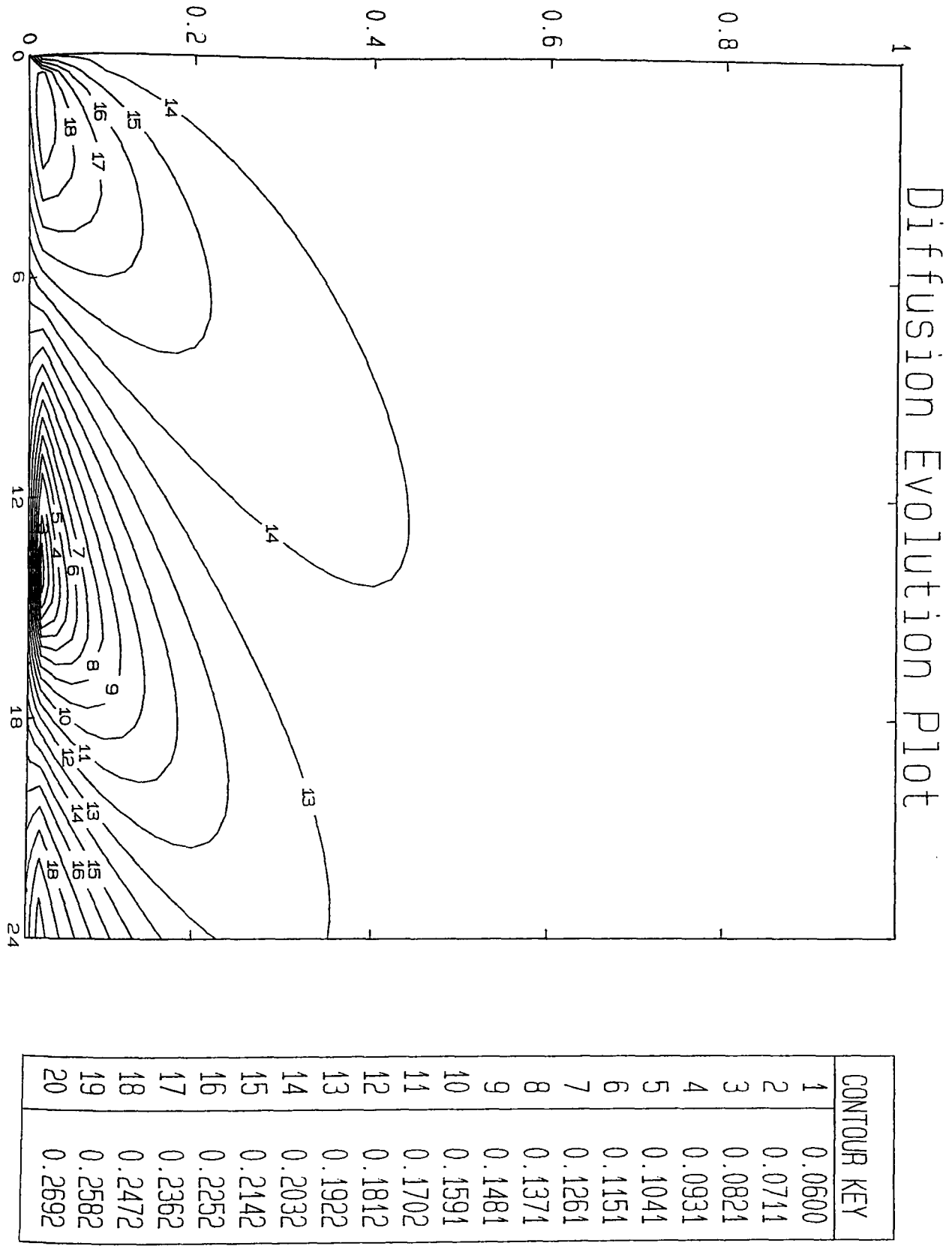

Fig. VIII.12.(b). 2nd. Harmonic Resonance,

Time, *hrs.* v. Depth, *cms.* v. Moisture, *dimensionless.*

T_M=0.19; T_A=0.05; θ_M=0.2;θ_A=0.01.

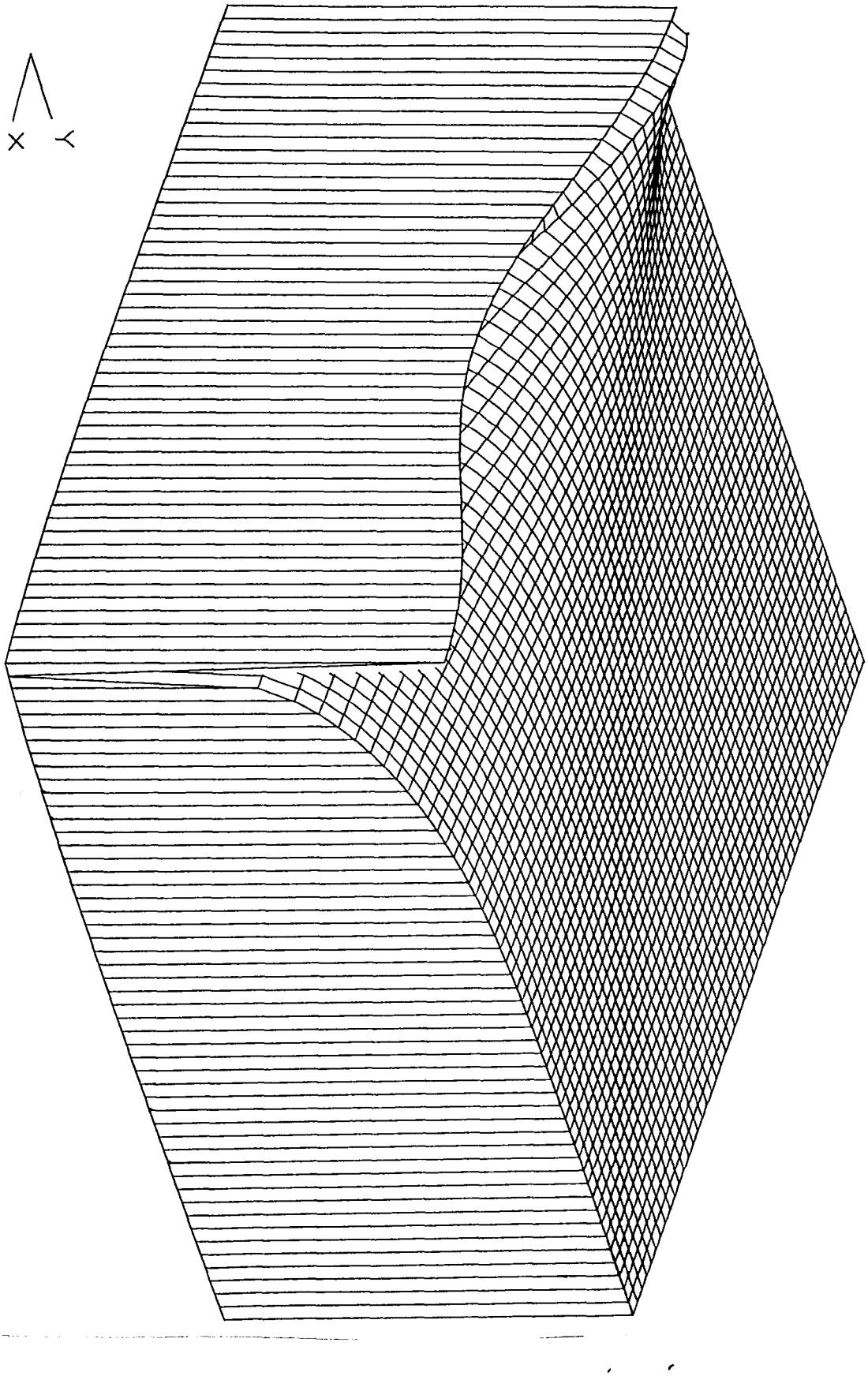

Fig. VIII.13.(a). 2nd. Harmonic Resonance,
$T_M = 0.18$; $T_A = 0.05$; $\theta_M = 0.2$; $\theta_A = 0.01$.

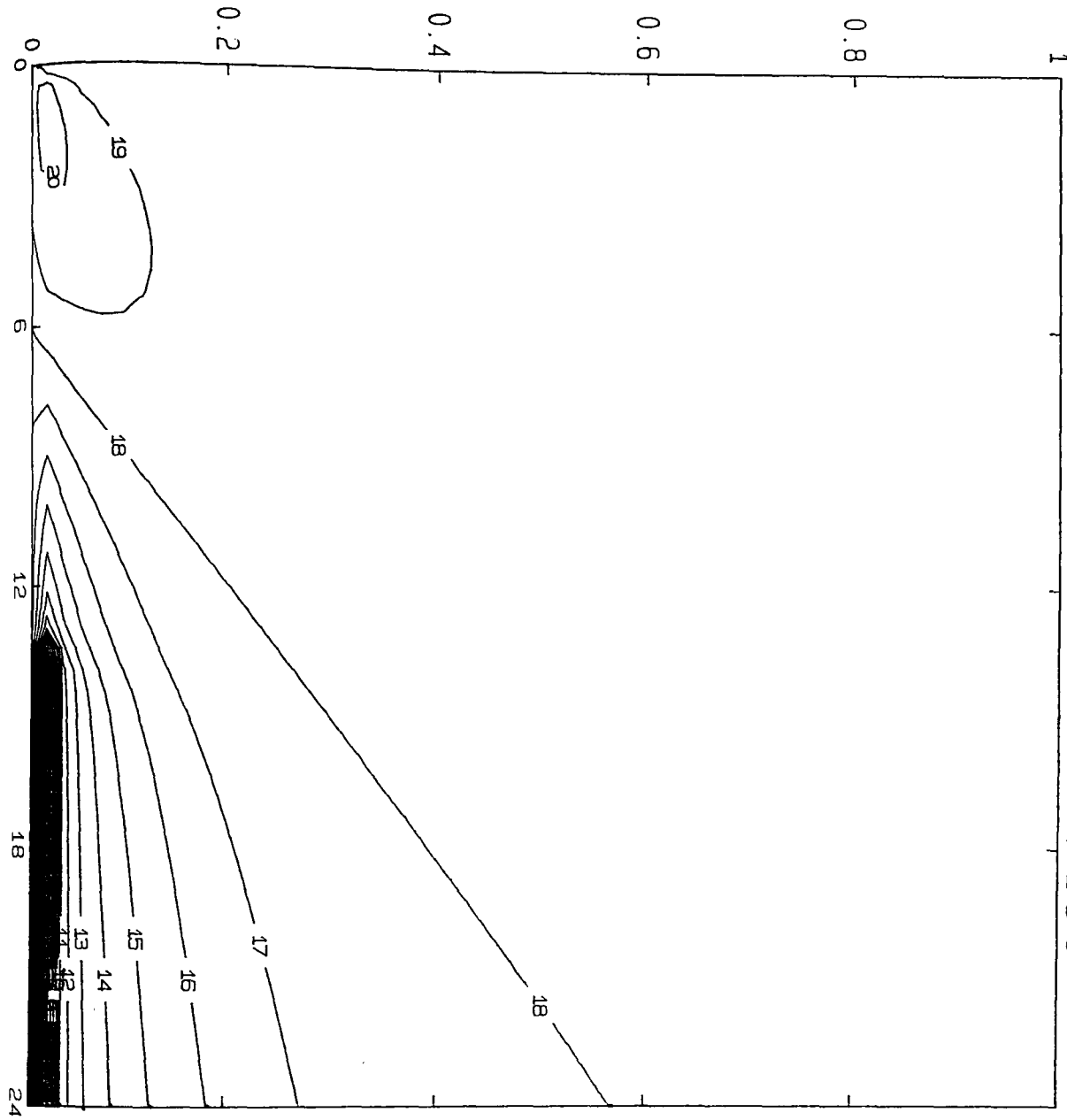

CONTOUR KEY	
1	-0.2860
2	-0.2580
3	-0.2300
4	-0.2021
5	-0.1741
6	-0.1461
7	-0.1181
8	-0.0901
9	-0.0621
10	-0.0342
11	-0.0062
12	0.0218
13	0.0498
14	0.0778
15	0.1057
16	0.1337
17	0.1617
18	0.1897
19	0.2177
20	0.2457

Fig. VIII.13.(b). 2nd. Harmonic Resonance,

Time, *hrs.* v. Depth, *cms.* v. Moisture, *dimensionless.*

T_M=0.18; T_A=0.05; θ_M=0.2;θ_A=0.01.

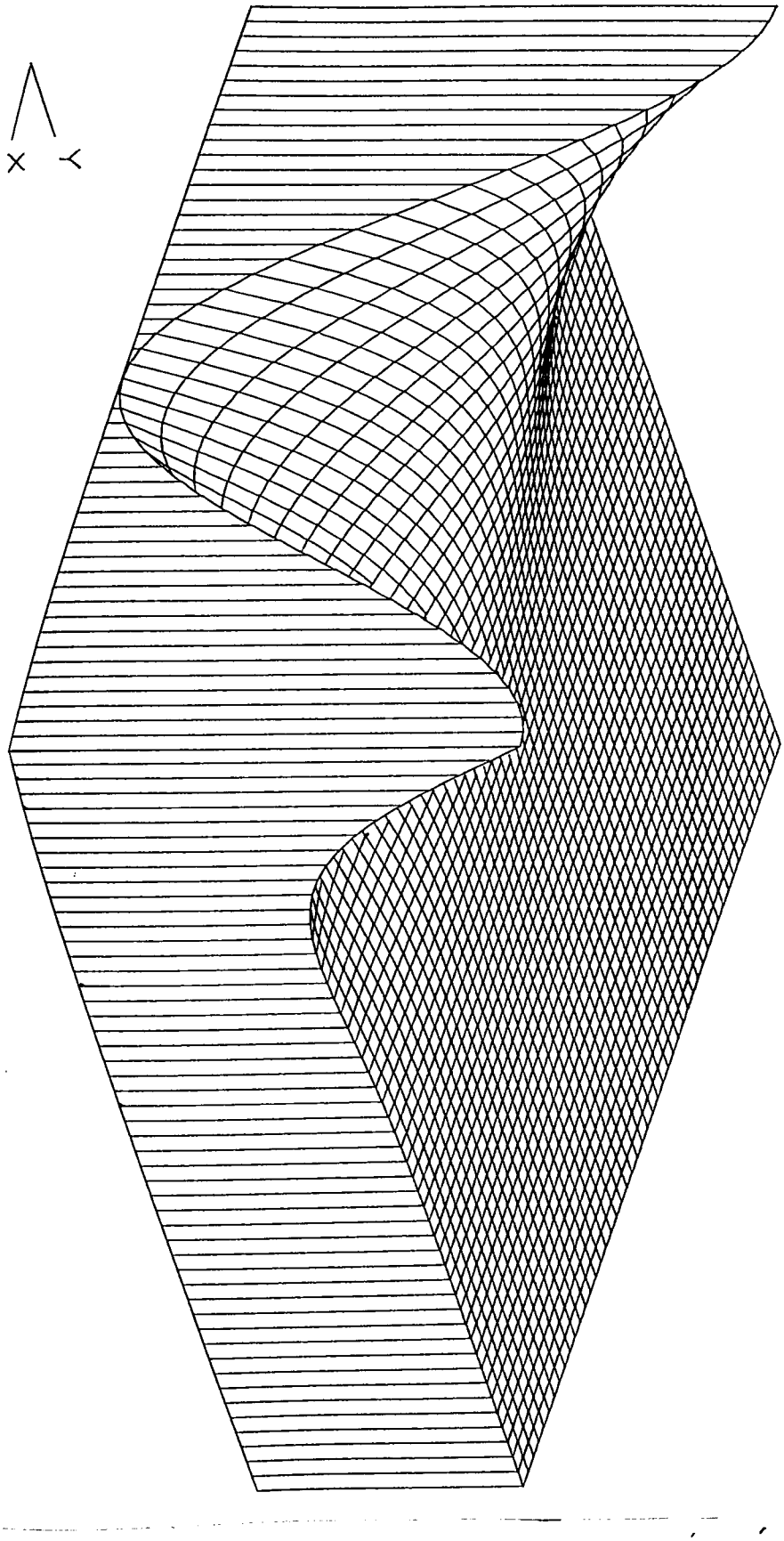

Fig. VIII.13.(a). 2nd. Harmonic Resonance,
$T_M = 0.18$; $T_A = 0.05$; $\theta_M = 0.2$; $\theta_A = 0.0$.

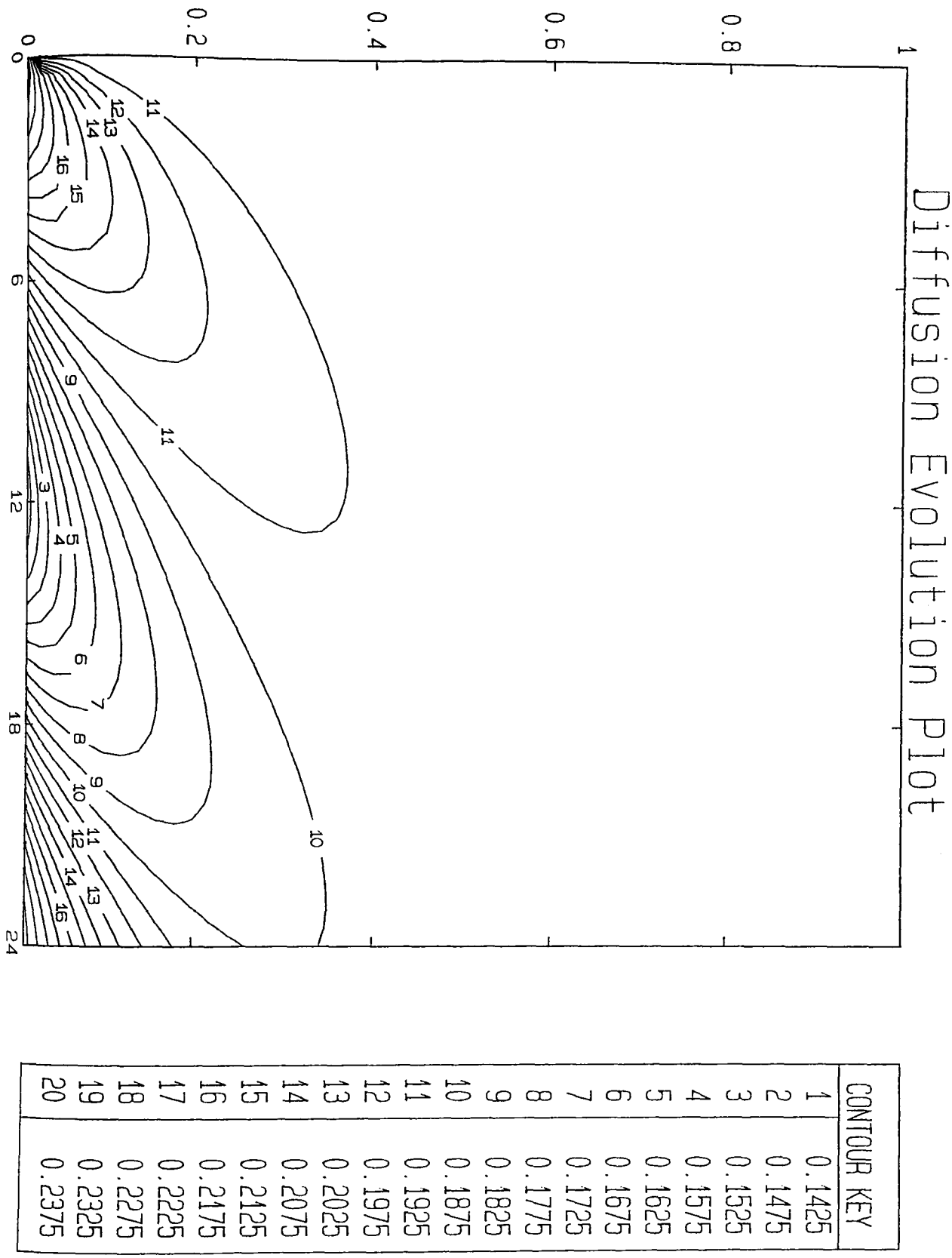

Fig. **VIII**.14.(b). 2nd. Harmonic Resonance,

Time, *hrs.* v. Depth, *cms.* v. Moisture, *dimensionless.*

T_M=0.18; T_A=0.05; θ_M=0.2;θ_A=0.0.

YYYY

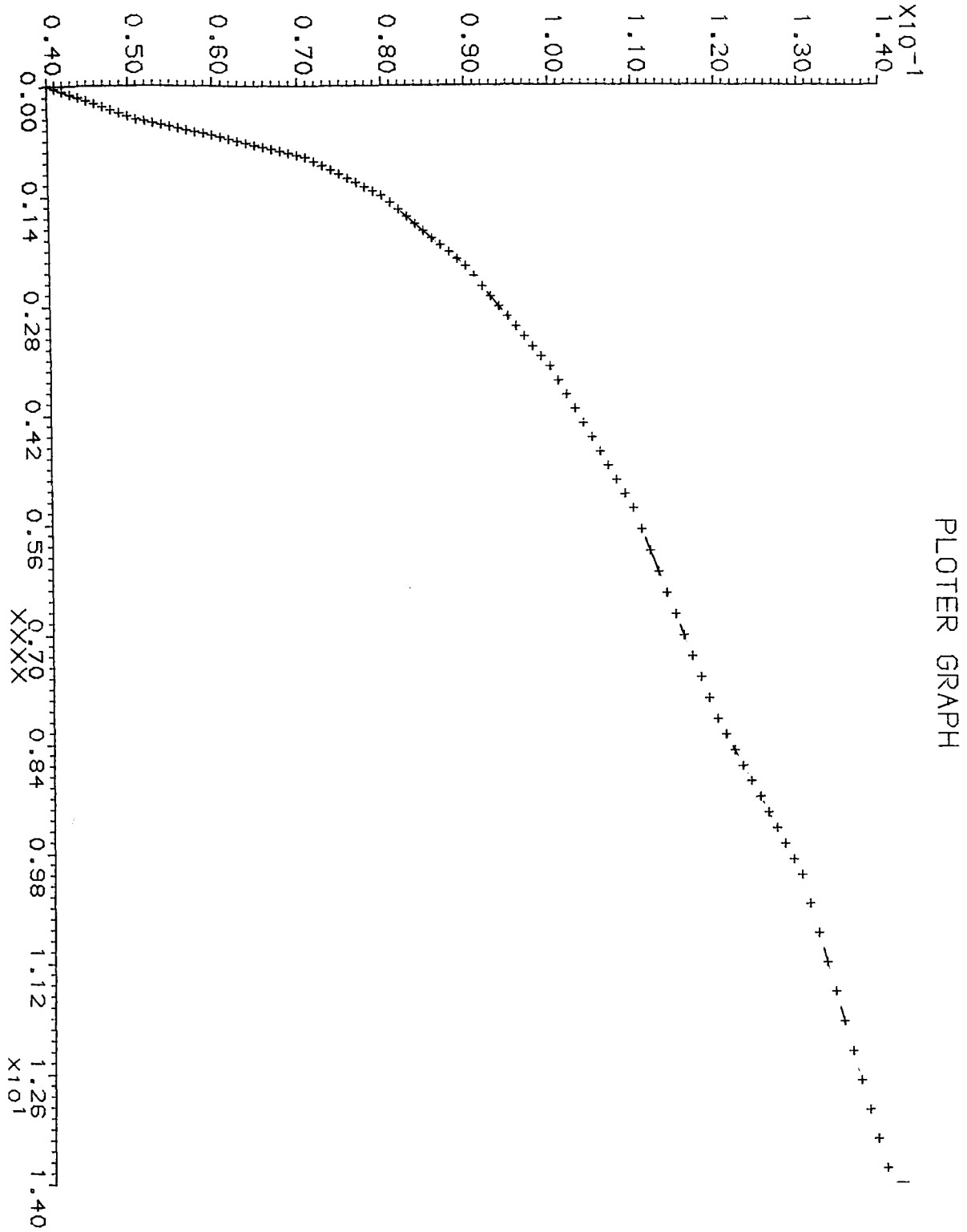

Fig.IX.1. Mean Moisture Profile, Day 4 of the Rose Experiment.

Depth, *cms.* v. Moisture Content, *dimensionless.*

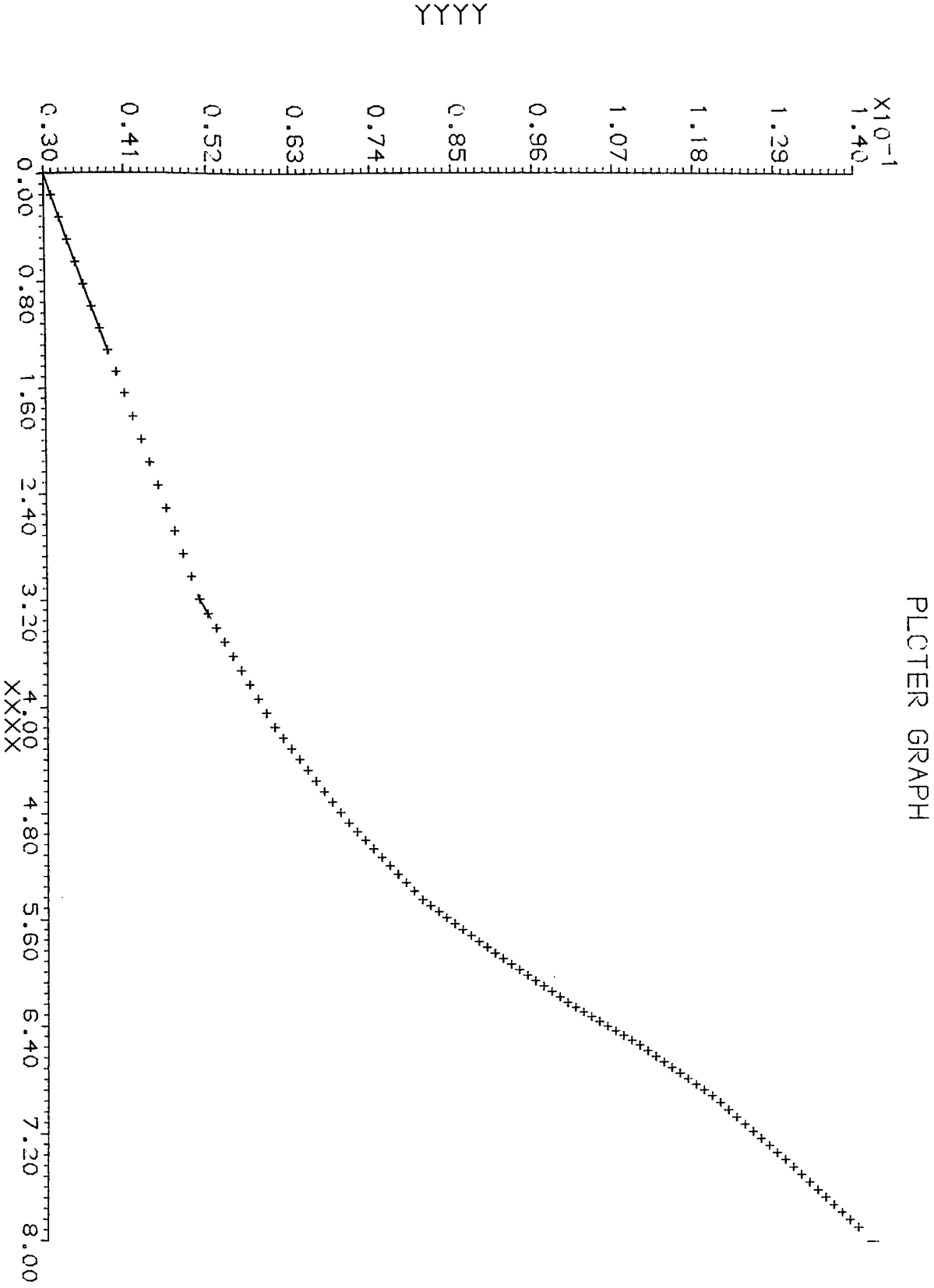

Fig.IX.2. Mean Moisture Profile, Day 7 of the Jackson Experiment.
Depth, *cms.* v. Moisture Content, *dimensionless.*

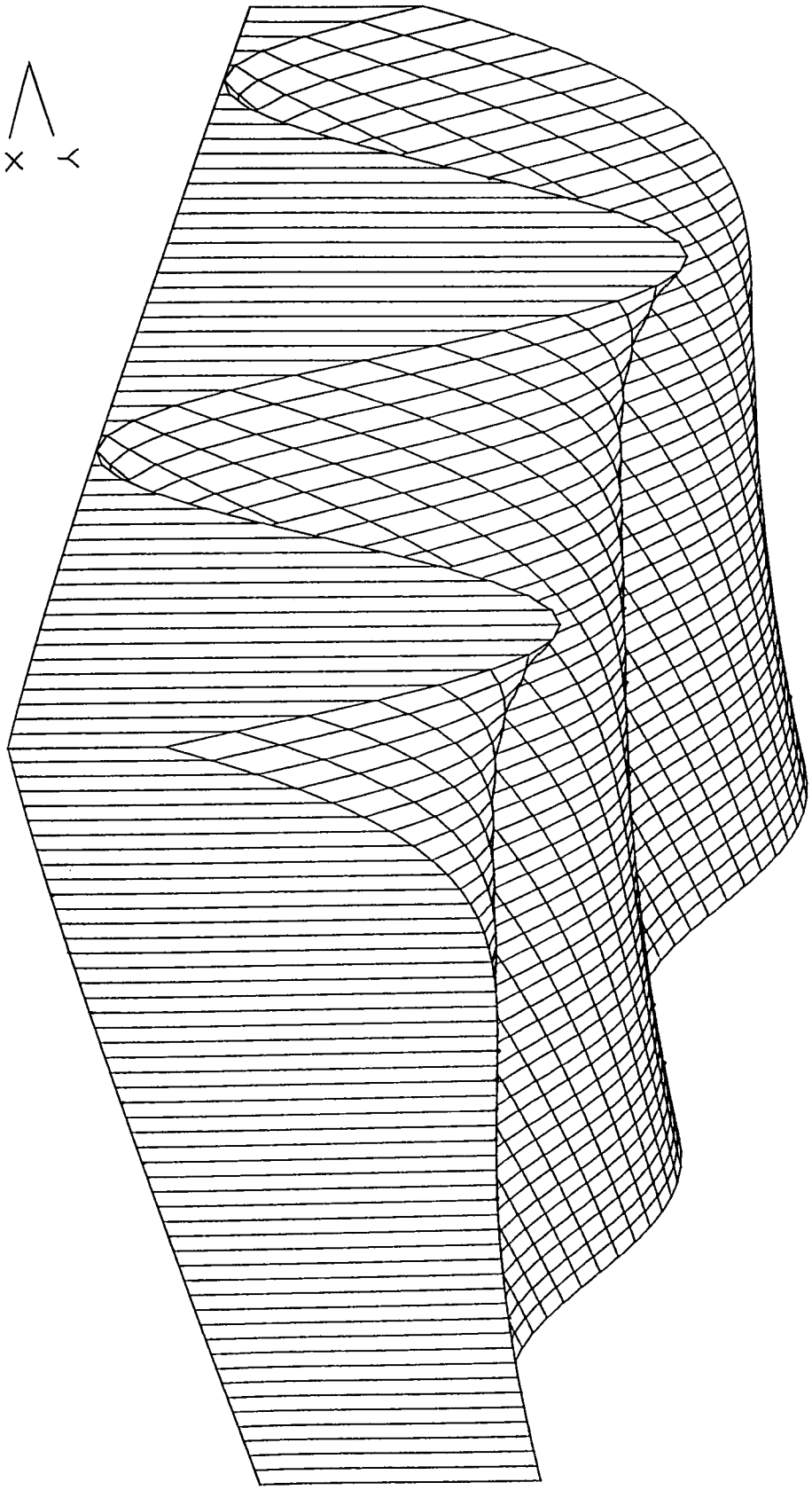

Fig. IX.6.(a). Analytical Surface Plot,
Surface Layer, Day 4 of the Rose Experiment.

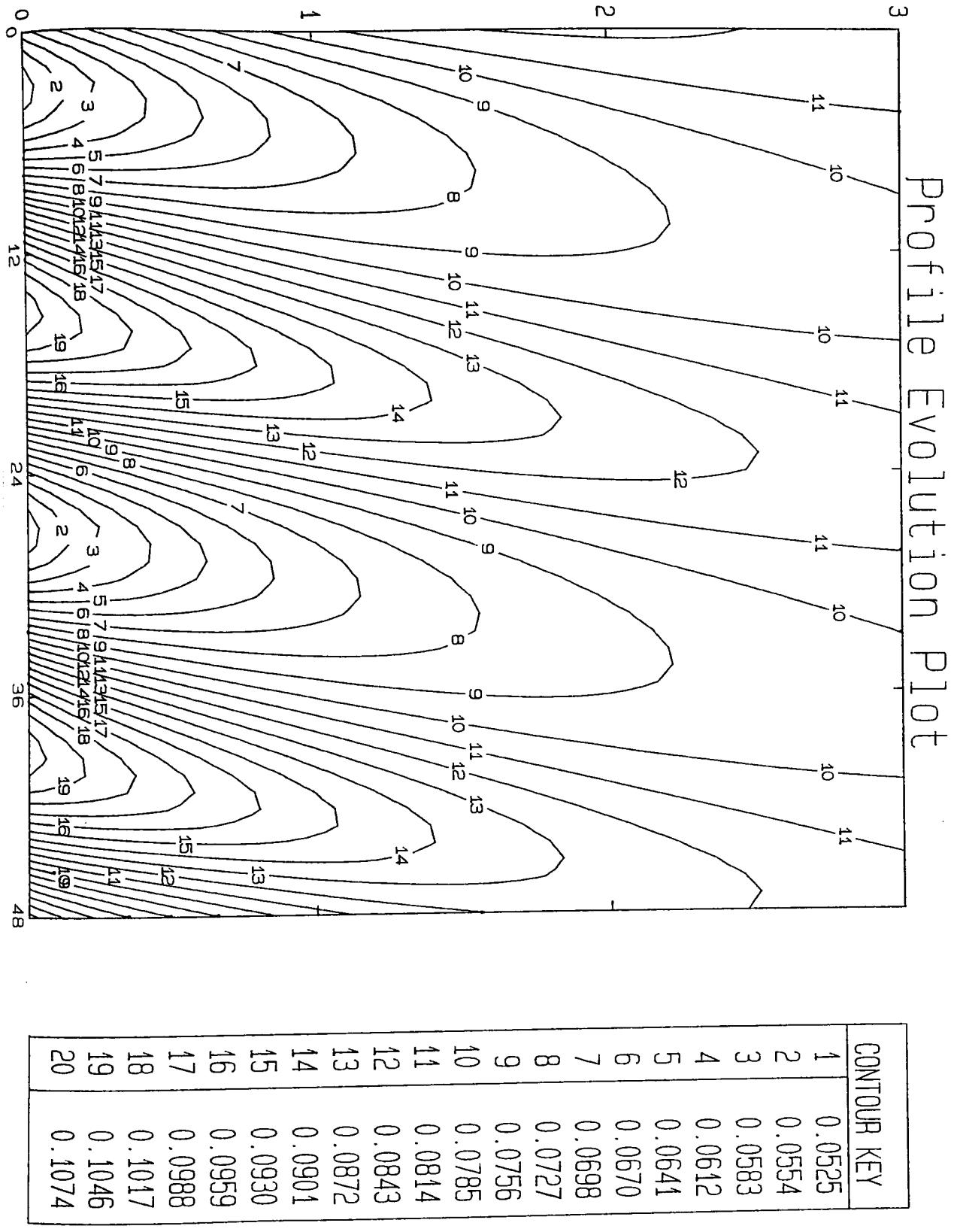

CONTOUR KEY	
1	0.0525
2	0.0554
3	0.0583
4	0.0612
5	0.0641
6	0.0670
7	0.0698
8	0.0727
9	0.0756
10	0.0785
11	0.0814
12	0.0843
13	0.0872
14	0.0901
15	0.0930
16	0.0959
17	0.0988
18	0.1017
19	0.1046
20	0.1074

Fig. IX.6.(b). Analytical Contour Plot to 3 *cms.*,
Day 4 of the Rose Experiment.
Time, *hrs.* v. Depth, *cms.* v. Moisture, *dimensionless.*

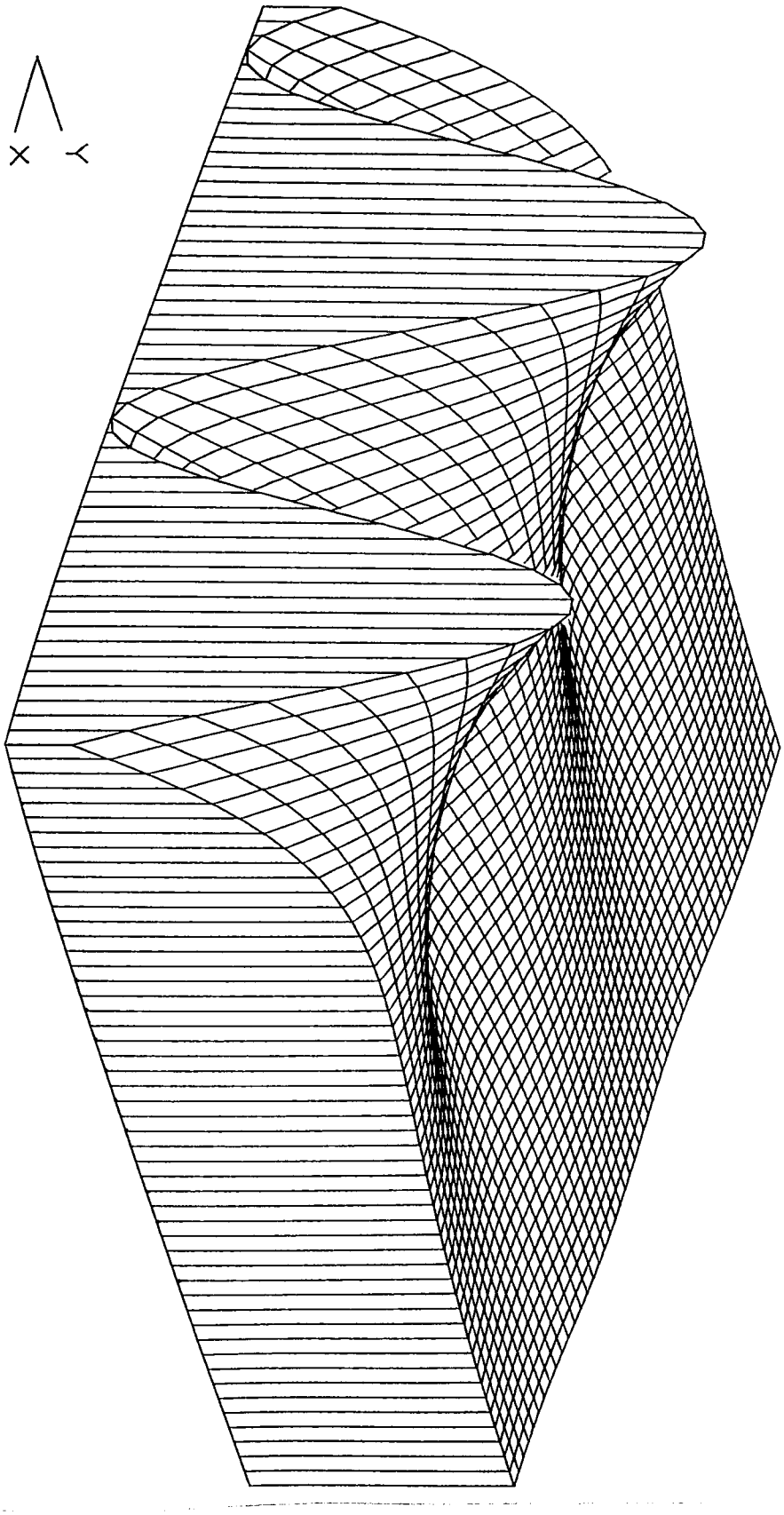

Fig. IX.7.(a). Analytical Surface Plot,
Intermediate Layer, The Rose Experiment,
No Enhancement.

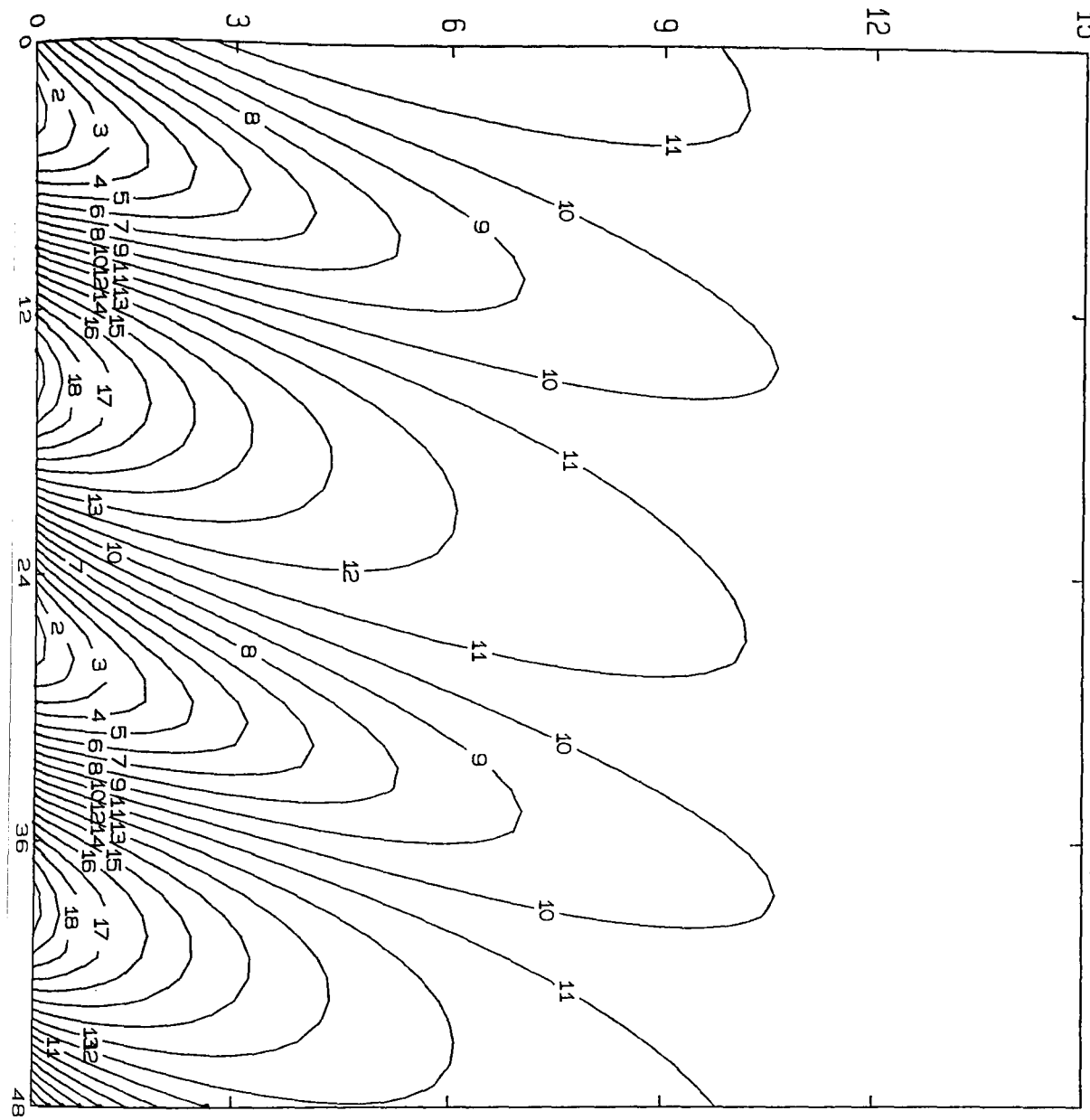

CONTOUR KEY	
1	0.1115
2	0.1145
3	0.1175
4	0.1205
5	0.1235
6	0.1265
7	0.1295
8	0.1325
9	0.1355
10	0.1384
11	0.1414
12	0.1444
13	0.1474
14	0.1504
15	0.1534
16	0.1564
17	0.1594
18	0.1624
19	0.1654
20	0.1684

Fig. IX.7.(b). Analytical Contour Plot to 15 *cms.*,
The Rose Experiment, No Enhancement.
Time, *hrs.* v. Depth, *cms.* v. Moisture, *dimensionless.*

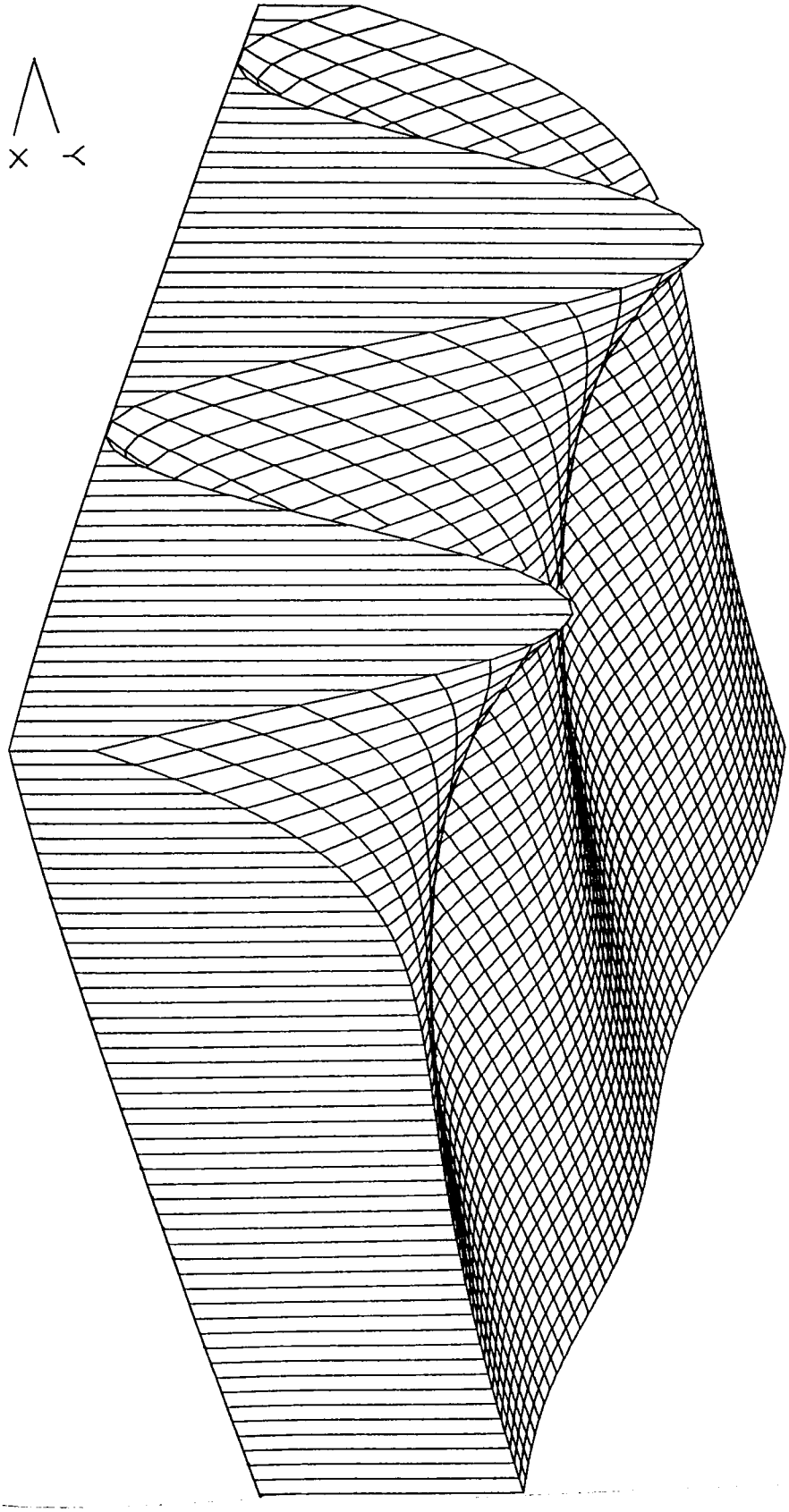

Fig. IX.8.(a). Analytical Surface Plot,
Intermediate Layer,
The Rose Experiment, Enhancement=10.0.

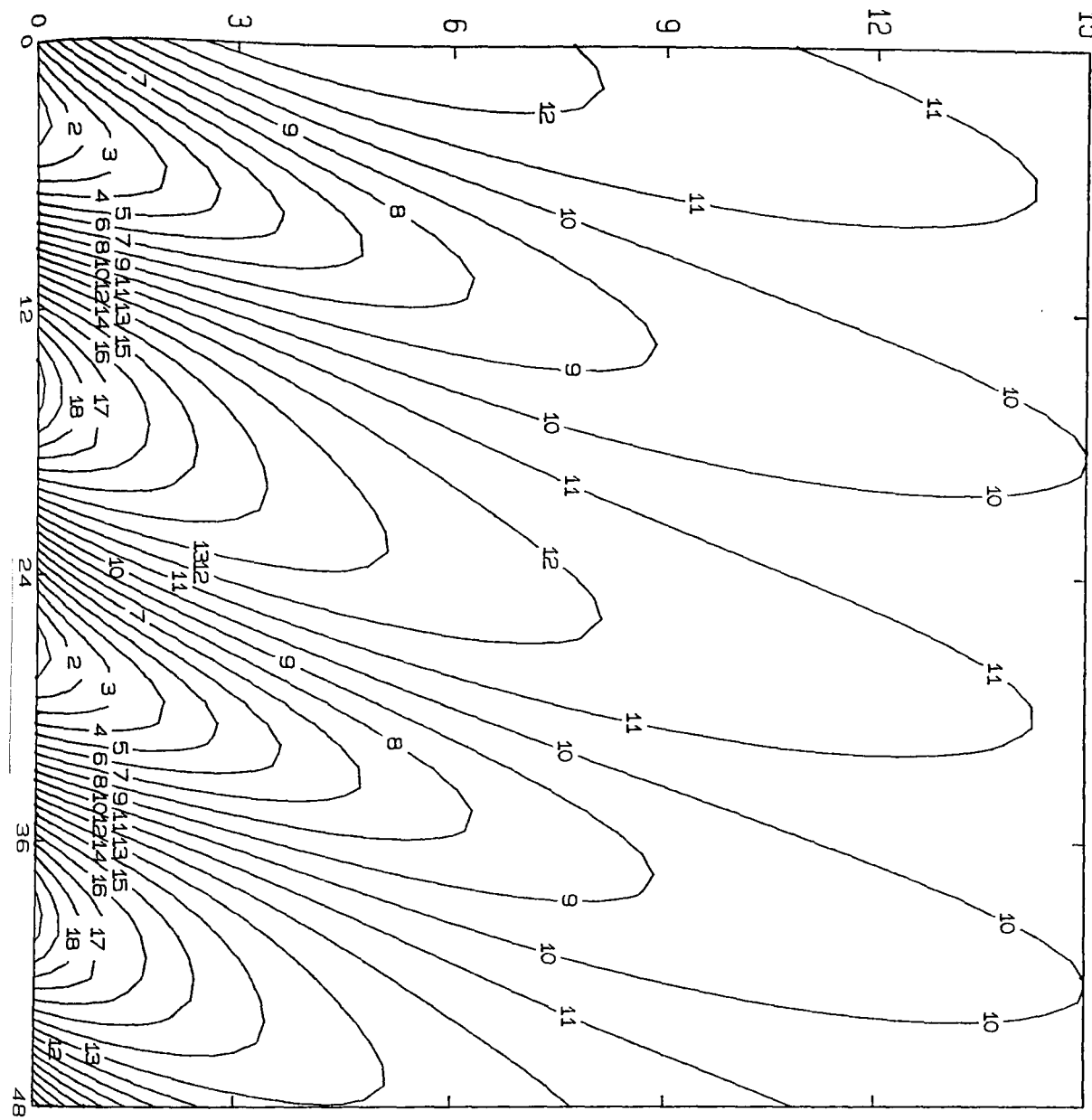

CONTOUR KEY	
1	0.1177
2	0.1201
3	0.1224
4	0.1248
5	0.1271
6	0.1295
7	0.1318
8	0.1342
9	0.1365
10	0.1389
11	0.1412
12	0.1436
13	0.1459
14	0.1483
15	0.1506
16	0.1530
17	0.1553
18	0.1577
19	0.1600
20	0.1624

Fig. IX.8.(b). Analytical Contour Plot to 15 *cms.*,

The Rose Experiment, Enhancement=10.0.

Time, *hrs.* v. Depth, *cms.* v. Moisture, *dimensionless.*

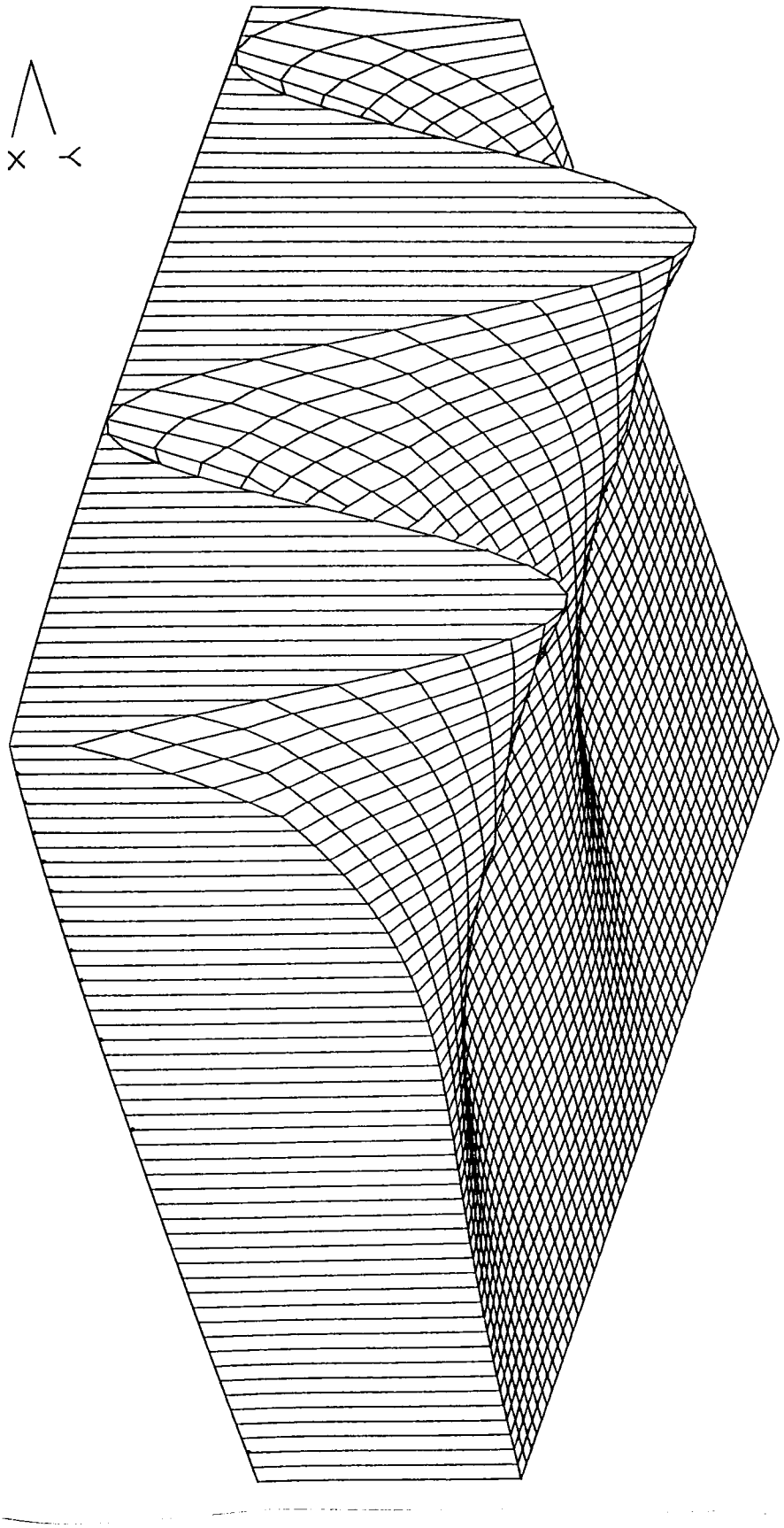

Fig. IX.8.(c). Simulated Surface Plot,
Intermediate Layer,
The Rose Experiment, Enhancement=10.0.

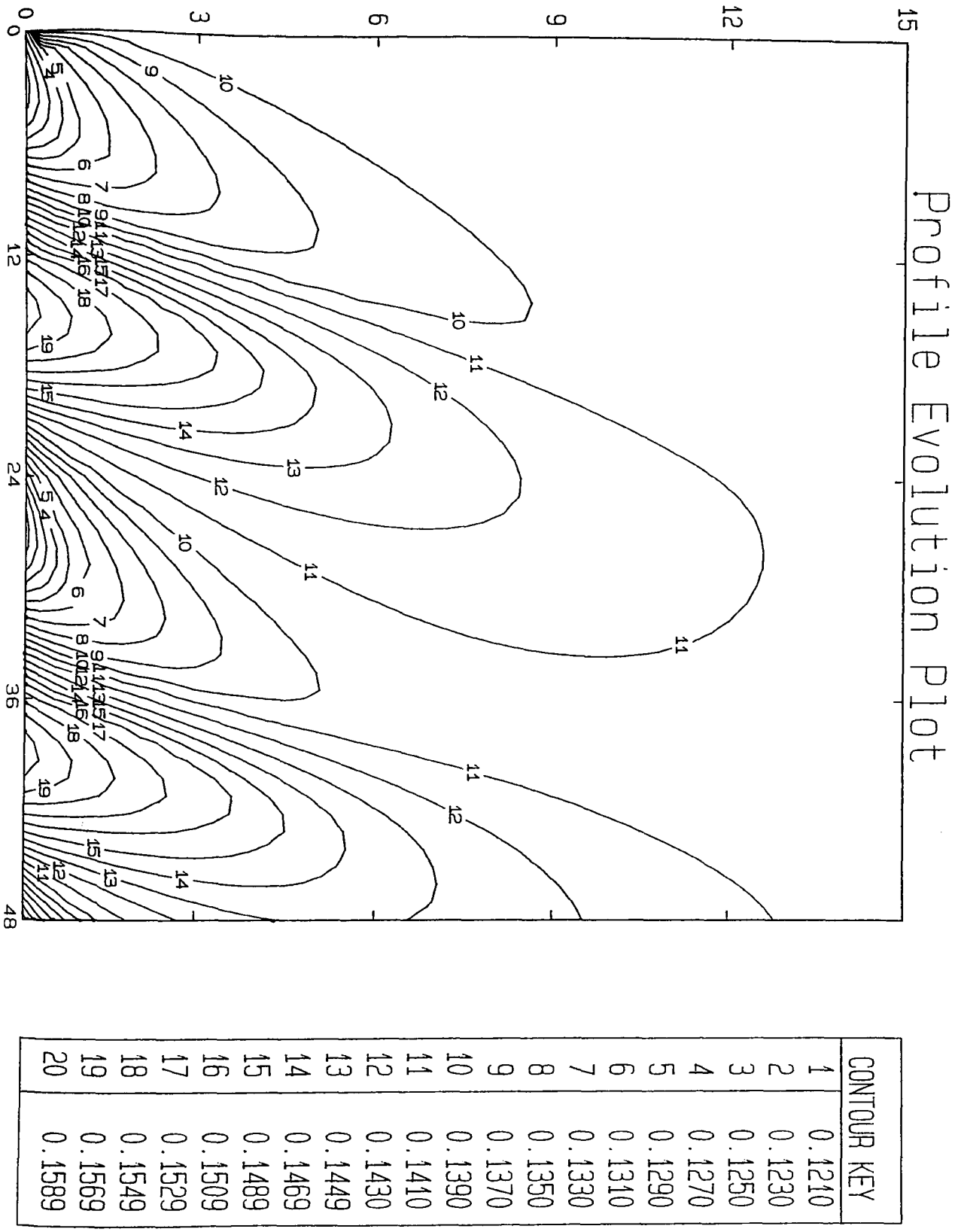

CONTOUR KEY	
1	0.1210
2	0.1230
3	0.1250
4	0.1270
5	0.1290
6	0.1310
7	0.1330
8	0.1350
9	0.1370
10	0.1390
11	0.1410
12	0.1430
13	0.1449
14	0.1469
15	0.1489
16	0.1509
17	0.1529
18	0.1549
19	0.1569
20	0.1589

Fig. IX.8.(d). Simulated Contour Plot to 15 *cms.*,
The Rose Experiment, Enhancement=10.0.
Time, *hrs.* v. Depth, *cms.* v. Moisture, *dimensionless.*

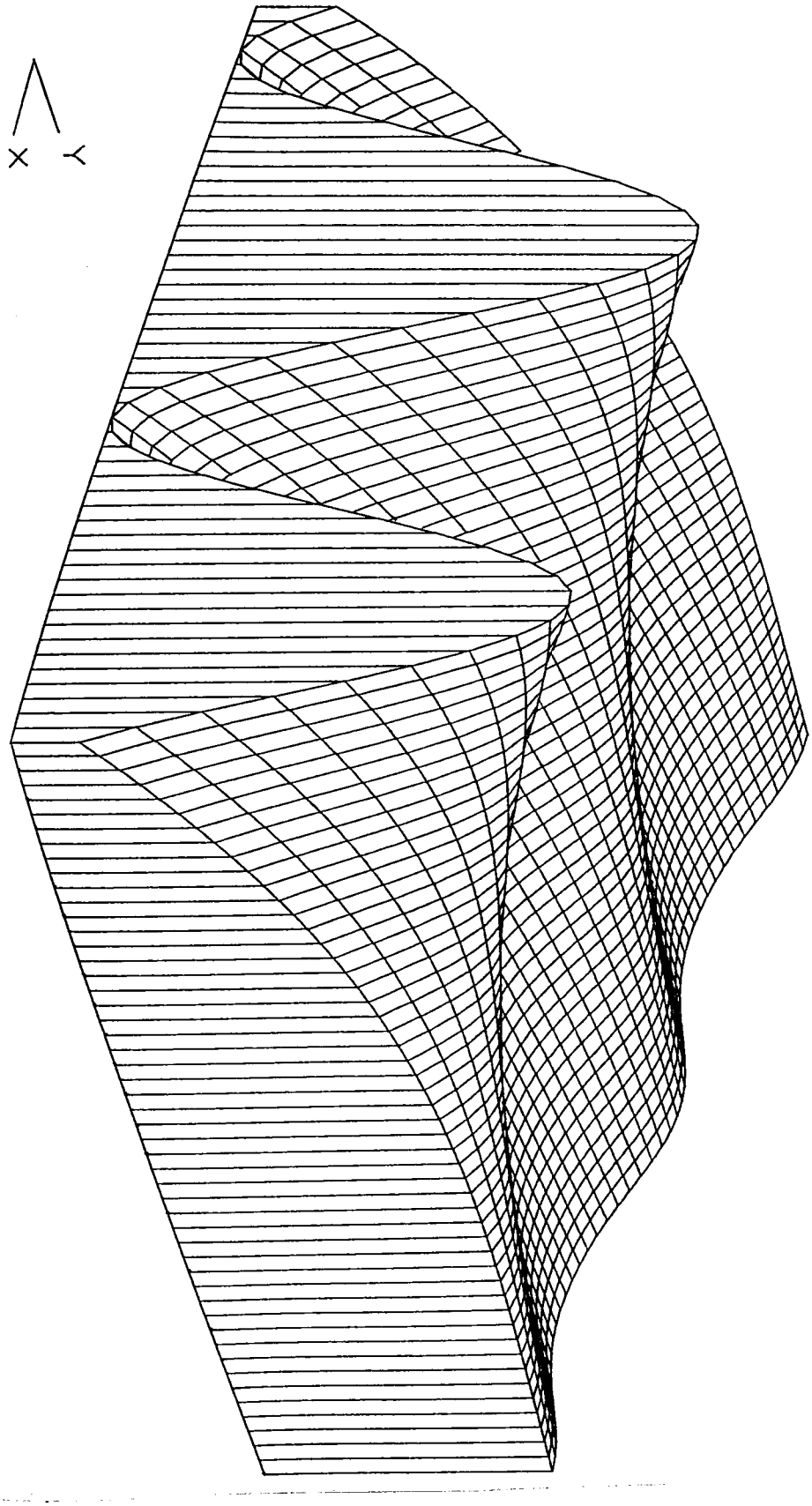

Fig. IX.9.(a). Analytical Surface Plot,
Intermediate Layer, The Rose Experiment,
Enhancement=50.0.

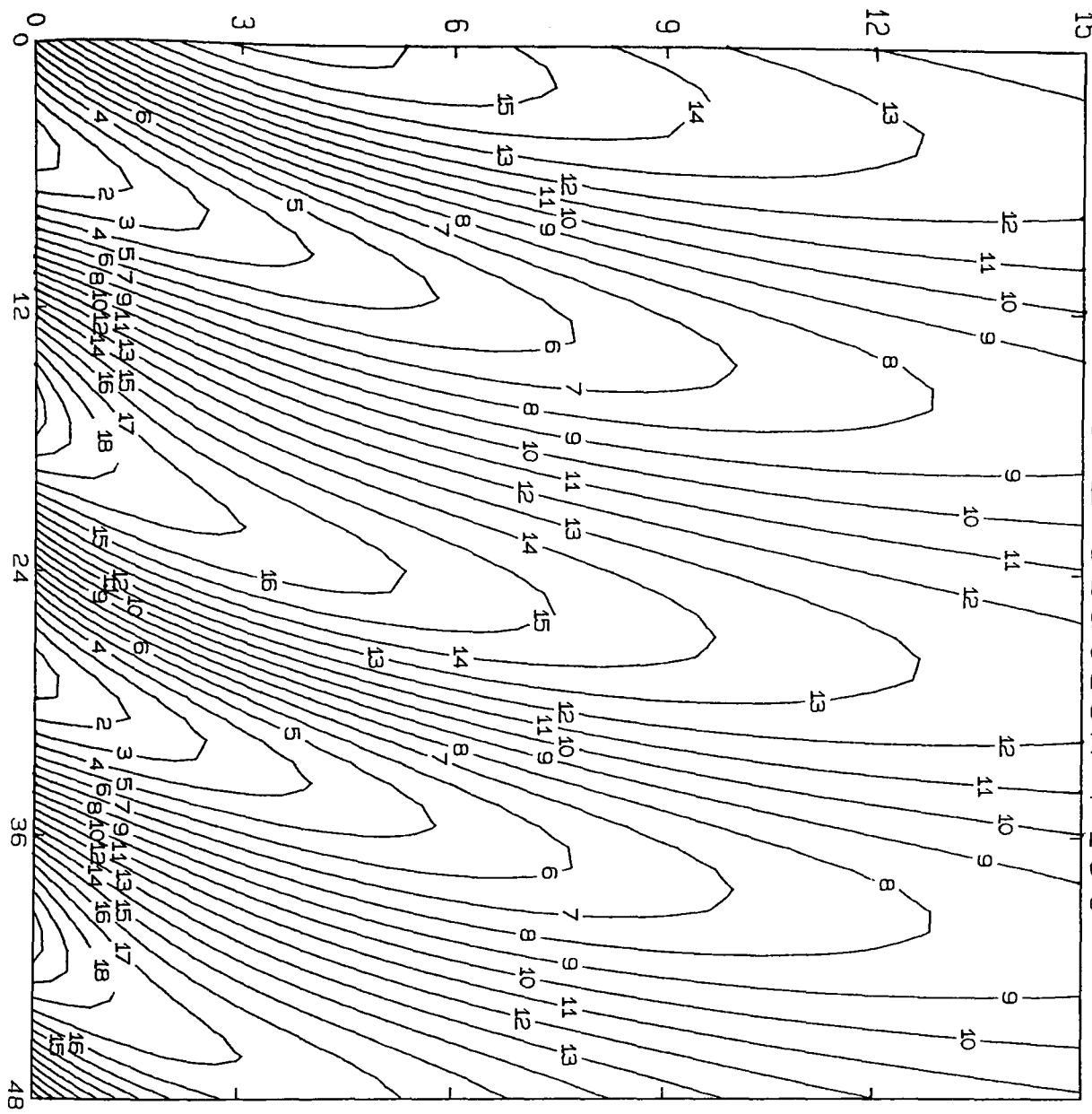

CONTOUR KEY	
1	0.1252
2	0.1267
3	0.1283
4	0.1298
5	0.1314
6	0.1330
7	0.1345
8	0.1361
9	0.1376
10	0.1392
11	0.1408
12	0.1423
13	0.1439
14	0.1454
15	0.1470
16	0.1486
17	0.1501
18	0.1517
19	0.1532
20	0.1548

Fig. IX.9.(b). Analytical Contour Plot to 15 *cms.*,
The Rose Experiment, Enhancement=50.0.
Time, *hrs.* v. Depth, *cms.* v. Moisture, *dimensionless.*

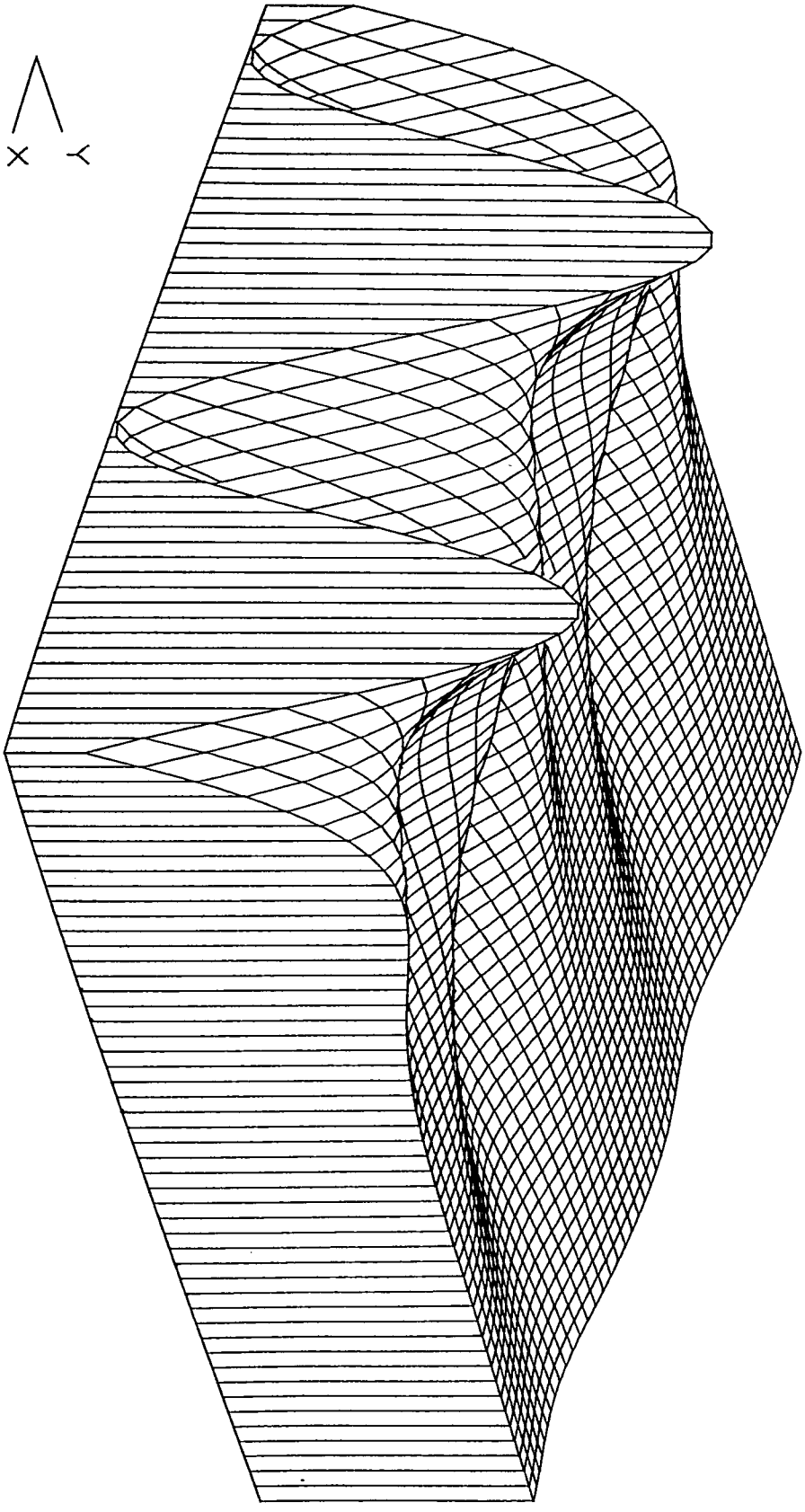

Fig. IX.11.(a). Analytical Surface Plot,
The Jackson Experiment, No Enhancement.

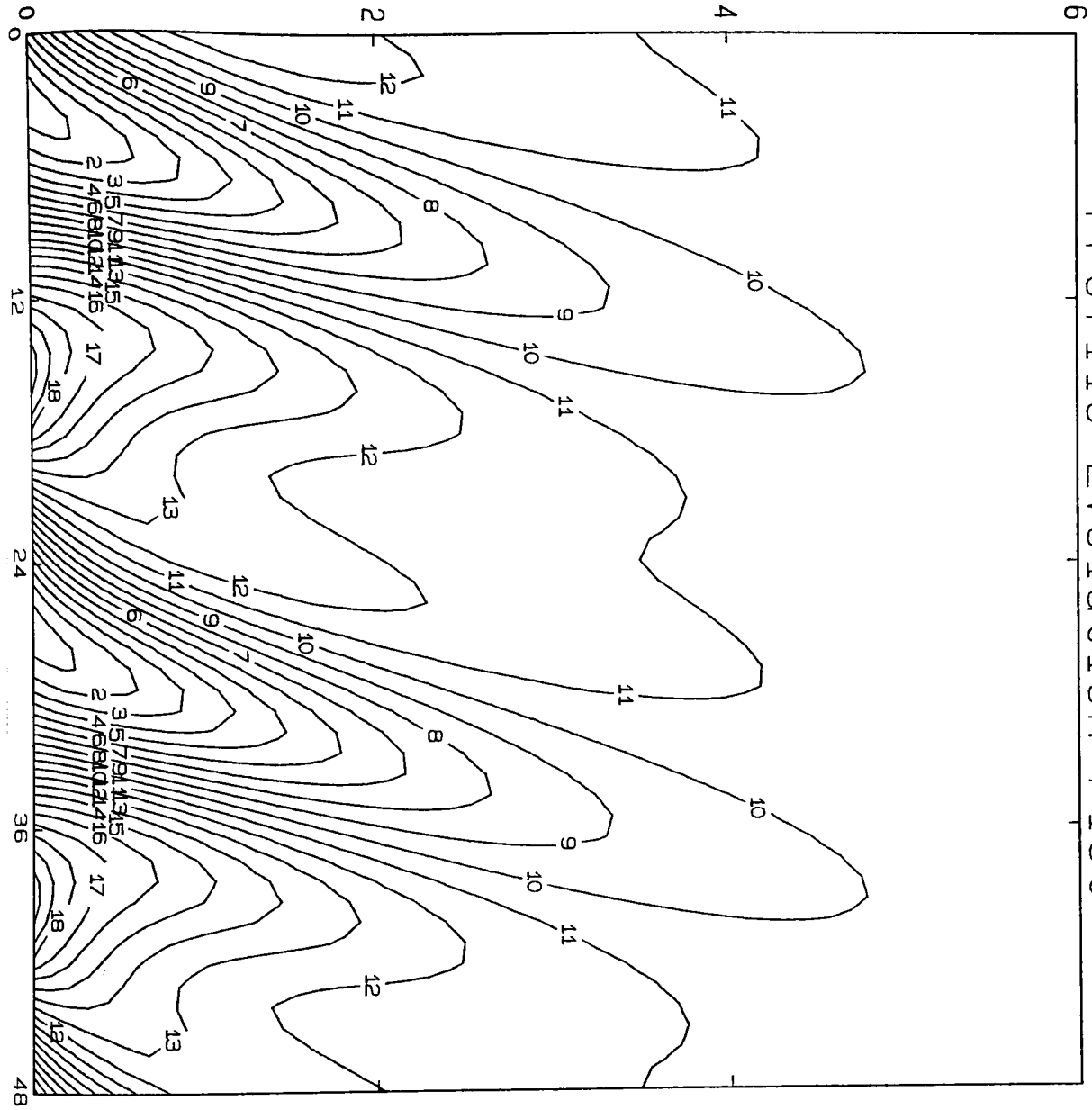

CONTOUR KEY	
1	0.1613
2	0.1633
3	0.1652
4	0.1672
5	0.1692
6	0.1711
7	0.1731
8	0.1751
9	0.1770
10	0.1790
11	0.1810
12	0.1829
13	0.1849
14	0.1868
15	0.1888
16	0.1908
17	0.1927
18	0.1947
19	0.1967
20	0.1986

Fig. IX.11.(b). Analytical Contour Plot to 6 *cms.*,
The Jackson Experiment, No Enhancement.
Time, *hrs.* v. Depth, *cms.* v. Moisture, *dimensionless.*

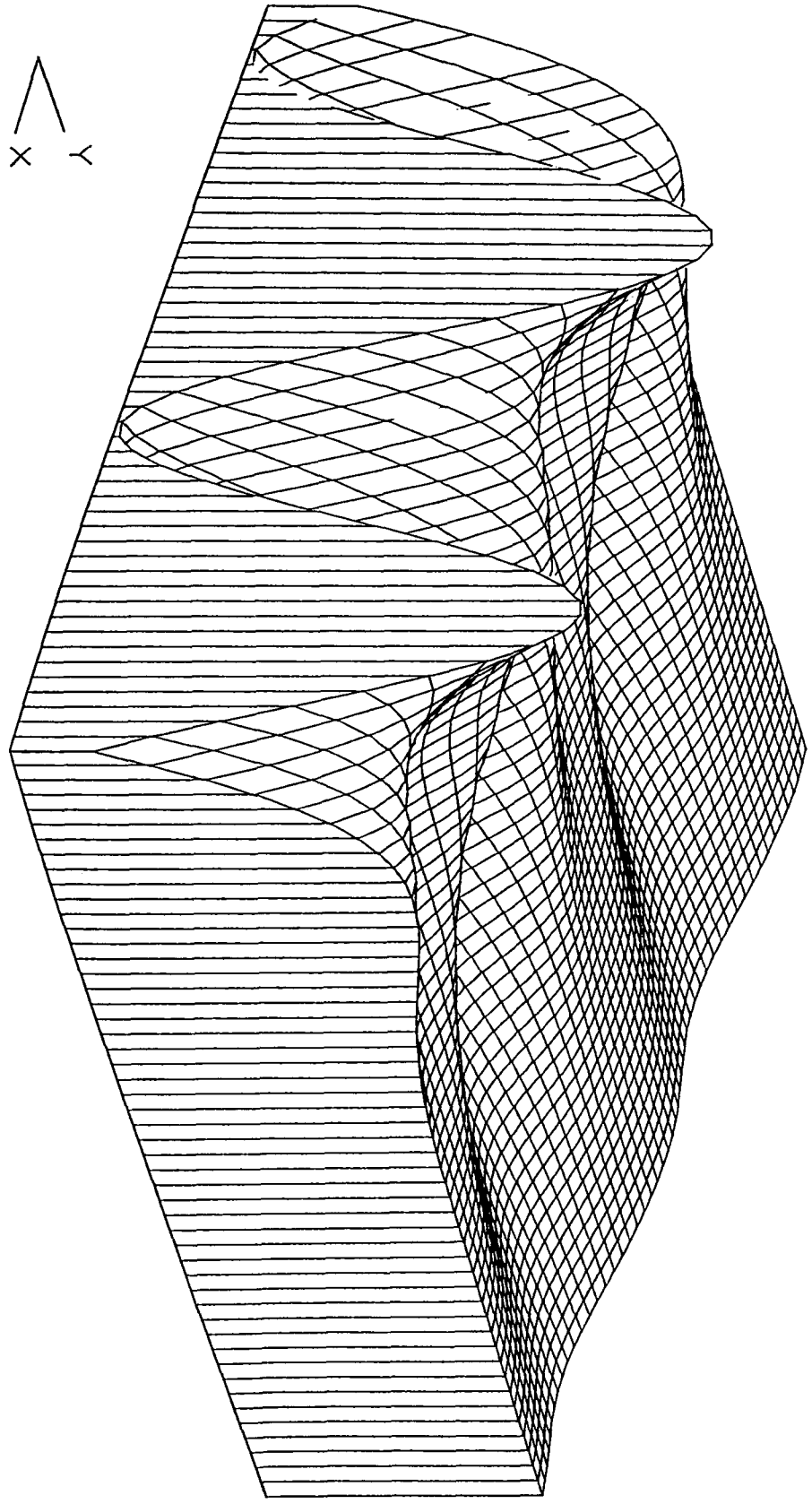

Fig. IX.12.(a). Analytical Surface Plot,
The Jackson Experiment, Enhancement = 10.0.

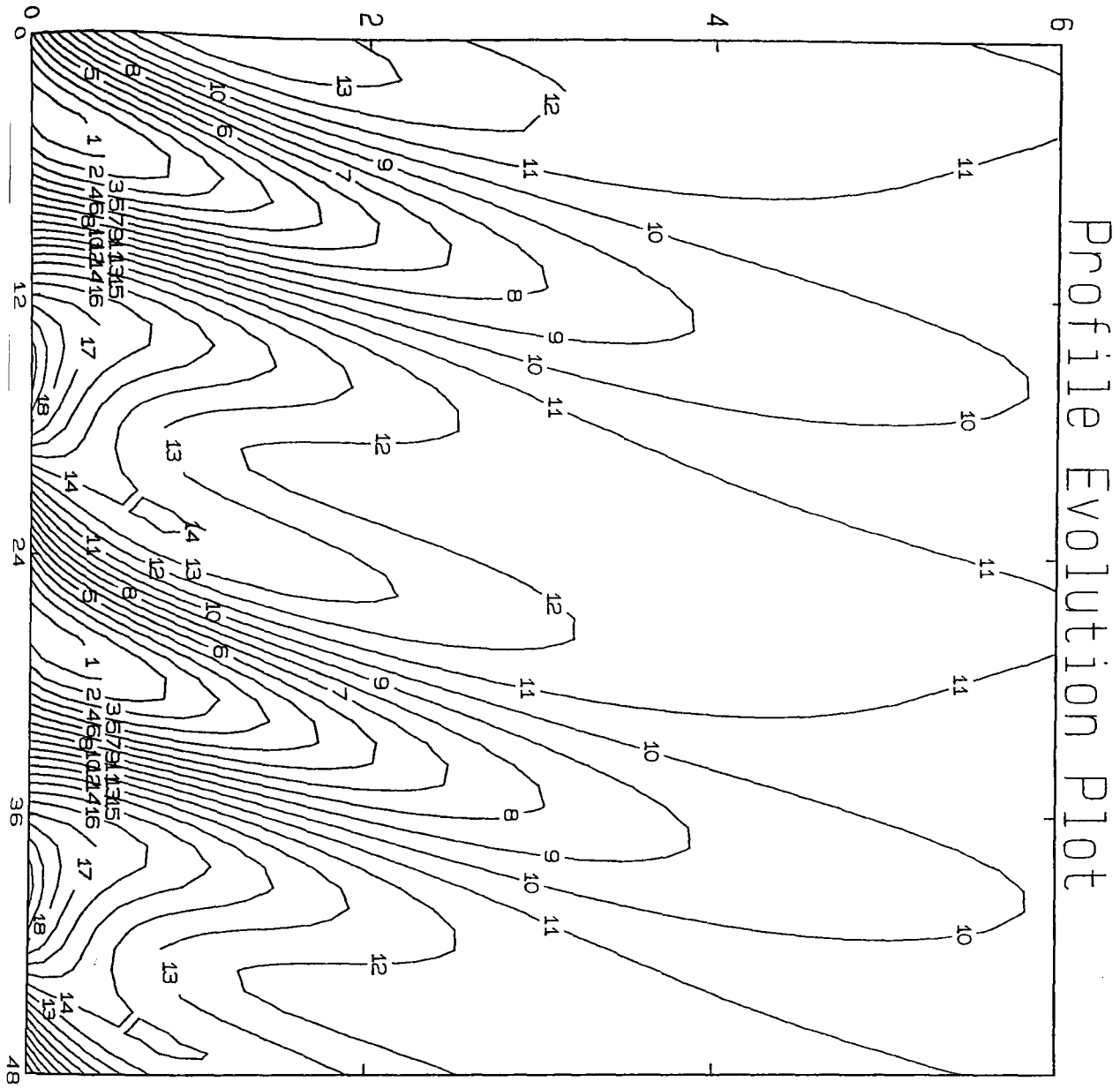

CONTOUR KEY	
1	0.1587
2	0.1610
3	0.1632
4	0.1654
5	0.1676
6	0.1699
7	0.1721
8	0.1743
9	0.1765
10	0.1787
11	0.1810
12	0.1832
13	0.1854
14	0.1876
15	0.1899
16	0.1921
17	0.1943
18	0.1965
19	0.1987
20	0.2010

Fig. IX.12.(b). Analytical Contour Plot to 6 *cms.*,
The Jackson Experiment, Enhancement = 10.0.
Time, *hrs.* v. Depth, *cms.* v. Moisture, *dimensionless.*

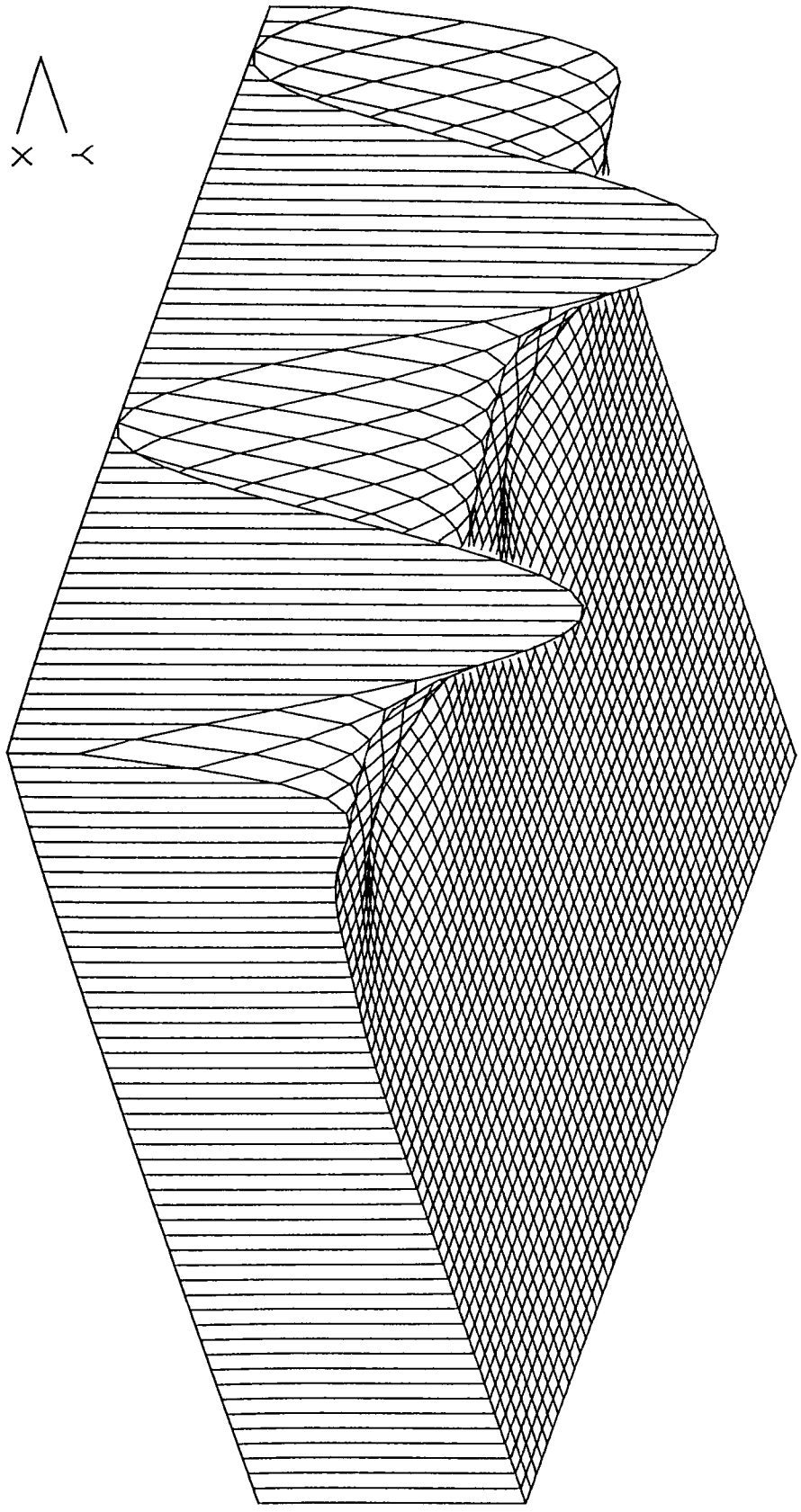

Fig. IX.13.(a). Analytical Surface Plot to 15cms.
The Jackson Experiment, No Enhancement.

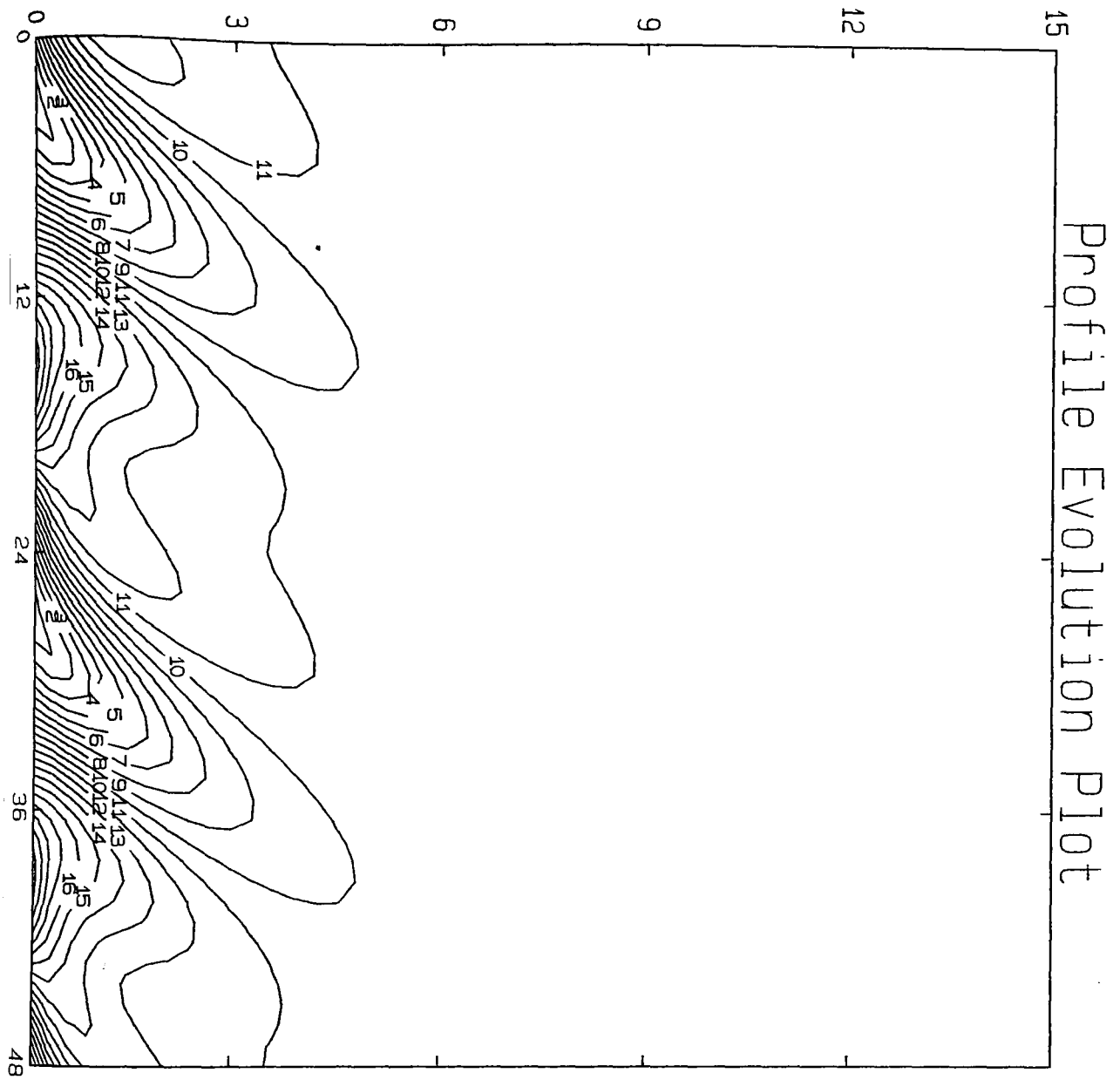

CONTOUR KEY	
1	0.1613
2	0.1633
3	0.1652
4	0.1672
5	0.1692
6	0.1711
7	0.1731
8	0.1751
9	0.1770
10	0.1790
11	0.1810
12	0.1829
13	0.1849
14	0.1868
15	0.1888
16	0.1908
17	0.1927
18	0.1947
19	0.1967
20	0.1986

Fig. IX.13.(b). Analytical Contour Plot to 15*cms.*,
The Jackson Experiment, No Enhancement.
Time, *hrs.* v. Depth, *cms.* v. Moisture, *dimensionless.*

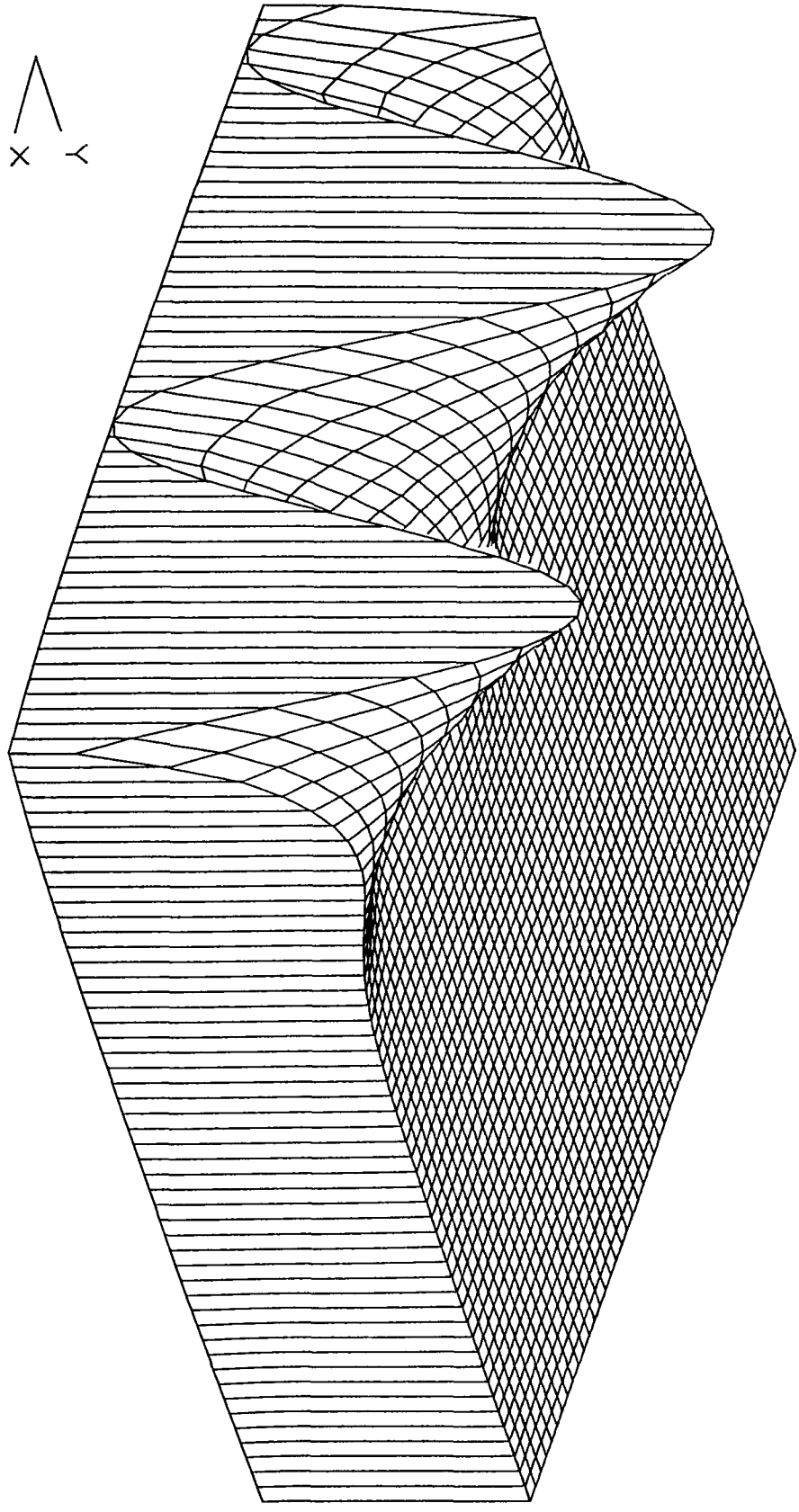

Fig. IX.13.(c). Simulated Surface Plot to 15*cms.*,
The Jackson Experiment, No Enhancement.

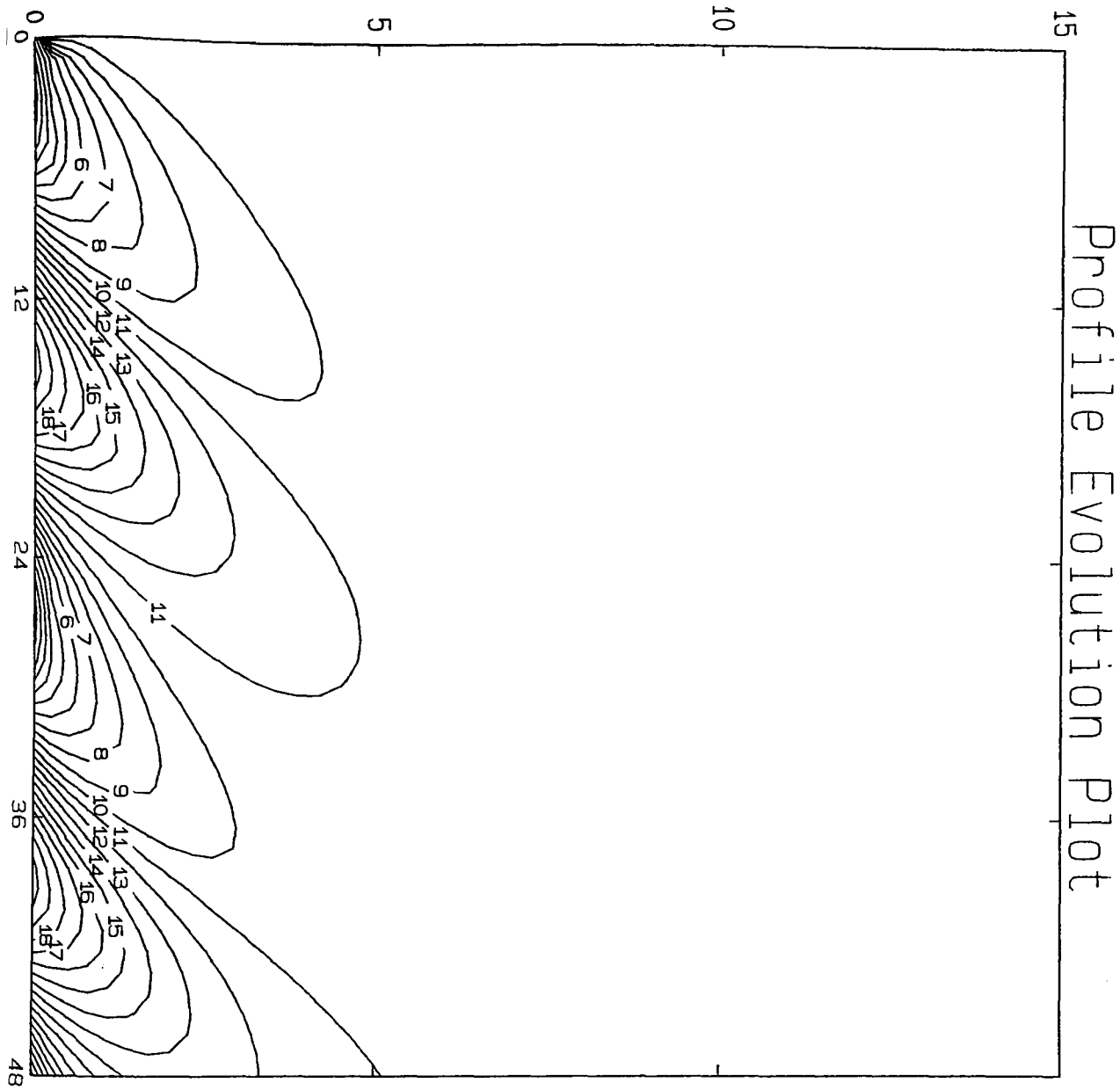

CONTOUR KEY	
1	0.1610
2	0.1630
3	0.1650
4	0.1670
5	0.1690
6	0.1710
7	0.1730
8	0.1750
9	0.1770
10	0.1790
11	0.1810
12	0.1830
13	0.1849
14	0.1869
15	0.1889
16	0.1909
17	0.1929
18	0.1949
19	0.1969
20	0.1989

Fig. IX.13.(d). Simulated Contour Plot to 15*cms.*,
The Jackson Experiment, No Enhancement.
Time, *hrs.* v. Depth, *cms.* v. Moisture, *dimensionless.*

YYYY

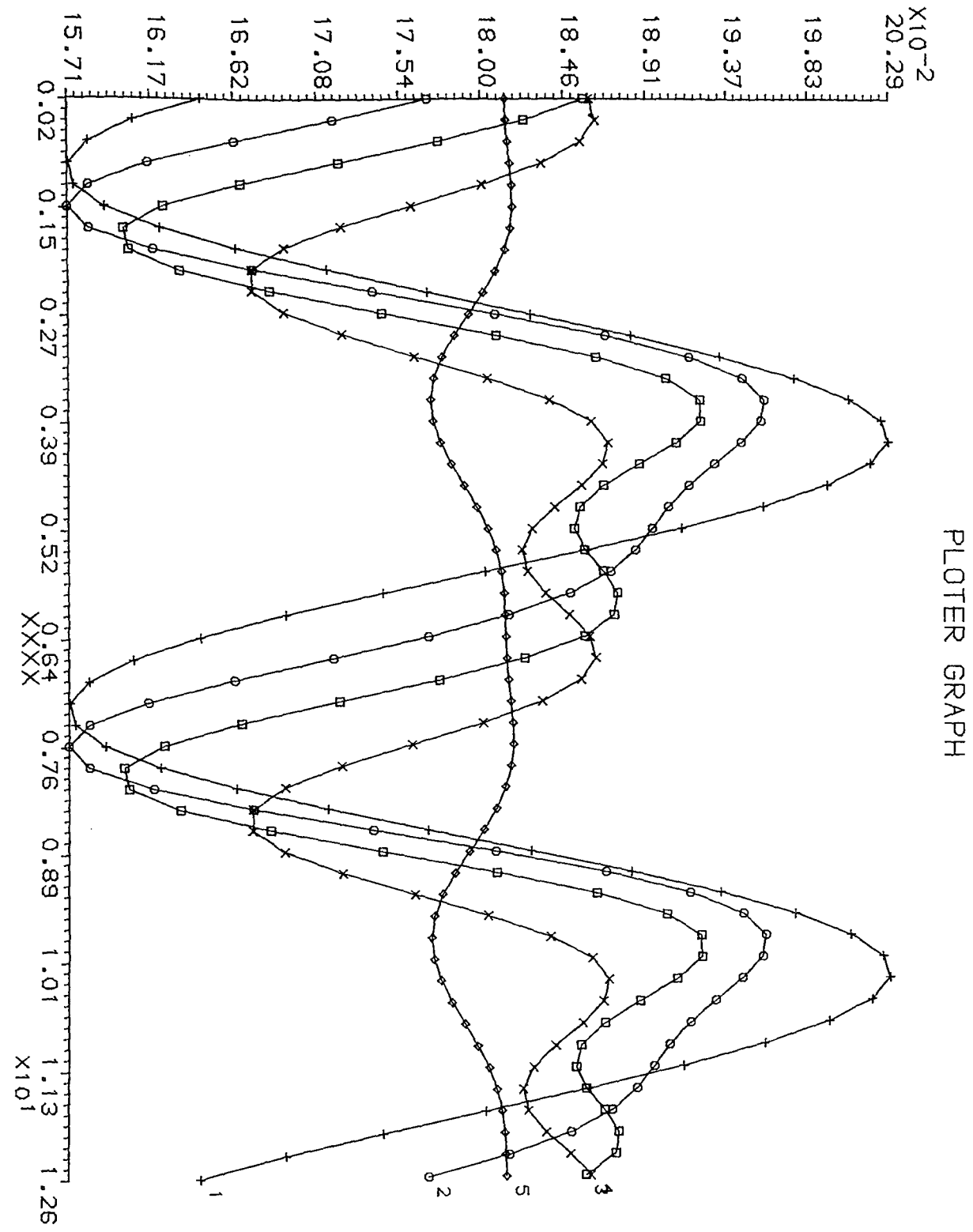

Fig. IX.14. Cross-sections of the Analytical Surface Plot.,

The Jackson Experiment, Fig.IX.12.(a).

Time, 2 cycles (4π) v. Moisture, *dimensionless*.